6 March 2008 | www.nature.com/nature | $10

THE INTERNATIONAL WEEKLY JOURNAL OF SCIENCE

nature

ASTROPHYSICS
Can LISA rule the gravity waves?

PLASMASPHERIC HISS
Starting in the chorus

ALGAL BLOOMS
When to see red

FEAST OR FAMINE

The unpredictability of the Lake Myvatn midges

NATUREJOBS
Focus on physics

$10.00US $12.99CAN

nature 452, 1-126 6 March 2008

www.nature.com/nature

no.7183

npg

R&D Systems NEW PlusCellect™ Kits

Positively the BEST in Cell Selection.

✓ Positive selection for the isolation of rare cell populations ✓ Flexible – compatible with several magnetic systems
✓ Selection and detection antibodies included ✓ Fast – enrichment in about 1 hour ✓ Specific & simple

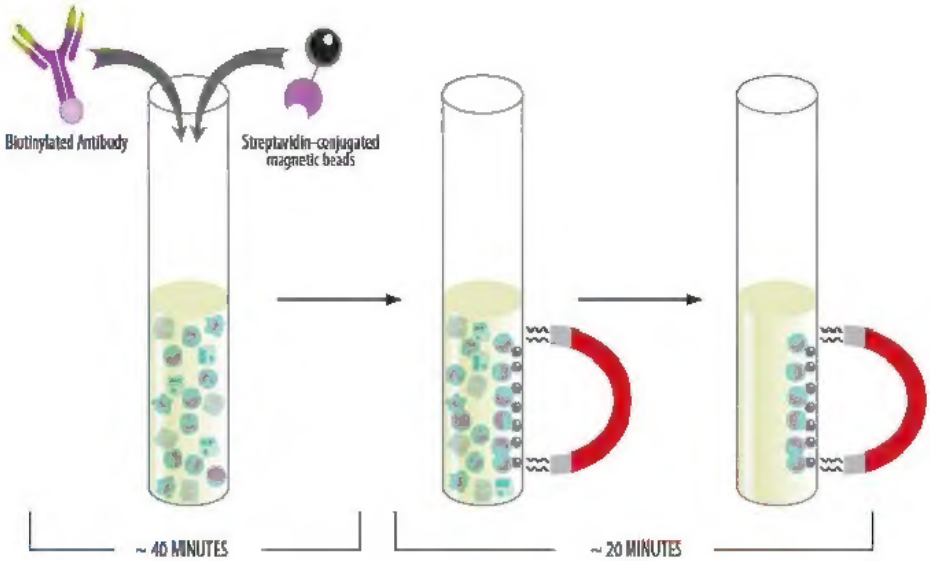

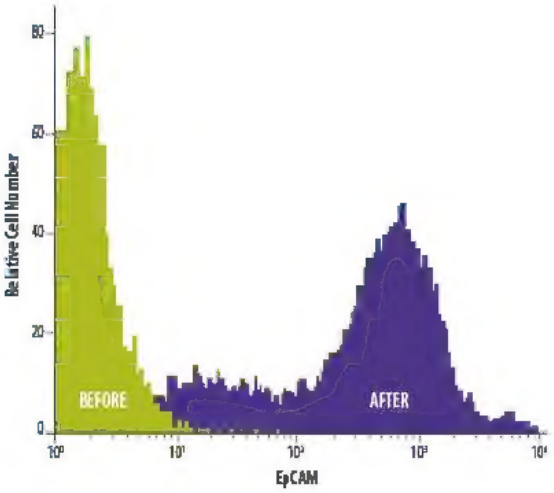

The human EpCAM PlusCellect Kit (Catalog # PLS960) was used to enrich for EpCAM+ cells in a culture containing human whole blood cells spiked with MCF-7 human breast cancer cells. Cells were stained with PE-conjugated anti-human EpCAM detection antibody both before (green) and after (purple) selection.

Kits for these markers are currently available:

- ACE/CD143
- CCR5
- CD3
- CD4
- CD45
- E-Selectin/CD62E
- CXCR4
- E-Cadherin
- Endoglin/CD105
- EpCAM
- IntegrinαV/CD51
- MCAM/CD146
- NCAM-1/CD56
- PECAM-1/CD31
- VE-Cadherin/CD144
- VCAM-1/CD106
- VEGF R2

For more information visit our website at www.RnDSystems.com/go/PlusCellect

For research use only. Not for use in diagnostic procedures.

R&D Systems Tools for Cell Biology Research™

USA & Canada **R&D Systems, Inc.** Tel: (800) 343-7475 info@RnDSystems.com
Europe **R&D Systems Europe, Ltd.** Tel: +44 (0)1235 529449 info@RnDSystems.co.uk

Selection expanding weekly—visit www.RnDSystems.com to sign up for weekly new product updates.

R&D SYSTEMS®


Shhh. It's the Innova AFM.
No noise. Higher resolution. This kind of news doesn't stay quiet for long.
www.veeco.com/innova
Veeco
Come see us at APS, Booth # 616

www.roche-applied-science.com

Genome Sequencer FLX System

Longer sequencing reads mean more applications.

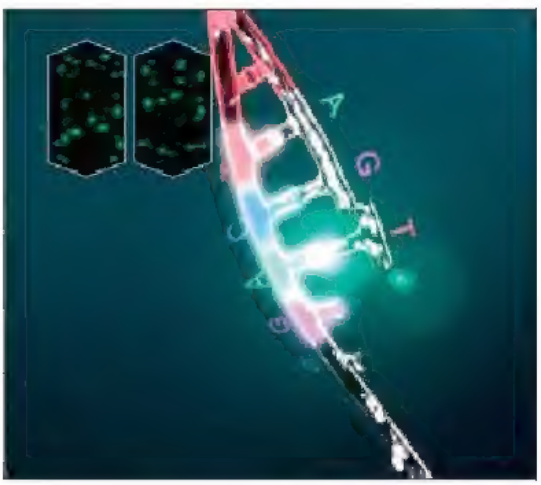

Sequencing-by-Synthesis: Using an enzymatically coupled reaction, light is generated when individual nucleotides are incorporated. Hundreds of thousands of individual DNA fragments are sequenced in parallel.

In 2005, the Genome Sequencer 20 System was launched

- Read length: 100 bases
- 20 million bases in less than 5 hours

In 2007, the Genome Sequencer FLX System was launched

- Read length: 250 to 300 bases
- 100 million bases in less than 8 hours

Available in 2008, the Genome Sequencer FLX with improved chemistries

- Read length: >400 bases
- 1 billion bases in less than 24 hours

More applications lead to more publications.

Proven performance with an expanding list of applications and more than 130 peer-reviewed publications.
Visit ***www.genome-sequencing.com*** to learn more.

454 LIFE SCIENCES

Roche Diagnostics
Roche Applied Science
Indianapolis, Indiana

Roche

For life science research only. Not for use in diagnostic procedures.

Nature Publishing Group
The Macmillan Building,
4 Crinan St, London N1 9XW, UK
e-mail: nature@nature.com

NATURE'S MISSION, 1869:
'The objective which it is proposed to attain by this periodical may be broadly stated as follows. It is intended, first, to place before the general public the grand results of scientific work and scientific discovery; and to urge the claims of science to move to a more general recognition in education and in daily life…Secondly, to aid scientific men [sic] themselves, by giving early information of all advances made in any branch of natural knowledge throughout the world, and by affording them an opportunity of discussing the various scientific questions which arise from time to time.'

Nature's mission statement was updated in 2000:
www.nature.com/nature/about
Submissions and Guide to Authors:
www.nature.com/nature/authors

Author and referee policies and services:
www.nature.com/authors

Nature® (ISSN 0028-0836) is published by Nature Publishing Group, a division of Macmillan Publishers Ltd (The Macmillan Building, 4 Crinan Street, London N1 9XW). Registered as a newspaper at the British Post Office.
North and South American orders to *Nature*, Subscription Dept, 342 Broadway PMB 301, New York NY 10013-3910, USA.
Other orders to *Nature*, Brunel Road, Basingstoke, Hants RG21 2XS, UK.

Identification code for *Nature*: 0028-0836/03
CPC PUB AGREEMENT #40032744
In the US, *Nature* (ISSN 0028-0836) is published weekly on Thursday, except the last week in December by Nature Publishing Group, 75 Varick St, 9th Fl, New York NY 10013-1917, USA. US Periodicals postage paid at New York NY, and additional mailing post offices.
US POSTMASTER: send address changes to *Nature*, Subscription Dept, 342 Broadway PMB 301, New York NY 10013-3910, USA.
Published in Japan by NPG Nature Asia-Pacific, Chiyoda Building, 2-37 Ichigayatamachi, Shinjuku-ku, Tokyo 162-0843, Japan.

nature publishing group

nature

D. VEN NERBECK

The age of steampunk: a clash of technologies, p. **32**.

W. LAWLER/ECOSCENE/CORBIS

Too late for some: deforestation is still on UN agenda, p. **8**.

Microsoft®
HealthVault™
Be Well Fund

It's time to bring healthcare into the Internet Age.

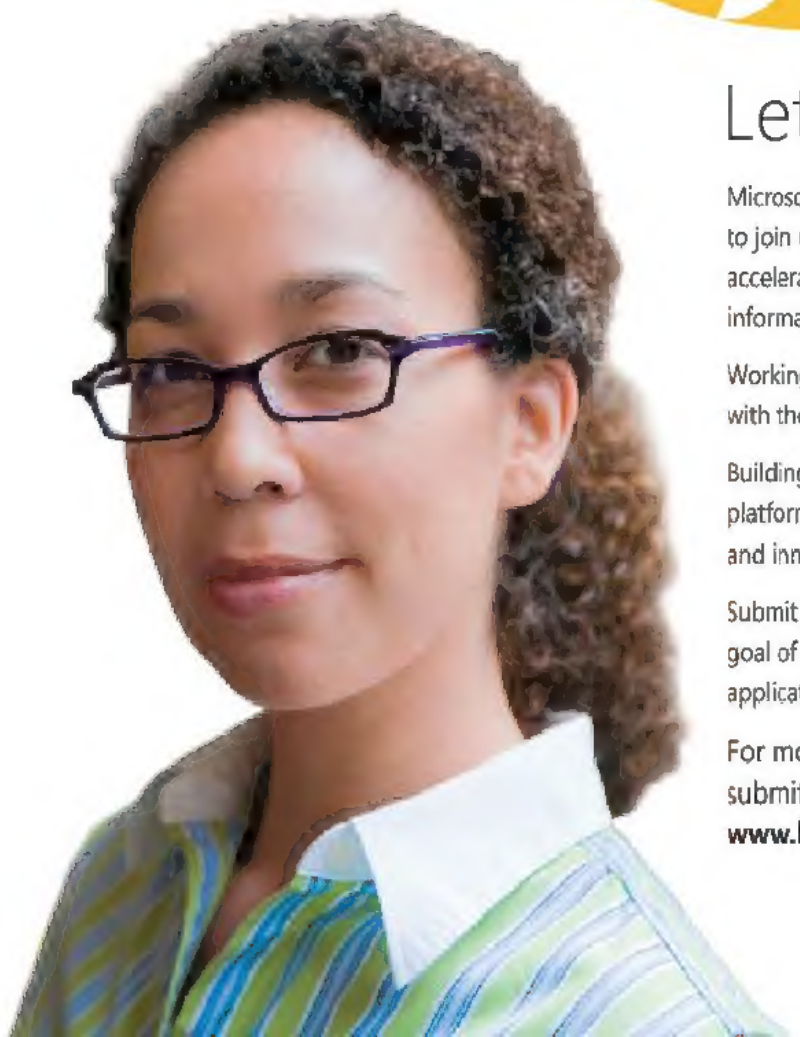

Let's do it *together*.

Microsoft is calling on research and academic health institutions to join us in the search for new, innovative health applications that accelerate connections between consumers and physicians and the information they need to make informed and personalized decisions.

Working together, we can empower physicians and patients with the solutions they need to make a difference.

Building on the Microsoft® HealthVault™ consumer health platform, you have the potential to enable fundamentally new and innovative scenarios.

Submit your ideas to the HealthVault Be Well Fund and join our goal of identifying and developing new, yet-to-be-imagined Web applications that will help people live longer, healthier lives.

For more information on how your institution can submit a proposal to the HealthVault Be Well Fund, visit:
www.healthvault.com/fund

Microsoft

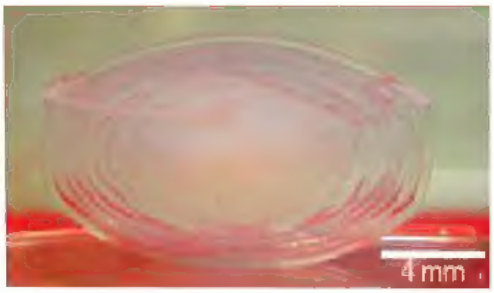

Advanced hydrogels: onioned-shaped gels mix well with living tissue, p. 72.

ARTICLES

LETTERS

NATURE ONLINE

ADVANCE ONLINE PUBLICATION

PUBLISHED ON 2 MARCH 2008

Localization and functionality of microsporidian iron–sulphur cluster assembly proteins
A V Goldberg, S Molik, A D Tsaousis, K Neumann, G Kuhnke, F Delbac, C P Vivares, R P Hirt, R Lill & T M Embley
doi:10.1038/nature06606

A skin microRNA promotes differentiation by repressing 'stemness'
R Yi, M N Poy, M Stoffel & E Fuchs
doi:10.1038/nature06642

Biodiversity and biogeography of phages in modern stromatolites and thrombolites
C Desnues *et al.*
doi:10.1038/nature06735

PUBLISHED ON 5 MARCH 2008

Broad phylogenomic sampling improves resolution of the animal tree of life
C W Dunn *et al.*
doi:10.1038/nature06614

Memory CD4 T cells emerge from effector T-cell progenitors
L E Harrington, K M Janowski, J R Oliver, A J Zajac & C T Weaver
doi:10.1038/nature06672

Identifying natural images from human brain activity
K N Kay, T Naselaris, R J Prenger & J L Gallant
doi:10.1038/nature06713

X-ray structure of a prokaryotic pentameric ligand-gated ion channel
R J C Hilf & R Dutzler
doi:10.1038/nature06717

Isolation of an active step I spliceosome and composition of its RNP core
S Bessonov, M Anokhina, C L Will, H Urlaub & R Lührmann
doi:10.1038/nature06842

BRIEF COMMUNICATIONS ARISING

PUBLISHED ON 6 MARCH 2008

Arising from 'Behavioural improvements with thalamic stimulation after severe traumatic brain injury' by N D Schiff *et al.* *Nature* **448**, 600–603 (2007).

Arousal by stimulation of deep-brain nuclei
H Staunton doi:10.1038/nature06574

Reply: N D Schiff *et al.* doi:10.1038/nature06575

PODCAST NEWS

Lake Myvatn in northern Iceland is popular with tourists seeking subarctic scenery and wildlife. It is also a remarkable example of an ecosystem dominated by one species — the midges featured on this week's cover and discussed in the podcast. Luckily for the tourists, these midges don't bite.
www.nature.com/podcast
For the podcast archive in mp3 format, visit:
http://tinyurl.com/k62cvt

Enabling Technologies for Cancer Research

A Comprehensive Oncology Toolkit

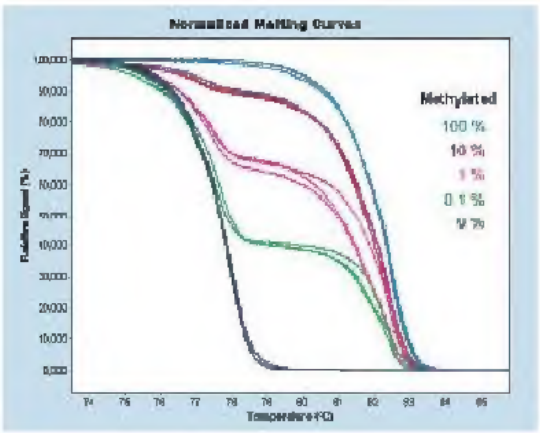

Analysis of tumor suppressor gene methylation with the LightCycler® 480 System. Mixtures of unmethylated and fully methylated genomic DNA were treated with bisulfite. A fragment of the MGMT tumor suppressor gene was then amplified and analyzed by high-resolution melting. This allowed semi-quantitative determination of the portion of methylated DNA contained in each case.

Data kindly provided by Tomasz K. Wojdacz and Alexander Dobrovic.

Drive your cancer research discoveries with Roche Applied Science's innovative, accurate, and versatile instruments and applications. We combine world-class technologies for real-time PCR, microarrays, and DNA sequencing to provide you with the most comprehensive cancer research toolkit available:

LightCycler® 480 Real-Time PCR System – Investigate genetic and epigenetic variation patterns with powerful real-time PCR applications, including high-resolution mutation screening, HRM methylation detection (Figure 1), and quantitative ChIP analysis.

NimbleGen® DNA Microarrays – Target and evaluate oncogenes and other regions of interest with long oligos at high resolution (2.1 million probes).

Genome Sequencer FLX System – Identify rare (<1%) cancer-associated somatic mutations at the molecular level from heterogeneous tissue samples.

Discover... Analyze... Validate.
Visit ***www.roche-applied-science.com*** for more information or to find a local representative.

Roche Diagnostics GmbH
Roche Applied Science
68298 Mannheim, Germany

Roche

THIS ISSUE

THREE'S COMPANY LISA, the Laser Interferometer Space Antenna, is one of the most ambitious space missions ever mounted. A joint effort between NASA and ESA, its job will be to measure the so-far invisible gravitational waves predicted by Einstein's general theory of relativity. In fact there are three 'LISAs', designed to travel 5 million kilometres apart at the corners of a giant equilateral triangle. Trudy Bell reports on the pre-launch preparations. [News Feature p. 18]

ESA

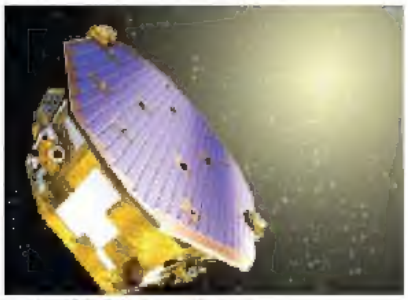

ESA's Pathfinder, a try-out for LISA

SPRING BOOK In *The Hot Topic*, science writer Gabrielle Walker and former UK government science adviser Sir David King outline the scientific 'party line' on the causes of climate change. And, says our reviewer David Reay, when turning to the solutions and politics of climate change, the book really shows its pedigree. Here it earns its subtitle — *How to Tackle Global Warming and Still Keep the Lights On*. Climate change, says Reay, has found its *Silent Spring*. [Books & Arts p. 31]

AIMING HIGH New York University's newly created Institute for the Study of the Ancient World (ISAW) intends to become a world-class archaeological institute, and has had $220 million to spend in pursuit of that goal. But some

ISAW/NYU

New Yorker: the Greek god Pan, now in Fifth Avenue.

in the archaeological establishment are not as excited at the prospect as you would expect, voicing concerns about the involvement of ISAW's principal patron with the world market in antiquities. Rex Dalton reports. [News Feature p. 22]

Iceland's Lake Myvatn ecosystem is remarkable in that it is so dominated by a single species. Myvatn translates as 'midge lake', and it is the midge *Tanytarsus gracilentus* that dominates, comprising two-thirds of the lake's secondary productivity. Midge numbers undergo extreme fluctuations of almost six orders of magnitude with an irregular period of 4 to 7 years. A new analysis of 25 years of population monitoring shows that this phenomenon can be explained by alternative dynamical states with the amplitude of the fluctuations set by small subsidies of food entering the habitat. Small decreases in food supply due to human disturbances could explain recent increases in midge fluctuations. In conservation terms, midge populations are inherently unpredictable and are much more vulnerable to small disturbances in the lake than was expected. The Lake Myvatn midges illustrate the fundamental complexities of natural ecosystems and the difficulties in managing them. The cover shows mating swarms of male midges waiting for females to join them. [Letter p. 84; Author page; www.nature.com/podcast]

ÁRNI EINARSSON

Turning the tide in Florida

The 'red tides' or algal blooms cause by rapid accumulation of algae in surface waters are potentially hazardous. Florida red tides in particular are associated with the neurotoxin brevetoxin, produced by the marine algae *Karenia brevis*, which can be fatal to fish, birds and marine mammals. Bathers finding themselves in a red tide can suffer skin irritation and other reactions. Despite extensive monitoring there is still much to be learned

FWC

Red alert: an algal bloom washes ashore.

about the origins and growth of red tides. As Mark Schrope reports, Florida's new Center for Prediction of Red Tides plans to raise the profile of red tide research and to improve forecasting accuracy. [News Feature p. 24]

DNA changes tack

Two papers in this issue report cycles of DNA methylation and demethylation of CpG dinucleotides at gene promoters. The findings contrast sharply with the prevailing view of DNA methylation as a stable epigenetic 'mark' capable of transmitting a specific pattern of gene expression through mitosis and into the daughter cells. Métivier *et al.* [Article p. 45] observed DNA methylation/demethylation cycles at the *pS2* gene promoter during its activation by oestrogen, accompanied by cycling of DNA methyltransferases and other factors. And Kangaspeska *et al.* report cyclical DNA methylation at five active promoters including *pS2* and the oestrogen receptor α. [Letter p. 112]

Touching all the bases

It is difficult to predict RNA structures from a base sequence, partly because of the presence of 'non-Watson–Crick' base pairs such as guanine bound to uracil; these mismatches are thought to contribute to the RNA's structural stability. With the importance of small RNA molecules in cellular regulation now clear, the need to find better ways of determining RNA structure is urgent. Marc Parisien and François Major present a series of algorithms that represents a significant technical advance in determining RNA structure from sequence alone. The algorithms take into account all base-pairing interactions to yield three-dimensional structures. [Article p. 51]

Cadmium fills a niche

A major part of the carbon export from the atmosphere to the deep ocean is carried out by marine phytoplankton, using carbonic anhydrase to catalyse the reversible hydration of carbon dioxide. The active site of this enzyme usually contains zinc, but some diatoms substitute cadmium — usually regarded as a toxic element — as the catalytic metal atom. The X-ray crystal structures of four forms of this enzyme from the diatom *Thalassiosira weissflogii* — cadmium-bound, zinc-bound, metal-

This month in *Nature Reviews*

Telomerase and cancer therapeutics
C. B. Harley

A specific telomerase inhibitor and several telomerase therapeutic vaccines are in clinical trials, and other telomerase-based therapies are in preclinical development. What are the advantages and disadvantages of these approaches and which cancer patients might benefit most?

www.nature.com/reviews/cancer

Genome-wide association studies: progress and potential for drug discovery and development
S. F. Kingsmore et al.

Genome-wide association (GWA) studies have recently identified common genetic variants associated with a range of common complex diseases such as diabetes. This article highlights selected successes with this novel approach and discusses the potential for GWA studies to identify therapeutic targets and genetic biomarkers.

www.nature.com/reviews/drugdisc

Genome-wide approaches to studying chromatin modifications
D. E. Schones & K. Zhao

Chromatin structure is subject to various modifications that have profound influences on gene expression. This article reviews the recently developed techniques to study chromatin modifications at a genome-wide scale, which are allowing researchers to probe the complex components that make up epigenomes.

www.nature.com/reviews/genetics

Discovering susceptibility genes for asthma and allergy
D. Vercelli

A number of susceptibility genes for asthma and allergy have been identified in recent years. Here, Donata Vercelli discusses these genes and reviews the techniques used by geneticists to identify them. She also highlights the outstanding challenges in the field.

www.nature.com/reviews/immunology

Physiological heterogeneity in biofilms
P. S. Stewart & M. J. Franklin

Stewart and Franklin discuss the processes that generate chemical gradients in biofilms, the genetic and physiological responses of the bacteria as they adapt to these gradients and the techniques that can be used to visualize and measure physiological heterogeneity in biofilms.

www.nature.com/reviews/micro

Small non-coding RNAs in animal development
G. Stefani & F. J. Slack

Our understanding of the biological functions of small non-coding RNAs stems from the analysis of genetic deletions of individual microRNAs (miRNAs) in mammals. These studies show that miRNAs are key regulators of animal development and are potential human disease loci.

www.nature.com/reviews/molcellbio

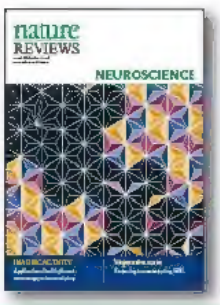

Pyramidal neurons: dendritic structure and synaptic integration
N. Spruston

The unique dendritic morphology of pyramidal neurons is likely to have an impact on their function. Spruston discusses how the properties of these neurons' distinct dendritic domains might contribute to their integration of synaptic inputs.

www.nature.com/reviews/neuro

***Nature Reviews Immunology* Focus on Allergy and Asthma**

This Focus issue of *Nature Reviews Immunology* highlights the latest advances in our understanding of the immune bases of these respiratory diseases and how this knowledge can be translated into effective treatment strategies.

www.nature.com/nri/focus/allergyandasthma

nature REVIEWS
www.nature.com/reviews
nature publishing group npg

free and acetate bound — have now been determined. The enzyme can easily exchange metals at its catalytic centre, suggesting that marine diatoms use of cadmium when zinc is rare, a considerable competitive advantage in the metal-poor environment of the oceans. [Article p. 56]

Plasmaspheric chorus line

Plasmaspheric hiss is a type of electromagnetic wave found in the dense plasma region — the plasmasphere — that encircles the Earth. This hiss is a dominant factor in controlling the two-zone structure of the Van Allen radiation belts, and since it removes high-energy electrons from the plasmasphere, it plays a pivotal role in reducing the radiation hazards to satellites and humans in space. Many theories have been proposed to explain the origin of the hiss, but none have stood the test of time. Bortnik *et al.* have used data from the CRRES satellite to develop a new model that explains hiss as a derivative of another wave type called chorus. Previously thought to be unrelated to hiss, chorus can propagate into the plasmasphere and subsequently evolve into hiss. [Letter p. 62, News & Views p. 41]

Cool quantum science

In recent years micromechanical devices have been developed that can strongly couple to light, by integrating them within optical cavities. A main goal has been to cool the devices optomechanically, freezing out all thermal vibrations, so that the object's motion eventually becomes limited by quantum mechanical fluctuations. This would make it possible to study a new range of quantum behaviour of mechanical objects. Thompson *et al.* report an improved design of such a system, involving a movable membrane sandwiched between two rigid high-quality mirrors. In previous

Mirror image: a new window into the quantum world

designs one of the mirrors had to double-up as a microresonator. The new device achieves substantial cooling, from room temperature to 6.8 mK. It should eventually be possible to reach the quantum-limited ground state with this system. [Letter p. 72]

A tissue of hydrogels

Polysaccharide-based hydrogels show potential for drug delivery and tissue engineering applications, for instance as a matrix to boost natural tissue regeneration. Ladet *et al.* use a multi-step interrupted gelation process to generate complex hydrogels with multi-membrane onion-like and tubular architectures. The new structures are made from chitosan or alginates, biocompatible natural polymers, and their novel layered structure creates vacant 'inter-membrane' spaces suitable for cell or drug introduction. The starting hydrogel can have any shape, and in principle any number of layers can be created. Initial experiments with chondrocyte cells cultured within a chitosan hydrogel suggest that the material has potential as a base for artificial tissues. [Letter p. 76]

A symbiont genome

The fungus *Laccaria bicolor* — seen in its above-ground fruiting body presence as the 'bicoloured deceiver' mushroom — lives symbiotically on the roots of trees. Its genome has now been sequenced, and the key features of the genome characterized by transcript profiling. The study throws light on the mechanism of mycorrhizal symbiosis, the union of

D. VAIRELLES

Fruits of the forest: with Douglas fir for company

roots and soil fungi that is of vital important to plant productivity. And it will be of keen interest to evolutionary and plant biologists for its revelations about plant–fungus interactions shaping genomes over time. [Letter p. 88; News & Views p. 42; Author page]

Psychosis complex isolated

New-generation antipsychotic drugs such as olanzapine and risperidone act by blocking neurotransmission by serotonin 2AR receptors; hallucinogens such as LSD also act via these receptors. And drugs that mimic the excitatory neurotransmitter glutamate at its mGluR2 receptor are also powerful antipsychotics. These and other lines of evidence suggest that the serotonin and glutamate neurotransmitter systems function abnormally in the brain in schizophrenia. This would seem to be confirmed with the surprising discovery of a functional complex containing the serotonin 2AR and mGluR2 receptors that is involved in the unique effects of chemical hallucinogens in cultured cells and mice. The balance of these two receptors is disrupted in the brains of schizophrenic subjects, further implicating this complex as a promising potential target for the treatment of psychosis. [Letters p. 93; News & Views p. 38]

Abstractions

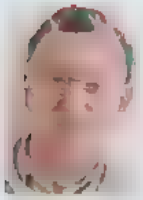

FIRST AUTHOR

About 85% of all plant species, most notably trees, depend on partnerships with soil fungi to thrive. The resulting mycorrhizal fungi scavenge hard-to-access nutrients and pass them on to the trees in exchange for the plants' store of carbon-rich sugar. On page 88, a team of international researchers reports some of the secrets of the genome of the mycorrhizal *Laccaria bicolor*. Francis Martin, a microbiologist at the French National Institute of Agricultural Research in Nancy, tells *Nature* how the genome sequence reveals an underground molecular dialogue that controls important ecosystem functions.

Was it difficult to get funding to sequence the genome of a mycorrhizal fungus?

I've worked with mycorrhizae for 25 years, but I wouldn't have bet a penny that we could get the €5-million worth of funding needed to sequence this genome. I worked on a collaborative effort, funded by the California-based Joint Genome Institute (JGI), to sequence the poplar tree's genome. After that, we were able to convince the JGI that sequencing *Laccaria* would provide a better understanding of ecosystem function.

Was this your first choice of species?

Yes. We wanted an ecologically relevant species that interacts with seedlings as well as mature trees found in Europe and North America. There were only a handful of such species with the minimal set of genetic resources required for sequencing, such as cDNA libraries. *Laccaria* is also economically relevant because it is used to promote the growth of conifer seedlings in nurseries.

Did the genome generate new hypotheses?

Many. For example, the genome has some features that are common to saprotrophs — organisms that consume dead organic matter — as well as genes required for symbiotic interactions, so we speculate that *Laccaria* may be an ancestral species of both groups. We also found genes encoding hundreds of small peptides, which we suspect the fungi may use to manipulate plant gene expression.

Are there any other mycorrhizal genome sequences on the horizon?

Yes, we are sequencing the genome of the black truffle mushroom, another mycorrhizal fungus. There are two main evolutionary branches of fungi, and the black truffle and *Laccaria* belong to different ones. By comparing the two genome sequences, we can see whether the two fungal kingdoms used the same tools to develop mycorrhizal symbioses with trees during evolution. We hope to get that paper out before Christmas — when truffles will reach the market. ■

MAKING THE PAPER

Anthony Ives

A mathematical model reveals the fragility of ecosystems.

The midges of Lake Myvatn — literal translation, 'Midge Lake' — in northern Iceland make up two-thirds of the lake's biomass, and often form swarms that hover like clouds over the surface of the water. Anthony Ives, a theoretical ecologist at the University of Wisconsin–Madison, puts their abundance into perspective by describing it as being "like going into prairie grasslands and having the majority of the animals there be a single species of grasshopper". But despite their dominance, the numbers of these tiny insects fluctuate wildly. And a mathematical model Ives developed to explain the population dynamics of the lake's midges suggests that they are extremely sensitive to both natural and human-induced change.

Ives began collaborating with Árni Einarsson and Arnthor Gardarsson at the University of Iceland in Reykjavik 10 years ago. Since 1977, these researchers had been gathering data on the population density of the midges, *Tanytarsus gracilentus*, living in Lake Myvatn. The data showed that the abundance of these midges, which feed on algae, fluctuates by almost six orders of magnitude. "The thing that really struck me was not just the extent of these fluctuations, but the fact that they're not random, nor are they regular. They're something in between," says Ives. Although some other animals also show dramatic population outbreaks, these typically occur in a regular fashion; outbreaks and crashes of Lake Myvatn's midges occur irregularly, 4 to 7 years apart.

To understand the phenomenon, Ives cobbled together statistical tools normally used to monitor stock market activity or the trajectories of interplanetary satellites, and applied them to Einarsson and Gardarsson's field data. The model showed unusual mathematical properties, so they enlisted Vincent Jansen at Royal Holloway, University of London, Epsom, to help interpret what these meant. In the model they designed, which is described on page 84, population abundance shifts between a constant state and one that is cyclical.

"It's this shifting from one type of dynamic [constant] to another type [cyclical] that can produce high-amplitude cycles and make the frequency of these cycles unpredictable or irregular," says Ives. Even small changes in the weather, or other environmental events, including those caused by human activities, may result in wild fluctuations in population density, he adds.

Ives's model also helps to explain the impact that historical dredging for the mineral diatomite may have had on the lake. The operation, which started in 1967, was abandoned in 2004 after becoming what Ives describes as "an environmental cause célèbre" when the fish populations started to diminish drastically. His mathematical model suggests that such dredging could have increased the size of the fluctuations in the midge population. Because these organisms are the main source of food for Lake Myvatn's fish, a crash in the midge population would have left fish with nothing to eat.

Ives hopes to continue this collaboration, and expand it to include other researchers, allowing them to gather further basic ecological information about the midges and the entire ecosystem that they affect. ■

FROM THE BLOGOSPHERE

With more than 100 members, the neuroscience group (http://tinyurl.com/2s356r) is one of the fastest growing areas of Nature Network. It recently started an online journal club for neuroscientists to discuss the latest research and trends.

As with a traditional journal club, interesting papers from any journal are featured, beginning with an account of the paper by a student or postdoc in the neuroscience discipline concerned who was not involved in the work being discussed.

This journal club is designed to teach non-specialists about certain neuroscience subfields that may be of interest to them, as well as to highlight important findings for specialists. Participants ask questions about data and conclusions, or the implementation of particular methodologies, discuss why additional data would help solidify conclusions, and suggest next steps.

It is almost two months since the journal club began, and five papers have already been discussed. Topics range from delivering anaesthesia to manufacturing hair cells, as well as controversial debate about glia, flies and sexual preference. ■

Visit Nautilus for regular news relevant to *Nature* authors ▸ http://blogs.nature.com/nautilus and see Peer-to-Peer for news for peer reviewers and about peer review ▸ http://blogs.nature.com/peer-to-peer.

nature

www.nature.com/nature

Vol 452 Issue no. 7183 6 March 2008

EDITORIAL

LONDON nature@nature.com
The Macmillan Building, 4 Crinan Street, London N1 9XW
Tel: +44 (0)20 7833 4000 Fax: +44 (0)20 7843 4596/7
EDITOR-IN-CHIEF: Philip Campbell
PUBLISHING EXECUTIVE EDITOR: Maxine Clarke
EDITORIALS: Philip Campbell, M Mitchell Waldrop
NEWS/FEATURES/ONLINE NEWS: Oliver Morton, Geoff Brumfiel, Daniel Cressey, Michael Hopkin, Nicola Jones, Anna Petherick, Katharine Sanderson, Sarah Tomlin, Gaia Vince
BOOKS & ARTS/CORRESPONDENCE & ESSAYS/COMMENTARIES: Sara Abdulla, Joanne Baker, Lucy Odling-Smee, Sarah Tomlin
NEWS AND VIEWS: Tim Lincoln, Andrew Mitchinson, Sadaf Shadan, Richard Webb
PHYSICAL, CHEMICAL AND EARTH SCIENCES: Karl Ziemelis, Rosamund Daw, Joshua Finkelstein, Magdalena Helmer, Juliane Mössinger, Karen Southwell, John VanDecar, Liesbeth Venema
BIOLOGICAL SCIENCES: Ritu Dhand, Lesley Anson, Tanguy Chouard, Henry Gee, Marie-Thérèse Heemels, Rory Howlett, Claudia Lupp, Barbara Marte, Deepa Nath, Ursula Weiss **INSIGHTS/REVIEWS/PROGRESS:** Lesley Anson
SUBEDITORS: Colin Sullivan, Sarah Archibald, Anne Blewett, Catherine Cassidy, Davina Dadley-Moore, Isobel Flanagan, Paul Fletcher, Jenny Gillion, Dinah Loon, David Price, Chris Simms, Anna York
EDITORIAL PRODUCTION: James McQuat, Alison Hopkins, Marta Rusin, Charles Wenz, Lauren Wethmar
MANUFACTURING PRODUCTION: Jenny Henderson, Stewart Fraser, Susan Gray, Jocelyn Hilton, Yvonne Strong
ART AND DESIGN: Martin Harrison, Wesley Fernandes, Madeline Hutchinson, Barbara Izdebska, Paul Jackman, Fern McNulty, Nik Spencer
ADMINISTRATION: Pauline Haslam, Karen Jones, Helen Anthony, Jayne Henderson, Diane Kempinski, Aimee Knight, Alison McGill, Jenny Meyer, Nichola O'Brien, Naomi Thornhill, Holly Welham
PRESS OFFICE: Ruth Francis, Katherine Anderson, Jen Middleton, Rachel Twinn

WASHINGTON DC nature@naturedc.com
968 National Press Building, 529 14th St NW, Washington DC 20045-1938
Tel +1 202 737 2355 Fax: +1 202 628 1609
EDITORIAL: Eric Hand, Gene Russo, Leslie Sage, Jeff Tollefson, M Mitchell Waldrop, Alexandra Witze **ADMINISTRATION:** Katie McGoldrick, Kenneth Simpson

NEW YORK nature@natureny.com
75 Varick St, 9th Floor, New York, NY 10013-1917
Tel +1 212 726 9200 Fax: +1 212 696 9006
EXECUTIVE EDITOR: Linda Miller
EDITORIAL: I-han Chou, Chris Gunter, Kalyani Narasimhan, Helen Pearson

BOSTON nature@boston.nature.com
25 First Street, Suite 104, Cambridge, MA 02141
Tel: +1 617 475 9275 Fax: +1 617 494 4960
EDITORIAL: Angela Eggleston, Joshua Finkelstein, Heidi Ledford **ADMINISTRATION:** Eric Schwartz

SAN FRANCISCO nature@naturesf.com
225 Bush Street, Suite 1453, San Francisco, CA 94104
Tel +1 415 403 9027 Fax: +1 415 781 3805
EDITORIAL: Erika Check Hayden, Natalie DeWitt, Alex Eccleston
ADMINISTRATION: Jessica Kolman

SAN DIEGO r.dalton@naturesf.com
3525 Del Mar Heights Road, PMB No. 462, San Diego, CA 92130
Tel. +1 858 755 6670 Fax. +1 858 755 8779
EDITORIAL: Rex Dalton

MUNICH a.abbott@nature.com
Josephspitalstrasse 15, D-80331 München
Tel +49 89 549057-13 Fax. +49 89 549057-20
EDITORIAL: Alison Abbott, Quirin Schiermeier

PARIS d.butler@nature.com
2 rue Moreau Vincent, 37270 Véretz Tel. +33 2 47 35 72 15
EDITORIAL: Declan Butler

TOKYO editnature@natureasia.com
Chiyoda Building 5-6th Floor, 2-37 Ichigaya Tamachi, Shinjuku-ku, Tokyo 162-0843
Tel +81 3 3267 8751 Fax +813 3267 8754
EDITORIAL: David Cyranoski, Mika Nakano, Akemi Tanaka

CONTRIBUTING CORRESPONDENTS
AUSTRALASIA: Carina Dennis Tel: +612 9404 8255
INDIA: K. S. Jayaraman Tel: +9180 2696 6579
ISRAEL: Haim Watzman Tel +972 2 671 4077
SOUTH AFRICA: Michael Cherry Tel: +27 21 886 4194
WASHINGTON DC: Meredith Wadman Tel +1 202 626 2514
MISSOURI: Emma Marris Tel: +1 573 256 0611

NATURE ONLINE

www.nature.com/nature

CHIEF TECHNOLOGY OFFICER: Howard Ratner **PUBLISHING DIRECTOR, NATURE.COM:** Timo Hannay
WEB PRODUCTION/DESIGN: Jeremy Macdonald, Glennis McGregor, Alexander Thurrell
WEB PRODUCTION TECHNOLOGIES: Heather Rankin **APPLICATION DEVELOPMENT:** Peter Hausel
NATURE PODCAST: Adam Rutherford, Kerri Smith, Sara Abdulla

PUBLISHING

LONDON feedback@nature.com
The Macmillan Building, 4 Crinan Street, London N1 9XW
Tel: +44 (0)20 7833 4000 Fax: +44 (0)20 7843 4596/7
MANAGING DIRECTOR: Steven Inchcoombe
PUBLISHER: Steven Inchcoombe
ASSISTANT PUBLISHER: Samia Mantoura
PUBLISHING ASSISTANT: Claudia Banks

TOKYO feedback@natureasia.com
Chiyoda Building 5-6th Floor, 2-37 Ichigaya Tamachi, Shinjuku-ku, Tokyo, 162-0843
Tel: +81 3 3267 8751 Fax. +81 3 3267 8754
PUBLISHING DIRECTOR — ASIA-PACIFIC: David Swinbanks
ASSOCIATE DIRECTOR — ASIA-PACIFIC: Antoine E Bocquet

DISPLAY ADVERTISING

MANAGEMENT: John Michael

NORTH AMERICA display@natureny.com
NEW ENGLAND: Sheila Reardon Tel: +1 617 494 4900 Fax +1 617 494 4960
NEW YORK/MID-ATLANTIC/SOUTHEAST: Jim Breault Tel: +1 212 726 9334 Fax: +1 212 696 9481
MIDWEST: Mike Rossi Tel: +1 212 726 9255 Fax: +1 212 696 9481
WEST COAST SOUTH: George Lui Tel: +1 415 781 3804 Fax: +1 415 781 3805
WEST COAST NORTH: Bruce Shaver Tel +1 415 781 6422 Fax +1 415 781 3805

EUROPE/REST OF WORLD display@nature.com
GERMANY/SWITZERLAND/AUSTRIA/OTHER EUROPE: Sabine Hugi-Fürst
Tel: +41 52 761 3386 Fax: +41 52 761 3419
UK/IRELAND/FRANCE/BELGIUM: Jeremy Betts
Tel: +44 (0)20 7843 4959 Fax +44 (0)20 7843 4749
SCANDINAVIA/THE NETHERLANDS/ITALY/SPAIN/PORTUGAL/ISRAEL/ICELAND: Graham Combe
Tel: +44 (0)20 7843 4914 Fax, +44 (0)20 7843 4749

ASIA-PACIFIC display@natureasia.com
JAPAN: Kate Yoneyama, Ken Mikami
Tel: +813 3267 8765 Fax +813 3267 8746
GREATER CHINA/SINGAPORE: Gloria To
Tel: +852 2811 7191 Fax: +852 2811 0743

SPONSORSHIP

EUROPE/NORTH AMERICA e.green@nature.com
NATURE BUSINESS DEVELOPMENT EXECUTIVE: Emma Green
Tel: +44 (0)20 7833 4000 Fax: +44 (0)20 7843 4749

NATUREJOBS

naturejobs@nature.com

Please refer to panel at the start of the *NatureJobs* section at the back of the issue

MARKETING & SUBSCRIPTIONS

USA/CANADA/LATIN AMERICA subscriptions@natureny.com
Nature Publishing Group, 75 Varick St, 9th Floor, New York, NY 10013-1917
Tel: (USA/Canada) +1 866 363 7860; (outside USA/Canada) +1 212 726 9365
MARKETING: Sara Girard **FULFILMENT:** Karen Marshall

JAPAN/CHINA/KOREA subscriptions@natureasia.com
Chiyoda Building 5-6th Floor, 2-37 Ichigaya Tamachi, Shinjuku-ku, Tokyo, 162-0843
Tel: +81 3 3267 8751 Fax: +81 3 3267 8746
MARKETING/PRODUCTION: Keiko Ikeda, Takesh Murakami

EUROPE/REST OF WORLD subscriptions@nature.com
Nature Publishing Group, Subscriptions, Brunel Road, Basingstoke, Hants RG21 6XS, UK
Tel: +44 (0)1256 329242 Fax +44 (0)1256 812358
MARKETING: Katy Dunningham, Elena Woodstock

INDIA npgindia@nature.com
Nature Publishing Group, 3A, 4th Floor, DLF Corporate Park, Gurgaon 122002
Tel: +91 124 2881053/54 Fax: +91 124 2881052
HEAD OF BUSINESS DEVELOPMENT, INDIA: Jaishree Srinivasan **MARKETING:** Harpal Singh Gill

Annual subscriptions (including post and packing)

INSTITUTIONAL/CORPORATE RATE:	$2,730
PERSONAL RATE:	$199
STUDENT RATE:	$99
POSTDOC RATE:	$119

Printed in USA. Individual rates available only to subscribers paying by personal check or credit card. Orders for student/postdoc subscriptions must be accompanied by a copy of student ID. Rates apply to USA, Canada, Mexico/Central & South America.
Add 7% GST tax in Canada (Canadian GST number 140911595).
BACK ISSUES: US$20.00

SITE LICENSES FULFILMENT & CUSTOMER SERVICES

feedback@nature.com
SITE LICENSES: npg.nature.com/libraries
FULFILMENT: Dominic Pettit
CUSTOMER SERVICE: Gerald Coppin

MILLIPORE

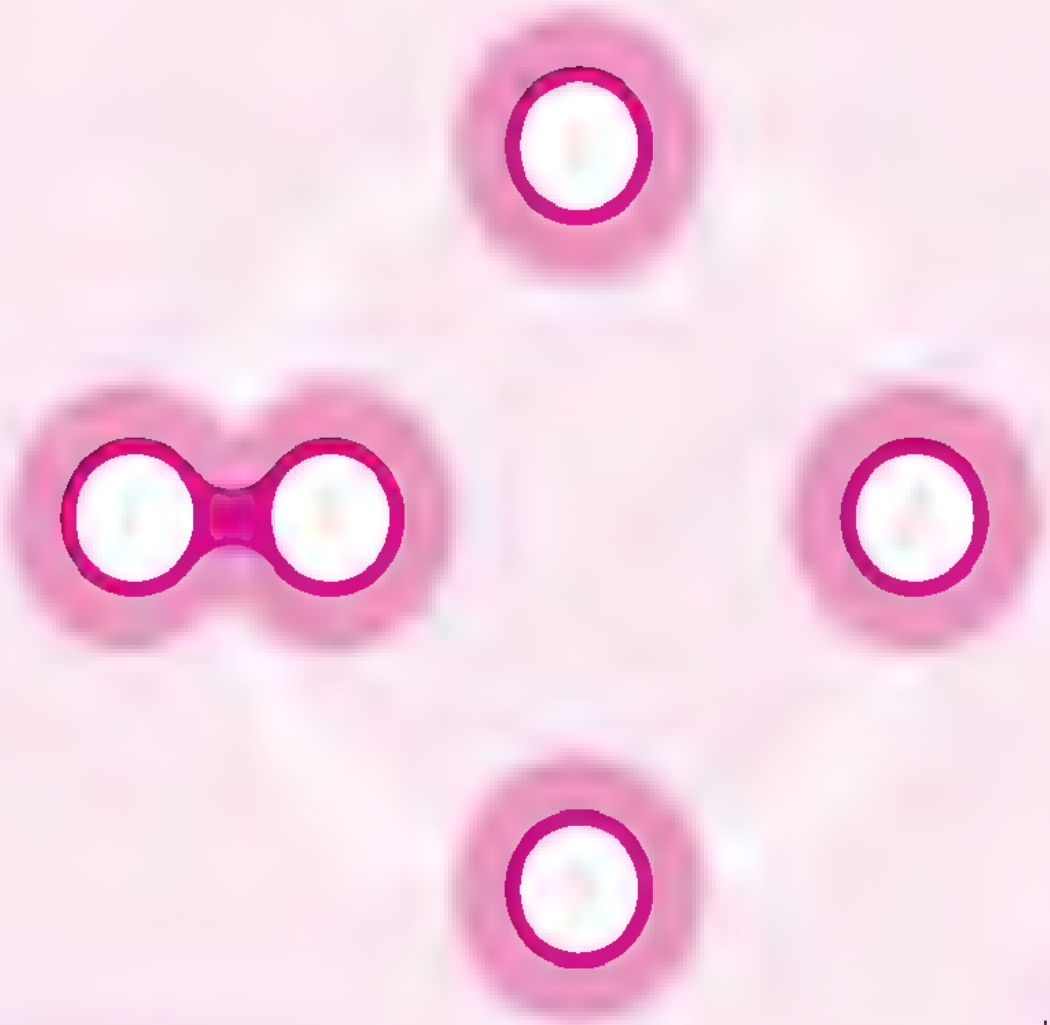

ALIVE AND WELL?

Control your cells.

CELL BIOLOGY
CELL SIGNALING
DRUG DISCOVERY
IMMUNODETECTION
LAB WATER
PROTEIN BIOMARKERS
STEM CELL RESEARCH

It's not always easy to know what your cells are doing. By combining Upstate and Chemicon products and services with our years of experience supporting Life Science research, we can help with your entire workflow, from media and cell preparation to analysis and screening.

ADVANCING LIFE SCIENCE TOGETHER

Visit www.millipore.com for more information on this and other ways Millipore supports Life Science research.

THE EXPERTISE OF
CHEMICON® & UPSTATE®
IS NOW A PART OF MILLIPORE

nature

www.nature.com/nature

Vol 452 Issue no. 7183 6 March 2008

No more scavenger hunts

The recent media flap over antidepressants highlights the need for data to be transparent — and for a mandatory database of all clinical trials.

It was not the media's finest hour. When a study was released last week challenging the effectiveness of several popular antidepressant drugs, some news outlets, particularly in the United Kingdom, responded with headlines blaring 'the drugs don't work' — even though the drugs often do work. Yes, the study showed that the drugs often performed no better than a placebo. But what many of the media missed was that the placebo effect can be remarkably strong in psychological and neurological disorders, especially in mild depression. Doctors scrambled to assure patients that they should not abandon treatment.

Almost buried in the hubbub, though, was a more important story. To access the data needed for this study — a meta-analysis of 35 clinical trials — the researchers had to file a Freedom of Information Act request with the US Food and Drug Administration. And the information they finally received was incomplete: crucial data were missing for several studies that failed to find a significant benefit of the drug compared with the placebo. The missing data limited the analysis, and forced the researchers to abandon their investigation of two drugs altogether.

Such data chaos has become all too familiar in the world of clinical trials. And that fact, combined with recent scandals about antidepressants, diabetes drugs and cholesterol medications, has spurred an outcry to make clinical-trial registries mandatory.

That outcry has not been ignored — the past few years have seen dramatic improvements in data transparency. The International Committee of Medical Journal Editors took a valuable step forward in 2004 when it demanded that authors list and describe their clinical trials in an accepted registry. The number of clinical trials registered in the US National Institutes of Health database rose from 13,153 to 22,714 in a single month, and now stands at more than 52,000 trials spanning 153 countries. Other databases are also active, including an international trial registry hosted by the World Health Organization, which has declared the registration of all interventional trials a "scientific, ethical and moral responsibility".

That responsibility remains unfulfilled. The existing databases are neither comprehensive nor mandatory. Researchers in search of clinical-trial data still have to embark on a scavenger hunt through missing trials and incomplete database entries. Yet the taste of success has been enough to move some open-access advocates to the next step: asking for a description not only of a trial's protocol, but also its results.

"Researchers still have to embark on a scavenger hunt through missing trials and incomplete database entries."

Critics argue that results databases could undermine the peer-review process, reveal competitive information or enable sloppy meta-analyses that set off public panics. They have a point: public registries are no substitute for peer-reviewed literature. But such results databases would still serve an important purpose — as repositories for the negative data that often go unpublished, but that can reveal a drug or treatment regime as ineffective. These data are crucial for meta-analyses, and could improve the design of subsequent trials. Despite reluctance by some pharmaceutical companies to participate, the registries could be helpful to them.

So what can be done to encourage recalcitrant investigators to deposit their data? Several prominent medical journals have removed one barrier by reassuring authors that depositing an abstract or table of results will not be considered 'prior publication'. Politicians in several countries have expressed interest in mandating clinical-trial registries, with some emphasizing the importance of depositing trial results as well. But true fulfilment of that moral responsibility will require international cooperation and enforcement by regulatory authorities — an unprecedented degree of organization and commitment. It is a daunting goal, but one worthy of the struggle. ■

Time to connect

More than ever, academics in Iran and in nations hostile to it should communicate with each other.

This week's address by Mohamed ElBaradei, director-general of the International Atomic Energy Agency (IAEA), to the 35 member states on the agency's governing board highlighted the urgent need for Iran to allow the agency broader inspection powers. But it also highlighted the importance of continuing constructive dialogue amid the bellicose words of national leaders.

There is plenty to alienate Western countries on the one hand and Iran on the other. Iranian President Mahmoud Ahmadinejad's threats against Israel, the nation's fatwa against the writer Salman Rushdie and current domestic violations of human rights are deplorable. But many in the West are ignorant of the depth of resentment, even among the most moderate Iranians, at Western foreign policy in the region. Particularly remembered are the 1953 overthrow by the United States and Britain of the elected government of Mohammed Mossadegh after he nationalized the Anglo-Iranian Oil Company, and the decades of despotic rule that ensued under the Shah.

Nevertheless, Iran's current hard-line leadership masks the county's rich veins of democracy, education and free thinking, which are more developed than those of most of its neighbours in the Middle East. Moreover, Iranian and US politics are both more diverse and pragmatic towards foreign policy than the respective presidents are.

Détente is no longer inconceivable as the national interests — the driver of *Realpolitik* — of both converge, not least in Iraq.

But as tensions run high, academics on all sides can try and help defuse them. Some, in particular physicists, are already active in back-channel diplomacy, encouraging détente by opening up informal, person-to-person communications that bypass their stiff-necked leaders. The US National Academy of Sciences is also expanding scientific cooperation and dialogue with Iran. Such efforts are to be applauded.

A crucial imperative is to find a way out of the international crisis over Iran's nuclear programme. Academics have a role here, too. From historians and nuclear physicists to national academies, they can help to elevate the level of debate above that conveyed by Fox News or Iran's state television. They can explain the complex geopolitical realities that have led to the current escalation, but also inject much-needed scientific facts and objectivity into the debates about the purposes of Iran's nuclear efforts.

It is important to unpack the issues. Iran needs to come clean on any past military aims. But the key challenge is to deal with the here and now: regimes' past intents can be changed by forceful diplomacy. Many nuclear experts argue that the most important goal is for the international community to have confidence that Iran's current programme is not diverted to military ends. And so the priority is to persuade Iran to agree to the 1997 'additional protocol' to the IAEA's safeguards agreement. The protocol gives the agency extra powers, such as short-notice inspections of any site — not just of declared nuclear facilities — and so guards against the biggest worry: clandestine diversion of nuclear expertise.

Iran has not ratified the additional protocol, although it voluntarily allowed equivalent broad access from May 2004 to January 2006. But after United Nations resolutions required it to suspend uranium enrichment, Iran stopped its extended cooperation with the IAEA, and reaped popular domestic support in the process by portraying the actions as foreign threats to their right to nuclear energy.

Earlier this week the United Nations Security Council agreed to further sanctions against Iran in the hope of forcing a suspension of enrichment. Such an aim is indeed desirable for many reasons, but an insistence that there can be no negotiations until Iran ceases enrichment is futile and counterproductive. A negotiated solution would strengthen the hand of reformers in Iran, because it would dilute Ahmadinejad's ability to wield external threats and divert domestic attention from his dire human-rights and economic record.

Many of Iran's democratic forces have their roots in a vibrant scientific community, which too often has been subjected to humiliating visa refusals and actively or passively ostracized by colleagues elsewhere. An experiment for Iranian and US scientists: follow the example of fellow researchers, find a counterpart in your field, and connect with them. ■

The EPA's tailspin

The director of the Environmental Protection Agency is sabotaging both himself and his agency.

The US Environmental Protection Agency (EPA) is fast losing the few shreds of credibility it has left. The Bush administration has always shown more zeal in protecting business interests than the environment (see *Nature* **447**, 892–893; 2007). But the agency's current administrator, Stephen Johnson, a veteran EPA toxicologist who was promoted to the top slot in 2005, has done so with reckless disregard for law, science or the agency's own rules — or, it seems, the anguished protests of his own subordinates.

On 27 February, to take the first of two examples that surfaced last week, Senator Barbara Boxer (Democrat, California) used a routine budget hearing to give Johnson a grilling. Why hadn't he given her state permission to regulate the carbon dioxide emissions of vehicle exhausts? California needs a waiver from the EPA to regulate in this way, and in the past such waivers have been granted easily. And, Boxer reminded him via a series of leaked memos and PowerPoint presentations, Johnson's own top-level staff begged him to sign the waiver in this case. "This is a choice only you can make," one colleague wrote to him. "But I ask you to think about the history and the future of the agency in making it. If you are asked to deny this waiver, I fear the credibility of the agency that we both love will be irreparably damaged."

In December, Johnson announced he would refuse the waiver, an act that would also deny permission to more than a dozen other states seeking to base their exhaust regulations on California's. Johnson argued that climate change is not a local phenomenon, so dealing with it isn't what the authors of the Clean Air Act intended for the waiver system.

Although logical, this argument is similar to that made by Johnson's EPA in an earlier case involving Massachusetts, when the agency fought against CO_2 regulation all the way to the Supreme Court — and lost. His insistence on using it again can perhaps best be understood from the fact that Johnson answers to a White House that is hostile to regulation on principle. It is also worth noting that his refusal documentation, made official on 29 February, extensively quotes an industry trade association, the Alliance of Automobile Manufacturers.

The second example came on 29 February, in the form of a joint letter to Johnson from the four labour unions representing most of the EPA's professional staff. Listing examples of alleged bad faith by Johnson, the unions essentially refused to work with him until he cleans up his act. Among the complaints was an assertion that he repeatedly ignored the EPA's official Principles of Scientific Integrity, citing "fluoride drinking water standards, organophosphate pesticide registration, control of mercury emissions from power plants" — and the waiver refusal.

In a rational world, Johnson would resign in favour of someone who could at least feign an interest in the environment. Alas, it seems that he will probably stay on until January 2009, refusing waivers, fighting lawsuits and further depressing employees' morale. In the meantime, we can only offer those employees a fantasy: the White House doesn't want the agency to do anything, so shut it down until next January. Take some fully paid sabbatical time to relax, and prepare for a return to the old-fashioned protecting of the environment that so many of you joined the agency for. ■

RESEARCH HIGHLIGHTS

In hot water

Geophys. Res. Lett. 35, L03613 (2008)

The warmest regions of open ocean on Earth may be protecting reefs from exposure to temperature spikes that cause corals to 'bleach' — that is, eject the colourful algae that live in their tissues and provide them with sustenance.

Joan Kleypas at the National Center for Atmospheric Research in Boulder, Colorado, and her colleagues analysed sea-surface-temperature records between 1950 and 2006 and a quarter-century of data on coral bleaching. They found that coral bleaching was less common in a region of the Pacific Ocean known as the western Pacific warm pool, where temperatures were high — around 30 °C — but had remained relatively constant.

Negative feedback mechanisms in areas of naturally warm open ocean may hold back warming beyond a threshold temperature, the authors suggest.

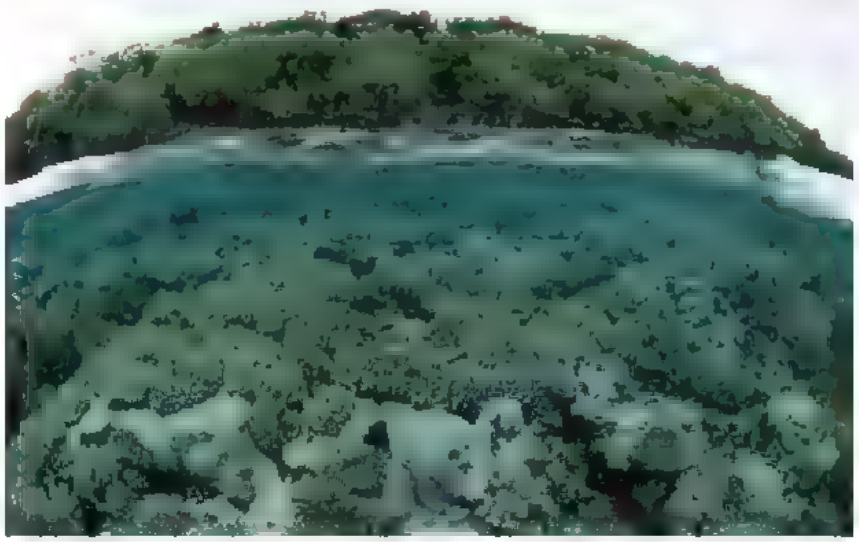

N. W. J./FLPA

MATERIALS SCIENCE

Stirred, not shaken

Phys. Rev. Lett. 100, 078002 (2008)

Frank Rietz and Ralf Stannarius of the Otto-von-Guericke University in Magdeburg, Germany, have added a new pattern to the menagerie of arrangements into which grains can spontaneously separate.

Shaken or sliding grains are a rich source of patterns, many of which are seen in nature — such as segregation by size or shape in wind-blown sand — and in industrial powder processing.

The researchers produced their pattern by confining tiny glass beads between two closely spaced long, narrow, horizontal plates that rotate around the long horizontal axis. When the space between the plates is almost full, most grains can only slide in compact clusters, and the 'slab' of grains develops a series of regularly spaced cells that circulate between the top and bottom of the container (pictured, over time, below; from the top, after 2,000, 4,000, 6,000 and 12,000 rotations). This circulation is analogous to that of convection cells that form in fluids with temperature gradients, yet seems to demand a new mechanism.

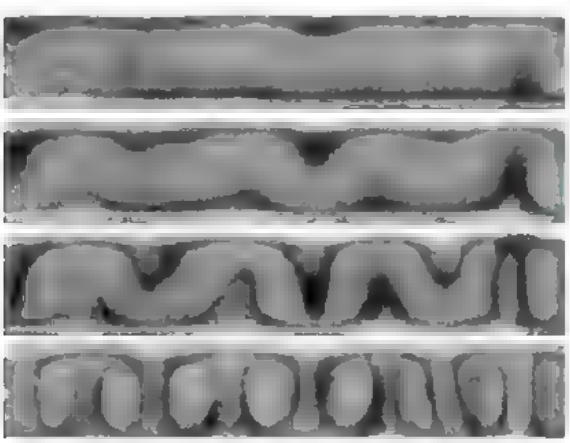

F. RIETZ

EVOLUTIONARY BIOLOGY

Modelling malaria

Proc. R. Soc. B doi:10.1098/rspb.2007.1545 (2008)

After infecting people, malaria parasites form many more merozoites — which cause red blood cells to burst — than gametocytes, sexual forms that do not harm the host but can transmit the infection to mosquitoes. This contributes greatly to the severity of the disease, and perplexes evolutionary biologists.

Nicole Mideo and Troy Day from Queen's University in Kingston, Canada, have adapted a model of malarial infection, and their calculations suggest that there are two possible explanations for the high number of merozoites. Either the host's immune response varies according to the number of gametocytes, or parasites from one strain need to fend off others. It follows from the latter that interventions that reduce the incidence of multiple infections — and thus reduce the risk of inter-strain competition — could favour gametocytes and improve the clinical course of the disease.

PLANETARY SCIENCE

Coming up dry

Geology 36, 211–214 (2008)

High-resolution topographic models of Mars's surface cast doubt on the idea that recently formed gullies are evidence for transient flows of liquid water.

Jon Pelletier at the University of Arizona in Tucson and his colleagues used data from the HiRISE camera now orbiting Mars to produce three-dimensional representations of a crater in which a gully formed between 2001 and 2005. They then applied software that models fluid or granular flow; modelling of dry, dusty flows produced features closer in appearance to the observed gully than did the wet models.

This work, the authors say, shows that gullies and similar formations could be made without water in at least one region of the planet, thus calling into question the watery origins of gullies elsewhere.

SOLID STATE PHYSICS

Making silicon shine

Nature Nanotech. doi:10.1038/nnano.2008.7 (2008)

Silicon is a mainstay of the electronics industry. It is also weakly luminescent — a property that has huge potential for devices such as those used in communication networks, which have long exploited the element's electrical properties. Now researchers have worked out what makes silicon nanocrystals luminesce.

Whether these nanocrystals glow because of quantum effects that are confined to each tiny crystal, or owing to defects in the material joining the nanocrystals together, has been debated for more than a decade.

Manus Hayne at Lancaster University, UK, and his colleagues distinguished between the two mechanisms by looking for subtle changes in the colour of the light emitted by silicon nanocrystals in a strong magnetic field. Such changes would be caused by the quantum-confinement mechanism. The authors found that both explanations were

valid, and that the dominant mechanism depended upon the number of defects in a structure. The team was also able to manipulate the origin of the light by controlling the number of defects.

SYSTEMS BIOLOGY

A powerhouse dissected

Nature Biotechnol. doi:10.1038/nbt1387 (2008)
A compendium detailing how an organelle involved in cellular energy production responds to a catalogue of compounds, two-thirds of which are marketed drugs, has been made freely available online.

Vamsi Mootha at Harvard Medical School in Boston and his colleagues developed a rapid technique for monitoring changes in the activity of mitochondria in cultured muscle cells in response to almost 2,500 compounds. They also measured alterations in the expression of 25 genes involved in the organelle's function.

People with heart disease are often prescribed propranolol to treat high blood pressure, and statins to lower cholesterol. The researchers found that when propranolol is applied to cell cultures in combination with several statins, this can drastically reduce mitochondrial function. This may explain why some people who take statins experience muscle pain.

ANTHROPOLOGY

An infectious idea

Proc. R. Soc. B doi:10.1098/rspb.2008.0094 (2008)
Historical patterns of the prevalence of nine major infectious diseases predict some social attitudes in today's societies better than do contemporary patterns of illness. This finding, from Corey Fincher at the University of New Mexico in Albuquerque and his colleagues, lends weight to the idea that certain social attitudes — such as distrust of outsiders, or high regard for behavioural conformity (pictured, right) — develop in response to disease.

The authors compare historical data on pathogen distribution with several surveys of cultural attitudes. They also factor in an analysis that statistically controls for other likely predictors, including income and inequality, to support a causal link between historical pathogens and cultural values.


© HIV/AFP/GETTY

QUANTUM PHYSICS

Magnetic gas

Nature Phys. doi:10.1038/nphys887 (2008)
Bose–Einstein condensates are weird clumps of extremely cold atoms. Normally, the condensates are made of atoms that interact with only neighbouring atoms, bouncing off each other like billiard balls. A team of physicists at the University of Stuttgart in Germany has now demonstrated that they can make stable clumps with long-range interactions.

Tobias Koch and his colleagues made a Bose–Einstein condensate by cooling a gas of chromium-52 to just above absolute zero. The atoms of this condensate had strong magnetic dipoles, and the team applied an external magnetic field to eliminate contact forces between the atoms. This left only the interaction between the magnetic dipoles.

Because the dipoles have a preferred direction, these clumps of atoms are only stable in certain configurations.

METEOROLOGY

Bacteria make rain

Science 319, 1214 (2008)
Fresh snow contains a surprisingly large amount of cells or cell fragments, a team of researchers has found. For the ice crystals that produce rain and snow to form, the high atmosphere must contain tiny particles on which moisture can condense.

Brent Christner of Louisiana State University in Baton Rouge and his colleagues sampled fresh snow collected at mid and high latitudes in North America, Europe and Antarctica. They found small amounts of biological ice nucleators in all of the samples, indicating that snow- and rain-making particles, such as certain plant pathogens, are able to travel long distances and that their effect on precipitation is not limited to vegetation-covered regions.

Health and plant growth have been linked to atmospheric processes, so changes in forestry or agriculture may have a large and direct impact on global precipitation, the authors add.

JOURNAL CLUB

Keith Devlin
Center for the Study of Language and Information, Stanford University, California

A mathematician considers the early signs of mathematical ability.

Have you ever wondered whether there is any reliable way to predict whether a three- or four-year-old child will be good at mathematics when he or she goes to school? Many people find it surprising that an early aptitude for arithmetic is not a terribly good indicator.

A 2004 paper by the psychologist Daniela O'Neill and her colleagues at the University of Waterloo in Ontario, Canada, suggested something better. O'Neill and her team showed three- and four-year-old children a picture book and asked them to tell a story about what they saw. The researchers then measured many parameters of the children's story-telling, including the diversity of vocabulary used and the length of the sentences constructed. Two years later, the team set the same children various tests of academic achievement (D. K. O'Neill *et al. First Lang.* 24, 149–183; 2004).

O'Neill and her co-workers found that vocabulary and sentence length in the initial study bore little relation to the test performances a couple of years later. However, the sophistication with which the children told their stories was important. The most significant feature of this sophistication was children's ability to switch perspectives as they related the stories. Crucially, the correlation that the researchers found pertained not to later performance in reading, spelling or general knowledge, but to future mathematical ability.

I have long thought that the human capacity for mathematical thinking must predate symbolic arithmetic, because numbers are a relatively recent invention. This study backs up this idea, because it suggests that the ability to solve mathematical problems has co-opted other innate capacities that have been important for much longer in our evolution.

Discuss this paper at **http://blogs.nature.com/nature/journalclub**

NEWS

Crunch time for peer review in lawsuit

A US magistrate is set to rule next week on whether the drugmaker Pfizer can force *The New England Journal of Medicine* (*NEJM*) to hand over confidential peer reviews as part of litigation involving two controversial painkillers.

Pfizer, the world's largest drug company, subpoenaed the medical journal last May to surrender peer reviews, the names of peer reviewers and internal editorial deliberations for 11 recent papers related to the painkillers Celebrex (celecoxib) and Bextra (valdecoxib). It also wants all other manuscripts the journal has received involving either drug. Most of the studies were published in 2005 and 2006 after Bextra and Vioxx (another drug in the same class of COX-2 inhibitors) were withdrawn because of serious side effects.

Pfizer, based in New York, is defending Celebrex and Bextra in lawsuits charging that they caused heart attacks and strokes. Bextra was pulled from the market in 2005, Celebrex is still available. The drugmaker is trying to obtain the *NEJM* reviews as part of its defence in the US district court in northern California, where several lawsuits relating to the drugs have been consolidated.

In November, the *NEJM* turned over 246 pages of documents, but included only its communications with the named authors of the papers, and their financial disclosures.

Pfizer offered to remove the names of individual peer reviewers from any documents the journal provided — but the *NEJM* still resisted. In January, the drug company filed a motion to force the *NEJM* to hand over the peer reviews and any other manuscripts "Scientific journals such as *NEJM* may have received manuscripts that contain exonerating data for Celebrex or Bextra, which would be relevant for Pfizer's causation defence," its lawyers wrote. "The public has no interest in protecting the editorial process of a scientific journal, particularly not when doing so prevents a defendant from access to potentially exonerating evidence."

Pfizer wants to obtain peer reviews relating to Celebrex.

M. NGAN/AFP/GETTY IMAGES

Responding in an affidavit, Jeffrey Drazen, *NEJM* editor-in-chief, argued that if the company prevails, there could be "serious adverse consequences" for the scientific peer-review process, including the ability of journals to recruit reviewers, who will be wary of "the possibility that their volunteer work would land them in the middle of litigation". He wrote that removing names would not be enough to disguise reviewers, given the

Bright hopes pervade dark matter

Physicists have again returned empty-handed from a search for the 'dark matter' that is thought to fill the cosmos. But the latest null result hasn't dimmed their enthusiasm — or their plans for a new generation of detectors.

Since the 1970s, theorists have predicted the existence of massive particles that rarely, if ever, interact with normal matter. This dark matter is believed to be responsible for slowing the rotation of galaxies and makes up about 85% of matter in the Universe. Physicists have devised a host of experiments to find dark matter, but to date, nobody has been able to detect it directly (see *Nature* **448**, 240–248; 2007).

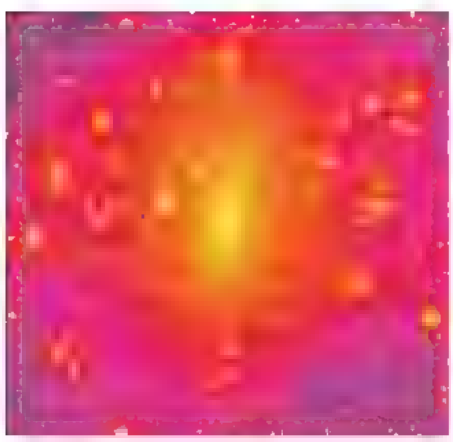
NST THEOR. PHYS., UNIV. ZURICH

Computer simulation of the distribution of dark matter that is thought to fill the Universe.

The latest non-findings met with spontaneous applause at a conference on 22 February in Marina del Rey, California. The results came from Cryogenic Dark Matter Search II (CDMSII) — one of the world's most advanced dark matter detectors, located in the Soudan mine in Minnesota. CDMSII uses giant crystals of germanium and silicon that physicists hope will ring out when struck by a dark-matter particle.

The crystals are kept more than 700 metres underground in order to shield them from disruptive cosmic radiation. A previous generation of CDMS detectors delivered nothing, and the new bigger and better crystals are only now beginning to reach sensitivities at which they might realistically see a dark-matter particle, says Bernard Sadoulet, a physicist at the University of California, Berkeley, who leads the CDMSII collaboration. "We really are entering the core of the interesting territory."

The results are not entirely surprising, says Elena Aprile, a physicist at Columbia University in New York city who is working on a rival experiment called XENON10. The dark-matter particles could still be well below the experiment's threshold, she says. "Maybe it's just a little too insensitive still."

Sadoulet says the CDMSII detector should reach up to four times its present sensitivity later this year, and Aprile says a new, larger XENON100 detector could do better still. But detecting the particles may require sensitivities hundreds of times beyond even these levels. That will probably mean a next generation of detectors. Sadoulet and Aprile both say they have proposals for third generation detectors, which are expected to cost tens of millions of dollars.

But the lack of detection and rising costs raise another spectre for the dark-matter hunters — what if the particles aren't there? Or what if they don't interact with regular matter?

small number of experts in any one area, who can easily identify each other through their arguments.

Similarly, he argued, free-flowing discussion among *NEJM* editors would be stemmed "if litigants were able to pick apart this internal editorial process to serve their own needs".

Scientists and editors have rallied to the *NEJM*'s cause. Donald Kennedy, editor-in-chief of *Science*, calls Pfizer's efforts a "fishing expedition" because of its failure to specify what it is looking for. If Pfizer prevails, says Marcia Angell, a senior lecturer in social medicine at Harvard Medical School and a former editor of the *NEJM*, "it would undermine the whole system of peer review, which depends utterly on confidentiality".

Aravinda Chakravarti, a computational biologist and geneticist at Johns Hopkins University in Baltimore, Maryland, says that he can imagine "exceptional circumstances" in which a manuscript review could be submitted as part of litigation, with any potentially identifying information removed. But with Pfizer requesting all of the reviews on 11 papers and possibly more, he says: "I am worried about the precedent. This may benefit Pfizer, but science loses in a big way."

A ruling is expected on 13 March. ■

Meredith Wadman

Nobody knows exactly where dark matter lives in the Milky Way, although it is likely to exist in our Solar System in some shape or form, according to Ben Moore, a theorist at the University of Zurich in Switzerland. But he adds that many proposed versions of the stuff would never interact with a germanium crystal — or anything else. "It's a gamble," he says. "If dark matter is one of those alternative candidates, then they're not going to see anything."

Sadoulet is the first to admit that this may be the case. Still, he hastens to add, there is good reason to look, especially because several other experiments may soon provide further clues. A satellite called the Gamma-ray Large Area Space Telescope will launch later this year, and may provide evidence of dark matter 'annihilating' in the cosmos. Also this year, the Large Hadron Collider, the world's largest particle accelerator, which is located at CERN near Geneva in Switzerland, will start looking for signals that could confirm the existence of some classes of dark-matter particle.

The risk of coming up empty-handed nags at the field, Sadoulet says. But if something is found, "it will be a new start for particle physics". ■

Geoff Brumfiel

HAVE YOUR SAY
Comment on any of our news stories, online.
www.nature.com/news

Entomologists stifled by Indian bureaucracy

An international collaboration to study insects in the Western Ghats mountains in southern India has been unable to get off the ground because of government concerns over biopiracy.

The Indian–American project aims to sample insects from different ecosystems at various elevations, and incorporate about 200,000 specimens into national insect collections. "We have already identified 24 taxonomists from all over the world who are willing to work on this project," says Priyadarsanan Dharmarajan, a taxonomist at the Ashoka Trust for Research in Ecology and the Environment in Bangalore, who leads the Indian team.

But the project has stalled because India's National Biodiversity Authority (NBA) has denied the Ashoka Trust permission to export the specimens, despite assurances that they would be returned to India after identification. "We have to send the specimens abroad for identification as we do not have the expertise at home," Dharmarajan says.

Indian biodiversity rules guiding foreign collaborations require permission from the NBA before specimens can be exported. Under the Biological Diversity Act, specimens must not be deposited in international museums but kept only in designated repositories in India.

Now Paul Tinerella, insect collection manager at the Illinois Natural History Survey in Champaign, which is involved in the project, has informed the Ashoka Trust that the venture is "doomed" without the exit permits from the NBA or relevant supporting documents from the Indian government. "Biodiversity assessment is critical to wise land-use planning and without the basics of a sound taxonomic framework across the spectrum of life, biodiversity assessment is extremely faulty," says Michael Irwin, an insect ecologist at the Illinois Natural History Survey.

The draconian regulations on the free exchange of specimens could isolate Indian biodiversity researchers, says K. D. Prathapan, a taxonomist at the Kerala Agricultural University. "This could totally isolate Indian biodiversity researchers." Prathapan's own recent discovery of three new species of flea beetle in India "would have been impossible" but for the loan of specimens from five international museums in four countries.

Krishnamoorthy Venkataraman, secretary of the NBA, says that the rules aim to fight biopiracy and not to stop basic research. "There is no restriction on collection or export of a few specimens for research," he told *Nature*. "But exporting 200,000 specimens is not permissible." The NBA encourages Indian scientists to send photographs or digital images to collaborators abroad instead of actual specimens, he says.

Dharmarajan hopes that the Indian government will follow the example of Brazil, which repealed its initially tough rules for biological specimens after protests by scientists. ■

K. S. Jayaraman

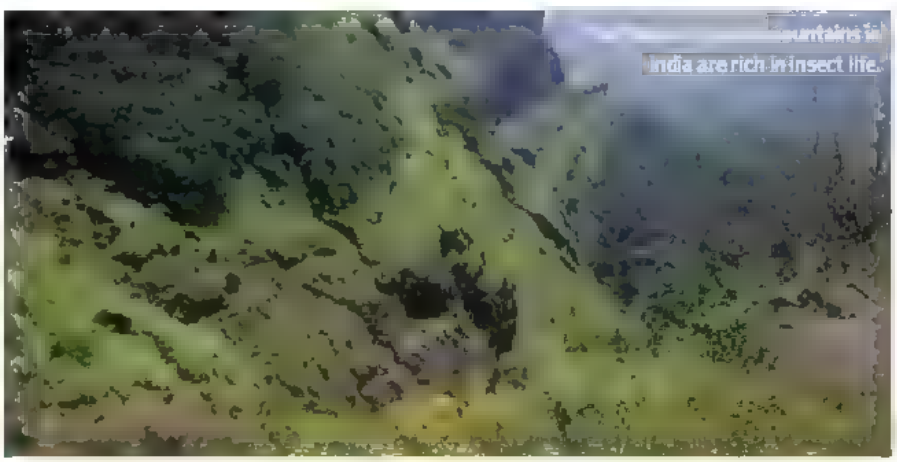

D NODIA

Vol 452|6 March 2008

SPECIAL REPORT

Save the trees

Scientists and policy-makers will meet in Bonn this June to discuss one of the most pressing concerns to come out of December's United Nations climate meeting — how to manage the world's trop cal forests. **Jeff Tollefson** examines some of the proposa s.

Rainforest nations walked away from the United Nations (UN) climate meeting in Indonesia last December with pretty much all they had hoped for: a place at the negotiating table and an acknowledgement that deforestation belongs in a future global-warming treaty.

The landmark decision in Bali was accompanied by an outpouring of concern — and in some cases money — from the international community. Little more than a month later, however, the European Commission released a proposal that would ban forestry credits of any kind from the world's largest carbon market until 2020. The document highlights old divisions over whether to integrate forestry issues into the cap-and-trade programme for reducing greenhouse-gas emissions or to tackle problems such as deforestation separately through government programmes. Rather than open up the European market, the commission proposes funnelling a portion of the proceeds from the carbon market into deforestation programmes.

Advocates of rainforest conservation have in the past focused on issues of biodiversity and the preservation of indigenous communities. The climatic implications of deforestation, which releases the carbon stored in plants and soils into the atmosphere, both heightens the urgency and opens the door to potential solutions. Yet although the Bali declarations endorse the idea of including forest protection in the next climate agreement, they say nothing about which avenue to take — an issue that is now being hotly debated.

Monitoring emissions

The discussions kicked off in Kyoto in 1997, when the United States pushed to make forestry part of the market-based cap-and-trade programme. Europe eventually accepted the programme, but was sceptical about including deforestation, unconvinced that the technology was advanced enough to monitor and quantify emissions resulting from deforestation. Reforestation projects were included in the final agreement, but avoiding deforestation was left out.

Ten years later, with the scientific community generally agreed that satellite monitoring is ready for prime time, rainforest nations banded together in favour of a market-based approach tied to national baselines — similar to the way developed nations would certify industrial emissions (see 'Taking steps at a local level'). Brazil seemed to be out in the cold last year when it continued to push for the creation of an international fund, independent of an eventual carbon market, that could be tapped in support of programmes to halt deforestation.

In the end, however, UN negotiators failed to settle the issue. "When we went into Bali, we all thought that carbon markets would win, but after Bali there are more and more voices saying, 'maybe the market doesn't work that well here'," says Fred Stolle, a researcher with the World Resources Institute, an environmental think tank based in Washington DC. Stolle says the European proposal puts the whole idea of a market-based forestry programme "on shaky ground", because where Europe leads, others may follow.

This dilemma has advocates of a market-based approach looking to the United States for leadership. The leading global-warming legislation in the Senate would set aside 2.5% of the credits in an eventual cap-and-trade system for forestry and deforestation projects. A coalition of businesses and environmental groups, represented by the lobbying firm Covington and Burling, based in Washington DC, is pushing to expand that and other provisions that would allow forestry to play a greater role.

An international fund such as that backed by Brazil might be useful to help pay for infrastructure issues as nations develop the expertise to track and police deforestation, sceptics argue, but the resources necessary to address such a problem can be raised only if avoiding deforestation becomes a private economic enterprise. "In global markets, forests are worth more dead than alive, and this is what we need to turn around," says Andrew Mitchell, director of the Global Canopy Programme in Oxford,

Taking steps at a local level

After more than a decade of work, scientists say today's computer models could allow virtually any nation to monitor deforestation rates and participate in some kind of international treaty. Greg Asner, who studies rainforests at the Carnegie Institution in Stanford, California, says the latest validation on his model suggests an error margin of about 0.5% for broad deforestation; that margin increases to around 10% for selective logging.

The question faced by delegates at the next United Nations climate talks will be how to translate such information into a workable system that rewards countries for reducing deforestation. The Coalition for Rainforest Nations, led by Papua New Guinea and Costa Rica, has proposed national baselines to ensure that problems do not migrate from one region to another.

Costa Rica, India and other nations are pushing for ways to reward countries that have already halted or prevented deforestation, including building a tourism industry around the natural resource. Advocates say this would ensure the problem doesn't move from one country to another while providing additional assistance for countries that are managing their resources properly.

All of these countries will probably need to build up expertise in running their own monitoring programmes, but Asner says his computer model is simple enough for him to be able to train his technicians in a couple of months. "I think that the key is planting the seed and building the scientific capacity within these nations," he says. **J.T.**

W. LAWLER/ECOSCENE/CORBIS

Logging in West Kalimantan, Borneo.

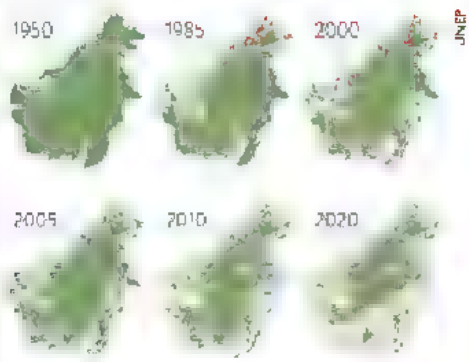

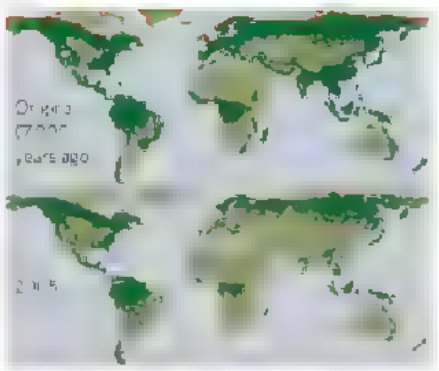

The extent of the problem: changes in forest cover in Borneo (left) and the human impact globally.

UK. "Philanthropy and governments won't do it. You have to look to markets to overturn what is in fact a market failure."

Moreover, having developing nations sign up to cap-and-trade commitments in the forestry sector will build momentum and increase pressure on countries such as China as well, says Stuart Eizenstat, a partner with Covington and Burling who served as chief negotiator for the US delegation to Kyoto. "This could open up a way of breaking this impasse between developed and developing countries."

To market

But perhaps the biggest fear among sceptics is that an endless stream of deforestation credits will simply allow companies in the developed world to pay a little extra and pass costs on to consumers without otherwise changing their policies. Artur Runge-Metzger, who is in charge of climate issues at the European Commission, says deforestation accounts for 5–6 gigatonnes of carbon dioxide annually, compared with 2 gigatonnes in the entire European trading scheme. "That would flood the market," he says, revealing a major reason behind Europe's stance. "We want to see real emissions reductions in Europe."

Eric Bettelheim, executive chairman of Sustainable Forestry Management in London, calls this logic "nonsense", saying forestry projects will come online over time as countries develop their monitoring systems, link up to the international system and work through projects. Moreover, as some 20% of global greenhouse-gas emissions come from deforestation each year, from a theoretical standpoint, deforestation can't make up more than 20% of the solution if it represents only 20% of the problem. "It is not the purpose of a market to punish industry," he says. If reducing emissions through deforestation is the cheapest option, "it's the logical thing to do".

Kevin Conrad, director of the New York-based Coalition of Rainforest Nations, plays down the European Commission's move to bar forestry projects, expressing confidence in the UN talks. He says developing nations would be suspicious of any new non-market initiative, such as the millennium development goals for deforestation, that would be perennially under-funded and bureaucratic. "Developing countries are trying to test the sincerity of developed countries, saying 'Don't try to fool us dangling some new-fangled fund in front of us'," Conrad says. "What we want is just our right to be at the table in the markets that are already in the tens of billions of dollars per year."

> "In global markets, forests are worth more dead than alive, and this is what we need to turn around."

How much money would flow into this sector ultimately depends on the actual cost of curbing deforestation, and for this there is a range of estimates. Doug Boucher, director of the tropical forests and climate initiative for the non profit Union of Concerned Scientists based in Cambridge, Massachusetts, is in the process of compiling and analysing various studies on the issue. He says the numbers vary from a few dollars per tonne of carbon dioxide for individual projects to $10–30 per tonne for some of the economic models. For perspective, carbon dioxide credits are currently trading at more than $30 per tonne in Europe, although they have been much lower in recent months.

In principle, Boucher says, the calculation is easy: saving a forest costs at least as much as a person would have earned cutting it down. And there will be additional costs for developing monitoring systems, administering programmes and enforcing laws, many of which already exist. Such aspects could benefit from traditional international aid, especially as countries gear up. Brazil recently sent a special police unit into the Amazon as part of an effort to bring illegal clearing under control — and to demonstrate its commitment to the problem.

Others are looking at financing mechanisms, including some form of carbon insurance that could be activated if a project that had been paid for turned sour for any reason. New financial institutions would be needed to link the global capital markets to people on the ground. Annie Petsonk, an attorney with Environmental Defense, a non-profit advocacy group in New York, says farmers might even be able to take out a project loan from "forest carbon" banks. "Could you use all of the learning that has been developed in the past 10–15 years in micro-finance?" she asks. "Could you apply that to carbon?"

But developed nations contribute to the emissions too. The expansion of palm-oil plantations in Indonesia, driven in part by European demand for biofuels, is a primary cause of deforestation. When it comes to timber, it is perfectly legal to ship illegally cut logs to the United States and Europe (although efforts are under way to change that). Cattle ranching is a leading cause of deforestation in the Amazon, and two-thirds of Brazil's beef goes to Europe, says Mitchell of the Global Canopy Programme. "Europe's markets are causing these emissions and, more and more, the developing world is saying that it doesn't want to be blamed."

But a well-designed and focused programme could markedly affect global deforestation. More than half of the emissions from deforestation come from two states in the Brazilian Amazon and one province in Indonesia, according to a preliminary analysis of deforestation trends between 2000 and 2005 by the World Resources Institute and South Dakota State University in Brookings. Whether such a programme could garner the political will and international backing to succeed remains to be seen. ■

What if staying up to date with the latest technology published in journals and patents were as easy as pushing a button?

It is.

With the "Keep Me Posted" alerting feature, SciFinder sends you automatic updates on areas you—and your competitors—are interested in.

You can monitor specific research topics, companies, authors, substances, or sequences, and choose how frequently you receive notifications: daily, monthly, or weekly.

The service isn't just convenient, it's incredibly current. Journal article records often appear in SciFinder before they're even in print. New references, substances, and sequences are added daily. Patents from all the major offices are added within two days of issuance.

As with all SciFinder features, Keep Me Posted is integrated with your workflow. At any point in a search (including the beginning), simply click on the Keep Me Posted button. SciFinder tracks your steps and will generate the appropriate alert—even for complex topics. When you receive a notification, you can follow each reference as you would in a search: find citing or cited articles (with links to the electronic full text), and follow referenced substances and reactions for further information.

Comprehensive, intuitive, seamless—SciFinder doesn't just alert you, it's part of the process. To find out more, call us at 800-753-4227 (North America) or 614-447-3700 (worldwide) or visit www.cas.org.

SciFinder®
Part of the process.™

HIV'S ANCIENT LEGACY
Lentiviruses may have vexed nonhuman primates for millions of years.
www.nature.com/news

PUNCHSTOCK

Magnets touted as fix for fusion reactor

Physicists and engineers are poised to deliver their proposals for resolving a serious design flaw in the flagship international fusion reactor ITER, which is overdue to begin construction in Cadarache, France.

The €10-billion (US$15-billion) reactor involving seven international partners has been on the drawing board since the mid-1980s, but around five years ago it emerged that there was a worrying fault with the design. Violent bursts of energy are expected to rocket out of ITER's plasma core, threatening to damage the reactor. Whether and how to solve the problem is proving controversial, as any solution will cost and delay the project further.

ITER aims to test the feasibility of fusion as an energy source. It will heat a plasma gas to around 100 million degrees so that heavy hydrogen nuclei fuse to become helium, releasing energy. The project has been beset with delays, including Japan and the European Union squabbling over the location, and partners such as the United States jumping in and out. By 2006, when all parties formally agreed to fund ITER, "they were blowing the cobwebs and dust off the design, while the science had marched on. Now they have to retrofit it", says Rick Moyer, a plasma physicist at the University of California, San Diego. Moyer was one of those who discovered that the bursts — known as edge localized modes, or ELMs — posed such a problem.

At a key meeting on 18 March, the working group charged with solving the issue will deliver its recommendations for last minute tweaks to Norbert Holtkamp, the project's construction leader. It is expected to call for a complex arrangement of magnets to dampen the effects of the ELMs.

Experiments now suggest that, in ITER, these chaotic eruptions will occur once every second. Although they last only a microsecond, each eruption has a power of 20 gigawatts — about the expected capacity of China's Three Gorges Dam. This energy needs to be absorbed by a device called a diverter, or the walls of the tokamak — the doughnut shaped vessel that contains the plasma — may be damaged. "This is like throwing a handful of hand grenades into the diverter every second," says Todd Evans, a physicist at General Atomics in San Diego and a member of the ELM working group.

Magnetic solution

Scientists have contained ELM bursts in smaller tokamaks using a technique called 'pellet pacing'. They inject frozen pellets of heavy hydrogen into the edge of the plasma, triggering smaller ELM like bursts. But experts are sceptical that any rate of pellet pacing — ITER scientists are considering rates as high as 40 pellets per second — could adequately dampen the ELMs.

In 2006, Evans and Moyer and their colleagues came up with an alternative solution involving magnetic coils. ITER already depends on magnetic loops that keep the plasma tightly confined within the tokamak. But the researchers found that they could suppress ELMs by adding a set of magnetic coils, shaped like picture frames, in rings around the vessel (T. E. Evans *et al. Nature Phys.* **2**, 419–423; 2006). The magnets seem to defuse the ELM bombs by allowing some energy to leak out, but not enough to threaten the critical density of the plasma core. It is like poking holes in a bucket, says Moyer. "We are just trying to bleed it."

But finding space to place the magnets within the tokamak has been a challenge. Last year, ITER scientists looked at putting them into 14 'port plugs' — windows in the tokamak that were already factored into the design. But 14 coils wouldn't be able to generate a strong enough field to reliably suppress the ELMs, and there was concern that the coils would interfere with the instruments that the ports were designed to use.

In January, the researchers proposed a new arrangement: four rings of nine magnets. This suggestion was rejected after costs were estimated at €50 million, with construction delays of up to a year. Gary Johnson, deputy director-general of the tokamak, expects that the current option being considered — 27 magnets in three rings — will be less costly and incur fewer delays. The magnets would be placed a little closer to the plasma, which helps with the suppression. They would also be easier to install — so purchasing the vessel can go ahead as planned, which is essential if the project is to be completed by its scheduled deadline of 2016.

Johnson declined to say whether the ELM working group, which he heads, would endorse the 27-magnet proposal at the March meeting, saying that many options are available, including merely leaving space to add the magnets in the future. But Ned Sauthoff, director of the US ITER office at Oak Ridge National Laboratory in Tennessee, says he expects the working group will recommend the added magnets. ■

Eric Hand

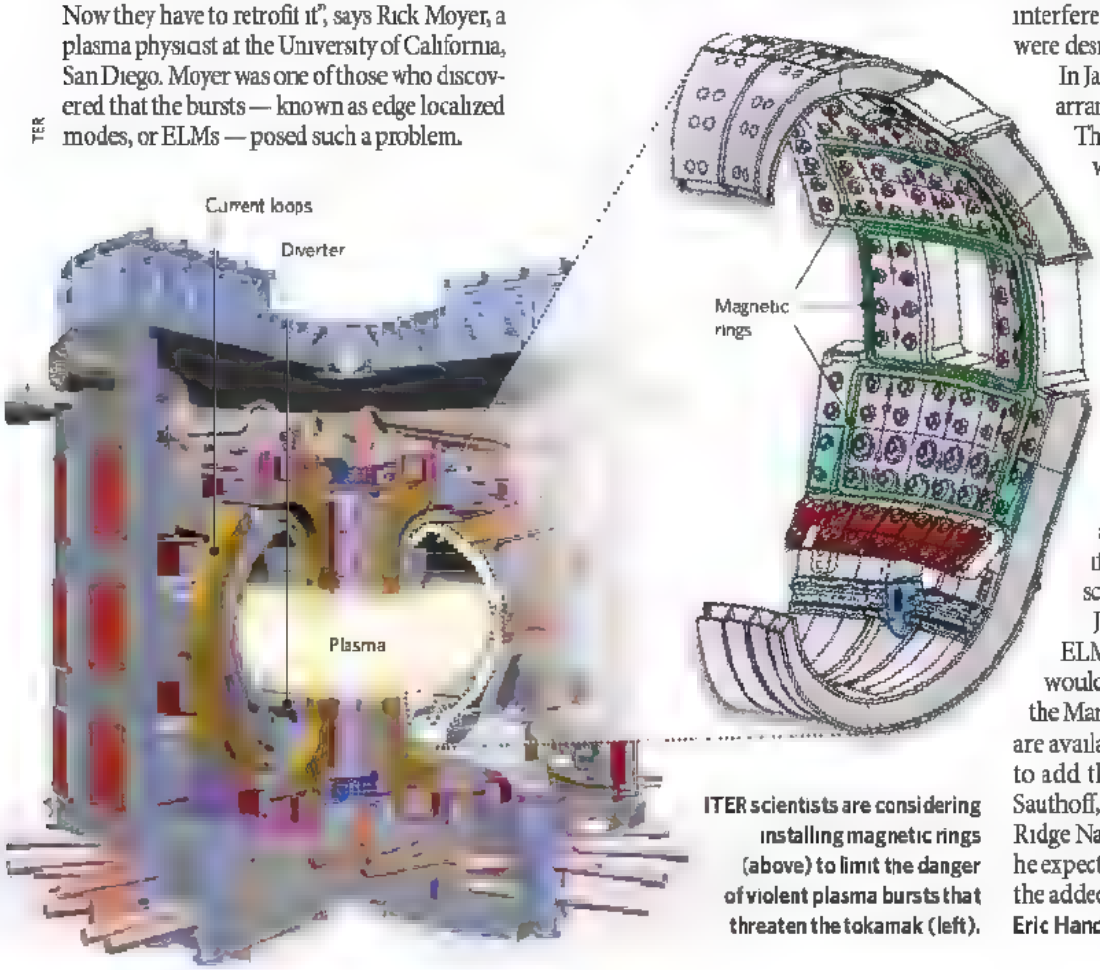

TER

ITER scientists are considering installing magnetic rings (above) to limit the danger of violent plasma bursts that threaten the tokamak (left).

SCORECARD

Energy-saving boat A boat propelled solely by the up-and-down motion of waves is about to set sail on a three-month voyage from Hawaii to Japan.

Energy-sapping day Britons used more power (0.1%) in a day than average during the nation's first Energy Saving Day, when people were encouraged to switch off unnecessary electric devices. UK officials blamed the disappointing outcome on the cold weather — this was perhaps unsurprising for 27 February...

ROBOT NEWS

Unthinking slaughter? Artificial-intelligence expert Noel Sharkey has declared himself "really scared" of potential developments in military robots over the coming decade. Worrying, given that the University of Sheffield professor was one of the brains behind popular BBC TV show *Robot Wars*.

MYUNG JUNG-H/AP

WORDWATCH

Planetary pedantry Ten-year-old Montana schoolgirl Maryn Smith has won a *National Geographic* competition to come up with a mnemonic for the names of the 11 recognized planets in the Solar System, in order of orbital radius. Her effort, 'My Very Exciting Magic Carpet Just Sailed Under Nine Palace Elephants', will now be immortalized in song, although being a pedant, Sidelines would point out that the Solar System has only eight proper planets (the other three being the dwarf planets Ceres, Pluto and Eris).

Sources: Daily Telegraph, popsci.com, BBC, Associated Press

SIDELINES

Hobbit was 'a cretin'

The 'hobbit' could be a cretin, Australian scientists say. But this latest assertion in the ongoing row over the identity of the small human skeleton found on the island of Flores in Indonesia is already being challenged — not least because the Australians used only cast images and never examined the actual skeleton. And they misinterpret a crucial skull component, according to three researchers who created casts of the remains.

Peter Obendorf of RMIT University in Melbourne and his colleagues say[1] that the cast shows an impression (called a fossa) of an enlarged pituitary gland at the base of the skull behind the nasal region. This, they say, is evidence that the skeleton is not from a new species (called *Homo floresiensis*) but from a *H. sapiens* with cretinism — a condition in which a person is born with a deficient thyroid gland. Untreated, such people often have an enlarged pituitary gland as well as severely stunted growth and a small brain.

The Australians call their idea "a tentative hypothesis", although Obendorf says he thinks they "are on the right track". They now are seeking access to the original specimen.

But Dean Falk, an anthropologist at Florida State University in Tallahassee who was the lead author on the first analysis of the skull cast[2], says that the pituitary fossa is small. "There is no way they can reach the conclusions they did," she argues. And Ralph Holloway, a neuroanatomist at Columbia University in New York who has a cast created from data from the original skull, says that his model also shows a small pituitary.

> "I'm the only person on the planet to have seen what's left of the pituitary fossa."

The disagreement highlights an often criticized practice whereby anthropologists examine secondary sources and publish conflicting reports, which many think clouds the course to verifiable results.

Since the discovery[3] in 2003 of the skull and partial skeleton of *H. floresiensis*, the anthropology community has sprouted numerous theories to explain its characteristics. Just over 1 metre tall, the 18,000-year-old creature had a brain one-quarter the size of modern humans and primitive skeletal features similar to those of earlier human relatives. Stone tools have also been found in the same cave.

Indonesia's leading palaeoanthropologist, Teuku Jacob, then of the University of Gadja Mada in Yogyakarta, and his colleagues initially analysed the bones and decided that the creature, known as 'the hobbit', was in fact a human who had a developmental disorder called microcephaly, in which the head is smaller than usual[4].

J. KAY/PETER ARNOLD INC./SPL

The stunted growth seen in cretinism may offer clues to the nature of the 'hobbit' remains.

Palaeoanthropologist Peter Brown and archaeologist Michael Morwood, both of the University of New England in Armidale, Australia, stand by their proposal that the skeleton is a new species. Morwood notes that bones from 12 separate hobbits had been unearthed in the original Liang Bua cave, although so far only the one skull has been found. Brown is critical of the cretin theory. "I am the only person on the planet to have seen what's left of the pituitary fossa," he declares. "It is very poorly preserved and not capable of meaningful measurement."

Last year, an Israeli team[5] published a report proposing that the hobbit had a growth disorder called Laron syndrome. Those authors also never examined the original skeleton and their report was branded "a joke" by Falk, who is preparing a rebuttal for presentation at the annual meeting of the American Association of Physical Anthropologists on 9–12 April in Columbus, Ohio.

With just one skull, the row over whether the creature was a human with a congenital abnormality or a new species will probably continue for some time. ■

Rex Dalton

1. Obendorf, P. *et al. Proc. R. Soc. B* doi 10.1098/rspb.2007.1488 (2008)
2. Falk, D. *et al. Science* **308**, 242–245 (2005)
3. Brown, P. *et al. Nature* **431**, 1055–1061 (2004)
4. Jacob, T. *et al. Proc. Natl Acad. Sci. USA* **103**, 13421–13426 (2006)
5. Hershkovitz, I., Kornreich, L. & Laron, Z. *Am. J. Phys. Anthropol.* **134**, 198–208 (2007).

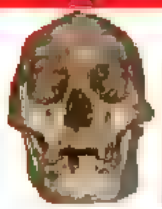

FLORES MAN
Visit our special report from the time of the discovery.
www.nature.com/news/specials/flores/index.html

Nobel prizewinner's paper retracted

A paper in *Nature* co-authored by Nobel prizewinning scientist Linda Buck has been retracted after the researchers were unable to reproduce the results. The authors now report that they have found "inconsistencies" between the original data and the data published in 2001.

The retracted paper (Z. Zou, L. F. Horowitz, J. -P. Montmayeur, S. Snapper and L. B. Buck *Nature* **414**, 173–179; 2001) describes tracing individual neural pathways from scent receptors in the nose through to the brain's olfactory cortex. Researchers in Buck's lab, then at Harvard Medical School in Boston, Massachusetts, produced transgenic mice that expressed a plant protein in neurons that have a specific odour receptor. The plant protein can travel across the junctions between neurons, allowing researchers to map neuronal networks by pinpointing the protein's location.

But researchers in Buck's lab, now at the Fred Hutchinson Cancer Research Center in Seattle, Washington, have since been unable to reproduce the original results. A subsequent review cast doubt on the validity of the published data. "There were inconsistencies in the data that were in figures contributed to the paper by the first author compared to the original data," says Buck. "I would say that we have totally lost confidence in the conclusions of that paper."

A synopsis of author contributions, published together with the retraction (see page 120), lists co-first-author Zhihua Zou as solely responsible for providing data and figures for the paper. Zou, now a researcher at the University of Texas Medical Branch in Galveston, did not respond to *Nature*'s requests for comment. Lisa Horowitz, who shared first authorship with Zou and continues to work in Buck's lab, was credited only with providing reagents and designing experiments.

Harvard Medical School has formed an ad hoc committee to review the retraction, and Buck has asked the Fred Hutchinson Cancer Research Center to review two later publications on which Zou was the lead author. "It's disappointing of course," says Buck. "The important thing is to correct the literature." The retracted paper has been cited 138 times, according to Thomson Scientific's ISI Web of Knowledge.

But the retraction will probably have only a minor effect on the field, says olfactory-neuron researcher Hitoshi Sakano of the University of Tokyo, Japan. Other researchers have corroborated some of the paper's results using other techniques, he notes. Neuroscientist Gilles Laurent of the California Institute of Technology in Pasadena, whose work on insect olfactory networks has occasionally conflicted with the results reported by Buck's lab, says that this has not hindered his research. "These questions are sufficiently complex and require such large amounts of data at high resolution that I have never considered them convincingly resolved in any system," he says. ■

Heidi Ledford

Coming Soon!

SIGMA Life Science

The 3rd edition of the Sigma Cell Culture Manual will be a hybrid reference and product guide that is designed to be a foundation for your discovery efforts.

- Extensive cell culture technical information and formulas
- Our most popular cell culture products and equipment
- Invaluable tool to help advance your research goals

Reserve your copy of the 2008-2009 Cell Culture Manual by visiting *sigma.com/ccmanual*

Our Innovation, Your Research — Shaping the Future of Life Science

SIGMA-ALDRICH

UK scientists keep access to the Gemini telescopes

Britain has reached an agreement that will allow UK astronomers continued access to the Gemini Observatory.

In November, the UK Science and Technology Facilities Council (STFC) announced its intention to withdraw from the observatory — which has 8-metre telescopes in Mauna Kea in Hawaii and Cerro Pachon in Chile — because of a budget shortfall (see *Nature* 450, 468; 2007). Subsequent negotiations to retain access to the Hawaiian telescope failed, raising fears that British astronomers would have no access to a large telescope in the Northern Hemisphere.

But on 27 February the STFC announced that it would remain in the Gemini partnership. It plans to save money by selling a portion of its nearly £4 million (US$7.9 million) annual subscription for telescope time to other interested nations.

"I welcome this announcement," says Michael Rowan-Robinson, president of the Royal Astronomical Society. Dropping out, he says, would have been "very bad for the United Kingdom's reputation as an international partner".

Massachusetts gears up to boost cash for life sciences

A. HINGER/REUTERS

Deval Patrick.

House lawmakers in Massachusetts on 27 February passed a bill that would provide $1 billion to life sciences in the state over ten years. The state Senate is expected to take up the bill next week. If it passes as expected, Massachusetts will be behind only California and Texas in state dollars recently earmarked for biological research.

The Massachusetts package features $250 million in grants, including $25 million in paediatric stem-cell research training grants; $250 million in tax credits for life-sciences firms that promise to create jobs in the state; and $500 million for bonding for capital investments, including $90 million and $95 million for building life-sciences facilities at the Worcester and Amherst campuses of the University of Massachusetts. Among the grant monies are $5.7 million for a stem-cell bank and registry at the University of Massachusetts Medical School in Worcester.

Governor Deval Patrick introduced the measure last spring.

Lunar pole is revealed in high resolution

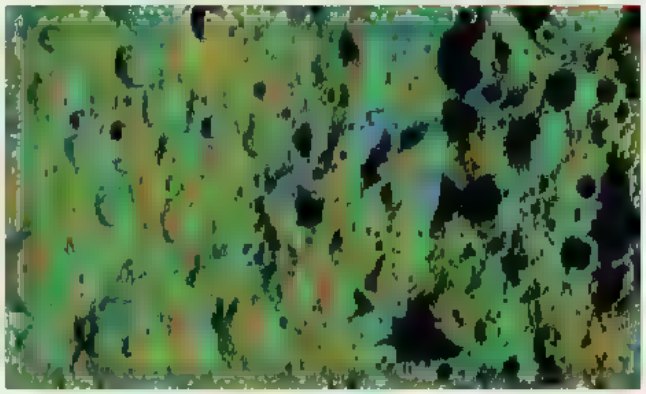

NASA

NASA has released radar pictures of the Moon's south polar region — the best ever, with a resolution of 40 metres, showing up the steep slopes and rugged topography (see right).

Taken using the Goldstone Solar System Radar facility in California's Mojave Desert, the pictures could help NASA to find smooth, flat landing areas for future rovers, or suitable spots for a lunar base. The south polar region is of particular interest because some areas, particularly those deep inside craters, are in perpetual shadow and may contain permanently frozen water that could be used as a resource.

But the Goldstone pictures, released on 27 February, do nothing to resolve the debate about whether there is water ice buried beneath the surface because the radar wavelengths used (3 centimetres) do not penetrate the surface well and an analysis of the polarization of the returning signal wasn't performed. Scientists hope that the Lunar Reconnaissance Orbiter, scheduled to launch later this year, will settle the ice question.

First of three contested stem-cell patents upheld

In a dispute over three stem-cell patents, Wisconsin Alumni Research Foundation (WARF) is claiming victory, after an interim decision from the US Patent and Trademark Office to uphold one of its patents.

On 28 February, WARF said that the claims of a 2001 patent on a method for growing and sustaining cultures of embryonic stem cells had been upheld. The patent is one of three on work led by James Thomson of the University of Wisconsin. The other two cover methods for deriving primate embryonic stem cells — including human ones — and the cells themselves.

In 2006, after critics challenged the patents on the basis that they were too broad and hindered the field of embryonic stem-cell research, the patent office said it would re-examine the three. The critics played down last week's decision, saying that WARF has already limited its claims in the upheld patent, and that the other two patents are more important. Rulings on those are still pending.

India to propose regulatory body to curb misconduct

India is to consider creating a national body to investigate plagiarism and misconduct in science after a string of high-profile frauds.

C. N. R. Rao, who heads the national science advisory committee, told *Nature* that he will discuss the proposal at his next meeting with Prime Minister Manmohan Singh. Rao was reacting to the news that Sri Venkateswara University in southern India is to reopen a massive fraud case involving chemistry professor, Pattium Chiranjeevi. Last month, Chiranjeevi was found guilty of plagiarizing or falsifying more than 70 research papers published in a variety of Western scientific journals between 2004 and 2007. Some of the journals have started retracting the articles.

US$50 billion agreed for Bush's global AIDS plan

Lawmakers in the US House of Representatives reached a key compromise last week clearing the way for a vote that could more than triple US funding to fight AIDS, malaria and tuberculosis.

The bill renews the President's Emergency Plan for AIDS Relief, a $15-billion, five-year law created by President Bush in 2003. Its new incarnation would provide $50 billion over the next five years, with $9 billion of that earmarked for fighting tuberculosis and malaria, which often affect patients with AIDS. Crucially, it does not require, as did its predecessor, that one-third of HIV/AIDS prevention money be spent on advocating abstinence. Instead, it asks countries to justify to Congress any decision to spend less than 50% of prevention dollars on promoting abstinence and faithfulness.

The Senate Foreign Relations Committee is working on its own version of the bill aiming for a similar compromise on the abstinence language.

Correction

The Editorial 'Time to take control' (*Nature* 451, 1030; 2008) failed to make it clear that Mark Grabowsky's assertion that "the billion-dollar malaria effort is flying blind" relates specifically to a lack of disease surveillance. Apologies.

UNIVERSITY OF OXFORD

Vice-Chancellor

The University of Oxford is seeking a new Vice-Chancellor to succeed Dr. John Hood in the autumn of 2009. Working closely with the Colleges, the appointee will lead an independent and self-governing institution committed to unrivalled academic standards.

Candidates must be of exceptional calibre with academic credibility and outstanding leadership qualities. They will have strong management skills gained at a senior level in a complex institution. The ability to promote the University in a regional, national and international context will be critical.

To apply for this position, or to receive further particulars, please contact Gill Lewis or Benjamin Tucker, Heidrick and Struggles (UK) Ltd., 3 Burlington Gardens, London W1S 3EP.

Email: oxford@heidrick.com Telephone: +44 (0)20 7075 4083.

Closing date for receipt of applications is 20 March 2008.

The University is an Equal Opportunities Employer.

HEIDRICK & STRUGGLES

126274A

OFFICES IN PRINCIPAL CITIES OF THE WORLD

McGILL UNIVERSITY

Director, Meakins-Christie Laboratories

The Department of Medicine of McGill University and of the McGill University Health Centre (MUHC) is inviting applications for the position of Director of the Meakins-Christie Laboratories (www.meakins.mcgill.ca/meakins/) a major International centre for research in respiratory diseases. The Meakins-Christie Laboratories are supported by an endowment and have a history of producing outstanding research in the area of respiratory diseases. The MUHC (www.muhc.ca) is one of the largest academic health providers in Canada with new and visionary leadership dedicated to the expansion of clinical, research, and community services. McGill University (www.mcgill.ca) is an English-speaking institution located in Montreal, one of North America's most cosmopolitan cities.

The Director of the Meakins-Christie Laboratories is expected to have an international reputation in research related to respiratory diseases. The successful candidate will be forward-looking, able to forge collaborative scientific relationships, and possess a solid understanding of and commitment to translational research. Applicants holding an MD degree who wish to engage in clinical practice must be eligible for licensure in the province of Quebec.

Compensation will be commensurate with qualifications and experience. An attractive package will be provided to the successful candidate including start-up funds. The candidate will be eligible for a tenured or tenure-track position at the Full Professor level.

Please submit a curriculum vitae including a list of publications, an outline of current research interests, and the names, addresses and contact numbers of three references within 30 days of publication of this advertisement to:

Dr. Barry I. Posner
Chair, Meakins-Christie Search Committee
Polypeptide Hormones Research Lab
3640 University Street, Room W3-15
Montreal, Quebec, H3A 2B2
E-mail: barry.posner@mcgill.ca

McGill University is committed to equity in employment and diversity. It welcomes applications from indigenous peoples, visible minorities, ethnic minorities, persons with disabilities, women, persons of minority sexual orientations and gender identities and others who may contribute to further diversification. All qualified applicants are encouraged to apply; however, in accordance with Canadian immigration requirements, priority will be given to Canadian citizens and permanent residents of Canada.

NW125848A

The scientist delusion

Religious resistance to science is often exaggerated, but fresh problems may lie ahead, says **David Goldston**.

PARTY OF ONE

Cosmologist Rocky Kolb began a public lecture last month with a slide amusingly titled "The View of Cosmology 1,000 Years Ago (and In Present-Day Kansas)". The joke, a reference to recent battles over teaching evolution in the state of Kansas, was telling. Many scientists today feel that they are confronted with an ever more religious and irrational public in the United States that reflexively rejects the views of scientists. But scientists tend to underestimate both the public receptivity to science and the battles that religious concerns may prompt in the years ahead.

It is true, of course, that the US population is far more religious than that of, say, western Europe, and this has created significant resistance to the acceptance of evolution in particular. Yet although a remarkably high percentage of Americans do not believe that humans evolved from earlier life forms — polls generally place the number at 40–50% — the figure has held relatively steady for at least a quarter of a century. Moreover, those statistics mask a number of attitudes that are far more favourable to science. For example, a 2006 poll conducted for a science organization asked who the respondents would be "interested in hearing from" about evolution, creationism and intelligent design. The two categories that ranked highest were scientists (77%) and science teachers (76%). Clergy ranked high, but 15 percentage points lower than scientists; and only half as many people were "very interested" in hearing from clergy compared with scientists.

Even the nature of the intelligent-design crusade reflects the high stature of scientists. Intelligent-design advocates try to sell their wares as science rather than religion partly as a legal gambit; the Supreme Court has ruled that religion cannot be taught in US public schools. But intelligent design is also framed as science because its purveyors know that science and scientists are held in high esteem and epitomize modern, forward looking, hopeful aspects of US society.

More generally, the United States is probably becoming less religious, not more so. A new study by the Pew Forum on Religion in Public Life found that 16% of Americans say that they are not part of any organized faith — a record high, although the study noted that the number includes many individuals who believe in God or are agnostic. Also, most Americans do not belong to religions that have any doctrinal quarrel with evolution. Some opposition to evolution is due as much to religious ignorance as scientific; most surveys find that Americans are not especially adept at answering specific questions about the Bible or theology.

The point here is not that there's nothing for scientists to worry about or that they should cease their efforts to teach evolution. But it is important for scientists to understand that they do not face a public inherently hostile to science (even among the relatively small percentage who are fundamentalists), and that public attitudes towards both science and religion are complicated and often contradictory. It's not even clear what most people mean when they say they don't believe that humans have evolved. Is this detail a matter of some concern to them, or is this just a casual way to say that they viscerally reject the notion of a random Universe? Evolution is largely a symbolic issue to the public, and may be a poor measure of how religious attitudes affect the reception of science more generally.

Recognizing the complexity of public attitudes, a number of scientists and other scholars are trying to develop language to discuss evolution in ways that might build bridges to the religious. These efforts were the subject of a well attended panel I moderated at last month's annual meeting of the American Association for the Advancement of Science in Boston, Massachusetts. Some panellists, in effect, advocated co-opting the language of religion. For example, Kenneth Miller of Brown University in Providence, Rhode Island, the author of a leading textbook on evolution and a practising Catholic, talked about embracing the notion of life having a design, but explaining it as the result and embodiment of evolution. Others, such as Matthew Nisbet, a communications scholar at American University in Washington DC who organized the panel, suggested moving the discussion away from scientific theory and talking about the medical and other benefits that have resulted from understanding evolution.

No doubt all these approaches are worth trying, and the general message of the panel — that scientists should address the public with respect rather than contempt — is well taken. But the panel failed to grapple with two important facets of the way science and religious attitudes intersect.

First, battles over science in general, and evolution in particular, tend not to reflect concerns about science, but about society more generally. Ever since Darwin there has been a small corps of people interested in attacking evolution, but noteworthy public crusades arise only periodically. They erupt most intensely at times when the culture is changing in ways that many find confusing and disconcerting — the Roaring '20s, the 1960s and today. Scientists must continue to carry out their educational mission, but evolution will disappear from the headlines only when the whole constellation of social issues that animate the religious right recedes from public concern.

Second, the panellists tiptoed around the fact that scientific discovery can genuinely undermine religious beliefs. The focus of the panel was on teaching evolution, but discoveries in genetics and neuroscience are likely to be far more problematic in the long run. The two fields are verging on drawing the ultimate materialist picture of human nature — humans as nothing more than proteins and electrical impulses, all machine and no ghost, to play off Descartes' formulation. This view will challenge not only fundamentalist views about the soul, but more widely held notions about what it means to be a person. That will further complicate age-old questions about the nature of individual responsibility and morality.

Responding to these issues will be difficult for scientists and non-scientists alike. New discoveries about the human genome and neuroscience will no doubt be clearly linked to potential medical advances, but they may also raise new questions about what kinds of interventions are appropriate. The conundrums may leave even atheists longing for some theological guidance on how to decide what is moral. And wandering about this uncharted territory may make the well-rehearsed battles over evolution seem like the good old days. ■

David Goldston is a visiting lecturer at Harvard University's Center for the Environment. Reach him at partyofonecolumn@gmail.com.

NATURE Vol 452 6 March 2008

HEARING THE HEAVENS

The cosmos is thought to be awash with gravitational waves to which humanity is, as yet, deaf. **Trudy E. Bell** reports on LISA, an experiment on an unprecedented scale designed to put that right.

Imagine a new constellation — a narrow triangle about as deep as the scoop of the Big Dipper But this constellation, unlike the familiar natural ones, moves through the sky, always appearing in the evening sky after sunset. The new constellation slowly rotates, each component circling around the centre once every year. And as it does so, it also expands and contracts.

Unaided earthly eyes will never actually see the Laser Interferometer Space Antenna (LISA), as this artificial constellation is to be named. Its three component spacecraft will be too small, and the light with which they shine will be invisible infrared. Unseen as it may be, though, it will still be humanity's largest ever creation — 5 million kilometres on a side. And the aspirations it embodies are similarly grandiose. In 2018, or thereabouts, it will try to detect extraordinary cosmic events, such as the births of galaxies and the deaths of black holes, in a fundamentally new way

LISA is perhaps the most ambitious space mission envisaged for the coming decades. A recent assessment of astrophysics research proposed for NASA's Beyond Einstein programme by America's National Research Council (NRC)[1] gave the "extraordinarily original and technically bold" project its highest scientific ranking. Under joint development by NASA and the European Space Agency (ESA), LISA's goal is to detect gravitational waves — fluctuations in the fabric of space and time — by measuring the relative motions of three spacecraft with great precision. Although that assessment carried out by the NRC saw LISA as the "least scientifically risky" of the proposals for future flagship missions, there is no getting away from the fact that no one has ever tried anything remotely similar before.

LISA is designed to measure the gravitational waves predicted by Einstein's general theory of relativity. Relativity defines gravity in terms of the geometry of space and time; gravitational waves are transient fluctuations that stretch and compress that geometry. Although they have never yet been observed directly, indirect evidence for them was enough to earn a Nobel Prize. Over three decades Russell Hulse and Joseph Taylor, now of Princeton University, New Jersey, observed a system in which two neutron stars whirl round each other once every 8 hours. Over the years, their spinning speeded up — evidence that the system was losing energy. The rate at which energy was lost matched exactly the power with which relativity predicted that the pair of stars would be emitting gravitational waves.

Geodesics and gigantism

Even when gravitational waves are generated by massive objects and ungodly accelerations, such as those involved in that neutron-star doublet, detecting them requires almost unthinkable attention to detail. In relativity, the shape of spacetime is defined as the path taken by a body falling free under no influence but that of gravity — a 'geodesic'. Gravitational waves affect these geodesics, and can thus be detected, but only through careful comparisons. "You cannot demonstrate that one particle is freely falling and following a geodesic," explains Stefano Vitale, a physics professor at the University of Trento in Italy. "You must have two particles, and compare the shapes of their paths by exchanging a ray of light between them." The small amplitude of gravitational waves means that detecting them by comparing geodesics in this way requires immense precision. The long wavelengths of the gravitational waves that most interest astrophysicists means that the geodesics being compared must be separated from each other by astronomical distances.

Using freely falling objects to spot gravitational waves in this way, as LISA is intended to do, is a three-step process. First you set up a situation in which masses can fall freely along their geodesics without being disturbed by magnetic fields or other spurious forces. Then you must measure with extraordinary precision how the distance between their geodesics changes when passing gravitational waves distort the local curvature of space. The last step is analysing these changes to determine the exact shape, frequency and intensity of the distortions to the curvature of space, so as to learn about the nature of distant events producing them.

> "We hope to use gravitational waves to peer through this dark fog to listen to the birth of the first galaxies."
> — Scott Hughes

To provide Vitale's geodesic-joining rays of light, LISA uses neodymium-YAG lasers, which shine at a wavelength of a little more than a micrometre, a wavelength they stick to with extreme precision. These will illuminate cubes four kilograms in mass but just four centimetres on a side — polished 'test masses' of gold-coated gold -platinum alloy as beautiful as fine jewellery and much more costly. The test masses respond to gravity and not much else. "The gold-platinum alloy has a magnetic susceptibility almost as low as glass," explains Paul McNamara, an ESA project scientist in Noordwijk, the Netherlands. Once in space, the test masses' sole purpose is to follow their own paths, each falling freely along its geodesic within one of the LISA spacecraft while reflecting the laser light with which the other spacecraft illuminate it.

LISA will be arranged so that these geodesics are 5 million kilometres apart, with the spacecraft falling around the Sun 20° behind the Earth in the same orbit. That will put them about 50 million kilometres from their planet of origin. Once during every annual orbit the triangle will 'breathe', its sides taking turns to grow and shrink by about 50,000 kilometres.

Hearing double

LISAs spacecraft do not need to measure the exact distance between the test masses each contains any more than a police officer with a radar gun needs to know the exact distance to a car before he can tell whether it is speeding. The system's 'breathing' causes a predictable Doppler shift — similar to the lowered tone of a receding train's whistle, or the redshift of a distant galaxy's light — in the light reflected from the test mass in one spacecraft to the instruments in another when the distance between them grows, and an opposite shift on contraction.

A passing gravitational wave will impose a variation on this predictable Doppler signal, because it will curve space between spacecraft and lengthen the route that the light connecting them has to take. Compared with the changes in the Doppler shift caused by the breathing, however, frequency changes due to gravitational waves happen much faster — over periods of between 10 seconds and 3 hours. It is here that the unprecedented precision of LISA's metrology will come into play. LISA's detectors will treat the infrared laser beam in the same way that an FM radio in a car treats a radio signal. An FM radio station transmits a steady high frequency signal (typically around 100 megahertz, or 10^8 cycles per second) modulated by lower-frequency audio programming (in the kilohertz range, or about 10^3 cycles per second). A home or car radio receiver contains a local oscillator that generates a signal at roughly the same higher frequency as the transmitter. Subtracting the signal received over the air from the local oscillator signal, a process called heterodyning, unmasks the much lower-frequency signal of the audio programming. That audio-frequency signal then drives the radio's speakers.

Optical heterodyning within LISA, using the million-times higher frequencies of infrared laser light (about

L COOK

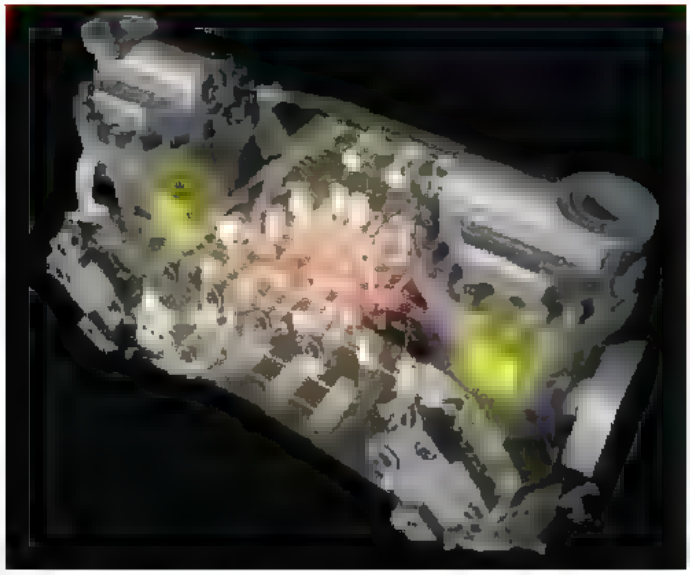

LISA Pathfinder in artists' impressions with test masses and laser light revealed in cutaway (left) and reaching its Lissajous orbit (right).

300 terahertz — 3×10^{14} cycles per second), will do much the same but with unprecedented precision. The incoming laser beam (as reflected off a distant test mass) will be combined with some light from the outgoing laser beam (treated as the reference signal) on a photodetector. The comparison will reveal the expected lower-frequency (1 megahertz) 'hum' of LISA's regular breathing. Gravitational waves would show up as a modulation of that hum at really low frequencies (a millihertz, or 0.001 cycles per second). Using signal processing akin to that in satellite-navigation receivers, LISA will measure that low-frequency signal to a precision of a few millionths of a cycle, corresponding to a few picometres in distance.

Finding the path

Unsurprisingly, some wonder whether this wizardry can be pulled off in practice. Specifically, can external disturbances — for example, the solar wind and the radiation pressure of the Sun's light — be understood and avoided well enough for LISA to achieve the sensitivity it needs?

"The devil is truly in the details," cautions Robin Stebbins, LISA project scientist at NASA's Goddard Space Flight Center in Greenbelt, Maryland. "When doing precision measurements, an instrumentalist must estimate all possible errors, verify in the lab that those estimates are correct, and constantly search for errors that may have been overlooked. We have a list of about 50 physical phenomena that could disturb LISA's test masses, of which perhaps 35 are significant."

There is, however, nothing as convincing as actually trying the technology out. That's where LISA Pathfinder comes in. LISA Pathfinder, currently being assembled by contractor EADS Astrium in Stevenage, UK, is a spacecraft designed to demonstrate LISA's underlying technologies: reflecting infrared laser beams off freely falling masses following their own geodesics, picometre metrology, and reducing unwanted disturbances to the test masses. "Flight hardware is being delivered almost every day for launch in 2010," says McNamara, who is LISA Pathfinder's project scientist.

Lissajous orbit

LISA Pathfinder will be launched into an elaborate Lissajous (pronounced, by coincidence, "Lisa-ju") orbit around the 'L-1' point 1.5 million kilometres sunwards of Earth, where the pull of the Earth and Sun mostly cancel each other out. "We want to get out of the gravitational pull of the Moon or away from the temperature drop of being eclipsed by Earth's shadow," McNamara says. "L-1 has constant solar power and constant temperature, and is relatively cheap to get to."

Once the spacecraft is in this orbit, two test masses just like those to be used in LISA will be gently released from the cages that have held them in place. This is no easy task: "A caging mechanism that would release the cubes with zero velocity was one of the toughest engineering problems — we've been working on it since '94," says McNamara. Once released the test masses, just like the ones in LISA, will fall freely along their own geodesics; only they'll do so separated by a few tens of centimetres, rather than a few million kilometres.

The rest of the LISA Pathfinder spacecraft will serve to shield the masses within from several dozen forces that would otherwise disturb any measurements. Like a parent holding an umbrella over a child in a rainstorm, the spacecraft will follow the test masses without touching them, continuously correcting its position by firing micronewton thrusters so gentle that their force is "the same as your breath from 200 metres away", McNamara says. If Pathfinder can protect its test masses, leaving them to fall

Meanwhile, back on Earth...

LISA is not the only gravitational wave detector: there are five laser interferometers at various stages of development and operation on Earth's surface, although they have yet to detect anything — and may never do so. The Laser Interferometer Gravitational-Wave Observatory (LIGO) consists of a pair of detectors in Hanford Washington and a third in Livingston, Louisiana, in the United States. Geo — the name is simply a reminder that the detector is located on Earth — sits near Hannover, Germany. Virgo — not an acronym but the name of a constellation that contains a cluster of active galaxies predicted to be a major source of gravitational waves — is near Pisa, Italy. Tama is named after a western suburb of Tokyo, Japan, where the detector is located. AIGO, the Australian International Gravitational Observatory, is in Gingin near Perth, Western Australia. Because they are on Earth, these detectors are much smaller than LISA, with arm lengths that range from 300 metres to 4 kilometres, and thus are sensitive only to short wavelength (high-frequency) signals. Their sensitivity is impaired by seismic noise issues that LISA will avoid, although LISA has its own noise challenges. Ground-based detectors at current levels of sensitivity are not expected to detect gravitational waves because of the rarity and weakness of the stellar-mass gravitational-wave sources found at high frequencies; however, planned improvements (specifically Advanced LIGO, to be finished in 2013) will increase sensitivity by more than a factor of 10. At that point some high-frequency detections are expected — if the cosmos plays ball. **T. E. B.**

as freely as if they were the only things in the Universe, then LISA's three spacecraft should be able to do the same.

LISA Pathfinder — a single spacecraft with a 90-day mission quite close to Earth — has a budget of €300 million ($440 million). LISA itself — three spacecraft with a 5- to 10-year lifetime, optical heterodyning equipment, deep-space communications and additional intricacies — is put at around US$2 billion. The cost is one reason why LISA is being pursued jointly by NASA and ESA, and why it has taken so long to get into space. "To get any mission into space, one must first convince the space community of its scientific value, because space is a zero-sum game," explains Karsten Danzmann, director of the Albert Einstein Institute in Hannover, Germany, and co-chair of the LISA science team. "In the early 1980s [when ideas for a mission such as LISA were first mooted] the astronomers and planetary scientists had neatly divided the cake. No one wanted to share the cake with the gravitational-wave physicists because it would mean getting a narrower slice. Also, no one at the time could see how to measure such small changes over such vast distances."

LISA made its first formal appearance in 1992, when ESA issued a request for proposals for medium sized scientific missions and Danzmann and his colleagues — about half of them in the United States — proposed a version of the idea with six small spacecraft. The European agency had taken the lead because NASA was more focused on repercussions from the space shuttle Challenger accident and the faulty mirror aboard the Hubble Space Telescope. But by 1997, NASA and ESA were anticipating a joint mission through coordinated studies of the concept that are still under development today.

Screaming stars

So if LISA finally starts to resonate with the Universe's gravitational radiation at the end of the next decade, as is currently planned, what new science will be revealed? Making a presentation to the NRC panel last year, Scott Hughes, a physicist at the Massachusetts Institute of Technology in Cambridge, provided a striking answer. Without warning, he played an audio recording of a tiger attacking and devouring a live monkey. As the monkey's screams echoed throughout the auditorium, "every primate in the room came to attention", recalls Stebbins.

Hughes was demonstrating just how much one can learn from sound as a way of emphasizing the extent to which LISA's unique output can be thought of in terms of noise, rather than vision. The analogy between LISA and human hearing "works surprisingly well", he says. A pair of star-sized black holes spiralling into each other would be expected to radiate gravitational waves of frequencies in human audio range. If human ears were sensitive to gravitational waves, the final merging of the black holes would sound like a rising warbling that ends in a mouse squeak, if not quite a monkey scream. That final squeak is what gravitational-wave detectors on Earth are trying to hear (see 'Meanwhile back on Earth').

At the much longer wavelengths to which LISA is sensitive, merging supermassive black holes within star clusters would emit a rising roar "more energetic than all the stars in all the galaxies", Stebbins adds. And the source of the waves should be apparent through LISA rather as the direction of a tiger's kill is obvious to a listener in the jungle. Just as with two human ears, "you can tell roughly where a sound originates, because the sound wave hits one ear before the other", says Hughes, so the distance between the LISA spacecraft allows any waves that it detects to be traced back towards their source. The three LISA spacecraft, 13 times as far from each other as the Moon is from Earth, will be 17 seconds from each other at the speed of light — which is also the speed of gravitational waves. Time lags in the signals measured across the different edges of the triangle should allow LISA to discern the approximate direction of a source of gravitational waves, in part so radio and optical telescopes could take a look. It is a triangle that triangulates.

> "Gravitational waves will throw open doors to an entirely new and vast vista of the Universe."
> — Peter Bender

The infancy of the Universe

LISA is expected to hear back to when the Universe was younger than a billion years old. "Half a billion years after the Big Bang was the cosmic dark ages, when the Universe was filled with neutral hydrogen gas that absorbed photons," Hughes explains. "We hope to use gravitational waves to peer through this dark fog to listen to the birth of the first galaxies." (In speech, LISA scientists go back and forth between auditory and visual metaphor.)

In addition, there will be a constant background "hissing and crackling" of higher-frequency gravitational waves from "20 million more ordinary white-dwarf star binaries that fill our galaxy," Danzmann says. But there will be deeper tones, too — notably, the booming collisions of entire galaxies. LISA's sensitivity to such events is one reason for being sure there is something for LISA to hear. "There are supermassive black holes of a million or 10 million solar masses in the centre of virtually every galaxy. And we see from photographs that galaxies are colliding everywhere," says Rainer Weiss, an emeritus physics professor at the Massachusetts Institute of Technology. "So at the wavelength range of LISA, we know there are sources."

The project's promise goes beyond astronomy into fundamental physics. "Since the beginning of the Copernican revolution, astronomy has posed challenges to physics. And we've used physics to understand astronomical objects," said Charles Kennel, a former NASA associate administrator, now director of the Scripps Institution of Oceanography in San Diego, California, who served as co-chair of the NRC report. "LISA will be able to find merging black holes and test general relativity in the strong field limit." That's a relativist's term for situations where gravity is so powerful — that is, the geometry of space is so sharply curved — that phenomena that cannot be observed in any laboratory, or by any observations of nearby astrophysical objects, come into play.

Relativity's predictions about this limit could be tested, though, by observing how matter and the fabric of space and time are wrenched apart near supermassive black holes in the centres of galaxies. General relativity predicts that when smaller black holes, with masses of ten times the Sun's, fall into these much vaster monsters, the geometry of space and time is also being wrenched and kinked in ways never seen anywhere more mundane — and the specifics of the gravitational waves given off should reveal the theoretical limits of general relativity. Only at the edges of masses capable of such acts of cosmic cannibalism — second in violence only to the Big Bang itself — are gravitational waves anticipated to reveal the theoretical limits of general relativity.

"People often say that gravitational waves will open a new window for astronomy," says Peter Bender, a physicist at the University of Colorado's institute JILA in Boulder. "More accurately, gravitational waves will throw open whole doors onto an entirely new and vast vista of the Universe." ■

Trudy E. Bell is the author of a dozen books on astronomy, space science, history and cycling.

1. Committee on NASA's Beyond Einstein Program, *NASA's Beyond Einstein Program: An Architecture for Implementation* (Nat. Acad. Press, Washington DC, 2007).

NATURE Vol 452|6 March 2008

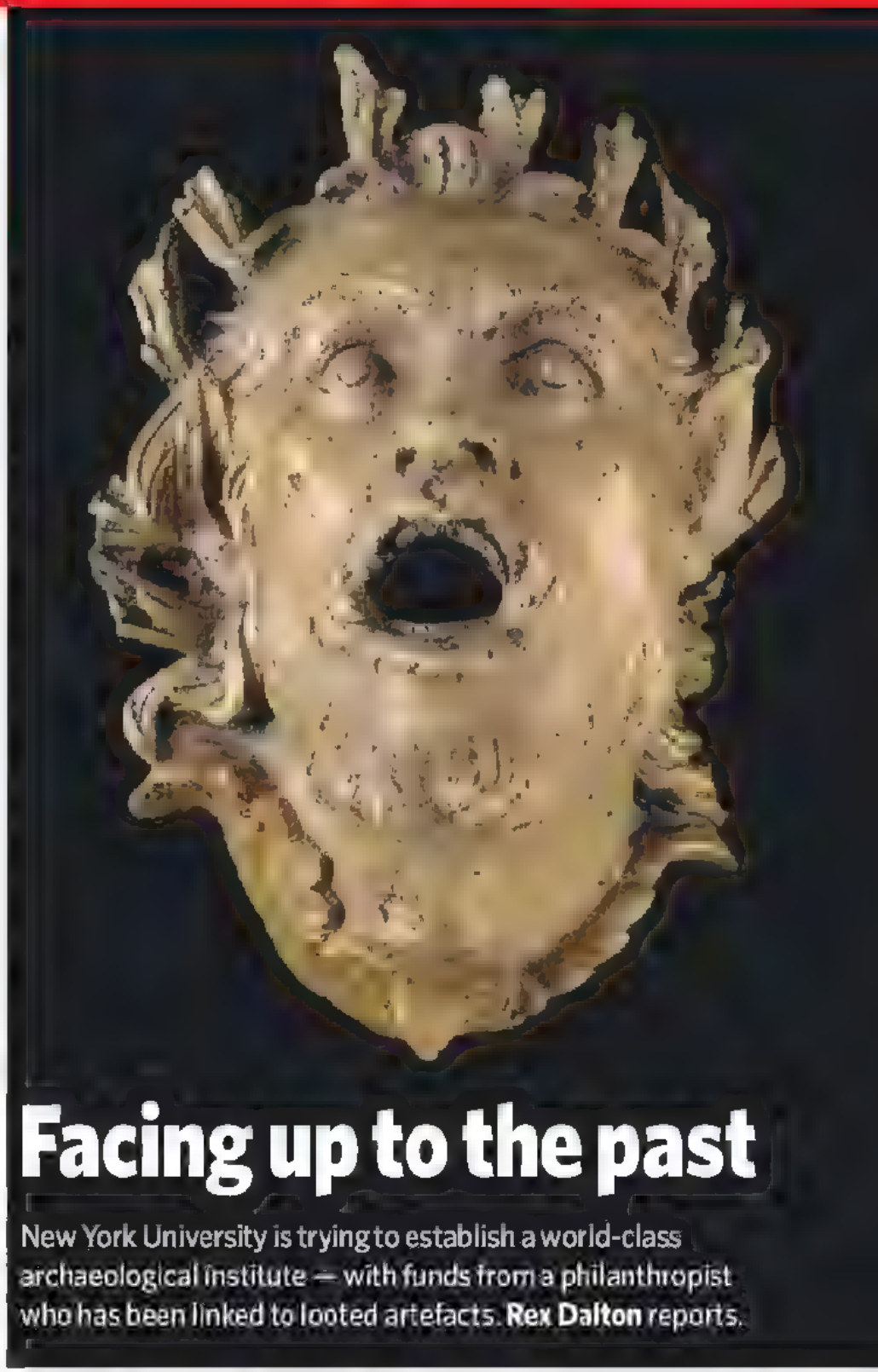

Facing up to the past

New York University is trying to establish a world-class archaeological institute — with funds from a philanthropist who has been linked to looted artefacts. Rex Dalton reports.

Unearthed last summer at an ancient crossroads in central Asia, two bronze lamps hark back to the Greek myth of the Golden Fleece. They come from the region once known as Colchis, in present-day Georgia, where Jason and the Argonauts are said to have searched for the precious wool[1]. The lamps also reflect the multitude of cultures that passed through the region — with an unusual intermingling of elephants, a woman's snake-wrapped torso and gods decorating their sides.

The lamps, which date from between the third and first century BC, are now bringing their story to the United States, where they and other stunning Georgian antiquities will form the inaugural show at the newly opened $220-million Institute for the Study of the Ancient World at New York University (NYU). The 130 artefacts include gold jewellery, bronze masks, sculptures and wine goblets, all dating from the last few centuries BC.

But while the public admires the artefacts in the institute's gallery, many in the archaeology community are still sputtering over its financial creator — Shelby White, a wealthy New York connoisseur whose name has been linked with looted antiquities. Last month, she returned nine major artefacts to Italy, from where they were looted decades ago; a Greek vessel will also be returned in 2010. White has insisted that she had no knowledge of their illicit route to her world-class collection.

The worldwide market for antiquities, which collectors such as White underpin, thrives on unprovenanced historical artefacts, sold to collectors as drawing-room 'art' or donated to museums as tax write-offs. Objects that move from the archaeological dig to the auction house are often lost to scientific study. Some observers even argue that, by raising demand for such antiquities, collectors are the real looters[2].

Objects and objections

White is one of the most high-profile private collectors, as she regularly lends her artefacts to museums for display. That visibility has drawn extra scrutiny of her collecting habits. "She is an unrepentant collector, whose approach to the past I believe is misguided," says Colin Renfrew, a British archaeologist and former director of the McDonald Institute for Archaeological Research at the University of Cambridge, UK. "I look at anything she funds with suspicion."

By chance, Renfrew will lecture next week at NYU's main campus in Greenwich Village, where some senior members of the university's anthropology department are similarly sceptical. Randall White, an NYU anthropologist who studies Palaeolithic cave art and is no relation to Shelby White, notes that the new institute was created without the involvement of the anthropology department, one of the top dozen in the nation. He resigned in protest from NYU's Center for Ancient Studies after university authorities accepted the $200 million endowment from Shelby White's foundation two years ago. In his resignation letter, he wrote that "NYU's acceptance of such support tells the world we condone the collection of unprovenanced antiquities that may have been clandestinely exported from their country of origin".

Others at the university are also distancing themselves. "The institute is built more around the interests of Shelby White," says Fred Myers, chair of the anthropology department. "We weren't involved in its development." Privately, a prominent department member voiced concerns that an affiliation with the institute might taint a career: "If we wanted to work anywhere in the world, we couldn't be associated with the institute."

NYU spokesman John Beckman says that such an assessment "overstates" the campus rift. "There was wide consultation among the faculty about the establishment of the institute," he says. "The response was generally, but not universally, favourable."

Jaw-dropping: this bronze portrait of Pan will form part of the inaugural show at the Institute for the Study of the Ancient World in New York.

Despite — or perhaps because of — the doubts in the community, the institute has set about establishing itself as an academic powerhouse in New York's posh Upper East Side. Housed in a six-storey limestone town house built a century ago, the institute has offices for five initial faculty members, space for future analytical facilities, a conference centre and a library headed by a specialist from the American School of Classical Studies at Athens in Greece. A new doctoral programme is planned, hopefully to start in 2009. For its first faculty hire, the institute's search committee, which included Shelby White, recruited Roger Bagnall from Columbia University in New York as director. An authority on ancient texts, Bagnall is widely respected for his scholarship and professionalism.

Last year, he created an advisory panel of half-a-dozen international authorities to begin hiring; it recruited Alexander Jones, a historian of mathematics and astronomy who came from the University of Toronto in Canada. Jones, who will start as a fully tenured NYU professor in July, says he was attracted by the centre's cross-cultural nature. "The institute is very exciting because it isn't centred around an individual idea or culture, like many university departments," he says.

"We wanted to create a place where different cultures could be studied to appreciate their interdependence," affirms Shelby White, whose former personal curator, archaeologist Jennifer Chi, is an associate director at the centre. "Thats the underlying uniqueness of the institute."

Looking back

For now, the institute's research mission has yet to be defined, beyond the general outline that it will focus on the time period from about 3000 BC to AD 1000. "Archaeology and history will be our core," says Bagnall.

As the institute takes shape, White's shadow is ever-present. She is well known in collection circles for her work with her financier husband, Leon Levy, who died in 2003. They regularly lent parts of their private collection of antiquities to major museums, including the Metropolitan Museum of Art (the Met), just blocks away from the new NYU institute. Yet they have also received some of the most public criticism questioning the provenance of their artefacts.

White herself has drawn fire for more than a decade. In 2000, President Bill Clinton nominated her to sit on a panel meant to fight the trade in illegal artefacts, a decision that triggered an outcry from many archaeologists. The then-president of the Archaeological Institute of America, Nancy Wilkie, wrote that White's "collecting practices certainly would not meet with the public's approval". White's nomination eventually died when President George W. Bush took office and dropped all of Clinton's nominees for such appointments.

In recent decades the archaeological community has fought back against looting, helping to craft new legislation to block trade in antiquities, launching international investigations, and even helping to close down some artefact auctions in London. Oscar Muscarella, an archaeologist at the Met who speaks out regularly on artefact provenance, says White and her husband seemed to live in the past, when collecting was seen more of an art initiative and less of a force that drives illicit looting. Muscarella recalls his last talk with Levy. "I liked him as a person," he says. "He wanted me to be his curator. But I read him the riot act on all the plundered stuff. He smiled, we shook hands and never spoke again."

> "The institute is very exciting because it isn't centred around an individual idea or culture."
> — Alexander Jones

Today, Shelby White remains active at the Met, where she is a benefactor and sits on the search committee to replace recently resigned director Philippe de Montebello. Renfrew, for one, says it is "amazing" that any museum would continue contact with anyone linked to questionable artefacts. "Instead of asking themselves how their policies could be so inadequate," he says, "the Met and some other museums are in denial."

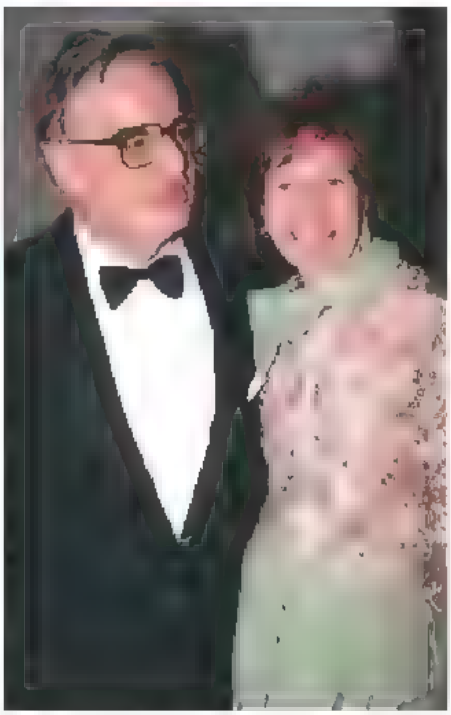

Shelby White (right) and Leon Levy's antiquities collection has been criticized by archaeologists.

B. CUNNINGHAM/NEW YORK TIMES

Coincidentally, similar issues have arisen recently in California, where last month 200 federal agents raided four major museums, including the Los Angeles County Museum of Art, as part of a criminal investigation into smuggling and alleged tax-donation violations involving artefacts from southeast Asia and Native American lands. A financier's private museum outside Chicago was also raided. During the five-year probe, undercover agents tape-recorded a network of buyers, gallery owners and museum curators engaged in alleged scams — including purchasing smuggled artefacts and donating others to museums for inflated tax write-offs. Federal search warrants indicate that some museum officials knew the objects were looted and values falsely inflated.

At the NYU institute's inaugural exhibition, the Georgian artefacts have a much clearer history. They have mostly come on loan as part of an arrangement worked out by David Lordkipanidze, director of the Georgian National Museum in Tbilisi. Lordkipanidze, renowned for his discovery[4] of early hominin fossils dating back 1.7 million years in Dmanisi, Georgia, says that he sees the exchanges as a way to advance studies in his homeland. Georgian conservators will receive training at the new institute. And in the catalogue for the upcoming show, he pays special tribute to White, writing that her "unstinting care for the archaeology of antiquity provides an amazing example of leadership and demonstrates what philanthropy and public–private partnership can do"

Most of the Georgian artefacts were on display at the Arthur M. Sackler Gallery of the Smithsonian Institution in Washington DC until last month, they have been supplemented for the NYU opening with some new finds, including candelabra, incense burners and the bronze lamps adorned with elephants.

In the future, academic archaeologists will be watching closely to see how the institute evolves — particularly in terms of what antiquities can be exhibited or accessioned. If artefacts with suspect credentials are showcased, the outcry is likely to be swift and savage. ■

Rex Dalton is a US West Coast correspondent for *Nature*.

1. Feresin, E. *Nature* **448**, 846–847 (2007)
2. Watson, P. & Todeschini, C. *The Medici Conspiracy* (PublicAffairs, New York, 2006)
3. Wilkie, N. C. *Archaeology* **53** (6), 10 (2000).
4. Lordkipanidze, D. *et al. Nature* **449**, 305–310 (2007)

FISH-WILDLIFE.CONSERV.COM

Algal blooms can make life miserable for coastal dwellers and wreak havoc on marine ecosystems. **Mark Schrope** reports on Florida's efforts to predict these red tides.

RED TIDE RISING

On 3 January 2005, a fisherman working 25 kilometres off the southwest coast of Florida noticed that the baitfish in his seawater tank were spinning and dying. He had seen this strange behaviour before, and knew that it meant more than just a ruined fishing trip. He called the authorities to warn them, and within days a 'red tide' swamped the coast. In the weeks that followed, potent levels of an algal species called *Karenia brevis* flooded the water with toxins.

Soon, tourists and residents alike were dodging beaches covered in dead fish and a salt spray that made eyes water and throats instantly raspy. Visits to hospital emergency departments spiked. Manatees, sea turtles, dolphins and other animals began to die; the scourge lasted for more than a year.

Red tides occur around the world, from Europe to New Zealand, and are caused by blooms of similar algal species. *Karenia brevis* is, however, a particularly nasty one; its outbreaks have afflicted the coast of Florida since as far back as the 1500s, and now do so almost every year to varying degrees. The state and federal governments spend millions of dollars each year trying to research and monitor the outbreaks. Yet despite all the money and effort put into developing sophisticated monitoring systems, for now the solitary fisherman offshore has as good a chance of catching the birth of a red tide as a satellite does.

"We have had a name for this [organism] now for decades, and we have evidence of humans coughing ever since [Hernando] de Soto took his trek around the Gulf of Mexico," says Bob Weisberg, an oceanographer at the University of South Florida (USF) in St Petersburg. "But we still don't have a good handle on what leads to a bloom, what sustains a bloom, and ultimately what leads to the demise of a bloom."

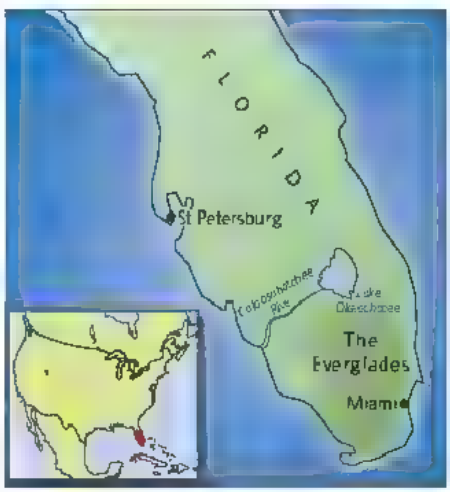

Weisberg and his colleagues are hoping to change that, with a new US$1.25-million Center for Prediction of Red Tides. The centre is a collaborative effort based at the USF's College of Marine Science, a series of low, non-descript, 1950s-era white buildings overlooking Tampa Bay. Its goal is to improve existing models to explain more accurately and then predict the complex progression of a red tide bloom. Successful forecasts could, for instance, allow fishermen to scoop up shellfish before a bloom takes hold, warn businesses to brace for a drop in beach tourism or alert managers to which environmentally sensitive areas they should be monitoring most closely. "From an environmental management standpoint, forecasting gives us huge benefits," says Cindy Heil, who leads work on red tides at the Florida Fish and Wildlife Research Institute in St Petersburg, which provided the funds for the new centre and is a partner in the work.

But monitoring and modelling *Karenia* are not simple tasks. The dinoflagellate, which has plate-shaped cells measuring 18–45 micrometres across, is found throughout the submerged shelf that extends from west Florida

out to the deeper basin of the Gulf of Mexico. Physical models have to account for factors such as its ability to grow at various depths and in a range of salinities, and how ocean currents affect its spread and growth. "We have got to get the ocean currents right so that we can get the rest of it right, and the rest of it is a lot more complicated," says Weisberg.

Practical applications

For years, Weisberg and his colleagues have maintained a growing collection of open-ocean buoys from the southern tip of Florida up to the Florida panhandle. As well as these buoys — which may actually go offline soon, as their funding dries up — the team uses tools such as an ocean-bottom profiler that rises into the water column at programmed intervals, then sinks back to the bottom, measuring temperature, salinity and currents as it goes. Weisbergs group also uses two-metre-long autonomous underwater vehicles (AUVs) that can be programmed to roam large swaths of the ocean gathering data. The data gathered with these tools are then combined with an evolving model developed by the US Navy to create a working physical model focused on red tides, but with numerous other applications. These include identifying favourable conditions for fishermen or for search and-rescue efforts.

In nearby Sarasota, collaborators at the Mote Marine Laboratory have outfitted their own AUVs, and one USF buoy, with instruments dubbed 'breve busters'. The breve busters are designed to detect the presence of *Karenia* and collect data that allow rough calculation of its concentrations. Still, says Mote's Gary Kirkpatrick, "we are certainly nowhere near what we envision as an operational system that can provide a quick look at where *Karenia* is or isn't on a minute-by minute basis". Such capabilities, he thinks, could arrive within a few years.

The work to understand the physical aspects of red tides, though, still has gaping holes: the physical models used do not incorporate any biology. They can track where a bloom is likely to spread on the basis of winds, currents, and the like, but they can't account for the algae growing, for instance. The group is now working to feed such biological factors into physical models retroactively, to see how well an output matches what actually happened. Such 'hindcasting' allows the researchers to test theories about how blooms might be controlled.

Like all dinoflagellates, *Karenia* has characteristics that blur taxonomic lines, which makes modelling challenging. It is an alga, so it photosynthesizes, but like an animal it can also move under its own momentum, using structures called flagella. Much has been learnt about *Karenia* biology, such as how fast the cells can multiply and swim and what nutrients they need. The current challenge is to understand what fuels the transition to the bloom stage, the explosive growth that follows and the bloom's ultimate demise.

Normally, *Karenia* are found in concentrations of about 1,000 cells per litre of water. Once the concentration hits 5,000 cells per litre, shellfish can become so contaminated with the toxins produced by the algae that they become off-limits for collecting and eating. A bad red tide can mean millions of cells per litre.

Where the nutrients come from to sustain such a massive bloom, especially the nitrogen that usually limits *Karenia*'s growth, is one major unknown. The alga is unusual in that it can use organic and inorganic forms of nitrogen, expanding the number of potential sources.

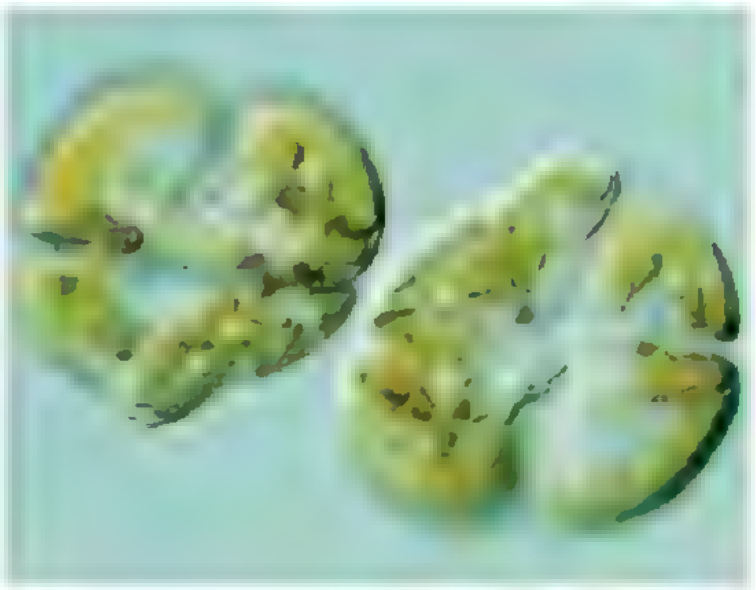

Karenia brevis can photosynthesize like a plant, yet moves like an animal.

FISH WILDLIFE CONSERV.COM

Several possible explanations are being investigated, and more than one of the possible nutrient sources could have significant roles. One idea is that dust carried from Africa by winds contributes iron, stimulating the growth of the bacterium *Trichodesmium*, which in turn converts atmospheric nitrogen into more bioavailable forms that support *Karenia*[1]. A more recent hypothesis is that nutrients from the Mississippi River drive cycles of plankton growth and nutrient recycling that, under the right wind and current conditions, eventually carry nutrients to the West Florida Shelf[2]. Still another idea, supported by some initial hindcasting work, is that the early stages of a bloom might be fuelled by bacteria such as *Trichodesmium*; then, as *Karenia* proliferates, the fish it kills start to decompose, producing new nutrients to fuel the bloom[3]. "We do have testable hypotheses," says Weisberg, "but like any other complex problem in nature, every time we think we understand red tide it surprises us."

> "Every time we think we understand red tide it surprises us."
> — Bob Weisberg

Nutrient pollutants

Perhaps the most contentious explanation has been the idea that run-off from land is a major contributor to algal blooms. In Florida, one important source could be the nutrient-rich water that at times pours out of the Caloosahatchee River into the Gulf of Mexico during heavy rains and when managers release water from the massive Lake Okeechobee inland reservoir as a flood-control measure. Much of this water would once have been filtered by the Florida Everglades, but for decades now, much of it has been diverted via a canal to the river and on to the sea, laden with nutrient pollution from the cities and farms that portions of the Everglades were drained to create. Fully addressing this problem would be a complex and expensive prospect, affecting powerful lobby groups such as developers and sugar farmers. Still, some work is already under way, including the multi-billion-dollar Everglades restoration programme, which could eventually prevent much of the water from being released into the Caloosahatchee, although the work is many years from being completed.

Environmentalists and researchers have charged for years that the state has not adequately examined the potential connections between run-off and algal blooms. As the state's red-tide leader, Heil has been a lightning rod for the dissent, sometimes accused of intentionally playing down a human contribution.

The fact that red tides have occurred in the region for centuries makes it clear that humans don't have to be involved. But some researchers, such as Larry Brand from the University of

M. SCHROPE

Funding for buoys used to monitor the ocean could soon dry up.

Miami, believe strongly that at least some of the time, the nutrients from the Caloosahatchee dramatically exacerbate the problem. Brand and his colleague Angela Compton recently reviewed a database of red tide research since the 1950s and concluded that *Karenia* concentrations have risen about 15-fold[4]. Heil doesn't dismiss the possibility, but says that limitations in the data set, such as sampling bias, hamper interpretation of the data. She becomes visibly shaken when discussing the review, which analysed a data set compiled by Karen Steidinger, her long-time colleague and *Karenia*'s namesake. "It's hard to see her database misinterpreted," says Heil. For his part, Brand says he has yet to see anything to convince him that his analysis wasn't sound.

In work not yet published, Brand has also worked with a physical modeller to conclude that water from the Caloosahatchee could have driven some recent blooms. In other unpublished work, although the calculations are only rough, Brand also says that data he has collected through several years of sampling suggest that at times the amount of nitrogen making it from the river to the sea would be enough to support a bloom.

Lee County, through which the Caloosahatchee flows, has helped fund some of Brand's work, as officials there have been unhappy with the state's level of attention to the topic. The county also supported work by Brand's collaborator Brian Lapointe, from the Harbor Branch Oceanographic Institution in Fort Pierce, to study related ties between Caloosahatchee nutrients and recent massive blooms of red-drift algae that periodically clog beaches in the area[5].

Back in time

Lapointe says that research as far back as the 1950s showed a strong tie between the Caloosahatchee and red-tide blooms[6], but was later ignored. Indeed, a 1962 report for the Army Corps of Engineers[7] refers to the connection as a given. Heil and others say that the older work was set aside in large part because it was conducted before the view emerged that the red tides initiate 20–60 kilometres offshore — rather than around the river mouths, as was thought at the time. Brand argues that that is essentially a moot point in terms of managing the problem. "The Caloosahatchee is not causing the blooms, so to speak," he says, "but if we dump more nutrients in, then whenever conditions are right for a red tide [the nutrients] make it worse." Heil allows that coastal inputs may indeed promote blooms. "Some are natural probably, and some are not," she says. Her main argument, for which she has been criticized, is that there simply aren't enough data to settle the question.

At one point, the local branch of the environmental group the Sierra Club considered filing a lawsuit against the state to try to force more research into the purported link between run-off and red tides, but has since decided not to. "We have moved past those points of real serious contention on those issues — we have a much more collaborative relationship now," says Stuart Decew, the club's red-tide campaign leader. "Although we could still do a great deal more to fully answer questions the public is asking."

Decew says encouraging recent developments include nearly $5 million in new funding on the nutrient issue from the National Oceanic and Atmospheric Administration, and a comprehensive Florida red-tide review released last August by a new Marine Policy Institute at the Mote Marine Laboratory[8]. Among many conclusions and recommendations, the report acknowledged the extreme difficulty of reliably pinpointing the nutrient sources for blooms, but suggests that available data warrant action to reduce nutrient inputs.

Weisberg laments that red tide research isn't further along, which he believes is at least partly due to state- and federal-level funding and research decisions being driven more by politics than by a comprehensive, science-based plan. "I think we can proceed with a lot more speed and efficiency if the agencies kind of changed their ways," he says. "I don't know how to say that nicely. The problem is not just here, but everywhere around the United States."

Heil has high hopes for what will be accomplished in the coming years. "We're at that stage where we're progressing fairly rapidly," she says, "and [the Center for Prediction of Red Tides] is the first step in trying to transition all these research products to management." Although unravelling the factors that drive the blooms, and putting technologies in place to monitor them better, pose significant challenges, she and Weisberg are optimistic that the work will lead to the ability to forecast the rise and fall of blooms, long before the fishermen see their baitfish doing death spins. "That's where we're heading," says Weisberg. "It may take a while to get there, but this is the starting point." ■

"Forecasting gives us huge benefits." — Cindy Heil

Mark Schrope is a freelance writer on Florida's east coast who wheezed this winter through a red tide.

1. Mulholland, M. R., Bernhardt, P. W., Heil, C. A., Bronk, D. A. & O'Neil, J. M. *Limnol. Oceanogr.* **51**, 1762–1776 (2006)
2. Stumpf, R. P., Taker, R. W., Lanerolle, L. & Tester, P. A. *Cont. Shelf Res.* **28**, 189–213 (2008)
3. Walsh, J. J. *et al. J. Geophys. Res.* **111**, C11003 (2006)
4. Brand, L. E. & Compton, A. *Harmful Algae* **6**, 232–252 (2007)
5. Lapointe, B. E. & Bedford, B. J. *Harmful Algae* **6**, 421–437 (2007)
6. Slobodkin, L. B. *J. Mar. Res.* **12**, 148–155 (1953)
7. *A Report to the District Engineer, Jacksonville District, US Army Corps of Engineers* Ser. no. 33 (1962)
8. Alcock, F. *Mote Marine Lab. Tech. Rep.* 1190 (Mote, FL, 2007)

Chemistry podcast from nature

Fourth chemistry podcast now live

In the January/February 2008 show, we find out how DNA is helping researchers build crystals out of nanoparticles, discover a clever chemical trick for manipulating uranium, explore the controversial field of DNA conductivity and talk to chemist Bruce Gibb about re-building life and lab after hurricane Katrina.

Free to download, listen to it today!

www.nature.com/chemistry/podcast

Sponsored by

SIGMA-ALDRICH

nature publishing group

Who stands to lose from double-blind review?

SIR — Why do journals expect scientists to use double-blind methods in their research, but refuse to apply a double-blind approach in evaluating that same research? The Editorial 'Working double-blind' (*Nature* **451**, 605–606; 2008) addresses this long-standing puzzle, arguing in defence of the current system of single-blind review.

This echoes the attitude of most journals over the years. The reasons offered in support of this stance have gradually mutated with time — from the burden of removing author names, through the inefficiency of masking author identity, to the potential downsides of author anonymity. The underlying attitude has remained fundamentally unchanged.

This makes me wonder whether the invariable position of leading journals on double-blind review may in fact be the result of an invariable reason, the mention of which is consistently avoided. To venture a guess: could that reason be pressure from prominent members of the research community who are opposed to a system in which they cannot fully rely on the benefits of their reputation?

Boyan K. Garvalov
Max Planck Institute of Neurobiology, Am Klopferspitz 18, 82152 Martinsried, Germany

Double-blind review: the paw print is a giveaway

SIR — In your Editorial 'Working double-blind' (*Nature* **451**, 605–606; 2008), you suggest that authors may be vulnerable to bias if referees guess their identities — for example, bias about their previous work, their gender, their nationality or their being new to a field. A high reputation could inhibit impartial assessment, although this bias is more likely to disarm than antagonize a reviewer.

The days when the gender or the nationality of a scientist could always be ascertained by her/his name are long gone; for example, try guessing my gender or nationality. I have met people from a non-European background who thought that the French name Jean-Marie was a female name.

An author (or an entire team) embarking on a new area of research is easily spotted: the bibliography will contain no or few references to previous works by the author(s) of the paper under review. Scientists who frequently refer to their own work are readily identified; one does not have to be a Newton to be recognized by one's paw prints (*Nature* **333**, 592; 1988). Double-blinding will not curb excessive self-citation because those who succumb to vanity know that they will be recognized anyway.

Regarding the open sharing of information, readers of a paper could benefit not just from the published paper, but also from the referees' reports if these were pithy and incisive.

Once upon a time, some journals appended to each paper the comments and the names of the reviewers. How about adopting this as an alternative to double-blind review, and rewarding scholars for all their contributions, original as well as critical?

K. Razi Naqvi
Department of Physics, Norwegian University of Science and Technology, N-7491 Trondheim, Norway

Double-blind review: easy to guess in specialist fields

SIR — I work in a field, replicon dynamics in microbes, in which the cooperation-to-competition ratio is, I would guess, relatively high. Subject, technique, citation habits and writing style would subvert more than 80% of attempts to conceal author identity, just as authors guess referee identity correctly in about 50% of cases. I doubt whether double-blinding, as discussed in your Editorial 'Working double-blind' (*Nature* **451**, 605–606; 2008), would be worth doing in such a situation.

Is it really just at the journal–reviewer interface where reputation works most insidiously? One hears of big names stamping their foot over the telephone to intimidate editors into acceptance. Even if such tactics are occasionally tried, author–editor anonymity is too impracticable to consider as a corrective measure.

David Lane
Laboratoire de microbiologie et génétique moléculaires, CNRS bât. IBCG, 118 route de Narbonne, 31062 Toulouse, France

Double-blind review: let diversity reign

SIR — The aim of blinding in peer-review is to improve the quality of reviews by removing any bias that might arise from knowing the identity of the authors. As your Editorial 'Working double-blind' (*Nature* **451**, 605–606; 2008) acknowledges, reviewing is not genuinely blind. You cite a study in which blinded reviewers identified at least one author on some 40% of papers (M. K. Cho *et al. J. Am. Med. Assoc.* **280**, 243–245; 1998). The recognizable authors were presumably well-known, and anecdotally, these are the authors favoured by single-blinding. So the effect of double-blinding may be to increase the bias towards well-known researchers.

We need definitive data on this score. Meanwhile, journals are plentiful and varied and (although most use single blinding) they offer a choice from totally open to double-blind reviewing. Switching to a different practice might help some journals to attract good manuscripts from scientists influenced by the type of review process.

Diversity is rated highly in ecology and economists lecture us about the benefits of free markets. Why not apply the same norms to the way we decide which papers to publish?

Bob O'Hara
Department of Mathematics and Statistics, PO Box 68 (Gustaf Hällströmin katu 2b), FIN-00014 University of Helsinki, Finland

Readers' comments on double-blinding are welcomed at http://tinyurl.com/2bzmvj.

Tibet's seeds must be stored as climate changes

SIR — The Tibet–Qinghai plateau is an area where climate change may have huge effects as glaciers retreat, leading to large decreases in water supply in the mega-rivers of India, southeast Asia and China by the middle of the century. For the 6,000 or more species of higher plants, including the widely admired Himalayan alpines, the effects will be even more severe as vegetation zones move upwards by several hundred metres. The movement of regions suitable for growth will be followed, not accompanied, by the vegetation suited to them, increasing the risk of extinctions.

In Tibet, few of the practices adopted in many other countries are in place. Although there are 38 nature reserves, covering a third of the country, there are no botanical gardens. The preservation of seeds of Tibetan plants is virtually non-existent. The Millennium Seed Bank at Kew in the United Kingdom stores seed from only three Tibetan species, and China's largest seed bank, the Southwest China Germplasm Bank of Wild Species in the Kunming Institute of Botany, has none.

We and researchers at other institutions are addressing this gap. We hope we'll be in time.

W. John Cram*, Yang Zhong†, Tashi Tersing‡, Jie Cai‖
*China–UK HUST–RRes Genetic Engineering and Genomics Joint Laboratory, Huazhong University of Science and Technology, Wuhan, Hubei 430074, China
†School of Life Sciences and Center for Evolutionary Biology, Fudan University, Shanghai 200433, China
‡Institute of Biodiversity Science and Geobiology, Tibet University, Lhasa 850000, China
‖Millennium Seed Bank Project, Royal Botanic Gardens, Kew, Wakehurst Place, Ardingly, West Sussex RH17 6TN, UK

Duplication: stop favouring applicant with longest list

SIR — The issue discussed in Mounir Errami and Harold Garner's Commentary 'A tale of two citations' (*Nature* **451**, 397–399; 2008) is a real problem, although I don't believe there are more duplicate papers than 10 years ago. This problem will only go away if grants and jobs are no longer given to those with the longest publication record.

Alternatives? Ask applicants to select their best three, five or ten papers.

Martin Fenner
Department of Haematology, Haemostaseology and Oncology, Hannover Medical School, 30625 Hannover, Germany

Duplication spreads the word to a wider audience

SIR — Self plagiarism seems to be an endemic phenomenon in biomedical journals, according to a recent *Nature News* discussion (http://tinyurl.com/2fcnfg) of the Commentary 'A tale of two citations' (*Nature* **451**, 397–399, 2008). Classical examples include redundant publication, duplicate publication and text recycling. But is self plagiarism really a bad thing?

We should try to disseminate scientific knowledge to the largest audience possible in order to help people solve their problems. This principle should be constrained only by legal issues such as copyright — not by ethical norms and/or constraints that violate this humanistic principle.

Some argue that self plagiarism represents ethical misconduct: for example, duplicated data can affect meta-analyses and waste precious publication space. But self plagiarism is currently not a legal issue; it does not meet the US Public Health Service research misconduct standards.

As editor of an international journal, *The Journal of Cognitive and Behavioral Psychotherapies*, I believe that a comprehensive ban on self-plagiarism is a fundamental error.

The reader assumes, unless told otherwise, that the text is written by the author, and that it is novel and accurate. I believe that ethical writing in relation to self plagiarism should be defined by: full disclosure if the new and/or derivative work incorporates text previously published, citing the old work in the new; and ensuring that there is no violation of copyright law.

If duplication of content within these constraints helps the author to reach a new or larger readership, and/or if text recycling within these constraints helps to present the same idea more accurately across several publications, they become legitimate conduct. Efforts to suppress the dissemination of scientific knowledge by overregulation call to mind the Inquisition, which was established to prevent spiritual wrong-doing in the Middle Ages.

Daniel David
Babes-Bolyai University, No. 37 Republicii St, 400015, Cluj-Napoca, Romania

Duplication and plagiarism increasing among students

SIR — Mounir Errami and Harold Garner make the point in their Commentary (*Nature* **451**, 397–399; 2008) that plagiarism in scientific writing is on the increase. Ready access to electronic copy makes it easy to snip out that handy phrase that encapsulates a thought, or that neat introductory paragraph, and then why not the whole section, and so on. We have all been tempted.

Undergraduates regularly expropriate whole articles from Wikipedia. They are not scared by anti-plagiarism software, as they know it is not routinely applied. As today's undergraduates will become tomorrow's researchers, the problem can only get worse.

As a referee who is used to reviewing papers in particular niche areas, I have occasionally identified duplicate or seriously overlapping content in manuscripts, often intended for high profile journals. In one instance, I received almost identical papers for review and in another I received a duplicate of an online pre-publication paper. The authors cannot be named, as that would violate referee confidentiality, but they were from well known institutions in the developed world.

What these duplications had in common (apart from the text!) was that the authors were relatively junior and newly appointed. Younger academics seem to feel under a great deal of pressure to publish. In my own institution, I believe that my younger colleagues place an unhealthy emphasis on impact factor when considering where to publish their work.

How to prevent plagiarism? Journal editors must refuse plagiaristic pieces and explain why. Identification of duplication post-publication should lead to high profile withdrawal of the papers by the journal that was misused. Plagiarism should be identified as a disciplinary offence in the employment contract of academic and research staff.

Brian Derby
School of Materials, University of Manchester, Grosvenor Street, Manchester M1 7HS, UK

Duplication: most cases on database are innocent

SIR — In a super-egotistical response to the Commentary about duplication (*Nature* **451**, 397–399; 2008), I decided to check the Déjà vu database (http://spore.swmed.edu/dejavu) to see whether anybody was copying my data. A search for "Brennan, P." revealed 31 citations, but this came as no surprise, because my name is quite common. However, I was more surprised when I went through the list and found only two significant incidents of plagiarism. This indicates a 93% false-positive rate for genuine duplication on my small sample. The Commentary authors themselves report a false-positive rate of 27%, after manually checking a much larger sample of 2,600 entries.

Some false positives could be excluded with a little effort. Four of the 31 articles were a series — more of a rarity today, but quite common in the past; sometimes the word 'part' appears in the title, so these could be excluded. Seven of the 31 were clinical updates and four were updates of reviews or opinion pieces. However, reviews and clinical trials are indicated in Medline and could probably be excluded from analysis. Clinical updates are often three or more years apart but have similar authors; the Déjà vu database has a 'time lag' field that can help to identify this type of duplication.

Errami and Garner ask whether it is reasonable to publish the same information in different languages, enabling a piece of work to reach different audiences. In terms of promoting good practice in medicine or other fields, local languages are important. These could be excluded within Medline.

Of the remaining articles I uncovered, there were one-off explanations: research on similar and related topics that seemed like duplicates but were, to me, distinct; re-publication of an article with corrections; and one example of an administrative error causing the journal to publish the article twice. One reprint was an homage to classic citation with permission. The Déjà vu database's tagging system is too simple to differentiate all of these contributions.

Paul Brennan
Medical Biochemistry and Immunology, School of Medicine, Cardiff University, Heath Park, Cardiff CF14 4XN, UK

Join in the duplication debate at http://tinyurl.com/2koto4.

BOOKS & ARTS

Physics to Bragg about

The first joint biography of the father and son who developed X-ray crystallography.

William and Lawrence Bragg, Father and Son: The Most Extraordinary Collaboration in Science
by John Jenkin
Oxford University Press: 2007 474 pp. £35

Jeff Hughes

William Bragg and his son Lawrence Bragg shared the Nobel Prize in Physics in 1915 for their joint development of X-ray crystallography. Lawrence was then 25 years old, and remains the youngest scientist to win a Nobel prize. X-ray crystallography transformed molecular structure determination in the physical and biological sciences, and both Braggs went on to long and successful careers in their respective laboratories and as public spokesmen for British science.

Beyond the usual obituaries and reminiscences, surprisingly little has been written about this unusual father–son scientific team. William Bragg is the focus of an affectionate but partial biography by his daughter. In 2004, Graeme Hunter wrote a much more substantial biography of Lawrence Bragg. John Jenkin's new book is the first joint biography of the two men, which puts their work on X-ray crystallography into a familial, as well as a scientific, context.

Born in 1862, William Bragg studied mathematics at the University of Cambridge, UK. In 1885, he was appointed professor of mathematics and physics at the University of Adelaide in Australia, where he became a key member of the nascent intellectual community in South Australia's capital. He married into the colonial élite, and began to establish both a family — Lawrence was born in 1890, Robert Charles in 1892 and Gwendolen Mary in 1907 — and his scientific career.

Williams first research, on radioactivity, brought him into contact with Ernest Rutherford and other luminaries of the new physics. Working in antipodean isolation, Bragg relied on advocates in the European and North American research communities to engage with and promote his work. His controversial 'neutral pair' interpretation of X- and γ-rays involved him in debate in the pages of *Nature* and elsewhere in 1908. This brought him to wider notice and back to Britain. In 1909, he was appointed professor of physics at the University of Leeds, UK, where he continued his research on radiation.

Educated initially under his father's auspices at the University of Adelaide, Lawrence Bragg then studied maths and physics at the University

Professional interactions between Lawrence Bragg (top) and his father (bottom) were often fraught.

TOPFOTO; SCIENCE MUSEUM/SSPL

of Cambridge, UK, followed by research work there in J. J. Thomson's Cavendish Laboratory on the eve of the First World War. During this period, Lawrence and his father drew on work by Max von Laue and others to develop the theory and technique of X-ray diffraction. Their pioneering research on crystal structures, and thereby the Nobel prize, followed. Neither Bragg travelled to Stockholm to collect their prize as both were involved in war research: William worked on submarine detection, Lawrence on sound ranging. They were the lucky ones; Robert Bragg died at Gallipoli in 1915.

The crystallography work is the climax of Jenkin's detailed account of the Braggs' early careers. The bulk of *William and Lawrence Bragg, Father and Son* focuses on the family's life in Australia. Jenkin, himself from Adelaide, has assiduously mined Australian and British archives and gives us a wonderfully rich picture of the Braggs in Adelaide — a useful corrective to later UK-centred accounts. Although only one of the 19 chapters is devoted to the prizewinning collaboration, Jenkin draws on unpublished material to throw some new light on this work.

Despite a slight tendency to romanticize the Braggs, Jenkin deals effectively with the difficulties of being on the geographical margins of a research community and of establishing credibility from a position of intellectual isolation. Brief comparisons with analogous academics working in other fields might have added a broader sense of perspective here. He also opens for debate the issue of relations between father and son over the allocation of credit for X-ray crystallography. Lawrence seems to have felt unjustly treated, and professional and social contacts with his father were often fraught. Again, a comparative study — on the atomic physicists J. J. Thomson and his son George Paget Thomson, for example — might have helped us to get a better sense of the validity of Jenkin's argument.

In 1915, William accepted the professorship of physics at University College, London, from where he hoped to play a more prominent part in national scientific administration. In 1923, he became director of the Royal Institution. There, he oversaw the growth of X-ray crystallographic research and what is now called public engagement until his death in 1942. He was one of the most prominent spokesmen for science in the interwar period, and president of the Royal Society between 1935 and 1940.

Notwithstanding its early brilliance, most of Lawrence's career came after the events described in the book. In 1919, he succeeded Rutherford as professor of physics at the University of Manchester, UK, and created his own research school to study the X-ray crystallography of inorganic molecules. After a brief period as director of the National Physical Laboratory, UK, he again followed Rutherford to become head of the Cavendish Laboratory. There, he encouraged the efflorescence of molecular biology, which led to the elaboration of the structure of DNA in 1953.

Given all this, and his emphasis on the father–son relationship, it is a pity that Jenkin squeezes the entirety of the Braggs' post-1920 careers into two short chapters, and that he chooses to use his brief epilogue to quarrel with Hunter's recent interpretation of Lawrence's relationships with his parents. Perhaps there is scope for a follow-up volume dealing more fully with the Braggs' later careers and the elaboration of Jenkin's views of the darker side of this 'extraordinary collaboration'. ■

Jeff Hughes is senior lecturer at the Centre for the History of Science, Technology and Medicine, University of Manchester, Manchester M13 9PL, UK. He is author of *The Manhattan Project: Big Science and the Atom Bomb*.

Climate change for the masses

The Hot Topic
By Gabrielle Walker and David King
Bloomsbury: 2008. 309 pp. £9.99
Harvest Books. 2008. 288 pp. $14.00

David S. Reay

Two years ago, I wrote in these pages about the need for a book on climate change that could engage millions, equivalent to the forcefulness and accessibility of Rachel Carson's classic *Silent Spring*. Since that time, the Stern Review, the Fourth Assessment Report from the Intergovernmental Panel on Climate Change and Al Gore's *An Inconvenient Truth* have joined the groaning shelves of works about global warming. Public awareness of climate change is soaring, and political parties increasingly vie for the greenest ground. So do we really need yet another mass-market climate-change book? When it is this good, unequivocally yes.

Misinformation and unsupported statements abound on both sides of the debate. Myriad shades of green advice on planet-friendly living compete for our attention with end-is-nigh hyperbole and diatribes from climate sceptics. *The Hot Topic* has an authoritative clarity that scythes through the junk science and brushes aside the brigades of doom-mongers and overly earnest environmentalists.

Its authors — geophysics writer and broadcaster Gabrielle Walker and ex-UK government science adviser David King — have chosen a simple format. They guide the reader systematically through the history of climate science, the projections and uncertainties, the solutions and politics. After an engaging discussion of the greenhouse effect and its discovery, taking in key players such as Joseph Fourier and John Tyndall, they examine the palaeological record and the evidence for human-induced changes in climate.

So far, so unremarkable. These topics are the bread-and-butter of books on climate change and many readers will be familiar with the content. Similarly, the brief chapter on climate-change effects is covered in much more depth in Mark Lynas's recent book *Six Degrees*. It is when Walker and King get into the solutions and politics of climate change that their book really begins to show its pedigree.

First the authors ask: can we actually avoid a 2 °C rise in average global temperature — in other words, dangerous climate change? They think it unlikely, but stress that this figure isn't an all-or-nothing doomsday trigger, and that it is still possible to stabilize greenhouse-gas concentrations in the atmosphere at a level that should avoid the most catastrophic impacts. On how to achieve this, their message is loud and clear: only a concerted global effort that makes use of new and established tools will do.

Walker and King give short thrift to geoengineering proposals, such as injecting clouds of sulphur dioxide into the atmosphere, labelling them dangerous tinkerings that trade one kind of pollution for another. Instead, they draw together an impressive and upbeat portfolio of possible efficiency boosters, renewable energy sources and emerging technologies, such as carbon capture and storage.

They advocate feeding more nuclear power into this mix, urging the reader to consider the arguments carefully. They contend that a new generation of more efficient nuclear power plants would create much less waste, adding just 10% to existing UK levels. But for a country that is already home to 100,000 tonnes of radioactive waste, this additional material would prompt a hefty rise in the cost of long-term storage. Their positive view of the nuclear option also fails to square with their justified scepticism over the pollution-swapping risks of geoengineering.

On climate economics and policy, Walker's writing skills and King's first-hand knowledge make for an informative and accessible package. Their empowering approach leaves no room for despair or inaction. A section on personal solutions necessarily goes over ground that will be familiar to most readers, but adds to the inspirational tone. In truth, I have never enjoyed reading a book on climate change more. The balance of accessible writing and peer-reviewed science — including a myth-busting appendix — should put a skip in the step of even the most jaded climatologist. The search for a climate-change equivalent of *Silent Spring* is over. ■

David S. Reay is a Natural Environment Research Council Fellow in the School of GeoSciences, University of Edinburgh, Crew Building, West Mains Road, Edinburgh EH9 3JN, UK. He is author of *Climate Change Begins at Home*.

D VENNERBECK

Doctoral student Alan Rorie aims to instil 'a sense of wonder and whimsy' through his machine art.

HACKING

Crafters tinker with technology

Krista Zala

A new crafts movement is afoot. Growing numbers of tinkerers are creating custom machines following their own aesthetics. Dabbling with electronics, electrolysis and etching, these contraption-hackers gleefully ignore warranties and dig in, here overhauling a lap-top to achieve a century-old look, or there wiring a pair of contemporary headphones into a gutted antique pair.

Capturing the spirit of the emerging culture, the O'Reilly Emerging Technology Conference that took place this week in San Diego, California, ran sessions on how to make aerial drones and on hacking — beyond gadgets to the body, brain and food. In May, just south of San Francisco, the third annual Maker Faire will bring together craft geeks usually united in cyberspace for a weekend of workshops and tip-swapping.

One subset of these twenty-first century creators looks back to an era when handcrafters designed everyday tools with an elegant flourish. For example, using old gas-lamp arms and chime levers scrounged from a grandfather clock, Sean Slattery, the computer guy at a chemical research and development company in Burlington, Massachusetts, retooled his keyboard and flat-screen monitor to imbue it with vintage Victorian style. "Steampunk is a general rejection of the sameness that globalization is bringing to the world," says Slattery (or Hieronymus Isambard Jake von Slatt, as he is known in steampunk circles)

"Steampunk is to science what civil war re-enactions are to history," Slattery explains. The people involved — many of them scientists and engineers — are interested in learning about the history of science. They do so by re-creation, converting electrical lamps to kerosene or fashioning telegraph sounders to tap out web content updates. Their engagement thus becomes personal, tactile and satisfying.

The trend emerged in the 1970s and 1980s as a subgenre of science fiction, which set Victorian characters amid today's technology or in a parallel future universe, where analogue triumphed over digital and the airship prevailed over the aeroplane. The fantastical sensibilities spread from literature into film and video games across Europe, Japan and the United States. The past few years have even seen steampunk pervade fashion and music. The style plays with the parallels between the Industrial Revolution and the Information Revolution — both eras of intense technological and social change. Now part of the wider culture of uploading, downloading, copying, pasting, swapping and re-ordering the world, steampunk applies the philosophy of open-source software to hardware.

"Steampunk is to science what civil war re-enactions are to history."

Aficionados combine an appreciation of good simple engineering, as embodied by the steam engine, with the 'do it your way' ethos of punk. Steampunk aesthetics, in contrast with the hidden mechanisms and functions of today's gadgets, expose and celebrate intricate machine workings. That said, the builders happily draft plans using modern software and materials

Tinkering has always been a key way into science. Inquisitive minds bent on learning how the world works have long gone at it with a screwdriver first. Now teachers are enhancing their lessons on electrolysis using Slattery's etchings on confectionery tins and iPods.

For purists, "it's not really steampunk unless it has a steam engine attached to it", says Sean Orlando, artistic director of the Steampunk Tree House, the interactive sculpture installed last year at the Burning Man arts festival in Nevada. The nine-metre-tall tree fashioned from steel pipes, I-beams and an 8,000-kilogram steam engine took five hours to generate the power to run a steam organ; its lights were powered by a solar array.

In San Francisco, the eighth annual Edwardian Ball Weekend this January showcased boiler-powered antique engines. A horizontal engine drove a novelty 'time machine' designed and built by Alan Rorie, a neurobiology doctoral student at Stanford University, California. The 'dihemispheric chronaether agitator' (pictured) is a polished copper sphere, the size of a desk globe, the hemispheres of which spin in opposing directions around a system of gears.

"I want to create interactive art that communicates science to people," says Rorie. Scientists physically experience the world to gain an understanding of systems, he explains, but share only the facts that they find, which deprives their audience of the feel of research. He aims to instill "a sense of wonder and whimsy" with his artwork. His next project is an interactive neuron to teach people about receptive fields. ■

Krista Zala is a science writer based in Victoria, Canada.

HACKING

Home cooking with a twist

Jascha Hoffman

"I think of cooking as hacking," says Californian computer programmer Marc Powell, who led a 'Kitchen Hack Lab' demonstration at the O'Reilly Emerging Technology Conference in San Diego this week.

In the kitchen, we're all amateur chemists. Protein, carbohydrate, fat and water react to changes in pressure and temperature during cooking. Just as a hardware hacker adapts an electronic device to a new purpose, a food hacker recombines ingredients in unconventional ways.

Powell wants to bring "the red-headed stepchild of molecular gastronomy" to the masses. At Unicorn Precinct XIII in San Francisco, he hosts a 'collaborative supper club'. Guests can sample blood ice cream, chocolate monkfish

liver and savoury bubble tea with squid ink tapioca pearls (http://up13.org).

A chemical logic underpins Powell's odd blend of ingredients: one batch of gumdrops used raspberry, rum and ant venom because they all contain derivatives of formic acid, which has a strong, tangy taste.

After the dot-com bust, Powell trained in the kitchen of Heston Blumenthal, head chef of The Fat Duck in Berkshire, UK. Blumenthal founded his own research laboratory to refine such culinary techniques as sous vide, or slow cooking in vacuum-sealed bags. In recent years, a handful of molecular chefs — including Ferrán Adria at Spain's El Bulli and Homaru Cantu at Moto in Chicago, Illinois — have used liquid nitrogen, lasers and inkjet printers to expand the range of possible flavours and textures.

Ultramodern kitchen experimentation has largely bypassed the amateur because of the high cost of equipment, such as rotary evaporators or an 'anti griddle' that chills to –34 °C. But vacuum-sealers and smoking guns are relatively cheap and, as food scientists such as Harold McGee and Hervé This have shown, there is also room for innovation using standard ingredients and appliances.

What sets Powell apart is his home-grown approach. He invites strangers to bring their own ingredients into his kitchen and hack alongside him. "I think food cooked at home is always better than what's cooked in a restaurant," he says.

Plus, unlike many restaurant chefs who keep their recipes secret, Powell encourages 'open-source recipe development' (http://wiki.foodhacking.com). For when inspiration fails, his website program (http://deliciouscorpse.com) generates random recipes — such as 'grub-injected wasp caviar with salt-baked spider bun' — that can be tailored to the contents of your larder.

It remains to be seen whether the invention of such new dishes, as the French epicure Jean-Anthelme Brillat-Savarin wrote in 1825, "does more for human happiness than the discovery of a new star." ■

Jascha Hoffman is a writer based in New York.

HACKING

Toys, bugs and rock 'n' roll

Joanne Baker

"I like listening to insects," says Thomas Truax. A nominee for Britain's 2008 Indy Music Award for best live act, Truax is making a name for himself by building his own instruments from gramophone horns and pull-string toys. He sings about ants, the ozone layer, the Internet and dogs howling at the Moon.

Truax grew up in Colorado and became fascinated with insect sounds. "I was at a camp in the jungle in Mexico and I heard this insect that sounded like a Volkswagen that couldn't get started," he says. Truax explains how he also records bat chirps near his home in London, editing them to make sample loops.

One of Truax's songs tells the story of an injured butterfly that has escaped being pinned to a specimen board by an entomologist. To evoke the sound of its wings, he plays the guitar with a hand held rotary fan, creating fluttering arpeggios. To avoid working with difficult musicians, Truax builds and plays his own instruments, such as a drum machine crafted from spinning fly-wheels and tiny cymbals.

Other instruments are created from reclaimed junk. Truax is inspired by toys and simple experiments, such as the two-way 'telephones' kids make from string and paper cups. On stage, he sings down a gramophone horn that is wired up with a Slinky to distort his voice, or he amplifies the percussion of clockwork and the vibrations of a single string held taut by an audience member. "I want to make people think about what music is," he says.

"We are at a point in history where computers can do so much but people are losing touch with tactile things," he says. If electronic instruments and digital editing are depersonalizing sound, Truax is making his own noise. ■

Joanne Baker is *Nature*'s Books & Arts editor.

Thomas Truax's single *Stranger On A Train* is out on SL Records (UK) on 31 March, and will be online from 14 April (www.thomastruax.com).

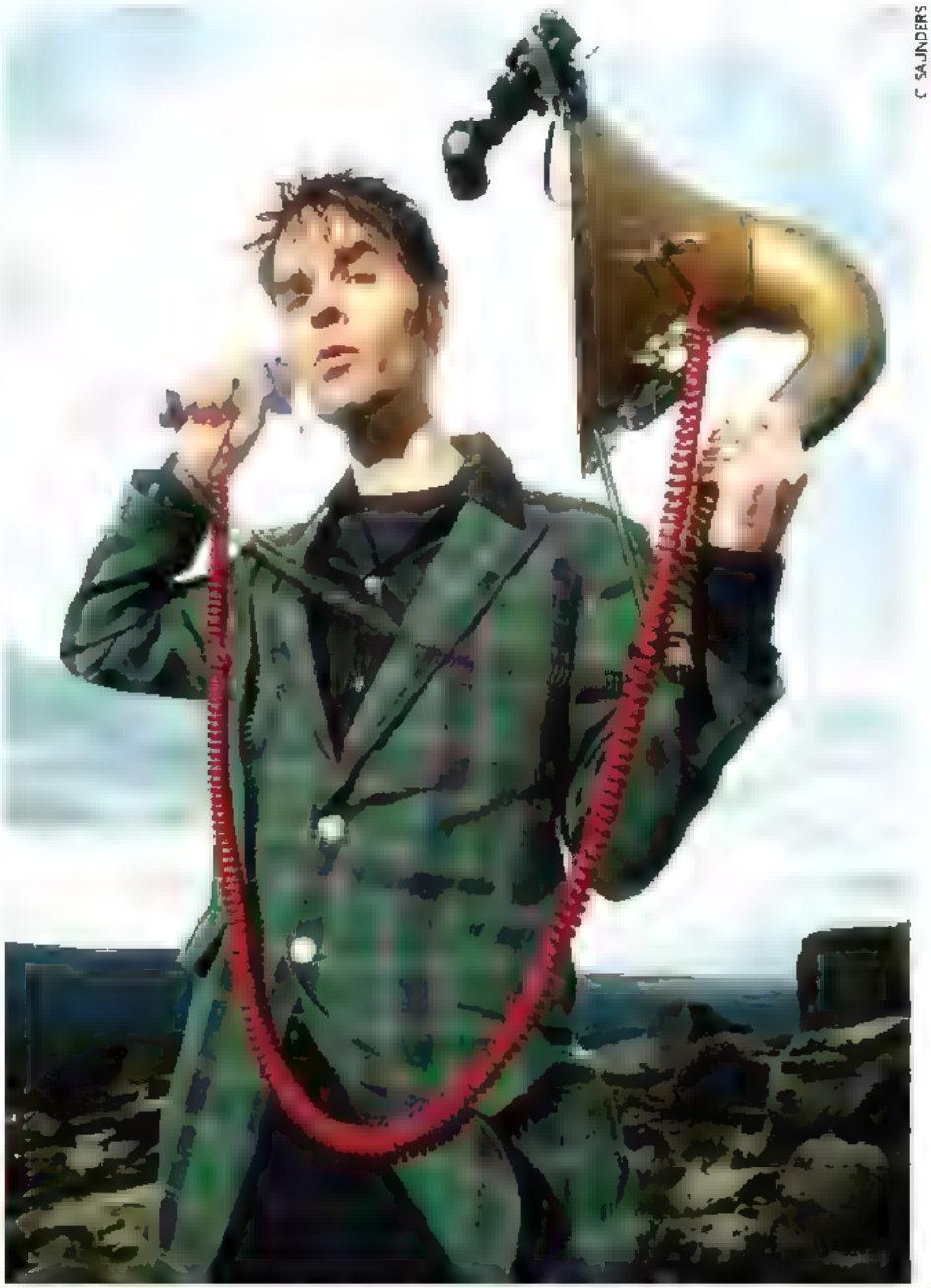

© SAUNDERS

Thomas Truax crafts instruments from junk to create a new sound inspired by insect noises.

IN RETROSPECT

The book that began invasion ecology

Charles Elton's 50-year-old text founded a field and is now cited more than ever.

The Ecology of Invasions by Animals and Plants
by Charles S. Elton
Methuen. 1958. 181 pp

Anthony Ricciardi and Hugh J. MacIsaac

Human activities have introduced alien animals, plants and microbes to all but the remotest regions of Earth. These biological invasions threaten ecosystems, economies and human health, and are the focus of a highly productive subdiscipline of ecology, the origin of which can be traced to a book that was published 50 years ago.

The Ecology of Invasions by Animals and Plants by British ecologist Charles S. Elton is, remarkably, not a scientific treatise or an academic text, but an expansion of a short series of BBC radio broadcasts aimed at the public. At the time, Elton was the most influential figure in animal ecology, having pioneered studies on population dynamics and food chains. He was particularly interested in what he called "ecological explosions" — enormous, uncontrolled increases in population.

Previously, ecologists had treated invasions as anomalies. Elton characterized them as being symptomatic of a process that could alter the biological landscape of the planet. "We are seeing one of the great historical convulsions of the world's fauna and flora," he wrote. In an effort to move the study of invasions beyond natural historical accounts, Elton produced testable generalizations drawing from disparate disciplines, including biogeography, epidemiology and human history. He also identified large-scale patterns, such as the higher number of invaders in temperate regions compared with tropical regions, and on islands versus mainland areas of equivalent size (both recently verified by statistical analyses).

Most importantly, Elton demonstrated the profound influence of human activities in reshaping species distributions. For example, decades before other scientists began to focus on the spread of invading alien aquatic species, Elton drew attention to the transport of organisms in ships' ballast tanks, the intercontinental movement of oysters and their associated flora and fauna, and the role of canals in linking regions formerly isolated from each other for millions of years.

Many of the concepts raised in *The Ecology of Invasions by Animals and Plants* have flourished into important research themes that continue to be vigorously debated. Most notable of these is the 'biotic resistance' hypothesis: that species-rich communities

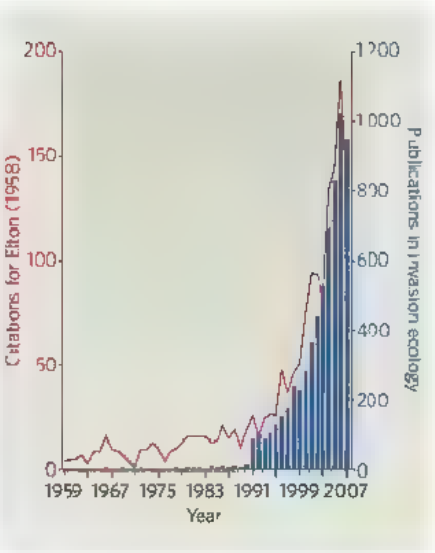

DATA FROM THOMSON SCIENTIFIC WEB OF SCIENCE

are more resistant to invasion. Elton proposed that diverse communities use resources more fully, leaving fewer niches for potential colonists to exploit. Recent studies have found that invaders in small, species-rich areas do indeed fare worse than those in areas of low biodiversity. But the pattern often reverses over large areas, apparently driven by external environmental conditions that affect native and alien species alike.

Elton also argued that complex food webs are likely to contain predators or parasites that can control invaders, whereas simpler food webs are more vulnerable to population explosions. As evidence, he pointed to the disproportionate numbers of invaders in environments such as remote islands and boreal forests, and those on cultivated land and in other environments that have been drastically simplified by human disturbance. These ideas have had a huge influence on subsequent ecological research into the link between a community's diversity and its stability. Elton further suggested that many species are invasive because they arrive in areas without their natural enemies, another controversial hypothesis that has generated many recent studies. His book is cited by more than 40% of published papers that address biotic resistance, enemy release or diversity–stability, according to Thomson Scientific's Web of Science.

Elton demonstrated the key role that some invasions have had in the reduction and extinction of native populations — an effect that became widely recognized only in the 1980s. "The eventual state of the biological world will become not more complex but simpler and poorer," he wrote. "Instead of six continental realms of life ... there will only be one world." This stark prediction may have inspired yet another current research theme: the consequences of the replacement of unique assemblages of plants and animals by widespread alien species that coexist with humans, such as rats, starlings and carp.

Half a century on, invasion ecology has progressed well-beyond the scope of Elton's book. Several topics that are now crucial to our current understanding were overlooked or only touched on by Elton. These include: the number of introductions or individuals a population requires to become established; the evolutionary effects of invasions; and interactions among alien species that enhance each other's success. Commerce in agriculture, aquaculture, ornamental plants and pets has opened up the world to thousands of potential invaders, often aided by rapid unregulated trade through the Internet. The release of genetically modified organisms has added another dimension. To try to predict invasions, researchers are examining traits that predispose species to interface with and survive transport by humans. Invasion ecology has had to embrace risk analysis, resource economics, computer modelling and molecular genetics.

Yet Elton's influence on the field continues to grow. The citation rate of his book (pictured, red line) has risen dramatically since the early 1990s after a time lag of some 30 years (a rise that, incidentally, could be compared to the exponential population explosion of an alien species). Why did the surge in journal publications in this discipline take so long to occur? Perhaps a few devastating and well-documented invasions lit the fuse that Elton laid down years before — such as those involving the Nile perch in Lake Victoria, the 'killer alga' *Caulerpa taxifolia* in the Mediterranean and the zebra mussel in North America. Perhaps the interest in biodiversity in the 1980s — the 'conservation of variety' that Elton stridently advocated — brought broader recognition to invasions as a major cause of extinction.

Or perhaps the delay illustrates how far ahead of its time *The Ecology of Invasions by Animals and Plants* was. Elton died in 1991, just as the field he founded began to flourish (pictured, blue bars). His book sounded an early warning that, having gone largely unheeded for three decades, has become a clarion call that resonates in the work of invasion ecologists worldwide. ■

Anthony Ricciardi is an associate professor at the Redpath Museum, McGill University, Montreal, Quebec, Canada H3A 2K6. Hugh J. MacIsaac is a professor at the Great Lakes Institute for Environmental Research, University of Windsor, Ontario, Canada N9B 3P4.

Supplier **Showcase**

nature REVIEWS IMMUNOLOGY

Focus on Allergy and asthma, March 2008

Respiratory disorders, including allergies, asthma and chronic obstructive pulmonary d sease (COPD), are a major public health burden worldwide. The latest WHO statistics (2007) estimate that 300 million people worldwide have asthma, 210 million people have COPD, and millions of people are affected by allergies. Each year, 250,000 people die of asthma. The prevalence of these diseases is increasing, and there is a continued need for new and improved therapies.

This Focus issue of *Nature Reviews Immunology* highlights the latest advances in our understanding of the immune bases of these respiratory diseases and how this knowledge can be translated into effective treatment strategies.

The Focus includes the following Review articles by leaders in the field:

Immunology of asthma and chronic obstructive pulmonary disease
Peter J. Barnes

Treatment strategies for allergy and asthma
Stephen T. Holgate and Riccardo Polosa

Discovering susceptibility genes for asthma and allergy
Donata Vercelli

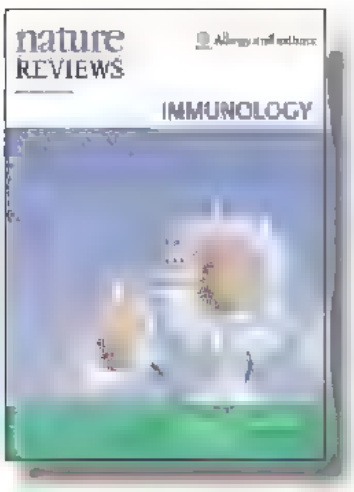

These Reviews and other Focus articles will be freely available online for the month of March at:

www.nature.com/reviews/immunol

NEWS & VIEWS

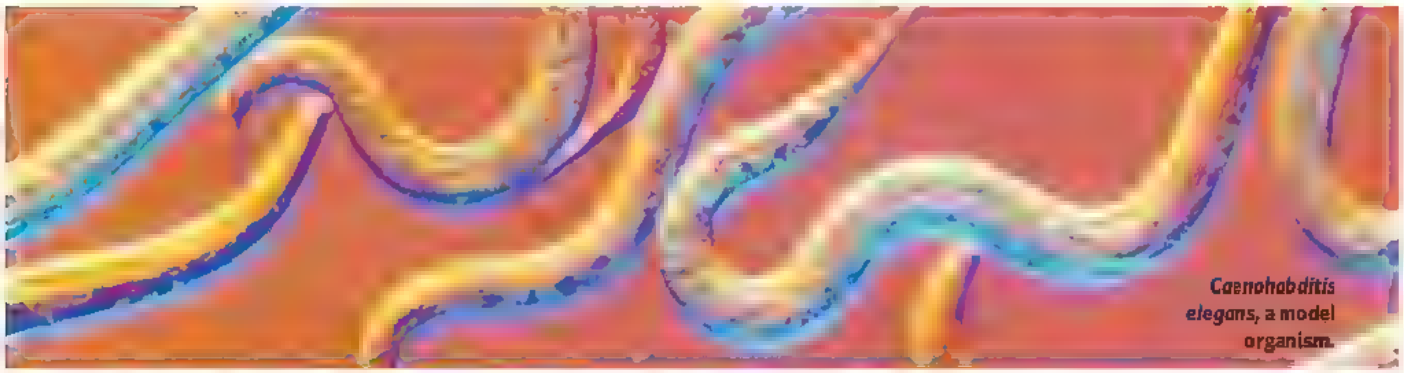

S STAMMERS/SPL

Caenorhabditis elegans, a model organism.

PHYSIOLOGY

Keeping it regular with protons

Laura M. Prolo & Miriam B. Goodman

Muscle coordination is mostly governed by motor programs built into the nervous system. But one program — the defecation cycle in a worm — has a mechanism that avoids nerves completely and uses protons as signals.

For athletes in a race, the crack of the starters pistol signals an intense burst of physical effort and mental concentration — but at least they don't have to think about coordinating their legs. After the initial impulse from the brain to start running, limb control is mostly unconscious, governed by a motor program in which motor neurons direct muscle fibres to contract in the right sequence. But a simple roundworm, *Caenorhabditis elegans*, is forcing us to question our neurocentric view of motor programs. In this animal, a rhythmic series of muscle contractions during another motor program, the defecation cycle, is initiated without the influence of neurons. Two reports now shed fresh light on this vital behaviour. Reporting in *Cell*, Beg *et al.*[1] show that intestinal cells dictate muscle contraction using an unusual chemical signal: the lowly proton. In *Current Biology*, Pfeiffer *et al.*[2] show that protons enter intestinal cells from the lumen of the intestine, driven by a proton-concentration gradient across the cell membrane.

Caenorhabditis elegans is an excellent organism in which to study the genetic basis of motor programs. Its defecation cycle consists of a three-step pattern of muscle contractions that moves food along the worm's digestive tract, culminating in the expulsion of waste. The three steps — muscle contractions in the tail (posterior), head (anterior) and anus — are independent of one another, as gene defects can disrupt one step while leaving the other two intact. The cycle repeats every 50 seconds with striking precision, and the clock that controls its timing runs even when the motor program shuts off in the absence of food[3].

In 1999, a remarkable discovery was made about this most humble of processes: the muscle contractions correlate with the release of calcium ions in the intestinal cells, with ion concentrations fluctuating with the same 50-second period as the defecation cycle[4]. This suggests that the intestine is the timekeeper of the defecation cycle. Accepted dogma would predict that the intestine must signal to neurons (using chemical signals known as neurotransmitters) to control the resulting muscle contraction. But neither typical neurotransmitters, nor proteins that regulate their release, were required. Most surprisingly of all, not even neurons were needed for posterior muscle contractions, suggesting that a previously unknown mechanism of muscle control was in operation.

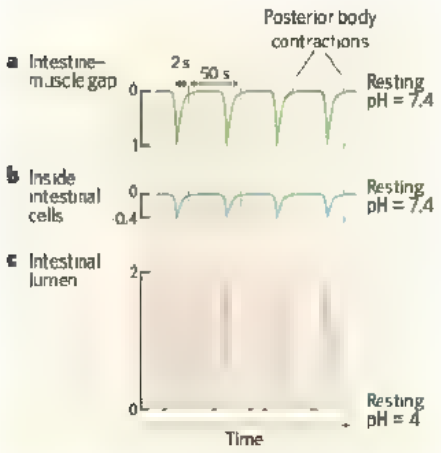

Figure 1 | Proton concentrations and worm defecation. In *C. elegans*, the defecation cycle consists of a precise pattern of posterior and anterior muscle contractions, culminating in expulsion of waste. Pfeiffer *et al.*[2] measured the change in pH in the intestine–muscle gap (**a**), inside intestinal cells (**b**) and in the intestinal lumen (**c**) during the defecation cycle. Drops in pH indicate a transient increase in proton concentration, whereas peaks in pH indicate transient falls in proton concentration. The changes in pH correlate with pulses of protons that trigger muscle contraction. Beg *et al.*[1] show that the proton pulses in the intestine–muscle junction precede posterior body muscle contraction by about 2 seconds.

Beg *et al.*[1] set out to discover how a biological clock in the intestines can control a rhythmic motor pattern without help from the nervous system. Their entry point was provided by two genes, *pbo-4* (also known as *nhx-7*) and *pbo-5*, that are specifically required for posterior body contraction. The PBO-4 protein is one of nine in *C. elegans* predicted to catalyse the exchange of sodium ions for protons (which are hydrogen ions, H^+) across cell membranes. The authors found that PBO-4 is expressed in epithelial cells that form the posterior intestine; specifically, they found it in the membrane facing the body-wall muscle. This raised the question of whether such cells control muscle contraction directly — perhaps by harnessing PBO-4 to release protons, which could then serve as transmitters that initiate contraction of nearby posterior muscles.

To test this idea directly, Beg *et al.* engineered a fluorescent, pH-sensitive PBO-4 protein and used *in vivo* optical imaging to show that a transient decrease in pH outside the cells

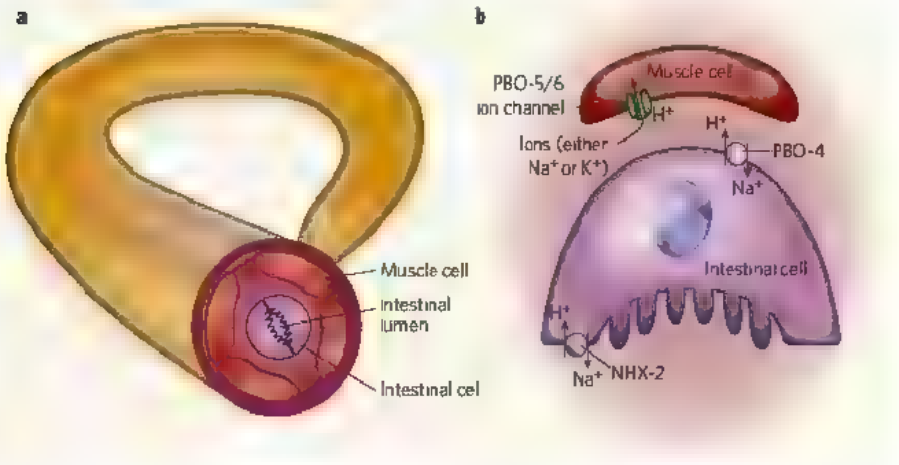

Figure 2 | Communication between cells in a worm's defecation cycle. **a**, Cross-section of the posterior section of *C. elegans* showing the arrangement of body wall muscles and the intestine. **b**, Unlike other known rhythmic motor programs, which are controlled by signals from neurons, the defecation cycle in *C. elegans* involves direct communication between the intestine and adjacent muscle cells. Beg *et al.*[1] show that the PBO-4 protein is expressed on the part of the intestinal cell membrane that faces muscle cells in the worm's body wall. PBO-4 exchanges protons (H^+) in the cell for sodium ions (Na^+) in the space between the intestinal and muscle cells. The released protons act as chemical signals, activating ion channels (formed from PBO-5 and PBO-6 proteins) on the surface of muscle cells. This activation might lead to muscle contraction. Another sodium–proton exchanger, NHX-2, is expressed in the part of the intestinal cell membrane that faces the intestinal lumen. Pfeiffer *et al.*[2] show that NHX-2 allows protons to enter the cell just before muscle contraction.

precedes muscle contraction. pH is a measure of proton concentration, with low pH indicating high proton concentration and vice versa. Beg and colleagues' results thus showed that each posterior body contraction is heralded by the release of a pulse of protons into the gap between the intestine and muscle (Fig. 1). Pfeiffer *et al.*[2] observed something similar using a different protein. Significantly, Beg *et al.*[1] were able to induce muscle contraction in the absence of PBO-4 simply by exposing the muscle cells to artificial proton pulses.

Pfeiffer and colleagues[2] investigated the source of the protons by monitoring the pH of three compartments: inside the intestinal lumen, inside intestinal cells, and in the gap between the intestine and muscle. They found that, between posterior body contractions, protons are 1,000-fold more concentrated in the intestinal lumen than they are in the cells. But just before contractions, the concentration of protons in the lumen decreases, whereas that in the cells increases (Fig. 1). This suggests that protons are transported from the lumen to the intestine–muscle junction via the intestinal cell (a process called transcellular transport), giving rise to muscle contraction.

To test this idea, Pfeiffer *et al.*[2] used RNA interference to reduce the expression of NHX-2 — a sodium–proton exchanger found in intestinal cells (specifically, in the membrane that faces the intestinal lumen). Surprisingly, this didn't reduce the number of protons released into the intestine–muscle junction or eliminate posterior body contractions. Instead, it reduced the size of proton pulses inside the cells and increased the period of both the defecation cycle and the intracellular calcium-ion pulses. NHX-2 therefore seems to be critical for timekeeping, but not necessary for PBO-4-dependent proton release. The next steps will be to discover which proteins set up and maintain such steep proton gradients, and how the loss of NHX-2 regulates the defecation-cycle period.

So how do protons activate muscles? Again, genetic analysis provides the necessary insight, in the guise of a candidate proton receptor: the PBO-5 protein, which is expressed in posterior muscle cells. Beg *et al.*[1] analysed *C. elegans pbo-5* mutants, and found that the worms no longer underwent posterior body contraction during the defecation cycle. This is consistent with the idea that PBO-5 is required for muscles to recognize the PBO-4-dependent proton signal. The *pbo-5* mutants were also unresponsive to artificial proton pulses, unlike worms that lacked the mutation.

When Beg and colleagues[1] co-expressed PBO-5 with PBO-6, a closely related protein, in cells *in vitro*, the proteins formed channels through the cell membranes that open in response to protons. The researchers found that these channels are needed for the defecation cycle. It remains unclear how PBO-4-dependent proton signals are terminated. Perhaps protons simply diffuse away from the intestinal–muscle junction, or are actively transported into the intestine or muscle.

The picture emerging from these studies[1,2] is that some epithelial cells harness transcellular proton transport and sodium–proton exchangers to release pulses of protons; the variations in proton concentration then activate muscle contraction using a proton-gated ion channel (Fig. 2). Such signalling is linked to the calcium-ion release in intestinal cells that keeps time during the defecation cycles, as mutations that alter the period of the calcium-ion pulses also affect the period of intracellular proton pulses in parallel[2]. The next crucial step will be to determine whether the bursts of calcium ions observed inside intestinal cells correlate with the proton release outside the cells. Are the calcium pulses alone enough to trigger proton release, or is another factor required?

Other questions remain. Do calcium ions directly regulate PBO-4 activity? Possibly, as PBO-4 contains several putative calcium-dependent regulation sites whose functions are yet to be examined. There might also be an indirect link: changes in calcium-ion concentrations could drive changes in cytoplasmic sodium-ion concentrations, these, in turn, could determine whether PBO-4 releases protons or retrieves them from the surrounding environment. In support of this idea, mutations in the *flr-1* gene (which encodes an epithelial sodium channel) double the speed of the defecation cycle[3]. Whether the link is direct or indirect, these studies[1,2] suggest that exchangers in the cell membrane may have more widespread roles in communication between cells than was previously believed[6].

An open question now is whether protons function as transmitters more generally. Rapid changes in proton concentrations have been reported in mammalian brain slices[7], and protons packaged into synaptic vesicles — spherical structures that release packets of neurotransmitters from neurons — have long been proposed to serve as neuromodulators. Beg and colleagues' work[1] suggests that sodium–proton exchangers, which are widely expressed in mammalian brains, could be an alternative or complementary source of protons. Proton signals in mammalian brains could be detected by proton-sensitive ion channels, such as the acid-sensing ion channels, some of which seem to play a part in learning and memory[8].

The two studies[1,2] extend the current understanding of how motor programs are controlled and challenge our definition of neurotransmitters. By providing an eloquent demonstration of protons as transmitters, they have fired the starting pistol in the race to discover more non-classical mechanisms of neurotransmission. With so many challenges on the horizon, it looks as if that race could be a marathon. ■

Laura M. Prolo is in the Neurosciences Program, and Miriam B. Goodman is in the Department of Molecular and Cellular Physiology, Stanford University School of Medicine, Stanford, California 94305, USA.
e-mail: mbgoodman@stanford.edu

1. Beg, A. A., Ernstrom, G. G., Nix, P., Davis, M. W. & Jorgensen, E. M. *Cell* **132**, 149–160 (2008)
2. Pfeiffer, J., Johnson, D. & Nehrke, K. *Curr. Biol.* **18**, 297–302 (2008)
3. Branicky, R. & Hekimi, S. *Trends Genet.* **22**, 571–579 (2006)
4. Dal Santo, P., Logan, M. A., Chisholm, A. D. & Jorgensen, E. M. *Cell* **98**, 757–767 (1999)
5. Take-uchi, M. *et al. Proc. Natl Acad. Sci. USA* **95**, 11775–11780 (1998)
6. Barnstable, C. J. *Curr. Opin. Neurobiol.* **3**, 520–525 (1993)
7. Krishtal, O. A., Osipchuk, Y. V., Shelest, T. N. & Smirnoff, S. V. *Brain Res.* **436**, 352–356 (1987)
8. Lingueglia, E. *J. Biol. Chem.* **282**, 17325–17329 (2007)

QUANTUM PHYSICS

Tangled memories

Lene Vestergaard Hau

The latest quantum trick — mapping two entangled photon states onto two separate regions of an atomic cloud, and then retrieving them — could be a fillip for applications, among them quantum cryptography.

On page 67 of this issue, Choi *et al.*[1] recount how they store two 'entangled' photon states in a memory consisting of a cloud of cold atoms, and then, after a certain delay, retrieve those self-same states from the cloud. The optical modes are stored in spatially separated regions of a single atom cloud, but there is no reason why the technique should not be used to imprint the same quantum states on two distinct atom clouds separated by a macroscopic distance. That would allow the controlled entanglement of two distant atomic samples — a step that might be of great importance for the practical implementation of quantum protocols to generate secure keys for the transfer of information over public networks.

Choi and colleagues' experiments start off with a light pulse containing a single photon. Like most of us, this photon soon comes to a point in life — in its case, a beam splitter — at which it is faced with a choice between two paths. In such a situation, the quantum world is kinder than the classical: it allows the photon to take both paths at the same time. If we set up a light detector to monitor one of the two paths, we will register a click (a photon hit) or no click, each with a 50% chance. But say some other (possibly distant) observer sets up a detector to monitor the other path. In this case, if this second observer detects a click, that instantaneously affects our own measurement: we will detect 'no click' with 100% probability (or vice versa, an absolutely certain click if the remote observer has detected no click).

This is entanglement: the strange correlation of two spatially separated quantum states. Entangled states are hard to maintain, because interactions with the environment destroy the entanglement. As a result, they are rare in our macroscopic world. But that doesn't stop them being essential to quantum information processing, for computing, teleportation and encryption applications.

In a classical computer, information is stored in strings of bits of value 0 or 1. The quantum bits of a quantum computer, on the other hand, can be in 'superposition states' — they can be 0 and 1 at the same time. Here, entanglement comes into its own. Let's say the quantum computer is set up to calculate the output value of a function that varies periodically with its input value (a sine wave, for example); we wish to find that period. The quantum computation leaves the system in a superposition of matched pairs, in which the output register holds the function value for the corresponding input.

The two registers are in fact entangled: a measurement of the output register will immediately affect the input register. For a periodic function, in which many input values correspond to a particular output value, the input register ends up in a superposition of precisely these inputs. After just one run-through of the calculation, therefore, global information

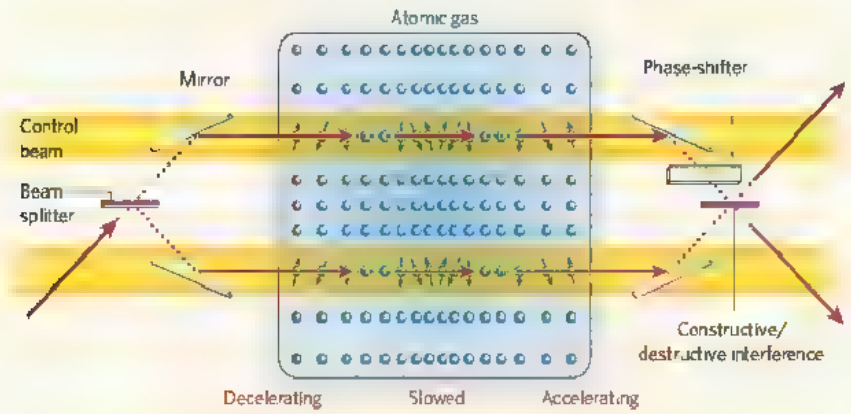

Figure 1 | Light split and slowed. In Choi and colleagues' experimental apparatus[1], a light pulse (red arrow) is split into two entangled states and fed into an atomic gas. There, under the influence of controlling laser beams, the split pulse is slowed, and the two entangled quantum states are imprinted onto two separate regions of the gas — effectively creating entanglement between the atoms of these regions. The light is then extinguished, and after a delay the photonic quantum states are regenerated from the information stored in the atoms. The amount of remaining entanglement is measured through the degree of constructive or destructive interference when the regenerated optical fields are recombined.

50 & 100 YEARS AGO

50 YEARS AGO

"A three-dimensional model of the myoglobin molecule obtained by X-ray analysis." By Drs J. C. Kendrew *et al.* — Until five years ago, no one knew how, in practice, the complete structure of a crystalline protein might be found by X-rays, and it was realized that the methods then in vogue among protein crystallographers could at best give the most sketchy indications about the structure of the molecule. This situation was transformed by the discovery, made by Perutz and his colleagues, that heavy atoms could be attached to protein molecules in specific sites and that the resulting complexes gave diffraction patterns sufficiently different from normal to enable a classical method of structure analysis, the so-called 'method of isomorphous replacement', to be used to determine the relative phases of the reflexions .. The present article describes the application, at low resolution, of the isomorphous replacement method in three dimensions to type *A* crystals of sperm whale myoglobin. The result is a three-dimensional Fourier, or electron-density, map of the unit cell, which for the first time reveals the general nature of the tertiary structure of a protein molecule . Perhaps the most remarkable features of the molecule are its complexity and its lack of symmetry. The arrangement .. is more complicated than has been predicated by any theory of protein structure.
From *Nature* 8 March 1958

100 YEARS AGO

It is reported by The Hague correspondent of the *Globe* (March 3) that Prof. Kamerlingh Onnes, professor of physics in the University of Leyden, has succeeded in liquefying helium.

ALSO:

In the report of the Maidstone Museum, Library, and Art Gallery for 1907, attention is directed to the unprecedentedly large number of visitors during the year.
From *Nature* 5 March 1908.

about the function — its period — is contained in the input register. After some 'fiddling', this period can be read out with many fewer operations than a classical computer requires[2]. (In a classical calculation we would have to run the computation many times, once for each input value, to slowly, step by step, build up global information about the function.)

Encoding this information in material quantum states, such as those of atomic clouds, is a particularly promising avenue towards implementing quantum-computational schemes. the interactions between atoms can be strong, and processing (through controlled changes to the quantum states) can happen fast. Long-distance transmission of the resulting output quantum states, on the other hand, works better with light: light can travel fast and with minimal losses in optical fibres. Reliable and efficient ways of mapping quantum information between light and matter are therefore an essential component of any quantum information network.

In their experiments, Choi *et al.*[1] achieve this transfer using 'slow light'[3]. Under particular conditions dictated by quantum mechanics, the speed of a light pulse that has been injected into an atom cloud illuminated by a control laser can be reduced by many orders of magnitude. As the pulse slows, its spatial extent shrinks, and it ultimately fits snugly inside the atom cloud (Fig. 1). The pulse affects the internal states of atoms within its localized region, creating a hologram-like imprint of itself in the atom cloud. If the control laser is turned off, the light pulse is halted and extinguished, but its atomic imprint remains in the cloud. If the control laser is turned back on, the same process runs backwards: the light pulse is regenerated and moves on, exits the atom cloud and speeds back up. Such storage of optical information has been demonstrated for classical light pulses containing many photons[4,5] and for single-photon light pulses[6,7].

The authors show that the entanglement of two light fields also survives such storage. They create their single-photon pulse by generating a single atomic excitation in a separate 'source' atom cloud, using the slow-light effect to read it out. The entangled optical modes generated at the beam splitter are injected into the main atomic sample, separated by 1 millimetre. After a microsecond, the authors are able to regenerate the optical fields. They then introduce a phase shift into one before the two modes recombine at a second beam splitter. Depending on the phase shift introduced, constructive or destructive quantum interference between the two optical paths is measured at a detector after the second beam splitter. The contrast of the fringes obtained as the phase is varied tells us the quality of the entanglement.

So what is the next step? Separate control of the phase relationship between the two optical modes' input to the atom cloud would allow the controlled storage and revival of actual quantum bits. Choi *et al.*[1] use cold atoms for their experiments, laser cooled to about 125 microkelvin above absolute zero to avoid thermal smearing of the stored holographic imprints, but it would be interesting to cool things down further, forming the phase-coherent state of atomic matter known as a Bose–Einstein condensate, which offers much-increased possibilities for storage and controlled processing[8]. The storage of entangled optical fields in two separated atom clouds also needs to be formally demonstrated. Such entanglement would allow the efficient sharing of quantum keys for secure encryption[9], and the transfer (teleportation) of quantum bits between two atomic clouds by simple transmission of pairs of classical bits[10].

Will any or all of this ever get to a stage at which it can be used in practical devices? That remains to be seen. We can state, however, that a century after quantum mechanics was discovered, the possibilities it offers continue to boggle our minds. ■

Lene Vestergaard Hau is in the Lyman Laboratory, Physics Department, Harvard University, 17 Oxford Street, Cambridge, Massachusetts 02138, USA.
e-mail hau@physics.harvard.edu

1 Choi, K. S., Deng, H., Laurat, J. & Kimble, H. J. *Nature* **452**, 67–71 (2008)
2 Shor, P. W. in *Proc. 35th Annu. Symp. Found. Comput. Sci.* (ed. Goldwasser, S.) 124–134 (IEEE Computer Soc. Press, Los Alamitos, CA, 1994)
3 Hau, L. V. *Sci. Am.* **285** (1), 66–73 (2001)
4 Liu, C., Dutton, Z., Behroozi, C. H. & Hau, L. V. *Nature* **409**, 490–493 (2001)
5 Phillips, D. F., Fleischhauer, A., Mair, A., Walsworth, R. L. & Lukin, M. D. *Phys. Rev. Lett.* **86**, 783–786 (2001)
6 Chanelière, T. *et al. Nature* **438**, 833–836 (2005)
7 Eisaman, M. D. *et al. Nature* **438**, 837–841 (2005)
8 Ginsberg, N. S., Garner, S. R. & Hau, L. V. *Nature* **445**, 623–626 (2007)
9 Ekert, A. *Phys. Rev. Lett.* **67**, 661–663 (1991)
10 Bennett, C. H. *et al. Phys. Rev. Lett.* **70**, 1895–1899 (1993)

NEUROSCIENCE

A complex in psychosis

Solomon H. Snyder

The molecular basis of psychoses such as schizophrenia remains largely mysterious. The interaction between two of the brain receptors involved adds to evidence that will help in the search for explanations.

This is a story that involves three types of receptor in the brain that influence human perception and behaviour (those for the neurotransmitters dopamine, serotonin and glutamate), and the drugs that block or enhance their activity. Such drugs are used by researchers to investigate the causes of psychotic disorders such as schizophrenia, and by clinicians to treat patients. Classical antipsychotic drugs, designated 'typical neuroleptics', act predominantly by blocking dopamine D2 receptors. A new generation of more effective 'atypical neuroleptics' also blocks a subtype of serotonin receptor known as 5-HT_{2A}, or more simply as 2AR. And last year we had the promising report[1] of a drug that mimics the effect of glutamate at a subtype of one of its receptors, metabotropic glutamate receptor 2 (mGluR2), and that seems to be as effective as atypical neuroleptics.

This is the background against which the paper by González-Maeso *et al.*[2] appears (page 93 of this issue): these authors show that

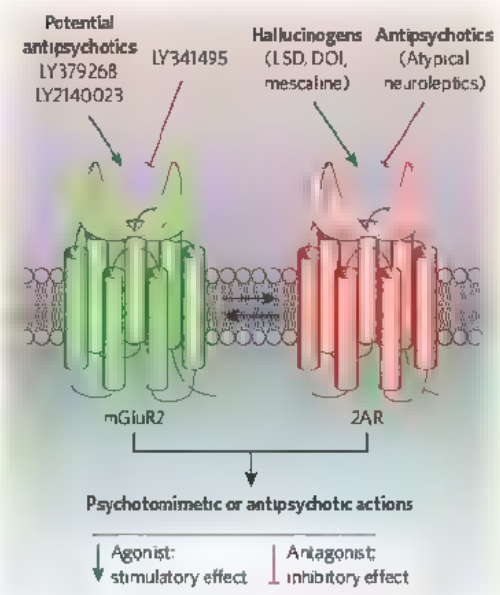

Figure 1 | Receptor interaction. González-Maeso *et al.*[2] find that the metabotropic glutamate receptor 2 (mGluR2) and serotonin 5-HT_{2A} receptor (2AR) physiologically bind each other, leading to reciprocal regulation of their functions. Agonists that stimulate mGluR2 are antipsychotic, whereas 2AR agonists, such as hallucinogens, have the opposite effect. It is conceivable that the clinically significant antischizophrenic effects of LY2140023, an mGluR2 agonist[1], derive from reducing the excessive — and hence hallucinogen-like — activity of 2AR. DOI, 2,5-dimethoxy-4-iodoamphetamine.

there are direct molecular interactions between 2AR and mGluR2, and that the interactions have functional effects. Besides helping to elucidate drug actions, these findings may shed light on fundamental aspects of the causes and consequences of schizophrenia.

In the absence of definitive evidence for the molecular causes of psychosis, biological psychiatrists have long relied largely on drugs as probes. If a drug is psychotomimetic (that is, elicits a psychotic state that resembles schizophrenia), then knowing how it acts might clarify aberrations in the brains of patients with schizophrenia. Conversely, if a drug selectively alleviates symptoms of schizophrenia, understanding its mode of action will also be illuminating.

The structure and action of diverse psychotomimetic drugs have led to different models of psychosis. For example, hallucinogens such as LSD (lysergic acid diethylamide), psilocybin and dimethyltryptamine resemble the indoleamine structure of serotonin, leading to a 'serotonin concept' of psychosis, which holds that perturbation of serotonin signalling is the main cause. Although phenethylamine hallucinogens such as mescaline and methoxyamphetamines are not indoleamines, their native conformation resembles that of serotonin and they elicit psychotic states much like that produced by LSD (ref. 3). Hallucinogens are agonists (stimulating agents) at 2ARs, which are blocked by atypical neuroleptics.

High doses of amphetamines, which act by releasing dopamine, evoke a psychosis that often resembles acute paranoid schizophrenia, and low doses selectively exacerbate schizophrenic symptoms. The typical neuroleptics block dopamine D2 receptors with potencies closely paralleling the effectiveness of their antipsychotic actions, leading to the 'dopamine hypothesis' of schizophrenia[4]. The effects of agents that block the NMDA subtype of glutamate receptor, such as phencyclidine (PCP, also known as angel dust), usually mimic schizophrenic symptoms better than any other drug-induced psychosis. The most recent development[1] in this pot-pourri of drug effects involves the striking antischizophrenic actions of LY2140023, an mGluR2 agonist.

González-Maeso *et al.*[2] wondered whether the similar therapeutic actions of 2AR antagonists and mGluR2 agonists reflect a specific molecular interaction between the two receptors. Like many neurotransmitter receptors, mGluR2 and 2AR are coupled to G proteins, which sit inside the cell membrane and act as molecular switches that regulate intracellular signalling pathways. During the past decade, Devi[5] and others have shown that different G-protein-coupled receptors can form functional complexes.

The advance made by González-Maeso *et al.* is the direct demonstration, using several techniques, of the existence of complexes between 2AR and mGluR2 (Fig. 1). These authors conclude that the complex is functionally relevant by showing that mGluR2 agonists increase the affinity of hallucinogens for 2AR binding, whereas 2AR agonists decrease the affinity of mGluR2 agonists for glutamate receptor binding. Moreover, activation of G proteins by 2AR was altered by co-expression of mGluR2. Induction of a gene (*egr 2*) that is selectively stimulated by hallucinogenic 2AR agonists was blocked by an mGluR2 agonist, whereas induction of *c-fos*, which responds both to hallucinogenic and non-hallucinogenic 2AR agonists, was unaffected by the same treatment.

The authors' observations of behavioural responses in mice also support the idea of mGluR2–2AR interaction, as the effects of an mGluR2 antagonist on movement were diminished in mice with targeted deletion of 2AR. Finally, post-mortem analysis of the brains of humans with schizophrenia revealed increased numbers of 2ARs and decreased numbers of mGluR2s.

What do we learn from these findings? Using various approaches, González-Maeso *et al.*[2] have provided a compelling case that 2AR and mGluR2 interact physically and physiologically, and that drugs influencing one of the receptors will alter the behaviour of the other. Neuronal wiring links between various transmitter circuits, and crosstalk between receptors regulated by agents called scaffolding proteins, are well known. González-Maeso and colleagues provide a new concept — that direct physical coupling of two receptors mediates complex pharmacological and behavioural responses.

Given this conclusion, researchers will be scurrying to explore what effect drugs that target 2ARs have on glutamate signalling and, conversely, to ascertain whether alterations in mGluR2s influence events mediated by serotonin. From a behavioural and clinical perspective, one would predict that drugs acting at these two different receptors would have similar influences. This possibility fits with the finding[1] that the antipsychotic actions of the mGluR2 agonist LY2140023 resemble those of the atypical neuroleptics that target 2ARs. Because drugs blocking dopamine D2 receptors also act similarly, they may have some link to the receptor complex. Finally, the new results may provoke a reassessment of the effects of hallucinogens as useful models of the brain disturbances that characterize schizophrenia. ■

Solomon H. Snyder is in the Solomon H. Snyder Department of Neuroscience, Johns Hopkins School of Medicine, 725 North Wolfe Street, Baltimore, Maryland 21205-2185, USA.
e-mail: ssnyder@jhmi.edu

1. Patil, S. T. *et al. Nature Med.* **13**, 1102–1107 (2007)
2. González-Maeso, J. *et al. Nature* **452**, 93–97 (2008)
3. Aghajanian, G. K. & Marek, G. J. *Brain Res. Rev.* **31**, 302–312 (2000)
4. Snyder, S. H., Banerjee, S. P., Yamamura, H. I. & Greenberg, D. *Science* **184**, 1243–1253 (1974)
5. Devi, L. A. *Trends Pharmacol. Sci.* **22**, 532–537 (2001)

AGEING

Rushed decisions

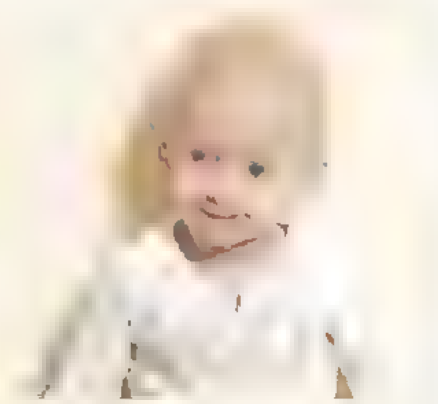

J. DURK N/REX FEATURES

People who have Hutchinson–Gilford progeria syndrome (HGPS), such as the two-year-old girl pictured, grow old before their time. This distressing condition of premature ageing is a rare but fatal genetic disorder, which is caused by the continuous production of progerin, an abnormal form of the nuclear protein lamin A. But what effects does excess progerin have? Paola Scaffidi and Tom Misteli report that the protein triggers a feature that resembles premature ageing at a cellular level: untimely stem-cell differentiation (P. Scaffidi & T. Misteli *Nature Cell Biol.* doi:101038/ncb1708, 2008).

The authors took a genome-wide approach to identify the genes concerned. They found that, 5 days after production of progerin was increased, the expression of almost 200 genes was dramatically affected, a number that rose to more than 1,000 by day 10. To interpret this striking effect, they searched for cellular pathways in which several progerin-responsive misregulated genes function; this led them to the Notch signalling cascade, which regulates stem-cell differentiation and cell fate. In cells derived from patients with HGPS, the components of Notch signalling were also abnormally active.

The main tissues affected in HGPS are those of mesenchymal origin, including bone, fat and cartilage. The authors looked at the effect of progerin overexpression — and so Notch activation — on normal human mesenchymal stem cells and found that it led to sporadic but spontaneous differentiation of these cells. Next, they triggered differentiation of mesenchymal stem cells into specific lineages in the presence of progerin: increased stem-cell differentiation into the bone lineage was the result. By contrast, progerin seemed to hinder stem cells' transformation into fat cells. These results are consistent with the fact that patients with HGPS have a high turnover of bone but suffer from a loss of subcutaneous fat.

Scaffidi and Misteli's work unravels at least some of the consequences of increased progerin levels associated with premature ageing. But their observations also have implications for understanding the normal process of ageing, as low levels of progerin are present in healthy individuals.

Sadaf Shadan

PALAEONTOLOGY

Modern life in ancient mats

Michael M. Tice

Microbial communities seem to have inhabited tidal sediments 2.9 billion years ago much as they do today — but what organisms were involved, and how they made their living, remain intriguing questions.

Establishing from fossil records how microbes and microbial ecosystems evolved is not an easy task: although 'microfossils' have been used to infer the presence and identity of microbes in particular environments[1,2], their simple shapes and comparative rarity limit what they can tell us. An alternative approach is to look for traces of products from communities of microorganisms[3,4]. Research by Noffke *et al.*[5], reported in *Geobiology*, illustrates this possibility. These authors have discovered evidence of 'microbial mats' in 2.9-billion-year-old sedimentary rocks from South Africa — a find that significantly augments the record of such structures from the Archaean eon, which ended 2.5 billion years ago.

Microbial mats are communities of microorganisms that grow in or on otherwise loose sediments, giving their substrate cohesiveness and tensile strength. Their consolidating effect means that they can produce a trace fossil record in sandstones and mudstones — even when no organic matter or microfossils are preserved. Structures that owe their existence to the stabilizing influence of mats can thus be important markers of ancient microbial ecosystems that would otherwise remain undetected.

Noffke *et al.*[5] describe sandstones of the Sinqueni Formation, part of the Pongola Supergroup of eastern South Africa. These rocks were formed from sandy sediments deposited in a tidal environment 2.9 billion years ago, but several features preserved in them demonstrate a cohesiveness not seen in unconsolidated sand. Three structures seem to point particularly conclusively to an overlying microbial mat (Fig. 1). First, anomalously coherent, deformed chunks of sandy bed would have originated as chips of mat ripped up by energetic tidal currents and subsequently redeposited (Fig. 1a). Second, overfolded chips of rock (clasts) indicate where pieces of mat were rolled over on themselves, unexpected behaviour for layers of loosely associated sand grains (Fig. 1b). Third, oscillation cracks are present; these features would have been formed above the normal tidal range when pockets of gas periodically accumulated under, and escaped from, the mats (Fig. 1c). Such processes caused the mats' surfaces to expand and contract, forming cracked beds with upturned edges.

The Sinqueni rocks formed from mud-poor, quartz-rich sediments, and there was little else other than microbial mats that could have provided the material strength to form these features. The observation that specific structures were formed in the same places, relative to the tidal range, where they are found today adds confidence to this interpretation. This particularly well-preserved and diverse set of mat-related structures thus adds to a growing record of sedimentary microbial communities extending from 3.4 billion years ago to the present. Remarkably, many of the physical properties of mats and the environments in which they grew seem not to have changed over most of that time.

So what can this record tell us about microbial evolution? Noffke *et al.*[5] conclude that the mat features they observe are consistent with, but not necessarily indicative of, construction by photosynthesizing cyanobacteria. Evidence of the existence of these organisms 2.9 billion years ago would be intriguing. Cyanobacteria are the only organisms to have independently evolved the ability to produce oxygen during photosynthetic growth; algae and green plants ultimately acquired their capability for oxygenic photosynthesis through symbiotic associations with cyanobacteria. The production of oxygen by cyanobacteria and its consequent accumulation in surface environments drove many organisms to evolve to exploit oxygen in their metabolism and biosynthesis[6]. This process ultimately allowed the incredible diversification of macroscopic body plans that began about 600 million years ago. The oldest evidence so far of oxygenic photosynthesis by cyanobacteria comes from 2.7-billion-year-old molecular fossils found in Western Australia[7], and the interpretation of even these fossils is not completely resolved[8,9].

Unfortunately, Noffke and colleagues' older mat structures tell us nothing about the metabolism of the organisms that constructed them. The stability they gave to the sands of the Sinqueni Formation could, as studies of modern microbial mats bear witness, be the result of at least two processes. First, filamentous bacteria can form meshes that trap and bind sand grains; second, microbially produced slime can encase sediments[10]. Neither mechanism is specific to organisms growing by oxygenic photosynthesis, and there is no known general

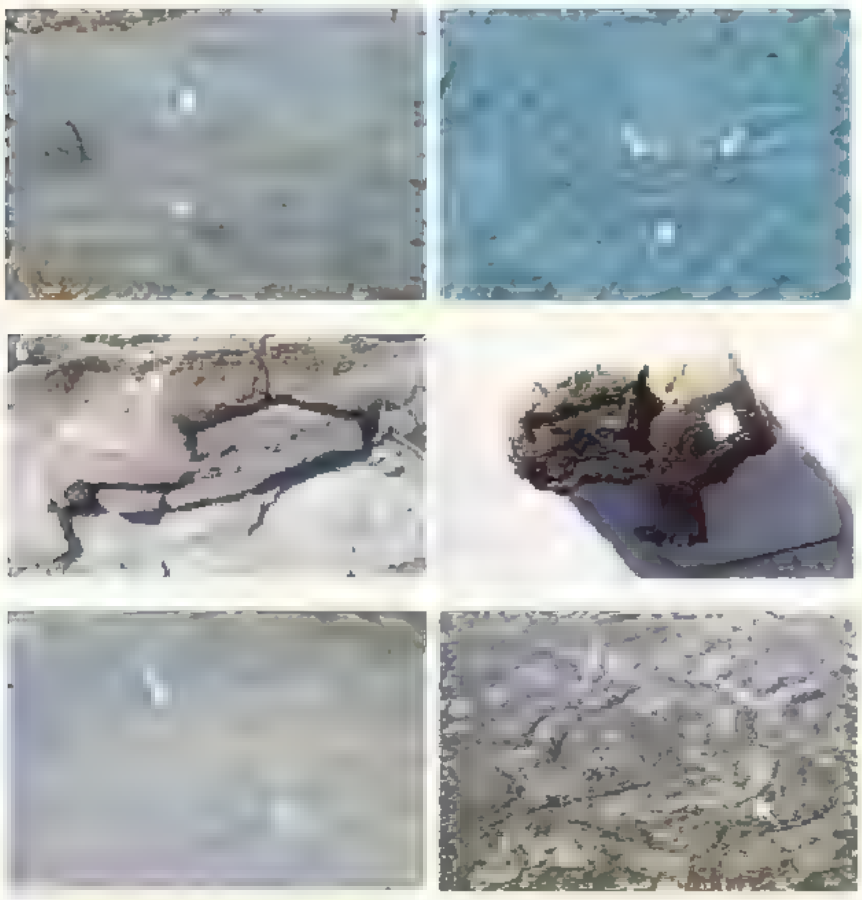

Figure 1 | Mat finish. Noffke *et al.*[5] find features in 2.9-billion-year-old rocks from the Pongola Supergroup in South Africa that are similar to those caused by microbial mats in intertidal zones today (left, fossil Pongola feature; right, contemporary feature for comparison). **a**, uprooted and redeposited mat chips, **b**, overfolded rock chips, **c**, oscillation cracks.

link between metabolism and the details of mat construction.

Most of what is currently known about microbial mats and their effect on sedimentation comes from studies of mats constructed primarily by cyanobacteria in modern, oxygen-rich environments. But oxygen did not accumulate in the atmosphere and the surface ocean in appreciable amounts until at least 2.5 billion years ago[11]. Before that time, might other organisms — such as the ancestors of modern anoxygenic photosynthetic bacteria or methane-producing microorganisms — have constructed similar mats in shallow environments, in which water currents are present, that have since come to be dominated by oxygenic organisms? Does evidence for cohesive sandy sediments even imply that sediment-binding behaviour by filamentous microbes, and slime production, were necessarily operating in the same way 2.9 billion years ago as they do now?

Noffke and colleagues' observations[5] help fill in the geological record of microbial communities and ecosystems at a potentially critical stage in their evolution. They tell us that microbes were constructing cohesive mats in early tidal environments much as they do today. But what this means in detail for the physiology and behaviour of the organisms involved is an open question, and one that awaits future studies of the mechanisms of mat construction in both aerobic and anaerobic environments. ■

Michael M. Tice is in the Department of Geology and Geophysics, Texas A&M University, College Station, Texas 77843-3115, USA.
e-mail: tice@geo.tamu.edu

1. Amard, B. & Bertrand-Sarfati, J. *Precamb. Res.* **81**, 197–221 (1997)
2. Hofmann, H. J. *J. Paleontol.* **50**, 1040–1073 (1976)
3. Noffke, N., Eriksson, K. A., Hazen, R. M. & Simpson, E. L. *Geology* **34**, 253–256 (2006)
4. Tice, M. M. & Lowe, D. R. *Nature* **431**, 549–552 (2004)
5. Noffke, N. *et al. Geobiology* **6**, 5–20 (2008)
6. Raymond, J. & Segrè, D. *Science* **311**, 1764–1767 (2006)
7. Brocks, J. J., Logan, G. A., Buick, R. & Summons, R. E. *Science* **285**, 1033–1036 (1999)
8. Kopp, R. E., Kirschvink, J. L., Hilburn, I. A. & Nash, C. Z. *Proc. Natl Acad. Sci. USA* **102**, 11131–11136 (2005)
9. Rasmussen, B., Fletcher, I. R., Sheppard, S., Sessions, A. L., Summons, R. E. & Newman, D. K. *Proc. Natl Acad. Sci. USA* **104**, 15099–15104 (2007)
10. Krumbein, W. E., Paterson, D. F. & Stal, L. J. (eds) *Biostabilization of Sediments* (BIS, Univ. Oldenburg, 1994)
11. Anbar, A. D. *et al. Science* **317**, 1903–1906 (2007)

MAGNETOSPHERIC PHYSICS

Hiss from the chorus

Craig J. Rodger and Mark A. Clilverd

What is the origin of the broadband, low-intensity radio waves thought to control the radiation belts that surround Earth? The latest suggestion sees this 'hiss' emerging from an unsuspected quarter.

Hard on the heels of the Soviet Union, the United States entered the space race fractionally over 50 years ago. The scientific instrumentation of America's first Earth-orbiting satellite, Explorer 1, launched on 31 January 1958, was designed and built under the direction of one James Van Allen of the University of Iowa. It included a Geiger counter, the first recordings from which reportedly moved one of Van Allen's team to utter an exclamation ripe for a science-fiction movie[1]: "My God, space is radioactive!" Since that first entirely unexpected revelation about our near neighbourhood, the belts of radiation that envelop Earth — the Van Allen belts — have only slowly yielded their secrets. The latest development is recounted by Bortnik *et al.*[2] on page 62 of this issue: a new explanation for how the gap found in their midst arises.

The Van Allen belts consist of a cloud (a 'plasma') of highly energetic charged particles, mainly electrons and protons, trapped by Earth's magnetic field. During 'quiet' times, the energetic electrons of the radiation belt are distributed into two regions: the inner belt, at altitudes above Earth's Equator of between around 1,500 and 10,000 km; and the outer belt, between around 19,000 and 64,000 km up (Fig. 1). These two belts are separated by the 'electron slot', in which the population of energetic electrons drops by between 10 and 100 times. Disturbances in Earth's magnetic field, known as geomagnetic storms, can lead to the slot becoming filled with energetic electrons, probably from the outer belt. But the slot rapidly clears, principally as electrons precipitate along magnetic field lines (thus bypassing the inner belt) into the underlying atmosphere. Because of its low population of energetic electrons, the slot is a relatively benign environment, and is favoured for 'medium Earth orbiting' satellites that are used extensively for telecommunications.

What causes the depletion of electrons in the slot is unclear, but it's probably some form of resonance between high-energy electrons and radio waves propagating through space. It has become clear that one variety of radio wave, plasmaspheric hiss, is crucial to the process[3]. Hiss is aptly named: it is a noisy emission, spread over a limited frequency band from about 100 hertz to 1 kilohertz, and it fills the cold, dense plasma of low-energy particles — the plasmasphere — that encircles Earth's atmosphere.

But what causes hiss? A recent study[4] into the statistical patterns in the amplitudes of radio emissions observed by spacecraft resuscitated an old idea[5]: that hiss might be the product of radio waves from terrestrial lightning that leak into the plasmasphere and progressively disperse there. The initial radio pulse from lightning is well known to interact with electrons in the inner Van Allen belt[6], but the idea that its influence extends farther, into the slot, proved controversial[7]. Shortly afterwards, the

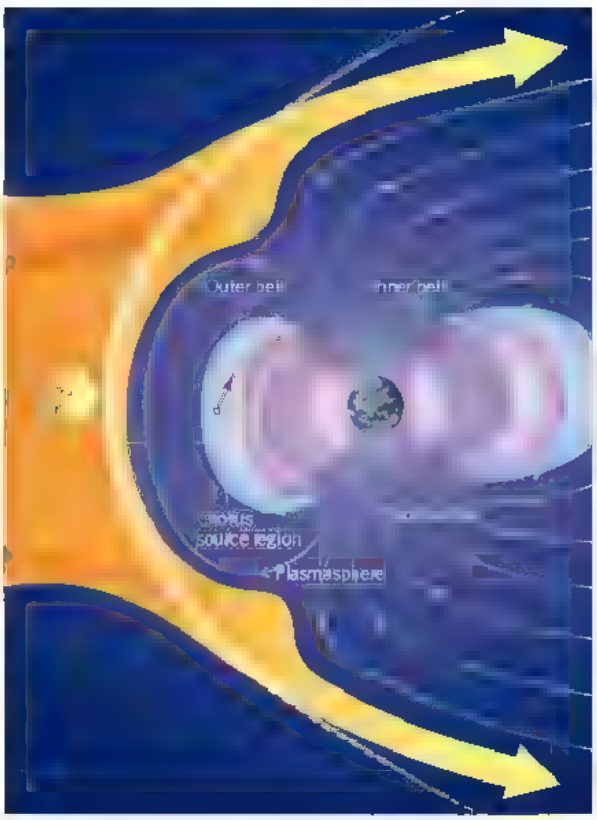

Figure 1 | Earth's engirdling belts. The Van Allen radiation belts (light blue) consist of 'hot' energetic particles trapped in Earth's magnetic field. Owing to the flow of the wind from the Sun, Earth's field, and hence also the belts, are compressed on the side facing the Sun and stretched out on the side facing away. The electron slot region lies between the inner and outer electron belts, and is located inside the plasmasphere (magenta), which is filled with 'cold', dense plasma. The red line shows the ray-traced path of a radio-wave chorus emission outside the plasmasphere. Bortnik *et al.* propose[2] that chorus emissions, originating in the outer Van Allen belt outside the plasmasphere, can gain access to the plasmasphere and drive processes that lead to the formation of the electron slot.

possibility seemed laid to rest when extended satellite data sets indicated that lightning-generated radio waves might indeed be responsible for noise in the plasmasphere at higher frequencies above 2 kHz, but could not be responsible for hiss's lower-frequency noise[8].

Another source for hiss that has been considered over the years is *in situ* amplification of random background thermal noise, a seemingly obvious candidate given hiss's broadband nature. But this mechanism has been effectively ruled out because insufficient amplification would be generated under typical conditions.

Bortnik *et al.*[2] provide a new, self-consistent explanation for the generation of plasmaspheric hiss that reproduces its fundamental properties. Their suggestion stems from modelling the propagation of high-intensity, coherent 'chorus' radio waves found outside the plasmasphere. Again, the name is apt: when these emissions are played back through an audio speaker, they sound like a dawn chorus of birds. The authors provide convincing arguments for the way in which this high-intensity, narrow-band chirping can 'evolve' into low-intensity broadband noise, filling the plasmasphere and ultimately being observed as hiss.

Chorus waves are rapidly gaining a reputation as the driver of large, rapid changes in populations of energetic electrons when they are dumped in the atmosphere during geomagnetic storms[9]. Such events are followed a few hours later by the chorus-driven acceleration of lower-energy electrons in the outer belt to relativistic energies, which increases the population of energetic electrons there hundreds or thousands of times[10]. These electrons have been nicknamed killer electrons, owing to their ability to disrupt, damage or destroy satellites in the outer radiation belt — principally those in geostationary orbits some 36,000 km up, in the heart of the outer Van Allen belt. If Bortnik and colleagues[2] are correct, chorus not only plays an important part in electron acceleration, but also drives some of the most significant loss processes that occur in the belts.

This modelling study is unlikely to be the final word on the formation of the electron slot, or indeed on the origins of plasmaspheric hiss; an experimental confirmation will, of course, be required. Nonetheless, the idea has the potential to be a 'circuit breaker' in our understanding of the radiation belts, pointing us at last towards a new and more convincing generation mechanism. The possibility that the drivers for phenomena in the Van Allen belts might be processes occurring tens of thousands of kilometres away from Earth is a fascinating one. The next generation of satellite missions designed to investigate these questions — among them NASA's Radiation Belt Storm Probes mission and the Canadian Space Agency's Outer Radiation Belt Injection, Transport, Acceleration and Loss Satellite (ORBITALS) — might well provide a definitive answer. ■

Craig J. Rodger is in the Department of Physics, University of Otago, PO Box 56, Dunedin 9054, New Zealand. Mark A. Clilverd is in the Physical Sciences Division, British Antarctic Survey, Madingley Road, Cambridge CB3 0ET, UK.
e-mails: crodger@physics.otago.ac.nz; macl@bas.ac.uk

1 Hess, W. N. *The Radiation Belt and Magnetosphere* (Blaisdell, Waltham, MA, 1968)
2 Bortnik, J., Thorne, R. M. & Meredith, N. P. *Nature* **452**, 62–66 (2008).
3. Lyons, L. R. & Williams, D. J. *Quantitative Aspects of Magnetospheric Physics* (Kluwer, Dordrecht, 1984)
4 Green, J. L. *et al. J. Geophys. Res.* **110**, doi:10.1029/2004JA010495 (2005)
5. Dowden, R. L. *Planet. Space Sci.* **19**, 374–376 (1971)
6. Rodger, C. J., McCormick, R. J. & Clilverd, M. A. *Geophys. Res. Lett.* **31**, doi:10.1029/2004GL019501 (2004)
7 Thorne, R. M., Horne, R. B. & Meredith, N. P. *J. Geophys. Res.* **111**, doi:10.1029/2005JA011477 (2006)
8 Meredith, N. P. *et al. J. Geophys. Res.* **111**, doi:10.1029/2006JA011707 (2006)
9 Clilverd, M. A. *et al. J. Geophys. Res.* **112**, doi:10.1029/2007JA012416 (2007)
10. Horne, R. B. *et al. J. Geophys. Res.* **110**, doi:10.1029/2004JA010811 (2005)

GENOMICS

Fungal symbiosis unearthed

Dan Cullen

Associations between plant roots and fungi are a feature of many terrestrial ecosystems. The genome sequence of a prominent fungal partner opens new avenues for studying such mycorrhizal interactions.

Plants and fungi often form marriages of convenience. In one form of this symbiotic relationship — an ectomycorrhizal association — long, branching fungal filaments known as hyphae ramify between cells of the root's outer layers, form a sheath around the root, and radiate outwards into the surrounding soil and litter. This transport network then allows the fungus to derive photosynthetically produced sugars from the host and in turn to transfer nitrogen and phosphorus to the plant. The ectomycorrhizal fungus *Laccaria bicolor* has been widely studied, in part because it is easy to grow in culture and establishes mycorrhizal associations with tree roots in laboratory experiments (Fig. 1). In a giant step forward, an international team of investigators report the genome analysis of this fungus. The analysis, published by Martin *et al.* on page 88 of this issue[1], reveals a mix of the intriguing and the unexpected.

At 65 million base pairs, the genome of *L. bicolor* is bigger than that of previously published fungal genomes. The size may be partly explained by the large number of mobile DNA sequences, known as transposable elements, that constitute more than 20% of the genome. Using a combination of gene-prediction tools, the authors[1] identify 20,614 protein-encoding genes. Of these, about 70% (14,464) show significant similarity to sequences in protein databases, particularly those from other homobasidiomycetes, the major fungal taxon to which *L. bicolor* belongs. Compared with other fungal genomes, the *L. bicolor* genome contains both more and larger gene families. Most of them have clear orthologues in other fungi — that is, they are genes that evolved from a common ancestor. Others, however, are unique to *L. bicolor*. Perhaps reflecting the complex exchange of nutrients between *L. bicolor* and its hosts, there is an especially large number of predicted membrane-bound transporter proteins.

An expectation of fungi that colonize forest litter is that they should secrete enzymes that break down cellulose and perhaps also lignin, two of the main components of plant cell walls. A voluminous literature and recent genome analysis of cellulolytic organisms[2–4] and aggressive plant pathogens[5,6] affirm a common strategy for efficient cellulose degradation.

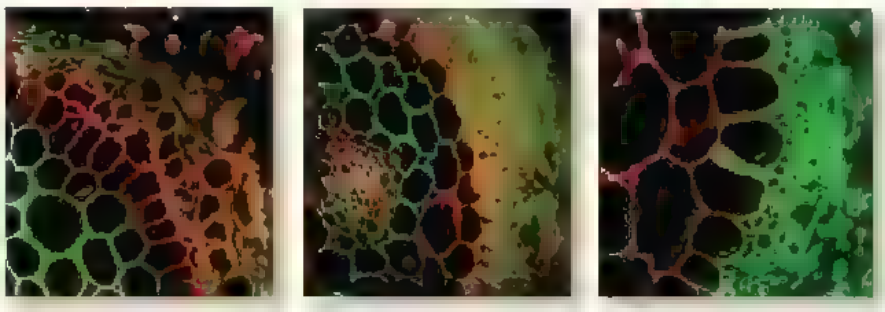

Figure 1 | *Laccaria bicolor* in action. This sequence of micrographs shows the colonization of poplar (*Populus* sp.) roots by this fungus. The images, from left to right, were taken 3, 10 and 28 days after initial fungus–root contact. By day 28, hyphal cells (green) form a dense external sheath and penetrate between host cells. (Photos are ×120 and are courtesy of J. Richter and V. Legue, INRA Nancy.)

Minimally, this strategy involves a synergistic attack by exocellobiohydrolases and endoglucanases, and the activities of these extracellular enzymes are often enhanced by their having cellulose-binding structural domains. Unexpectedly, given the capacity of *L. bicolor* to persist in litter, the genome of this fungus reveals only a single gene encoding an endoglucanase with a cellulose-binding domain, and no genes for exocellobiohydrolases. There is also little evidence of the oxidative systems necessary for lignin degradation, genes encoding lignin-depolymerizing peroxidases, which generally occur as multigene families in efficient lignin-degrading fungi, are absent.

Thus, *L. bicolor* seems to be poorly adapted for efficient degradation of carbon-rich lignocellulose, which may reflect a reliance on host-supplied carbon. In contrast, the high number of genes encoding various glycoside hydrolases and proteinases that are predicted by the authors may indicate a capacity to use alternative nutrient sources (such as insects, bacteria and decomposed organic matter) and to transfer nitrogen and phosphorus to the host. In this connection, interactions within the broad microbial community, including bacteria present inside the fungal cells[7], may have an important role in mobilizing soil nutrients.

A paucity of predicted enzymes that degrade plant cell walls has also been observed in the genome of *Ustilago maydis*[8], a distantly related basidiomycete that is the causal agent of corn smut. The hyphae of this amazing pathogen proliferate within the plant, but rather than causing rapid cell death and necrosis, the fungus induces spectacular, spore-filled tumours. Kämper *et al.*[8] presciently suggested parallels between such pathogens and "plant-growth-promoting mycorrhizal fungi"; the absence of conventional cellulases in *L. bicolor* and *U. maydis* supports this view.

Another intriguing similarity with *U. maydis* is the impressive number of sequences predicted to encode secreted proteins of fewer than 300 amino acids in length. In *U. maydis*, the genes for these 'secreted small proteins' are extensively clustered and the proteins are implicated in pathogenesis. Gene clustering is not as pronounced in *L. bicolor*, but it is tempting to speculate that in *L. bicolor* some of these proteins are involved in establishing and maintaining symbiotic interactions. Consistent with this possibility, the whole-genome expression microarrays carried out by Martin *et al.*[1] show that several genes encoding secreted small proteins are expressed during symbiosis. Another analytical technique used by the authors was immunofluorescence microscopy, through which one such secreted small protein was localized to hyphae within colonized roots, but was not evident in the free-living fungus.

With the genome of *L. bicolor* in hand, we should see rapid progress in elucidating the molecular processes involved in symbiotic interactions[9]. In addition to the expression microarrays and immunofluorescence studies described by Martin *et al.*[1], direct genetic manipulation of *L. bicolor* may be within reach[10]. Further, the ability of *L. bicolor* to form mycorrhizae with *Populus trichocarpa*, which is the only tree whose genome has been sequenced to date[11], offers unique opportunities for comprehensive investigations of a complete ectomycorrhizal system. ■

Dan Cullen is at the USDA Forest Products Laboratory, One Gifford Pinchot Drive, Madison, Wisconsin 53726, USA.
e-mail: dcullen@facstaff.wisc.edu

1. Martin, F. *et al. Nature* **452**, 88–92 (2008)
2. Martinez, D. *et al. Nature Biotechnol.* **22**, 695–700 (2004).
3. Galagan, J. E. *et al. Nature* **422**, 859–868 (2003)
4. Galagan, J. E. *et al. Nature* **438**, 1105–1115 (2005)
5. Dean, R. A. *et al. Nature* **434**, 980–986 (2005)
6. Cuomo, C. A. *et al. Science* **317**, 1400–1402 (2007)
7. Bertaux, J. *et al. Environ. Microbiol.* **7**, 1786–1795 (2005)
8. Kämper, J. *et al. Nature* **444**, 97–101 (2006)
9. Martin, F., Kohler, A. & Duplessis, S. *Curr. Opin. Plant Biol.* **10**, 204–210 (2007)
10. Kemppainen, M., Circosta, A., Tagu, D., Martin, F. & Pardo, A. G. *Mycorrhiza* **16**, 19–22 (2005)
11. Tuskan, G. A. *et al. Science* **313**, 1596–1604 (2006)

SOLID-STATE PHYSICS

How does your quasicrystal grow?

Paul J. Steinhardt

Somewhere between the amorphous glasses and the rigidly regimented periodic crystals lie the quasicrystals: ordered, predictable, yet non-periodic arrangements of atoms. How do these strange structures form?

Just as it's easy to construct a mosaic of square tiles simply by adding tiles one at a time, so it's little trouble for atoms to arrange themselves into an analogous, perfectly periodic pattern: a crystal. The rules for constructing another class of mosaic — a quasicrystal — seem to be much more complex. So how is it that atoms can rapidly organize themselves into quasicrystalline solids with seemingly little extra effort? Using computer simulations, Keys and Glotzer, writing in *Physical Review Letters*[1], take a fresh look at this long-standing puzzle.

To get an idea of what a quasicrystal looks like, one need only look at a mosaic of so-called Penrose tiles (Fig. 1). These patterns, invented by Roger Penrose in the 1970s, consist of two differently shaped tiles for which there are certain rules constraining how they can join edge-to-edge. These rules can be satisfied everywhere only if they are arranged in a tiling with five-fold rotational symmetry — the same as a regular pentagon. This symmetry is mathematically incompatible with forming a periodic pattern. The Penrose tiling is non-periodic: if you shift it by any amount to the right or left, or up or down, the pattern will never overlay the original exactly. Yet the sequence of tiles is not random either. It can be described by a finite sum of periodic functions the ratio of whose periods is irrational (it cannot be expressed as the ratio of two whole numbers) — a kind of spatial disharmony.

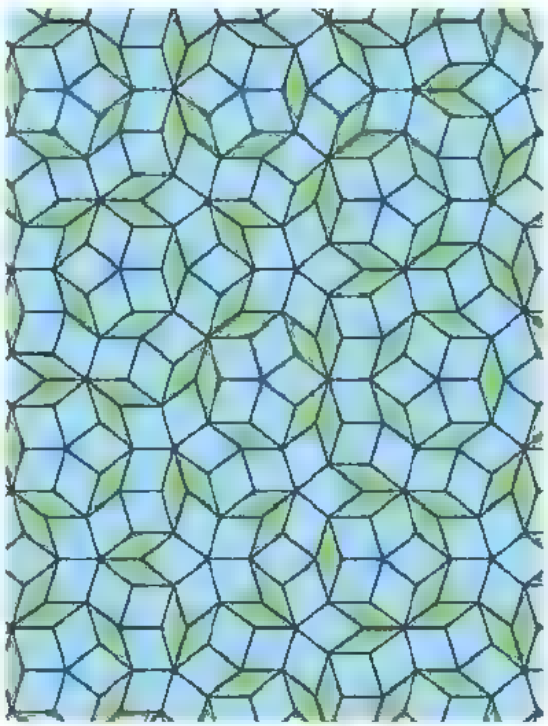

Figure 1 | Quasicrystalline mosaic. A Penrose tiling, which has five-fold symmetry, is constructed from two types of tile (blue and green), each decorated with white lines. The rules for joining the tiles edge-to-edge equate to requiring the lines to match and form a straight line across their common edge. Furthermore, for a site on the surface of the tiling to be 'sticky', the short-range forces between tiles require that there be only one way to add tiles that satisfies the rules. Keys and Glotzer[1] have modelled simple interatomic forces that cause atom clusters to arrange themselves in quasicrystal layers analogous to a Penrose tiling, but with 12-fold symmetry.

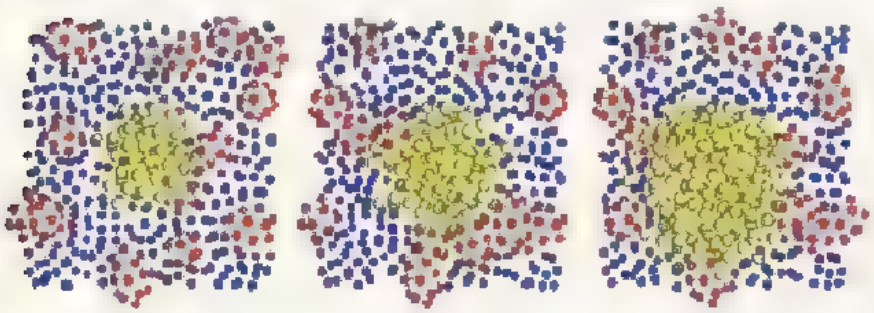

Figure 2 | Assimilation simulation. According to Keys and Glotzer's model[1], a quasicrystal nucleus (yellow atoms) grows from a bulk liquid (blue) by assimilating icosahedral clusters (red) whose formation is favoured in a supercooled liquid. (Atoms are shown at 60% of their actual size relative to the space they occupy.)

A similar sum of functions describes the arrangement of atoms in a quasicrystal solid.

In the quasicrystalline arrangement, no two atoms (or tiles) occupy equivalent positions: they might have the same arrangements of nearest neighbours, but if the surrounding atomic configurations are compared out to an arbitrary distance, differences inevitably crop up. Although Penrose's rules allow a perfect space-filling mosaic pattern to form, experimenting for a few minutes shows that actually constructing that pattern is difficult. Even if you begin from a seed cluster of tiles that is part of a perfect Penrose pattern, adding tiles randomly according to the rules leads to frequent mismatches and defects. The attachment of one tile may conflict with what is needed for the ideal configuration surrounding another tile a great distance away.

By analogy, for some time after the idea of quasicrystals was first proposed[2], it was argued that highly perfect quasicrystalline solids could never be formed. Physically unrealistic long-range interactions would be required to ensure that each atom attaches properly to its unique position. And indeed, the first quasicrystals observed in the laboratory[3] were highly imperfect.

Then, in 1988, theorists used Penrose tiles to show that local interactions suffice to grow perfect quasiperiodic patterns[4]. The proof relied on constructing short-range forces between tiles that allow perfect growth to occur stochastically: a vertex on the surface of a finite Penrose pattern is chosen at random and a tile is added depending on whether the interaction between the new tile and the existing tiles at the vertex is 'sticky' or 'non-sticky' according to short-range forces acting there. If the seed from which the tiling grows contains a particular kind of point-like topological defect, there are guaranteed to be sticky sites on the surface no matter how many tiles are added. A quasicrystal tiling can then grow rapidly ad infinitum without the need for any further defects or mismatches. Analogously, real atoms or groups of atoms should be able to attach to a seed atomic cluster when a quasicrystalline solid grows from a liquid.

Coincidentally, soon afterwards new combinations of elements were discovered (such as an alloy mixture of aluminium, iron and copper) that form large, faceted, highly perfect quasicrystals; many physical examples can now be grown in the laboratory[5]. Notably, it has also been shown that similar growth results can be obtained using a single decagonal (ten-sided) tile instead of the two Penrose tiles, and simpler local forces that distinguish sticky from non-sticky sites[6]. The relationship between these idealized mathematical studies of tilings and real quasicrystal growth has never been fully established.

Keys and Glotzer[1] use computer simulations to move the issue of quasicrystal growth out of the abstract realm of two-dimensional tilings, and into the more realistic world of atoms interacting in three dimensions. Their starting point is a supercooled liquid in which the interactions between pairs of atoms are governed by a simple, isotropic potential[7,8]. In the supercooled liquid, these potentials favour the formation of icosahedral (20-faced) clusters of atoms. In the solid state, a regular crystal will form under thermal-equilibrium conditions. On rapid supercooling, however, the outcome is a dodecagonal quasicrystal that has 12-fold symmetry in one plane and is periodic in its third dimension. The rapid growth of the quasicrystal occurs by the assimilation of icosahedral clusters from the liquid (Fig. 2) — a process similar in spirit to the production of two-dimensional tilings using only decagonal tiles and simple, short range forces[6].

Beginning from the same small seed nucleus each time, Keys and Glotzer show that they can repeatedly grow almost the same structure each time — near perfect quasicrystals — even though the growth process itself is stochastic, in the sense that the order in which the clusters join varies randomly from trial to trial. That indicates that the structure is strongly determined by the local forces between clusters in the liquid and those in the seed tiling. The imperfections correspond to 'phason defects', local rearrangements of atomic clusters relative to the ideal structure, whose positions vary from trial to trial, indicating an element of randomness. The authors do not make the connection between simulations and the abstract tiling studies, but their results are markedly similar to what would be found for mosaics if occasional violations of local rules and attachments to non-sticky sites were allowed.

One should be careful not to read too much into non-equilibrium simulations of a few thousand atoms, as this is a minute fraction of the number in a real quasicrystal sample. Nevertheless, the results raise many questions that should fuel future studies. Can the simple interatomic potential used by Keys and Glotzer — or other simple potentials — induce the growth of solids with truly long-range quasicrystalline order? If so, does that growth occur through local interactions that distinguish sticky and non-sticky sites on the seed cluster, in agreement with the tiling theory? If not, what mechanism accounts for the degree of order found in the simulations?

One way to explore these questions would be to study growth from a seed possessing a topological defect to see if it leads to the kind of perfect and reproducible results found with tilings[4]. One might also ask whether there are local growth rules for quasicrystals with symmetries other than the 12-fold symmetry of Keys and Glotzer's dodecahedra, and whether such growth processes can also be simulated with simple interatomic potentials. Then there is the issue of whether this analysis can be extended to the more realistic case of alloys of two or three elements.

Such investigations could provide a new understanding of why quasicrystals form, and make it possible to grow even more highly perfect quasicrystalline solids, as well as quasicrystalline colloids and more general self-assembled heterostructures. Intriguing as such studies are on a fundamental level, there is also a strong practical interest in understanding these materials: quasicrystalline solids are stronger and less deformable than normal crystals made of similar elements, and the photonic bandgap structure in some quasicrystal dielectric heterostructures might make them immensely valuable in circuits that work on the basis not of electrons, but of light. ■

Paul J. Steinhardt is in the Department of Physics and the Center for Theoretical Physics, Princeton University, Princeton, New Jersey 08544-0708, USA
e-mail: steinh@princeton.edu

1. Keys, A. S. & Glotzer, S. C. *Phys. Rev. Lett.* **99**, 235503 (2007)
2. Levine, D. & Steinhardt, P. J. *Phys. Rev. Lett.* **53**, 2477–2480 (1984)
3. Shechtman, D., Blech, I., Gratias, G. & Cahn, J. W. *Phys. Rev. Lett.* **53**, 1951–1953 (1984)
4. Onoda, G., Steinhardt, P. J., DiVincenzo, D. P. & Socolar, J. E. S. *Phys. Rev. Lett.* **60**, 2653–2656 (1988)
5. Suck, J. B., Schreiber, M. & Häussler, P. *Quasicrystals: An Introduction to Structure, Physical Properties and Applications* (Springer, Berlin, 2002)
6. Jacobson, L. Senior thesis, Princeton Univ. http://library.princeton.edu/theses/thesesid.asp?ID=14573 (2006)
7. Dzugutov, M. *Phys. Rev. Lett.* **70**, 2924–2927 (1993)
8. Dzugutov, M. *Phys. Rev. Lett.* **79**, 4043 (1997)

ARTICLES

Cyclical DNA methylation of a transcriptionally active promoter

Raphaël Métivier[1], Rozenn Gallais[1], Christophe Tiffoche[1], Christine Le Péron[1], Renata Z. Jurkowska[2], Richard P. Carmouche[3], David Ibberson[3], Peter Barath[1]†, Florence Demay[1], George Reid[3], Vladimir Benes[3], Albert Jeltsch[2], Frank Gannon[3]† & Gilles Salbert[1]

Processes that regulate gene transcription are directly under the influence of the genome organization. The epigenome contains additional information that is not brought by DNA sequence, and generates spatial and functional constraints that complement genetic instructions. DNA methylation on CpGs constitutes an epigenetic mark generally correlated with transcriptionally silent condensed chromatin. Replication of methylation patterns by DNA methyltransferases maintains genome stability through cell division. Here we present evidence of an unanticipated dynamic role for DNA methylation in gene regulation in human cells. Periodic, strand-specific methylation/demethylation occurs during transcriptional cycling of the *pS2/TFF1* gene promoter on activation by oestrogens. DNA methyltransferases exhibit dual actions during these cycles, being involved in CpG methylation and active demethylation of ^{5m}CpGs through deamination. Inhibition of this process precludes demethylation of the *pS2* gene promoter and its subsequent transcriptional activation. Cyclical changes in the methylation status of promoter CpGs may thus represent a critical event in transcriptional achievement.

Differential expression of the eukaryotic genome through cell differentiation or response to environmental changes requires specific modulation of its nuclear organization. These processes enable regulated genes to prevail against regulatory constraints of chromatin structure[1,2] in which DNA is wrapped around core nucleosomes consisting of octamers of histones H2A, H2B, H3 and H4 (refs 3, 4). Overcoming the structural restriction of chromatin upon gene expression is achieved in part through the modulation of particular marks that define active or inactive chromatin domains. DNA methyltransferases (Dnmts) establish and maintain the pattern of genomic DNA methylation on cytosines of CpG dinucleotides. This epigenetic mark is linked to gene repression: hypomethylated DNA is associated with active genes, whereas hypermethylated genes are silent[5]. Although gene expression correlates with CpG demethylation[6,7], processes that either remove the 5-methyl group or that exchange methylated cytosines (^{5m}C) with cytosines are unclear in metazoa. Only multiple rounds of cell division without Dnmt-mediated remethylation have been demonstrated to erase these epigenetic marks[8,9]. By contrast, plants have two glycosylase/lyases that initiate active ^{5m}C demethylation[10]. Post-translational modification of histones by acetyl transferases (HATs), deacetylases (HDACs) or methyl transferases (HMTs) modulate histone/histone and DNA/nucleosome contacts. In addition, specific patterns of histone modification define a code that dictates the sequential and dynamic recruitment of transcription factors[11]. Chromatin plasticity is further modulated by ATP-dependent complexes such as SWI/SNF or NuRD that rearrange nucleosome organization along the chromatin fibre[12].

Important insights into mechanisms of transcriptional regulation were recently obtained with studies on oestrogen-receptor-α (ERα; NR3A1)-driven gene expression[13,14]. ERα belongs to the nuclear receptor superfamily of transcription factors[15] and binds to cognate DNA sequences (oestrogen responsive elements, EREs). The binding of oestradiol (E_2) into a carboxy-terminal hydrophobic pocket of ERα induces three-dimensional modulation of surfaces that interact with cofactors[16]. Studies using chromatin immunoprecipitation (ChIP) demonstrated that, once recruited to target promoters, E_2-bound ERα induces an ordered and cyclical recruitment of coactivator complexes, some of which contain HAT, HMT or ATP-dependent remodelling activities[14]. We demonstrate here that Dnmt-dependent variations of the methylation status of CpGs within the *pS2* gene promoter are integral components of the 'transcriptional clock'[14] that controls the progression through these cycles (concluding scheme in Supplementary Fig. 10).

CpG methylation of active *pS2* promoter

In MDA-MB231 cells stably expressing ERα (MDA::ERα), transcriptional cycles of the *pS2* gene promoter in the presence of E_2 (10^{-8} M) mirror those already observed in MCF-7 cells[14], as evaluated through ChIP experiments on G0/G1 synchronized cells (72 h of serum deprivation) initially treated with 2.5 μM α-amanitin for 2 h. This pre-treatment generates an initially transcriptionally silent experimental background that facilitates the observation of the transcriptional cycles of the *pS2* promoter[14]. Significantly, the NuRD complex engages the promoter 2 h after E_2 addition, as indicated by the mobilization of its Mi2 component (Fig. 1a). We envisioned that DNA methylation may target NuRD to the promoter at this specific time, as NuRD includes ^{5m}CpGs-binding domain (MBD) containing proteins (MBPs), such as MBD2 and/or MBD3[17]. Accordingly, MBD2, MBD3 and MeCP2, another MBP, engage the *pS2* promoter (Fig. 1a) when transcription of the *pS2* gene is reduced (run-on experiments shown within Fig. 1b). Sequential-ChIP (Supplementary Fig. 1) and kinetic ChIP assays summarized in Fig. 1c demonstrate that MBD2 and MBD3 engage the promoter when Mi2 is also present, in agreement with an inclusion within NuRD[17]. By contrast, but in accordance with a previously identified interaction[18], MeCP2 is simultaneously recruited to the *pS2* promoter with SWI/SNF (as

[1]Université de Rennes I, CNRS, UMR 6026 Equipe SPARTE, IFR 140 GFAS, Campus de Beaulieu, 35042 Rennes cedex, France. [2]Jacobs University Bremen, Campus Ring 1, 28759 Bremen, Germany. [3]EMBL Meyerhofstrasse 1, D-69117 Heidelberg, Germany. †Present addresses: Cancer Research Institute, Slovak Academy of Sciences, Vlarska 7, SK-833 91 Bratislava, Slovak Republic (P.B.); Science Foundation Ireland, Wilton Park House, Wilton Place, Dublin 2, Ireland (F.G.)

defined by the recruitment of its Brg1 component) at the end of each transcriptionally productive cycle.

MBPs may cyclically engage the *pS2* gene promoter in consequence of variations in the methylation status of some CpGs, which was therefore evaluated through bisulfite sequencing. Within the 19 CpGs located between −701/+25 of the *pS2* promoter, some exhibit a constant methylation state: −654, −609, −601, −544 CpGs are methylated, the −443 unmethylated and the −301 apparently hemi-methylated (Fig. 1d; methylation pattern of sequenced clones within Supplementary Fig. 2). By contrast, the methylation status of the 13 remaining CpGs changes with kinetics not consistent with replication-induced methylation[5] (Supplementary Fig. 3). Strand-specific demethylation of the −519, −507, −399, −354, −84, −56, +11 and +17 CpGs occurs at the end of the first cycle. In addition, cytosines at positions −399, −56 and +11 are remethylated when the *pS2* promoter becomes transcriptionally quiescent (70–80 and 110–120 min). Cytosines at −181, −20, −13 and −9 have peak methylation at 120 min, coincident with the departure of ERα from the *pS2* promoter. The cytosine located on the non-coding strand at position −387 becomes methylated at 120 min, and then demethylated on initiation of the following transcriptional cycles. Methylation of the −9 and −20 CpGs at 120 min is not strand specific and may result in hemi-methylation or complete methylation. Importantly, the methylation pattern of the *pS2* promoter is reset by serum deprivation, and cycles of methylation of the *pS2* promoter are observed in cells that were not treated with α-amanitin (Supplementary Figs S3 and S4). Transcriptional regulation of the *pS2* gene therefore involves cyclical variation in CpG methylation, with initial demethylation of CpGs affecting only the transcribed strand.

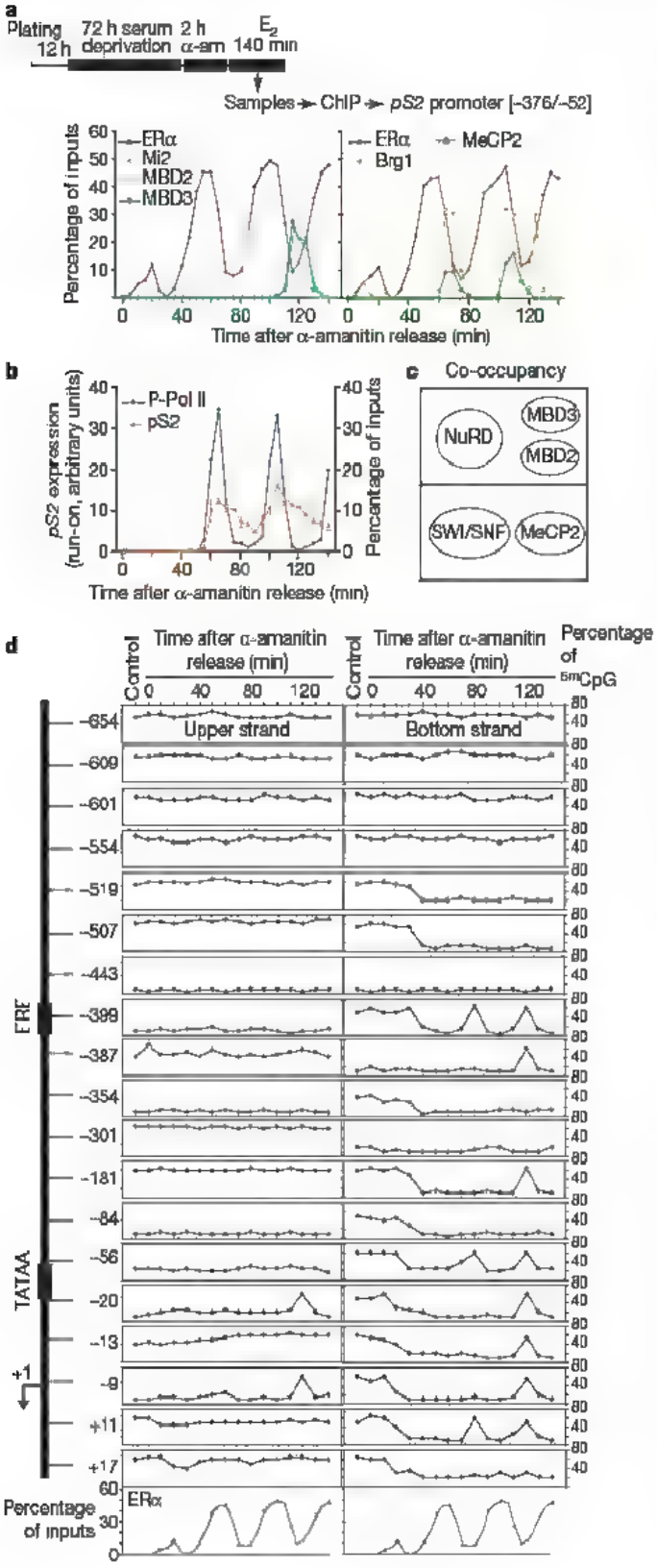

Figure 1 | Cyclical methylation of the *pS2* promoter. **a**, ChIP experiments were performed using the antibodies shown, on chromatin prepared from cells sampled at 5 min intervals after α-amanitin release (see flow chart). The amounts of immunoprecipitated *pS2* promoter (−376/−52) were quantified by real-time quantitative PCR (qPCR) and normalized to inputs. **b**, Run-on assays measuring *pS2* gene transcription. Data were normalized against control ribosomal phosphoprotein *RPLP0* (*PO*) messenger RNA, and presented as mean values ± s.e.m. ($n = 3$). Recruitment of phosphorylated polymerase II (P-Pol II) to the *pS2* promoter, as determined by ChIP, is also shown. **c**, Schematic summarizing sequential-ChIP experiments on the co-occupancy of the *pS2* promoter with MBPs, NuRD or SWI/SNF (Supplementary Fig. 1). **d**, Methylation status of individual CpG on upper (coding) and bottom (transcribed) strands as determined by bisulphite sequencing. 'Control' indicates initial methylation status before α-amanitin treatment. Occupancy of ERα to the *pS2* promoter, estimated by ChIP analysis, is indicated below.

Dual roles of Dnmts in *pS2* transcription

We then determined which Dnmt(s) were involved in methylation events through resolving their mobilization on the *pS2* promoter. Serum-deprived MDA::ERα cells were treated with 10 nM E_2 for 6 h. This is sufficient to observe an induction of *pS2* gene expression, and to generate a cell population in which we can observe all proteins that are present on E_2-activated *pS2* promoters. We detected an enrolment of Dnmt1, Dnmt3a and Dnmt3b, but not Dnmt2, on *pS2* promoters (Fig. 2a). Depletion of ERα protein, by treatment for 16 h with the ERα antagonist $ICI_{182,780}$ (ICI), reduced both *pS2* gene expression and the recruitment of Dnmt3a and 3b (Fig. 2a), indicating that conscription of these enzymes is linked to the transcriptional activity of the *pS2* gene. Addition of 1 μM 5-Aza-deoxycytidine (5-Aza-dC) for 24 h, which when incorporated into DNA prevents Dnmt action, stimulated the basal expression of the *pS2* gene, but reduced its induction by E_2. Conversely, treatment with 5-Aza-dC reduced recruitment of ERα and Dnmt3a in the presence of E_2, abrogated Dnmt1 engagement, and affected the mobilization of Dnmt3b to the *pS2* promoter (Fig. 2a). Sequential-ChIP experiments (Fig. 2b–d, summarized in Fig. 2e) indicate that, after E_2 exposure, and correlated with CpG methylation, *pS2* promoters are co-occupied by Dnmt1, MeCP2 and SWI/SNF, at the end of each transcriptionally productive cycle. In addition, at 80 and 105 min after oestrogenic stimulation, Dnmt3a/b are present on the *pS2* promoter. Significantly, Dnmt3a/b are also recruited at the beginning of each transcriptionally productive cycle, when demethylation of a subset of ^{5m}CpGs occurs.

These results suggest that Dnmt3a/b have roles in both methylation and demethylation. We used RG108, which directly blocks the activity of Dnmts without integrating into DNA[19,20], to probe the roles of Dnmts in the cyclical commitment of the *pS2* gene. Pre-treatment of MDA::ERα cells with RG108 for 1–8 h inhibited

induction of *pS2* gene transcription by E_2; however, *pS2* expression was increased two- to threefold after treatment for 24–72 h (Fig. 3a). Long-term exposure to RG108 also provoked re-expression of the *pS2* gene in native MDA cells, corroborating observations made using 5-Aza-dC[31]. RG108 did not affect expression of ERα (Supplementary Fig. 5). We then evaluated the impact of RG108 on the methylation status of three CCGG sites (−354, −84 and −20, Fig. 3b) using the methylation sensitive endonuclease *Hpa*II, which does not restrict hemi- or fully methylated $C^{5m}CGG$. Pre-treating cells with RG108 for 2 h before α-amanitin synchronization prevented demethylation of all three ^{5m}CpGs, whereas all became unmethylated after 72 h of RG108 pre-treatment (Fig. 3d). Additionally, co-treatment of MDA:ERα cells with RG108 and E_2 precluded the peak of methylation observed in E_2 treated cells at 120 min (Fig. 3d), without impairing the demethylation of the *pS2* promoter that occurs around 30–40 min after release from α-amanitin. Presumably, this would require almost all intracellular Dnmts to be inactivated by RG108, as it is likely to occur after the 2 h pre-treatment. Thus, RG108 provokes two transcriptional responses: (1) long-term stimulation, which may result from inhibition of CpG methylation occurring during cell replication, and (2) short-term inhibitory activity due to abrogation of cyclical methylation.

Transcriptional cycling of the *pS2* promoter is markedly affected by a 2 h pre-incubation with RG108 (Fig. 3e). In contrast to control

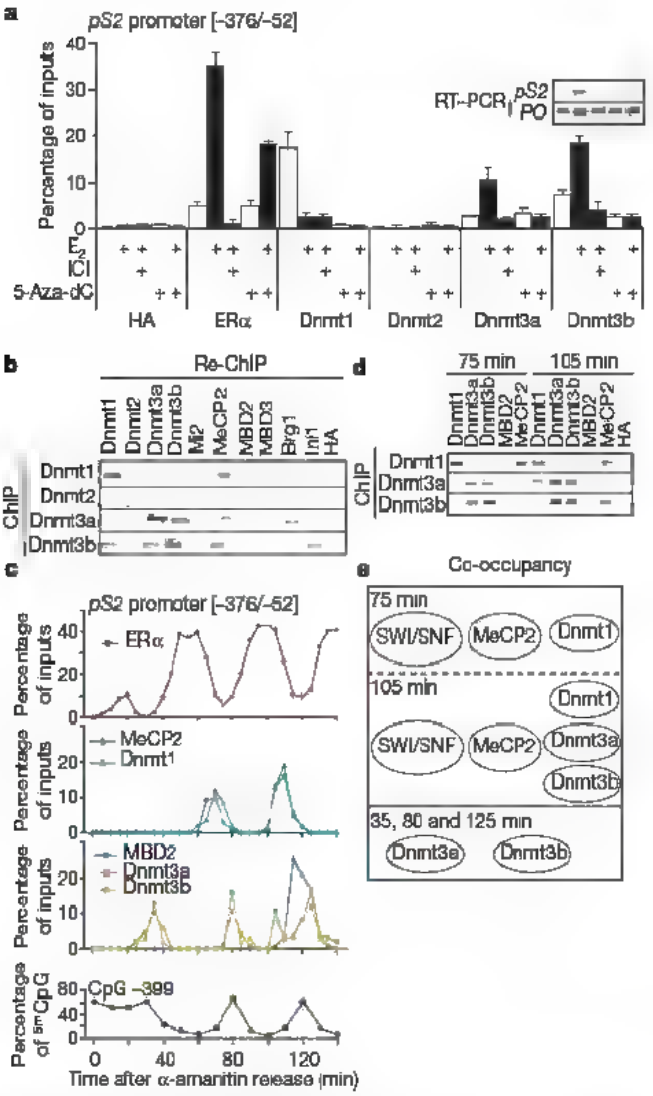

Figure 2 | Kinetic association of Dnmts with transcriptionally active *pS2* promoter in MDA::ERα cells. **a**, Cells were serum-deprived for 72 h and treated for 6 h with 10 nM E_2 or with ethanol (vehicle). When indicated, cells were pre-treated for 16 h with 1 μM $ICI_{182,780}$ or 24 h with 2 μM 5-Aza-deoxycytidine (5-aza-dC). The recruitment of ERα and Dnmts to the *pS2* promoter is shown as the percentage of *pS2* promoter bound to these proteins normalized to input and presented as means ± s.d. of two separated ChIP experiments performed in duplicate. HA antibody served as a negative control. In parallel, *pS2* and control *PO* mRNA amounts were evaluated by RT–PCR (inset). **b**, Sequential-ChIP analysis of chromatin prepared from cells after 72 h of serum deprivation and 6 h of treatment with 10 nM E_2. Antibodies used in the first ChIP are indicated on the left of the panel, and those used in the second ChIP (Re-ChIP) are on the top. **c**, Kinetic ChIP assays performed as in Fig. 1. **d**, Sequential-ChIP analysis of chromatin prepared from cells serum-deprived for 72 h, α-amanitin synchronized, and treated for 75 or 105 min with 10 nM E_2. **e**, Illustration of the co-occupancy of the *pS2* gene promoter with Dnmts and other proteins.

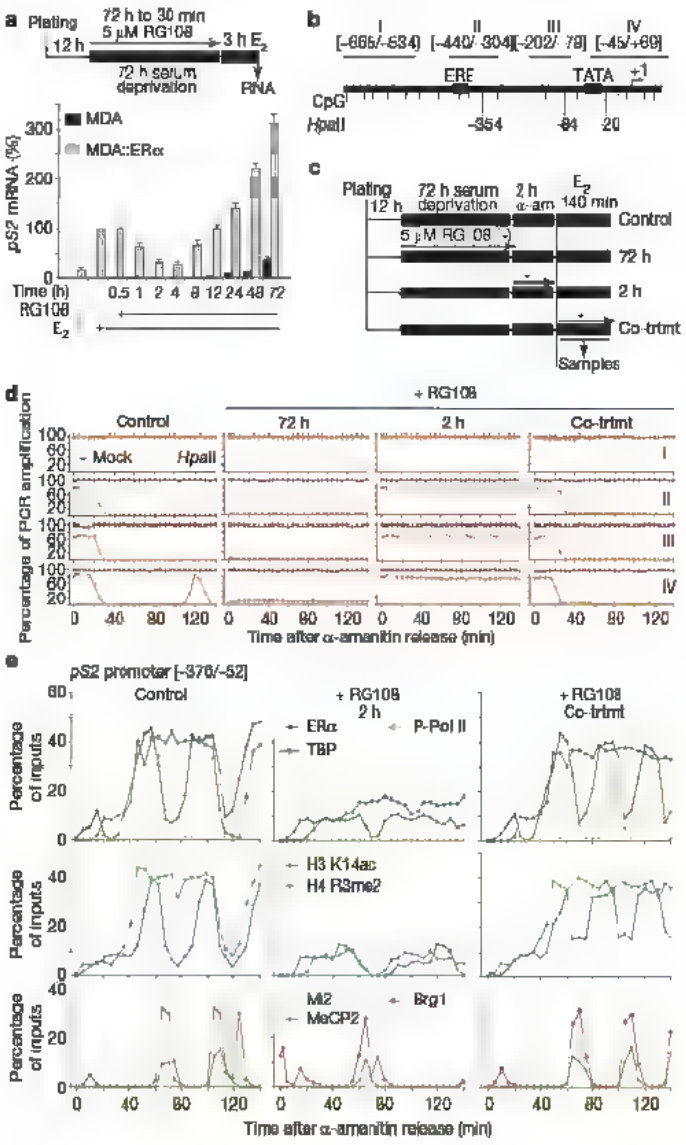

Figure 3 | Inhibition of Dnmt activity modifies *pS2* transcriptional cycling. **a**, qPCR of the relative expression of the *pS2* mRNA in MDA or MDA::ERα cells pre-treated for 0.5–72 h with 5 μM RG108 or DMSO before stimulation for 3 h with 10 nM E_2. Mean values ± s.e.m. obtained from three independent triplicate experiments are shown, normalized to *PO* mRNA. **b**, To analyse the methylation status of the CpGs located within the three CCGG *Hpa*II sites, restriction of the four depicted targets was evaluated by qPCR. Fragment I has no *Hpa*II site and served as internal control. **c**, Rationale of the different treatments subsequently performed: MDA::ERα cells were pre-treated or not with 5 μM RG108 (+), synchronized by α-amanitin and placed into medium containing 10 nM E_2 and 5 μM RG108 in the co-treatment condition (Co-trtmt). **d**, Genomic DNA prepared from cells sampled every 5 min after treatments was digested by *Hpa*II or not (Mock), and the four target sequences were amplified by real-time PCR. Results, expressed as the percentage of amplification, are mean values generated from assays repeated at least three times (s.d. less than 4%). **e**, Kinetic ChIP experiments using chromatin prepared from MDA::ERα cells treated as above.

(E_2 alone), the TATA-box binding protein (TBP) is never removed from the promoter in RG108-treated cells and phosphorylated RNA Polymerase II is never present (P-Pol II antibody; Fig. 3e). Also contrasting with control conditions, MeCP2 engages the promoter at the end of the first cycle, but NuRD never does (Mi2 protein; Fig. 3e). Furthermore, whereas Brg1 is recruited at the beginning of the first unproductive and second productive cycles to generate an appropriate nucleosomal conformation[14], Brg1 engages the promoter at the beginning of each cycle under RG108 treatment for 2 h. However, in these conditions, the inhibition of initial ^{5m}CpG demethylation prevents the *pS2* promoter chromatin structure from attaining a transcriptionally permissive state (data not shown). Co-treating cells with E_2 and RG108 reduces the periodicity of *pS2* transcriptional cycling from 50 to 35 min (Fig. 3e). Moreover, TBP and H4R3me2 are continuously present on the *pS2* promoter and NuRD is never recruited. These results are consistent with the hypotheses that (1) Dnmts have dual roles during transcriptional initiation of *pS2*; and that (2) the peak of methylation that occurs at 120 min after E_2 treatment serves as a signal for NuRD mobilization.

Coordinate actions of Dnmt3, TDG and BER

Bacterial Dnmts actively deaminate cytosine and ^{5m}C when methyl donor concentration is low[22,23]. Deaminated cytosines can be then repaired through base excision repair (BER). DNA glycosylases such as methyl-binding domain protein 4 (MBD4) or thymine DNA glycosylase (TDG) could recognize and cleave T:G mismatches generated by deamination of ^{5m}C. Generated abasic sites could then be repaired by the sequential activities of an AP endonuclease, DNA polymerase β, and a DNA ligase[24]. In accordance with such a mechanism, Dnmt3a associates with TDG in MDA::ERα cells (Supplementary Fig. 6), confirming previous observations[25,26]. The p68 RNA helicase (p68), a coactivator of ERα[27], also associated with TDG (Supplementary Fig. 6), in agreement with co-involvement in a putative 'demethylation' complex[28]. We therefore reasoned that if Dnmt3a/b were able to deaminate ^{5m}C, BER proteins might subsequently be recruited to the *pS2* promoter. This was evaluated through sequential-ChIP analysis on chromatin prepared from MDA::ERα cells treated with 10 nM E_2 for 6 h, after 72 h of serum deprivation (Fig. 4a), and through kinetic ChIPs on synchronized cells (Fig. 4b). A coordinated recruitment of Dnmt3a/b, TDG, p68, an AP endonuclease (REF-1), DNA polymerase β and DNA ligase I occurs at the beginning of each E_2-directed transcriptionally productive cycle of the *pS2* promoter (Fig. 4c). Additionally, short interfering RNA (siRNA) disruption of TDG expression for 72 h induced a 2.5-fold decrease in E_2-mediated induction of *pS2* gene transcription (Fig. 4d). This is associated with higher levels of methylation at positions −354, −84 and −20 (Fig. 4e). A reduction in TDG expression therefore impairs the demethylation process and reduces *pS2* promoter transcriptional activity.

We next assessed the potential deamination activity of Dnmt3a/b. Polymerase chain reaction (PCR)-synthesized DNA templates, fully methylated (M/M) or not (U/U) were treated with purified Dnmt3a/b catalytic domains. T:G or U:G mismatches resulting respectively from ^{5m}C or C deamination were then cleaved through treatment with UDG (uracil DNA glycosylase) that recognizes only U:G, or TDG that recognized both mismatches, followed by strand cleavage with NaOH. Two fragments from template DNA were amplified: a Φ control region devoid of CpG and a Σ test region whose amplification would be reduced if deamination and cleavage had occurred (Fig. 5a; additional controls within Supplementary Figs 7 and 8). We also controlled the ability of both Dnmt3 catalytic domains to methylate the U/U probe. Amplification of the Σ fragment after *Hpa*II restriction in the presence of S-adenosyl methionine (SAM) (Fig. 5b) reflected the methylation state of the probe and validated our experimental settings. Although TDG has been proposed to have ^{5m}C DNA glycosylase activity[28], this was not detected in our *in vitro* system. The amplification of the Σ fragment after TDG action on U/U or M/M probes (Fig. 5c) was reduced by Dnmt3a, and RG108 abrogated TDG-mediated cleavage of these templates. This indicated that deamination of cytosines and ^{5m}C was occurring. This activity might also explain Dnmt3a-mediated protection against *Hpa*II digestion observed within Fig. 5b in the absence of SAM. In agreement with their ability to increase the rate of CpG deamination by bacterial Dnmts[22,23], the SAM analogues sinefungin (Sinf) and 5′-aminoadenosine (AA) further reduced amplification of the Σ fragment (Fig. 5c). Under these conditions, the Dnmt3b catalytic domain was able to catalyse C and ^{5m}C deamination only in the presence of SAM analogues. UDG-mediated reduction of the Σ/Φ ratio was detected only on the U/U probe (Fig. 5c), thereby confirming that the observed cleavages are consequences of deamination events, and not of other base modifications that could be processed by TDG, which has a broader spectrum of glycosylase activity. Finally, 36% or 26% of probes incubated with Dnmt3a or Dnmt3b, respectively, harboured at least one C/T or G/A mutation within CpG motifs, thereby confirming that both proteins are able to deaminate C and ^{5m}C (Fig. 5d, e). These values agree with the PCR experiments (Fig. 5c), in which only one deamination event would prevent the amplification of the Σ fragment. Interestingly, within the 465 sequences analysed, all but two C and ^{5m}C mutations were within CpGs motifs. These two C to T transitions were observed within CpApG trinucleotides after Dnmt3b action on methylated probe, likely reflecting its ability to recognize and methylate CpA motifs[29]. Sequencing Dnmt3-treated DNA templates confirmed that, *in vitro*, Dnmt3s exhibit deamination activity. No statistically relevant preference for particular CpGs was detectable.

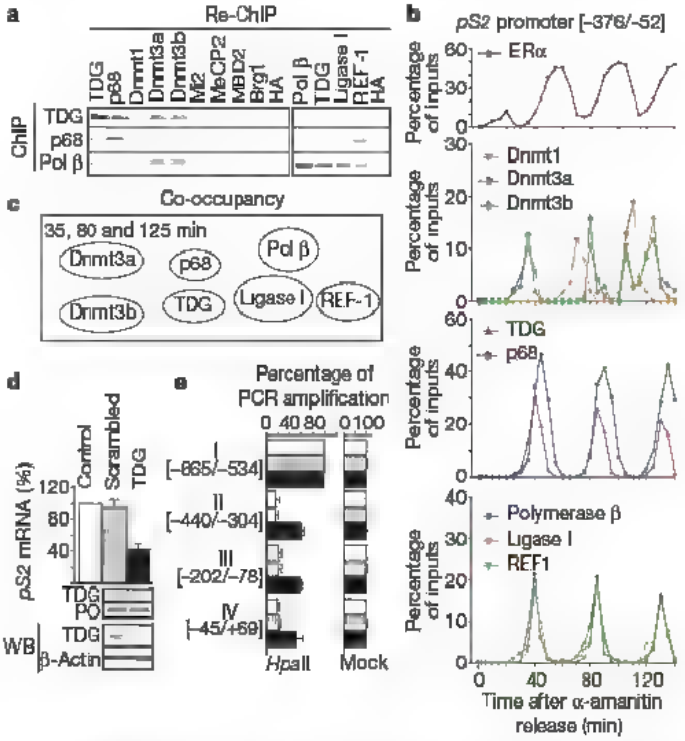

Figure 4 | Mobilization of TDG, p68, Dnmt3a/b and BER proteins during *pS2* promoter demethylation. **a**, Chromatin prepared from MDA::ERα cells serum-deprived for 72 h and treated for 6 h with 10 nM oestradiol (E_2) was used in sequential-ChIP experiments. **b**, Kinetic ChIP experiments performed as in Fig. 1. **c**, Scheme illustrating complexes co-recruited to the *pS2* promoter. **d**, **e**, MDA::ERα cells were transfected or not with scrambled siRNAs or siRNAs targeting TDG for 48 h, and then treated for 6 h with 10 nM E_2. Independent duplicate experiments were performed twice. Cells were then harvested for protein extraction and subsequent western blot experiments (WB, complete image in Supplementary Fig. 5), RNA preparation and RT–PCR of the indicated gene expression (mean values ± s.e.m. of qPCR are shown as the percentage of amplification, with 100% ascribed to the control sample value), or genomic DNA preparation to analyse the methylation status of the CpGs included in the three *Hpa*II sites.

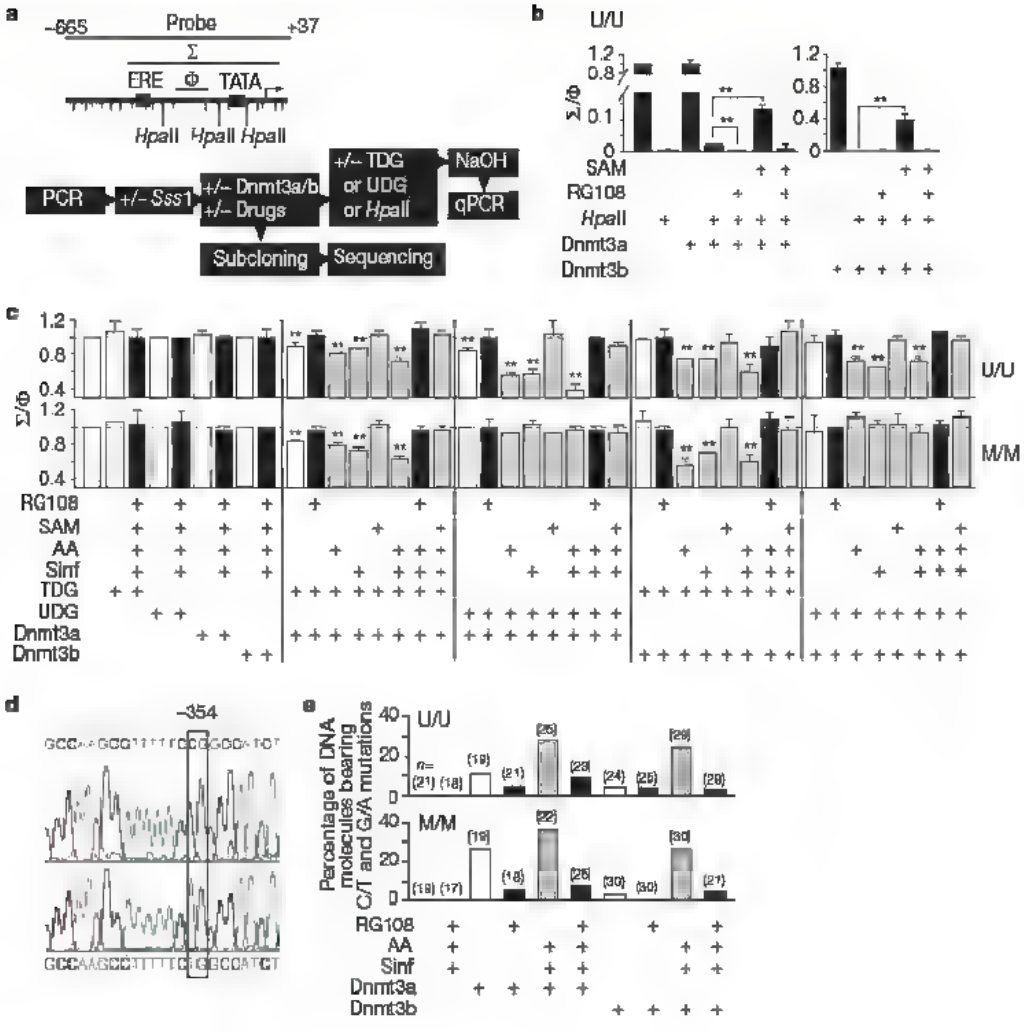

Figure 5 | Dnmt3a/b deaminate CpGs and ^{5m}CpGs. **a**, Scheme summarizing the *in vitro* deamination/methylation assays. Double-stranded probes (unmethylated or methylated; U/U and M/M, respectively) were incubated with purified wild-type Dnmt3a or Dnmt3b catalytic domain (**b** and **c**). Combinations of S-adenosyl methionine (SAM), 5′-aminoadenosine (AA), sinefungin (Sinf), RG108 or their corresponding solvents were included in the reactions, as indicated. Abasic sites generated by TDG or UDG after Dnmt3a-mediated deamination were cleaved by NaOH. Dnmt3a/b methylation activity was controlled by *Hpa*II digestion (**b**). Digested probes were subjected to real-time PCR of the Σ or control Φ fragments. Σ/Φ ratios are shown as mean values ± s.e.m. of experiments done at least three times in duplicate. Asterisks denote significant differences (**$P < 0.001$, by Student's *t*-test) between paired conditions (**b**) or with control samples (**c**). **d**, **e**, After incubation with Dnmt3s and drugs, probes were sequenced to check C/T and G/A mutations, which are indicative of C and ^{5m}C deamination occurring on either DNA strand. The number of sequences harbouring at least one mutation (illustrated on the sequence in **d**, characterized after Dnmt3a action), is summarized in **e**, with the number of sequenced clones in brackets.

Discussion

We show that CpG methylation is not only a stable epigenetic mark but also an integral component of transcription. Dynamic demethylation/methylation processes are inherent to transcriptional cycling of the *pS2* gene. The role of methylation in transcription might be an important feature for a significant proportion of genes, as we observed transcriptional cycling and methylation cycles on another ERα target gene, *Wisp-2*[30] (Supplementary Fig. 9).

Methylation of CpGs, which occurs at the end of each transcriptionally productive cycle (75 and 105 min after promoter synchronisation), is correlated with the presence of MeCP2, SWI/SNF, Dnmt1 and Dnmt3a/b on the *pS2* promoter. This is in accordance with a coordinated action of Dnmt3a/b and Dnmt1[31] on the remethylation of CpGs. Demethylation of *pS2* promoter CpGs involves the coordinate recruitment of Dnmt3a/b, p68, TDG and BER proteins. A reported association of ERα with TDG resulted in transcriptional activation of reporter genes, but this did not require a functional TDG catalytic domain[32]. However, others have shown that ERα interaction with TDG increases the glycosylase activity of the enzyme[33], with TDG suggested to be required for the hormonal control of transcription of a methylated template[34]. Although we cannot exclude an involvement of other proteins in demethylation, the concordant recruitment of TDG with BER proteins is in favour of a role for TDG in DNA repair after deamination, rather than in a coactivator role. We describe that, *in vitro*, Dnmt3a/b are able to deaminate cytosine and ^{5m}C. It is possible that, *in vivo*, selectivity towards ^{5m}CpGs might be imposed by local histone modifications, through association with proteins that transduce these marks, such as HP1[35]. Alternatively, as we performed these experiments with isolated catalytic domains and not full-length Dnmt3a/b, because of protein production and purity requirements, it is possible that their amino-terminal regions might direct the catalytic domain to given sites[36]. Recruitment of Dnmt3a/b is generally associated with targeted methylation of CpGs[37], as illustrated by their concomitant recruitment with MeCP2 and SWI/SNF at specific steps of the transcriptional cycles of the *pS2* promoter. This implies that Dnmt3a/b function in two alternative modes, involved in either cytosine methylation or deamination. The association of Dnmt3a/b with TDG and/or p68 may influence their activities, as Dnmt3a stimulates the glycosylase activity of TDG, whereas TDG inhibits the methylation activity of Dnmt3a *in vitro*[25]. Alternatively, it cannot be excluded that active Dnmt3a/b are required for the recruitment of an as yet unidentified deaminase.

Although reports have suggested rapid changes in CpG methylation[38], fast cyclical variation of CpG methylation is unanticipated and provides an additional level of regulation to genome expression. Demethylation of transcribed promoter DNA by Dnmt3a/b, TDG and BER complex could generate mismatches and strand-specific breaks that, if incorrectly repaired, would lead to mutations. DNA strand breaks or DNA repair processes have been reported during demethylation of CpGs in other experimental systems[39,40]. CpG methylation also influences the activity of topoisomerases[41] that generate and then repair double-strand DNA breaks in the early phase of *pS2* promoter cycling[42]. Understanding how these processes are linked and integrated is necessary to understand mechanisms underlying transcription commitment and attainment. Furthermore, the dual role of Dnmts in cyclical methylation expands the current understanding of the propagation and regulation of epigenetic marks through cell division and differentiation.

METHODS SUMMARY

Sequencing of bisulphite-modified DNA was performed on at least 25 clones generated in two to three independent bisulphite modifications. All ChIP assays shown are representative of experiments performed with minor modifications from our previous work[14], and repeated at least twice, with reproducible patterns (s.d. less than 5%). PCRs illustrated are representative of experiments performed at least three times. For the PCR with reverse transcription (RT–PCR) illustrated as gel pictures, PCR reactions were performed in semi-quantitative conditions, with 26–27 cycles being within the exponential phase of the amplification. As only a binary output is expected from sequential-ChIP experiments, PCRs performed on these samples followed 30–32 cycles of amplification, and are therefore only qualitative, answering the question of whether two proteins are co-recruited to the *pS2* promoter or not.

Full Methods and any associated references are available in the online version of the paper at www.nature.com/nature.

Received 21 September; accepted 12 December 2007.

1. Spector, D. L. The dynamics of chromosome organization and gene regulation. *Annu. Rev. Biochem.* 72, 573–608 (2003).
2. Casolari, J. M., Brown, C. R., Drubin, D. A., Rando, O. J. & Silver, P. A. Developmentally induced changes in transcriptional program alter spatial organization across chromosomes. *Genes Dev.* 19, 1188–1198 (2005).
3. Khorasanizadeh, S. The nucleosome: from genomic organization to genomic regulation. *Cell* 116, 259–272 (2004).
4. Dillon, N. Gene regulation and large-scale chromatin organization in the nucleus. *Chromosome Res.* 14, 117–126 (2006).
5. Klose, R. J. & Bird, A. P. Genomic DNA methylation: the mark and its mediators. *Trends Biochem. Sci.* 31, 89–97 (2006).
6. Oswald, J. *et al.* Active demethylation of the paternal genome in the mouse zygote. *Curr. Biol.* 10, 475–478 (2000).
7. Murayama, A. *et al.* A specific CpG site demethylation in the human interleukin 2 gene promoter is an epigenetic memory. *EMBO J.* 25, 1081–1092 (2006).
8. Rougier, N. *et al.* Chromosome methylation patterns during mammalian preimplantation development. *Genes Dev.* 12, 2108–2113 (1998).
9. Matsuo, K. *et al.* An embryonic demethylation mechanism involving binding of transcription factors to replicating DNA. *EMBO J.* 17, 1446–1453 (1998).
10. Morales-Ruiz, T. *et al.* Demeter and Repressor of Silencing 1 encode 5-methylcytosine DNA glycosylases. *Proc. Natl Acad. Sci. USA* 103, 6853–6858 (2006).
11. Kouzarides, T. Chromatin modifications and their function. *Cell* 128, 693–705 (2007).
12. Becker, P. B. & Horz, W. ATP-dependent nucleosome remodeling. *Annu. Rev. Biochem.* 71, 247–273 (2002).
13. Shang, Y., Hu, X., DiRenzo, J., Lazar, M. A. & Brown, M. Cofactor dynamics and sufficiency in estrogen receptor-regulated transcription. *Cell* 103, 843–852 (2000).
14. Metivier, R. *et al.* Estrogen receptor-alpha directs ordered, cyclical, and combinatorial recruitment of cofactors on a natural target promoter. *Cell* 115, 751–763 (2003).
15. Robinson-Rechavi, M., Escriva Garcia, H. & Laudet, V. The nuclear receptor superfamily. *J. Cell Sci.* 116, 585–586 (2003).
16. Brzozowski, A. M. *et al.* Molecular basis of agonism and antagonism in the oestrogen receptor. *Nature* 389, 753–758 (1997).
17. Zhang, Y. *et al.* Analysis of the NuRD subunits reveals a histone deacetylase core complex and a connection with DNA methylation. *Genes Dev.* 13, 1924–1935 (1999).
18. Harikrishnan, K. N. *et al.* Brahma links the SWI/SNF chromatin-remodeling complex with MeCP2-dependent transcriptional silencing. *Nature Genet.* 37, 254–264 (2005).
19. Christman, J. K. 5-Azacytidine and 5-aza-2′-deoxycytidine as inhibitors of DNA methylation: mechanistic studies and their implications for cancer therapy. *Oncogene* 21, 5483–5495 (2002).
20. Brueckner, B. *et al.* Epigenetic reactivation of tumor suppressor genes by a novel small-molecule inhibitor of human DNA methyltransferases. *Cancer Res.* 65, 6305–6311 (2005).
21. Sharma, D., Saxena, N. K., Davidson, N. E. & Vertino, P. M. Restoration of tamoxifen sensitivity in estrogen receptor-negative breast cancer cells: tamoxifen-bound reactivated ER recruits distinctive corepressor complexes. *Cancer Res.* 66, 6370–6378 (2006).
22. Zingg, J. M., Shen, J. C., Yang, A. S., Rapoport, H. & Jones, P. A. Methylation inhibitors can increase the rate of cytosine deamination by (cytosine-5)-DNA methyltransferase. *Nucleic Acids Res.* 24, 3267–3275 (1996).
23. Sharath, A. N., Weinhold, E. & Bhagwat, A. S. Reviving a dead enzyme: cytosine deaminations promoted by an inactive DNA methyltransferase and an S-adenosylmethionine analogue. *Biochemistry* 39, 14611–14616 (2000).
24. Waters, T. R., Gallinari, P., Jiricny, J. & Swann, P. F. Human thymine DNA glycosylase binds to apurinic sites in DNA but is displaced by human apurinic endonuclease 1. *J. Biol. Chem.* 274, 67–74 (1999).
25. Li, Y. Q., Zhou, P. Z., Zheng, X. D., Walsh, C. P. & Xu, G. L. Association of Dnmt3a and thymine DNA glycosylase links DNA methylation with base-excision repair. *Nucleic Acids Res.* 35, 390–400 (2007).
26. Gallais, R. *et al.* Deoxyribonucleic acid methyl transferases 3a and 3b associate with the nuclear orphan receptor COUP-TFI during gene activation. *Mol. Endocrinol.* 21, 2085–2098 (2007).
27. Endoh, H. *et al.* Purification and identification of p68 RNA helicase acting as a transcriptional coactivator specific for the activation function 1 of human estrogen receptor alpha. *Mol. Cell Biol.* 19, 5363–5372 (1999).
28. Jost, J. P. *et al.* A chicken embryo protein related to the mammalian DEAD box protein p68 is tightly associated with the highly purified protein-RNA complex of 5-MeC-DNA glycosylase. *Nucleic Acids Res.* 27, 3245–3252 (1999).
29. Suetake, I., Miyazaki, J., Murakami, C., Takeshima, H. & Tajima, S. Distinct enzymatic properties of recombinant mouse DNA methyltransferases Dnmt3a and Dnmt3b. *J. Biochem.* 133, 737–744 (2003).
30. Fritah, A., Redeuilh, G. & Sabbah, M. Molecular cloning and characterization of the human WISP-2/CCN5 gene promoter reveal its upregulation by oestrogens. *J. Endocrinol.* 191, 613–624 (2006).
31. Fatemi, M., Hermann, A., Gowher, H. & Jeltsch, A. Dnmt3a and Dnmt1 functionally cooperate during de novo methylation of DNA. *Eur. J. Biochem.* 269, 4981–4984 (2002).
32. Chen, D. *et al.* T·G mismatch-specific thymine-DNA glycosylase potentiates transcription of estrogen-regulated genes through direct interaction with estrogen receptor alpha. *J. Biol. Chem.* 278, 38586–38592 (2003).
33. Jost, J. P., Thiry, S. & Siegmann, M. Estradiol receptor potentiates, *in vitro*, the activity of 5-methylcytosine DNA glycosylase. *FEBS Lett.* 527, 63–66 (2002).
34. Zhu, B. *et al.* 5-methylcytosine-DNA glycosylase activity is present in a cloned G/T mismatch DNA glycosylase associated with the chicken embryo DNA demethylation complex. *Proc. Natl Acad. Sci. USA* 97, 5135–5139 (2000).
35. Fuks, F. DNA methylation and histone modifications: teaming up to silence genes. *Curr. Opin. Genet. Dev.* 15, 490–495 (2005).
36. Oka, M., Rodic, N., Graddy, J., Chang, L. J. & Terada, N. CpG sites preferentially methylated by Dnmt3a *in vivo*. *J. Biol. Chem.* 281, 9901–9908 (2006).
37. Li, F. *et al.* Chimeric DNA methyltransferases target DNA methylation to specific DNA sequences and repress expression of target genes. *Nucleic Acids Res.* 35, 100–112 (2007).
38. Lucarelli, M., Fuso, A., Strom, R. & Scarpa, S. The dynamics of myogenin site-specific demethylation is strongly correlated with its expression and with muscle differentiation. *J. Biol. Chem.* 276, 7500–7506 (2001).
39. Kress, C., Thomassin, H. & Grange, T. Active cytosine demethylation triggered by a nuclear receptor involves DNA strand breaks. *Proc. Natl Acad. Sci. USA* 103, 11112–11117 (2006).
40. Barreto, G. *et al.* Gadd45a promotes epigenetic gene activation by repair-mediated DNA demethylation. *Nature* 445, 671–675 (2007).
41. Leteurtre, F. *et al.* Effects of DNA methylation on topoisomerase I and II cleavage activities. *J. Biol. Chem.* 269, 7893–7900 (1994).
42. Ju, B. G. *et al.* A topoisomerase IIbeta-mediated dsDNA break required for regulated transcription. *Science* 312, 1798–1802 (2006).

Supplementary Information is linked to the online version of the paper at www.nature.com/nature.

Acknowledgements We thank B. Brueckner for the gift of the RG108 compound, P. Chambon for the pSG5-TDGwt plasmid, F. Fuller-Pace for the anti-p68 RNA helicase antibody, and V. Legagneux and U. K. Laemmli for the anti-CAPD2 and anti-CAPH antibodies, respectively. This work was supported by funds from the Ministère de l'Education Nationale de l'Enseignement Supérieur et de la Recherche (MENESR), the Centre National de la Recherche Scientifique (CNRS), the University of Rennes I, the Association pour la Recherche contre le Cancer (ARC), the Ligue contre le Cancer, and by funding from EMBO and EMBL. R.G. was supported by a grant from the MENESR and a fellowship from the Ligue Nationale Contre le Cancer. We also thank C. Rallière for DNA sequencing, C. Martin, F. Percevault and C. Tascon for their technical assistance, and B.Stride and S. Kangaspeska for their comments during the writing of the manuscript.

Authors Contributions ChIP, sequential-ChIP experiments, bisulphite and run-on assays were performed by R.M. Methylation/deamination assays were set up by R.G. and performed by R.G. and R.M. C.T. ran all RT-PCR experiments on siRNA-treated cells, and set up the analysis on the *Wisp-2* gene. Co-immunoprecipitations and proteomic controls were performed by C.L.P., R.G. and R.M. Synthesis and purification of TDG protein were performed by P.B. and F.D., as the preparation of the anti-TDG antibody. R.Z.J. purified all the Dnmt3 catalytic domains. R.P.C. and D.I. were involved, under the supervision of V.B., in the mass sequencing of the clones generated during the bisulphite-mediated analysis of CpG methylation and through the *in vitro* deamination assays. G.R. introduced R.M. to FACS analysis and bisulphite-modification of DNA. R.M., G.R., A.J., F.G. and G.S. were responsible for the overall project management, strategy and data interpretation. R.M., G.R. and G.S. prepared the manuscript. All authors discussed the results and commented on the manuscript.

Author Information Reprints and permissions information is available at www.nature.com/reprints. Correspondence and requests for materials should be addressed to R.M. (Raphael.Metivier@univ-rennes1.fr).

ARTICLES

The MC-Fold and MC-Sym pipeline infers RNA structure from sequence data

Marc Parisien[1] & François Major[1]

The classical RNA secondary structure model considers A•U and G•C Watson–Crick as well as G•U wobble base pairs. Here we substitute it for a new one, in which sets of nucleotide cyclic motifs define RNA structures. This model allows us to unify all base pairing energetic contributions in an effective scoring function to tackle the problem of RNA folding. We show how pipelining two computer algorithms based on nucleotide cyclic motifs, MC-Fold and MC-Sym, reproduces a series of experimentally determined RNA three-dimensional structures from the sequence. This demonstrates how crucial the consideration of all base-pairing interactions is in filling the gap between sequence and structure. We use the pipeline to define rules of precursor microRNA folding in double helices, despite the presence of a number of presumed mismatches and bulges, and to propose a new model of the human immunodeficiency virus-1 −1 frame-shifting element.

The number of RNAs found to be involved in non-coding cellular roles is increasing rapidly and persistently[1,2], and many RNA transcripts of unknown function have recently been detected in eukaryotic cell maps[3]. RNAs can be grouped into families that share structural features and function. Therefore, unravelling the structure provides crucial insights into the way in which RNA works. However, producing RNA high-resolution structures by X-ray crystallography and NMR spectroscopy is slow compared to sequencing, thus creating an important gap between the number of known tertiary (three-dimensional, 3D) structures[4] and that of sequences[5].

In the search for an effective RNA structure-determination approach, we examined different theoretical schemes and studied their relative merit to attain our goal. Hope came from the fact that secondary structures would provide enough structural constraints to automate 3D building[6]. A secondary structure describes the stems of RNA—crucial building blocks that form when two complementary regions of the sequence base pair and adopt a double-helix structure. A legitimate approximation of secondary structures considers stems that consist of A•U and G•C Watson–Crick base pairs as well as G•U wobble base pairs. These base pairs are called 'canonicals'.

Secondary structures can be derived from a sequence by using a combination of free-energy minimization[7] and covariation analysis[8]. However, the presence of a few key non-canonical base pairs blurs predictions, because they contribute energies and complicate covariation interplay[9]. Even when experimental data are considered (for example, enzymatic or chemical probing), selecting the native amongst many suboptimal secondary structures remains elusive[10]. More importantly, secondary structures deprived of non-canonical base pairs are neither adequate to determine 3D structures nor sufficient to faithfully align sequences of the same family[6,11,12]. Recent attempts to replace thermodynamics by statistical scores resulted in either similar[13] or only slightly improved[14] predictive power. Furthermore, empirical scoring of 3D structures applies only to very short sequences and requires covariation data[4,5]. Taken together, these shortcomings and increasing needs for RNA genome-wide annotation prompted us to develop a new approach.

We extended the classical rationale underlying RNA structure prediction by incorporating all base pairs. To do so, we introduced a new first-order object to represent nucleotide relationships in structured RNAs: the nucleotide cyclic motif (NCM). The NCMs became apparent to us from an analysis of the X-ray crystallographic structure of the 23S ribosomal RNA of *Haloarcula marismortui*[16]. Adjacent NCMs share common base pairs—a property providing enough base-pairing context information to derive an effective scoring function and making possible the use of the same algorithm for predicting secondary and tertiary structures.

We propose a new RNA-structure-prediction method based on NCMs, implemented as a pipeline of two computer programs: MC-Fold and MC-Sym (Supplementary Fig. 1). We illustrate the predictive power of the pipeline by reproducing experimentally determined 3D structures from a single sequence, building 3D structures of precursor microRNA (pre-miRNA) that are compatible with Dicer docking, and proposing a new 3D structure of the human immunodeficiency virus (HIV-1) *cis*-acting −1 frame-shifting element. In practice, judicious pipeline predictions from a single sequence are expected for fragments of up to approximately 150 nucleotides.

Folding single sequences

We evaluated the predictive power of MC-Fold by comparing the base pairs in the lowest-energy (best) predicted structure of each sequence with those found in experimental hairpin loop structures (Table 1). Compared to the thermodynamic approach, MC-Fold predicts over 6% more canonical base pairs, despite a lower positive predictive value, concurrently makes less false positives and negatives, and obtains a higher Matthews correlation coefficient ratio (MCCR) (see Supplementary Table 1). In addition, the optimal solution for each hairpin includes more than 60% of the non-canonical base pairs, and this number goes up to more than 80% if the top five solutions are considered. The low rate of false negatives is a prerequisite for building 3D structures.

We evaluated the predictive power of the MC-Fold and MC-Sym pipeline by analysing and comparing the best predictions for thirteen experimental 3D structures (Table 2). Eleven of the thirteen examples rank first (that is, match the lowest-energy structure). Eight of the thirteen examples have MCCRs of 100% (average = 98.2%). Seven of

[1]Institute for Research in Immunology and Cancer (IRIC), Department of Computer Science and Operations Research, Université de Montréal, PO Box 6128, Downtown Station, Montréal, Québec H3C 3J7, Canada

Table 1 | MC-Fold predictive power

Predicted base pairs (%)	Zipper (lower bound)	RNAsubopt (thermodynamics)	MC-Fold (NCM)
PPV $= \frac{TP}{(TP + FP)}$	59.6	**91.8**	83.4
STY $= \frac{TP}{(TP + FN)}$	74.1	74.8	**89.9**
Matthews $= \sqrt{\frac{TP}{(TP+FN)}\frac{TP}{(TP+FP)}}$	66.5	82.9	**86.6**

Best predictions over 2,093 base pairs (1,784 canonical base pairs) in 264 hairpin loops extracted from 182 different PDB structures. Columns show programs and rows show coefficients. Zipper is a program that implements a greedy algorithm that folds a sequence from bottom-up using exclusively tandems of base pairs. This gives a lower bound on the predictive power. RNAsubopt implements the current thermodynamics model and enumerates systematically all suboptimal structures. The numbers of nucleotides in these hairpin loops vary from 8 to 35 base pairs (average = 19.6). The best value for each row is shown in bold. FN, number of false negatives; FP, number of false positives; TP, number of true positives; Matthews, Matthews correlation coefficient ratio; PPV, positive predictive value; and STY, sensitivity.

Table 2 | MC-Fold and MC-Sym pipeline predictive power

RNA (PDB code)	Size (nucleotides)	Rank	Matthews (%)	r.m.s.d. (Å)
Hairpins				
Loop E (430D†)	29	1	100	1.7
IRE (1NBR)	29	1	100	2.4
Classical swine fever virus IRES domain III (2HUA*)	40	4	100	2.6
RNA thermometer (2GIO*)	29	1	100	1.7
Eel *UnaL2* LINE 3′ element (2FDT*)	36	1	100	2.0
Telomerase RNA domain IV (2FEY*)	43	1	94	3.3
RNase P RNA P4 (2CD1*)	27	2	96	2.1
GNYA tetraloop (2EVY*)	14	1	100	1.8
U2 snRNA (2O33*)	20	1	100	2.0
Group II intron branchsite (2AHT*)	27	1	96	1.9
Y-shape				
Hammerhead ribozyme (1NYI†)	36	1	100	2.7
5S rRNA (2HGH*)	47	1	96	2.9
Pseudo-knot				
Yellow leaf virus (2AP5*)	18	1	94	2.7

The MC-Fold and MC-Sym pipeline is applied to single sequences. Three different RNA topologies were tested: hairpin, multi-branch (Y-shape) and pseudo-knot. The best predictions (best MCCRs) are reported. The r.m.s.d. values were calculated over all heavy atoms. The average MC-Fold real time for all but one sequence is 7 s on a typical workstation processor (AMD Athlon 64, 2.2 GHz); real time for the 5S rRNA sequence is 143 s. The best 3D models are selected amongst all models generated using a probabilistic search over a period of 12 h.
* A recent NMR structure.
† X-ray crystallographic structure.

the thirteen examples combine first rank and 100% MCCRs. The average root mean squared deviations[17] (r.m.s.d.) of the thirteen examples when optimally superimposed on their corresponding experimental structures are near 2 ångströms (Å) (Fig. 1). The nucleotides that increase the r.m.s.d. are those with more degrees of freedom, that is, those not involved in base-pairing interactions (see, for instance, nucleotides A14 and U16 in the iron-responsive element (IRE) hairpin loop in Fig. 1a). Another source of high r.m.s.d. is the presence of false positives and negatives. For instance, the telomerase RNA domain IV has an MCCR of 94% and a r.m.s.d. of 3.3 Å (Fig. 1b). Interestingly, the false positive and the false negative are made in the hairpin loop. The NMR structure has a single-nucleotide bulge, A22, which stacks inside the helix on the 5′ side of a CUAU tetra-loop. The C23•U26 base pair that closes the tetra-loop is stabilized by a single hydrogen bond, and the two bases are perpendicular to each other. Although relatively stable, these features are

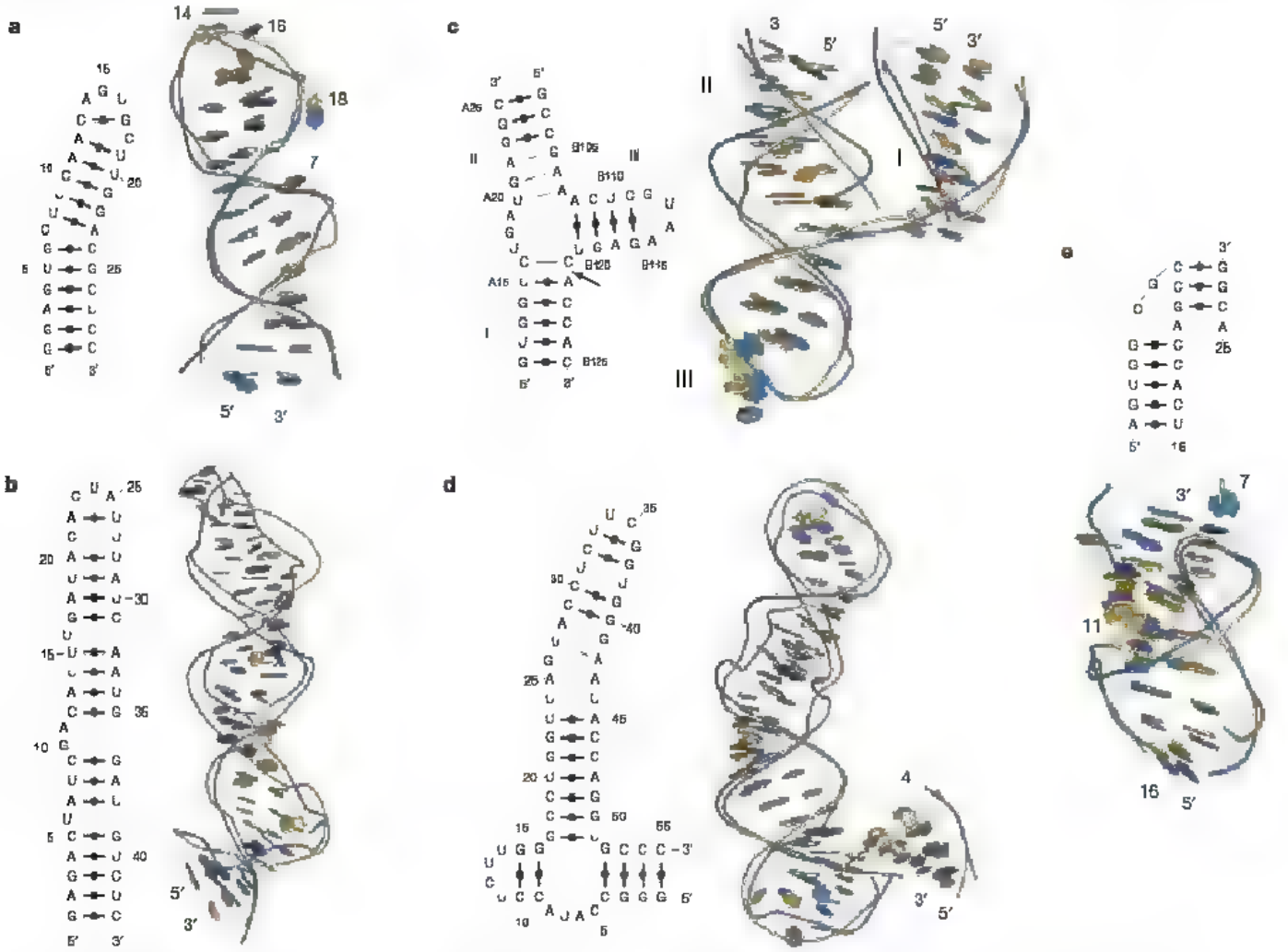

Figure 1 | A selection of 3D structures predicted from sequence. The canonical (bold lines, black dots) and non-canonical (non-bold lines) base pairs predicted by MC-Fold are shown on the left of the 3D structures. The closest structure (minimum r.m.s.d.) over all heavy atoms is shown (blue) is superimposed on its respective experimental structure (gold). **a**, IRE. **b**, Telomerase RNA domain IV. **c**, Pre-catalytic conformation of a hammerhead ribozyme. The arrow points the cleavage site. **d**, Subdomain of the *X. laevis* 5S rRNA. **e**, Yellow leaf virus pseudo-knotted element

rather rare and might be induced by particular experimental conditions or structure resolution methods. The NMR hairpin loop is less stable than the penta-loop proposed by the MC-Fold and MC-Sym pipeline.

When the experimental structure does not correspond to the lowest-energy structure, it is generally due to the formation of extra base pairs in the latter. The lowest-energy structure is often referred to the 'ground state'. The base pair formation/disruption phenomenon is known to be dependent on conformational changes induced by cofactors[18], which are difficult to represent in any scoring scheme. Consequently, polymorphic structures are found in MC-Fold's suboptimal solutions.

The conserved sequence of the *Deinococcus radiodurans* and *Escherichia coli* 23S rRNA helix 40 (ref. 19) contains an interior loop, 5′−CUAAG−3′ / 3′−GAAGC−5′, the structure of which differs whether it is solved by NMR or by X-ray crystallography. The NMR conditions favour the formation of a non-canonical A•A/A•G base-pair tandem, which MC-Fold ranks first (shown in bold above). The X-ray crystallographic structure is bound to a protein that possibly induces the disruption of the A•A non-canonical base pair and the apparition of a single bulged-out A (shown in bold-italic above), which MC-Fold ranks fifth.

The 'on' and 'off' conformational states of the cytoplasmic eukaryotic rRNA A site[20] contains an interior loop, 5′−CGC−U−3′ / 3′ AAAAG 5′, the structure of which differs whether the ribosome is active in protein translation (on) or not (off). X-ray crystallographic data of the *Homo sapiens* A site reveal these two distinct structures[20]. The on state has two unpaired A nucleotides that bulge out of the main helix (shown in bold above), whereas only one A, 3′ of the two bulges in the on state, is unpaired in the off state (shown in italic above). MC-Fold ranks the on state as sixth and the off state as fourth.

Multi-branched RNAs are made of more than two helical stems that are joined by a multi-branch loop. We used the pipeline to reproduce the 3D structure of a pre-catalytic conformation of the hammerhead ribozyme[21] (Fig. 1c), as well as that of the recent NMR structure of the *Xenopus laevis* 5S rRNA bound to zinc fingers[22] (Fig. 1d). When more than two stems are selected by MC-Fold, the coaxial energies are computed and accounted for in the final score (Supplementary Methods). The key base pairs to project properly the hammerhead in 3D space are located near the multi-branch: the three base pairs at the bottom of stem II and the C•C base pair in stem I. The C•C base pair is particularly important to avoid coaxial stacking between stem I and stem III.

Finally, inserting a stem that creates a nested structure generates a pseudo-knot, as shown in the structure of the yellow leaf virus[23] (Fig. 1e). In this model, a false positive non-canonical A•A base pair is made at the bottom of the upper stem. Nevertheless, the closest generated model shares 2.7 Å of r.m.s.d. when optimally superimposed on the NMR structure.

Folding human precursor microRNAs

When we submitted the pre-miRNA sequences of let-7c, mir-19a and mir-29a, our predictions were almost identical, and were similar to the A-RNA double helix (Fig. 2). In fact, we did not find any pre-miRNA sequence in mirBase[24] that could not be folded in the double helix (data not shown), despite an overrepresentation of U•U and U•C mismatches. The double helix offers a fixed and stable reference to the scissile phosphates that are cleaved by the Drosha complex upstream of the pre-miRNA[25], as well as by Dicer near the terminal loop[26].

The pre-miRNA double helix of let-7c (Fig. 2a) is bulge-free and presents to Dicer the expected docking surface[26], despite the non-canonical base pairs. In the 3D structure of mir-29a (Fig. 2b), the unpaired C23 nucleotide stacks inside the helix, acting as a lever to push the scissile phosphate of A26 into its proper position. Finally, in the 3D structure of mir-19a (Fig. 2c), the two unpaired nucleotides, A56 and U57, form a bulge behind the docking surface, and hence do not interfere with Dicer binding. These strict 3D structural restraints should further help in distinguishing between RNA stem-loop structures that can be processed by Dicer.

The presumed microRNA mismatches, in fact, adopt a geometry isosteric to Watson–Crick base pairs[27]. Their energies are less than that of canonical ones, which may facilitate the unwinding of the double helix and loading of the mature miRNA into the RNA-induced silencing complex (RISC). Interestingly, we find very few G•A mismatches in the miRNA region interfacing Dicer because their propensity for the sheared conformation is not isosteric to Watson–Crick base pairs. The sheared geometry distorts the backbone path of the double helix and, thus, might interfere with Dicer binding. The natural selection for non-canonical base pairs increases the diversity of possible pre-miRNA sequences, while increasing target specificity and, simultaneously, decreasing off targeting.

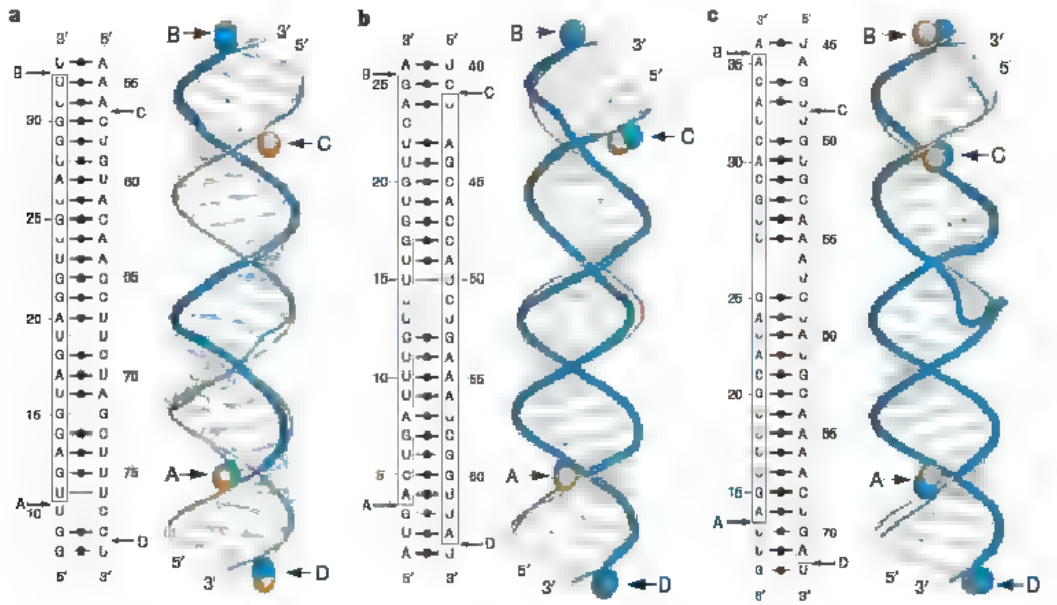

Figure 2 | A selection of pre-miRNA 3D structures. The predicted structures (blue) are optimally superimposed on a theoretically generated A-RNA double helix (gold). For each pre-miRNA, the nucleotides that form the mature miRNA are shown inside boxes. The spheres represent the scissile phosphate atoms: Drosha complex cleavage (A and D) and Dicer (B and C). **a**, Human let-7c. **b**, Human miR-29a. **c**, Human miR-19a.

Folding using probing data

As shown above, MC-Fold does not always rank experimental and activated structures first. Reaching these structures is nevertheless of principal importance. Here we show how experimental data can be incorporated to restrain the conformational space of MC-Fold to identify such induced structures.

For example, a recent study investigated the yeast transfer RNA^{Asp} structure by selective 2′-hydroxyl acylation and primer extension (SHAPE)[28]. SHAPE data reveal the flexible and constrained nucleotides, subject to experimental conditions. The tRNA sequence tested is deprived of the modified nucleotides, and has been shown to adopt the cloverleaf structure[29]. The top MC-Fold prediction of this $tRNA^{Asp}$ sequence is a hairpin, not a cloverleaf.

If we introduce high- and medium-flexibility SHAPE constraints (Supplementary Fig. 2), MC-Fold generates cloverleaf structures and ranks the native one sixth. The D-stem–loop sequence of this tRNA has a positive folding free energy under the thermodynamic model. Amongst the solutions, one includes a correct D-stem base-pairing registry (MCCR of 100%) and the A14•A21 base pair, whereas all other solutions base pair U13 with A21. The A14 inflexibility demonstrated by SHAPE is thus sufficient to discriminate the native amongst all solutions.

Similarly, by introducing dimethyl sulphate (DMS) data[10], all known canonical (with the exception of G56•C28) and all non-canonical base pairs of the *E. coli* 5S rRNA are captured in the correct *in vivo* Y-shaped topology (Supplementary Fig. 3a). Interestingly, the MC-Fold optimal solution (Supplementary Fig. 3b) of sub-sequence 16 to 69 has a marked resemblance to the *in vitro* structure that was probed by chemical modifications[30] and by NMR[31]. The latter suggests further a bias towards structures in the ground state.

Consensus structural assignments

Sequences that are functionally related are another source of structural data. Consider the IRE, a hairpin loop found in the 3′ untranslated region of the ferritin and transferrin receptor mRNAs. IREs are involved in maintaining iron homeostasis in vertebrate cells by acting as post-transcriptional factors[32]. MC-Fold and MC-Sym best predictions of several IRE sequences reveal the base pairs and nucleotides found to be involved in receptor binding (Fig. 1a): an upper stem of six base pairs[33], a single unpaired nucleotide 3′ of the hairpin-loop-flanking base pair[34] and a single (V) or double (W) bulge in the 5′ strand of the stem.

MC-Cons computes a structural assignment, that is, it assigns to each sequence the structure that maximizes the overall sum of pairwise structural similarities. The structural assignment returned when 30 IRE sequences available at Rfam (RNA families database)[35] and their top ten MC-Fold predictions are input to MC-Cons (see Supplementary Methods) reveals two IRE subclasses (Supplementary Fig. 4), corresponding to both helix-bending motifs, V and W. The two subclasses have been shown to be important in selective repressor binding, in particular to the human iron responsive protein 2 (ref. 36). Similarly, using ten yeast tRNA sequences, MC-Cons identified the cloverleaf structure for each sequence (see Supplementary Fig. 5).

Multiple-sequence and low-resolution data can be used in combination. Using fourteen 5S rRNA *E. coli* sequences and DMS data, the *in vivo* 5S rRNA structure is captured (Supplementary Fig. 6). In this case, a high rate of non-canonical false positives is made in the large hairpin (nucleotides 35–47). This is probably due to the fact that the RNA in the crystal structure is bound to the ribosomal complex, in which the large hairpin makes several contacts with the ribosomal protein L5. However, the consensus structural assignment of the *E. coli* 5S rRNA sequences without DMS probing data predicts the *in vitro* structure (Supplementary Fig. 7). Similarly, the Selenocysteine Insertion Sequence (SECIS) structure is also predicted using seven sequences and various RNase probing data[37] to block the base pairing of 13 out of 151 nucleotides (Supplementary Fig. 8).

Modelling HIV-1 frame-shifting element

HIV-1 is known for encoding two proteins, pol and gag-pol[38], using the same mRNA and a −1 *cis*-acting frame-shifting mechanism owing to the formation of a structure downstream of the slippery sequence[39,40]. Recent NMR data suggest that this structure could be a hairpin loop with an asymmetric bulge of three nucleotides, 5′-GGA-3′. In a first study, clear NMR signals were obtained by modifying the sequence to include GC base pairs in the lower stem, therefore introducing a coerced registry. In a second study the native sequence was used. However, it was extracted from the mRNA so that the lower stem was also constrained. Besides, when MC-Fold is run with both NMR sequences, the best solutions match the structures obtained by NMR.

However, using 50 randomly selected sequences out of the 753 reported in Rfam, a single and different structure makes the consensus assignment amongst these sequences. The principal difference between the new structure and those obtained by NMR is in the bulge: MC-Fold predicts a double-A bulge, 5′-AA-3′, instead of a 5′-GGA-3′ bulge (Fig. 3). This is a minor difference, but several arguments support it (see Supplementary Discussion).

Discussion

Our results highlight the fact that for effective RNA structure predictions, dealing with all base-pairing types in both secondary and tertiary structures is of the utmost importance. A difference between our study and other recent attempts is the use of a first-order object based on NCMs, which incorporates more base-pairing context-dependent information; this suggests that it is key in scoring secondary structures.

The lowest free-energy states determined by MC-Fold often differ from active and experimental states. Furthermore, solving the consensus structural assignment using MC-Cons occasionally predicts such ground rather than active structures (for example, *in vitro E. coli* 5S rRNA). However, we showed that few low-resolution experimental data could be introduced to bias the search towards experimental and *in vivo* structures (for example, tRNA, *in vivo* 5S rRNA and a SECIS element). Predicting both ground state and induced fit structures for the same sequence is a strong indication that MC-Fold

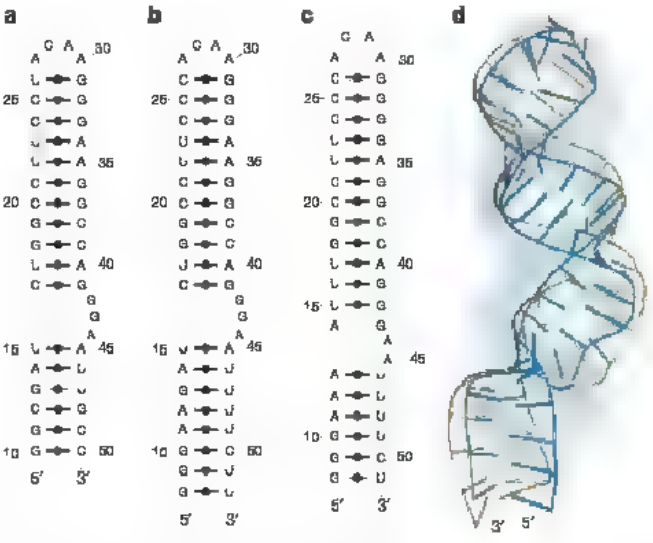

Figure 3 | HIV-1 −1 frame-shifting-element models. **a**, Secondary structure of the first NMR study (Protein Data Bank, PDB, code 1ZC5) **b**, Second NMR study (PDB code 1Z2J) **c**, MC-Cons best secondary structure prediction. The sequence used is EMBL AJ535040.1 from patient PT747 that expresses the pol and gag proteins. **d**, MC-Sym tertiary structures. The closest model (minimum r.m.s.d. of 3.4 Å over all heavy atoms) is shown in blue, optimally superimposed on the NMR structure resolved in the second study (gold), as well as ten representative structures of the conformational space of MC-Sym (light blue).

predicts correct structures, as well as structures that are accessible to any given sequence. This is reflected in the high rate of false positives when compared to experimental structures.

Thanks to the pipeline, RNA modelling is now more accurate and simpler than ever. The secondary structures generated by MC-Fold are more informative than those deprived of non-canonical base pairs and include very few false negatives. Producing 3D models consistent with these secondary structures is now a straightforward and accessible-to-all online activity. This should translate into keener RNA function hypotheses and less experimental work to verify them.

METHODS SUMMARY

The three algorithms and the scoring function are fully described in the Supplementary Information. A web service of the three algorithms has been made publicly available on the Internet at http://www.major.iric.ca. The protocols to produce secondary and tertiary structures using the website are described elsewhere (submitted).

Received 7 January 2007; accepted 11 January 2008.

1. *The RNA World* 3rd edn (eds Gesteland, R. F., Cech, T. R. & Atkins, J. F.) (CSHL, Cold Spring Harbor, 2006).
2. Griffiths-Jones, S. *et al.* Rfam: annotating non-coding RNAs in complete genomes. *Nucleic Acids Res.* 33, D121–D124 (2005).
3. Kapranov, P. *et al.* RNA maps reveal new RNA classes and a possible function for pervasive transcription. *Science* 316, 1484–1488 (2007).
4. Berman, H. M. *et al.* The protein data bank. *Nucleic Acids Res.* 28, 235–242 (2000).
5. Benson, D. A. *et al.* GenBank. *Nucleic Acids Res.* 35, D21–D25 (2007).
6. Shapiro, B. A. *et al.* Bridging the gap in RNA structure prediction. *Curr. Opin. Struct. Biol.* 17, 157–165 (2007).
7. Mathews, D. H. & Turner, D. H. Prediction of RNA secondary structure by free energy minimization. *Curr. Opin. Struct. Biol.* 16, 270–278 (2006).
8. Gutell, R. R., Lee, J. C. & Cannone, J. J. The accuracy of ribosomal RNA comparative structure models. *Curr. Opin. Struct. Biol.* 12, 301–310 (2002).
9. Mathews, D. H. Revolutions in RNA secondary structure prediction. *J. Mol. Biol.* 359, 526–532 (2006).
10. Mathews, D. H. *et al.* Incorporating chemical modification constraints into a dynamic programming algorithm for prediction of RNA secondary structure. *Proc. Natl Acad. Sci. USA* 101, 7287–7292 (2004).
11. Major, F. *et al.* The combination of symbolic and numerical computation for three-dimensional modeling of RNA. *Science* 253, 1255–1260 (1991).
12. Lescoute, A. *et al.* Recurrent structural RNA motifs, isostericity matrices and sequence alignments. *Nucleic Acids Res.* 33, 2395–2409 (2005).
13. Dima, R. I., Hyeon, C. & Thirumalai, D. Extracting stacking interaction parameters for RNA from the data set of native structures. *J. Mol. Biol.* 347, 53–69 (2005).
14. Do, C. B., Woods, D. A. & Batzoglou, S. CONTRAfold: RNA secondary structure prediction without physics-based models. *Bioinformatics* 22, e90–e98 (2006).
15. Das, R. & Baker, D. Automated *de novo* prediction of native-like RNA tertiary structures. *Proc. Natl Acad. Sci. USA* (2007).
16. Lemieux, S. & Major, F. Automated extraction and classification of RNA tertiary structure cyclic motifs. *Nucleic Acids Res.* 34, 2340–2346 (2006).
17. Kabsch, H. A discussion of the solution for the best rotation to relate two sets of vectors. *Acta Crystallogr. A* 34, 827–828 (1978).
18. Williamson, J. R. Induced fit in RNA-protein recognition. *Nature Struct. Biol.* 7, 834–837 (2000).
19. Shankar, N. *et al.* The NMR structure of an internal loop from 23S ribosomal RNA differs from its structure in crystals of 50S ribosomal subunits. *Biochemistry* 45, 11776–11789 (2006).
20. Kondo, J., Urzhumtsev, A. & Westhof, E. Two conformational states in the crystal structure of the *Homo sapiens* cytoplasmic ribosomal decoding A site. *Nucleic Acids Res.* 34, 676–685 (2006).
21. Pley, H. W., Flaherty, K. M. & Mckay, D. B. Three-dimensional structure of a hammerhead ribozyme. *Nature* 372, 68–74 (1994).
22. Lee, B. M. *et al.* Induced fit and "lock and key" recognition of 5S RNA by zinc fingers of transcription factor IIIA. *J. Mol. Biol.* 357, 275–291 (2006).
23. Giedroc, D. P., Theimer, C. A. & Nixon, P. L. Structure, stability and function of RNA pseudoknots involved in stimulating ribosomal frameshifting. *J. Mol. Biol.* 298, 167–185 (2000).
24. Griffiths-Jones, S. *et al.* miRBase: microRNA sequences, targets and gene nomenclature. *Nucleic Acids Res.* 34, D140–D144 (2006).
25. Han, J. *et al.* Molecular basis for the recognition of primary microRNAs by the Drosha–DGCR8 complex. *Cell* 125, 887–901 (2006).
26. Macrae, I. J. *et al.* Structural basis for double-stranded RNA processing by Dicer. *Science* 311, 195–198 (2006).
27. Leontis, N. B., Stombaugh, J. & Westhof, E. The non-Watson-Crick base pairs and their associated isostericity matrices. *Nucleic Acids Res.* 30, 3497–3531 (2002).
28. Merino, E. J. *et al.* RNA structure analysis at single nucleotide resolution by selective 2′-hydroxyl acylation and primer extension (SHAPE). *J. Am. Chem. Soc.* 127, 4223–4231 (2005).
29. Perret, V. *et al.* Conformation in solution of yeast $tRNA^{Asp}$ transcripts deprived of modified nucleotides. *Biochimie* 72, 735–743 (1990).
30. Brunel, C. *et al.* Three-dimensional model of *Escherichia coli* ribosomal 5S RNA as deduced from structure probing in solution and computer modeling. *J. Mol. Biol.* 221, 293–308 (1991).
31. Leontis, N. B. & Moore, P. B. NMR evidence for dynamic secondary structure in helices II and III of the RNA of *Escherichia coli*. *Biochemistry* 25, 3916–3925 (1986).
32. Hentze, M. W. & Kuhn, L. C. Molecular control of vertebrate iron metabolism: mRNA-based regulatory circuits operated by iron, nitric oxide, and oxidative stress. *Proc. Natl Acad. Sci. USA* 93, 8175–8182 (1996).
33. Jaffrey, S. R. *et al.* The interaction between the iron-responsive element binding protein and its cognate RNA is highly dependent upon both RNA sequence and structure. *Nucleic Acids Res.* 21, 4627–4631 (1993).
34. Sierzputowska-Gracz, H., Mckenzie, R. A. & Theil, E. C. The importance of a single G in the hairpin loop of the iron responsive element (IRE) in ferritin mRNA for structure: an NMR spectroscopy study. *Nucleic Acids Res.* 23, 146–153 (1995).
35. Griffiths-Jones, S. *et al.* Rfam: an RNA family database. *Nucleic Acids Res.* 31, 439–441 (2003).
36. Leipuviene, R. & Theil, E. C. The family of iron responsive RNA structures regulated by changes in cellular iron and oxygen. *Cell. Mol. Life Sci.* (in the press).
37. Clery, A. *et al.* An improved definition of the RNA-binding specificity of SECIS-binding protein 2, an essential component of the selenocysteine incorporation machinery. *Nucleic Acids Res.* 35, 1868–1884 (2007).
38. Jacks, T. *et al.* Characterization of ribosomal frameshifting in HIV-1 *gag-pol* expression. *Nature* 331, 280–283 (1988).
39. Gaudin, C. *et al.* Structure of the RNA signal essential for translational frameshifting in HIV-1. *J. Mol. Biol.* 349, 1024–1035 (2005).
40. Staple, D. W. & Butcher, S. E. Solution structure and thermodynamic investigation of the HIV-1 frameshift inducing element. *J. Mol. Biol.* 349, 1011–1023 (2005).

Supplementary Information is linked to the online version of the paper at www.nature.com/nature.

Acknowledgements We thank P. Thibault for updating MC-Sym and P. Gendron for helping us with the Condor and web services. We thank D. D'Amours, M.-F. Gaumont-Leclerc and V. Lisi for making suggestions to improve the manuscript. We thank D. H. Mathews and E. Westhof for discussions about MC-Fold. This project was supported by grants from the Canadian Institutes of Health Research (CIHR) and from the Natural Sciences and Engineering Research Council (NSERC) of Canada. M.P. holds Ph.D. scholarships from the NSERC and the Fonds Québécois de la Recherche sur la Nature et les Technologies. F.M. is a member of the Centre Robert-Cedergren of the Université de Montréal.

Author Contributions Both authors were involved in every aspect of the research. M.P. programmed MC-Fold and MC-Cons.

Author Information Reprints and permissions information is available at www.nature.com/reprints. Correspondence and requests for materials should be addressed to F.M. (francois.major@umontreal.ca).

ARTICLES

Structure and metal exchange in the cadmium carbonic anhydrase of marine diatoms

Yan Xu[1]*, Liang Feng[2]*†, Philip D. Jeffrey[2]*, Yigong Shi[2] & François M. M. Morel[3]

Carbonic anhydrase, a zinc enzyme found in organisms from all kingdoms, catalyses the reversible hydration of carbon dioxide and is used for inorganic carbon acquisition by phytoplankton. In the oceans, where zinc is nearly depleted, diatoms use cadmium as a catalytic metal atom in cadmium carbonic anhydrase (CDCA). Here we report the crystal structures of CDCA in four distinct forms: cadmium-bound, zinc-bound, metal-free and acetate-bound. Despite lack of sequence homology, CDCA is a structural mimic of a functional β-carbonic anhydrase dimer, with striking similarity in the spatial organization of the active site residues. CDCA readily exchanges cadmium and zinc at its active site—an apparently unique adaptation to oceanic life that is explained by a stable opening of the metal coordinating site in the absence of metal. Given the central role of diatoms in exporting carbon to the deep sea, their use of cadmium in an enzyme critical for carbon acquisition establishes a remarkable link between the global cycles of cadmium and carbon.

Vertical profiles of cadmium (Cd) concentrations in the oceans show that this metal is cycled in the water column like an algal nutrient: it is impoverished at the surface by phytoplankton uptake and regenerated at depth by remineralization of sinking organic matter[1,2]. Part of the explanation for this nutrient-like behaviour is the use of Cd as a catalytic metal atom in carbonic anhydrase (CA) in marine diatoms[3–5]. These organisms, which are responsible for some 40% of net marine primary production[6], have adapted to life in a medium containing vanishingly small concentrations of essential metals. The expression of a CDCA is a remarkable example of this adaptation.

CA, which catalyses the reversible hydration of carbon dioxide (CO_2), was one of the first proteins for which a crystal structure was obtained[7–9]. In phytoplankton, CA plays an essential part in the acquisition of inorganic carbon for photosynthesis[10,11]. CA is categorized into three main classes: α, β and γ, which share no significant similarity in primary sequence or overall structure[12], but which all rely on Zn for activity. Whereas α- and γ-CA use three histidine residues to coordinate the Zn atom, β-CA uses two cysteine residue and one histidine residue[12–16]. Two new classes of CA have been discovered in marine diatoms, both isolated from the model species *Thalassiosira weissflogii*: δ-CA, represented by TWCA1, with similar enzymes identified in other classes of phytoplankton[12,17,18] and an active site similar to that of α-CA[19]; and ζ-CA, represented by CDCA1, which naturally uses Cd as its catalytic metal[12,20]. CDCA1 consists of three tandem CA repeats (R1–R3), which share 85% identity in their primary sequences[20]. Genes coding for similar proteins have been identified in other cultured diatoms and in natural samples of sea water[21].

Here we report the high-resolution crystal structures of CDCA1 repeats and associated biochemical characterization. Although CDCA1 was initially isolated as a Cd enzyme, it is actually a cambialistic enzyme—that is, it can use either Zn or Cd for catalysis—and spontaneously exchanges the two metals. Structural analysis reveals a plausible explanation for this facile metal exchange. Though less efficient than the Zn form, Cd-bound CDCA is a fast enzyme that can support the catalytic needs of fast growing diatoms.

Overall structure and active site

We crystallized the Cd-bound second repeat of CDCA1 (CDCA1-R2, residues 223–432) and determined its structure at 1.45 Å resolution using single anomalous dispersion signal from the bound Cd atom (Supplementary Table 1). The structure of CDCA1-R2 has an overall ellipsoidal shape, with seven α-helices and nine β-strands (Fig. 1a and Supplementary Fig. 1). Seven β-strands are located in the centre of the structure, constituting two β-sheets that appear to be contiguous with each other. One β-sheet contains four strands (β1, β6, β8 and β9), whereas the other β-sheet comprises three strands (β3, β4 and β5). All seven α-helices are located on one side of the contiguous β-sheets. The structure can be divided into two lobes, each nucleated by a β-sheet. One lobe (residues 223–257 and 370–432) consists of the four-stranded β-sheet, strands β2 and β7, and helices α1, α6 and α7. The other lobe (residues 258–369) contains the three-stranded β-sheet, and helices α2–α5. On the surface of the ellipsoid between the two lobes, there is a deep cleft that leads to the active site pocket.

In the active site, Cd is coordinated by three invariant residues in CDCA of all diatom species[21]: Cys 263, His 315 and Cys 325 (Fig. 1b and Supplementary Fig. 1). The distances between Cd and the metal-binding atoms of these residues (Sγ of Cys 263, Nε of His 315 and Sγ of Cys 325) are 2.46 Å, 2.34 Å and 2.51 Å, respectively (Fig. 1c, left panel). Notably, despite their conservation in other CDCAs, His 310 and His 318 are not involved in binding to Cd. The tetrahedral coordination of Cd is completed by a water molecule 2.35 Å away. A second water molecule also contributes to Cd binding, with a distance of 2.65 Å. These two water molecules are hydrogen-bonded to a third water molecule, which is connected to a number of well-ordered water molecules above the active site.

A search of the Protein Data Bank using the program Dali[22] did not yield any entry with significant structural similarity; thus CDCA1 appears to represent a previously unreported protein fold. Despite a lack of sequence homology and overall structure, the active site conformation in CDCA1-R2 closely resembles that of the β-CA from *Pisum sativum*[23] (Fig. 1b). There are five highly conserved residues at the active site of CDCA1: three involved in coordinating Cd and an

[1]Department of Ecology and Evolutionary Biology, [2]Department of Molecular Biology, [3]Department of Geosciences, Princeton University, New Jersey 08544, USA. †Present address: Laboratory of Molecular Neurobiology and Biophysics, Rockefeller University, New York 10065, USA.
*These authors contributed equally to this work.

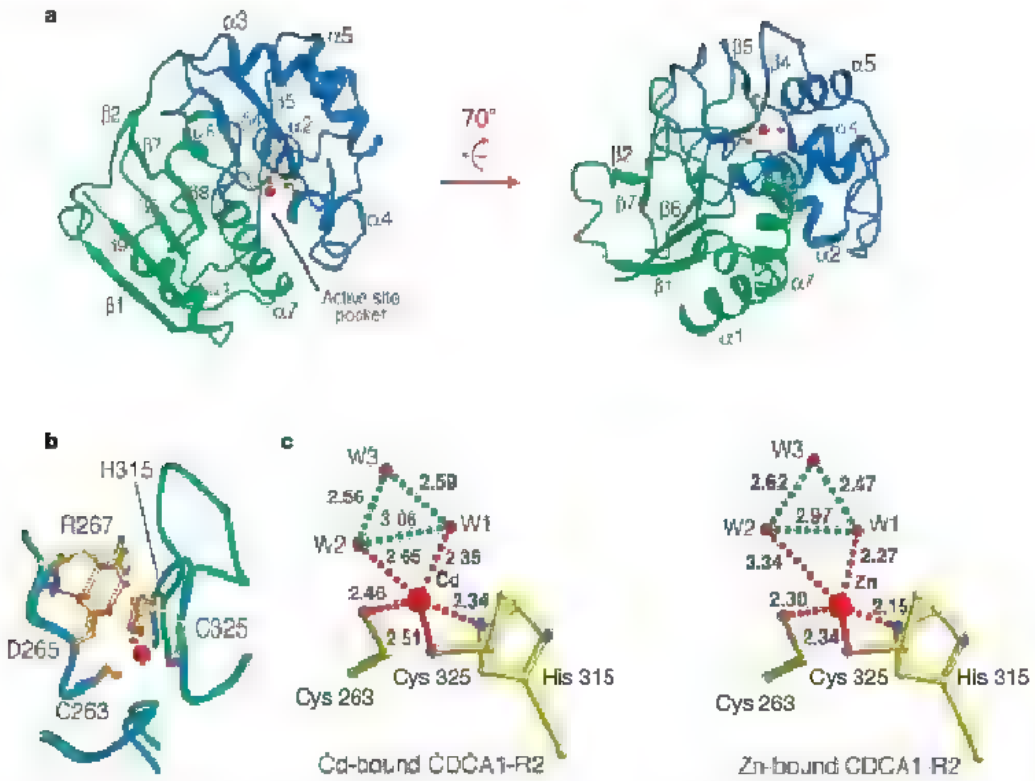

Figure 1 | Structure of the second CA repeat of CDCA1 (CDCA1-R2). **a**, Overall structure of the Cd-bound CDCA1-R2. Two lobes of the structure are coloured blue and green. Cd is highlighted in red, and Cd-coordinating residues are coloured yellow. **b**, Comparison of the active site conformation between CDCA-R2 (green) and β-CA (blue). The active site residues in CDCA-R2 and β-CA are coloured yellow and orange, respectively. Hydrogen bonds are represented by red dashed lines. Cd and the water ligand are shown in large and small red spheres, respectively. (A stereo view is shown in Supplementary Fig. 1b.) **c**, Comparison of Cd- and Zn-coordination in CDCA1-R2. Metal coordination and hydrogen bonds are indicated by red and green dashed lines, respectively; numbers indicate bond lengths in Å. W1–W3, water molecules. Structural images were prepared using MOLSCRIPT[44] and GRASP[45].

Asp 265–Arg 267 pair (Supplementary Fig. 1). The Cα atoms of these five residues can be superimposed with those of β-CA[23] with an r.m.s. deviation of 0.73 Å. The locations of the catalytic metal ion and its tetrahedrally bound water molecule are also nearly identical between CDCA1 and β-CA. In addition, the role of the Asp–Arg pair is also identical. The carboxylate side chain of Asp 265 accepts one hydrogen bond from the tetrahedrally bound water molecule and two hydrogen bonds from the guanidinium group of Arg 267, which is further buttressed by a fourth hydrogen bond from the amide nitrogen of Arg 267 to the side chain of Asp 265 (Fig. 1b). CDCA1 is inactivated by mutation of any of these five conserved residues (data not shown). These structural features suggest a common catalytic mechanism.

Mimicry of a β-CA dimer

Although CDCA1-R2 shares little structural similarity with a β-CA monomer, it can be superimposed with a functional dimer of β-CA[23] with an r.m.s. deviation of 1.93 Å over 102 Cα atoms (Fig. 2a). Strikingly, the three-stranded lobe only superimposes with one β-CA monomer whereas the four-stranded lobe aligns well with the adjacent β-CA monomer. The functional unit of β-CA is a homodimer[23]; yet each CA repeat of CDCA1 exhibits robust catalytic activity as a monomer (see below). Thus, a single molecule of CDCA1-R2 is a structural and functional mimic of a β-CA dimer. This structural mimicry emanates from the active site between the two lobes of CDCA1-R2 and becomes less apparent with increasing distance away from the active site.

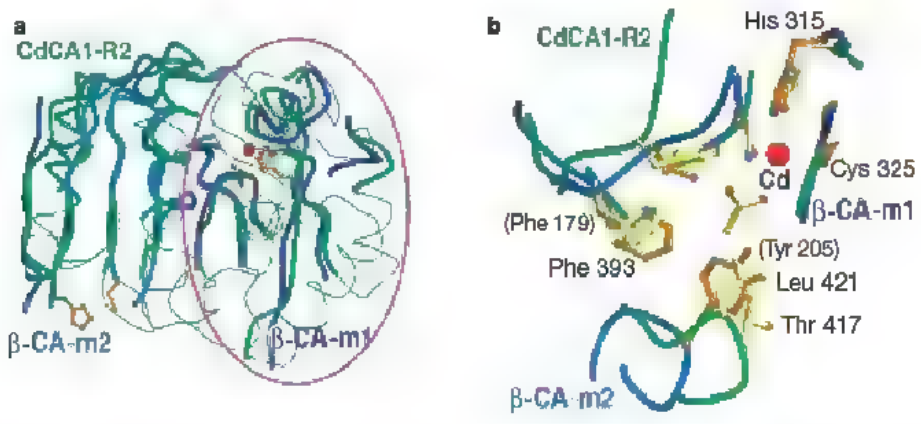

Figure 2 | CDCA1-R2 is a structural mimic of a functional dimer of β-CA. **a**, Superposition of the CDCA1-R2 structure (green) with that of a functional β-CA dimer. The two monomers of β-CA (β-CA-m1 and β-CA-m2) are coloured dark and light blue, respectively. For clarity, only the aligned portion of β-CA structure is shown. Zn-binding residues are shown in the β-CA dimer to indicate the orientation of the molecules. **b**, A close-up view of the active site comparison between Cd-bound CDCA1-R2 (green) and a functional β-CA dimer bound to acetate[23] (blue). (Stereo views are shown in Supplementary Fig. 2a and b.)

Analysis of the active site conformation in CDCA1-R2 reveals distinct contributions from the two lobes and hence provides a rational basis for why CDCA1 needs to be a structural mimic of a β-CA dimer. The three metal-coordinating residues as well as the conserved Asp–Arg pair are all located in the three-stranded lobe. However, the putative substrate-binding residues are mostly contained within the four-stranded lobe. The residues Phe 179 and Tyr 205, which directly interact with the substrate analogue acetate in β-CA[23], are replaced by Phe 393, Leu 421 and Thr 417 in CDCA1-R2, all located in the four-stranded lobe (Fig. 2b). In confirmation of this analysis, missense mutation of any of these three residues cripples catalytic activity (Supplementary Fig. 2). Thus the two-lobe architecture of CDCA1-R2, and hence its structural mimicry of a β-CA dimer, are necessitated by the catalytic activity.

Substrate binding

To support the structural analysis, we crystallized the Cd-bound CDCA1-R2 in the presence of acetate, a known substrate analogue and weak inhibitor of β-CA, and determined its structure at 1.4 Å resolution (Supplementary Table 2). As reported for β-CA[23], acetate is bound at the bottom of the catalytic cleft (Supplementary Fig. 3), and is well-ordered (as judged by the electron density; Fig. 3a). The bound acetate replaces one of the two water molecules that were hydrogen-bonded to the metal ion in the acetate-free CDCA1-R2 structure (Figs 1c, 3b). Consequently, one oxygen atom of acetate is 2.47 Å away from Cd, and the carboxylate moiety of acetate is within hydrogen-bond distances of the remaining water molecule (Fig. 3b). This water molecule is presumably deprotonated owing to Cd coordination and a hydrogen bond from Asp 265. The resulting hydroxide ion is the nucleophile that attacks the electrophilic carbon atom in CO_2. The orientation of acetate is further stabilized by a hydrogen bond from the backbone amide of Phe 327.

Cd is located at the bottom of a funnel-shaped active site pocket. Intriguingly, the funnel continues to traverse the hydrophobic core of CDCA1-R2 through an elongated channel (Fig. 3c). This channel has an inner diameter of 4–5 Å and is surrounded exclusively by 12 hydrophobic amino acids which are conserved in CDCA (Supplementary Fig. 1): Ile 229 and Leu 233 on helix α1, Val 264 and Phe 327 on α4, Val 374 and Ile 376 on β6, Phe 393 and Val 395 on β8, and Leu 411, Ala 414, Val 418 and Leu 421 on α7. The acetate molecule is situated at one end of the hydrophobic channel, whose conserved nature suggests functional significance. The channel being large enough to accommodate a carbon dioxide molecule, we speculate that it might be the entry or escape route for the reaction substrate or product.

Facile metal exchange

Although Cd was the catalytic metal ion in CDCA1 isolated from *T. weissflogii*, it can be substituted by Zn, yielding an even more efficient enzyme. In the absence of supplemental Cd in growth medium (which contains 15 μM Zn and <3 nM Cd), *Escherichia coli* incorporates Zn into CDCA1 and its monomers. We determined the structure of Zn-bound CDCA1-R2 at 1.8 Å resolution (Supplementary Table 2). As anticipated, the overall structure remains nearly identical to that of the Cd-bound CDCA1-R2, with an r.m.s. deviation of 0.11 Å over all 209 Cα atoms. However, the distances between Zn and the metal-binding atoms of the three coordinating residues are reduced by approximately 0.16–0.19 Å (Fig. 1c).

With increasing concentrations of Cd in the medium, Cd gradually replaces Zn in the enzyme until an essentially pure Cd form (Zn < 2% of Cd) is obtained at a Cd concentration of 500 μM (Fig. 4a). Either metal can also be incorporated *in vitro* into the apoprotein. The β-CA of the diatom *Phaeodactylum tricornutum*, PtCA1[24], which has a metal binding centre practically identical to that of CDCA, incorporates Cd only to a small extent when overexpressed in *E. coli* in the presence of 500 μM Cd.

The dissociation constants of CDCA1-R2, measured by competition with 4-(2-pyridylazo) resorcinol, are $10^{-8.9}$ M for Zn^{2+} and less than 10^{-10} M for Cd^{2+}. In the presence of Cd^{2+} chelated with an excess of nitrilotriacetic acid (NTA), the Zn-bound CDCA1 spontaneously exchanges Zn for Cd (Fig. 4b). But in the reciprocal experiment, Zn bound to NTA failed to replace Cd in the enzyme (Fig. 4c). In the presence of excess phytochelatin dimer (PC2 = (γ-Glu-Cys)$_2$-Gly, whose thiol groups confer a high affinity for Cd^{2+}), Zn^{2+} or Cd^{2+} was able to replace a large fraction of the other metal in the protein within 24 h (Fig. 4b, c). Previous studies have documented very slow metal exchange kinetics in CAs[25]. The presence of some ligands can greatly accelerate the removal of the metal from the active centre of CAs, but metal re-insertion appears to necessitate an equimolar or higher metal-to-ligand ratio[26,27]. We observed inefficient replacement of Zn by Cd in PtCA1 in the presence of Cd bound to excess NTA or PC2 (Fig. 4b). The metal-binding and metal exchange properties of CDCA thus appear unusual: it is a cambialistic enzyme that can incorporate either Zn or Cd as its metal centre and readily exchange one metal for the other. As the synthesis of phytochelatins is constitutive in diatoms and responds to very low concentrations of Cd and Zn (refs 5, 28), it seems possible that these peptides play a part in incorporating metals into CDCA *in vivo*.

To elucidate the structural basis for the facile metal exchange in CDCA, we determined the structure of metal-free CDCA1-R1 at 1.45 Å resolution (Supplementary Table 2). For comparison, we also determined the structure of the Cd-bound CDCA1-R1 at 1.7 Å resolution (Supplementary Table 2). Although most of the structural elements are extremely well superimposed between these two structures (r.m.s. deviation of 0.515 Å over 202 Cα atoms), the active site pocket takes on two distinct conformations (Fig. 5a, b). Compared to the Cd-bound CDCA1-R1, the sequence element between the last

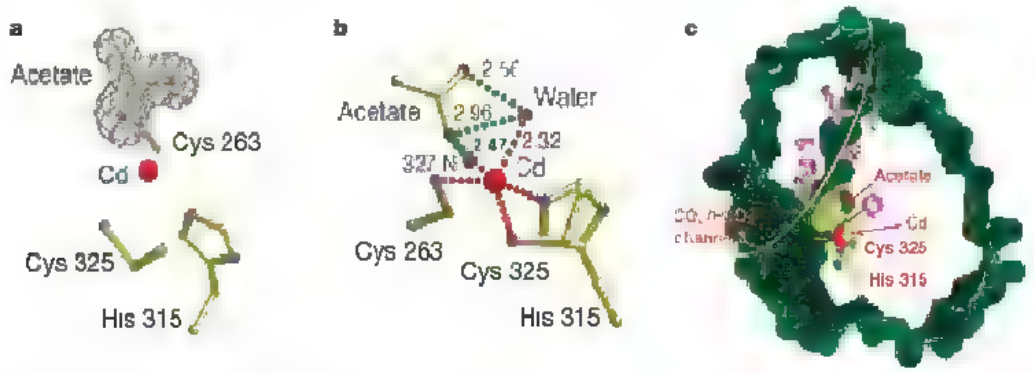

Figure 3 | Structure of CDCA1-R2 bound to substrate analogue acetate. **a**, A close-up view of the region around acetate. The $F_o - F_c$ electron density map surrounding acetate was calculated using simulated annealing with the omission of acetate and was contoured at 5σ. **b**, A close-up view of the active site conformation. Metal coordination and hydrogen bonds are indicated by red and green dashed lines, respectively. Relevant distances are indicated (Å). **c**, A hydrophobic channel traverses through CDCA1-R2. Cd is highlighted in red. Acetate is shown in yellow. The conserved hydrophobic residues that line the channel are shown in magenta. (Stereo views of **a** and **b** are shown in Supplementary Fig. 3b and c.)

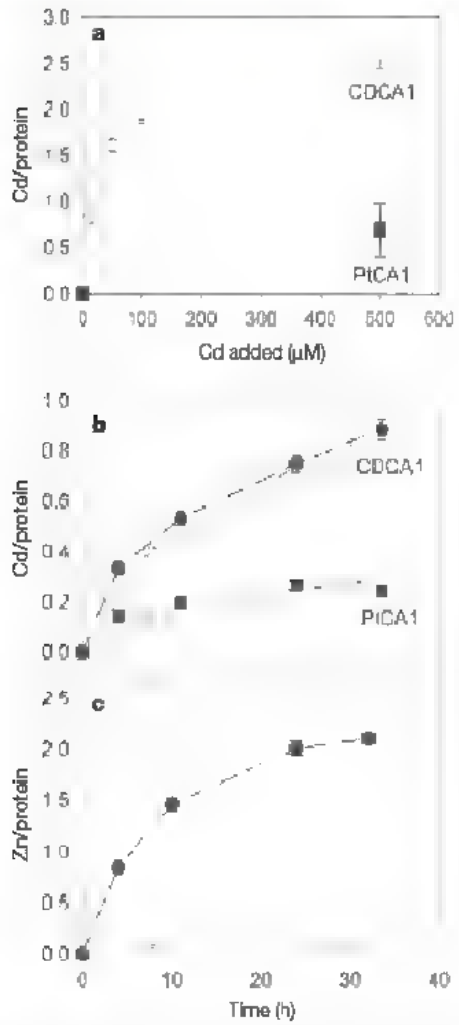

Figure 4 | Facile metal exchange in CDCA1. **a**, Cd incorporation in CDCA1 (circles) and PtCA1 (squares) in *E. coli* expression system. **b**, *In vitro* Cd replacement for Zn in Zn-CDCA1 (circles) and Zn-PtCA1 (squares) over time. 12 μM Cd-NTA (open symbols) or Cd-phytochelatin (filled symbols) complex was incubated with 3.3 μM Zn-CDCA1 or 5 μM Zn-PtCA1. **c**, *In vitro* Zn replacement for Cd in Cd-CDCA1 over time. 12 μM Zn-NTA (open circles) or Zn-PC2 (filled circles) complex was incubated with 3.3 μM Cd-CDCA1. In **b** and **c**, the ligands were in excess of the metals by a factor of 2 (phytochelatin) or 3 (NTA). Error bars (s.d.) represent duplicate measurements of a single experiment except PtCA1 in **a**, which shows the mean and s.d. from three separate experiments.

two Cd-binding residues (amino acids 106–114) in the metal-free structure has a much more open conformation. Cys 125 is translocated from its metal-coordinating position by approximately 4 Å and undergoes a 90° rotation. In addition, the Sγ atom of Cys 53 is flipped away from its metal-binding position (Fig. 5b). Thus, in contrast to other known CAs such as CAII[29], the active site conformation of metal-free CDCA1 is stable and different from that of the metal-bound form. Accordingly, the free energy minimum of the metal-free CDCA1-R1 corresponds to an active site conformation that is different from that of the metal-bound form. This unique thermodynamic characteristic probably facilitates metal exchange in CDCA1 by stabilizing the transitional, metal-free conformation.

To allow the opening of the metal-binding site, the linker sequence between the metal-coordinating His 105 and Cys 115 must be sufficiently flexible. Significantly, the two ends of this sequence are made up of Gly residues (Supplementary Fig. 4), which are known to provide flexibility to polypeptide chains[30] and may serve as hinges for the conformational change. Supporting this analysis, mutation of either Gly 316 or Gly 324 to Ala in CDCA1-R2 resulted in a loss of ability to exchange the metals (Fig. 5c).

Enzyme kinetics

We performed a preliminary kinetic analysis of CDCA1 and studied the rate of CO_2–HCO_3^- interconversion at equilibrium by mass spectrometry[31]. Both the CA repeats and the full-length CDCA1 exhibit high CA activity with either Cd or Zn as the catalytic metal (Fig. 6 and Supplementary Fig. 5). The catalytic efficiency of the zinc enzyme is remarkably high, perhaps even higher than CAII[32], approaching the diffusion limit at high pH ($k_{cat}/K_m = 8.7 \times 10^8\ M^{-1}\ s^{-1}$ for CO_2 hydration, where k_{cat} is the turnover number and K_m the half saturation constant). The decreasing efficiency at lower pH is typical of many CAs and resembles an acidimetric titration with pK_a values around 7 and 9 (refs 13, 33, 34). Though lower than that of Zn-CDCA1, the catalytic efficiency of the Cd-CDCA1 protein is still very high ($k_{cat}/K_m = 1.4 \times 10^8\ M^{-1}\ s^{-1}$ for CO_2 hydration at pH 9). The catalytic efficiency reported for Cd-substituted CAs is generally very low, about 2% or less of the Zn enzyme at circumneutral pH[35,36]. In assays of PtCA1 with partial substitution of Cd for Zn, the reduced activity corresponded to the fraction of Zn in the enzyme. We observed no effect on CDCA1 activity of the concentration of HEPES used as a buffer over the range 2.5 to 50 mM (data not shown).

Discussion

Collectively, the five related structures of CDCA1 we report here reveal a coherent molecular basis for the function of CDCA. The structural mimicry between CDCA1 and a functional β-CA dimer ensures the formation of a complete active site. Structural analysis provides a plausible explanation for spontaneous exchange of Zn and Cd in the active site of CDCA1. A conserved sequence between two metal-coordinating residues adopts a stable open conformation in

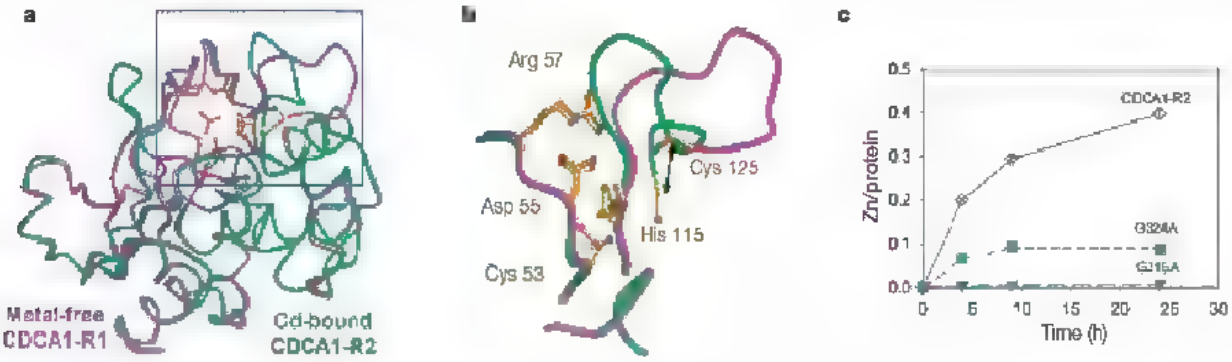

Figure 5 | Structural basis of efficient metal exchange in CDCA1. **a**, Overlay of the structure of metal-free CDCA1-R1 (magenta) with that of the Cd-bound CDCA1-R1 (green). Details of the area indicated by the blue rectangle is shown in **b**. **b**, Comparison of the active site conformation between meta-free CDCA1-R1 (magenta) and the Cd-bound CDCA1-R1 (green). (A stereo view is shown in Supplementary Fig. 4a.) **c**, Effect of the mutation of Gly 316 and Gly 324 flanking the linkage sequence between two metal binding residues, His 315 and Cys 325, on Zn replacement for Cd in Cd-bound CDCA1-R2. Data shown for wild-type (open diamonds), G316A (green triangles) and G324A (blue squares). 12 μM Zn-PC2 complex was incubated with 10 μM Cd-CDCA1-R2 and Cd-mutants in the presence of excess phytochelatin (PC2). Error bars (s.d.) represent duplicate measurements of a single experiment.

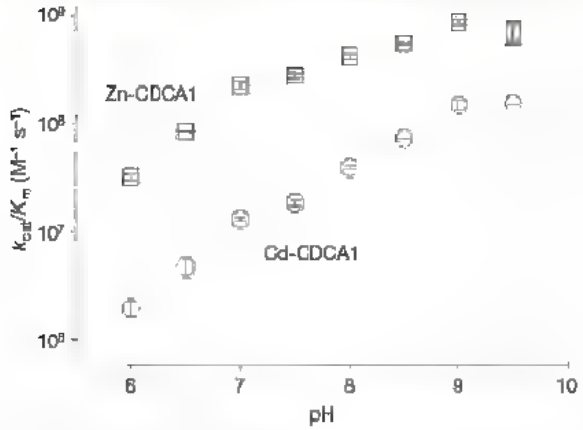

Figure 6 | pH dependence of k_{cat}/K_m for the Cd-bound (circles) and Zn-bound (squares) CDCA1. Error bars (s.d.) represent duplicate measurements of a single experiment.

the metal-free protein which effectively lowers the free energy penalty of releasing the bound metal and hence facilitates metal exchange.

The CDCA of diatoms readily exchanges metals at its catalytic centre and retains better activity in the Cd form than other CAs. These properties have presumably evolved in response to the low metal environment of the oceans. But our kinetic data show that the replacement of Zn by Cd results nonetheless in a decrease in catalytic efficiency. Whereas the addition of Cd is clearly beneficial to Zn-limited laboratory cultures, increasing both *in vivo* CA activity and growth rate[3], how effective can Cd replacement of Zn be in the ocean where Cd is even more scarce than Zn? Phytoplankton growing at, say, 0.5 d^{-1} need a photosynthetic carbon turnover rate of nearly 2 d^{-1} ($=2\times10^{-5}$ s^{-1}) during daylight to support both their growth and their light and dark respiration. On the basis of the catalytic efficiency of Cd-CDCA1 (taken at $k_{cat}/K_m = 3\times10^7$ $M^{-1}s^{-1}$, Fig. 6), and an intracellular CO_2 concentration of ~1 μM (taken as the half saturation constant for photosynthesis[37]), we estimate that a cellular CDCA1 concentration of 0.6 μmol enzyme per mol C is needed to catalyse the hydration/dehydration of all inorganic carbon fixed photosynthetically. This corresponds to a cellular Cd/C ratio of 2 μmol Cd per mol C, similar to the Cd/C ratio measured in the phytoplankton biomass[38]. The replacement of Zn by Cd in CDCA in the ocean can indeed satisfy a substantial fraction of the catalytic needs of fast growing diatoms.

The remarkable ability to make use of an element previously known only for its toxicity is presumably a significant competitive advantage for diatoms in the metal-poor environment of the oceans. CA is a key enzyme in the carbon uptake machinery of these organisms, which are responsible for a large fraction of the carbon export from the atmosphere to the deep ocean. The biochemical use of Cd may thus have played a part in the global radiation of diatoms during the Cenozoic era and the concomitant decrease in atmospheric CO_2.

METHODS SUMMARY

The various CA coding sequences were overexpressed in *E. coli* and purified by metal affinity chromatography and gel filtration. Metal content of purified protein was measured by inductively coupled plasma-mass spectrometry. The kinetics of ^{18}O exchange from trip,y labelled CO_2 ($^{13}C^{18}O^{18}O$) were followed in a membrane-inlet mass spectrometer and the rate constants calculated as reported[31]. The metal binding affinity assay was as described[39] with minor modifications. The metal exchange experiment was performed by incubating CAs with CdY or ZnY (Y = NTA or PC2) with tracer ^{109}Cd or ^{65}Zn and then removing aliquots for protein assay and radioactivity counting.

Various CA repeats were crystallized by the hanging-drop vapour-diffusion method. Diffraction data were processed using the HKL suite[40]. The structure of the Cd-bound CDCA1-R2 was determined by Cd-SAD (single wavelength anomalous diffraction) using SHELX[41], all other structures were solved by molecular replacement. Model building and refinement were performed using ARP/wARP[42] and CNS[43], respectively.

Full Methods and any associated references are available in the online version of the paper at www.nature.com/nature.

Received 3 July 2007; accepted 10 January 2008.

1. Boyle, E. A., Sclater, F. & Edmond, J. M. Marine geochemistry of cadmium. *Nature* 263, 42–44 (1976).
2. Bruland, K. W., Knauer, G. A. & Martin, J. H. Cadmium in Northeast Pacific waters. *Limnol. Oceanogr.* 23, 618–625 (1978).
3. Lane, T. W. & Morel, F. M. M. A biological function for cadmium in marine diatoms. *Proc. Natl Acad. Sci. USA* 97, 4627–4631 (2000).
4. Morel, F. M. M. *et al.* Zinc and carbon co-limitation of marine phytoplankton. *Nature* 369, 740–742 (1994).
5. Price, N. M. & Morel, F. M. M. Cadmium and cobalt substitution for zinc in a marine diatom. *Nature* 344, 658–660 (1990).
6. Falkowski, P. G. *et al.* The evolution of modern eukaryotic phytoplankton. *Science* 305, 354–360 (2004).
7. Fridborg, K. *et al.* Crystal structure of human erythrocyte carbonic anhydrase C.3 Molecular structure of enzyme and of one enzyme-inhibitor complex at 5.5 Å resolution. *J. Mol. Biol.* 25, 505–516 (1967).
8. Kannan, K. K. *et al.* Crystal structure of human erythrocyte carbonic anhydrase C.6. 3-dimensional structure at high resolution in relation to other mammalian carbonic anhydrases. *Cold Spring Harb. Symp. Quant. Biol.* 36, 221–231 (1971).
9. Liljas, A. *et al.* Crystal structure of human carbonic anhydrase C. *Nature New Biol.* 235, 131–137 (1972).
10. Badger, M. The roles of carbonic anhydrases in photosynthetic CO_2 concentrating mechanisms. *Photosynth. Res.* 77, 83–94 (2003).
11. Reinfelder, J. R., Kraepiel, A. M. L. & Morel, F. M. M. Unicellular C4 photosynthesis in a marine diatom. *Nature* 407, 996–999 (2000).
12. Tripp, B. C., Smith, K. & Ferry, J. G. Carbonic anhydrase: New insights for an ancient enzyme. *J. Biol. Chem.* 276, 48615–48618 (2001).
13. Cronk, J. D. *et al.* Identification of a novel noncatalytic bicarbonate binding site in eubacterial beta-carbonic anhydrase. *Biochemistry* 45, 4351–4361 (2006).
14. Mitsuhashi, S. *et al.* X-ray structure of beta-carbonic anhydrase from the red alga, *Porphyridium purpureum*, reveals a novel catalytic site for CO_2 hydration. *J. Biol. Chem.* 275, 5521–5526 (2000).
15. Sawaya, M. R. *et al.* The structure of beta-carbonic anhydrase from the carboxysomal shell reveals a distinct subclass with one active site for the price of two. *J. Biol. Chem.* 281, 7546–7555 (2006).
16. Strop, P., Smith, K. S., Iverson, T. M., Ferry, J. G. & Rees, D. C. Crystal structure of the "cab"-type beta class carbonic anhydrase from the archaeon *Methanobacterium thermoautotrophicum*. *J. Biol. Chem.* 276, 10299–10305 (2001).
17. Roberts, S. B., Lane, T. W. & Morel, F. M. M. Carbonic anhydrase in the marine diatom *Thalassiosira weissflogii* (Bacillariophyceae). *J. Phycol.* 33, 845–850 (1997).
18. Soto, A. R. *et al.* Identification and preliminary characterization of two cDNAs encoding unique carbonic anhydrases from the marine alga *Emiliania huxleyi*. *Appl. Environ. Microbiol.* 72, 5500–5511 (2006).
19. Cox, E. H. *et al.* The active site structure of *Thalassiosira weissflogii* carbonic anhydrase 1. *Biochemistry* 39, 12128–12130 (2000).
20. Lane, T. W. *et al.* A cadmium enzyme from a marine diatom. *Nature* 435, 42 (2005).
21. Park, H., Song, B. & Morel, F. M. M. Diversity of the cadmium-containing carbonic anhydrase in marine diatoms and natural waters. *Environ. Microbiol.* 9, 403–413 (2007).
22. Holm, L. & Sander, C. Protein structure comparison by alignment of distance matrices. *J. Mol. Biol.* 233, 123–138 (1993).
23. Kimber, M. S. & Pai, E. F. The active site architecture of *Pisum sativum* beta-carbonic anhydrase is a mirror image of that of alpha-carbonic anhydrases. *EMBO J.* 19, 1407–1418 (2000).
24. Satoh, D., Hiraoka, Y., Colman, B. & Matsuda, Y. Physiological and molecular biological characterization of intracellular carbonic anhydrase from the marine diatom *Phaeodactylum tricornutum*. *Plant Physiol.* 126, 1459–1470 (2001).
25. Coleman, J. E. Human carbonic anhydrase. Protein conformation and metal ion binding. *Biochemistry* 4, 2644–2655 (1965).
26. Ejnik, J., Munoz, A., Gan, T., Shaw, C. F. & Petering, D. H. Interprotein metal ion exchange between cadmium-carbonic anhydrase and apo- or zinc-metallothionein. *J. Biol. Inorg. Chem.* 4, 784–790 (1999).
27. Pocker, Y. & Fong, C. T. O. Kinetics of inactivation of erythrocyte carbonic anhydrase by sodium 2,6-pyridinedicarboxylate. *Biochemistry* 19, 2045–2050 (1980).
28. Ahner, B. A., Price, N. M. & Morel, F. M. M. Phytochelatin production by marine phytoplankton at low free metal ion concentrations — Laboratory studies and field data from Massachusetts Bay. *Proc. Natl Acad. Sci. USA* 91, 8433–8436 (1994).
29. Hakansson, K., Carlsson, M., Svensson, L. A. & Liljas, A. Structure of native and apo carbonic anhydrase II and structure of some of its anion-ligand complexes. *J. Mol. Biol.* 227, 1192–1204 (1992).

30. Okoniewska, M., Tanaka, T. & Yada, R. Y. The pepsin residue glycine76 contributes to active-site loop flexibility and participates in catalysis. *Biochem. J.* **349**, 169–177 (2000).
31. Silverman, D. N. Carbonic anhydrase-O^{18} exchange catalyzed by an enzyme with rate contributing proton transfer steps. *Methods Enzymol.* **87**, 732–752 (1982).
32. Christianson, D. W. & Cox, J. D. Catalysis by metal-activated hydroxide in zinc and manganese metalloenzymes. *Annu. Rev. Biochem.* **68**, 33–57 (1999).
33. Alber, B. E. *et al.* Kinetic and spectroscopic characterization of the gamma-carbonic anhydrase from the methanoarchaeon *Methanosarcina thermophila*. *Biochemistry* **38**, 13119–13128 (1999).
34. Fisher, S. Z. *et al.* Speeding up proton transfer in a fast enzyme: Kinetic and crystallographic studies on the effect of hydrophobic amino acid substitutions in the active site of human carbonic anhydrase II. *Biochemistry* **46**, 3803–3813 (2007).
35. Coleman, J. E. Metal ion dependent binding of sulphonamide to carbonic anhydrase. *Nature* **214**, 193–194 (1967).
36. Tibell, L. & Lindskog, S. Catalytic properties and inhibition of Cd^{2+}-carbonic anhydrases. *Biochim. Biophys. Acta* **788**, 110–116 (1984).
37. Burkhardt, S., Amoroso, G., Riebesell, J. & Sultemeyer, D. CO_2 and HCO_3^- uptake in marine diatoms acclimated to different CO_2 concentrations. *Limnol. Oceanogr.* **46**, 1378–1391 (2001).
38. Kuss, J. & Kremling, K. Spatial variability of particle associated trace elements in near-surface waters of the North Atlantic (30 degrees N/60 degrees W to 60 degrees N/2 degrees W), derived by large volume sampling. *Mar. Chem.* **68**, 71–86 (1999).
39. Liu, J. B., Stemmler, A. J., Fatima, J. & Mitra, B. Metal-binding characteristics of the amino-terminal domain of ZntA. Binding of lead is different compared to cadmium and zinc. *Biochemistry* **44**, 5159–5167 (2005).
40. Otwinowski, Z. & Minor, W. Processing of X-ray diffraction data collected in oscillation mode. *Methods Enzymol.* **276**, 307–326 (1997).
41. Sheldrick, G. A short history of SHELX. *Acta Crystallogr. A* **64**, 112–122 (2008).
42. Perrakis, A., Morris, R. & Lamzin, V. S. Automated protein model building combined with iterative structure refinement. *Nature Struct. Biol.* **6**, 458–463 (1999).
43. Brunger, A. T. *et al.* Crystallography & NMR system: A new software suite for macromolecular structure determination. *Acta Crystallogr. D* **54**, 905–921 (1998).
44. Kraulis, P. J. Molscript: A program to produce both detailed and schematic plots of protein structures. *J. Appl. Crystallogr.* **24**, 946–950 (1991).
45. Nicholls, A., Sharp, K. A. & Honig, B. Protein folding and association: Insights from the interfacial and thermodynamic properties of hydrocarbons. *Proteins Struct. Funct. Genet.* **11**, 281–296 (1991).

Supplementary Information is linked to the online version of the paper at www.nature.com/nature.

Acknowledgements We thank A. Saxena at the NSLS for assistance and Patrick McGinn for help with CA assays. This work was supported by start-up funds from Princeton University (to Y.S.), the NSF and the NSF-funded Center for Environmental Bioinorganic Chemistry (to F.M.M.M.).

Author Contributions Y.X. performed all the biochemical experiments; L.F. crystallized all forms of CDCA1; P.D.J. solved the structures, and F.M.M.M. and Y.S. supervised the work and wrote the paper. All authors discussed the results and commented on the manuscript.

Author Information Atomic coordinates have been deposited with the Protein Data Bank with the accession numbers 3BOB (R2-Cd), 3BOC (R2-Zn), 3BOE (R2-Cd-Acetate), 3BOH (R1-Cd-acetate) and 3BOJ (R1-metal free). Reprints and permissions information is available at www.nature.com/reprints. Correspondence and requests for materials should be addressed to F.M.M.M. (morel@princeton.edu) or Y.S. (yshi@princeton.edu).

LETTERS

The unexpected origin of plasmaspheric hiss from discrete chorus emissions

Jacob Bortnik[1], Richard M. Thorne[1] & Nigel P. Meredith[2]

Plasmaspheric hiss[1] is a type of electromagnetic wave found ubiquitously in the dense plasma region that encircles the Earth, known as the plasmasphere[2]. This important wave is known to remove[3–5] the high-energy electrons that are trapped along the Earth's magnetic field lines[6], and therefore helps to reduce the radiation hazards to satellites and humans in space. Numerous theories to explain the origin of hiss have been proposed over the past four decades, but none have been able to account fully for its observed properties. Here we show that a different wave type called chorus[7,8], previously thought to be unrelated to hiss, can propagate into the plasmasphere from tens of thousands of kilometres away, and evolve into hiss. Our new model naturally accounts for the observed frequency band of hiss, its incoherent nature, its day–night asymmetry in intensity, its association with solar activity and its spatial distribution. The connection between chorus and hiss is very interesting because chorus is instrumental in the formation of high-energy electrons outside the plasmasphere[9], whereas hiss depletes these electrons at lower equatorial altitudes[3,4].

Early spacecraft observations beginning in the late 1960s, of wideband electromagnetic noise at frequencies below a few kiloHertz established the presence of a steady, incoherent noise band in the frequency range between ~200 Hz and ~1 kHz (refs 7, 8 and 10). This emission was named plasmaspheric hiss[1] because of its unstructured nature, spectral resemblance to audible hiss, and confinement to the plasmasphere. Hiss occurs at all local times, but intensities are strongest on the day side[1,10,11], and further increase when geomagnetic activity (such as storms and substorms, ultimately driven by solar activity) is increased[11]. There have been a number of different hypotheses attempting to explain the origin of hiss[12] (see Supplementary Information for further discussion), but only two have emerged as the most likely candidates: (1) the *in situ* growth and amplification of background electromagnetic turbulence, driven by unstable energetic electron populations[1,13], and (2) the evolution of a spectrum of electromagnetic waves injected into the plasmasphere by terrestrial lightning strikes, into the observed hiss band[14–17]. However, there are observational difficulties with both leading models for the origin of hiss. Typical wave growth rates inside the plasmasphere are too modest[13] to generate the observed emissions. Alternatively, if plasmaspheric hiss originated from lightning, the emissions would be stronger over the continents than over the oceans because lightning activity is more prevalent over land. A recent study[18] of the geographic association of plasmaspheric emissions above 3 kHz led to substantial controversy[19,20], and a more extensive study[21] showed that hiss below 2 kHz, where the emission power is strongest, has no correlation with landmass. In addition, a lightning source of hiss cannot account for the pronounced association of wave intensities with geomagnetic activity. Clearly, an alternative explanation is required that is theoretically viable and can simultaneously account for all the observed features of hiss.

Figure 1b shows a dynamic spectrogram of an electromagnetic emission known as chorus[7,8,22], which, unlike hiss, occurs in the unstable region outside the plasmasphere. The intensity and spectral characteristics of chorus are very different to those of hiss (Fig. 1c). Chorus wave power is typically greater than that of hiss[1,11,23], and consists of discrete spectral features, which rise at a rate of the order of 1 kHz s^{-1} over a well-defined frequency band controlled by the equatorial electron gyrofrequency (f_{ce}, defined as the frequency with which electrons gyrate about the Earth's magnetic field line, and which is proportional to the magnetic field strength). Chorus typically occurs in two frequency bands: a lower, more intense, band in the range ~0.1–0.45f_{ce}, and an upper band at ~0.5–0.7f_{ce}. In contrast, hiss remains in a roughly constant frequency band of ~0.2–1 kHz throughout the entire plasmasphere.

The propagation of chorus has been modelled as shown in Fig. 1a, using numerical ray tracing for a set of rays initiated at the geomagnetic equator, consistent with observations[22]. The rays are injected at $L = 5$, where L is the distance in Earth radii ($1\ R_E = 6{,}370$ km) from the centre of the Earth to the equatorial crossing of a given magnetic field line, at the lower end of the chorus frequency spectrum, $0.1f_{ce}$, corresponding to a frequency of 704 Hz. Each ray is initiated with a slightly different wave normal angle ψ_0 (defined as the angle between the Earth's magnetic field, and the normal to the plane of the wave, with negative angles pointed towards the Earth), and colour-coded accordingly. The damping experienced by each ray is accurately calculated[23], and each ray is plotted until it decays to 1% of its initial power.

The rays exhibit a variety of behaviours. Those rays with ψ_0 near $-70°$ or $+20°$ are completely damped before they reach high latitudes (for example, $\lambda \approx 50°$), while the rays with $\psi_0 \approx -25°$ to $+10°$ (day side) magnetospherically reflect at high latitudes, and propagate away from the Earth, probably contributing to an emission previously reported as extremely low frequency hiss[8,24]. However, a key range of rays with $\psi_0 \approx -30°$ to $-60°$ (day side), magnetospherically reflect towards lower L[25], and propagate into the plasmasphere. Once inside the plasmasphere, the damping rate is dramatically reduced owing to the high cold electron density, and low electron fluxes which produce the damping. The rays internally reflect many times before being completely damped, and in so doing, fill the plasmasphere with wave energy down to $L \approx 1.6$, consistent with observations[1] (see Supplementary Information for a detailed ray path and discussion). Each ray has a slightly different entry point into the plasmasphere, so the chorus rays which propagated coherently outside the plasmasphere become completely randomized after only one or two internal reflections inside the plasmasphere, leading to the incoherent nature of hiss. Also clearly evident is the dramatic

[1]Department of Atmospheric and Oceanic Sciences, University of California, Los Angeles, 405 Hilgard Avenue, Los Angeles, California 90095, USA. [2]British Antarctic Survey, Natural Environment Research Council, Madingley Road, Cambridge, CB3 0ET, UK.

difference between day and night in the access of rays into the plasmasphere, due primarily to the different electron fluxes responsible for the damping.

To quantify the plasmaspheric access of chorus, rays were traced for different initial values of L, ψ_0 and frequency, and the lifetime τ (defined to be the time taken for the ray to reach 1% of its initial power) was recorded. The results (shown in Fig. 2) can be interpreted as follows: rays that are completely damped before they reach high latitudes typically have $\tau < 1$ s, those that reflect and propagate to higher latitudes typically have $\tau < 5$ s, but rays that enter the plasmasphere have much longer lifetimes. A certain set of rays, marked by the letter I, originating at $L \approx 4.5$–6.5, have lifetimes exceeding 30 s, and coincidentally have frequencies in the range ~0.2–1 kHz, identical to the observed hiss spectrum. On the night side, fewer waves are able to access the plasmasphere, and those that do have much shorter lifetimes, typically $\tau \approx 10$ s. As the frequency of the source population of chorus is increased (day side in Fig. 2c and e; night side in Fig. 2d and f), access into the plasmasphere becomes more restricted, and τ is lowered to less than 10 s, accounting for the reduced intensities of hiss above 1 kHz, and the weaker emissions observed on the night side. The power spectral intensity of those waves that access the plasmasphere is enhanced, owing to the multiple magnetospheric reflections and the reduced magnetospheric volume occupied by hiss compared to that occupied by chorus. Consequently, only a small fraction of the chorus wave power needs to leak into the plasmasphere to account for typical hiss intensities. Interestingly, we also note in Fig. 1a that

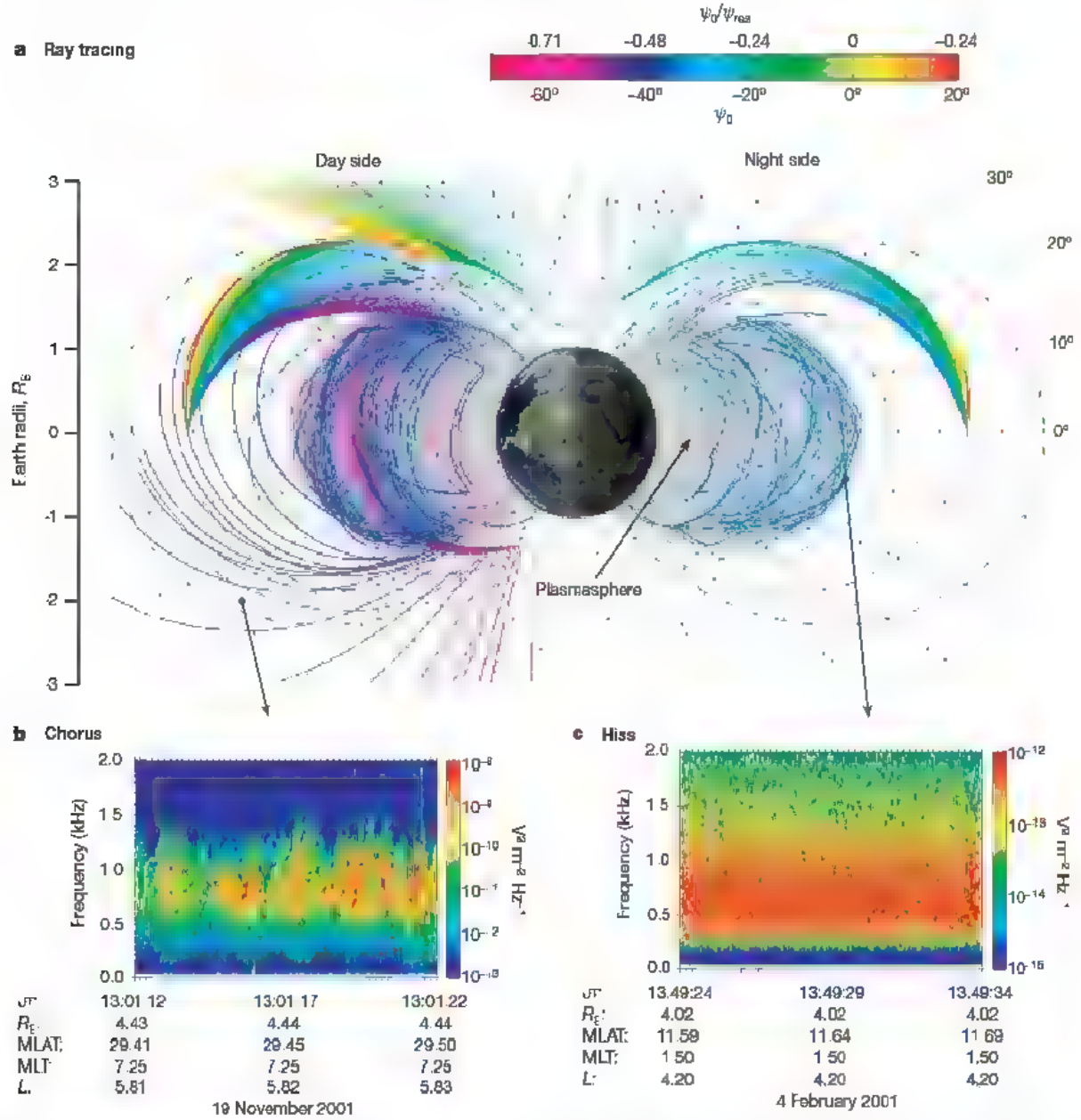

Figure 1 | Evolution of chorus into plasmaspheric hiss. a, A schematic of the near-Earth space environment, with the grey regions indicating the typical location of the dense plasmasphere. A set of 91 rays is launched from the geomagnetic equator (that is, $\lambda = 0°$) at $L = 5$, with $f = 0.1 f_{ce}$ (704 Hz), in the wave normal range −70° to +20°, at every 1°. Each ray is traced until its power decreases to 1% of its initial value, at which point the ray is terminated. Chorus originating with a different frequency and starting location will have a similar set of ray paths, which will merge together into an incoherent emission to fill the outer plasmasphere with hiss. **b**, A 10-s-long spectrogram showing the intensity of a typical series of rising chorus elements, as a function of frequency and time, observed by the Wideband instrument on the Cluster II satellite on the day side outside the plasmasphere. **c**, A similar 10-s-long spectrogram showing plasmaspheric hiss intensity, on the night side inside the plasmasphere. There is a sharp lower frequency cut-off at ~200 Hz, and a more gradual upper frequency cut-off at ~1 kHz, and no apparent structure in the spectrum. The abscissas shown represent: UT, Universal time; MLT, magnetic local time, which is the local time of equatorial crossing of the magnetic field-line passing through the satellite, and can be slightly different to the actual local time; and MLAT, magnetic latitude, the latitude of CRRES relative to the geomagnetic equator.

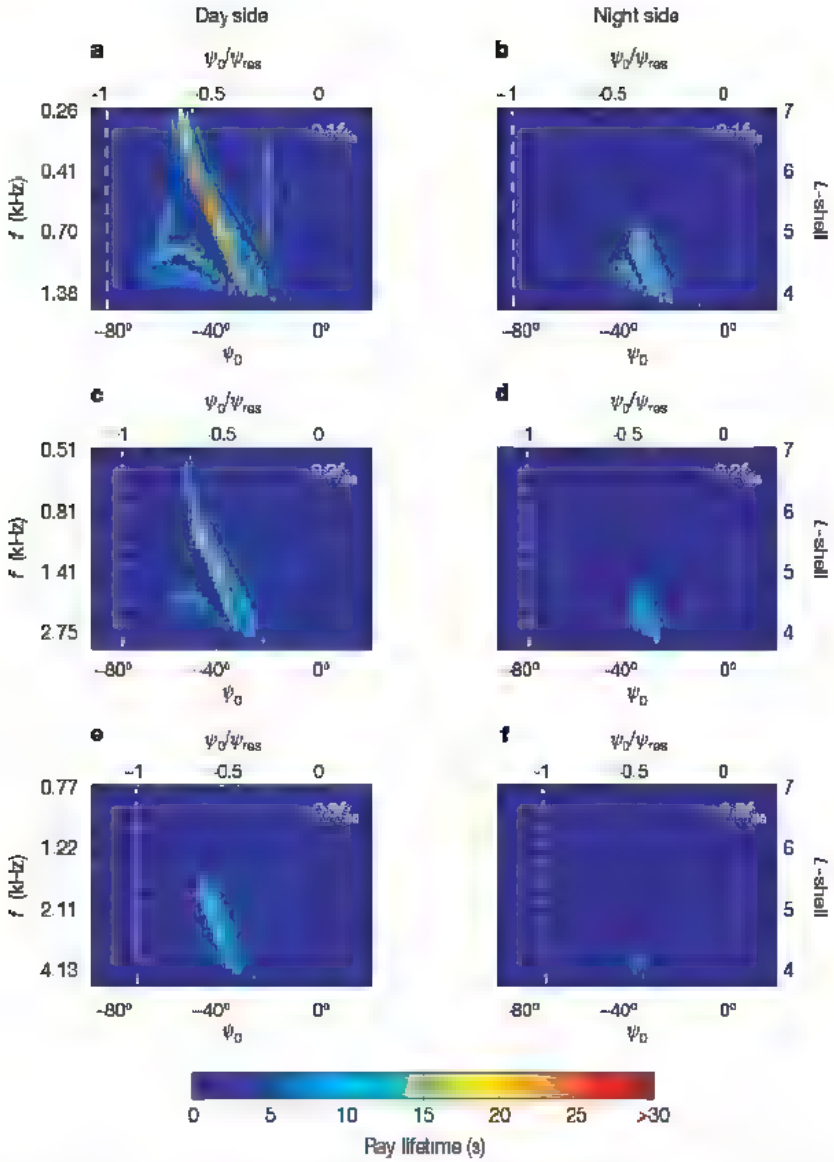

Figure 2 | Penetration characteristics of chorus rays. Each pixel represents a single chorus ray, initiated at the geomagnetic equator at the location L and the wave normal ψ_0 shown. Each chorus ray is ray-traced until its power decreases to 1% of its initial value, and the time is recorded, and displayed using the colour scale at the bottom of the figure. The day side and night side cold plasma distribution is modelled after ref. 28, the field is assumed to be dipolar, and the suprathermal flux distribution used in the calculation of Landau damping outside the plasmasphere is obtained from the CRRES, following the methodology of ref. 23, taking the distribution to be MLT and L-dependent. Inside the plasmasphere, the flux distribution from ref. 29 is assumed. **a–f**, Each panel shows chorus ray lifetimes, for frequencies $f/f_{ce} = 0.1$, 0.2 and 0.3 as shown, normalized to the electron gyrofrequency, with the actual wave frequency f associated with the ray's initial L value. ψ_0 normalized to the resonance-cone angle ψ_{res}, beyond which propagation in the cold-plasma whistler-mode is not possible, is also shown. Rays with lifetimes over 5 s have all entered and remained in the plasmasphere (Fig. 1a), with some rays reaching lifetimes well over 50 s.

some of the chorus rays pass through the plasmasphere, exit and return to the outer magnetosphere. Such emissions have been observed and referred to as exo-hiss in past studies[1] but their origin appears to be chorus.

An observation of hiss and chorus waves from the Combined Release and Radiation Effects Satellite (CRRES) is shown in Fig. 3. During the inbound leg of the orbit (after ~11:00 UT), the satellite travels from higher to lower L and enters the plasmasphere on the day side. Although individual chorus elements cannot be distinguished on this timescale, the frequency band of chorus clearly follows the equatorial gyrofrequency, increasing in frequency as the satellite moves to lower L, and remaining confined roughly to the band ~0.1–0.45f_{ce}. On entering the plasmasphere, the chorus emissions are abruptly cut off at ~14:40 UT, and are replaced by the typical plasmaspheric hiss band, which has a peak intensity near the outer boundary of the plasmasphere and becomes weaker closer to the Earth. Many of the features discussed above are evident in this plot, including the increased intensity of hiss on the day side versus the night side, and the approximate location of the chorus source region, which is believed to leak into the plasmasphere and evolve into hiss (marked by the letter 'S' in Fig. 3), indicating that the rays responsible for the most intense portion of the hiss spectrum are generated well outside the plasmasphere, and not adjacent to it. Also visible is exo-hiss, at ~14:00–14:40, f≈ 0.2–0.5 kHz, outside the plasmasphere, which is believed to have leaked out, as described above. The upper frequency cut-off of both the hiss and chorus waves near the plasmasphere boundary shows a very close correspondence, suggesting that it is these higher-frequency chorus waves that have leaked into the plasmasphere and evolved into the hiss spectrum, but at much lower intensities than the components at less than 1 kHz, as is clearly reproduced in our simulations.

The present modelling study is the first to link chorus to the origin of plasmaspheric hiss. Much detailed modelling remains to be done in this area, but our results naturally account for the essential features of hiss, such as the observed frequency spectrum, its incoherent nature, the day–night asymmetry in intensity, the distribution in L,

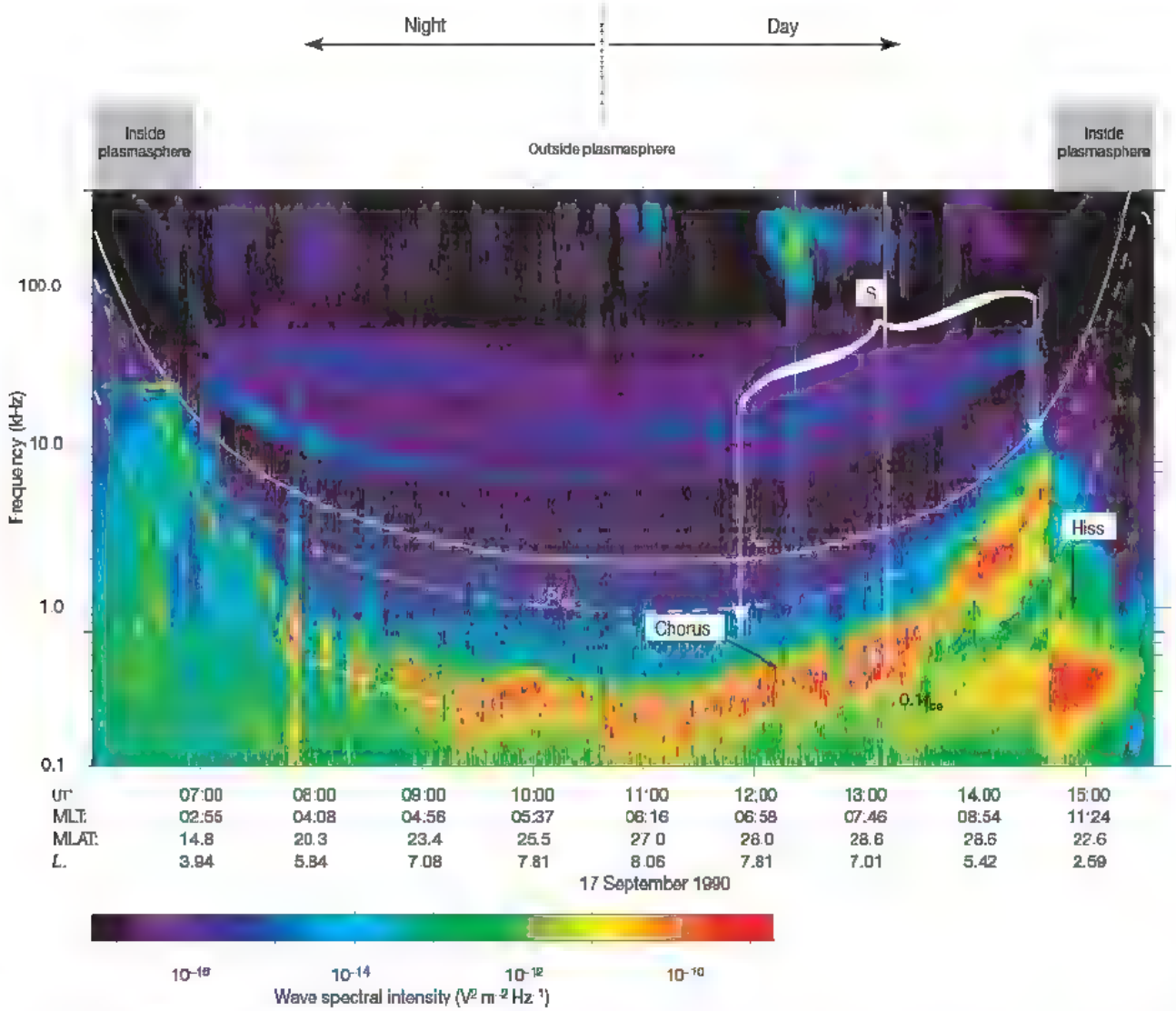

Figure 3 | CRRES satellite data showing chorus and hiss emissions. Survey plot (~9 h) of the wave spectral intensity for orbit 130 from the CRRES Plasma Wave Experiment. The region marked "S" is the source region of chorus from which waves propagate into the plasmasphere and evolve into hiss. We note that there is not a perfect correspondence between the observed chorus and the hiss, because the CRRES satellite was changing its local time rapidly, observing the chorus on the dawn side of the Earth, and the hiss close to noon, so the chorus waves that evolve into the hiss shown would have been produced on the day side, and are different from those shown in the spectrogram (though they would have been qualitatively very similar). The L value of CRRES is calculated using the Olson–Pfitzer tilt-dependent static model[30] and the IGRF 85 model.

the geomagnetic control[11,26,27], as well as other ancillary features, such as exo-hiss and extremely low frequency hiss. We thus contend that chorus waves are the dominant source of plasmaspheric hiss.

Received 1 May 2007; accepted 16 January 2008.

1. Thorne, R. M., Smith, E. J., Burton, R. K. & Holzer, R. E. Plasmaspheric hiss. *J. Geophys. Res.* 78, 1581–1595 (1973).
2. Carpenter, D. L. & Park, C. G. What ionospheric workers should know about the plasmapause/plasmasphere. *Rev. Geophys.* 11, 133–154 (1973).
3. Lyons, L. R., Thorne, R. M. & Kennel, C. F. Pitch-angle diffusion of radiation belt electrons within the plasmasphere. *J. Geophys. Res.* 77, 3455–3474 (1972).
4. Abel, B. W. & Thorne, R. M. Electron scattering loss in Earth's inner magnetosphere. 1. Dominant physical processes. *J. Geophys. Res.* 103, 2385–2396 (1998).
5. Lyons, L. R. & Thorne, R. M. Equilibrium structure of radiation belt electrons. *J. Geophys. Res.* 78, 2142–2149 (1973).
6. Van Allen, J. A. in *Discovery of the Magnetosphere* (eds Gillmor C. S. & Spreiter, J. R.) *History of Geophysics* Vol. 7 235–251 (American Geophysical Union, Washington DC, 1997).
7. Dunckel, N. & Helliwell, R. A. Whistler mode emissions on the Ogo 1 satellite. *J. Geophys. Res.* 74, 6371–6385 (1969).
8. Russell, C. T., Holzer, R. E. & Smith, E. J. OGO 3 observations of ELF noise in the magnetosphere: 1. Spatial extent and frequency of occurrence. *J. Geophys. Res.* 74, 755–777 (1969).
9. Horne, R. B. *et al.* Timescales for radiation belt electron acceleration by whistler mode chorus waves. *J. Geophys. Res.* 111, A03225, doi:10.1029/2004JA010811 (2005).
10. Taylor, W. W. L. & Gurnett, D. A. The morphology of VLF emissions observed with the Injun 3 satellite. *J. Geophys. Res.* 73, 5615–5626 (1968).
11. Meredith, N. P. *et al.* Substorm dependence of plasmaspheric hiss. *J. Geophys. Res.* 109, A06209, doi:10.1029/2004JA010387 (2004).
12. Hayakawa, M. & Sazhin, S. S. Mid-latitude and plasmaspheric hiss: a review. *Planet. Space Sci.* 40, 1325–1338 (1992).
13. Church, S. R. & Thorne, R. M. On the origin of plasmaspheric hiss: ray path integrated amplification. *J. Geophys. Res.* 88, 7941–7957 (1983).
14. Sonwalkar, V. S. & Inan, U. S. Lightning as an embryonic source of VLF hiss. *J. Geophys. Res.* 94, 6986–6994 (1989).
15. Draganov, A. B., Inan, J. S., Sonwalkar, V. S. & Bell, T. F. Magnetospherically reflected whistlers as a source of plasmaspheric hiss. *J. Geophys. Res.* 19, 233–236 (1992).
16. Bortnik, J., Inan, U. S. & Bell, T. F. Frequency-time spectra of magnetospherically reflecting whistlers in the plasmasphere. *J. Geophys. Res.* 108 (A1) 1030 doi:10.1029/2002JA009387 (2003).
17. Bortnik, J., Inan, U. S. & Bell, T. F. Energy distribution and lifetime of magnetospherically reflecting whistlers in the plasmasphere. *J. Geophys. Res.* 108 (A5), 1199, doi:10.1029/2002JA009316 (2003).
18. Green, J. L. *et al.* On the origin of whistler mode radiation in the plasmasphere. *J. Geophys. Res.* 110, A03201, doi:10.1029/2004JA010495 (2005).
19. Thorne, R. M., Horne, R. B. & Meredith, N. P. Comment on "On the origin of whistler mode radiation in the plasmasphere" by Green *et al.* *J. Geophys. Res.* 111, A09210, doi:10.1029/2005JA011477 (2006).
20. Green, J. L. *et al.* Reply to "Comment on "On the origin of whistler mode radiation in the plasmasphere" by Green *et al.*" *J. Geophys. Res.* 111, A09211, doi:10.1029/2006JA011622 (2006).

21 Meredith, N. P. *et al.* Origins of plasmaspheric hiss. *J. Geophys. Res.* **111**, A09217, doi:10.1029/2006JA011707 (2006)
22 Burtis, W. J. & Helliwell, R. A. Magnetospheric chorus: occurrence patterns and normalized frequency. *Planet. Space Sci.* **24**, 1007–1024 (1976)
23. Bortnik, J., Thorne, R. M. & Meredith, N. P. Modeling the propagation characteristics of chorus using CRRES suprathermal electron fluxes. *J. Geophys. Res.* **112**, A08204, doi:10.1029/2006JA012237 (2007)
24. Santolik, O. *et al.* Propagation of whistler mode chorus to low altitudes: Spacecraft observations of structured ELF hiss. *J. Geophys. Res.* **111**, A10208, doi:10.1029/2005JA011462 (2006)
25. Thorne, R. M. & Kennel, C. F. Quasi-trapped VLF propagation in the outer magnetosphere. *J. Geophys. Res.* **72**, 857–870 (1967)
26. Smith, E. J., Frandsen, A. M. A., Tsurutani, B. T., Thorne, R. M. & Chan, K. W. Plasmaspheric hiss intensity variations during magnetic storms. *J. Geophys. Res.* **79**, 2507–2510 (1974)
27. Thorne, R. M., Smith, E. J., Fiske, K. J. & Church, S. R. Intensity variation of ELF hiss and chorus during isolated substorms. *Geophys. Res. Lett.* **1**, 193–196 (1974)
28. Carpenter, D. L. & Anderson, R. R. An ISEE/whistler model of equatorial electron density in the magnetosphere. *J. Geophys. Res.* **97** (A2), 1097–1108 (1992)
29. Bell, T. F., Inan, U. S., Bortnik, J. & Scudder, J. D. The Landau damping of magnetospherically reflected whistlers within the plasmasphere. *Geophys. Res. Lett.* **29**, 15, doi:10.1029/2002GL014752 (2002)
30. Olson, W. P. & Pfitzer, K. *Magnetospheric Magnetic Field Modeling* Annual Scientific Report, AFOSR Contract No. F44620-75-c-0033 (1977)

Supplementary Information is linked to the online version of the paper at www.nature.com/nature.

Acknowledgements J.B. acknowledges support from the National Science Foundation's (NSF) Geospace Environment Modeling (GEM) post-doctoral award and NASA, and R.M.T. acknowledges support from an NSF GEM grant. N.P.M. acknowledges support from the Natural Environment Research Council, UK. We thank Roger R. Anderson for provision of the CRRES plasma wave data used in this study.

Author Contributions J.B. performed all the calculations shown in the paper, wrote the manuscript and Supplementary Information section, and composed all the figures. R.M.T. provided consultation on the theoretical aspects of the work and manuscript writing. N.P.M. provided global models of CRRES/LEPA data used in the Landau damping calculations, the dynamic spectrogram shown in Fig. 3, and input into the manuscript writing.

Author Information Reprints and permissions information is available at www.nature.com/reprints. Correspondence and requests for materials should be addressed to J.B. (jbortnik@gmail.com)

LETTERS

Mapping photonic entanglement into and out of a quantum memory

K. S. Choi[1], H. Deng[1], J. Laurat[1]† & H. J. Kimble[1]

Developments in quantum information science[1] rely critically on entanglement—a fundamental aspect of quantum mechanics that causes parts of a composite system to show correlations stronger than can be explained classically[2]. In particular, scalable quantum networks require the capability to create, store and distribute entanglement among distant matter nodes by means of photonic channels[3]. Atomic ensembles can play the role of such nodes[4]. So far, in the photon-counting regime, heralded entanglement between atomic ensembles has been successfully demonstrated through probabilistic protocols[5,6]. But an inherent drawback of this approach is the compromise between the amount of entanglement and its preparation probability, leading to intrinsically low count rates for high entanglement. Here we report a protocol where entanglement between two atomic ensembles is created by coherent mapping of an entangled state of light. By splitting a single photon[7–9] and performing subsequent state transfer, we separate the generation of entanglement and its storage[10]. After a programmable delay, the stored entanglement is mapped back into photonic modes with overall efficiency of 17%. Together with improvements in single-photon sources[11], our protocol will allow 'on-demand' entanglement of atomic ensembles, a powerful resource for quantum information science.

In the quest to achieve quantum networks over long distances[3], there has been considerable interest in the interaction of light with atomic ensembles consisting of a large collection of identical atoms[4]. In the regime of continuous variables, a notable advance has been the teleportation of quantum states between light and matter[12]. For discrete variables with photons taken one by one, important achievements include the efficient mapping of collective atomic excitations to single photons[13–16], the realization of entanglement between distant ensembles[5,17] and, recently, entanglement distribution involving two pairs of ensembles[6]. The first step towards entanglement swapping has been made[18] and light–matter teleportation has been demonstrated[19].

In all these cases, progress has relied on probabilistic schemes following the measurement-induced approach developed by Duan *et al.*[4] and subsequent extensions. For this protocol, heralded entanglement is generated by detecting a single photon emitted indistinguishably by one of two ensembles. Intrinsically, the probability p of preparing entanglement with only one excitation shared between two ensembles is related to the quality of entanglement, because the likelihood for contamination of the entangled state by processes involving two excitations likewise scales as p (ref. 17), and results in low probability of success. Although the degree of stored entanglement can approach unity for the (rare) successful trials[17], the condition $p \ll 1$ dictates reductions in the count rate and compromises in the quality of the resulting entangled state (for example, as $p \to 0$, processes such as stray light scattering and detector dark counts become increasingly important). Furthermore, for finite memory time, subsequent connection of entanglement becomes increasingly challenging[18].

The separation of processes for the generation of entanglement and for its storage enables this drawback to be overcome. Here, we demonstrate this by reversible mapping of an entangled state into a quantum memory. The mapping is obtained by using adiabatic passage based on dynamic electromagnetically induced transparency (EIT)[20–23] (see Methods). Storage and retrieval of optical pulses have been demonstrated previously, for both classical pulses[24,25] and single-photon pulses[26,27]. Adiabatic transfer of a collective excitation has been demonstrated between two ensembles coupled by a cavity mode[28], which can provide a suitable approach for generating on-demand entanglement over short distances. However, to assist efficient distribution of entanglement over quantum networks, reversible mapping of an entangled state between matter and light, as illustrated in Fig. 1a, has not been addressed until now.

In our experiment, entanglement between two atomic ensembles L_a,R_a is created by first splitting a single photon into two modes L_{in},R_{in} to generate an entangled state of light[7–9]. This entangled field state is then coherently mapped to an entangled matter state for L_a,R_a. On demand, the stored atomic entanglement for L_a,R_a is converted back into entangled photonic modes L_{out},R_{out}. As opposed to the original scheme of Duan *et al.*[4], our approach is inherently deterministic, suffering principally from the finite efficiency of mapping single excitations to and from an atomic memory. An efficiency of about 50% has been achieved (see Methods). Moreover, the contamination of entanglement for L_a,R_a from processes involving two excitations can be arbitrarily suppressed (independent of the mapping probabilities) with continuing advances in on-demand single-photon sources[11]. Our experiment thereby provides a promising tool for distributing and storing entanglement over remote atomic ensembles for quantum networks[10].

The experimental setup is depicted in Fig. 1. Our single-photon source is based on Raman transitions in an optically thick caesium ensemble[4,13] (see Methods). This system generates 28-ns-long single photons (resonant with the $6S_{1/2}, F = 4 \leftrightarrow 6P_{3/2}, F' = 4$ transition) in a heralded fashion where successful photoelectric detection of a single photon unambiguously signals ('heralds') the presence of a single collective excitation, and enables subsequent triggered generation of single photons[13]. The single photons are polarized at 45° from the eigen-polarizations of the beam displacer BD_1 (Fig. 1b) which splits them into entangled optical modes L_{in},R_{in} (called the signal modes) to produce, in the ideal case, the following state:

$$\frac{1}{\sqrt{2}}\left(|0_{L_{in}}\rangle|1_{R_{in}}\rangle + e^{i\phi_{rel}}|1_{L_{in}}\rangle|0_{R_{in}}\rangle\right) \quad (1)$$

The next stage consists of coherently mapping the photonic entanglement for L_{in},R_{in} into atomic ensembles L_a,R_a (called the memory ensembles) within a single cloud of cold caesium atoms in a magneto-optical trap (MOT) (Fig. 1c). Ensembles L_a,R_a are defined by the well-separated optical paths of the entangled photonic modes

[1]Norman Bridge Laboratory of Physics 12-33, California Institute of Technology, Pasadena, California 91125, USA. †Present address: Laboratoire Kastler Brossel, Université P. et M. Curie, Ecole Normale Superieure et CNRS, UPMC Case 74, 4 place Jussieu, 75252 Paris Cedex 05, France.

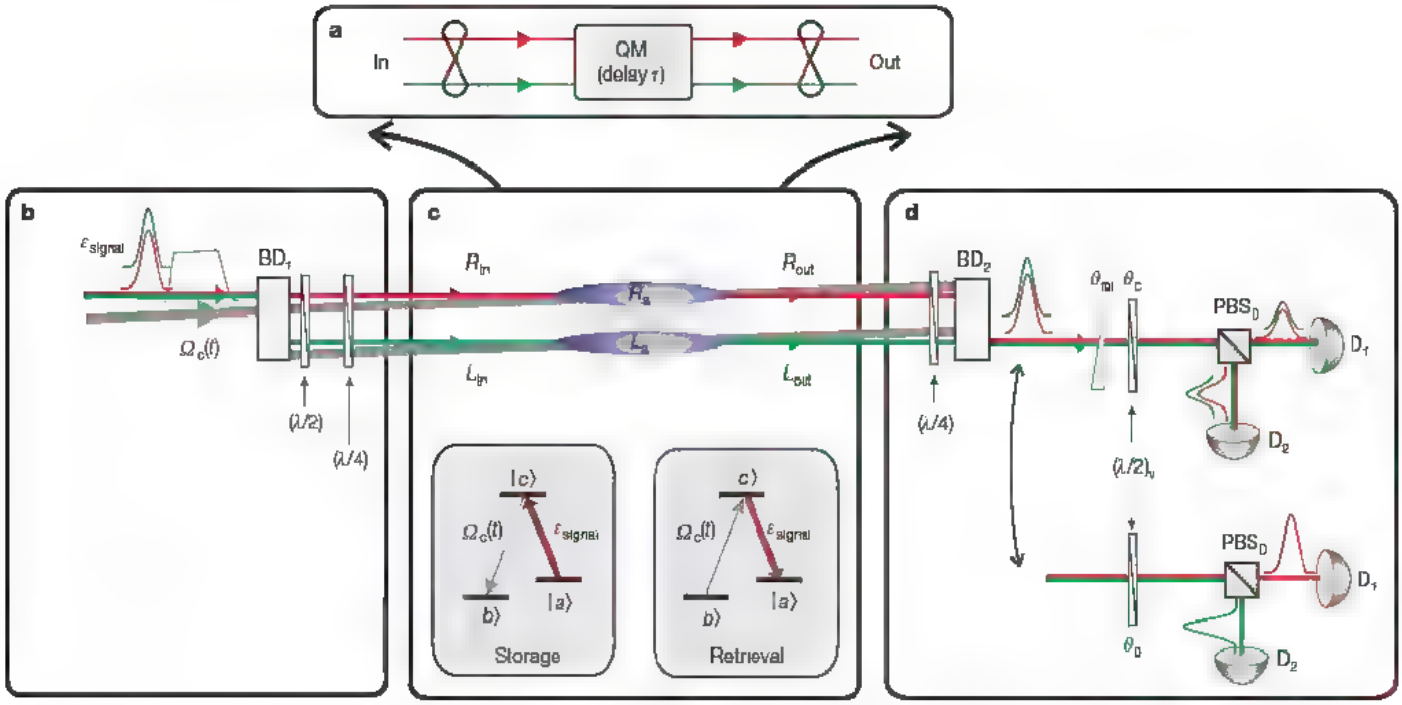

Figure 1 | Overview of the experiment. **a**, Reversible mapping. Illustration of the mapping of an entangled state of light into and out of a quantum memory (QM) with storage time τ. **b**, Photonic 'entangler'. A beam displacer BD_1 splits an input single photon into two orthogonally polarized, entangled modes L_{in},R_{in}, which are spatially separated by 1 mm. With wave plates $\lambda/2$ and $\lambda/4$, the signal fields ε_{signal} for L_{in},R_{in} and the two control fields $\Omega_c^{(L,R)}(t)$ are transformed to circular polarizations with the same helicity along each path L, R, and copropagate with an angle of 3°. **c**, Quantum interface for reversible mapping. Photonic entanglement between L_{in},R_{in} is coherently mapped into the memory ensembles L_a,R_a by switching $\Omega_c^{(L,R)}(t)$ off adiabatically. After a programmable storage time, the atomic entanglement is reversibly mapped back into optical modes L_{out},R_{out} by switching $\Omega_c^{(L,R)}(t)$ on. Relevant energy diagrams for the storage and retrieval processes are shown in the insets. States $|a\rangle$, $|b\rangle$ are the hyperfine ground states $F = 4$, $F = 3$ of $6S_{1/2}$ in atomic caesium; state $|c\rangle$ is the hyperfine level $F' = 4$ of the electronic excited state $6P_{3/2}$. **d**, Entanglement verification. After a $\lambda/4$ plate, the beam displacer BD_2 combines modes L_{out},R_{out} into one beam with orthogonal polarizations. With the verification wave plate $(\lambda/2)_v$ at $\theta_c = 22.5°$ before the polarization beamsplitter (PBS_D), single-photon interference is recorded at detectors D_1,D_2 by varying the relative phase ϕ_{rel} with a Berek compensator. With $(\lambda/2)_v$ at $\theta_0 = 0°$, photon statistics for each mode L_{out},R_{out} are measured independently.

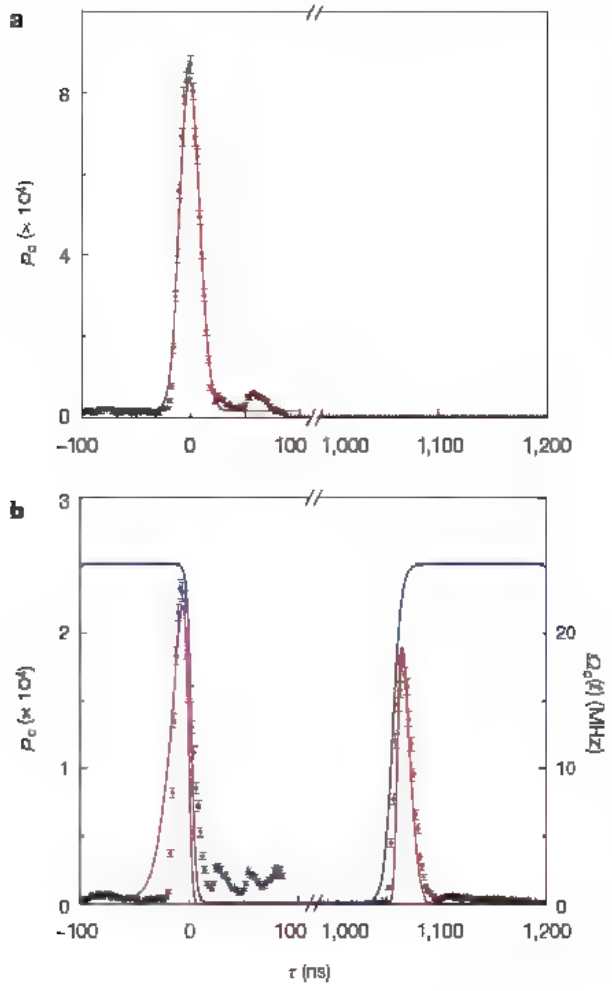

L_{in},R_{in}. To avoid dissipative absorption for the fields in modes L_{in},R_{in} for our choice of polarization[26], we spin-polarize the atomic ensemble into one Zeeman sublevel of a hyperfine ground state $|F = 4, m_F = 0\rangle$. Initially, the strong control fields $\Omega_c^{(L,R)}(t)$ (resonant with $6S_{1/2}$, $F = 3 \leftrightarrow 6P_{3/2}$, $F' = 4$ transition) open transparency windows $\Omega_c^{(L,R)}(0)$ in L_a,R_a for the signal modes. As the wave packet of the signal field propagates through each ensemble, the control fields $\Omega_c^{(L,R)}(t)$ are turned off in 20 ns by an electro-optical intensity modulator, thus coherently transforming the fields of the respective signal modes to collective atomic excitations within L_a,R_a. This mapping leads to heralded entanglement between L_a,R_a. After a user-defined delay, chosen here to be 1.1 μs, the atomic entanglement is converted back into entangled photonic modes by switching on the control fields $\Omega_c^{(L,R)}(t)$ (see Methods). Alternate algorithms for quantum control of the conditional readout allow extensions for entanglement connection and distribution by way of asynchronous preparation[6,18].

For a given optical depth γ, there is an optimal Rabi frequency $\Omega_c(t)$ for the control field. In our experiment, γ and $\Omega_c(0)$ are 15 and 24 MHz, respectively. An example of our measurements of the EIT process for a single ensemble is presented in Fig. 2. Because of finite γ, the small length (~3 mm) of the ensemble and the turn-off time of the intensity modulator, there is considerable loss in the storage process, as

Figure 2 | Single-photon storage and retrieval for a single ensemble. **a**, Input. The data points are the measured probabilities p_c for the signal field, a single photon generated from a separate atomic ensemble[15]. The red solid line represents a gaussian fit of 1/e width 28 ns. **b**, Storage and retrieval. The points around $\tau = 0$ μs represent 'leakage' of the signal field due to the finite optical depth and length of the ensemble. The points beyond $\tau = 1$ μs show the retrieved signal field. The overall storage and retrieval efficiency is $(17 \pm 1)\%$. The blue solid line is the estimated Rabi frequency $\Omega_c(t)$ of the control pulse. The red solid curve is from a numerical calculation solving the equation of motion of the signal field in a dressed medium[25]. Error bars give the statistical error of 1σ for each point.

evidenced by the counts around $\tau = 0$ μs in Fig. 2b. The peak beyond $\tau = 1$ μs represents the retrieved pulse after 1.1 μs of storage. Overall, we find good agreement between our measurements and numerical calculations following the methods in ref. 23. We use the fitted function of the input signal field (Fig. 2a) as the initial condition with all other parameters from independent measurements (see Methods). We find an overall storage and retrieval efficiency of $\eta_r = 17 \pm 1\%$, also in agreement with the simulation of $\eta_r^{\text{theory}} = 18\%$.

With these results in hand for the individual L_a,R_a ensembles, we next turn to the question of verification of entanglement for the optical modes of L_{in},R_{in} and L_{out},R_{out}. We follow the protocol introduced in ref. 5 by (1) reconstructing a reduced density matrix ρ constrained to a subspace containing no more than one excitation in each mode, and (2) assuming that all off-diagonal elements between states with different numbers of photons vanish, thereby obtaining a lower bound for any purported entanglement. In the photon-number basis $|n_L,m_R\rangle$ with $\{n,m\} = \{0,1\}$, the reduced density matrix ρ is written as[5]

$$\rho = \frac{1}{P}\begin{pmatrix} p_{00} & 0 & 0 & 0 \\ 0 & p_{10} & d & 0 \\ 0 & d^* & p_{01} & 0 \\ 0 & 0 & 0 & p_{11} \end{pmatrix} \quad (2)$$

Here, p_{ij} is the probability of finding i photons in mode L_k and j in mode R_k, $d \approx \frac{1}{2}V(p_{10} + p_{01})$ is the coherence between $|1_L 0_R\rangle_k$ and $|0_L 1_R\rangle_k$, $P = p_{00} + p_{10} + p_{01} + p_{11}$, and V is the visibility for interference between modes L_k,R_k with $k \in \{\text{in, out}\}$. The degree of entanglement of ρ can be quantified in terms of concurrence, $C = \frac{1}{P}\max\left(0, 2|d| - 2\sqrt{p_{00}p_{11}}\right)$, which is a monotone function of entanglement, ranging from 0 for a separable state to 1 for a maximally entangled state[29].

We first perform tomography on the input modes L_{in},R_{in} to verify that they are indeed entangled. To this end, we remove the memory ensembles to transmit the signal fields directly into the verification stage, following our protocol of complementary measurements as described in Fig. 1d. The interference fringes between the two input modes are shown in Fig. 3a. From the independently determined propagation and detection efficiencies (see Methods), we use the measurements at D_1,D_2 to infer the quantum state for the input modes L_{in},R_{in} entering the faces of L_a,R_a (ref. 5), with the reconstructed density matrix ρ_{in} given in Fig. 3a. The concurrence derived from ρ_{in} is $C_{in} = 0.10 \pm 0.02$, so the fields for L_{in},R_{in} are indeed entangled. The value of the concurrence is in good agreement with the independently derived expectation of $C_{in}^{\text{theory}} = 0.10 \pm 0.01$, which depends on the quality of the single photon and the vacuum component (that is, the overall efficiency)[17]. Given a heralding click from our single-photon source, the probability of having a single photon at the face of either memory ensemble is 15%, leading to a vacuum component of 85%. We also independently characterize the suppression w of the two-photon component relative to a coherent

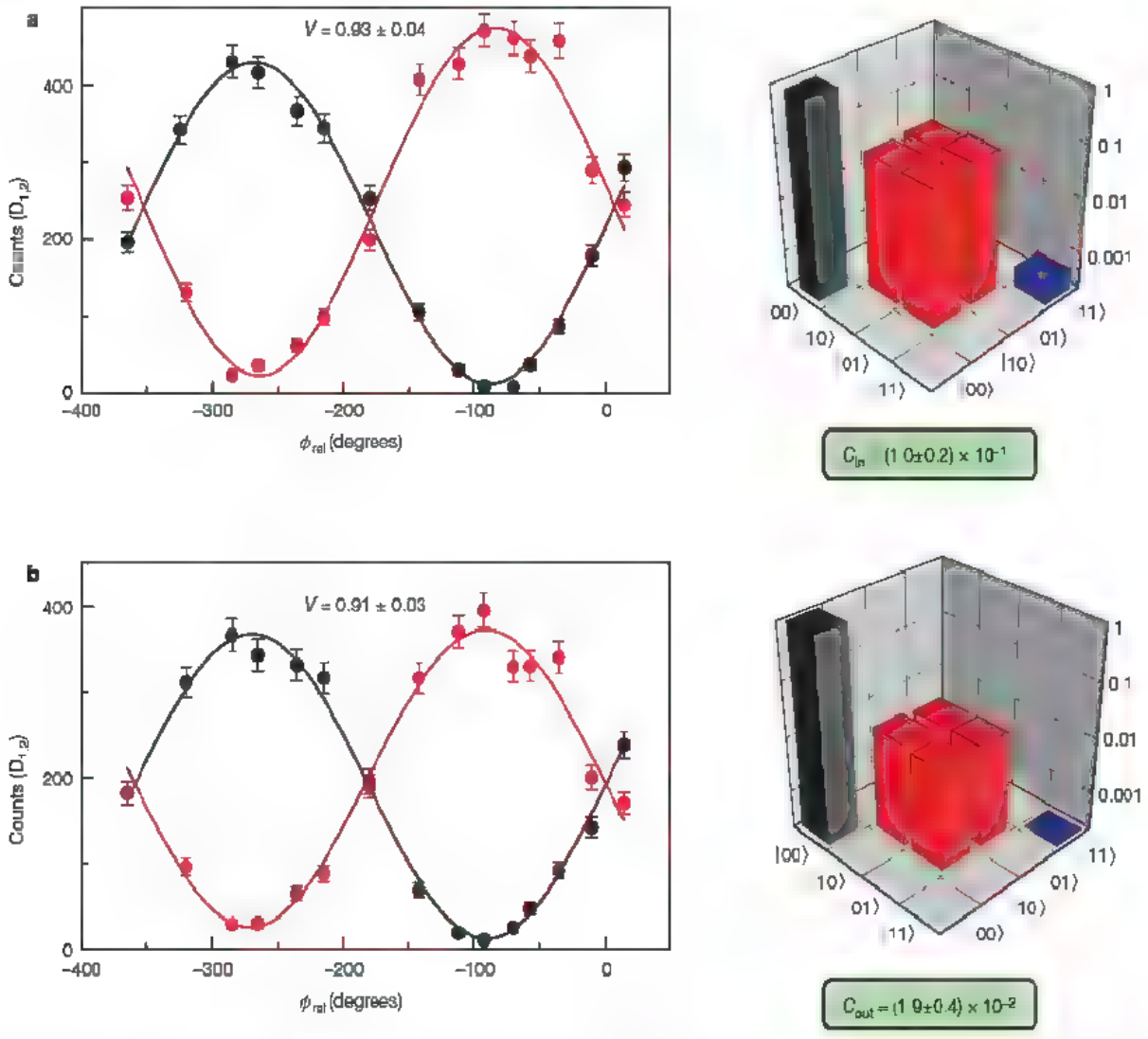

Figure 3 | Entanglement for the input and output optical modes. To verify entanglement, complementary measurements are made: interference leading to a fringe when the relative phase ϕ_{rel} is scanned and independent photon statistics for each light mode. Interference fringes and the reconstructed density matrices (in log scale) are shown for the photonic modes: **a**, at the input of the memory and **b**, the output after storage and retrieval. The estimated concurrence is given in each case. Each point of the fringe is taken for 20,000 (100,000) heralding events for the input (output) state. The red and black data points correspond to detection events in detectors D_1,D_2, respectively. Error bars indicate statistical errors of 1σ.

state (for which $w = 1$) and find $w = 0.09 \pm 0.03$. Our input entanglement is limited only by the current properties of our single-photon source, which will be improved with the rapid advances in sources of single photons[11].

Having verified entanglement for the input modes L_{in},R_{in}, we next map this photonic entanglement into L_a,R_a, which serve as a quantum memory (Fig. 1c). After storing the entanglement for 1.1 μs, we transfer the resulting atomic excitation from the memory to the output modes L_{out},R_{out} and perform quantum-state tomography to determine ρ_{out} as for ρ_{in}. As shown in Fig. 3, the visibility for interference of the fields after storage and retrieval shows no appreciable degradation (from $V_{in} = 0.93 \pm 0.04$ to $V_{out} = 0.91 \pm 0.03$). From the measurements at D_1,D_2, we infer the quantum state ρ_{out} at the output faces of L_a,R_a, as displayed in Fig. 3b. The associated concurrence $C_{out} = (1.9 \pm 0.4) \times 10^{-2}$ is in agreement with $C_{out}^{theory} = (1.7 \pm 0.1) \times 10^{-2}$. Because mapping of atomic states from L_a,R_a into field modes L_{out},R_{out} is a local operation, this measurement provides a lower bound for the entanglement between the L_a,R_a ensembles[5]. Thus, we demonstrate the reversible mapping of an entangled state of the electromagnetic field to and from a material system. For completeness, Table 1 gives the diagonal elements and concurrences of $\bar{\rho}_{in}$,$\bar{\rho}_{out}$ determined directly at D_1 and D_2 without correction for propagation and detection efficiencies.

We emphasize that although the entanglement associated with ρ_{out} is heralded (because of the nature of our single-photon source), our protocol for generation and storage of entanglement is intrinsically deterministic. The transfer efficiency of entanglement from input modes to output modes of the quantum memory is limited by the storage and retrieval efficiency η_r of the EIT process. This transfer can be quantified by the ratio λ of the concurrence C_{out} for the output state ρ_{out} to C_{in} for the input state ρ_{in}. For an ideal source of single photons on-demand (with no vacuum component), the input concurrence is approximated by $C_{in} \approx \alpha V$, where α denotes the transmission efficiency of the single photon from the source to the entangler in Fig. 1b (ref. 17). Similarly, for the output, $C_{out} \approx \alpha\eta_r V$, where we assume that the visibility V is preserved by the mapping processes. Thus, $\lambda = C_{in}/C_{out} \approx \eta_r$, which therefore estimates the maximum amount of entanglement in modes L_{out},R_{out} for the case of an ideal single photon generated deterministically. In our experiment, the entanglement transfer reaches $\lambda = (20 \pm 5)\%$. By optimal pulse shaping and improved optical depth, the entanglement transfer could be greatly improved (see Methods).

The performance of our quantum interface also depends on the memory time τ_m over which one can faithfully retrieve a stored quantum state. For our system, independent measurements of η_r made by varying the storage duration τ allow us to determine $\tau_m = (8 \pm 1)$ μs, as limited by inhomogeneous Zeeman broadening and misalignment of the quantization axis. Active and passive compensation of the residual magnetic field would improve τ_m, along with optical trapping techniques (see Methods).

In conclusion, our work provides the first realization of mapping an entangled state into and out of a quantum memory. Our protocol alleviates the significant drawback of probabilistic protocols[4], where low preparation probabilities prevent its potential scalability[18], and thus our strategy can be incorporated into extensions of ref. 4 for efficient scaling for high-fidelity quantum communication[10]. Our results are limited by the large vacuum component of our available single-photon source, which reduces the degree of entanglement in the input, and by the limited retrieval efficiency of the EIT process, which limits the entanglement transfer to $\lambda = (20 \pm 5)\%$. With improved retrieval efficiency and memory time, along with the rapid development of on-demand single-photon sources[11], our protocol will make possible the generation, storage and distribution of entanglement among remote quantum memories for scalable quantum networks. Such networks have diverse applications in quantum information science, including quantum metrology, where quantum sensing is provided by the atomic entanglement and readout by coherent mapping to the photonic modes.

In the broader context of quantum information theory, our experiment contributes to the lively debate about 'single-particle' entanglement[7,8,30]. Part of the discussion centres on a gedanken experiment in which an entangled state for a single particle is mapped into a two-particle system by local operations, verifying the presence of entanglement for the original 'single-particle' state[30]. Our experiment demonstrates that an entangled state with one photonic excitation shared between two optical modes (see equation (1)) can be converted into an entangled state for two atomic ensembles by way of coherent mapping. The presence of entanglement between the two atomic ensembles is explicitly quantified by the lower bound $C_{out} = (1.9 \pm 0.4) \times 10^{-2}$, thereby realizing the proposal of ref. 30.

Table 1 | Experimentally determined $\bar{\rho}_{ij}$ and concurrences $\bar{C}_{in}$, $\bar{C}_{out}$

	$\bar{\rho}_{in}$	$\bar{\rho}_{out}$
$\bar{\rho}_{00}$	0.9800 ± 0.0001	0.99625 ± 0.00003
$\bar{\rho}_{10}$	$(1.043 \pm 0.008) \times 10^{-2}$	$(2.09 \pm 0.02) \times 10^{-3}$
$\bar{\rho}_{01}$	$(0.957 \pm 0.008) \times 10^{-2}$	$(1.67 \pm 0.02) \times 10^{-3}$
$\bar{\rho}_{11}$	$(8 \pm 2) \times 10^{-6}$	$(2 \pm 2) \times 10^{-7}$
$\bar{C}$	$(1.28 \pm 0.09) \times 10^{-2}$	$(2.5 \pm 0.5) \times 10^{-3}$

The diagonal elements $\bar{\rho}_{ij}$ and concurrences $\bar{C}_{in}$, $\bar{C}_{out}$ for the density matrices $\bar{\rho}_{in}$, $\bar{\rho}_{out}$ are those derived directly from detectors D_1,D_2 without correction for losses and detection efficiencies. Statistical errors of 1σ are also given.

METHODS SUMMARY

After loading the atoms into a magneto-optical trap and subsequent cooling, the atomic ensembles are optically pumped to $|F = 4, m_F = 0\rangle$ by Zeeman pumping beams (close to $4 \leftrightarrow 4'$ transition and linearly polarized along the quantization axis, and a hyperfine pumping beam. Each trial starts at a repetition rate of 1.7 MHz. The single-photon source is a cold atomic ensemble (called the source ensemble) located 3 m from the memory ensembles, synchronized by a fast clock signal. We apply a sequence of write and read laser pulses to the source ensemble which generates sequentially a pair of Raman scattered fields 1, 2, where field 2 is collectively enhanced. The detection of field 1 is used to trigger a logic circuit which terminates the write and read lasers during the storage process at the quantum interface. All data are taken conditioned on a field-1 detection for the source ensemble. The single photon propagates through the memory ensembles where the group velocity of the field is adiabatically reduced and stopped by reducing the intensity of the control laser[23]. On demand, the single excitation shared between L_a,R_a is retrieved back to photonic modes by time-reversing the control laser. The operational procedures for constructing the reduced density matrix (equation (2)) are based on the analysis in ref. 5 and are further elaborated.

Full Methods and any associated references are available in the online version of the paper at www.nature.com/nature.

Received 16 October 2007; accepted 3 January 2008.

1. Zoller, P. *et al.* Quantum information processing and communication. Strategic report on current status, visions and goals for research in Europe. *Eur. Phys. J. D* **36**, 203–228 (2005).
2. Clauser, J. F. & Shimony, A. Bell's theorem: Experimental tests and implications. *Rep. Prog. Phys.* **41**, 1881–1927 (1978).
3. Briegel, H.-J., van Enk, S. J., Cirac, J. I. & Zoller, P. Quantum networks and multi-particle entanglement. in *The Physics of Quantum Information* (eds Bouwmeester, D., Ekert, A. K. & Zeilinger, A.) (Springer, Berlin, 2000).
4. Duan, L.-M., Lukin, M. D., Cirac, J. I. & Zoller, P. Long-distance quantum communication with atomic ensembles and linear optics. *Nature* **414**, 413–418 (2001).
5. Chou, C. W. *et al.* Measurement-induced entanglement for excitation stored in remote atomic ensembles. *Nature* **438**, 828–832 (2005).
6. Chou, C. W. *et al.* Functional quantum nodes for entanglement distribution over scalable quantum networks. *Science* **316**, 1316–1320 (2007).
7. Tan, S. M., Walls, D. F. & Collett, M. J. Nonlocality of a single photon. *Phys. Rev. Lett.* **66**, 252–255 (1991).
8. Hessmo, B., Usachev, P., Heshang, H. & Gunner, B. Experimental demonstration of single photon nonlocality. *Phys. Rev. Lett.* **92**, 180401 (2004).
9. Jacques, V. *et al.* Experimental realization of Wheeler's delayed-choice gedanken experiment. *Science* **315**, 966–968 (2007).
10. Sangouard, N. *et al.* Long-distance entanglement distribution with single-photon sources. *Phys. Rev. A* **76**, 050301(R) (2007).
11. Lounis, B. & Orrit, M. Single-photon sources. *Rep. Prog. Phys.* **68**, 1129–1179 (2005).

12. Sherson, J. F. *et al.* Quantum teleportation between light and matter *Nature* **443**, 557–560 (2006)
13. Laurat, J. *et al.* Efficient retrieval of a single excitation stored in an atomic ensemble. *Opt. Express* **14**, 6912–6918 (2006).
14. Thompson, J. K., Simon, J., Loh, H. & Vuletić, V. A high-brightness source of narrowband, identical photon pairs. *Science* **313**, 74–77 (2006).
15. Matsukevich, D. N. *et al.* Deterministic single photons via conditional quantum evolution *Phys. Rev. Lett.* **97**, 013601 (2006).
16. Chen, S. *et al.* Deterministic and storable single-photon source based on a quantum memory *Phys. Rev. Lett.* **97**, 173004 (2006)
17. Laurat, J., Choi, K. S., Deng, H., Chou, C.-W. & Kimble, H. J. Heralded entanglement between atomic ensembles: Preparation, decoherence, and scaling. *Phys. Rev. Lett.* **99**, 180504 (2007)
18. Laurat, J. *et al.* Towards experimental entanglement connection with atomic ensembles in the single excitation regime. *New J. Phys.* **9**, 207–220 (2007).
19. Chen, Y.-A. *et al.* Memory-built-in quantum teleportation with photonic and atomic qubits. *Nature Phys.* **4**, 103–107 (2008)
20. Harris, S. E. Electromagnetically induced transparency *Phys. Today* **50**, 36–40 (1997).
21. Hau, L. V., Harris, S. E., Dutton, Z. & Behroozi, C. H. Light speed reduction to 17 metres per second in an ultracold atomic gas *Nature* **397**, 594–598 (1999).
22. Kash, M. M. *et al.* Ultraslow group velocity and enhanced nonlinear optical effects in a coherently driven hot atomic gas. *Phys. Rev. Lett.* **82**, 5229–5232 (1999).
23. Fleischhauer, M. & Lukin, M. D. Dark-state polaritons in electromagnetically induced transparency *Phys. Rev. Lett.* **84**, 5094–5097 (2000).
24. Liu, C., Dutton, Z., Behroozi, C. H. & Hau, L. V. Observation of coherent optical information storage in an atomic medium using halted light pulses *Nature* **409**, 490–493 (2001)
25. Phillips, D. F., Fleischhauer, A., Mair A., Walsworth, R. L. & Lukin, M. D. Storage of light in atomic vapor *Phys. Rev. Lett.* **86**, 783–786 (2001)
26. Chanelière, T. *et al.* Storage and retrieval of single photons transmitted between remote quantum memories. *Nature* **438**, 833–836 (2005).
27. Eisaman, M. D. *et al.* Electromagnetically induced transparency with tunable single-photon pulses. *Nature* **438**, 837–841 (2005).
28. Simon, J., Tanji, H., Ghosh, S. & Vuletic, V. Single-photon bus connecting spin-wave quantum memories. *Nature Phys.* **3**, 765–769 (2007).
29. Wootters, W. K. Entanglement of formation of an arbitrary state of two qubits. *Phys. Rev. Lett.* **80**, 2245–2248 (1998)
30. van Enk, S. J. Single-particle entanglement. *Phys. Rev. A.* **72**, 064306 (2005)

Supplementary Information is linked to the online version of the paper at www.nature.com/nature.

Acknowledgements We acknowledge our ongoing collaboration with S. J. van Enk. This research is supported by the Intelligence Advanced Research Projects Activity and by the National Science Foundation. H.D. acknowledges support as Fellow of the Center for the Physics of Information at Caltech. J.L. acknowledges financial support from the European Union (Marie Curie Fellowship).

Author Contributions K.S.C. and H.D. are the principal contributors to the experiment in equal measure.

Author Information Reprints and permissions information is available at www.nature.com/reprints. Correspondence and requests for materials should be addressed to H.J.K. (hjkimble@caltech.edu).

LETTERS

Strong dispersive coupling of a high-finesse cavity to a micromechanical membrane

J. D. Thompson[1], B. M. Zwickl[1], A. M. Jayich[1], Florian Marquardt[2], S. M. Girvin[1,3] & J. G. E. Harris[1,3]

Macroscopic mechanical objects and electromagnetic degrees of freedom can couple to each other through radiation pressure. Optomechanical systems in which this coupling is sufficiently strong are predicted to show quantum effects and are a topic of considerable interest. Devices in this regime would offer new types of control over the quantum state of both light and matter[1–4], and would provide a new arena in which to explore the boundary between quantum and classical physics[5–7]. Experiments so far have achieved sufficient optomechanical coupling to laser-cool mechanical devices[8–12], but have not yet reached the quantum regime. The outstanding technical challenge in this field is integrating sensitive micromechanical elements (which must be small, light and flexible) into high-finesse cavities (which are typically rigid and massive) without compromising the mechanical or optical properties of either. A second, and more fundamental, challenge is to read out the mechanical element's energy eigenstate. Displacement measurements (no matter how sensitive) cannot determine an oscillator's energy eigenstate[13], and measurements coupling to quantities other than displacement[14–16] have been difficult to realize in practice. Here we present an optomechanical system that has the potential to resolve both of these challenges. We demonstrate a cavity which is detuned by the motion of a 50-nm-thick dielectric membrane placed between two macroscopic, rigid, high-finesse mirrors. This approach segregates optical and mechanical functionality to physically distinct structures and avoids compromising either. It also allows for direct measurement of the square of the membrane's displacement, and thus in principle the membrane's energy eigenstate. We estimate that it should be practical to use this scheme to observe quantum jumps of a mechanical system, an important goal in the field of quantum measurement.

Experiments and theoretical proposals aiming to study quantum aspects of the interaction between optical cavities and mechanical objects have focused on cavities in which one of the cavity's mirrors is free to move (for example, in response to radiation pressure exerted by light in the cavity). A schematic of such a setup is shown in Fig. 1a. Although quite simple, Fig. 1a captures the relevant features of nearly all optomechanical systems described in the literature, including cavities with 'folded' geometries, cavities in which multiple mirrors are free to move[5], and whispering gallery mode resonators[14] in which light is confined to a waveguide. All these approaches share two important features. First, the optical cavity's detuning is proportional to the displacement of a mechanical degree of freedom (that is, mirror displacement or waveguide elongation). Second, a single device must provide both optical confinement and mechanical pliability.

In these systems, optomechanical coupling can be strong enough to laser-cool their brownian motion by a factor of 400 via passive cooling[13]. But the coupling has been insufficient to observe quantum

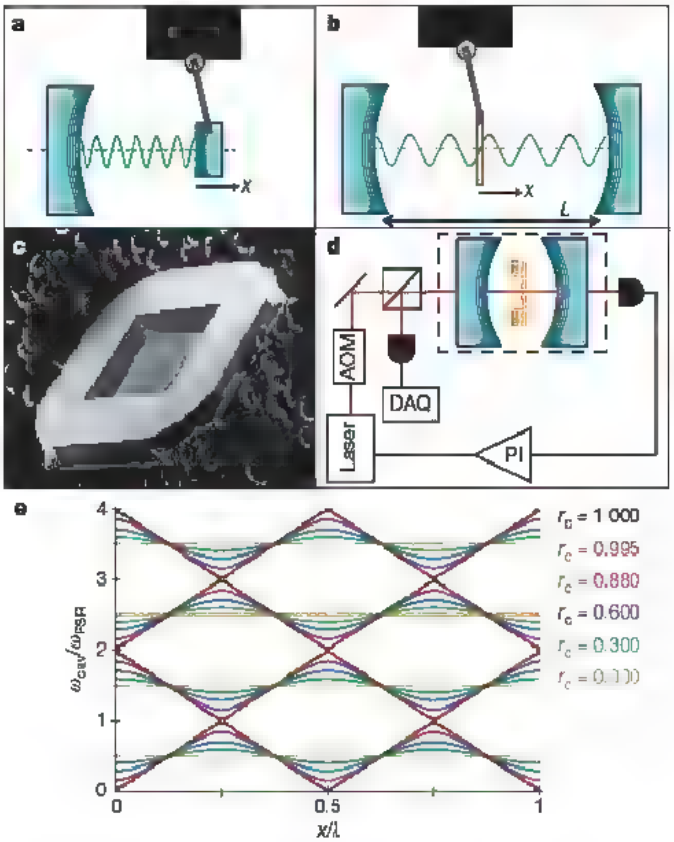

Figure 1 | Schematic of the dispersive optomechanical set-up. **a**, Conceptual illustration of 'reflective' optomechanical coupling. The cavity mode (green) is defined by reflective surfaces, one of which is free to move. The cavity detuning is proportional to the displacement x. **b**, Conceptual illustration of the 'dispersive' optomechanical coupling used in this work. The cavity is defined by rigid mirrors. The only mechanical degree of freedom is that of a thin dielectric membrane (orange) in the cavity mode (green). The cavity detuning is periodic in the displacement x. The total cavity length is $L = 6.7$ cm. **c**, Photograph of a SiN membrane (1 mm × 1 mm × 50 nm) on a silicon chip. **d**, Schematic of the optical and vacuum setup. The vacuum chamber (dotted line) is ion-pumped to $\sim 10^{-6}$ torr. The membrane chip is shown in orange. The optical path includes an AOM for switching the laser beam on and off, and a proportional-integral (PI) servo loop for locking the laser to the cavity. The reflected laser power is recorded by a data acquisition system (DAQ). **e**, Calculation of the cavity frequency $\omega_{cav}(x)$ in units of $\omega_{FSR} = \pi c/L$. Each curve corresponds to a different value of the membrane reflectivity r_c. Extrema in $\omega_{cav}(x)$ occur when the membrane is at a node (or antinode) of the cavity mode. Positive (negative) slope of $\omega_{cav}(x)$ indicates the light energy is stored predominantly in the right (left) half of the cavity, with radiation pressure force acting to the left (right).

[1]Department of Physics, Yale University, 217 Prospect Street, New Haven, Connecticut, 06520, USA. [2]Physics Department, Center for Nano Science, and Arnold Sommerfeld Center for Theoretical Physics, Ludwig Maximilians University, Theresienstrasse 37, 80333, Munich, Germany. [3]Department of Applied Physics, Yale University, 15 Prospect Street, New Haven, Connecticut 06520, USA.

effects such as quantum fluctuations (shot noise) of the radiation pressure. To illustrate the connection between observing quantum effects and the properties of the devices in Fig. 1a we consider a figure of merit R, the ratio between the force power spectral densities of radiation pressure shot noise ($S_F^{(\gamma)}$) and thermal fluctuations ($S_F^{(T)}$): $R \equiv S_F^{(\gamma)}/S_F^{(T)} = 16\hbar P_{in} QF^2/\lambda c\pi k_b T m\omega_m$. Here P_{in} and λ are the laser power and wavelength incident on the cavity; F is the cavity finesse; Q, m and ω_m are the mechanical element's quality factor, motional mass and resonant frequency; and T is the temperature of the thermal bath. This expression highlights the importance of achieving both good optical properties (high F) and good mechanical properties (high Q, small m, spring constant k).

Simultaneously achieving good mechanical and optical properties has been the main technical barrier to realizing quantum optomechanical systems. In large part this is because high-finesse mirrors are not easily integrated into micromachined devices. These mirrors are typically SiO_2/Ta_2O_5 multilayers which are mechanically lossy[17] (limiting Q); they must also be ~2 μm thick and ~30 μm in diameter to avoid transmission and diffraction losses[18,19], setting lower limits on m and k; and the mirror's cleanliness and flatness must be maintained during micromachining. As a result most experiments (including those using whispering gallery mode resonators) reach a compromise between high-quality optical or mechanical properties.

Figure 1b shows a cavity layout that differs from Fig. 1a and is the focus of this paper. The cavity is a standard high-finesse Fabry–Perot which in our laboratory is formed between two macroscopic, rigid, commercial mirrors mounted to a rigid spacer. These mirrors are assumed to be fixed. The mechanically compliant element is a thin dielectric membrane placed at the waist of the cavity mode. We use a commercial SiN membrane 1 mm square by 50 nm thick. The membrane is supported by a silicon frame (a typical device is shown in Fig. 1c). The cavity is excited by a laser with $\lambda = 1{,}064$ nm. The beam path is shown in Fig. 1d.

Unlike the cavities illustrated in Fig. 1a, the coupling between the membrane and the optical cavity in Fig. 1b depends on where the membrane is placed relative to the nodes of the cavity mode (shown in green in Fig. 1b). This results in a cavity detuning $\omega_{cav}(x)$ which is periodic in the membrane displacement x, in analogy with the dispersive coupling in some atom-cavity experiments[20,21]. A one-dimensional calculation gives $\omega_{cav}(x) = (d/L)\cos^{-1}[r_c \cos(4\pi x/\lambda)]$ where L is the cavity length and r_c is the membrane's (field) reflectivity. Figure 1e shows a plot of $\omega_{cav}(x)$ for various values of r_c. This geometry is discussed in ref. 22, although not its connection to the fabrication and quantum non-demolition issues discussed here

The optical force on the membrane is proportional to $\partial\omega_{cav}/\partial x \propto r_c$, so using a membrane with modest r_c does not substantially reduce the optomechanical coupling. Thus our approach removes the need to integrate good mirrors into good mechanical devices. We have made use of the fact that the cavity mirrors set F, and the mechanical element's reflectivity only determines the fraction of intracavity photons that transfer momentum to the membrane. Our approach also relaxes the constraint on the mechanical element's thickness, although not on its lateral size.

For this 'membrane-in-the-middle' approach to work, the membrane must not diminish F through absorption or scatter, or by coupling light into lower-F modes. Figure 2a shows cavity ringdown measurements with the membrane removed (blue), and with the membrane inserted at an antinode (green) or node (red) of the intracavity field. Fitting the empty cavity data gives $F_0 = 16{,}100$. With the membrane at an antinode F drops to $F_{AN} = 6{,}940$, implying $\mathrm{Im}(n_{SiN}) = 1.6 \times 10^{-4}$ (n_{SiN} is the membrane's refractive index), consistent with tabulated optical properties[23] of SiN. But when the membrane is placed at a node, the finesse is $F_N = 15{,}200$, equal to F_0 to within the repeatability of the measurement (~10%).

Figure 2a thus highlights an additional important advantage of the 'membrane-in-the-middle' geometry. It allows us to use a membrane much thinner than λ and to position it at a cavity node, greatly reducing the overlap of the membrane with the optical field and making the membrane's already small optical losses essentially irrelevant. This is important both for maintaining high F and ensuring the mechanical device is not heated by absorption of light. By contrast, a cantilever-mounted mirror as in Fig. 1a must overlap with several antinodes[18]. A similar suppression is used in blue-detuned optical lattices where atoms are trapped at the optical field nodes and experience greatly reduced scattering[24]. Straightforward calculations show that with the measured SiN optical loss, commercially available end mirrors could allow $F > 5 \times 10^5$ if the membrane is placed at a node.

Figure 2b shows the transmission through the cavity as function of laser frequency and x. The bright bands correspond to cavity

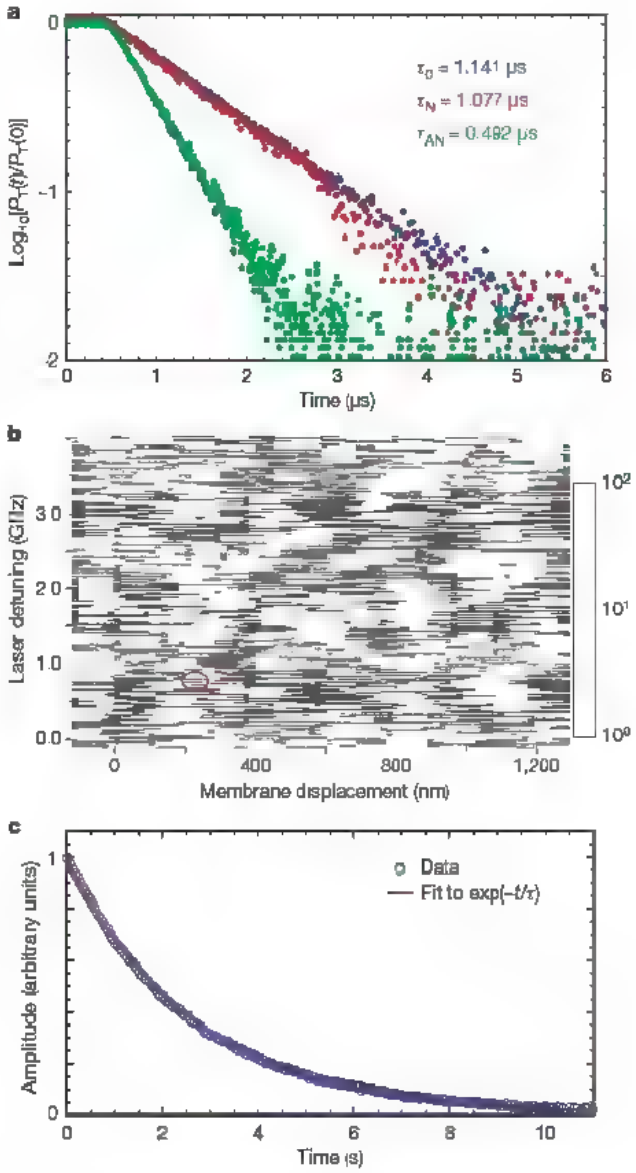

Figure 2 | Optical and mechanical characterization of the cavity. **a**, Ringdown measurements of the cavity with the membrane removed (blue), and with it placed at a cavity node (red) or at an antinode (green). The transmitted power P_T is plotted as a function of time. The laser is switched off at 400 ns. An offset has been subtracted from the data. The exponential time constants (τ_0, τ_N and τ_{AN}) fitted to the data correspond to cavity finesses $F_0 = 16{,}100$, $F_N = 15{,}200$ and $F_{AN} = 6{,}940$. **b**, Logarithmic greyscale plot of the cavity transmission versus laser detuning and membrane position. The two brightest curves correspond to the cavity's TEM_{00} mode. Fitting the data gives the membrane reflectivity $r_c = 0.42$ (see Fig. 1e). The fainter curves are higher-order transverse modes. **c**, Ringdown measurement of the membrane's lowest mechanical resonance. The fit gives a ringdown time $\tau = 2.67$ s, corresponding to $Q = \omega_m\tau/2 = 1.1 \times 10^6$

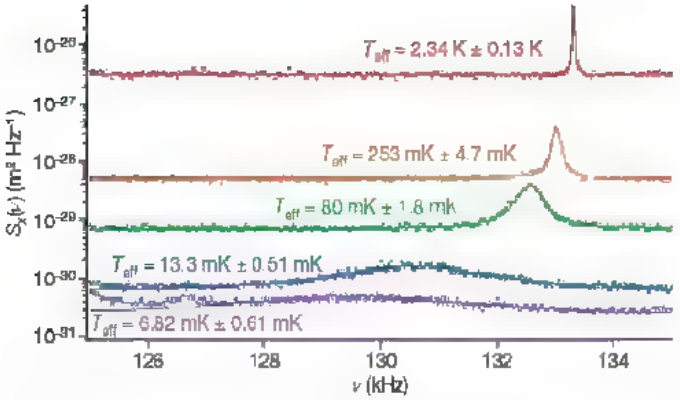

Figure 3 | Passive laser cooling of the membrane. The power spectral density S_x of the membrane's undriven motion at different values of the laser detuning (from top to bottom: 4.84, 2.18, 1.66, 1.00 and 0.71 cavity linewidths) and an incident optical power $P_{in} = 114\,\mu W$ (except for the uppermost curve for which $P_{in} = 359\,\mu W$). Solid lines are fits to a damped driven oscillator model. The effective temperature T_{eff} of the membrane is determined from Q_{eff} and is indicated on the figure (the quoted error is the statistical error in fitting Q_{eff}, as determined from the fit residuals). A broad feature partially visible at the left of the lowest two data sets is due to electrical noise and was excluded from the fits. The noise floor is set by stationary voltage noise at the detector. The noise floor differs in the curves because of the detuning dependence of the volts-to-metres conversion.

resonances. Fitting the data gives $r_c = 0.42$, consistent with the membrane thickness and $\mathrm{Re}(n_{SiN}) = 2.2$.

Figure 2c shows the mechanical ringdown of the membrane's lowest flexural resonance at $\omega_m = 2\pi \times 134\,\mathrm{kHz}$. From ω_m and m (calculated from the membrane dimensions to be 4×10^{-8} g) we find the spring constant $k = 28\,\mathrm{N\,m^{-1}}$. Fitting the data in Fig. 2c gives $Q = 1.1 \times 10^6$.

For small oscillation amplitudes the membrane is well described as a harmonic oscillator and $\omega_{cav}(x)$ is linear to lowest order in x (except at an extremum of $\omega_{cav}(x)$). Thus this device can mimic the traditional optomechanical systems illustrated in Fig. 1a, but without the technical challenge of integrating mirrors into cantilevers.

To illustrate this point, we use the mechanism described in refs 9–12 to laser-cool the membrane's brownian motion. Figure 3 shows the power spectral density of the membrane's undriven motion $S_x(\nu)$ when the laser is slightly red-detuned from the cavity resonance. The membrane's motion is monitored by means of the light reflected from the cavity while the laser detuning and P_{in} are varied. As described elsewhere[9–12], the radiation pressure exerted by the red-detuned laser damps the membrane's brownian motion.

We extract the membrane's effective temperature T_{eff} from the data in Fig. 3 in two ways: $T_{eff}^{(x)} = m\omega_m^2\langle x^2\rangle/k_B$ or $T_{eff}^{(Q)} = TQ_{eff}/Q$ where $\langle x^2\rangle = \int S_x(\nu)\mathrm{d}\nu$ and the effective Q factor Q_{eff} is found by fitting each curve. The values of $T_{eff}^{(x)}$ and $T_{eff}^{(Q)}$ agree to within a factor of ~2, with $T_{eff}^{(x)}$ systematically less than $T_{eff}^{(Q)}$. Because $T_{eff}^{(x)}$ may be affected by small errors in the absolute calibration of x, we cite $T_{eff}^{(Q)}$ in Fig. 3.

The lowest temperature achieved in Fig. 3 is 6.82 mK, a factor of 4.4×10^4 below the starting temperature of 294 K. This is a cooling ratio more than 100 times greater than has been achieved previously with passive laser cooling of mechanical devices[11]. It is made possible by the geometry of this system, which allows us to combine high-F cavities with high-Q, low-k mechanical oscillators.

The laser cooling in Fig. 3 was obtained by positioning the membrane so that $\omega_{cav}(x)$ is proportional to x. However, if the membrane is positioned at an extremum of ω_{cav} (red circle in Fig. 2b), then to lowest order $\omega_{cav}(x) \propto x^2$. In this case, light leaving the cavity carries information only about x^2. The ability to realize a direct x^2-measurement is a fundamental difference between our approach and previous work because it can be used as a quantum non-demolition readout of the membrane's phonon number eigenstate[13].

To see this we note that the Hamiltonian of the optomechanical system is $\hat{H} = \hbar\omega_{cav}(\hat{x})\hat{a}^\dagger\hat{a} + \hbar\omega_m\hat{b}^\dagger\hat{b}$ where $\hat{a}$ and $\hat{b}$ are the lowering operators for the optical and mechanical modes, $\hat{x} = x_m(\hat{b}^\dagger + \hat{b})$, and $x_m = \sqrt{\hbar/2m\omega_m}$. With the membrane at an extremum of ω_{cav} (for example, $x = 0$), we can expand $\hat{H} \approx \hbar(\omega_{cav}(0) + \frac{1}{2}\omega''_{cav}(0)x_m^2(\hat{b}^\dagger + \hat{b})^2)\hat{a}^\dagger\hat{a} + \hbar\omega_m\hat{b}^\dagger\hat{b}$ where $\omega''_{cav} = \partial^2\omega_{cav}/\partial x^2$. In the rotating wave approximation (valid when $\pi dLF \ll \omega_m$)[25], this becomes $\hat{H} \approx \hbar(\omega_{cav}(0) + \omega''_{cav}(0)x_m^2(\hat{b}^\dagger\hat{b} + \frac{1}{2}))\hat{a}^\dagger\hat{a} + \hbar\omega_m\hat{b}^\dagger\hat{b}$. Thus, within this approximation, $[\hat{H}, \hat{b}^\dagger\hat{b}] = 0$, and so the membrane's phonon number can be measured without back action. In principle $\hat{b}^\dagger\hat{b}$ can be read out by monitoring the optical cavity: it experiences a detuning-per-phonon $\Delta\omega_{cav} = x_m^2\omega''_{cav}(0)$ which can be monitored with a Pound–Drever–Hall circuit.

The presence of extrema in $\omega_{cav}(x)$ thus provides an optomechanical coupling of the form required for quantum non-demolition measurements of the membrane's phonon number. Whether such a measurement can be used to observe a quantum jump of the membrane depends on whether $\Delta\omega_{cav} = (16\pi^2 c x_m^2/L\lambda^2)\sqrt{2(1-r_c)}$ can be resolved in the lifetime of a phonon number state. The shot-noise-limited sensitivity of an ideal Pound–Drever–Hall detector is[26] $S_{\omega_{cav}} = \pi^3\hbar c^3/16F^2L^2\lambda P_{in}$, and the (power) signal-to-noise ratio for resolving a jump from the nth phonon state is $\Sigma^{(n)} = \tau_{tot}^{(n)}\Delta\omega_{cav}^2/S_{\omega_{cav}}$. For realistic parameters we find that the lifetime of the nth phonon state $\tau_{tot}^{(n)}$ is primarily limited by thermal excitations, with small corrections due to the rotating wave approximation and imperfect positioning of the membrane at $x = 0$. The relevant calculation is in the Supplementary Information.

For our estimates we assume that $T = 300\,\mathrm{mK}$, that the membrane is laser-cooled to its ground state[25], and that the cooling laser is then shut off. We calculate $\Sigma^{(0)}$, the signal-to-noise ratio for observing the quantum jump of the membrane out of its ground state. Table 1 shows two sets of experimental parameters giving $\Sigma^{(0)} \approx 1$. The parameters in Table 1, although challenging, seem feasible. We have measured $Q = 1.2 \times 10^7$ for these membranes at $T = 300\,\mathrm{mK}$, and have cryogenically cooled the brownian motion of similar devices[27] to 300 mK. The x^2-measurement can be realized with the membrane at a node, so $F > 3 \times 10^5$ should be possible. With the membrane at a node, we assume that P_{in} of a few microwatts would not lead to excessive heating. The mass $m = 5 \times 10^{-11}$ g is the motional mass of a membrane 50 nm thick and 40 μm in diameter. Remarkably, patterning such a membrane can lead to high r_c (ref. 28) and may allow for $r_c > 0.999$ (O. Solgaard, personal communication). The required picometre-scale placement of the membrane is within the stability and resolution of cryogenic positioning systems[29]. According to the standard theory of radiation pressure cooling[25,30], the parameters in Table 1 should allow laser cooling to the membrane's ground state ($n < 0.1$) using P_{in} as low as 0.1 nW. Experiments with higher-F mirrors and cryogenic pre-cooling are under way in our laboratory.

The new type of optomechanical coupling that we have developed resolves a number of the outstanding technical issues faced by previous approaches. It offers the new feature of allowing a sensitive

Table 1 | Parameters for observing a membrane's quantum jumps

Q	T (K)	F	P_{in} (μW)	m (pg)	$\omega_m/2\pi$ (Hz)	r_c	x_0 (pm)	λ (nm)	$\tau^{(0)}$ (ms)	$\Sigma^{(0)}$
1.2×10^7	0.3	3×10^5	10	50	10^5	0.999	0.5	532	0.3	1.0
1.2×10^7	0.3	6×10^5	1	50	10^5	0.9999	0.5	532	0.3	4.0

Two sets of experimental parameters that would allow observation of an individual quantum jump from the membrane's ground state to its first excited state.

x^2-measurement which should make it possible to measure the quantum jumps of micrometre-scale mechanical oscillators. This approach should make it straightforward to couple multiple mechanical devices to a single cavity mode. Stacking multiple chips like the one in Fig. 1c would give a self-aligned array of membranes which could be placed inside a cavity. Such a complex optomechanical system would be particularly interesting for studying entanglement between the membranes[4] or using one membrane to provide a quantum non-demolition readout of another.

METHODS SUMMARY

The optical cavity is formed between two commercial mirrors rigidly attached to an Invar spacer. The SiN membrane is mounted inside the cavity on a stage which allows us to adjust *in situ* the membrane's tilt relative to the cavity axis and its position along the cavity axis. The stage also includes a piezoelectric element which allows us to excite the lowest several vibrational modes of the membrane.

The cavity is illuminated by a continuous-wave Nd:YAG laser. The beam path includes an acousto-optic modulator (AOM) which is used to chop the laser beam in order to perform the cavity ringdown measurements in Fig. 2a.

To measure Q the membrane's lowest vibrational mode mode was excited by means of the piezoelectric drive. The drive was then abruptly switched off and the membrane's ringdown was monitored, as shown in Fig. 2c. For these measurements we used a laser with $\lambda = 1{,}550$ nm. At this wavelength, $F \approx 1$, ensuring that the laser light does not affect the membrane's mechanical properties. Measurements of Q at cryogenic temperatures were carried out in a ^{3}He refrigerator using a fibre-optic interferometer and $\lambda = 1{,}550$ nm laser light.

The calibration of the brownian motion signals in Fig. 3 is somewhat more complicated than for optomechanical systems using the 'usual' geometry. This is because the cavity detuning (shown in Fig. 1e) depends on the membrane reflectivity as well as its position relative to a node in the optical field. Our calibration procedure involves measuring the photodiode signal produced by a frequency modulation of the laser (equivalent to modulation of the cavity detuning or modulation of the membrane displacement) and then calibrating the cavity detuning in terms of the membrane displacement. This requires several intermediate steps described in the online Methods.

Full Methods and any associated references are available in the online version of the paper at www.nature.com/nature.

Received 11 July; accepted 20 December 2007.

1. Fabre, C. *et al.* Quantum-noise reduction using a cavity with a movable mirror. *Phys. Rev. A.* **49**, 1337–1343 (1994)
2. Giovannetti, V., Mancini, S. & Tombesi, P. Radiation pressure induced Einstein–Podolsky–Rosen paradox. *Europhys. Lett.* **54**, 559–565 (2001)
3. Vitali, D. *et al.* Optomechanical entanglement between a movable mirror and a cavity field. *Phys. Rev. Lett.* **98**, 030405 (2007)
4. Pinard, M. *et al.* Entangling movable mirrors in a double-cavity system. *Europhys. Lett.* **72**, 747–753 (2005).
5. Bose, S., Jacobs, K. & Knight, P. L. Scheme to probe the decoherence of a macroscopic object. *Phys. Rev. A.* **59**, 3204–3210 (1999).
6. Marshall, W., Simon, C., Penrose, R. & Bouwmeester, D. Towards quantum superpositions of a mirror. *Phys. Rev. Lett.* **91**, 130401 (2003)
7. Pereira, A., Guerreiro, A. & Vedral, V. Macroscopic thermal entanglement due to radiation pressure. *Phys. Rev. Lett.* **96**, 060407 (2006).
8. Höhberger, C. & Karrai, K. Cavity cooling of a microlever. *Nature* **432**, 1002–1005 (2004)
9. Gigan, S. *et al.* Self cooling of a micromirror by radiation pressure. *Nature* **444**, 67–70 (2006)
10. Arcizet, O., Cohadon, P.-F., Briant, T., Pinard, M. & Heidmann, A. Radiation-pressure cooling and optomechanical instability of a micromirror. *Nature* **444**, 71–74 (2006)
11. Corbitt, T. *et al.* An all-optical trap for a gram-scale mirror. *Phys. Rev. Lett.* **98**, 150802 (2007)
12. Schliesser, A., Del'Haye, P., Nooshi, N., Vahala, K. J. & Kippenberg, T. J. Radiation pressure cooling of a micromechanical oscillator using dynamical backaction. *Phys. Rev. Lett.* **97**, 243905 (2006).
13. Braginsky, V. B., Vorontsov, Y. I. & Thorne, K. S. Quantum nondemolition measurements. *Science* **209**, 547–557 (1980)
14. Santamore, D. H., Doherty, A. C. & Cross, M. C. Quantum nondemolition measurements of Fock states of mesoscopic mechanical oscillators. *Phys. Rev. B* **70**, 144301 (2004)
15. Martin, I. & Zurek, W. H. Measurement of energy eigenstates by a slow detector. *Phys. Rev. Lett.* **98**, 120401 (2007).
16. Jacobs, K., Lougovski, P. & Blencowe, M. Continuous measurement of the energy eigenstates of a nanomechanical resonator without a nondemolition probe. *Phys. Rev. Lett.* **98**, 147201 (2007)
17. Harry, G. M. *et al.* Thermal noise in interferometric gravitational wave detectors due to dielectric optical coatings. *Class. Quantum Grav.* **19**, 897–917 (2002).
18. Hood, C. J., Kimble, H. J. & Ye, J. Characterization of high-finesse mirrors: Loss, phase shifts, and mode structure in an optical cavity. *Phys. Rev. A.* **64**, 033804 (1999)
19. Kleckner, D. *et al.* High finesse opto-mechanical cavity with a movable thirty-micron-size mirror. *Phys. Rev. Lett.* **96**, 173901 (2006).
20. Brune, M., Haroche, S., Lefevre, V., Raimond, J. M. & Zagury, N. Quantum nondemolition measurement of small photon numbers by Rydberg-atom phase-sensitive detection. *Phys. Rev. Lett.* **65**, 976–979 (1990).
21. Wallraff, A. *et al.* Strong coupling of a single photon to a superconducting qubit using circuit quantum electrodynamics. *Nature* **431**, 162–167 (2004)
22. Meystre, P., Wright, E. M., McCullen, J. D. & Vignes, E. Theory of radiation-pressure-driven interferometers. *J. Opt. Soc. Am. B* **2**, 1830–1840 (1985).
23. Poenar, D. P. & Wolffenbuttel, R. F. Optical properties of thin-film silicon-compatible materials. *Appl. Opt.* **36**, 5122–5128 (1997)
24. Müller-Seydlitz, T. *et al.* Atoms in the lowest motional band of a three-dimensional optical lattice. *Phys. Rev. Lett.* **78**, 1038–1041 (1997)
25. Marquardt, F., Chen, J. P., Clerk, A. A. & Girvin, S. M. Quantum theory of cavity-assisted sideband cooling of mechanical motion. *Phys. Rev. Lett.* **99**, 093902 (2007)
26. Black, E. D. An introduction to Pound–Drever–Hall laser frequency stabilization. *Am. J. Phys.* **69**, 79–87 (2001)
27. Bleszynski, A. C., Shanks, W. E. & Harris, J. G. E. Noise thermometry and electron thermometry of a sample-on-cantilever system below 1 Kelvin. *Appl. Phys. Lett.* **92**, 013123 (2008).
28. Kilic, O. *et al.* Photonic crystal slabs demonstrating strong broadband supression of transmission in the presence of disorders. *Opt. Lett.* **29**, 2782–2784 (2004).
29. Stipe, B. C., Rezaei, M. A. & Ho, W. A variable-temperature scanning tunneling microscope capable of single-molecule vibrational spectroscopy. *Rev. Sci. Instrum.* **70**, 137–143 (1999).
30. Wilson-Rae, I., Nooshi, N., Zwerger, W. & Kippenberg, T. J. Theory of ground state cooling of a mechanical oscillator using dynamical backaction. *Phys. Rev. Lett.* **99**, 093901 (2007)

Supplementary Information is linked to the online version of the paper at www.nature.com/nature.

Acknowledgements We acknowledge funding by the NSF, the DFG NIM network and Emmy Noether programme (F.M.), and a fellowship from the Sloane Research Foundation (J.H.). We thank W. Shanks for the microscopy and cryogenic measurements, and C. Yang for assistance with the laser-cooling measurements.

Author Information Reprints and permissions information is available at www.nature.com/reprints. Correspondence and requests for materials should be addressed to J.G.E.H. (jack.harris@yale.edu).

LETTERS

Multi-membrane hydrogels

Sébastien Ladet[1], Laurent David[1] & Alain Domard[1]

Polysaccharide-based hydrogels are useful for numerous applications, from food[1] and cosmetic processing to drug delivery and tissue engineering[2,3]. The formation of hydrogels from polyelectrolyte solutions is complex, involving a variety of molecular interactions. The physical gelation of polysaccharides can be achieved by balancing solvophobic and solvophilic interactions[4]. Polymer chain reorganization can be obtained by solvent exchange, one of the processing routes forming a simple hydrogel assembly. Nevertheless, many studies on hydrogel formation are empirical with a limited understanding of the mechanisms involved, delaying the processing of more complex structures. Here we use a multi-step interrupted gelation process in controlled physico-chemical conditions to generate complex hydrogels with multi-membrane 'onion-like' architectures. Our approach greatly simplifies the processing of gels with complex shapes and a multi-membrane organization. In contrast with existing assemblies described in the literature, our method allows the formation of free 'inter-membrane' spaces well suited for cell or drug introduction. These architectures, potentially useful in biomedical applications, open interesting perspectives by taking advantage of tailor-made three-dimensional multi-membrane tubular or spherical structures.

Here we report on the processing of multi-membrane structured materials (Fig. 1) based on physical hydrogels of amphiphilic polymers obtained without external cross-linker. We have applied the approach to chitosan and alginate, but it could be generalized to numerous amphiphilic polyelectrolyte polymers. We mainly focused our work on chitosan, well known to be biodegradable[5], bioactive[6] and biocompatible[7]. Chitosan is an amphiphilic natural co-polymer in which the relative proportion of acetylated and de-acetylated residues plays an important role in the balance between hydrophilic and hydrophobic interactions[8–10]. In addition, chitosan is haemostatic[11], fungi- and bacterio-static[12], and is known to be important in cell proliferation and tissue regeneration[13,14]. For the processing of physical hydrogels made only of chitosan and a solvent, we previously proposed methods based on a simple hydrogel assembly[4,15]. Knowledge of the gelation mechanism, including physico-chemical events involved during gelation and the molecular organization at various levels, was essential to understand the formation of our multi-membrane 'onion-like' structures. This gelation process is applicable to a variety of other amphiphilic polymers, especially natural polyelectrolytes such as alginates or hyaluronic acid.

An alcohol gel is easily formed from a chitosan solution in a 50/50 water/1,2-propanediol mixture by water evaporation at 55 °C. This is not limited to propanediol and has been performed with several other alcohols[15]. A key parameter for the gelation is to keep the initial polymer concentration above the critical concentration for chain entanglements. When water is almost fully removed, a gel is formed. Neutralization in a sodium hydroxide solution and subsequent washings in water yield a physical hydrogel that contains only water (over 95 wt%) and chitosan in the free amine form. Although evaporation induces a decrease in the charge density of the polymer chains, when gelation is fully achieved almost 40% NH_3^+ groups are still present[15] and have to be neutralized to favour inter-chain interactions allowing the formation of a stable hydrogel. Indeed, an alcohol gel in contact with water before neutralization rapidly converts into a hydro-alcoholic solution. Therefore we investigated the neutralization step using different concentrations of aqueous solutions of NaOH.

Figure 2a illustrates the macroscopic shrinkage of the hydrogel during neutralization and reveals that an increase in the concentration

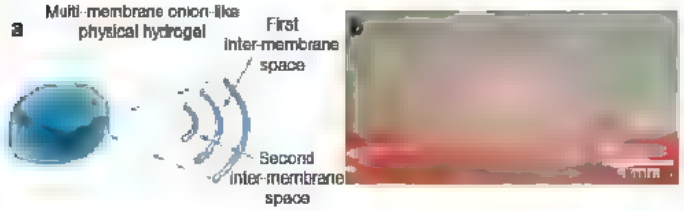

Figure 1 | Multi-membrane hydrogels. a, Schematic diagram of the multi-membrane onion-like structures, **b**, multi-membrane biomaterial with 'onion-like' structure based on chitosan

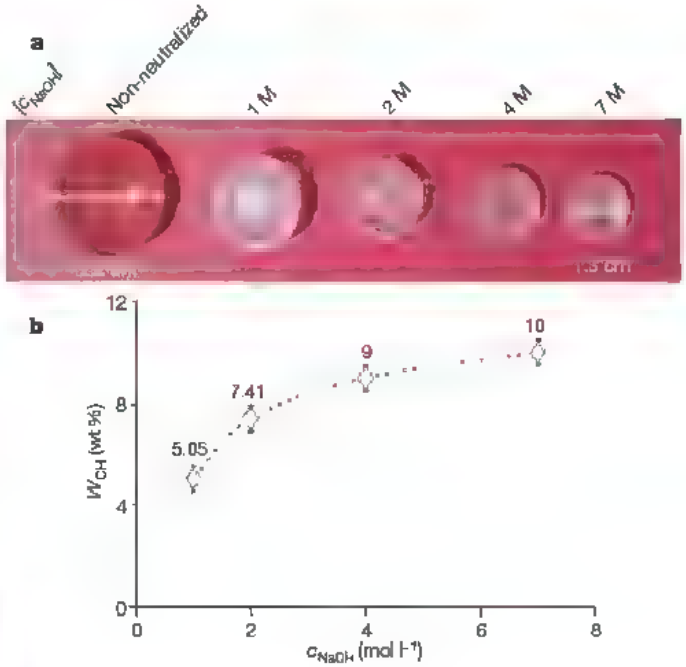

Figure 2 | Parameters influencing the polymer mass fraction of physical gels based on chitosan. a, Variation of hydrogel shrinkage during neutralization as a function of the concentration of sodium hydroxide. The initial polymer concentration in the non-neutralized alcohol gel is constant and close to 4.5wt% in each case. **b**, Evolution of the chitosan mass fraction in the gel (W_{CH}) at different steps of the hydrogel neutralization as a function of the NaOH concentration in the neutralization bath. Error bars represent ±1 standard deviation.

[1]Université de Lyon, Université Lyon 1, UMR CNRS 5223, Ingénierie des Matériaux Polymères (IMP), Laboratoire des Matériaux Polymères et des Biomatériaux, 15 Boulevard A Latarjet, Bâtiment ISTIL, F-69622 Villeurbanne Cedex, France.

of the neutralizing agent favours the gel depletion. Chitosan mass fractions in the hydrogels (W_{CH}) after neutralization for an initial alcohol gel with $W_{CH} \approx 4.5$ wt% are shown in Fig. 2b. The neutralization of NH_3^+ sites into NH_2 led to the disappearance of ionic repulsions between polymer chains so that physical cross-links corresponding to hydrogen bonding, hydrophobic interactions and crystallite formation were favoured. Volume changes in gels can also be driven by inter-chain interactions[16,17] and by pH variations for synthetic polyelectrolyte gels[18,19].

As previously discussed, this result can be interpreted by considering different contributions such as the change in the electrostatic potential during the neutralization inducing the formation of physical crosslinks, and ionic strength effects. The concentration of the neutralization agent (C_{NaOH}) also determines the kinetics of neutralization. At high C_{NaOH}, chains are rapidly and completely neutralized, and their condensation is maximum, leading to gels with a high physical cross-linking density. In contrast, for low C_{NaOH}, water diffusion within the alcohol gel must be considered, because it contributes to disturb hydrophobic interactions, influencing the final density of physical cross-links and thus W_{CH} of the neutralized hydrogel. Moreover, the presence of salts in a non-neutralized polyelectrolyte gel induces a screening of the electrostatic repulsions between polymer chains and should therefore favour physical junctions inside the gel. Additionally, the salting-out effect in amphiphilic polymer gels[20] could be considered. This effect corresponds to a displacement of water in the gel to form strongly hydrated ions (small electrolytes in solution), thus contributing to dehydrate polymer chains and increase hydrophobic inter-chain interactions, and increasing the density of cross-linking in the neutralized hydrogel. Nevertheless, the neutralization of an alcohol gel in a solution containing 1 M NaOH and 5 M NaCl only results in a slight increase (0.91%) in W_{CH} compared with the value obtained for an alcohol gel neutralized in the same conditions without NaCl. To summarize, different salt effects occur during neutralization but their contributions to the shrinkage of the gel are small compared with pure neutralization effects. The neutralization step seems complex, with several different phenomena acting simultaneously.

We used this mechanism of neutralization to generate multi-membrane onion-like architectures. As discussed above, the modification of the balance between hydrophobic and hydrophilic interactions induces a contraction of the neutralized gel (Fig. 3a–c),

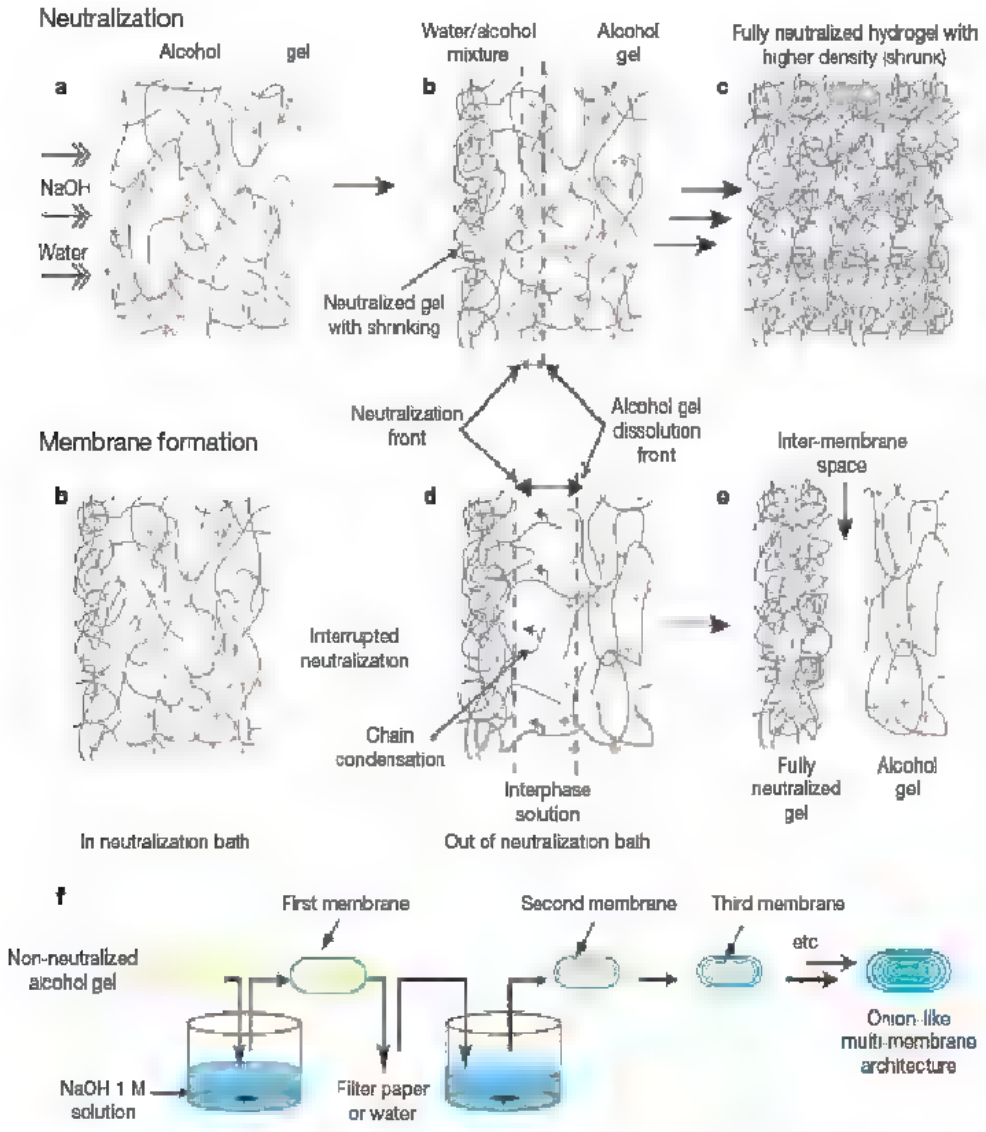

Figure 3 | Schematic representation of neutralization of a polyelectrolyte alcohol gel and derived methodology for building a multi-membrane structure. **a**, Non-neutralized alcohol gel introduced into the neutralization bath. **b**, Chain condensation and shrinkage of the alcohol gel with the disappearance of ionic repulsions during the neutralization step. **c**, Fully neutralized shrunk hydrogel after a classical neutralization step. **d**, Formation of the interphase solution and collapse of the polymer chains onto the neutralized shrunk gel during the interruption of the neutralization step. **e**, Inter-membrane space formation after complete condensation of the residual polymer chains in the interphase solution. At the end of the process, the multi-membrane system was thoroughly washed in distilled water to eliminate the excess of NaOH, the salts formed during neutralization and the alcohol. **f**, Overview of the multi-step neutralization process.

but to form separate gel membranes, an interphase that was less concentrated in polymer had to be generated between the neutralized and the alcohol gels (Fig. 3d). Control of the degree of entanglement across this interphase was essential to control the formation of separate membranes in the final structure (Fig. 3e). This, in turn, was determined by the kinetics of several phenomena occurring near the neutralization front, such as water diffusion within the alcohol gel. Indeed, going back to the gelation process, the sol–gel transition occurred after a complete water evaporation of a water/alcohol solution of chitosan. This transition is reversible after rehydration of the alcohol gel. As a result, during neutralization, if the water diffusion kinetics was fast enough in comparison with the neutralization kinetics, a thick interfacial solution could be formed in which the polymer hydration and mobility were high enough to allow disentanglement of the polymer chains and then their condensation onto the neutralized gel (Fig. 3d to e). In contrast, when the kinetics of neutralization was faster, a continuous entangled network existed between the alcohol and neutralized gels (Fig. 3c), without any possibility of forming a membrane and therefore a multi-membrane organization. The formation of inter-membrane spaces could be promoted by slowing down the neutralization simply by removing the gel from the neutralization bath or by washing with water. As discussed above, this resulted in (i) the formation of a water/alcohol solution between the neutralized and the alcohol gels, (ii) the disentanglement of chains located within the interphase, and (iii) condensation and contraction onto the neutralized gel.

The sequence including the neutralization and interruption steps could be repeated several times (Fig. 3f), for example 20 times, for a macroscopic gel of a few cubic centimetres, to build a multi-membrane onion-like structure composed of non-adherent and then fully independent gel membranes. The membranes were progressively formed from the periphery of the initial alcohol gel inwards, so it was possible to structure the gels fully into a succession of membranes, or to combine a continuous gel in the core (Fig. 1b) with a multi-membrane region at the periphery. Moreover, depending on the initial shape of the alcohol gel, which was easy to mould, various geometries of multi-membranes such as spherical, ovoid, cubic or tubular shapes (Fig. 4a) were possible, with a broad range of sizes (Fig. 4b). We varied the conditions of membrane formation by varying the initial polymer concentration in the alcohol gel, and the concentration and the nature of the neutralizing agent. Chitosan membrane formation occurred with NaOH ($pK_a = 14$), ethanolamine ($pK_a = 9.51$) or ethylamine ($pK_a = 10.81$) in specific conditions but was not observed with aqueous ammonia ($pK_a = 9.25$), for any concentration of the base ranging from 1 to 7 M and polymer concentration of the (1,2-propanediol) alcohol gel ranging from 2 to 6 wt%. These neutralization experiments led to gels with different polymer fractions ranging from 4.7 to 12.8 wt% (Supplementary Table 1) with an initial alcohol gel of 4.5 wt%, but with no direct relationship with the capacity to form membranes.

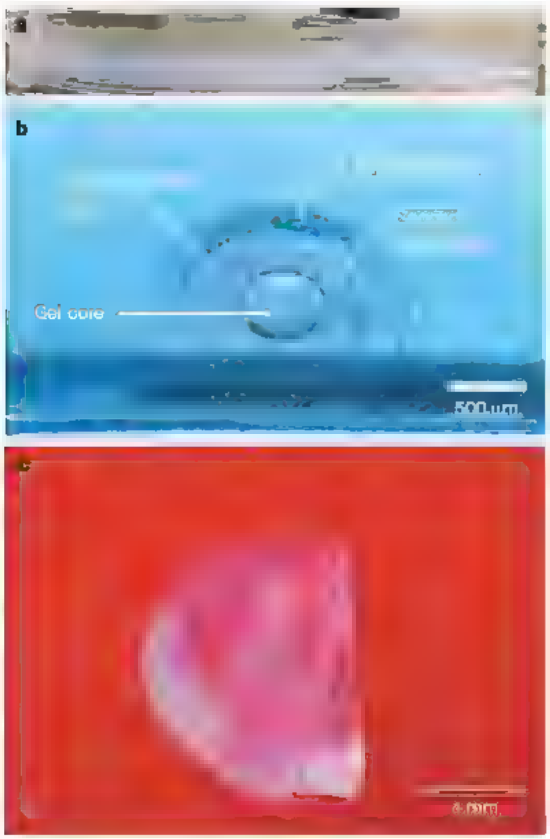

Figure 4 | Versatility of the multi-membrane architecture process. **a**, Multi-membrane tubular architecture, resembling a blood vessel. **b**, Microscopic multi-membrane capsule. **c**, Macroscopic multi-membrane architecture based on alginate hydrogel.

In contrast, the viscosity of the base/water/alcohol mixture was found to be closely related to the membrane formation (Supplementary Fig. 5). The viscosity of bases in water/1,2-propanediol mixtures was significantly larger than in water (Supplementary Fig. 5b and Supplementary Table 1), except in the case of aqueous ammonia for which the increase was very weak. For NaOH and NH_4OH, this trend was measured either as a function of the concentration of the base in a 50/50 mixture (by weight) (Supplementary Fig. 5a), or as a function of the 1,2-propanediol fraction at a fixed base concentration (Supplementary Fig. 5b). Consequently, the higher viscosity of NaOH/water/1,2-propanediol solutions resulted in lower diffusion kinetics of the base through the alcohol gel and thus slower neutralization kinetics, promoting the hydration of the alcohol gel and the formation of membranes. At a microscopic scale, the high viscosity of NaOH/water/1,2-propanediol mixtures could be related to specific interactions of 1,2-propanediol with the ionic species ('structure making effects'), as reviewed elsewhere[21]. Similar bridging effects have previously been described between polymers and ionic species[22]. Finally, the role of the alcohol viscosity was confirmed when 1,2-propanediol was replaced by glycerol, a more viscous solvent. In the latter case, multi-membrane processing became possible even with aqueous ammonia.

We also studied the membrane formation conditions, showing that chitosan membranes were only obtained for low initial polymer concentration in the alcohol gel (C_{pi}) and low NaOH concentrations (Supplementary Fig. 5c). At high concentrations of neutralization agent, the neutralizing flux entering the alcohol gel was high and the resulting neutralization kinetics fast. At high C_{pi}, the entangled network (in the alcohol gel) was dense and the disentanglement kinetics too slow, compared with the neutralization kinetics, to form membranes. We observed that C_{pi} appeared to have a weak influence on the membrane thickness, whereas the latter increased with the concentration of NaOH and the root square of the neutralization time (Supplementary Figs 6 and 7). This offers a way to control the width of the membranes and again illustrates the strong influence of the diffusion mechanism on the membrane formation. It showed that the increase of C_{pi} only affects the polymer chain mobility and their disentanglement, but not the NaOH diffusion within the gel, essentially governed by the concentration and viscosity of the neutralization bath.

The concept involved in the multi-step assembly process could also be applied to other natural polymers of polyanionic nature. We checked this with alginate hydrogels. Alcohol algmate gels were easily obtained by evaporation of water/1,2-propanediol mixtures, as in the case of chitosan alcohol gels, and multi-membrane architectures were generated by interrupted complex hydrogel assembly in $CaCl_2$ baths (Fig. 4c). The kinetics of hydrogel assembly played a dominant role, as the membrane architecture could only form for low concentrations in $CaCl_2$.

To validate the usefulness of our systems as biomaterials, we carried out chondrocyte culture within multi-membrane onion-like

hydrogels of chitosan (Supplementary Fig. 8). Cell aggregates were observed in several inter-membrane spaces, showing that cells can be introduced and cultured within these new systems for tissue engineering. Details of a biological study of rabbit chondrocytes cultured in our systems will be published elsewhere.

METHODS SUMMARY

Sample purification and characterization. We purified and characterized chitosan from squid pens (Mahtani Chitosan, batch 114) as described previously[4]. Its degree of acetylation was 2.5 ± 0.1%, with a weight-average molecular weight M_w = 550,000 ± 25,000 g mol^{-1}. Sodium alginate (System Bio-Industries, lot Satialgine SG800) had a mannuronic/guluronic ratio of 0.5.

Gelation. After purification, lyophilized chitosan or alginate were ground with a cryo-grinder, then dispersed in water. For chitosan, we added a stoichiometric amount of hydrochloric acid to neutralize the amino groups. After dissolution, we added an equivalent weight of 1,2-propanediol and stirred the mixture at room temperature for 1 h before evaporating the solution in a ventilated oven.

Chitosan multi-membrane structures. After collecting the gel from its mould, we placed it in 1 M NaOH for 5 min, then took it out of this medium for 3 min and carefully removed the excess NaOH from its surface with a filter paper. This sequence allowed the formation of both a first membrane and a first inter-membrane space, and could be repeated to produce several membranes and inter-membrane spaces. The 'onion' was then washed extensively in water to eliminate the alcohol and NaOH.

Alginate-based multi-membrane systems. After evaporation, the gel was at a concentration of 2%. We treated it alternately in a coagulation bath of 0.3 M $CaCl_2$, then in a water bath, for 5 min each.

Viscometry. We carried out viscometry at 25 °C with an automatic capillary viscometer (Viscologic TI1, SEMATech).

Full Methods and any associated references are available in the online version of the paper at www.nature.com/nature.

Received 25 June; accepted 17 December 2007.

1. Pilnik, W. & Rombouts, F. M. Polysaccharides and food processing. *Carbohydr. Res.* 142, 93–105 (1985).
2. Peppas, N. A., Hilt, J. Z., Khademhosseini, A. & Langer, R. Hydrogels in biology and medicine: From molecular principles to bionanotechnology. *Adv. Mater.* 18, 1345–1360 (2006).
3. Drury, J. L. & Mooney, D. J. Hydrogels for tissue engineering: scaffold design variables and applications. *Biomaterials* 24, 4337–4351 (2003).
4. Montembault, A., Viton, C. & Domard, A. Physico-chemical studies of the gelation of chitosan in a hydroalcoholic medium. *Biomaterials* 26, 933–943 (2005).
5. Varum, K. M., Myhr, M. M., Hjerde, R. J. & Smidsrod, O. *In vitro* degradation rates of partially N-acetylated chitosans in human serum. *Carbohydr. Res.* 299, 99–101 (1997).
6. Domard, A. & Domard, M. in *Polymeric Biomaterials* (ed. Dumitriu, S.) 187–212 (2002).
7. Hirano, S. & Noishiki, Y. The blood biocompatibility of chitosan and N-acetylchitosans. *J. Biomed. Mater. Res.* 19, 413–417 (1985).
8. Lamarque, G., Lucas, J.-M., Viton, C. & Domard, A. Physicochemical behavior of homogeneous series of acetylated chitosans in aqueous solution: role of various structural parameters. *Biomacromolecules* 6, 131–142 (2005).
9. Schatz, C., Viton, C., Delair, T., Pichot, C. & Domard, A. Typical physicochemical behaviors of chitosans in aqueous solution. *Biomacromolecules* 4, 641–648 (2003).
10. Sorlier, P., Denuziere, A., Viton, C. & Domard, A. Relation between the degree of acetylation and the electrostatic properties of chitin and chitosan. *Biomacromolecules* 2, 765–772 (2001).
11. Malette, W. G., Quigley, H. J., Gaines, R. D., Johnson, N. D. & Rainer, W. G. Chitosan, a new haemostatic. *Ann. Thorac. Surg.* 36, 55–61 (1983).
12. Strand, S. P., Vandvik, M. S., Varum, K. J. & Ostgaard, K. Screening of chitosans and conditions for bacterial flocculation. *Biomacromolecules* 2, 126–133 (2001).
13. Montembault, A. *et al.* A material decoy of biological media based on chitosan physical hydrogels: applications to cartilage tissue engineering. *Biochimie* 88, 551–564 (2006).
14. Boucard, N. *et al.* The use of physical hydrogels of chitosan for skin regeneration following third-degree burns. *Biomaterials* 28, 3478–3488 (2007).
15. Boucard, N., Viton, C. & Domard, A. New aspect of the formation of physical hydrogels of chitosan in a hydroalcoholic medium. *Biomacromolecules* 6, 3227–3237 (2005).
16. Vasquez, B., Gurruchaga, M., Goni, I. & San Roman, J. pH-sensitive hydrogel based on non-ionic acrylic copolymers. *Biomaterials* 18, 521–526 (1997).
17. Ilmain, F., Tanaka, T. & Kokufuta, E. Volume transition in a gel driven by hydrogen bonding. *Nature* 349, 400–401 (1991).
18. Siegel, R. A. & Firestone, B. A. pH dependent equilibrium swelling properties of hydrophobic polyelectrolytes copolymers gels. *Macromolecules* 21, 3254–3259 (1988).
19. Ostroha, J., Pong, M., Lowman, A. & Dan, N. Controlling the collapse swelling transition in charged hydrogels. *Biomaterials* 25, 4345–4353 (2004).
20. Porath, J., Sundberg, L., Fornstedt, N. & Olsson, I. Salting-out in amphiphilic gels as new approach to hydrophobic adsorption. *Nature* 245, 465–466 (1973).
21. Von Hippel, P. H. & Schleich, T. Ions effect on the solution of biological macromolecules. *Acc. Chem. Res.* 2, 257–265 (1969).
22. Pu, Q., Ng, S., Mok, V. & Chen, S. B. Ion bridging effects on the electroviscosity of flexible polyelectrolytes. *J. Phys. Chem. B* 108, 14124–14129 (2004).

Supplementary Information is linked to the online version of the paper at www.nature.com/nature.

Acknowledgements We thank M.-T. Corvol and K. Tahiri (Univ. Paris Descartes) for the chondrocyte cell culture study, and L. Bordenave and R. Bareille (Univ. Victor Segalen, Bordeaux) for additional endothelial/osteoprogenitor cell co-culture experiments. We also thank C. Viton, J.-M. Lucas and A. Crepet for technical assistance, and D. Gillet from Mahtani Chitosan for providing chitosan samples.

Author Information Reprints and permissions information is available at www.nature.com/reprints. Correspondence and requests for materials should be addressed to L.D. (laurent.david@univ-lyon1.fr) or A.D. (alain.domard@univ-lyon1.fr).

LETTERS

Near-isothermal conditions in the middle and lower crust induced by melt migration

Gabriela V. Depine[1], Christopher L. Andronicos[1] & Jason Phipps-Morgan[1]

The thermal structure of the crust strongly influences deformation, metamorphism and plutonism[1–3]. Models for the geothermal gradient in stable crust predict a steady increase of temperature with depth. This thermal structure, however, is incompatible with observations from high-temperature metamorphic terranes exhumed in orogens[1,4,5,6]. Global compilations[7] of peak conditions in high-temperature metamorphic terranes define relatively narrow ranges of peak temperatures over a wide range in pressure, for both isothermal decompression and isobaric cooling paths. Here we develop simple one-dimensional thermal models that include the effects of melt migration. These models show that long-lived plutonism results in a quasi-steady-state geotherm with a rapid temperature increase in the upper crust and nearly isothermal conditions in the middle and lower crust. The models also predict that the upward advection of heat by melt generates granulite facies metamorphism, and widespread andalusite–sillimanite metamorphism in the upper crust. Once the quasi-steady-state thermal profile is reached, the middle and lower crust are greatly weakened due to high temperatures and anatectic conditions, thus setting the stage for gravitational collapse[8], exhumation and isothermal decompression after the onset of plutonism. Near-isothermal conditions in the middle and lower crust result from the thermal buffering effect of dehydration melting reactions that, in part, control the shape of the geotherm.

Pressure–temperature estimates in andalusite–sillimanite metamorphic belts and middle crustal granulite terranes predict unreasonably hot geothermal gradients if one assumes a purely conductive geotherm, steadily increasing with depth (Fig. 1d). Here, we demonstrate the shape of a more realistic geotherm in crust that is undergoing extensive partial melting and high-temperature metamorphism. The abundance of plutons and batholiths associated with migmatites and granulites in these terranes suggest that heat transport by pervasive flow of magma through the crust helps to shape the metamorphic geotherm (refs 2, 6, 9 and references therein). Decompression melting caused by post-thickening crustal extension has often been used to explain the low-pressure, high-temperature metamorphism found in some of these terranes[1]. In contrast, field studies of terranes with isobaric cooling pressure–temperature paths demonstrate that migmatite formation, granulites, and plutonism formed before exhumation and uplift[10]. Concentration of radioactive elements during crustal thickening can, given enough time, cause melting of mica-rich lithologies[4,11]. However, additional heat sources are required to induce large degrees of anatexis in amphibolite bulk compositions[1,3,6]—the likely crustal protolith of calc-alkaline plutonic suites[1,12]. Mechanisms that have been proposed to increase the mantle heat flux in granulite terranes include: mantle plume activity[13,14]; post-thickening extensional collapse and/or erosional thinning[1,15]; pre-thickening extension[6]; lower crustal delamination[16]; or subduction of an active spreading ridge[17].

Here we model the thermal structure of thickened crust undergoing partial melting, which results in a melt-transport-elevated geotherm that fits many observed features of granulite–migmatite terranes. The results are applicable to continental arcs and collisional orogens. These models place constraints on the heat flux across the Mohorovičić discontinuity (Moho) that is necessary to trigger granulite metamorphism and anatexis in the absence of changes in crustal thickness due to erosion, crustal thickening, extension or addition of mantle derived melts to the crust. The models do not depend on crustal rheology; melt transport mechanism or the detailed nature of deformation. We focus on crustally derived magmas without the inclusion of melts or fluids that may be introduced by subduction zone processes. Although these processes are important, we choose to keep our models as simple as possible to emphasize the interaction between melt migration, melting in the crust, and upward heat transport across the Moho. The shape of the melt-enhanced geotherm is found to depend strongly upon the shape of the solidus curve for a specific composition, because equilibrium melting reactions buffer temperature until exhaustion of one (or more) of the melting phases. The models assume the presence of a fluid-absent amphibolite middle and lower crust (Fig. 1)[17]. If we assumed mica-rich lithologies or fluid-present compositions, melting would occur at lower temperatures.

Our models are constrained in particular by observations from the central gneiss complex (CGC) of western British Columbia[5,18–21]. The CGC is characterized by an amphibolitic lower crust[5,21], with widespread migmatitic gneiss and granulite intruded by calc-alkaline plutons[5] that were emplaced at middle crustal levels (~10–25 km deep), and which represent two magmatic pulses related to distinct tectonic episodes between 85–65 and 60–52 million years (Myr) ago[18]. During the first event plutons were emplaced, during transpressional to convergent tectonics associated with thickening of the crust, to at least 55 km. Both events are characterized by high-grade metamorphism and widespread migmatites. However, the second event is characterized by an additional magmatic flare-up of voluminous igneous plutons[20] that intruded during ongoing regional granulite-facies metamorphism[21]. Large-scale crustal extension dominated tectonics during the magmatic flare-up, so that rocks followed a 'clockwise' isothermal pressure–temperature–time path[5].

The one-dimensional numerical models generate predicted crustal thermal profiles for varying crustal melt fluxes and heat conduction across the Moho. Each simulation assumes that heat transfer is by conduction and by melt transport. The models solve the following advection–diffusion–melting equation

$$\rho c_p \partial T/\partial t + \rho c_p W \partial T/\partial y = \kappa \partial^2 T/\partial y^2 + \rho H(y) - \rho \Delta H \partial F/\partial t$$

Model parameters are listed in Table 1. Boundary conditions are surface $T = 0\,^{\circ}C$ and basal $T = 1{,}250\,^{\circ}C$. The maximum depth of the

[1]Department of Earth and Atmospheric Sciences, Snee Hall, Cornell University, Ithaca, New York 14853, USA.

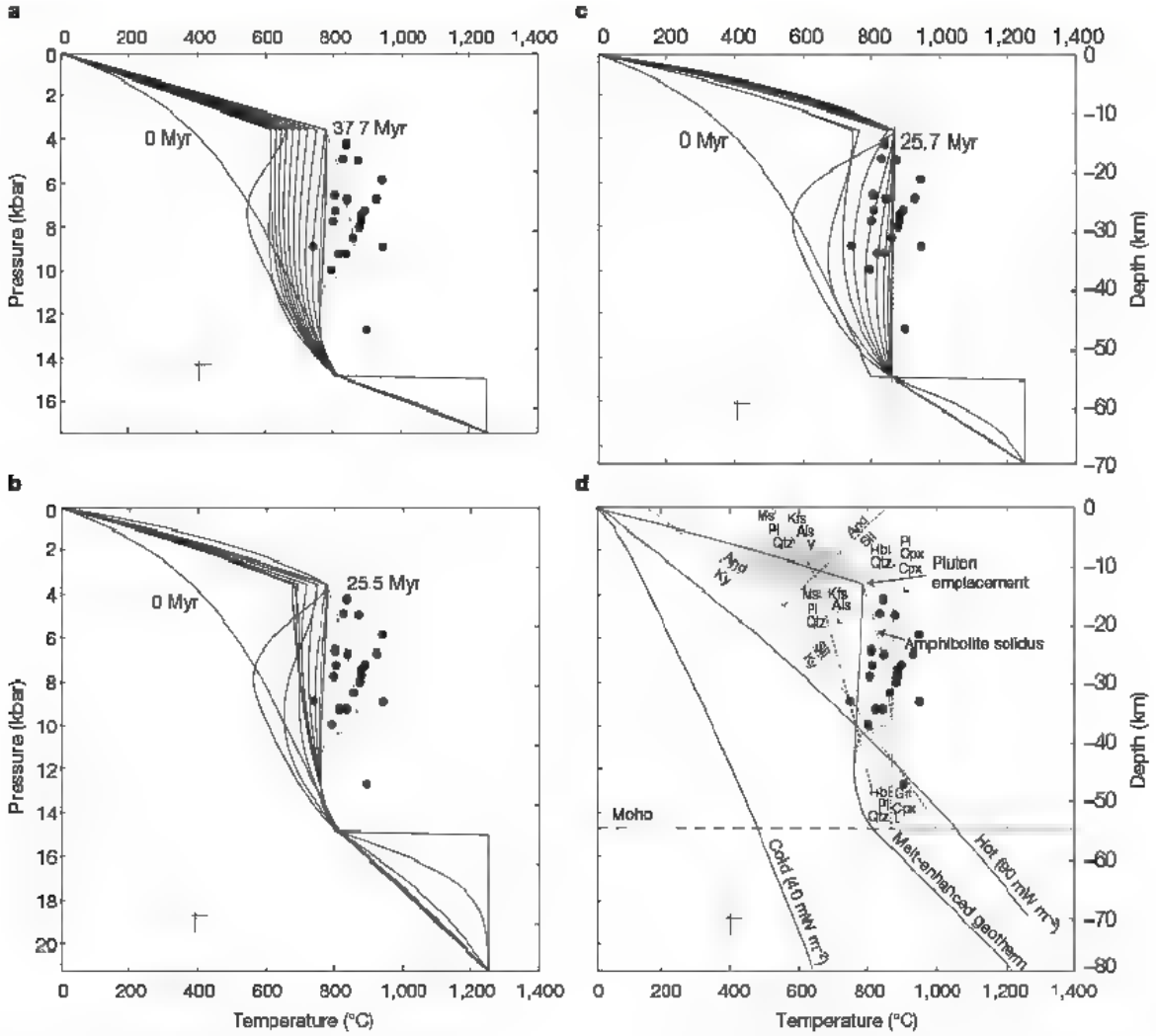

Figure 1 | One-dimensional numerical models showing evolution of predicted crustal geotherms through time as a function of mantle heat flux, melt focusing, and lower crustal solidus relations. Bold lines represent geotherms every 3 Myr, starting at the initial steadily-increasing with depth geotherm perturbed at 55 km with a temperature of 1,250 °C. The thin dashed lines represent the solidus curve in **a**–**d** and other metamorphic reactions in **d**. Dots represent pressure–temperature estimates of worldwide granulites corrected for retrograde exchange[7]. Three examples are shown (**a**–**c**). **a**, A model for a high mantle heat flux of 120 mW m^{-2} and amphibolite dehydration melting curve. The quasi-steady state is reached after 37.7 Myr. **b**, A model including melt focusing by a factor of two with a mantle heat flux of 47.5 mW m^{-2}; the quasi-steady state is reached after 25.5 Myr. **c**, A model using the hornblende + quartz ± plagioclase dehydration melting curve as the solidus for the crust. In this case focusing of the melt by a factor of two with a mantle heat flux of 65 mW m^{-2} is also required for the 'hot' threshold geotherm. The quasi-steady state is reached after 25.7 Myr. We note that this model best fits pressure–temperature estimates from worldwide granulite terranes. **d**, Comparison between geotherms predicted from surface heat flow measurements and calculated melt-enhanced geotherm from model 1. The grey field includes the general region of andalusite–sillimanite type metamorphism[32]. We note that simply conductive geotherms extrapolated from surface heat flow measurements do not intersect conditions recorded by most granulites or andalusite–sillimanite metamorphic belts. Also plotted are reaction curves relevant for granulite facies metamorphism[7]. And, andalusite; Ky, kyanite; Ms, muscovite; Pl, plagioclase; Qtz, quartz; Kfs, potassic feldspar; Als, aluminosilicate; V, vapour; Sil, sillimanite; Hbl, hornblende; Opx, orthopyroxene; Cpx, clinopyroxene; L, liquid; Grt, garnet. The crosses in the lower right-hand corners of each panel show the pressure–temperature arbitrary uncertainties of ±1 kbar and ±50 °C.

profile is varied to simulate different long-term basal mantle heat fluxes. Therefore, geotherms have a simple physical meaning from the top of the profile to the Moho; but below the Moho, the curve is a gradient representing specific mantle heat fluxes across the Moho that does not reflect the shape of the convective mantle geotherm.

Table 1 | Constants and values used in models

κ	Thermal diffusivity	7.91×10^{-7} m^2 s^{-1}
ρ	Density	2,700 kg m^{-3}
c_p	Heat capacity	1,170 J kg^{-1} °C^{-1} (ref. 19)
ΔH	Latent heat	320 kJ kg^{-1}
W	Velocity of flow	Function of melt fraction $\partial F/\partial t$
H	Radioactive heat production	$H = H_0 e^{-t/10,000}$ (ref. 34)
T	Temperature	
t	Time	
y	Depth	

($H_0 = 3.4 \times 10^{-10}$ W kg^{-1} calculated for 80 Myr ago.)

The larger the gradient, the higher the mantle heat flux, and the sooner the model reaches the steady-state equilibrium.

The model starts with 55-km-thick crust and a near-surface geothermal gradient of 35 °C km^{-1}, similar to the surface heat flow measured in modern arcs[22]. An initial temperature at the crust–mantle interface of 1,250 °C (Fig. 1) is equivalent to positioning the asthenosphere directly at the base of the crust. This could result from delamination, asthenospheric upwelling by steepening of a slab, impingement of a mantle plume or initiation of rifting. Our model does not depend on which process actually occurs. The outcome is rapid cooling of the uppermost mantle until the mantle heat flux achieves a quasi-steady-state value determined by the thickness of the mantle 'lid', which simulates the formation of a dynamically maintained layer of mantle lithosphere. Transfer of heat from the mantle to the crust triggers melting in the lower crust. The Moho evolves from 1,250 °C to the crustal solidus temperature, owing to thermal-buffering of melting. In amphibolite, melt is assumed to

accumulate to a threshold of 10 vol.%, at which point the melt migrates to 13 km, advecting upward heat in the crust-derived melts. The crust below 13 km is displaced downwards to replace the ascending melt, as a simple mass balance.

Two end-member scenarios occur, depending on the heat input from the mantle (Fig. 1 and 2a). In the first scenario, the depth to the 1,250 °C isotherm (bottom of the model) was chosen to produce a mantle heat flux of ~120 mW m^{-2} at the quasi-steady state (Fig. 1a). With these conditions, a pluton forms at 13 km within 5 Myr of the tectonic perturbation and starts diffusing heat downward into the colder lower crust. After 35 Myr, the model arrives at the quasi-steady-state profile. The mantle heat input needed is equivalent to that obtained from intruding 0.93 km of basalt per Myr for 35 Myr (that is, 32.5 km of basaltic underplating). This scenario would require extraordinarily hot mantle heat fluxes and/or volumes of basaltic underplating that are not often found in orogens.

For a mantle heat input lower than 120 mW m^{-2}, extensive crustal melting does not occur and granulites in the middle crust are not generated in realistic geological timescales (<35 Myr, Fig. 2a). To generate extensive crustal melting and granulite formation under conditions of reduced mantle heat input, we found that focusing of crustal melt into the column is needed to produce partial melting and high-temperature metamorphism, which results in our second end-member scenario. To simulate melt focusing, more melt is migrated from the model base to accumulate in a mid-crustal pluton than is generated in the one-dimensional crustal column. This is equivalent to bringing melt laterally from adjacent regions at the base of the crust. For common mantle heat fluxes in orogens (<100 mW m^{-2}) and geologically reasonable time spans (<35 Myr), we found that melt must be focused by a factor of at least 1.3 (Fig. 2a). As an example, if melt is focused by a factor of two, a quasi-steady state is predicted to occur after 25.5 Myr for a mantle heat flux of 47.5 mW m^{-2} (Fig. 1b). Therefore, melt focusing can greatly lower the requirement of a high heat flux across the Moho (Fig. 2a), indicating that this scenario is geologically more permissive.

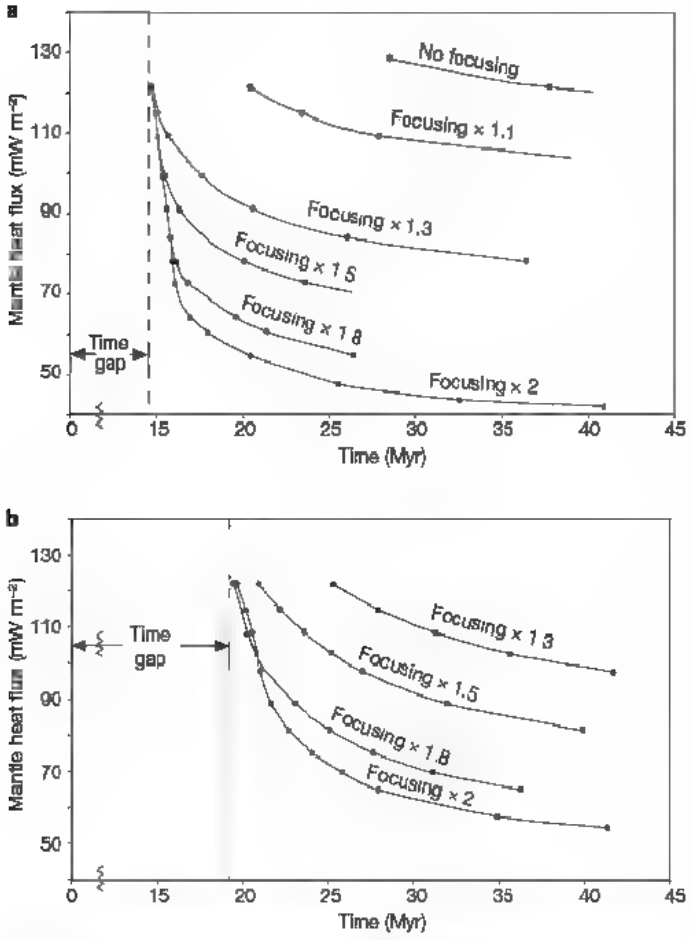

Figure 2 | Comparison between mantle heat fluxes and the time to the onset of the quasi-steady-state melt-enhanced geotherm. **a**, Results using the amphibolite solidus curve. Each curve represents different melt focusing factors. The top curve has no melt focusing and represents the first end-member discussed in the text, where extremely high mantle inputs (<120 mW m^{-2}) are required. The following curves represent the second case scenario discussed in the text, in which melt focusing leads to geotherms that match pressure–temperature estimates from the lower-temperature end of granulite terranes. **b**, Results using the hornblende + quartz ± plagioclase melting curve, which matches pressure–temperature estimates from many granulite terranes. In this case higher mantle heat fluxes are required as well as a longer time span (minimum 20 Myr) to generate the melt-enhanced geotherm. As seen in Fig. 1c, these conditions better match pressure–temperature data from granulite terranes.

The results of these models reproduce geotherms that pass at the lower temperature end of pressure–temperature data compiled from many granulite terranes (Fig. 1). This is probably due to the limitations of our models, which assume melting is continuous in a fixed composition and that no phases are exhausted. In nature, melting would change mineral composition and exhaust one or more phases in the rocks, incrementally changing the solidus to higher temperatures, which would relax the constraint of thermal buffering during melting. In Fig. 1c, we investigate melting of hornblende + quartz ± plagioclase, which occurs at higher temperature than the amphibolite solidus in Fig. 1d. Pressure–temperature estimates from natural (Fig. 1c) granulite terranes overlap this geotherm, but some record temperatures up to 200 °C hotter. This geotherm requires focusing of melt by a factor of 1.5 (Fig. 2b). For example, a minimum mantle heat flux of 65 mW m^{-2} is required when focusing by a factor of 2. The time to get to the quasi-steady-state geotherm using this solidus curve takes longer (>20 Myr) than when using the amphibolite solidus curve (>15 Myr, compare Fig. 2a with Fig. 2b). Clearly granulite terranes that record these conditions have undergone extraordinary processes to result in such high crustal temperatures.

A possible mechanism for melt focusing is crustal flow[18,20,23,24]. Many tectonic environments are thought to result in melt focusing, including spreading at mid-ocean ridges[25], continental arcs[18], extensional tectonic settings[26], mantle plumes[25], and transpressive fault zones[27]. Strike-slip shear zones can also act as corridors for melt focusing in ductile environments[28]. Orogen parallel transport is a common feature in modern convergent margins, where 31% of convergent margins have oblique convergence sufficient to generate transcurrent displacements[29]. Our thermal modelling can also capture the thermal effects of focused additions of basaltic magmas into a batholith, where the amount of focusing would reflect the ratio of basalt to calc-alkaline melts into the batholith. For simplicity, we have assumed that no basalt is added.

The models show that the thermal evolution in granulite crustal environments was profoundly shaped by melt migration and pluton construction. These results are similar to those from previous studies that concluded that partial melting in the crust and granulite facies metamorphism requires elevated mantle heat fluxes and pervasive melt migration through the crust[1,6,9,30]. Our models highlight the important roles of heat transport by melt migration, and of thermal buffering by crustal anatexis, as originally suggested by studies of metamorphism in the Himalaya[30], and modelled by Stüwe[31]. Extreme conditions in large hot orogens typified by granulite facies metamorphism, low-pressure high-temperature metamorphic belts and calc-alkaline batholiths are therefore likely to result from large fluxes of magma through the crustal column.

The processes of basaltic underplating, asthenospheric impingement and melt focusing remain cryptic in the geologic record, yet our models imply they may be common in orogenic settings, as has been inferred from numerous studies of high temperature metamorphic terranes[1,9,10,26]. The models show the predicted shape of the resultant geotherms, which have the following implications for metamorphic and tectonic process. The quasi-steady state profiles (Fig. 1d) have

very steep surface geothermal gradients of more than 50 °C km^{-1}, consistent with the generation of andalusite–sillimanite metamorphic terranes and also consistent with observations of peak conditions in many contact aureoles[32]. Melt migration and pluton construction cause the entire middle and lower crust to reach temperatures of ~800 °C and the lowest 12 km of the crust to be partially molten. These conditions are similar to those estimated for many high-grade metamorphic terranes[7,10].

Our models show that linear extrapolation of geothermal gradients is only applicable to the upper portions of the crust in active tectonic settings and that the middle and lower crust experience near-isothermal conditions buffered by the melting temperatures of the crustal rocks. Melt-laden middle and lower crust produce conditions that favour orogenic instability, and may be necessary preconditions for late orogenic extensional collapse and/or lower crustal flow. For terranes where collapse occurs, exhumation would follow the pressure peak and be nearly isothermal because the entire middle and lower crust is hot. Thus exceptionally fast exhumation rates are not necessary for nearly isothermal decompression. Slowly exhumed orogens that stay at high temperatures for long time periods (more than tens of millions of years)[33] can also be explained by exhumation along a quasi-steady-state melt-enhanced geotherm. For terranes that do not collapse, isobaric heating and cooling paths would be followed.

Received 25 September 2007; accepted 8 January 2008.

1. Thompson, A. B. in *Understanding Granites: Integrating New and Classical Techniques* (eds Castro, A., Fernandez, C. & Vigneresse, J. L.) 7–25 (Geol. Soc. Lond. Spec. Publ. 158, 1999)
2. Gerbi, C. C., Johnson, S. E. & Koons, P. O. Controls on low-pressure anatexis. *J. Metamorph. Geol.* 24, 107–118 (2006).
3. Sandiford, M., Martin, N., Zhou, S. & Fraser, G. Mechanical consequences of granite emplacement during high-T, low-P metamorphism and the origin of "anticlockwise" PT paths. *Earth Planet. Sci. Lett.* 107, 164–172 (1991)
4. Patiño-Douce, A. E., Humphreys, E. D. & Johnston, A. D. Anatexis and metamorphism in tectonically thickened continental crust exemplified by the Sevier hinterland, western North America. *Earth Planet. Sci. Lett.* 97, 290–315 (1990).
5. Hollister, L. S. Metamorphic evidence for rapid (2 mm/yr) uplift of a portion of the Central Gneiss Complex, Coast Mountains, B.C. *Can. Mineral.* 20, 319–332 (1982)
6. De Yoreo, J. J., Lux, D. R. & Guidotti, C. V. Thermal modelling in low-pressure/high-temperature metamorphic belts. *Tectonophysics* 188, 209–238 (1991).
7. Pattison, D. R. M., Chacko, T., Farquhar, J. & McFarlane, C. R. M. Temperatures of granulite-facies metamorphism: constraints from experimental phase equilibria and thermobarometry corrected for retrograde exchange. *J. Petrol.* 44, 867–900 (2003)
8. Molnar, P. & Lyon-Caen, H. Some simple physical aspects of the support, structure, and evolution of mountain belts. *GSA Spec. Pap.* 218, 179–207 (1988)
9. Leitch, A. M. & Weinberg, R. F. Modelling granite migration by mesoscale pervasive flow. *Earth Planet. Sci. Lett.* 200, 131–146 (2002)
10. Harley, S. L. The origins of granulites: a metamorphic perspective. *Geol. Mag.* 126, 215–247 (1989)
11. Huerta, A. D., Royden, L. H. & Hodges, K. V. The interdependence of deformational and thermal processes in mountain belts. *Science* 273, 637–639 (1996)
12. López, S. & Castro, A. Determination of the fluid-absent solidus and supersolidus phase relationships of MORB-derived amphibolites in the range 4–14 kbar. *Am. Mineral.* 86, 1396–1403 (2001)
13. Chardon, D., Peucat, J. J., Jayananda, M., Choukroune, P. & Fanning, C. M. Archean granite-greenstone tectonics at Kolar (South India): interplay of diapirism and bulk inhomogeneous contraction during juvenile magmatic accretion. *Tectonics* 21, doi:10.1029/2001TC901032 (2002).
14. Gibson, R. L. & Stevens, G. in *What Drives Metamorphism and Metamorphic Reactions?* (eds Treloar, P. J. & O'Brien, P. J.) 121–135 (Geol. Soc. Lond. Spec. Publ. 138, 1998
15. Thompson, A. B., Schulmann, K., Jezek, J. & Tolar, V. Thermally softened continental extensional zones (arcs and rifts) as precursors to thickened orogenic belts. *Tectonophysics* 332, 115–141 (2001).
16. Kay, R. W. & Mahlburg-Kay, S. Delamination and delamination magmatism. *Tectonophysics* 219, 177–189 (1993)
17. Brown, M. in *What Drives Metamorphism and Metamorphic Reactions?* (eds Treloar, P. J. & O'Brien, P. J.) 137–169 (Geol. Soc. Lond. Spec. Publ. 138, 1998).
18. Hollister, L. S. & Andronicos, C. L. Formation of new continental crust in western British Columbia during transpression and transtension. *Earth Planet. Sci. Lett.* 249, 29–38 (2006).
19. Hollister, L. S., Hargraves, R. B., James, T. S. & Renne, P. R. The paleomagnetic effects of reheating the Ecstall pluton, British Columbia. *Earth Planet. Sci. Lett.* 221, 397–407 (2004).
20. Andronicos, C. L., Chardon, D. H., Hollister, L. S., Gehrels, G. E. & Woodsworth, G. J. Strain partitioning in an obliquely convergent orogen, plutonism, and synorogenic collapse: Coast Mountains Batholith, British Columbia, Canada. *Tectonics* 22, 1–24 (2003)
21. Kenah, C. & Hollister, L. S. in *Migmatites, Melting and Metamorphism* (eds Atherton, M. P. & Gribble, C. D.) 142–162 (Shiva Geology Series, Cheshire, UK, 1983).
22. Furukawa, Y., Shinjoe, H. & Nishimura, S. Heat flow in the southwest Japan arc and its implication for thermal processes under arcs. *Geophys. Res. Lett.* 25, 1087–1090 (1998).
23. Beaumont, C., Jamieson, R. A., Nguyen, M. H. & Lee, B. Himalayan tectonics explained by extrusion of a low-viscosity crustal channel coupled to focused surface denudation. *Nature* 414, 738–742 (2001)
24. Rabinowicz, M. & Vigneresse, J. L. Melt segregation under compaction and shear channeling; application to granitic magma segregation in a continental crust. *J. Geophys. Res.* 109, B04407, 1–20 (2004)
25. Morgan, J. P. Melt migration beneath mid-ocean spreading centers. *Geophys. Res. Lett.* 14, 1238–1241 (1987).
26. MacCready, T., Snoke, A. W., Wright, J. E. & Howard, K. A. Mid-crustal flow during Tertiary extension in the Ruby Mountains core complex, Nevada. *Geol. Soc. Am. Bull.* 109, 1576–1594 (1997).
27. Brown, M. & Solar, G. S. Shear-zone systems and melts; feedback relations and self-organization in orogenic belts. *J. Struct. Geol.* 20, 211–227 (1998)
28. Hutton, D. H. W. Igneous emplacement in a shear-zone termination. The biotite granite at Strontian, Scotland. *Geol. Soc. Am. Bull.* 100, 1392–1399 (1988)
29. Patchett, P. J. & Chase, C. G. Role of transform continental margins in major crustal growth episodes. *Geology* 30, 39–42 (2002)
30. Hodges, K. V., Le Fort, P. & Pecher, A. Possible thermal buffering by crustal anatexis collisional orogens: Thermobarometric evidence from Nepalese Himalaya. *Geology* 16, 707–710 (1988).
31. Stüwe, K. Thermal buffering effects at the solidus. Implications for the equilibration of partially melted metamorphic rocks. *Tectonophysics* 248, 39–51 (1995)
32. Pattison, D. R. M. & Tracy, R. J. in *Contact Metamorphism* (ed. Kerrick, D. M.) 105–206 (Mineralogical Society of America, Washington DC, 1991)
33. Shaw, C. A., Heizler, M. T. & Karlstrom, K. E. in *The Rocky Mountain Region; an Evolving Lithosphere, Tectonics, Geochemistry, and Geophysics* (eds Karlstrom, K. E. & Keller, G. R.) 163–184 (American Geophysical Union, Washington DC, 2005)
34. Turcotte, D. L. & Schubert, G. *Geodynamics* (Cambridge Univ. Press, Cambridge, UK, 2002)

Supplementary Information is linked to the online version of the paper at www.nature.com/nature.

Acknowledgements This work was supported by the US National Science Foundation and Cornell University.

Author Information Reprints and permissions information is available at www.nature.com/reprints. Correspondence and requests for materials should be addressed to G. V. D. (gvd2@cornell.edu)

LETTERS

High-amplitude fluctuations and alternative dynamical states of midges in Lake Myvatn

Anthony R. Ives[1], Árni Einarsson[2], Vincent A. A. Jansen[3] & Arnthor Gardarsson[2]

Complex dynamics are often shown by simple ecological models[1,2] and have been clearly demonstrated in laboratory[3,4] and natural systems[5–9]. Yet many classes of theoretically possible dynamics are still poorly documented in nature. Here we study long-term time-series data of a midge, *Tanytarsus gracilentus* (Diptera: Chironomidae), in Lake Myvatn, Iceland. The midge undergoes density fluctuations of almost six orders of magnitude. Rather than regular cycles, however, these fluctuations have irregular periods of 4–7 years, indicating complex dynamics. We fit three consumer–resource models capable of qualitatively distinct dynamics to the data. Of these, the best-fitting model shows alternative dynamical states in the absence of environmental variability; depending on the initial midge densities, the model shows either fluctuations around a fixed point or high-amplitude cycles. This explains the observed complex population dynamics: high-amplitude but irregular fluctuations occur because stochastic variability causes the dynamics to switch between domains of attraction to the alternative states. In the model, the amplitude of fluctuations depends strongly on minute resource subsidies into the midge habitat. These resource subsidies may be sensitive to human-caused changes in the hydrology of the lake, with human impacts such as dredging leading to higher-amplitude fluctuations. *Tanytarsus gracilentus* is a key component of the Myvatn ecosystem, representing two-thirds of the secondary productivity of the lake[10] and providing vital food resources to fish and to breeding bird populations[11,12]. Therefore the high-amplitude, irregular fluctuations in midge densities generated by alternative dynamical states dominate much of the ecology of the lake.

Although the possibility of alternative states in ecological systems has been recognized for several decades[13,14], only recently have good empirical examples been established[9,15,16]. The most familiar type of alternative states is alternative stable states in which a system has two (or more) stable equilibria, with the system settling to one or the other depending on initial conditions[17]. Alternative stable states lead to the possibility that a system may be shifted from one state to another, less favourable, state by a sudden shock or other disturbance, with unfortunate ecological consequences. Once trapped in the new state, undoing the disturbance will not return the system to its original (desirable) state, because the system will remain trapped in the domain of attraction of its new state.

Alternative states, however, need not be stable equilibrium points; they may instead be dynamical structures such as cycles[18–22]. Here we investigate the possibility of alternative dynamical states, in which one state is an equilibrium point and the other is a high-amplitude stable cycle. Data on the long-term dynamics of the midge *Tanytarsus gracilentus* suggest these alternative states, because they show high-amplitude fluctuations that are not regularly periodic. In most populations in nature and in most simple models, if high-amplitude fluctuations occur, they occur as fairly regular cycles, with the strong ecological forces that drive the high amplitudes also entraining the dynamics into a stable limit cycle[23].

Tanytarsus gracilentus is the dominant herbivore/detritivore in Myvatn, comprising roughly 75% of the secondary consumers and 66% of secondary production in this shallow, naturally eutrophic lake in northern Iceland[10]. As larvae, *T. gracilentus* individuals feed from tubes they construct in the benthic sediment, grazing on both benthic diatoms (algae) and detritus[24] consisting largely of dead benthic and planktonic algae, and midge frass. They have two non-overlapping generations per year, with adults forming large swarms around the perimeter of the lake over two 1–2-week mating periods, the first in May and the second in July and early August. In generations with high midge abundance, larvae are limited by food, and adult size decreases for several generations before the population crashes. Detailed statistical evaluation of data on population density, body size and predator abundance suggests that fluctuations in *T. gracilentus* populations are driven by consumer–resource interactions, with midges being the consumers and algae/detritus the resources, as opposed to predator–prey interactions with midges being the prey[25].

We have collected data on the abundance of adult midges since 1977 by using window traps at two locations on the shore of the lake[26]. We have fitted these data to a model constructed to describe the fundamental interactions among midges, algae and detritus (Box 1). In the model, the midge population growth is dependent on density and is limited by the availability of food. Food consists of algae and detritus, which may differ in quality for midges. Algae have density-dependent growth, and detritus is formed from dead algae. In the model, midge populations are allowed to reach densities at which all algae are consumed, at which point the midge population crashes, with the rate of crash being moderated by the presence of detritus, which serves as an alternative food source. A feature crucial to the model is that if all algae are consumed, algal populations can recover through the input of small subsidies from outside the midge–algae–detritus system. These subsidies represent small influxes of algae and detritus into the muddy midge habitat from hard-bottom areas where midges are few. Although we have no direct measurement of this input, much of the algae and detritus in the lake occurs in areas inaccessible to midge larvae, and the hydrological mixing of the shallow lake[27] makes influxes of small amounts of this material into the midge habitat a certainty. We added environmental stochasticity to the model as random variation in per capita changes in abundances of midges, algae and detritus. Finally, we fitted the data by using a state-space version of the model[28] to incorporate the measurement error that we knew to be significant (Supplementary Methods). Predictions by the fitted model about changes in log (midge populations) from one generation to the next explain 74%

[1]Department of Zoology, University of Wisconsin–Madison, Madison, Wisconsin 53706 USA [2]Myvatn Research Station and Institute of Biology University of Iceland, Sturlugata 7 IS-101 Reykjavik, Iceland. [3]School of Biological Sciences, Royal Holloway, University of London, Egham, Surrey TW20 0EX, UK

Box 1 | The midge–algae–detritus model and alternatives

We constructed a midge–algae–detritus model to give a basic description of their interactions, attempting to have a minimum number of parameters that must be estimated from the data. The midge dynamics are

$$x(t+1)=r_1x(t)\left(1+\frac{x(t)}{R(t)}\right)^{-q}e^{\varepsilon_1(t)} \quad (1)$$

where $x(t)$ is the abundance of midges in generation t, r_1 is the intrinsic population growth rate, larger values of q produce stronger density dependence, and $\varepsilon_1(t)$ is a normal random variable representing stochastic environmental variability. The dimensionless measure of resource abundance in generation t, $R(t)=y(t)+pz(t)$, is composed of algae, $y(t)$, and detritus, $z(t)$, with the parameter p giving the quality of detritus for midge population growth relative to algae. Because we were interested in dynamics rather than mean abundance, we 'non-dimensionalized' midge densities to produce equation (1) and used a separate scaling parameter K when fitting the model so that the observed log(adult midge density) equalled $K+\log(x(t))$ (Supplementary Methods). Furthermore, the data showed a distinct seasonal pattern in which spring generations had mean densities 3.4 times higher than summer densities. This might reflect either true differences in survival and/or fecundity between generations or sampling bias due to differences in weather conditions and hence flight activity and catchability. Because we were interested in long-term, multi-generational dynamics, we factored out this consistent seasonal pattern by multiplying summer midge densities by 3.4 before statistical analyses.

Algae dynamics are

$$y(t+1)=\left[r_2y(t)(1+y(t))^{-1}-\frac{y(t)}{R(t)}x(t+1)+c\right]e^{\varepsilon_2(t)} \quad (2)$$

where r_2 is the algae intrinsic population growth rate and c is the influx of algae from outside the midge habitat. Because we have no data on algae abundance available to midges, $y(t)$ is not observed, therefore, in the model the mean value of $y(t)$ need not be included, and $y(t)$ is dimensionless. The term $[y(t)/R(t)]x(t+1)$ is the amount of resource consumed, $x(t+1)$, scaled by the proportion of that resource which is algae, $y(t)/R(t)$. A key feature of algae dynamics is that midge populations can build to sufficient abundance to consume all algae. When the term for the amount of algae consumed, $[y(t)/R(t)]x(t+1)$, is greater than the amount produced, $r_2y(t)[1+y(t)]^{-1}$, we assume that all algae come from influx, so $y(t+1)=c$.

The detritus dynamics are

$$z(t+1)=\left[dz(t)+y(t)-\left(\frac{pz(t)}{R(t)}\right)x(t+1)+c\right]e^{\varepsilon_3(t)} \quad (3)$$

where d gives the retention rate of detritus in the midge habitat. We assume that the influx rate of detritus equals that of algae, and that detritus is produced in proportion to the quantity of algae in the previous generation, $y(t)$. As with algae, if all detritus in the midge habitat is consumed, then $z(t+1)=c$. Because both algae and detritus were not measured, we assumed for estimation purposes that the standard deviations of $\varepsilon_2(t)$ and $\varepsilon_3(t)$ are equal: $\sigma_2=\sigma_3$.

We compared the midge–algae–detritus model to two additional models. The multidimensional Gompertz log-linear model[30] is

$$u_1(t+1)=b_{11}u_1(t)+b_{12}u_2(t)+b_{13}u_3(t)+\varepsilon_1(t) \quad (4)$$

$$u_2(t+1)=b_{21}u_1(t)+b_{22}u_2(t)+b_{23}u_3(t)+\varepsilon_2(t) \quad (5)$$

$$u_3(t+1)=b_{31}u_1(t)+b_{32}u_2(t)+b_{33}u_3(t)+\varepsilon_3(t) \quad (6)$$

where $u_1(t)=\log x(t)$, $u_2(t)=\log y(t)$ and $u_3(t)=\log z(t)$. The Lotka–Volterra model is

$$x(t+1)=r_1x(t)\exp(-d+b_{12}y(t)+b_{13}z(t)+\varepsilon_1(t)) \quad (7)$$

$$y(t+1)=r_2y(t)\exp(1+b_{21}x(t)+b_{22}y(t)+b_{23}z(t)+\varepsilon_2(t)) \quad (8)$$

$$z(t+1)=r_3z(t)\exp(1+b_{31}x(t)+b_{32}y(t)+b_{33}z(t)+\varepsilon_3(t)) \quad (9)$$

In equations (7)–(9), three parameters can be removed to non-dimensionalize the equations without changing the observed dynamics of midges, we therefore set $b_{12}=1$ and $b_{13}=1$ (assuming that midges benefit from both resources) and $b_{21}=-1$ (assuming that midges reduce algae abundance). As with the midge–algae–detritus model, for both alternative models we fitted the data with a scaling parameter K to factor out mean midge density. Fitting of all three models was performed with a state-space approach factoring in measurement error; see Supplementary Methods for details.

of the variance in generation-to-generation population fluctuations (Fig. 1 and Table 1).

When stripped of environmental stochasticity, the deterministic skeleton of the model shows alternative dynamical states (Fig. 2a). There is a relatively high stable point surrounded by a stable cycle of very high amplitude. The existence of alternative dynamical states pervades the biologically plausible range of parameter values (white areas in Fig. 3a), demonstrating that they are a common feature caused by the general structure of the model rather than phenomena requiring unlikely parameter values. In the fully stochastic model, produced by including the level of environmental stochasticity estimated in the fitted model, the population trajectory skips between the domains of attraction of the two alternative states (Supplementary Figs 1–9), for some stretches of time fluctuating around the stable point and for other stretches showing cycles (Fig. 2b). The amplitude of fluctuations is highly sensitive to the rate of influx of resources into the system; as the influx of algae and detritus, c, decreases from 10^{-3} to 10^{-9}, the amplitude increases from less than three orders of magnitude to more than ten orders of magnitude (Fig. 3b). This occurs because lower subsidies (lower values of c) allow midge populations to crash to lower levels before they are saved from extinction by the recolonization of algae. The amount of subsidy needed to save the population is low. The value of c in the model fitted to Myvatn data, $c=10^{-6.4}$, implies that inputs are six orders of magnitude lower than the abundance of algae at the stable equilibrium point. A full pictorial analysis of the deterministic and stochastic behaviours of the model is given in Supplementary Figs 1–9.

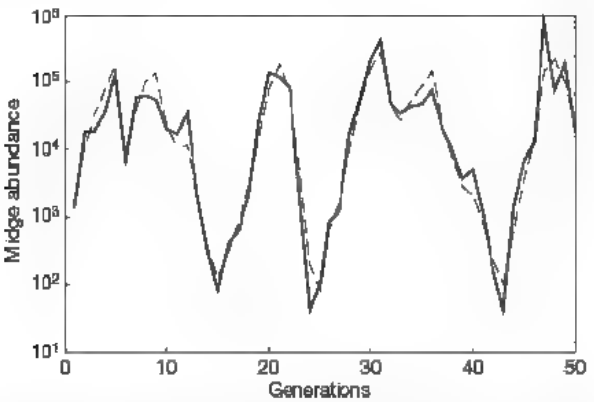

Figure 1 | Population dynamics of *T. gracilentus* in Myvatn. The solid line gives the abundance of midges in each generation, averaged between two traps. The dashed line gives the predicted 'true' (unobserved) abundances from the model given by Box 1 equations (1)–(3) with parameter values estimated by maximum likelihood: $r_1=3.873$, $r_2=11.746$, $c=10^{-6.435}$, $d=0.5517$, $P=0.06659$, $q=0.9026$, $K=9.613$, $\sigma_1=0.3491$ and $\sigma_2=\sigma_3=0.7499$.

Our midge–algae–detritus model is firmly anchored in biology and fits the data well. The model displays alternative dynamical states and high-amplitude fluctuations over a broad range of parameter values governing the influxes of resources into the system (Fig. 3). This strongly suggests the existence of alternative dynamical states in the real midge system. We obtained further statistical support for alternative dynamical states in two ways. First, the model contains a parameter, q, that dictates the strength of density dependence

Table 1 | Goodness-of-fit measures for the midge–algae–detritus and alternative models

Goodness of fit	Model			Description
	Midge–algae–detritus	Gompertz	Lotka–Volterra	
Number of parameters*	6	9	9	Parameters included in the model deterministic skeleton
−2 LL	156.2	174.7	185.5	−2 × log likelihood function
Total R^2	0.98	0.98	0.97	1 − var $E(t)$/var $X(t)$†
Prediction R^2 for $X(t+1)$	0.74	0.57	0.38	1 − var $E(t)$/var $[\hat{X}(t+1) - \hat{X}(t)]$‡
Prediction R^2 for $X(t+1)$	0.53	0.39	0.25	1 − var $E(t)$/var $[X(t+1) - X(t)]$

See Supplementary Methods for descriptions of measures, and Box 1 for descriptions of the models
*Number of parameters in the model determining the dynamics. There are six additional parameters in each model for the scaling term K, process variation for midges (σ_1) and algae/detritus ($\sigma_2 = \sigma_3$), and initial densities for midges, algae and detritus.
†$E(t) = X(t) - X_p(t)$, where $X_p(t)$ is the one-step-ahead prediction of log(midge abundance) made by models in Box 1
‡$\hat{E}(t) = \hat{X}(t) - X_p(t)$, where $\hat{X}(t)$ is the one-step-ahead prediction of log(midge abundance) after being updated by the observed value of $X(t)$ to account for measurement error

affecting midge growth and reproduction (Box 1). As q decreases and density dependence weakens in the model, the stable point is lost, leaving only the high-amplitude cycle. For the model fitted to the data, the value of q is 0.903, yet the value below which only the high-amplitude cycle remains is 0.737 (Supplementary Fig. 1). We refitted the model to the data constraining q to be small enough for only the high-amplitude cycle to occur, and the fit of the resulting model was statistically significantly worse than the fit with $q = 0.903$ (likelihood ratio test, $\chi^2 = 6.34$, d.f. = 1, $P < 0.012$; see Supplementary Methods). This represents a conservative test because, even for values of q low enough to rule out alternative dynamical states, the stochastic dynamics nevertheless show many of the same characteristics; although the deterministic skeleton of the model does not have alternative states, there is a residual 'ghost' that is still detected in the region surrounding the formerly stable point (Supplementary Fig. 9).

As a second line of statistical support, we fitted the data to two additional models and compared the fits with our midge–algae–detritus model (Box 1). We selected the additional models to have flexibility in fitting the Myvatn midge dynamics and yet to be incapable of producing alterative dynamical states. The first is a three-variable Gompertz (log–linear) model. This model has nine parameters governing the midge dynamics, in contrast with six in the midge–algae–detritus model. Furthermore, we did not constrain the sign of the parameters, so the interactions between the three variables could be positive or negative. Thus, the three-variable Gompertz model represents the most general three-dimensional log–linear model possible, yet because it is log–linear it cannot produce either stable limit cycles or alternative dynamical states. Our second additional model is a two-resource, one-consumer Lotka–Volterra model. Like the Gompertz model, it contains nine parameters governing midge dynamics, and these are fitted only with constraints to guarantee that midges are consumers of the two resource variables. The Lotka–Volterra model can produce stable limit cycles, although it cannot have alternative states. Our strategy was to select additional models that are overparameterized (nine parameters) and thus should have an advantage over the midge–algae–detritus model yet cannot produce alternative dynamical states.

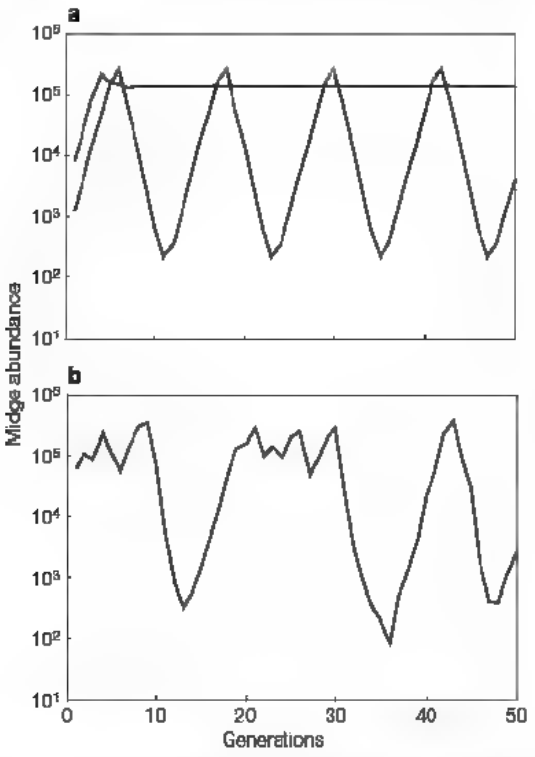

Figure 2 | Simulated dynamics of the model given by Box 1 equations (1)–(3) for 50 generations. **a**, Dynamics in the absence of environmental stochasticity ($\varepsilon_1(t) = \varepsilon_2(t) = \varepsilon_3(t) = 0$). **b**, Dynamics in the presence of environmental stochasticity. In **a**, two midge population trajectories starting from different initial values are illustrated. Parameter values are equal to those estimated from the data: $r_1 = 3.873$, $r_2 = 11.746$, $c = 10^{-6.435}$, $d = 0.5517$, $P = 0.06659$, $q = 0.9026$, $K = 9.613$; in **b**, $\sigma_1 = 0.3491$ and $\sigma_2 = \sigma_3 = 0.7499$

Despite the advantages of the additional models, the midge–algae–detritus model outperformed both of them (Table 1), giving evidence for the plausibility of alternative dynamical states underlying midge population dynamics. Further support for our model comes by applying it to a shorter data set from another shallow eutrophic lake nearby, Lake Vikingavatn (Supplementary Methods). The model fits well, and the parameter estimates are similar to those from Myvatn, with exceptions being explained by characteristics such as lake size.

A striking biological conclusion from the model is the sensitivity of the amplitude of midge fluctuations to very small amounts of resource input, c (Fig. 3); the resource input sets the lower boundary of midge abundance and hence the severity of population crashes. Thus, even though resource input might be six orders of magnitude less than the abundance of resources in the lake in most years, this vanishingly small source of resources is nevertheless critical in setting the depth of the midge population nadir and the subsequent rate of recovery. This sensitivity to resource subsidies might explain changes in midge dynamics that have apparently occurred over the last decades. Although Myvatn has supported a local charr (salmonid) fishery for centuries[29], this fishery collapsed in the 1980s, coincident with particularly severe midge population crashes[11]. Over the same period, waterbird reproduction in Myvatn was also greatly reduced during the crash years[12]. These changes might have been caused by dredging in one of the two basins in the lake that started in 1967 to extract diatomite from the sediment. Hydrological studies[27] indicate that dredging produces depressions that act as effective traps of organic particles, hence reducing algae and detritus inputs to the midge habitat. Our model predicts that even a slight reduction in subsidies can markedly increase the magnitude of midge fluctuations. Such slight environmental changes can then have seriously negative consequences for fish and bird populations.

Midges are central to the functioning of Myvatn, not only providing food for fish and birds but also representing most of the secondary production in the lake. Our analyses show that the marked, complex midge population dynamics can be explained by alternative

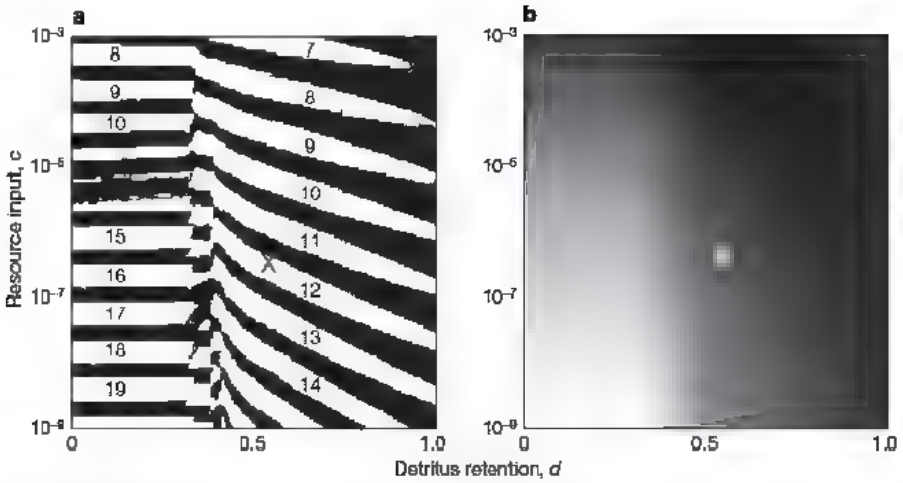

Figure 3 | Dynamics of the midge–algae–detritus model depending on resource input rate, *c*, and detritus retention, *d*. **a**, Alternative dynamical states in the deterministic skeleton (black, only a single stable point; white, stable point and stable cycle with integer period labelled). **b**, Amplitude of fluctuations in the stochastic model, with lighter shading corresponding to higher amplitude (black, 10^3, white, 10^{10}). The crosses mark values estimated from the data. Parameters are $r_1 = 3.873$, $r_2 = 11.746$, $c = 10^{-6.435}$, $d = 0.5517$, $P = 0.06659$, $q = 0.9026$, $K = 9.613$; in **b**, $\sigma_1 = 0.3491$ and $\sigma_2 = \sigma_3 = 0.7499$.

states, with one state a stable point and the other a stable cycle. Alternative dynamical states mean that the character of the dynamics (relatively constant versus cyclic) may change abruptly yet naturally. Moreover, the amplitude of the cycle is highly sensitive to small subsidies of resources into the midge habitat that rescue crashing midge populations. From a conservation perspective, this represents a challenge. Not only are midge dynamics inherently unpredictable, they may also be extremely and unexpectedly vulnerable to small disturbances to the lake.

Received 9 August; accepted 19 December 2007.

1. May, R. M. Simple mathematical models with very complicated dynamics. *Nature* 261, 459–467 (1976)
2. Hastings, A., Hom, C. L., Ellner, S., Turchin, P. & Godfray, H. C. J. Chaos in ecology: is Mother Nature a strange attractor? *Annu. Rev. Ecol. Syst.* 34, 1–33 (1993)
3. Dennis, B., Desharnais, R. A., Cushing, J. M., Henson, S. M. & Costantino, R. F. Estimating chaos and complex dynamics in an insect population. *Ecol. Monogr.* 71, 277–303 (2001)
4. Becks, L., Hilker, F. M., Malchow, H., Jürgens, K. & Arndt, H. Experimental demonstration of chaos in a microbial food web. *Nature* 435, 1226–1229 (2005)
5. Bjornstad, O. N. & Grenfell, B. T. Noisy clockwork: Time series analysis of population fluctuations in animals. *Science* 293, 638–643 (2001)
6. Dwyer, G., Dushoff, J. & Yee, S. H. The combined effects of pathogens and predators on insect outbreaks. *Nature* 430, 341–345 (2004)
7. Turchin, P. *Complex Population Dynamics: a Theoretical/Empirical Synthesis* (Princeton Univ. Press, Princeton, NJ, 2003)
8. Hanski, I., Turchin, P., Korpimaki, E. & Henttonen, H. Population oscillations of boreal rodents—regulation by mustelid predators leads to chaos. *Nature* 364, 232–235 (1993)
9. Scheffer, M., Carpenter, S., Foley, J. A., Folke, C. & Walker, B. Catastrophic shifts in ecosystems. *Nature* 413, 591–596 (2001)
10. Lindegaard, C. & Jonasson, P. M. Abundance, population dynamics and production of zoobenthos in Lake Mývatn, Iceland. *Oikos* 32, 202–227 (1979).
11. Gudbergsson, G. Arctic charr in Lake Myvatn: the centennial catch record in the light of recent stock estimates. *Aquatic Ecol.* 38, 271–284 (2004)
12. Gardarsson, A. & Einarsson, A. Resource limitation of diving ducks at Myvatn: Food limits production. *Aquatic Ecol.* 38, 285–295 (2004).
13. May, R. M. Thresholds and breakpoints in ecosystems with a multiplicity of stable states. *Nature* 269, 471–477 (1977).
14. Noy-Meir, I. Stability of grazing systems: an application of predator–prey graphs. *J. Ecol.* 63, 459–481 (1975).
15. Scheffer, M., Hosper, S. H., Meijer, M.-L., Moss, B. & Jeppesen, E. Alternative equilibria in shallow lakes. *Trends Ecol. Evol.* 8, 275–279 (1993).
16. Persson, L. *et al.* Culling prey promotes predator recovery—alternative states in a whole-lake experiment. *Science* 316, 1743–1746 (2007)
17. Carpenter, S. R. *Regime Shifts in Lake Ecosystems: Patterns and Variation* (International Ecology Inst., Oldendorf/Luhe, Germany, 2003).
18. Henson, S. M., Costantino, R. F., Desharnais, R. A., Cushing, J. M. & Dennis, B. Basins of attraction: population dynamics with two stable 4-cycles. *Oikos* 98, 17–24 (2002)
19. Ives, A. R., Gross, K. & Jansen, V. A. A. Periodic mortality events in predator–prey systems. *Ecology* 81, 3330–3340 (2000).
20. King, A. A. & Schaffer, W. M. The rainbow bridge: Hamiltonian limits and resonances in predator–prey models. *J. Math. Biol.* 39, 439–469 (1999)
21. Jansen, V. A. A. & Sabelis, M. W. Outbreaks of colony-forming pests in tri-trophic systems: consequences for pest control and the evolution of pesticide resistance. *Oikos* 74, 172–176 (1995).
22. Klebanoff, A. & Hastings, A. Chaos in three species food chains. *J. Math. Biol.* 32, 427–451 (1994)
23. Kendall, B. E. *et al.* Why do populations cycle? A synthesis of statistical and mechanistic modeling approaches. *Ecology* 80, 1789–1805 (1999).
24. Ingvason, H. R., Olafsson, J. S. & Gardarsson, A. Food selection of *Tanytarsus gracilentus* larvae (Diptera, Chironomidae), an analysis of instars and cohorts. *Aquatic Ecol.* 38, 231–237 (2004)
25. Einarsson, A., Gardarsson, A., Gislason, G. M. & Ives, A. R. Consumer–resource interactions and cyclic population dynamics of *Tanytarsus gracilentus* (Diptera: Chironomidae). *J. Anim. Ecol.* 71, 832–845 (2002)
26. Gardarsson, A. *et al.* Population fluctuations of chironomid and simulid Diptera at Myvatn in 1977–1996. *Aquatic Ecol.* 38, 209–217 (2004).
27. Kjaran, S. P., Hólm, S. L. & Myer, E. M. Lake circulation and sediment transport in Lake Myvatn. *Aquatic Ecol.* 38, 145–162 (2004)
28. Harvey, A. C. *Forecasting, Structural Time Series Models and the Kalman Filter* (Cambridge Univ. Press, Cambridge, 1989).
29. McGovern, T. H., Perdikaris, S., Einarsson, Á. & Sidell, J. Coastal connections, local fishing, and sustainable egg harvesting: patterns of Viking Age inland wild resource use in Mývatn district, Northern Iceland. *Environ. Archaeol.* 11, 187–205 (2006).
30. Ives, A. R., Dennis, B., Cottingham, K. L. & Carpenter, S. R. Estimating community stability and ecological interactions from time-series data. *Ecol. Monogr.* 73, 301–330 (2003)

Supplementary Information is linked to the online version of the paper at www.nature.com/nature.

Acknowledgements We thank K. C. Abbott, M. Duffy, K. J. Forbes, R. T. Gilman, J. P. Harmon and members of Zoo/Ent 540, Theoretical Ecology, University of Wisconsin – Madison, for comments on the manuscript. V.A.A.J. thanks R. A. Jansen-Spence for the time to do this research. This work was funded in part by National Science Foundation grants to A.R.I., and grants from the Icelandic Research Council and the University of Iceland Research Fund to A.E. and A.G.

Author Contributions A.E. and A.G. oversaw the data collection and are responsible for the long-term study on midge dynamics in Myvatn. A.E. and A.R.I. conceived the midge–algae–detritus model, and A.R.I. performed statistical analyses. V.A.A.J. and A.R.I. performed the mathematical analyses of the midge–algae–detritus model.

Author Information Reprints and permissions information is available at www.nature.com/reprints. Correspondence and requests for materials should be addressed to A.R.I. (arives@wisc.edu).

LETTERS

The genome of *Laccaria bicolor* provides insights into mycorrhizal symbiosis

F. Martin[1], A. Aerts[2], D. Ahrén[3], A. Brun[1], E. G. J. Danchin[4], F. Duchaussoy[1], J. Gibon[1], A. Kohler[1], E. Lindquist[2], V. Pereda[1], A. Salamov[2], H. J. Shapiro[2], J. Wuyts[1,5], D. Blaudez[1], M. Buée[1], P. Brokstein[2], B. Canbäck[3], D. Cohen[1], P. E. Courty[1], P. M. Coutinho[4], C. Delaruelle[1], J. C. Detter[2], A. Deveau[1], S. DiFazio[6], S. Duplessis[1], L. Fraissinet-Tachet[8], E. Lucic[1], P. Frey-Klett[1], C. Fourrey[1], I. Feussner[7], G. Gay[8], J. Grimwood[9], P. J. Hoegger[10], P. Jain[11], S. Kilaru[10], J. Labbé[1], Y. C. Lin[5], V. Legué[1], F. Le Tacon[1], R. Marmeisse[8], D. Melayah[8], B. Montanini[1], M. Muratet[11], U. Nehls[12], H. Niculita-Hirzel[13], M. P. Oudot-Le Secq[1], M. Peter[14], H. Quesneville[15], B. Rajashekar[3], M. Reich[1,10], N. Rouhier[1], J. Schmutz[9], T. Yin[16], M. Chalot[1], B. Henrissat[4], U. Kües[10], S. Lucas[2], Y. Van de Peer[5], G. K. Podila[11], A. Polle[10], P. J. Pukkila[17], P. M. Richardson[2], P. Rouzé[5,18], I. R. Sanders[13], J. E. Stajich[19], A. Tunlid[3], G. Tuskan[16] & I. V. Grigoriev[2]

Mycorrhizal symbioses—the union of roots and soil fungi—are universal in terrestrial ecosystems and may have been fundamental to land colonization by plants[1,2]. Boreal, temperate and montane forests all depend on ectomycorrhizae[1]. Identification of the primary factors that regulate symbiotic development and metabolic activity will therefore open the door to understanding the role of ectomycorrhizae in plant development and physiology, allowing the full ecological significance of this symbiosis to be explored. Here we report the genome sequence of the ectomycorrhizal basidiomycete *Laccaria bicolor* (Fig. 1) and highlight gene sets involved in rhizosphere colonization and symbiosis. This 65-megabase genome assembly contains ~20,000 predicted protein-encoding genes and a very large number of transposons and repeated sequences. We detected unexpected genomic features, most notably a battery of effector-type small secreted proteins (SSPs) with unknown function, several of which are only expressed in symbiotic tissues. The most highly expressed SSP accumulates in the proliferating hyphae colonizing the host root. The ectomycorrhizae-specific SSPs probably have a decisive role in the establishment of the symbiosis. The unexpected observation that the genome of *L. bicolor* lacks carbohydrate-active enzymes involved in degradation of plant cell walls, but maintains the ability to degrade non-plant cell wall polysaccharides, reveals the dual saprotrophic and biotrophic lifestyle of the mycorrhizal fungus that enables it to grow within both soil and living plant roots. The predicted gene inventory of the *L. bicolor* genome, therefore, points to previously unknown mechanisms of symbiosis operating in biotrophic mycorrhizal fungi. The availability of this genome provides an unparalleled opportunity to develop a deeper understanding of the processes by which symbionts interact with plants within their ecosystem to perform vital functions in the carbon and nitrogen cycles that are fundamental to sustainable plant productivity.

The 65-megabase genome of *Laccaria bicolor* (Maire) P. D. Orton is the largest sequenced fungal genome published so far[3–7] (Table 1). Although no evidence for large-scale duplications was observed within the *L. bicolor* genome, tandem duplication occurred within multigene families (Supplementary Fig. 4). Transposable elements comprised a higher proportion (21%) than that identified in the other sequenced fungal genomes and may therefore account for the relatively large genome of *L. bicolor* (Supplementary Table 3). Approximately 20,000 protein-coding genes were identified by combined gene predictions (Supplementary Information Section 2). Expression of nearly 80% (~16,000) of the predicted genes was detected in free-living mycelium, ectomycorrhizal root tips or fruiting bodies (Supplementary Table 4) using NimbleGen custom-oligoarrays (Supplementary Information Section 9). Most genes are activated in almost all tissues, whereas other more specialized genes are only activated in some specific developmental stages, such as the free-living mycelium, ectomycorrhizae or the fruiting body (Supplementary Table 5).

Only 14,464 *L. bicolor* proteins (70%) showed sequence similarity (BLASTX, cut-off *e*-value >0.001) to documented proteins. Most homologues were found in the sequenced basidiomycetes *Phanerochaete chrysosporium*[4], *Cryptococcus neoformans*[5], *Ustilago maydis*[6] and *Coprinopsis cinerea*[7] (Supplementary Table 6). The percentage of proteins found in multigene families was related to genome size and was the largest in *L. bicolor* (Fig. 2). This was mainly owing to the expansion of protein family size, but was also because of the larger number of protein families in *L. bicolor* compared with the other basidiomycetes (Supplementary Table 7). Expansion of protein family sizes in *L. bicolor* was prominent in the lineage-specific multigene families. Marked gene family expansions occurred in those genes predicted to have roles in protein–protein interactions (for example, WD40-domain-containing proteins) and in signal transduction

[1]UMR 1136, INRA-Nancy Université, Interactions Arbres/Microorganismes, INRA-Nancy, 54280 Champenoux, France. [2]US DOE Joint Genome Institute, Walnut Creek, California 94598, USA. [3]Microbial Ecology Lund University, SE-223 62 Lund, Sweden. [4]Architecture et Fonction des Macromolécules Biologiques, UMR 6098 CNRS-Universités Aix-Marseille I & II, 13288 Marseille Cedex 9, France. [5]Department of Plant Systems Biology, Flanders Interuniversity Institute for Biotechnology (VIB), Ghent University, B-9052 Ghent, Belgium. [6]Department of Biology, West Virginia University, Morgantown, West Virginia 26506, USA. [7]Department for Plant Biochemistry, Georg-August-Universität Göttingen, 37077 Göttingen, Germany. [8]Université Lyon 1, UMR CNRS - USC INRA d Ecologie Microbienne, 69622 Villeurbanne, France. [9]Stanford Human Genome Center, Department of Genetics, Stanford University School of Medicine, 975 California Avenue, Palo Alto, California 94304, USA. [10]Institute of Forest Botany, Georg-August-Universität, 37077 Göttingen, Germany. [11]Department of Biological Sciences, University of Alabama, Huntsville, Alabama 35899, USA. [12]Eberhard-Karls-Universität, Physiologische Oekologie der Pflanzen, 72076 Tübingen, Germany. [13]Department of Ecology & Evolution, University of Lausanne, 1015 Lausanne, Switzerland. [14]Swiss Federal Research Institute WSL, 8903 Birmensdorf, Switzerland. [15]Unité de Recherches en Génomique-Info, INRA-Evry, 91034 Évry Cedex, France. [16]Environmental Science Division, Oak Ridge National Laboratory, Oak Ridge, Tennessee 37831, USA. [17]Department of Biology, The University of North Carolina, Chapel Hill, North Carolina 27599-3280, USA. [18]Laboratoire Associé de l INRA, Ghent University, B-9052 Gent, Belgium. [19]Department of Plant and Microbial Biology, University of California, Berkeley, California 94720-3102, USA.

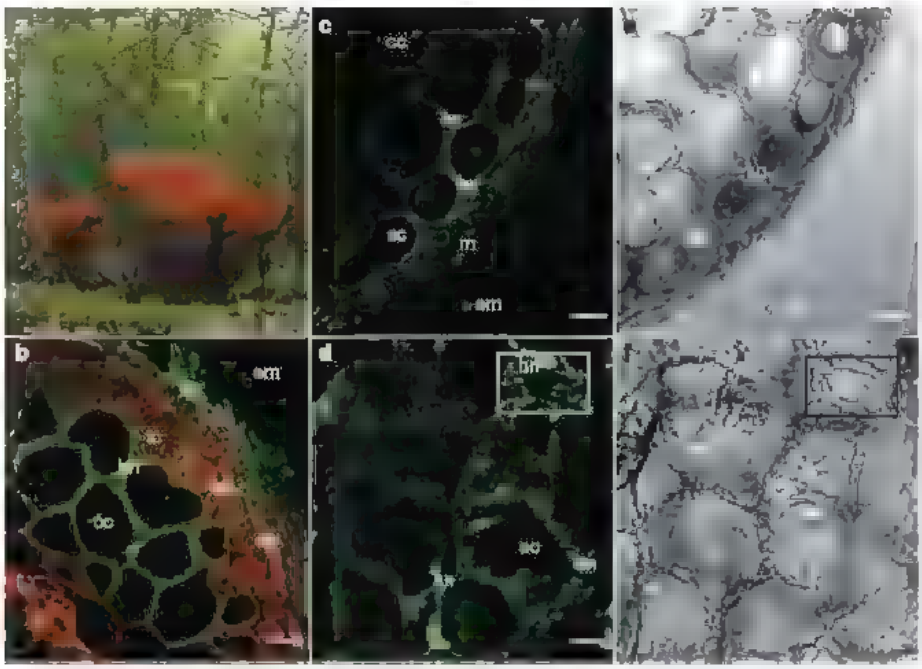

Figure 1 | Ectomycorrhizal symbiosis and the localization of the SSP MISSP7. **a**, Fruiting bodies of *L. bicolor* colonizing seedlings of Douglas fir (photograph courtesy of D. Vairelles). **b**, Laser-scanning confocal microscopy image of a transverse section of *Pseudotsuga menziesii–L. bicolor* ectomycorrhizae showing extramatrical mycelium (em), the mantle (m) and Hartig net hyphae (hn) between epidermal (ec), tannin (tc) and cortical (cc) root cells. Scale, 10 μm. **c–f**, Immunofluorescent localization of MISSP7. Transverse (**c**, **e**) and longitudinal (**d**, **f**) sections of *P. trichocarpa–L. bicolor* ectomycorrhizae. MISSP7 was detected in the hyphae of the mantle (m) and the Hartig net (hn) ensheathing epidermal cells (ec). Rectangles in **d** and **f** show the finger-like, labyrinthine hyphal system accumulating a large amount of MISSP7. **e**, **f**, Phase contrast images. Scale, 10 μm.

mechanisms (Supplementary Table 7). Two new classes of GTPase α genes were found and may be candidates for the complex communication that must occur between the mycobiont and its host plant during mycorrhizae establishment (Supplementary Table 8). Several transcripts coding for expanded and lineage-specific gene families were upregulated in symbiotic and fruiting body tissues, suggesting a role in tissue differentiation (Supplementary Tables 5 and 9).

In our analysis of annotated genes, in particular that of paralogous gene families, we highlighted processes that may be related to the biotrophic and saprotrophic lifestyles of *L. bicolor*. Twelve predicted proteins showed a similarity to known haustoria-expressed secreted proteins of the basidiomycetous rusts *Uromyces fabae*[8] and *Melampsora lini*[9], which are involved in pathogenesis (Supplementary Table 10). Out of the 2,931 proteins predicted to be secreted by *L. bicolor*, most (67%) cannot be ascribed a function, and 82% of these predicted proteins are specific to *L. bicolor*. Within this set, we found a large number of genes that encode cysteine-rich products that have a predicted size of <300 amino acids. Of these 278 SSPs, 69% belong to multigene families, but only nine groups comprising a total of 33 SSPs co-localized in the genome (Supplementary Fig. 5). The structure of two of these clusters is shown in Supplementary Fig. 6. Other SSPs are scattered all over the genome, and we found no correlation between SSP and transposable element genome localization (Supplementary Fig. 5). Transcript profiling revealed that the expression of several SSP genes is specifically induced in the symbiotic interaction (Table 2 and Supplementary Fig. 10). Five of the 20 most highly upregulated fungal transcripts in ectomycorrhizal root tips code for SSPs (Supplementary Table 5). These mycorrhiza-induced cysteine-rich SSPs (MISSPs) belong to *L. bicolor*-specific orphan gene families. Within the MISSPs, we found a family of secreted proteins with a CFEM domain (INTERPRO IPR014005) (Supplementary Figs 7 and 8), as previously identified in the plant pathogenic fungi *M. lini*[9] and *Magnaporthea grisea*[10] (Supplementary Table 10), and proteins with a gonadotropin (IPR0001545) or snake-toxin-like (SSF57302) domains related to the cysteine-knot domain. Expression of several SSPs was downregulated in ectomycorrhizal root tips (cluster E in Supplementary Fig. 10), suggesting a complex interplay between these secreted proteins in the symbiosis interaction.

The rich assortment of MISSPs may therefore act as effector proteins to manipulate host cell signalling or to suppress defence pathways during infection, as suggested for pathogenic rusts[8,9], smuts[6] (*U. maydis*) and *Phytophthora*[11] species. To have a role in symbiosis development, MISSPs should be expressed in *L. bicolor* hyphae colonizing the root tips. To test this assertion, we determined the tissue distribution of the mycorrhiza-induced cysteine-rich SSP of 7 kDa (MISSP7) (JGI identification number 298595) showing the highest induction in ectomycorrhizal tips (Table 2 and Supplementary Table 5). Two peptides, one of which is located in the amino-terminal and the other in the carboxy-terminal part of the mature protein, were selected as antigens for the production of anti-MISSP7 antibodies. The selected peptides were not found in the deduced protein sequences of other *L. bicolor* gene models, nor in the *Populus trichocarpa* genome[12]. MISSP7

Table 1 | Genome characteristics of *L. bicolor* and other basidiomycetes

Genome characteristics	*L. bicolor*	*C. cinerea*[7]	*P. chrysosporium*[4]	*C. neoformans*[5]	*U. maydis*[6]
Strain	S238N-H82	Okayama7#130	RP78	H99	521
Sequencing institution	JGI	Broad	JGI	Broad	Broad
Genome assembly (Mb)	64.9	37.5	35.1	19.5	19.7
GC content (%)	46.6	51.6	53.2	48.2	54
Number of protein-coding genes	20,614	13,544	10,048	7,302	6,522
Coding sequence <300 bp	2,191	838	163	313	58
Average gene length (bp)	1,533	1,679	1,667	1,828	1,935
Average coding sequence length (bp)	1,134	1,352	1,366	1,502	1,840
Average exon length (nt)	210.1	251	232	253	1,051
Average intron length (nt)	92.7	75	117	66	127

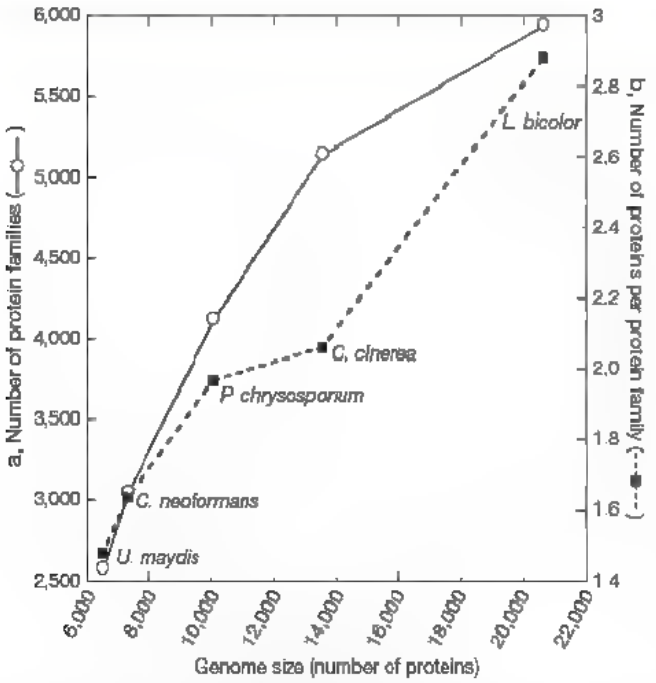

Figure 2 | Expansion of protein families in *L. bicolor*. **a**, Relationship between genome size and the number of protein families. **b**, Relationship between genome size and protein family sizes in five sequenced basidiomycetes. Protein sequences predicted from the genome sequences of *L. bicolor*, *C. cinerea*, *P. chrysosporium*, *C. neoformans* and *U. maydis* were clustered into families using the TRIBE-MCL algorithm (see Supplementary Information Section 5 for details).

localization in *L. bicolor–P. trichocarpa* ectomycorrhizal root tips by indirect immunofluorescence is illustrated in Fig. 1 and Supplementary Fig. 11. Control images in which the ectomycorrhizae sections were obtained by replacing primary anti-MISSP7 antibodies with pre-immune immunoglobulin (Ig)G are shown in Supplementary Fig. 12. For cases in which ectomycorrhizae were treated with anti-MISSP7 antibody followed by fluorescent-labelled secondary antibody, fluorescence was localized in the hyphae colonizing short roots (Fig. 1 and Supplementary Fig. 11) and was not detected in the free-living mycelium (Supplementary Fig. 12). Although MISSP7 was detected in the hyphal mantle layers ensheating the root tips, the protein mainly accumulated in the finger-like, labyrinthine branch hyphal system (Hartig net), which provides a very large area of contact between cells of the two symbionts. It accumulated in the cytosol and cell wall of the fungal cells. The MISSP7 protein could therefore interact with the plant components after secretion. MISSP7 shares no sequence similarity or protein motif with other SSPs.

Comparison of the MISSP sequences did not reveal a specific conserved motif that could potentially contribute to their function or to targeting to the host cell, such as the RXLR motif[11] of phytopathogenic *Phytophthora* or the malaria parasite. SSPs with upregulated expression in fruiting bodies (Supplementary Table 5 and Supplementary Fig. 10) may have a role in the differentiation of the sexual tissues and/or the aggregation of sporophore tissues. Interestingly, there is a large set of SSP genes showing significant changes in gene expression in both ectomycorrhizal root tips and fruiting bodies (cluster A in Supplementary Fig. 10), suggesting that both developmental processes recruit similar gene networks (for example, those involved in hyphal aggregation).

Host trees are able to harness the formidable web of mycorrhizal hyphae (which permeates the soil and decaying leaf litter) for their nutritional benefit. A process that is pivotal to the success of ectomycorrhizal interactions is therefore the equitable exchange of nutrients between the symbiont and its host plant[1,2,13]. A comparison with other basidiomycetes (Supplementary Table 12) revealed that the total number of predicted transporters is larger in *L. bicolor* compared with *C. cinerea* and *P. chrysosporium*. Interestingly, *L. bicolor* has multiple ammonia transporters, although it encodes a single nitrate permease. Ammonia is arguably the most important inorganic nitrogen source for ectomycorrhizal fungi[14]. One of the ammonia transporters (*AMT2.2*), for instance, is greatly upregulated in ectomycorrhizae (Supplementary Table 5). Therefore, *L. bicolor* shows an increased genetic potential in terms of nitrogen uptake compared with other basidiomycetes. These capabilities are consistent with *L. bicolor* being exposed to a range of nitrogen sources from the decay of organic matter[15].

Although the *L. bicolor* genome contains numerous genes coding for key hydrolytic enzymes, such as proteases and lipases, we observed an extreme reduction in the number of enzymes involved in the degradation of plant cell wall (PCW) oligosaccharides and polysaccharides. Glycoside hydrolases, glycosyltransferases, polysaccharide lyases, carbohydrate esterases and their ancillary carbohydrate-binding modules were identified using the carbohydrate-active enzyme (CAZyme) classification (http://www.cazy.org/). A comparison of the *L. bicolor* candidate CAZymes with fungal phytopathogens

Table 2 | Changes in expression of transcripts coding for MISSPs

Protein identification (JGI *Laccaria* database)	Family size	Length (amino acids)	Transcript concentration (FLM)	*P. menziesii* ECM/FLM ratio (fold)	*P. trichocarpa* ECM/FLM ratio (fold)	Features
298595	sc	68	ND	21,877	12,913	MISSP7
333839	5	129	ND	7,844	1,931	Glycosyl phosphatidylinositol (GPI)-anchored
298667	2	70	ND	1,906	1,407	
332226	8	181	43	847	780	CFEM domain (INTERPRO IPR014005)
311468	2	59	ND	191	ND	
295737	8	288	131	171	252	
334759	sc	101	ND	109	18	
395403	4	121	24	103	93	
333423	9	120	6	102	72	Gonadotropin domain (IPR0001545)
312262	4	106	85	69	53	
295625	4	199	325	66	48	
325402	8	238	310	49	74	Snake toxin-like (SSF57302)
316998	sc	56	137	29	57	
333197	3	148	266	17	8	
327918	2	154	763	13	4	Homologue in *C. cinerea*
307956	sc	74	336	13	90	Whey acidic domain (IPR008197)
327246	sc	194	1,025	10	18	Homologue in *C. cinerea*
303550	5	98	1,365	10	14	
300377	2	291	5,499	10	8	
293250	sc	224	127	9	10	Homologue in *C. cinerea*
298648	sc	64	1,108	8	12	
298646	2	73	1,028	7	14	
293729	3	210	3,000	7	7	

Transcript profiling was performed on free-living mycelium (FLM) and ectomycorrhizal root tips (ECM) of poplar (*P. trichocarpa*) and Douglas fir (*P. menziesii*). See Supplementary Information Section 9 for details. Abbreviations: ND, not detected; sc, single copy.

confirms the adaptation of its enzyme repertoire to symbiosis and reveals the strategy used for the interaction with the host (Supplementary Tables 13 and 14). The reduction in PCW CAZymes affects almost all glycoside hydrolase families, culminating in the complete absence of several key families. For instance, there is only one candidate cellulase (glycoside hydrolase 5, GH5) appended to the sole fungal cellulose-binding module (CBM1) found in the genome, and no cellulases from families GH6 and GH7 (Supplementary Table 14). Similar reductions or loss of hemicellulose- and pectin-degrading enzymes were also noted. These observations suggest that the inventory of *L. bicolor* PCW-degrading enzymes underwent massive gene loss as a result of its adaptation to a symbiotic lifestyle, and that this species is now unable to use many PCW polysaccharides as a carbon source, including those found in soil and leaf litter. The remaining small set of secreted CAZymes with potential action on plant polysaccharides (for example, GH28 polygalacturonases) is probably required for cell wall remodelling during fungal tissue differentiation because their expression was upregulated in both fruiting bodies and ectomycorrhizae (Supplementary Table 15 and Supplementary Fig. 13). By contrast, transcripts coding for proteins with an expansin domain were only induced in ectomycorrhizae, suggesting they may be used by *L. bicolor* for penetrating into the root apoplastic space.

To survive before its mycorrhizal association with its host, *L. bicolor* seems to have developed a capacity to degrade non-plant (for example, animal and bacterial) oligosaccharides and polysaccharides; this is suggested by retention of CAZymes from families GH79, polysaccharide lyase 8 (PL8), PL14 and GH88 (Supplementary Table 14). Interestingly, there is no invertase gene in the *L. bicolor* genome, implying that this fungus is unable to use sucrose directly from the plant. This is consistent with earlier observations[16] that *L. bicolor* depends on its host plant to provide glucose in exchange for nitrogen. We also noticed an expansion of CAZymes involved in the fungal cell wall biosynthesis and rearrangement, almost entirely owing to an increased number of putative chitin synthases and enzymes acting on β-glucans (Supplementary Table 14). Several of the corresponding genes are up- or down-regulated in developmental processes requiring cell wall alterations such as formation of fruiting bodies or mycorrhizae (Supplementary Table 15 and Supplementary Fig. 13).

Ectomycorrhizal fungi have an important role in mobilizing nitrogen from well-decomposed organic matter[2,15]. The hyphal network permeating the soil might therefore be expected to express a wide diversity of proteolytic enzymes. The total number of secreted proteases (116 members) identified (Supplementary Fig. 14) is relatively large compared with that in other sequenced saprotrophic basidiomycetes, such as *C. cinerea* and *P. chrysosporium*. Secreted aspartyl-, metallo- and serine-proteases may have a role in degradation of decomposing litter[15], confirming that *L. bicolor* has also the ability to use nitrogen of animal origin, as suggested previously[17]. They may also have a role in developmental processes because the expression of several secreted proteases is up- or down-regulated in fruiting bodies and ectomycorrhizal root tips (Supplementary Table 16). Mycelial mats formed by *L. bicolor* hyphae colonizing organic matter therefore possess the ability to degrade proteins from decomposing leaf litter.

Our analysis of the gene space reveals a multi-faceted mutualistic biotroph equipped to take advantage of transient occurrences of high-nutrient niches (living host roots and decaying soil organic matter) within a heterogeneous, low-nutrient environment. The availability of genomes from mutualistic, saprotrophic[4] and pathogenic[6] fungi, as well as from the mycorrhizal tree *P. trichocarpa*[12], now provides an unparalleled opportunity to develop a deeper understanding of the processes by which fungi colonize wood and soil litter, and also interact with living plants within their ecosystem, to perform vital functions in the carbon and nitrogen cycles[2] that are fundamental to sustainable plant productivity.

METHODS SUMMARY

Genomic sequence. Scaffolds and assemblies for all genomic sequences generated by this project are also available from the Joint Genome Institute (JGI) portal (http://genome.jgi-psf.org/Lacbi1/Lacbi1.download.ftp.html). A genome browser is available from JGI (http://www.jgi.doe.gov/laccaria). BLAST search of the genome is available at JGI (http://www.jgi.doe.gov/laccaria) and INRA LaccariaDB (http://mycor.nancy.inra.fr/IMGC/LaccariaGenome/).

Predicted gene models. Consensus gene predictions, produced by combining several different gene predictors, are available from JGI (http://www.jgi.doe.gov/laccaria) as General Feature Format (GFF) files. These gene models can also be accessed from the Genome Browser in the JGI *L. bicolor* portal (http://www.jgi.doe.gov/laccaria).

Gene annotations. Tables compiling KEGG, PFAM, KOG and best BLAST hits for predicted gene models, transposable element and CAZyme data, as well as Tribe-MCL gene families, are available from INRA LaccariaDB (http://mycor.nancy.inra.fr/IMGC/LaccariaGenome/)

Full Methods and any associated references are available in the online version of the paper at www.nature.com/nature.

Received 10 August; accepted 20 December 2007.

1. Smith, S. E. & Read, D. J. *Mycorrhizal Symbiosis* 2nd edn (Academic, London, 1996)
2. Read, D. J. & Perez-Moreno, J. Mycorrhizas and nutrient cycling in ecosystems — a journey towards relevance? *New Phytol.* 157, 475–492 (2003)
3. Galagan, J. E., Henn, M. R., Ma, L. J., Cuomo, C. A. & Birren, B. Genomics of the fungal kingdom: insights into eukaryotic biology. *Genome Res.* 15, 1620–1631 (2005)
4. Martinez, D. *et al.* Genome sequence of the lignocellulose degrading fungus *Phanerochaete chrysosporium* strain RP78. *Nature Biotechnol.* 22, 695–700 (2004)
5. Loftus, B. J. *et al.* The genome of the basidiomycetous yeast and human pathogen *Cryptococcus neoformans*. *Science* 307, 1321–1324 (2005).
6. Kämper, J. *et al.* Insights from the genome of the biotrophic fungal plant pathogen *Ustilago maydis*. *Nature* 444, 97–101 (2006)
7. *Coprinus cinereus* database (http://www.broad.mit.edu/annotation/genome/coprinus_cinereus/Home.html)
8. Wirsel, S. G. R., Voegele, R. T. & Mendgen, K. W. Differential regulation of gene expression in the obligate biotrophic interaction of *Uromyces fabae* with its host *Vicia faba*. *Mol. Plant Microb. Int.* 14, 1319–1326 (2001).
9. Catanzariti, A. M., Dodds, P. N., Lawrence, G. J., Aylifte, M. A. & Ellis, J. G. Haustorially expressed secreted proteins from flax rust are highly enriched for avirulence elicitors. *Plant Cel* 18, 243–256 (2006).
10. Kulkarni, R. D., Kelkar, H. S. & Dean, R. A. An eight-cysteine-containing CFEM domain unique to a group of fungal membrane proteins. *Trends Bioch. Sci.* 28, 118–121 (2003)
11. Kamoun, S. A. Catalogue of the effector secretome of plant pathogenic oomycetes. *Annu. Rev. Phytopathol.* 44, 41–60 (2006)
12. Tuskan, G. A. *et al.* The genome of black cottonwood, *Populus trichocarpa* (Torr & Gray). *Science* 313, 1596–1604 (2006)
13. Martin, F., Kohler, A. & Duplessis, S. Living in harmony in the wood underground: ectomycorrhizal genomics. *Curr. Opin. Plant Biol.* 10, 204–210 (2007)
14. Chalot, M., Blaudez, D. & Brun, A. Ammonia, a candidate for nitrogen transfer at the mycorrhizal interface. *Trends Plant Sci.* 11, 263–266 (2006)
15. Lindahl, B. D. *et al.* Spatial separation of litter decomposition and mycorrhizal nitrogen uptake in a boreal forest. *New Phytol.* 173, 611–620 (2007)
16. Nehls, U., Grunze, N., Willmann, M., Reich, M. & Küster, H. Sugar for my honey: carbohydrate partitioning in ectomycorrhizal symbiosis. *Phytochemistry* 68, 82–91 (2007)
17. Klironomos, J. N. & Hart, M. M. Animal nitrogen swap for plant carbon. *Nature* 410, 651 (2001)

Supplementary Information is linked to the online version of the paper at www.nature.com/nature.

Acknowledgements The genome sequencing of *L. bicolor* was funded by the US Department of Energy's Office of Science, Biological and Environmental Research Program and the by University of California, the Lawrence Berkeley National Laboratory, the Lawrence Livermore National Laboratory, and the Los Alamos National Laboratory. Annotation and transcriptome analyses were supported by INRA, the US Department of Energy, the US National Science Foundation, the European Commission, the Région Lorraine and the Swedish Research Council. We thank S. Rombauts, L. Sterck, K. Vandepoele, G. Werner and his colleagues, S. Pitluck and K. Zhou, B. Hilselberger and J. Gérard for their assistance. F.M. thanks N. Talbot for critical reading of an early draft of the manuscript.

Author Contributions A.A., D.A., A.B., E.G.J.D., F.D., J.G., A. K., E.L., V.P., A.S., H.J.S. and J.W. contributed equally to this work as second authors. M.C., B.H., U.K., S.L., Y.V.d.P., G.K.P., A.P., P.J.P., P.M.R., P.R., I.R.S., J.E.S., A.T., G.T. and I.V.G. contributed equally to this work as senior authors. Individual contributions were as follows. For the sequencing project, F.M. and G.T. initiated the sequencing project in the wake of the *Populus* genome project. F.M., I.V.G. and P.M.R. developed and coordinated the sequencing, annotation and transcriptome projects. S.L. and sequencing staff at

JGI performed the shotgun sequencing. H.J.S. and his staff at JGI performed the JAZZ assembly of the nuclear and mitochondrial genome. J.G. and J.S. performed the Arachne assembly, closed up repetitive gaps and fixed missassembled regions. A.A., A.S., J.W., M.M., P.R., Y.V.d.P. and I.V.G. did the *ab initio* annotation of protein-coding gene models. A.K., E.L., P.B., C.D., A.D., J.C.D., M.P., G.K.P., A.T. and F.M. provided expressed sequence tag/cDNA information for the *ab initio* and manual annotation. Genome statistics was performed by D.A., F.D., J.W., P.R., I.V.G. and F.M. A.A. and I.V.G., and F.D. and M.P.O.-L.S. were responsible for database design and maintenance at JGI and INRA, respectively. For genome analysis, D.C., M.P. and G.K.P. were responsible for DNA extraction and purification; D.A., F.D., Y.C.L., B.R., Y.V.P., P.R., A.S., J.E.S., A.T., I.V.G. and F.M. for comparative genome analysis; B.C., D.A. and A.T. for genome synteny; J.L., T.Y., G.T., F.M. and F.L.T. for construction of the genetic map; S.D.F. for single nucleotide polymorphisms; A.K., F.D. and F.M. for DNA arrays; A.D., B.C., P.F.K. and F.M. for high-GC sequences; J.W., P.R. and F.M. for tRNA, snRNA and rDNA; E.G.J.D., P.M.C., B.H. for carbohydrate active enzymes; A.D. and P.F.-K. for carbohydrate metabolism; J.G., P.H., L.K. and F.M. for cell wall proteins and secretome; L.F.-T., G.G., D.M. and R.M. for cytoskeleton and motor proteins; M.R., I.F. and A.P. for lipid metabolism; and H.N.-H., U.K. and I.R.S. for mating type genes. F.M. was responsible for genome analysis of the mitochondrion; P.E.C., P.H., M.B., S.K. and L.K. for the multi-copper oxidases, M.B., P.E.C. and F.M. for the proteases; N.R. for the redox genes; S.D., P.J. and G.K.P. for the signal transduction pathway; A.B., D.B., C.F., E.L., B.M., U.N., V.P. and M.C. for transporters; J.L., J.W., P.R., F.M. and H.Q. for transposable elements; V.P., J.G., A.B. and V.L. for immunolocalization of SSP; and J.E.S. and P.J.P. for the *Coprinopsis* genome. F.M. organized co-ordination between different groups. F.M. wrote and edited the paper with input from I.V.G., A.T., D.A., P.R., M.C. and B.H.

Author Information The whole-genome shotgun project has been deposited at GenBank/EMBL/DDBJ under project accession number ABFE00000000. The version described in this paper including assembly and annotation is the first version, ABFE01000000. The complete expression data set is available as a series under accession number GSE9784 at the Gene Expression Omnibus at NCBI (http://www.ncbi.nlm.nih.gov/geo/). Correspondence and requests for materials should be addressed to F.M. (fmartin@nancy.inra.fr)

LETTERS

Identification of a serotonin/glutamate receptor complex implicated in psychosis

Javier González-Maeso[1,2], Rosalind L. Ang[1], Tony Yuen[1], Pokman Chan[1], Noelia V. Weisstaub[5,6], Juan F. López-Giménez[8], Mingming Zhou[5], Yuuya Okawa[1], Luis F. Callado[9,10], Graeme Milligan[8], Jay A. Gingrich[5,6,7], Marta Filizola[3], J. Javier Meana[9,10] & Stuart C. Sealfon[1,4]

The psychosis associated with schizophrenia is characterized by alterations in sensory processing and perception[1,2]. Some antipsychotic drugs were identified by their high affinity for serotonin 5-HT_{2A} receptors (2AR)[3,4]. Drugs that interact with metabotropic glutamate receptors (mGluR) also have potential for the treatment of schizophrenia[5–7]. The effects of hallucinogenic drugs, such as psilocybin and lysergic acid diethylamide, require the 2AR[8–10] and resemble some of the core symptoms of schizophrenia[10–12]. Here we show that the mGluR2 interacts through specific transmembrane helix domains with the 2AR, a member of an unrelated G-protein-coupled receptor family, to form functional complexes in brain cortex. The 2AR–mGluR2 complex triggers unique cellular responses when targeted by hallucinogenic drugs, and activation of mGluR2 abolishes hallucinogen-specific signalling and behavioural responses. In post-mortem human brain from untreated schizophrenic subjects, the 2AR is upregulated and the mGluR2 is downregulated, a pattern that could predispose to psychosis. These regulatory changes indicate that the 2AR–mGluR2 complex may be involved in the altered cortical processes of schizophrenia, and this complex is therefore a promising new target for the treatment of psychosis.

The 2AR and mGluR2/3 show an overlapping distribution in brain cortex in autoradiography studies[13]. The mGluR2 and mGluR3 are not distinguished by autoradiographic ligands. We used fluorescent *in situ* hybridization (FISH) to determine whether either of these receptor subtypes is co-expressed by the same neurons. In layer V mouse somatosensory cortex (SCx), cells positive for *2AR* mRNA were mostly positive for *mGluR2* mRNA. The level of expression in SCx was much lower for *mGluR3* mRNA, which rarely co-localized with *2AR* mRNA (Fig. 1a). Control studies validated the sensitivity and specificity of the assay, and similar 2AR–mGluR2 mRNA co-localization was found in cortical primary cultures (Fig. 1a–c and Supplementary Fig. 1). Translation of 2AR protein in cortical pyramidal neurons was found to be necessary for normal mGluR2 expression. Mice with globally disrupted 2AR expression (*htr2A*$^{-/-}$ mice) showed reduced cortical mGluR2 binding and expression, whereas mice in which 2AR expression had been selectively restored in cortical pyramidal neurons[8,14] showed expression levels equal to those in the control (Supplementary Table 1 and Supplementary Fig. 2). The effects of mGluR2/3 activation on 2AR responses have generally been attributed to synaptic mechanisms[5,6,13,15]. However, the co-localization of *2AR* and *mGluR2* and the decrease in mGluR2 expression levels in *htr2A*$^{-/-}$ mice led us to examine whether a direct mechanism contributed to cortical cross-talk between these two receptor systems.

Recent studies have demonstrated that some G-protein-coupled receptors (GPCRs) belonging to the same sequence classes can form dimers[16] or, potentially, higher-order oligomers[17]. Although the 2AR and mGluR2 belong to different GPCR classes, we established the existence of 2AR–mGluR2 heterocomplexes by several methods: co-immunoprecipitation of human brain cortex samples (Fig. 1d) and of HEK-293 cells transfected with epitope-tagged receptors (Fig. 2b), bioluminescence resonance energy transfer (BRET) (Fig. 1e and Supplementary Fig. 3), and fluorescence resonance energy transfer (FRET) (Fig. 2d) studies in transfected cells.

To determine whether the formation of the 2AR–mGluR2 complex has functional consequences, we first examined, in mouse SCx membranes, the effects of an mGluR2/3 agonist on the competition binding of several hallucinogenic 2AR agonists (Fig. 1f, top) and of a 2AR agonist on the competition binding of several mGluR2/3 agonists (Fig. 1f, bottom) The agonist affinities for the 2AR and mGluR2/3 were decreased when receptor–G-protein complexes were uncoupled by GTP-γS (Supplementary Fig. 4 and Supplementary Tables 2 and 3). The glutamate agonist LY379268 increased the affinity of all three hallucinogens studied for the 2AR-binding site. Furthermore, the 2AR agonist DOI (1-(2,5-dimethoxy-4-iodophenyl)-2-aminopropane) decreased the affinity of the three mGluR2/3 agonists for the glutamate-receptor-binding site. The allosteric interactions observed were eliminated by antagonist for each modulator (see Supplementary Tables 2 and 3 and Supplementary Fig. 4 for additional concentrations of DOI and LY379268 and for the elimination of the allosteric effects by antagonists). Although the glutamate agonists studied do not distinguish between the mGluR2 and mGluR3 subtypes[18], the rarity of *mGluR3* and *2AR* mRNA co-expression in cortex, the absence of evidence for 2AR–mGluR3 complex formation by co-immunoprecipitation, BRET and FRET, and the detection of 2AR–mGluR2 complexes by these same assays all indicate that the cross-talk identified results from 2AR–mGluR2 complexes.

The differences in the capacity of the mGluR2 and mGluR3 to interact with the 2AR and their close sequence similarity provided the basis for identifying the specific mGluR2 domains responsible for heterocomplex formation. A study of a series of molecular chimaeras of the mGluR2 and mGluR3 (see Fig. 2a) demonstrated that the segment containing transmembrane (TM) helices 4 and 5 of the mGluR2 receptor was both necessary and sufficient for the formation of a complex with the 2AR. The mGluR3 receptor chimaera containing only this segment from the mGluR2 (mGluR3ΔTM4,5) was capable of co-immunoprecipitating with the 2AR (Fig. 2b), mediating

[1]Department of Neurology [2]Department of Psychiatry [3]Department of Structural and Chemical Biology and [4]Center for Translational Systems Biology, Mount Sinai School of Medicine, New York, New York 10029, USA [5]Department of Psychiatry, [6]Sackler Institute Laboratories and [7]Lieber Center for Schizophrenia Research, Columbia University, and the New York State Psychiatric Institute, New York, New York 10032, USA [8]Division of Biochemistry and Molecular Biology, Institute of Biomedical and Life Sciences, University of Glasgow, Glasgow G12 8QQ, UK [9]CIBER of Mental Health, and [10]Department of Pharmacology, University of the Basque Country, E-48940 Leioa, Bizkaia, Spain

allosteric cross-talk (Fig. 2c) and maintaining close proximity with the 2AR as indicated by FRET (Fig. 2d). In contrast, mGluR2ΔTM4,5 did not show evidence of complex formation with the 2AR (Fig. 2, Supplementary Figs 5 and 6, and Supplementary Tables 4 and 5 show complete curves, analysis and evidence of membrane expression of all chimaeras). The absolute and relative levels of expression of heterologous constructs were comparable to the physiological levels found in mouse SCx, and in cortical primary cultures (Supplementary Fig. 5 and Supplementary Table 4). Our data do not exclude the possibility that the predicted 2AR–mGluR2 heterodimer, a model of which is shown in Fig. 2f, assembles into tetramers or larger receptor oligomers[19,20].

The changes in high-affinity binding caused by 2AR–mGluR2 cross-talk suggested that this complex may serve to integrate serotonin and glutamate signalling and modulate G-protein coupling[21,22]. This hypothesis was tested by measuring the regulation of $G\alpha_{q/11}$ and $G\alpha_i$ proteins by 2AR. High-affinity activation of $G\alpha_{q/11}$ by the 2AR was decreased by co-expression of mGluR2 (Fig. 2e and Supplementary Table 6). The activation of $G\alpha_i$ by the 2AR was markedly enhanced by mGluR2 co-expression (Fig. 2e and Supplementary Table 7). The mGluR2-dependent effects on both $G\alpha_{q/11}$ and $G\alpha_i$ regulation by the 2AR were reversed in the presence of mGluR2 agonist (Fig. 2e and Supplementary Tables 6 and 7). Consonant with the results from co-immunoprecipitation, allosteric modulation and FRET, the functional assays of G-protein activity also show that the TM4–5 segment of the mGluR2, when substituted into the mGluR3, was sufficient for signalling cross-talk to occur (Fig. 2e). These data support the presence of functional and physiological 2AR–mGluR2 complexes that integrate serotonin and glutamate neurotransmission to specify the pattern of G-protein regulation.

Similar evidence for specification of G-protein subtype regulation was also observed for the endogenous brain 2AR–mGluR2 complex

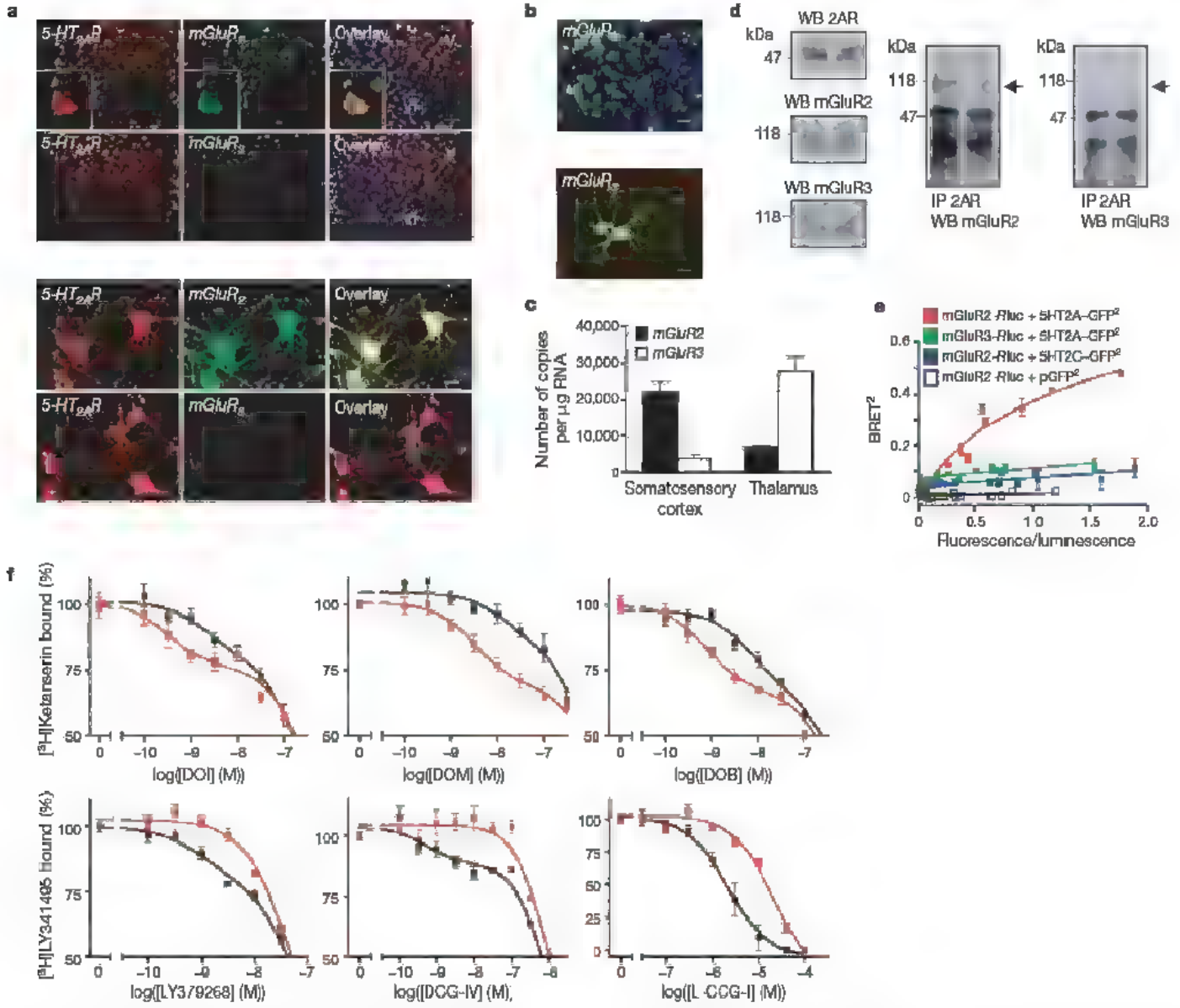

Figure 1 | 2AR and mGluR2 co-localize and interact. **a**, *2AR* and *mGluR2*, but not *mGluR3*, are co-expressed in cortical neurons. Top, mouse somatosensory cortex; bottom, mouse cortical primary culture. Scale bars, 50 µm (top) and 10 µm (bottom). Nuclei are blue. Inset: co-expressing neuron. **b**, FISH for *mGluR3* in thalamus. Top, mouse thalamus; bottom, thalamic primary culture. Scale bars, 25 µm (top) and 10 µm (bottom). **c**, mRNA levels measured by real-time PCR (Error bars show s.e.m., $n = 6$ per group). **d**, Specific co-immunoprecipitation of 2AR and mGluR2 in duplicate human frontal cortex samples (arrows). WB, western blot; IP, immunoprecipitation. **e**, BRET2 shows specific 2AR and mGluR2 interaction in HEK-293 cells. Data are means ± s.e.m. ($n = 3$). The mGluR2/2AR curve is fitted better by a saturation curve than by a linear regression, F test ($P < 0.001$). The other co-transfection data sets show linear regressions. **f**, Top, [^{3}H]ketanserin displacement curves in mouse SCx membranes. 2AR agonist affinities were higher in the presence of the mGluR2/3 agonist LY379268 at 10 µM (red) than in vehicle alone (black). [^{3}H]LY341495 displacement curves (bottom panels). mGluR2/3 agonist affinities were lower in the presence of the 2AR agonist DOI at 10 µM (red) than in vehicle alone (black). DCG-IV, (2*S*,2′*R*,3′*R*)-2-(2′,3′-dicarboxycyclopropyl)-glycine; L-CCG-I, (2*S*,1′*S*,2′*S*)-2-(carboxycyclopropyl)-glycine.

with membranes from cortical primary cultures (Fig. 3a). The pattern of G-protein regulation in cortical pyramidal neurons has been shown to predict specific behavioural responses to 2AR agonists. Hallucinogenic drugs and non-hallucinogenic drugs activate the same population of 2ARs in cortical pyramidal neurons but differ in the 2AR-dependent pattern of G-protein regulation and gene induction that they elicit[8,9]. In brain cortical neurons, the signalling elicited by hallucinogenic and non-hallucinogenic 2AR agonists causes the induction of c-*fos* and requires $G_{q/11}$-dependent activation of phospholipase C. However, the signalling of hallucinogens such as DOI and lysergic acid diethylamide (LSD) acting at the 2AR also induces *egr-2*, which is $G_{i/o}$-dependent. Thus, c-*fos* expression results from any 2AR signalling, and *egr-2* induction is a specific marker for hallucinogen signalling through the 2AR[8,9]. The finding that mGluR2 modulates the coupling of the 2AR to G_i (Fig. 3a and Supplementary Tables 6 and 7) indicated that this complex might be important for hallucinogen signalling. The induction of c-*fos* by hallucinogenic 2AR agonists or by structurally similar non-hallucinogenic 2AR agonists *in vivo* in mouse SCx and in cortical primary cultures (Fig. 3b and Supplementary Figs 8–10) was not affected by the mGluR2/3 agonist LY379268. In contrast, the hallucinogen-specific induction of *egr-2* was selectively blocked by LY379268 in both mouse cortex *in vivo* and in primary cortical cultures (Fig. 3b and Supplementary Figs 8–10 show FISH results with LSD treatment, and real-time PCR gene assay results with DOI, DOM (1-(2,5-dimethoxy-4-methylphenyl)-2-aminopropane), DOB (1-(2,5-dimethoxy-4-bromophenyl)-2-aminopropane), LSD, lisuride hydrogen maleate and ergotamine). We also studied the effects of LY379268 on the head-twitch response behaviour, which is hallucinogen-specific[8,9]. In a similar manner to its effects on G-protein activation and gene induction, the glutamate agonist LY379268 suppressed the induction of the head-twitch response by either DOI or LSD (Supplementary Fig. 11). These results suggest that LY379268 acts at the 2AR–mGluR2 complex to reduce the hallucinogen-specific $G_{i/o}$ signalling and behaviour. To establish further the functional relevance of 2AR–mGluR2 cross-talk, we compared the responses to the mGluR2/3 antagonist LY341494 in $htr2A^{+/+}$ and $htr2A^{-/-}$ mice. The locomotor and vertical activities elicited by LY341495 were significantly attenuated in the $htr2A^{-/-}$ mice (Fig. 3c), supporting the functional relevance of the 2AR–mGluR2 complex *in vivo* and suggesting that it also influences the endogenous response to glutamate.

The findings that $G_{i/o}$ regulation, which is necessary for the effects of hallucinogens[8], is enhanced by the formation of the 2AR–mGluR2 complex and that activation of the mGluR2 component suppresses hallucinogen-specific signalling implicate this complex in the effects of hallucinogens. The neuropsychological effects of hallucinogenic drugs present commonalities with the psychosis of schizophrenia, and both conditions are accompanied by disruptions of cortical sensory processing[10,11,23–27]. We investigated whether the components of the 2AR–mGluR2 signalling complex are dysregulated in the brain cortex of subjects with schizophrenia. We determined the density of binding sites for 2AR and for mGluR2/3 in cortex from schizophrenic subjects and in controls who were matched by gender, age and post-mortem delay (Supplementary Tables 8 and 9). The receptor densities in cortical membranes from untreated schizophrenic subjects were significantly altered, showing increased 2AR levels and decreased mGluR2/3 levels (Fig. 4a, b). mRNA assays showed that expression of *mGluR2* but not *mGluR3* was decreased in cortex from schizophrenic subjects (Fig. 4e). The studies in mouse show that

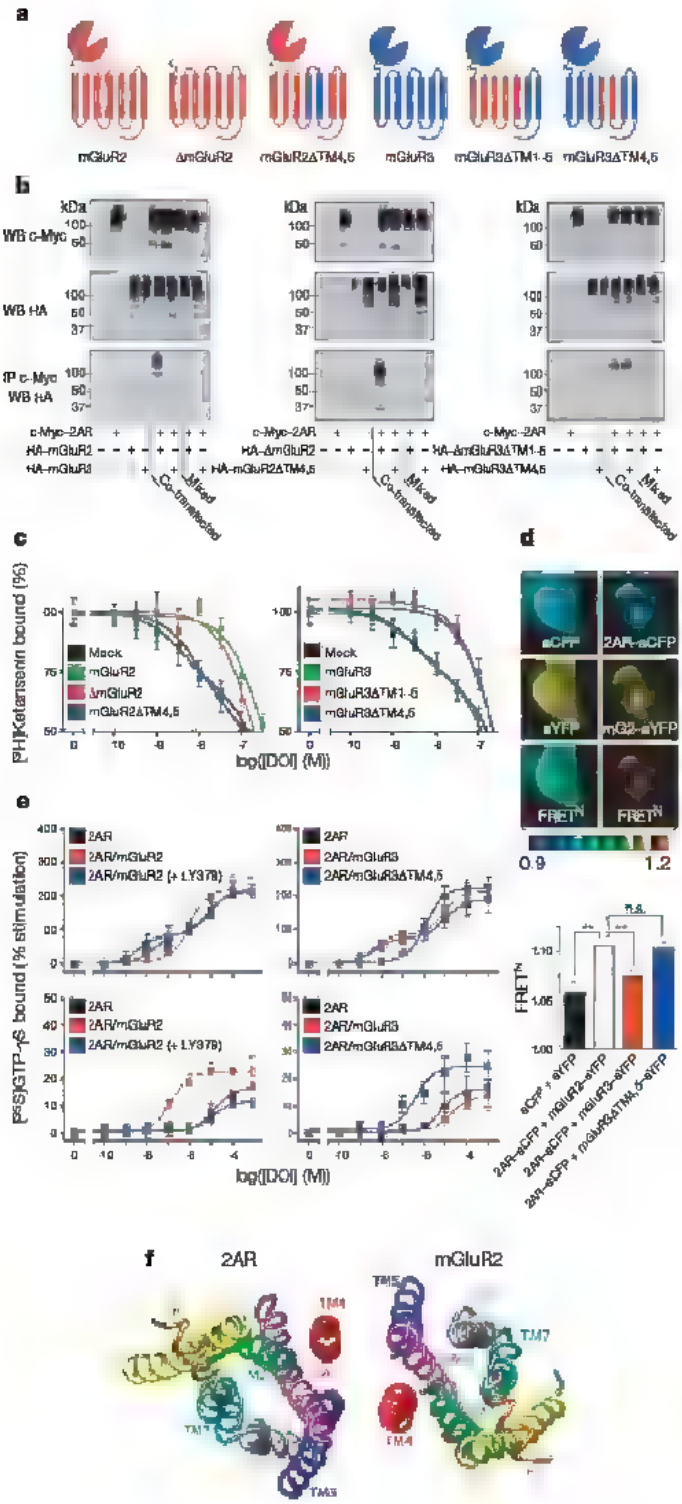

Figure 2 | mGluR2 transmembrane domains 4/5 mediate association with 2AR. **a**, mGluR2/mGluR3 chimaeras studied. **b**, c-Myc–2AR and haemagglutinin (HA)–mGluR2/mGluR3 chimaera co-immunoprecipitations. Cells separately expressing each construct were also mixed. WB, western blot; IP, immunoprecipitation. **c**, 2AR competition binding in cells stably expressing the 2AR and transfected with mGluR2/mGluR3 chimaeras. Error bars show s.e.m. ($n = 4$). **d**, FRET in cells expressing 2AR tagged with enhanced cyan fluorescent protein (eCFP) and either mGluR2, mGluR3 or mGluR3ΔTM4,5 chimaera, all tagged with enhanced yellow fluorescent protein (eYFP). Pseudocolour images represent normalized values ($FRET^N$). Numbers of samples: eCFP + eYFP, $n = 19$; 2AR–eCFP + mGluR2–eYFP, $n = 43$; 2AR–eCFP + mGluR3–eYFP, $n = 31$; 2AR–eCFP + mGluR3ΔTM4,5–eYFP, $n = 27$. Two asterisks, $P < 0.01$; analysis of variance with Dunnett's post hoc test. n.s., not significant. Error bars show s.e.m. **e**, DOI-stimulated [^{35}S]GTP-γS binding in membranes followed by immunoprecipitation with anti-$G\alpha_{q/11}$ (top) or anti-$G\alpha_{i1,2,3}$ (bottom). Cells stably expressing 2AR were transfected with mGluR2, mGluR3 or mGluR3ΔTM4,5. The potency of DOI activating $G\alpha_{i1,2,3}$ was significantly increased when the 2AR was co-expressed with either mGluR2 or mGluR3ΔTM4,5, an effect abolished by 10 μM LY379268 (LY379) ($P < 0.001$ by F test). Data are means ± s.e.m. for three experiments performed in triplicate. **f**, Ribbon backbone representation of the transmembrane helices of the 2AR–mGluR2 heteromer model, seen from the intracellular face.

activation of the mGluR2 component of the 2AR–mGluR2 complex eliminates the hallucinogen-specific component of the signalling responses to LSD-like drugs. Thus, the increased 2AR and decreased mGluR2 found in the brain in schizophrenia may predispose to a hallucinogenic pattern of signalling.

Many laboratories have attempted to determine the density of 2AR in post-mortem brain from subjects with schizophrenia, and some studies have reported decreased or unchanged 2AR densities[28]. To try to understand the basis for these discrepancies from our results, we first studied the effects of chronic antipsychotic treatment on the 2AR and mGluR2 in mouse. The chronic atypical antipsychotic clozapine specifically downregulated the level of expression of 2AR and of mGluR2 in mouse SCx (Supplementary Fig. 12). The downregulation of mGluR2 by clozapine required expression of the 2AR, because it did not occur in *htr2A*$^{-/-}$ mice (Supplementary Fig. 12) and was not induced by the chronic typical antipsychotic haloperidol (Supplementary Fig. 13). In concordance with the effects of clozapine in murine models, the density of 2AR was reduced to control levels in postmortem human brain cortex of schizophrenics treated with atypical antipsychotic drugs (Fig. 4c), and the mGluR2/3-binding sites were also downregulated (Fig. 4d). The onset of psychosis in schizophrenia usually occurs in later adolescence or early adulthood[1]. We studied the relationship of receptor densities with ageing: both [^{3}H]ketanserin and [^{3}H]LY341495 binding showed a highly significant negative correlation with age (Supplementary Fig. 14). Hallucinations and delusions typically attenuate with ageing[29], which correlates with the lower density of the components of the 2AR–mGluR2 complex that we observed in older subjects. Consequently, the marked dysregulation of both 2AR and mGluR2 expression in schizophrenia would be unlikely to be observed in samples from heterogeneous groups including treated patients[28] or in studies including older patients[28,30].

These studies identify the 2AR–mGluR2 complex as a possible site of action of hallucinogenic drugs. The glutamate and serotonin systems have both been implicated in psychotic disorders, and the components of this complex are found to be differentially regulated in cortex from individuals with schizophrenia. Our results are consistent with the hypothesis that the 2AR–mGluR2 complex integrates serotonin and glutamate signalling to regulate the sensory gating functions of the cortex, a process that is disrupted in psychosis.

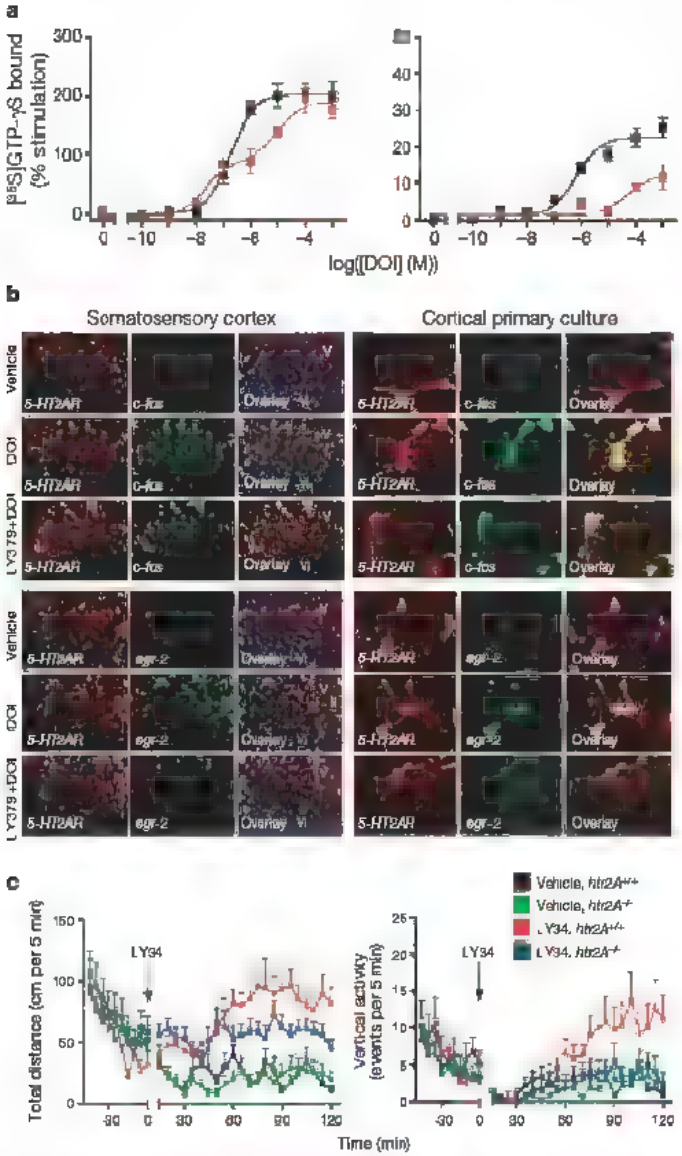

Figure 3 | 2AR–mGluR2 complex-dependent modulation of cellular and behavioural responses. **a**, DOI-stimulated [^{35}S]GTP-γS binding in primary culture membranes followed by immunoprecipitation with anti-$G\alpha_{q/11}$ antibodies (left) or anti-$G\alpha_{i1,2,3}$ antibodies (right). DOI $G\alpha_{i1,2,3}$ activation potency was significantly decreased by 10 μM LY379268 (red) compared with vehicle alone (black). Data are mean ± s.e.m. for three experiments performed in triplicate. **b**, FISH in mice injected with vehicle or 2 mg kg^{-1} DOI 15 min after injection with vehicle or 15 mg kg^{-1} LY379268 (left), and in primary cultures treated with 10 μM DOI 15 min after being pretreated with vehicle or 10 μM LY379268 (right). Nuclei are blue. Scale bars, 50 μm (left) and 10 μm (right). **c**, Distance and vertical activity induced in *htr2A*$^{+/+}$ and *htr2A*$^{-/-}$ mice by the mGluR2/3 antagonist LY341495 (LY34) at 6 mg kg^{-1}. In *htr2A*$^{-/-}$ mice, the effect of LY341495 on distance was decreased ($P < 0.05$, Bonferroni's post hoc test of two-factor analysis of variance), and its effect on vertical activity was absent ($n = 30$–32). Error bars show s.e.m.

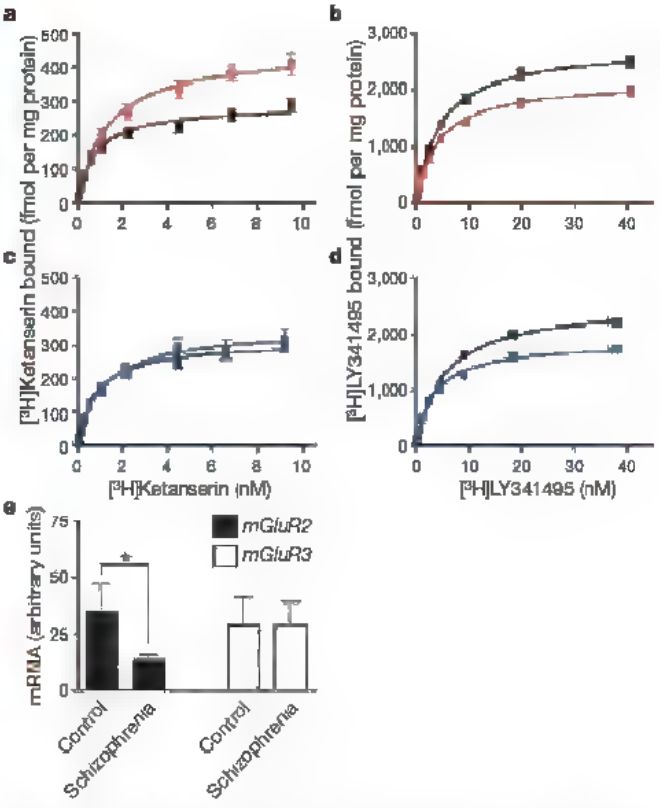

Figure 4 | 2AR is increased and mGluR2 is decreased in schizophrenia. **a**, **b**, Frontal cortex membrane receptor binding assays from untreated schizophrenic subjects (red, $n = 13$) and matched control subjects (black, $n = 13$). In schizophrenia, [^{3}H]ketanserin binding (**a**) was higher and [^{3}H]LY341495 binding (**b**) was lower ($P < 0.05$; Student's *t*-test). Error bars show s.e.m. **c**, **d**, Receptor binding in antipsychotic-treated schizophrenic subjects (blue; $n = 12$) and matched control subjects (black; $n = 12$). In treated schizophrenia, [^{3}H]ketanserin binding (**c**) was unaffected and [^{3}H]LY341495 binding (**d**) was lower ($P < 0.05$). Error bars show s.e.m. **e**, *mGluR2* mRNA expression is decreased in untreated schizophrenic subjects ($n = 7$) compared with matched control subjects ($n = 7$, asterisk, $P < 0.05$, error bars show s.e.m.)

METHODS SUMMARY

All reagents were purchased from commercial vendors except for LY379268 (Eli Lilly and Co.). Mouse lines, treatment protocols, behavioural studies, dissections, and primary neuronal cultures, approved by Institutional Use and Care Committees, have been described previously[8,9]. Protocols used for FISH[8], binding assays[8], real-time PCR[8], FRET[17] and co-immunoprecipitation[17] were performed as described previously or with minor modifications. Epitope-tagged, BRET2, FRET and chimaera receptor constructs were generated by using standard cloning techniques and were confirmed by sequencing. BRET2 using *Renilla* luciferase and green fluorescent protein (GFP2) was performed in HEK-293 cells. Matched schizophrenia and control human brains were obtained from autopsies performed in the Basque Institute of Legal Medicine, Bilbao, Spain, in compliance with policies of research and ethical review boards for post-mortem brain studies.

Full Methods and any associated references are available in the online version of the paper at www.nature.com/nature.

Received 2 November; accepted 20 December 2007.
Published online 24 February 2008.

1. Freedman, R. Schizophrenia. *N. Engl. J. Med.* 349, 1738–1749 (2003)
2. Sawa, A. & Snyder, S. H. Schizophrenia: diverse approaches to a complex disease. *Science* 296, 692–695 (2002)
3. Lieberman, J. A. *et al.* Serotonergic basis of antipsychotic drug effects in schizophrenia. *Biol. Psychiatry* 44, 1099–1117 (1998)
4. Miyamoto, S., Duncan, G. E., Marx, C. E. & Lieberman, J. A. Treatments for schizophrenia: a critical review of pharmacology and mechanisms of action of antipsychotic drugs. *Mol. Psychiatry* 10, 79–104 (2005)
5. Aghajanian, G. K. & Marek, G. J. Serotonin model of schizophrenia: emerging role of glutamate mechanisms. *Brain Res. Brain Res. Rev.* 31, 302–312 (2000)
6. Marek, G. J. Metabotropic glutamate 2/3 receptors as drug targets. *Curr. Opin. Pharmacol.* 4, 18–22 (2004)
7. Patil, S. T. *et al.* Activation of mGlu2/3 receptors as a new approach to treat schizophrenia: a randomized Phase 2 clinical trial. *Nature Med.* 13, 1102–1107 (2007)
8. Gonzalez-Maeso, J. *et al.* Hallucinogens recruit specific cortical 5-HT_{2A} receptor-mediated signaling pathways to affect behavior. *Neuron* 53, 439–452 (2007)
9. Gonzalez-Maeso, J. *et al.* Transcriptome fingerprints distinguish hallucinogenic and nonhallucinogenic 5-hydroxytryptamine 2A receptor agonist effects in mouse somatosensory cortex. *J. Neurosci.* 23, 8836–8843 (2003)
10. Vollenweider, F. X., Vollenweider-Scherpenhuyzen, M. F., Babler, A., Vogel, H. & Hell, D. Psilocybin induces schizophrenia-like psychosis in humans via a serotonin-2 agonist action. *Neuroreport* 9, 3897–3902 (1998).
11. Gouzoulis-Mayfrank, E. *et al.* Psychological effects of (*S*)-ketamine and *N,N*-dimethyltryptamine (DMT): a double-blind, cross-over study in healthy volunteers. *Pharmacopsychiatry* 38, 301–311 (2005).
12. Colpaert, F. C. Discovering risperidone: the LSD model of psychopathology. *Nature Rev. Drug Discov.* 2, 315–320 (2003).
13. Marek, G. J., Wright, R. A., Schoepp, D. D., Monn, J. A. & Aghajanian, G. K. Physiological antagonism between 5-hydroxytryptamine$_{2A}$ and group II metabotropic glutamate receptors in prefrontal cortex. *J. Pharmacol. Exp. Ther.* 292, 76–87 (2000)
14. Weisstaub, N. V. *et al.* Cortical 5-HT2A receptor signaling modulates anxiety-like behaviors in mice. *Science* 313, 536–540 (2006)
15. Benneyworth, M. A. *et al.* A selective positive allosteric modulator of metabotropic glutamate receptor subtype 2 blocks a hallucinogenic drug model of psychosis. *Mol. Pharmacol.* 72, 477–484 (2007)
16. Angers, S., Salahpour, A. & Bouvier, M. Dimerization: an emerging concept for G protein-coupled receptor ontogeny and function. *Annu. Rev. Pharmacol. Toxicol.* 42, 409–435 (2002).
17. Lopez-Gimenez, J. F., Canals, M., Pediani, J. D. & Milligan, G. The α1b-adrenoceptor exists as a higher-order oligomer: effective oligomerization is required for receptor maturation, surface delivery, and function. *Mol. Pharmacol.* 71, 1015–1029 (2007)
18. Wright, R. A., Arnold, M. B., Wheeler, W. J., Ornstein, P. L. & Schoepp, D. D. [^{3}H]LY341495 binding to group II metabotropic glutamate receptors in rat brain. *J. Pharmacol. Exp. Ther.* 298, 453–460 (2001)
19. Palczewski, K. *et al.* Crystal structure of rhodopsin: A G protein-coupled receptor. *Science* 289, 739–745 (2000).
20. Fotiadis, D. *et al.* Atomic-force microscopy: Rhodopsin dimers in native disc membranes. *Nature* 421, 127–128 (2003).
21. Kenakin, T. Efficacy at G-protein-coupled receptors. *Nature Rev. Drug Discov.* 1, 103–110 (2002)
22. Gonzalez-Maeso, J., Rodriguez-Puertas, R. & Meana, J. J. Quantitative stoichiometry of G-proteins activated by μ-opioid receptors in postmortem human brain. *Eur. J. Pharmacol.* 452, 21–33 (2002)
23. Carlsson, A. The neurochemical circuitry of schizophrenia. *Pharmacopsychiatry* 39 (Suppl. 1), S10–S14 (2006).
24. Vollenweider, F. X. & Geyer, M. A. A systems model of altered consciousness: integrating natural and drug-induced psychoses. *Brain Res. Bull.* 56, 495–507 (2001)
25. Vollenweider, F. X. *et al.* Positron emission tomography and fluorodeoxyglucose studies of metabolic hyperfrontality and psychopathology in the psilocybin model of psychosis. *Neuropsychopharmacology* 16, 357–372 (1997)
26. Umbricht, D. *et al.* Effects of the 5-HT_{2A} agonist psilocybin on mismatch negativity generation and AX-continuous performance task: implications for the neuropharmacology of cognitive deficits in schizophrenia? *Neuropsychopharmacology* 28, 170–181 (2003)
27. Gouzoulis-Mayfrank, E. *et al.* Inhibition of return in the human 5HT_{2A} agonist and NMDA antagonist model of psychosis. *Neuropsychopharmacology* 31, 431–441 (2006).
28. Dean, B. The cortical serotonin$_{2A}$ receptor and the pathology of schizophrenia: a likely accomplice. *J. Neurochem.* 85, 1–13 (2003).
29. Davidson, M. *et al.* Severity of symptoms in chronically institutionalized geriatric schizophrenic patients. *Am. J. Psychiatry* 152, 197–207 (1995).
30. Gurevich, E. V. & Joyce, J. N. Alterations in the cortical serotonergic system in schizophrenia: a postmortem study. *Biol. Psychiatry* 42, 529–545 (1997).

Supplementary Information is linked to the online version of the paper at www.nature.com/nature.

Acknowledgements We thank L. Devi and L. Ivic for critiquing the manuscript; S. Morgello and the Manhattan HIV Brain Bank for providing control brain cortex; I. Rodil, J. Urigüen and B. Lin for assistance with biochemical assays; the Mount Sinai Microscopy and Microarray, Real-Time PCR and Bioinformatics Shared Research Facilities, the staff members of the Basque Institute of Legal Medicine for their cooperation in the study; J. H. Prather for a gift of LY379268, and J.-P. Pin for providing the signalling peptide sequence of rat mGluR5. This study was supported by the National Institutes of Health, UPV/EHU and the Basque Government, the Spanish Ministry of Health, the REM-TAP Network, the Whitehall Foundation, the Gatsby Foundation and the American Foundation for Suicide Prevention.

Author Contributions J.G.M. and S.C.S. designed experiments, supervised research and wrote the manuscript. J.G.M. performed experiments. R.L.A. performed BRET experiments. T.Y. designed and cloned receptor chimaeras. Y.O. assisted with experiments. P.C. performed FISH studies. N.V.W. and M.Z., supervised by J.A.G., performed behaviour experiments and developed mutant mouse lines. J.L.G., supervised by G.M., performed FRET experiments. M.F. performed computer modelling. L.F.C. and J.J.M. performed schizophrenia post-mortem human brain studies. All authors discussed the results and commented on the manuscript.

Author Information Reprints and permissions information is available at www.nature.com/reprints. Correspondence and requests for materials should be addressed to J.G.M. (javier.maeso@mssm.edu) or S.C.S. (stuart.sealfon@mssm.edu).

LETTERS

Hax1-mediated processing of HtrA2 by Parl allows survival of lymphocytes and neurons

Jyh-Rong Chao[1], Evan Parganas[1], Kelli Boyd[2], Cheol Yi Hong[1], Joseph T. Opferman[1] & James N. Ihle[1]

Cytokines affect a variety of cellular functions, including regulation of cell numbers by suppression of programmed cell death[1]. Suppression of apoptosis requires receptor signalling through the activation of Janus kinases and the subsequent regulation of members of the B-cell lymphoma 2 (Bcl-2) family. Here we demonstrate that a Bcl-2-family-related protein, Hax1, is required to suppress apoptosis in lymphocytes and neurons. Suppression requires the interaction of Hax1 with the mitochondrial proteases Parl (presenilin-associated, rhomboid-like) and HtrA2 (high-temperature-regulated A2, also known as Omi). These interactions allow Hax1 to present HtrA2 to Parl, and thereby facilitates the processing of HtrA2 to the active protease localized in the mitochondrial intermembrane space. In mouse lymphocytes, the presence of processed HtrA2 prevents the accumulation of mitochondrial-outer-membrane-associated activated Bax, an event that initiates apoptosis. Together, the results identify a previously unknown sequence of interactions involving a Bcl-2-family-related protein and mitochondrial proteases in the ability to resist the induction of apoptosis when cytokines are limiting.

In a screen for genes that suppress apoptosis of Janus kinase 2 (*Jak2*)-null fetal liver cells, we identified *Hax1* full-length clones. Expression of *Hax1* rescued both erythroid-lineage-committed progenitors and, to a lesser extent, earlier multi-lineage progenitors (Supplementary Table 1). Hax1 was initially identified by its association with HS1 (also known as Hcls1), a Src kinase substrate[2]. It has anti-apoptotic activity and some structural similarities to Bcl-2 family members, including the presence of BH1- and BH2-like domains and a carboxyl transmembrane domain[3]. Like Bcl-2 family members, *Hax1* expression is induced by cytokines (Supplementary Fig. 1a, b) and the protein is mitochondrial[3]. In mitochondria, it is localized on the inner and outer mitochondrial membranes and exposed to the intermembrane space (unpublished data). Lastly, human mutations of Hax1 cause increased neutrophil apoptosis, resulting in autosomal recessive severe neutropenia[4] and in some cases has been suggested to be the basis for neurological impairments[5,6].

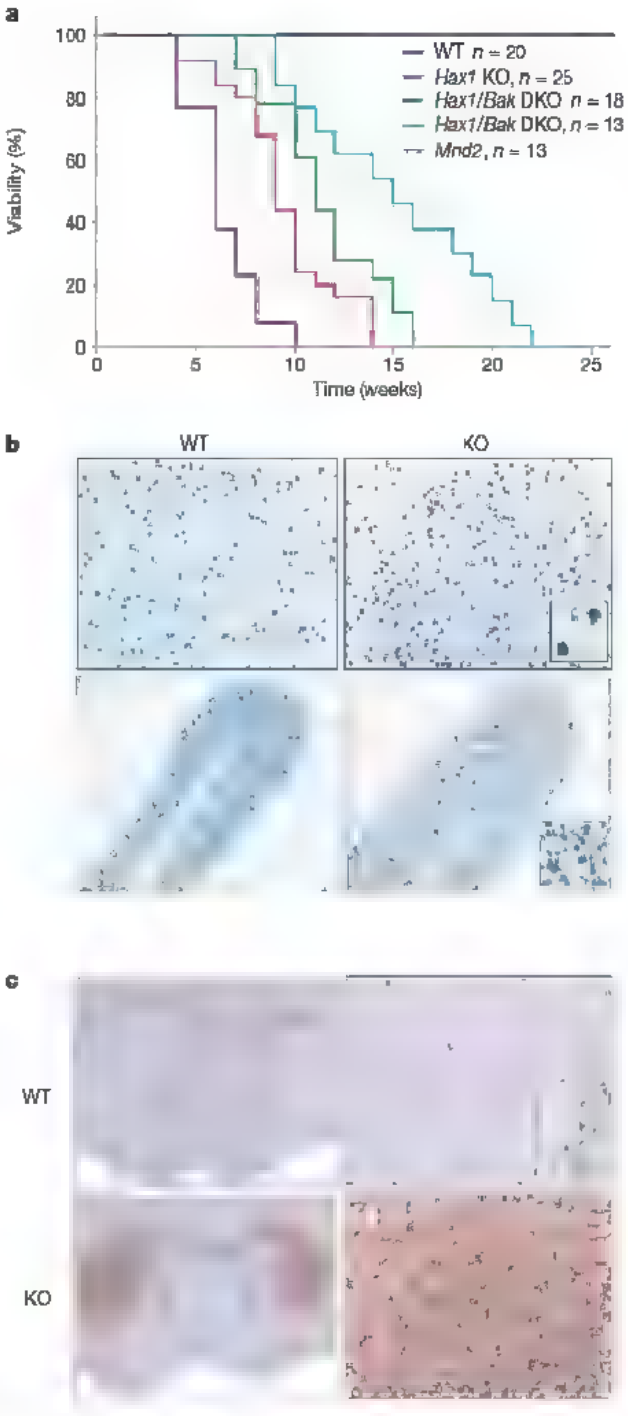

Figure 1 | Loss of *Hax1* results in postnatal lethality and neuronal apoptosis. **a**, Survival curves of wild-type (WT), *Hax1*-knockout (KO), *Mnd2*, and *Hax1/Bax* and *Hax1/Bak* double-knockout (DKO) mice. At least 13 mice per genotype were observed. The viability curves for *Hax1*-null versus *Hax1/Bax*-null are significantly different ($P < 0.0004$), as are those for *Mnd2* and *Hax1*-null ($P < 0.007$). **b**, Terminal deoxynucleotidyltransferase-mediated dUTP nick end labelling (TUNEL) staining was performed on ventral sections of brain including the striatum (top panels) and the cerebellum (lower panels). TUNEL-positive striatal neurons were brown in colour. Arrows indicate TUNEL-positive neurons. **c**, Immunohistochemical staining for GFAP as a marker of astrocyte infiltration on brain sections of wild-type (WT, top panels) or *Hax1*-null (KO) mice. Right panels illustrate a higher magnification relative to the left panels.

[1]Department of Biochemistry, [2]Animal Resources Center, St Jude Children's Research Hospital, Memphis, Tennessee 38105, USA.

To assess the functions of *Hax1*, null mice were produced by gene targeting (Supplementary Fig. 2). Heterozygous mice were viable and fertile whereas homozygous-null mice, although born at expected frequencies, failed to survive longer than 14 weeks (Fig. 1a). Lethality was caused by loss of motor coordination and activity, ultimately leading to failure to eat or drink. Histological analysis identified extensive apoptosis of neurons in the striatum and the cerebellum (Fig. 1b). Consistent with neuronal loss, staining for glial fibrillary acidic protein (GFAP) identified extensive infiltration of astrocytes in the striatum (Fig. 1c). A comparable phenotype was seen in *Hax1*/*Rag2*-null mice, ruling out a role for the immune system in neuronal apoptosis (data not shown).

Deletion of *Hax1* also resulted in the loss of lymphocytes with age in spleen, bone marrow and thymus (Fig. 2a). Loss of cellularity was associated with increased annexin-V-stained apoptotic cells (data not shown). In the thymus, both double- and single-positive populations were lost comparably (Supplementary Fig. 3a). In bone marrow there was a preferential loss of pro-B cell and pre-B cell populations (Supplementary Fig. 3b) and an associated increase in apoptotic cells (data not shown). In cultures of T or B cells there were no detectable differences between wild-type and *Hax1*-null cells in the presence of cytokines (interleukin (IL)-2 or IL-7, data not shown). However, with cytokine withdrawal, *Hax1*-null T and B cells lost viability more rapidly (Fig. 2b). Loss of viability of T cells could be rescued by retroviral introduction of *Hax1* (Supplementary Fig. 3c). The results demonstrate that *Hax1* extends the window of survival after cytokine withdrawal by approximately 8 h.

Hax1-null mice appeared phenotypically similar to mice with a mutation of the mitochondrial protease HtrA2 that inactivates protease activity (*Mnd2*, motor neurodegeneration 2) or to mice in which the gene was deleted by homologous recombination[7,8]. In a direct comparison with *Mnd2* mice, we found both the neuropathology (data not shown) and the loss of lymphocytes were identical, although more severe in *Mnd2* mice (Fig. 2a, b). Consistent with a potential functional relationship, *Hax1* was identified in a yeast two-hybrid screen for HtrA2-interacting proteins[9]. We confirmed this interaction and identified a carboxyl-terminal region, termed the Hax1 homology domain (HD1), as being essential for association (summarized in Fig. 3a; data shown in Supplementary Fig. 4a, b).

The Hax1–HtrA2 association could have several consequences. HtrA2 is synthesized as an inactive precursor containing a 133-amino-acid mitochondrial-targeting sequence (MTS). After mitochondrial import, the MTS is cleaved, releasing the active protease into the intermembrane space. Finally, protease activity is regulated by engagement of a C-terminal PDZ domain[10]. Because Hax1 only weakly interacts with the processed protease and not with the PDZ domain (summarized in Fig. 3b; data shown in Supplementary Fig. 4a, b), regulation of protease activity is unlikely. To explore import and processing, a protease inactive mutant (Ser 306A) protein was expressed with or without Hax1 (Fig. 3c). Only unprocessed HtrA2 was present in the cytosolic fraction and it was unaffected by Hax1 co-expression. In contrast, mitochondria contain both unprocessed and processed HtrA2, and co-expression of Hax1 markedly increased the amount of processed protease. Processing required the normal site, because a cleavage site mutant (LA133RR) was not processed. As summarized in Fig. 3a, processing required the HD1 domain as well as the HD2 domain. Together, the data support the conclusion that Hax1 associates with HtrA2 and facilitates its mitochondrial processing. Consistent with this, processed HtrA2 is markedly reduced in tissues from *Hax1*-null mice (Fig. 3d). Also, consistent with a position upstream of HtrA2, retroviral introduction of *Hax1* into *Mnd2*

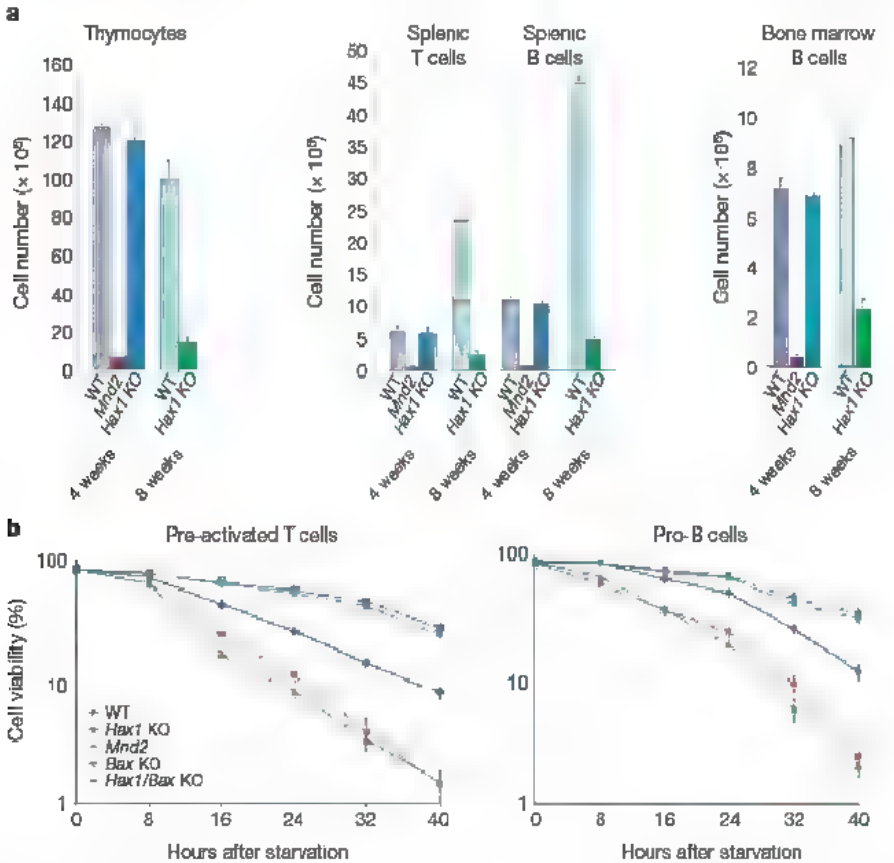

Figure 2 | *Hax1* deficiency results in loss of lymphocytes. a, The number of T or B lymphocytes from thymus (left), spleen (middle) or bone marrow (right) of mice at 4 or 8 weeks of age. Cell numbers were determined by trypan blue exclusion. The values represent standard deviation from the mean of four mice. The *Hax1*-null versus wild-type numbers at 4 weeks are not significantly different, whereas all other comparisons have probabilities of $P < 0.001$. **b**, Cell viabilities for pre-activated peripheral T cells or pro-B cells cultured in medium without IL-2 or IL-7, respectively, for 0, 8, 16, 24, 32 or 40 h. Error bars denote standard deviation of three independent experiments. The *Hax1*-null and *Mnd2* curves are not statistically different, nor are the *Bax*-null and *Bax*/*Hax1*-null curves. Others are significantly different from wild type $P < 0.001$.

mutant T cells did not rescue their loss of viability after IL-2 withdrawal (Supplementary Fig. 3c).

Recently, mice null for the mitochondrial inner membrane protease Parl were described that were also markedly similar to *Hax1*-null and *HtrA2*-mutant mice[11]. We therefore explored the possibility that Parl cooperates with Hax1 to process HtrA2. In co-expression studies, Hax1 interacts with Parl (summarized in Fig. 3c; data shown in Supplementary Fig. 4c), and this requires the HD1 and HD2 regions. Association could also be demonstrated with endogenous proteins (Fig. 3f). In contrast, no association between Parl and HtrA2 was demonstrable. This suggested that HtrA2 may be recruited to a Hax1–Parl complex for processing. Consistent with this, co-expression of HtrA2 with increasing concentrations of Parl resulted in progressively processed HtrA2 (Fig. 3e). This increase was not seen with a Parl protease inactive mutant (S277G). The amount of processed HtrA in *Parl*-deficient fibroblasts was reduced, comparable to that seen in *Hax1*-null fibroblasts (Fig. 3e).

The results support a model in which Hax1 associates with Parl on the inner mitochondrial membrane. When imported, unprocessed HtrA2 associates with the Hax1–Parl complex and, thereby, HtrA2 is 'presented' to Parl for processing. Once processed, the mature enzyme is released into the intermembrane space and provides protection from apoptosis.

Previous studies have focused on the pro-apoptotic functions of HtrA2 when the relatively non-specific protease is released into the cytosol after damage to the mitochondrial membrane[12]. Genetically, however, the normal physiological function is anti-apoptotic. One possibility was that Hax1–HtrA2 function is required for normal mitochondrial membrane integrity. This was intriguing because *Parl*-deficient mitochondria release cytochrome *c* more readily, perhaps related to effects on Opa1—a protein implicated in cristae integrity[11,13]. However, analysis of various parameters, including the amount, localization and state of oligomerization of Opa1 as well as mitochondrial morphology, membrane potential and sensitivity to induction of cytochrome *c* release, failed to identify inherent mitochondrial defects in *Hax1*-deficient or *HtrA*-mutant mitochondria (unpublished data).

The specific requirement for Hax1–HtrA2 after cytokine withdrawal suggested a role for pro-apoptotic Bcl-2 family proteins[14]. This was genetically assessed with gene-deficient mice. Deficiencies of *Bax*, *Bak* (also known as *Bak1*) (Fig. 1a) or *Bim* (also known as *Bcl2l11*) did not eliminate the neurodegenerative phenotype or neuronal apoptosis (data not shown). This was unexpected because *Bax* has been proposed to be a critical mediator of neuronal cell death after neuron tropic factor withdrawal[15–17]. However, absence of *Bax* or *Bim*, but not *Bak*, rescued the loss of lymphocytes (Supplementary Fig. 5). Consistent with this, T or B cells from *Hax1*/*Bax*-deficient (Fig. 2b) or *Hax1*/*Bim*-deficient (data not shown) mice were as resistant to cytokine withdrawal as *Bax*- or *Bim*-deficient lymphocytes.

Mitochondrial outer membrane permeabilization and apoptosis after cytokine withdrawal requires activation of Bax and/or Bak[18,19].

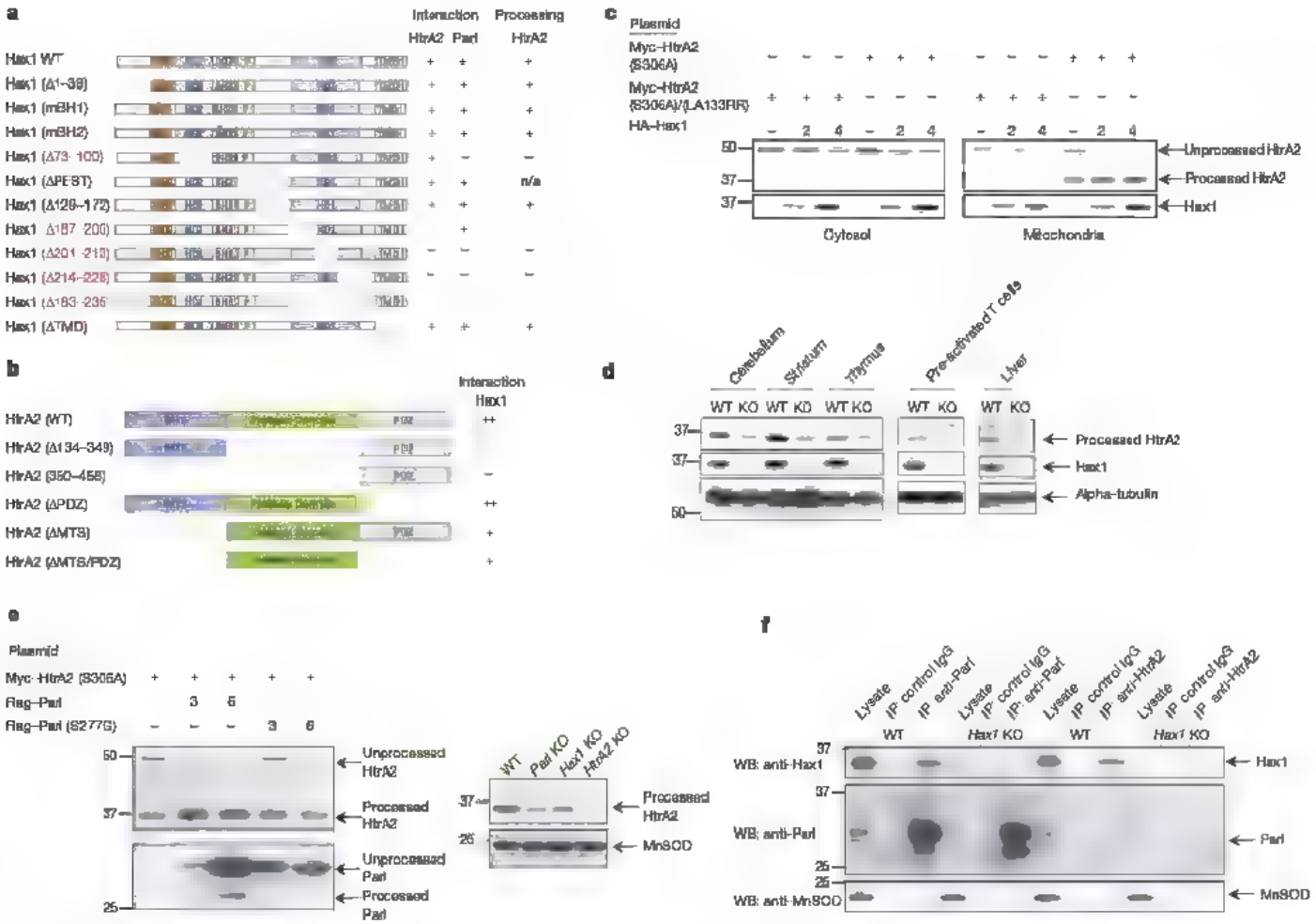

Figure 3 | Hax1 is required for Parl-mediated processing of HtrA2. **a**, Schematic of *Hax1* deletion mutants and ability to bind HtrA2, to enhance processing of HtrA2 or bind Parl. BH1 and BH2, Bcl-2 protein homology domains; HD1 and HD2, Hax1 domains conserved among species; P, PEST sequence; TMD, transmembrane-like domain. The box on the right indicates whether interactions or HtrA2 processing are observed with the various mutants. m, mutation; Δ, deletion. **b**, Schematic of *HtrA2*-deletion mutants and ability to bind Hax1. MTS, mitochondrial targeting sequence. For **a** and **b**, the data are illustrated in Supplementary Fig. 4. **c**, Immunoblots of lysates from cytosolic and mitochondrial fractions of transiently transfected COS-7 cells. **d**, Immunoblot of the indicated tissues from wild-type (WT) and *Hax1*-null (KO) mice at 3 weeks of age. **e**, Transient transfectants of COS-7 cells and MEFs established from wild type, *Parl*-null, *Hax1*-null or *HtrA2*-null mice with which association of endogenous proteins was examined. **f**, Mitochondrial lysates of wild-type or *Hax1*-null livers.

Activation of Bax is downstream of Bim activation, which occurs as a consequence of loss of anti-apoptotic partners and/or receptor-induced phosphorylation promoting turnover[20–23]. We therefore examined the consequences of *Hax1* deficiency or *HtrA2* mutation on these events. Neither mutation affected Bim accumulation or total Bax. Nor did the mutations affect the expression patterns of anti-apoptotic proteins Bcl-2, Bcl-x or Mcl-1 (Supplementary Fig. 6). However, both mutations greatly affected the rate of appearance of a conformation of Bax that is uniquely associated with the mitochondrial outer membrane and is responsible for mitochondrial-outer-membrane permeabilization[24,25]. Increases in activated Bax occurred at least 8 h sooner than in wild-type cells and correlated directly with loss of viability (data provided in Supplementary Fig. 6).

Our results provide mechanistic insights into one component of the events that determine how long lymphocytes can survive after cytokine withdrawal. In particular, withdrawal of cytokines reduces the levels of anti-apoptotic proteins including Hax1 (Fig. 4b). With loss of Hax1, the production of the processed HtrA2 is reduced (Fig. 4b). Conversely, the loss of other anti-apoptotic proteins and the accumulation of Bim contribute to the generation of activated Bax. Ultimately, it is the loss of HtrA2 activity that contributes to the accumulation of sufficient amounts of activated Bax to induce cytochrome *c* release and cell death. Although we have focused on lymphocytes, Hax1 also contributes to suppression of apoptosis of neutrophils deprived of G-CSF (Supplementary Fig. 7) and may function generally in protecting haematopoietic cells from cytokine withdrawal.

Several challenging questions are raised by the results. For example, although activated Bax may be the target in lymphocytes, genetically, any role in the neuronal apoptosis is not evident. Therefore, it will be important to identify pathways and potential mediators of apoptosis in neurons that are suppressed by Hax1–HtrA2 in both normal development and in conditions associated with Parkinson's disease[26]. Also it will be important to determine how HtrA2 suppresses the appearance of activated Bax. Activated Bax may be a substrate of HtrA2, however it is equally possible that Bax-associated proteins are substrates. The results raise the possibility that other mitochondrial proteases may be important in regulating programmed cell death.

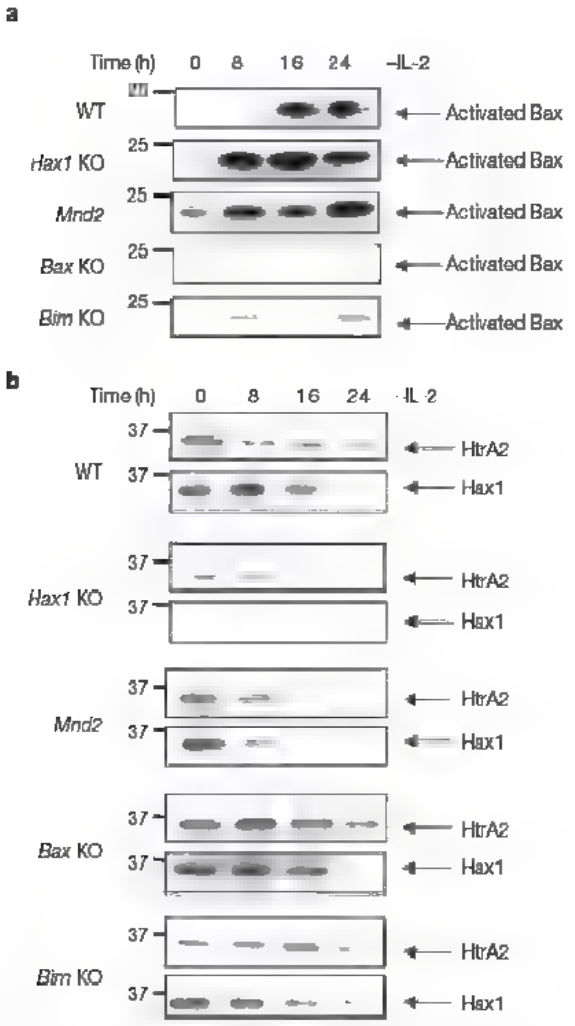

Figure 4 | HtrA2 has a role in controlling accumulation of activated Bax in peripheral lymphocytes. Pre-activated T cells from wild-type, *Hax1*-null, *Bax*-null, *Mnd2* or *Bim*-null mice were cultured in media without IL-2 for 0, 8, 16 or 24 h. Lysates were immunoblotted with the indicated antibodies **a**, Activated Bax was detected by lysing cells in 1% CHAPS lysis buffer (1% CHAPS, 20 mM Tris-Cl, pH 7.4, 137 mM NaCl, 10% glycerol and 1 mM EDTA), immunoprecipitation with mouse monoclonal anti-Bax antibody (6A7) and immunoblotting with rabbit polyclonal anti-Bax antibody **b**, Immunoblots for detection of HtrA2 or Hax-1. Loading controls (β-actin) and the results examining Bim, total Bax, Mcl-1, Bcl-x, Bcl-2 and Parl, as well as the percentage of viable T cells are presented in Supplementary Fig. 6.

METHODS SUMMARY

Immunoprecipitations, immunoblots and northern blots used standard techniques as described previously[27]. Expression constructs generally used pCDNA3 (Invitrogen), and deletion mutants were made by PCR-based, site-directed mutation and confirmed by DNA sequencing. Transfections used FuGENE6 (Roche) or standard calcium-phosphate methods. Pre-activated T cells were obtained by culture of splenocytes with anti-CD3ε monoclonal antibody, followed by culture in human IL-2 (200 U ml^{-1}) for 7 days. Pro-B cells were obtained by culturing bone marrow cells in stem cell factor (50 ng ml^{-1}) and IL-7 (10 ng ml^{-1}) for 14 days.

Full Methods and any associated references are available in the online version of the paper at www.nature.com/nature.

Received 24 October; accepted 21 December 2007.
Published online 20 February 2008.

1. Ihle, J. N. Cytokine receptor signalling. *Nature* 377, 591–594 (1995).
2. Suzuki, Y. *et al.* HAX-1, a novel intracellular protein, localized on mitochondria, directly associates with HS1, a substrate of Src family tyrosine kinases. *J. Immunol.* 158, 2736–2744 (1997).
3. Sharp, T. V. *et al.* K15 protein of Kaposi's sarcoma-associated herpesvirus is latently expressed and binds to HAX-1, a protein with antiapoptotic function. *J. Virol.* 76, 802–816 (2002).
4. Klein, C. *et al.* HAX1 deficiency causes autosomal recessive severe congenital neutropenia (Kostmann disease). *Nature Genet.* 39, 86–92 (2007).
5. Matsubara, K. *et al.* Severe developmental delay and epilepsy in a Japanese patient with severe congenital neutropenia due to HAX1 deficiency. *Haematologica* 92, e123–e125 (2007).
6. Carlsson, G. & Fasth, A. Infantile genetic agranulocytosis, morbus Kostmann: Presentation of six cases from the original 'Kostmann family' and a review. *Acta Paediatr.* 90, 757–764 (2001).
7. Jones, J. M. *et al.* Loss of Omi mitochondrial protease activity causes the neuromuscular disorder of *Mnd2* mutant mice. *Nature* 425, 721–727 (2003).
8. Martins, L. M. *et al.* Neuroprotective role of the Reaper-related serine protease HtrA2/Omi revealed by targeted deletion in mice. *Mol. Cell. Biol.* 24, 9848–9862 (2004).
9. Cilenti, L. *et al.* Regulation of HAX-1 anti-apoptotic protein by Omi/HtrA2 protease during cell death. *J. Biol. Chem.* 279, 50295–50301 (2004).
10. Li, W. *et al.* Structural insights into the pro-apoptotic function of mitochondrial serine protease HtrA2/Omi. *Nature Struct. Biol.* 9, 436–441 (2002).
11. Cipolat, S. *et al.* Mitochondrial rhomboid PARL regulates cytochrome c release during apoptosis via OPA1-dependent cristae remodeling. *Cell* 126, 163–175 (2006).
12. Vaux, D. L. & Silke, J. HtrA2/Omi, a sheep in wolf's clothing. *Cell* 115, 251–253 (2003).
13. Frezza, C. *et al.* OPA1 controls apoptotic cristae remodeling independently from mitochondrial fusion. *Cell* 126, 177–189 (2006).
14. Letai, A. Growth factor withdrawal and apoptosis: the middle game. *Mol. Cell* 21, 728–730 (2006).
15. Deckwerth, T. L. *et al.* BAX is required for neuronal death after trophic factor deprivation and during development. *Neuron* 17, 401–411 (1996).
16. Deckwerth, T. L., Easton, R. M., Knudson, C. M., Korsmeyer, S. J. & Johnson, E. M. Jr Placement of the BCL2 family member BAX in the death pathway of sympathetic neurons activated by trophic factor deprivation. *Exp. Neurol.* 152, 150–162 (1998).

17 White, F. A., Keller-Peck, C. R., Knudson, C. M., Korsmeyer, S. J. & Snider, W. D. Widespread elimination of naturally occurring neuronal death in Bax-deficient mice. *J. Neurosci.* 18, 1428–1439 (1998)
18. Lindsten, T. *et al.* The combined functions of proapoptotic Bcl-2 family members bak and bax are essential for normal development of multiple tissues. *Mol. Cell* 6, 1389–1399 (2000)
19. Wei, M. C. *et al.* tBID, a membrane-targeted death ligand, oligomerizes BAK to release cytochrome c. *Genes Dev.* 14, 2060–2071 (2000)
20. Harada, H., Quearry, B., Ruiz-Vela, A. & Korsmeyer, S. J. Survival factor-induced extracellular signal-regulated kinase phosphorylates BIM, inhibiting its association with BAX and proapoptotic activity. *Proc. Natl Acad. Sci. USA* 101, 15313–15317 (2004)
21. Ley, R. *et al.* Extracellular signal-regulated kinases 1/2 are serum-stimulated "Bim(EL) kinases" that bind to the BH3-only protein Bim(EL) causing its phosphorylation and turnover. *J. Biol. Chem.* 279, 8837–8847 (2004).
22. Luciano, F. *et al.* Phosphorylation of Bim-EL by Erk1/2 on serine 69 promotes its degradation via the proteasome pathway and regulates its proapoptotic function. *Oncogene* 22, 6785–6793 (2003)
23. Seward, R. J., von Haller, P. D., Aebersold, R. & Huber, B. T. Phosphorylation of the pro-apoptotic protein Bim in lymphocytes is associated with protection from apoptosis. *Mol. Immunol.* 39, 983–993 (2003)
24. Nechushtan, A., Smith, C. L., Hsu, Y. T. & Youle, R. J. Conformation of the Bax C-terminus regulates subcellular location and cell death. *EMBO J.* 18, 2330–2341 (1999)
25. Wolter, K. G. *et al.* Movement of Bax from the cytosol to mitochondria during apoptosis. *J. Cell Biol.* 139, 1281–1292 (1997)
26. Plun-Favreau, H. *et al.* The mitochondrial protease HtrA2 is regulated by Parkinson's disease-associated kinase PINK1. *Nature Cell Biol.* 9, 1243–1252 (2007)
27. Parganas, E. *et al.* Jak2 is essential for signaling through a variety of cytokine receptors. *Cell* 93, 385–395 (1998)

Supplementary Information is linked to the online version of the paper at www.nature.com/nature.

Acknowledgements This work was supported by grants from the National Institutes of Health to J.N.I. and the American Lebanese and Syrian Associated Charities (ALSAC) of SJCRH (St Jude Children's Research Hospital). We thank B. De Strooper for providing reagents and information regarding the properties of the *Parl*-null mice and L. Pellegrini for antisera against Parl. J.T.O. is a Pew Scholar in the Biomedical Sciences.

Author Contributions J.-R.C. planned the project, performed experimental work and helped to prepare the manuscript. E.P. and C.Y.H. performed experimental work. K.B. performed the animal histology. J.T.O. and J.N.I. planned and directed the project, analysed data and wrote the manuscript.

Author Information Reprints and permissions information is available at www.nature.com/reprints. Correspondence and requests for materials should be addressed to J.N.I. (james.ihle@stjude.org)

LETTERS

The inflammasome recognizes cytosolic microbial and host DNA and triggers an innate immune response

Daniel A. Muruve[1]*, Virginie Pétrilli[3]*, Anne K. Zaiss[2], Lindsay R. White[1], Sharon A. Clark[1], P. Joel Ross[4], Robin J. Parks[4] & Jurg Tschopp[3]

The innate immune system recognizes nucleic acids during infection and tissue damage. Whereas viral RNA is detected by endosomal toll-like receptors (TLR3, TLR7, TLR8) and cytoplasmic RIG-I and MDA5, endosomal TLR9 and cytoplasmic DAI bind DNA[1], resulting in the activation of nuclear factor-κB and interferon regulatory factor transcription factors. However, viruses also trigger pro-inflammatory responses[2], which remain poorly defined. Here we show that internalized adenoviral DNA induces maturation of pro-interleukin-1β in macrophages, which is dependent on NALP3 and ASC, components of the innate cytosolic molecular complex termed the inflammasome. Correspondingly, NALP3- and ASC-deficient mice display reduced innate inflammatory responses to adenovirus particles. Inflammasome activation also occurs as a result of transfected cytosolic bacterial, viral and mammalian (host) DNA, but in this case sensing is dependent on ASC but not NALP3. The DNA-sensing pro-inflammatory pathway functions independently of TLRs and interferon regulatory factors. Thus, in addition to viral and bacterial components or danger signals in general, inflammasomes sense potentially dangerous cytoplasmic DNA, strengthening their central role in innate immunity.

CpG-rich DNA from bacteria and viruses stimulates dendritic cells and macrophages to release considerable amounts of type I interferon (IFN) by activating the DNA-sensing protein TLR9 (ref. 1). However, there is ample evidence that DNA, including host (self) DNA, can be recognized independently of TLR9 (refs 2, 3). A double-stranded (ds)DNA-binding protein designated DAI was recently identified that detects both microbial and host DNA[4]. In the absence of DAI, the type I IFN response triggered by viral DNA is severely hampered, suggesting an important role of the DAI signalling pathway in the antiviral response. In addition to type I IFN, a successful anti-viral response is also dependent on a strong pro-inflammatory component controlled by two alarm cytokines, TNF and interleukin (IL)-1β (ref. 5). Although the mechanism of the type I IFN response has been intensively investigated, little is known about the mechanism of the virus-mediated inflammatory response.

Adenoviruses are non-enveloped DNA viruses that cause respiratory and gastrointestinal disease in humans. In addition, recombinant adenovirus vectors are studied and developed for gene and oncolytic therapy[6]. Adenovirus vectors trigger the innate immune system, which results in the rapid induction of inflammatory cytokines such as IL-1β and TNF[6] and acute inflammation *in vivo*[7,8]. In contrast to most RNA viruses, the signalling pathways that mediate this effect have not been fully defined.

The NALP proteins are cytoplasmic NOD-like receptors (NLRs)[9]. The best understood is NALP3 (also called cryopyrin, NLRP3), which senses exogenous and host ligands such as bacterial peptidoglycan, ATP or uric acid[9,10]. NALP3 recruits, via the adaptor protein ASC, the inflammatory caspase-1 into a molecular complex termed the inflammasome[10]. Once activated, caspase-1 processes pro-IL-1β and pro-IL-18 to their active and secreted forms. Other NLRs that are known to form IL-1β-processing inflammasomes include NALP1 and IPAF, the latter of which directly activates caspase-1 in response to bacterial flagellin[11]. Given the limited information on the inflammatory response to DNA viruses and DNA in general, we have explored here the role of the inflammasome in this pathway.

To test whether adenovirus can activate the inflammasome, differentiated human THP-1 cells were infected with wild-type human adenovirus (serotype 5) and the processing and secretion of caspase-1 and IL-1β protein was determined (Fig. 1a). Because antiviral antibodies enhance the interaction and internalization of adenovirus with leukocytes[12], adenovirus infections were also performed in the presence of human serum. Adenovirus infection induced robust processing of the 35-kDa pro-IL-1β protein to the mature, secreted 17-kDa IL-1β cytokine within 2 h, which increased over time. Similar results were obtained after infection with serotype 3 human adenovirus (Fig. 1b). To determine whether viral replication was necessary to activate IL-1β, THP-1 cells were incubated with the non-replicating adenovirus vectors AdLacZ or AdGFP. Both adenovirus vectors efficiently activated pro-IL-1β maturation (Fig. 1c). To examine further the role of the adenovirus virion in inflammasome activation, THP-1 cells were challenged with ultraviolet/psoralen-inactivated adenovirus, adenovirus vectors lacking CAR and integrin-binding capsid domains, or a helper-dependent adenovirus vector (Fig. 1d). All of the recombinant adenovirus vectors effectively induced IL-1β processing and secretion (Fig. 1d and Supplementary Fig. 1), confirming that the adenovirus virion activates the inflammasome, independent of the transgene or viral gene expression. IL-1β secretion on adenovirus transduction was not restricted to human cells, as cytokine release from murine macrophages was almost as efficient as that triggered by lipopolysaccharide (LPS) and ATP (Fig. 1e). Moreover, infection with HSV-1, a DNA virus of the Herpesviridae family, also caused potent caspase-1 and pro-IL-1β maturation, suggesting that DNA viruses in general may activate an IL-1β-based inflammatory response (Fig. 1f).

To determine more precisely the virion component responsible for IL-1β activation, THP-1 cells were incubated with infectious empty adenovirus capsids or adenovirus DNA. An increasing titre of empty viral capsids was incapable of inducing IL-1β processing (Fig. 2a). Because empty viral capsids retain the binding and internalization properties of mature adenovirus virions[13], these results suggested that the capsid proteins or the mere internalization event are probably not responsible for inflammasome activation. To test whether

[1]Department of Medicine, [2]Biochemistry and Molecular Biology, University of Calgary, Alberta T2N 4N1, Canada. [3]Department of Biochemistry, University of Lausanne, Epalinges, Switzerland. [4]Molecular Medicine Program, Ottawa Health Research Institute, Ottawa, Ontario K1Y 4E9, Canada.
*These authors contributed equally to this work

the adenovirus DNA could activate the inflammasome, THP-1 cells were incubated with purified adenovirus DNA. Under these conditions, no IL-1β activation was observed, suggesting that the viral components leading to IL-1β secretion were not detected by surface receptors (Fig. 2b). In contrast, adenovirus DNA, but not capsid, transfected using cationic liposomes efficiently activated IL-1β processing (Fig. 2b), implying that cytoplasmic adenovirus DNA is a major activating ligand for the inflammasome.

Because helper-dependent adenovirus vectors lack all viral DNA, these results suggested that the recognition of DNA by the inflammasome may not be virus specific. Indeed, transfected DNA isolated from *Escherichia coli* also potently activated IL-1β, which was abolished on treatment with DNase (Fig. 2c and Supplementary Fig. 2a). Moreover, microbe-unrelated mammalian genomic DNA, synthetic polymerase chain reaction (PCR)-generated DNA (576 base pairs (bp)), but not double-stranded short oligonucleotides (40 bp) were activators of the inflammasome (Fig. 2c). A more detailed size–activity analysis of PCR-generated DNA revealed that a minimal length of approximately 250 bp was required for inflammasome activation (Fig. 2d and Supplementary Fig. 2). Although the highly repetitive DNA sequence poly(dA:dT) also led to the production of IL-1β (corroborating a sequence unrelated sensing system), single-stranded (ss)DNA and CpG oligonucleotides did not, although activation of interferon regulatory factor (IRF)-3 by the latter remained intact (Fig. 2e and Supplementary Fig. 3). In keeping with this, transfection of macrophages with plasmid DNA resulted in the secretion of active IL-1β (Fig. 2f), indicating that transfection experiments expressing inflammasome components must be interpreted with caution. Activation of caspase-1 and IL-1β by cytoplasmic DNA also occurred in dendritic cells (Supplementary Fig. 4). In contrast to the activation of the inflammasome by DNA, we were unable to confirm inflammasome activation after cellular challenge with total mammalian RNA, poly(I:C)[14] or infection with the RNA viruses reovirus and vesicular stomatitis virus (Supplementary Fig. 4 and data not shown).

The strong IL-1β activation induced by adenovirus and HSV-1 strongly suggested that one of the inflammasome-forming NLRs was responsible for viral recognition of internalized virions. Thus, macrophages from ASC- and NALP3-deficient mice were transduced with AdLacZ (Fig. 3a). In contrast to wild-type cells, IL-1β maturation was completely absent in ASC- and NALP3-deficient macrophages. In contrast, TLR9- or MyD88-deficient macrophages still responded to AdLacZ and DNA-mediated IL-1β processing (Fig. 3a and Supplementary Fig. 5). AdLacZ also induced IL-1β processing and secretion in IPAF-deficient macrophages, excluding a role for this inflammasome (Fig. 3a)

Notably, NALP3 was not required for the sensing of adenovirus DNA that was delivered to the cytoplasm by lipid-mediated transfection as opposed to infection or transduction. Whether the DNA was of viral, bacterial, fish, or human origin, IL-1β activation still

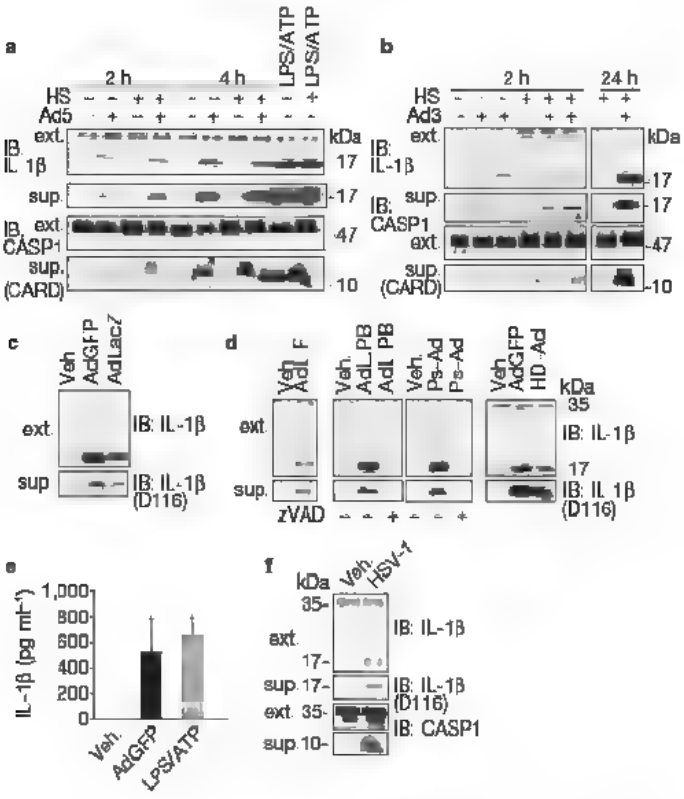

Figure 1 | Adenovirus infection activates IL-1β processing and secretion. **a**, **b**, Immunoblotting (IB) for IL-1β and caspase-1 in cell extracts (ext.) or tissue culture supernatants (sup.) from PMA-differentiated THP-1 cells infected with wild-type serotype 5 adenovirus (**a**) or wild-type serotype 3 adenovirus (**b**). Crude LPS (12.5 ng ml^{-1}) and ATP (5 mM) were used as positive controls. HS, human serum. **c**, PMA-differentiated THP-1 cells were transduced with AdLacZ, AdGFP or vehicle (veh.) for 6 h. IL-1β activation by AdGFP and AdLacZ confirms that the response is transgene independent. D116, antibody directed against mature (17 kDa) human IL-1β. **d**, IL-1β immunoblot of differentiated THP-1 cells transduced with tropism-modified (Ps-Ad, transcription-defective adenovirus vector; AdL.PB, RGD-deleted adenovirus vector, AdL.F, fibre-modified, CAR-ablated adenovirus vector) and helper-dependent adenovirus vector (HD-Ad) in human serum in the presence or absence of the pan-caspase inhibitor zVAD-fmk. **e**, IL-1β ELISA at 6 h from tissue culture supernatants of primary mouse macrophages transduced with AdGFP or stimulated with LPS and ATP (mean ± s.d.). **f**, Immunoblotting for IL-1β and caspase-1 in THP-1 cells infected with human HSV-1 at 6 h (multiplicity of infection 10:1).

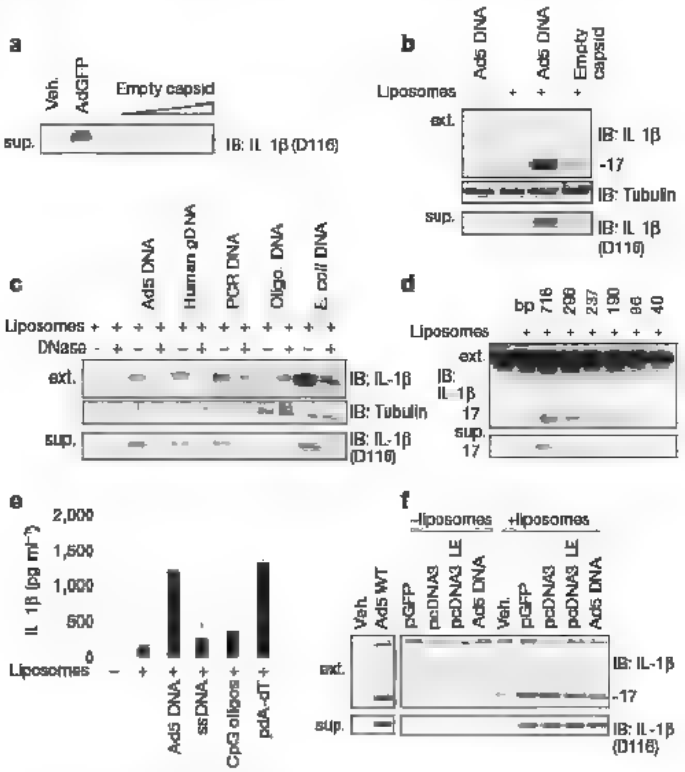

Figure 2 | Role of viral and non-viral DNA in IL-1β activation. Immunoblotting for IL-1β in cell extracts (ext.) or tissue culture supernatants (sup.). **a**, IL-1β activation in differentiated THP-1 cells challenged with an increasing concentration of empty adenovirus capsids. **b**, IL-1β activation in THP-1 cells transfected with Ad5 DNA or empty capsids at 6 h. **c**, Effect of liposome-mediated transfection of adenoviral (Ad5), human genomic (gDNA), PCR (576 bp), oligonucleotide (40 bp) and *E. coli* DNA with or without DNase treatment in THP-1 cells at 6 h. **d**, Immunoblotting for IL-1β in mouse peritoneal macrophages transfected with PCR-generated DNA of different length. **e**, ELISA for IL-1β in tissue culture supernatant of mouse peritoneal macrophages transfected with various forms of DNA (n = 3–4, mean ± s.d.). **f**, Effect of viral and plasmid DNA transfection in THP-1 cells at 6 h. The plasmid pcDNA3 LE is a low-endotoxin purified preparation.

occurred in the absence of NALP3 (Fig. 3b and Supplementary Fig. 6). However, ASC and caspase-1 were essential, suggesting that the DNA sensor is formed of an alternative inflammasome of the NALP family. We therefore tested macrophages from all other currently available NALP-deficient mice (NALP6 and NALP12, our own unpublished data) or mutant mice (C57/BL6, NALP1; ref. 15), but found no difference in their capacity to respond to cytoplasmic DNA (data not shown). Moreover, transfected DNA still triggered pro-IL-1β processing in IPAF- or TLR9-deficient macrophages as expected (Supplementary Fig. 7).

To gain some insight into the signals that couple intracellular DNA sensing with inflammasome activation, we investigated the role of cytoplasmic K^+ levels. Recently, K^+ efflux was found to be essential for the activation of NALP1 and NALP3 inflammasomes[16,17]. Blocking K^+ efflux through the addition of extracellular K^+ or glyburide, a blocker of ATP-dependent K^+ channels, resulted in the complete or partial inhibition of caspase-1 activation, independent of whether the signal was triggered by adenovirus or transfected DNA (Fig. 3c and Supplementary Fig. 8). This indicates that DNA-mediated inflammasome activation also involves this crucial change in ionic environment. The requirement for ASC but not NALP3 to recognize cytoplasmic DNA is reminiscent of inflammasome activation by the cytosolic pathogen *Francisella tularensis*[18]. Infection by *F. tularensis* results in the secretion of IFN-β; its signalling through the type I IFN receptor (IFNRI) is required for inflammasome activation and IL-1β secretion. Because cytoplasmic DNA is a strong activator of type I IFN, we explored the possibility that inflammasome activation was indirect and dependent on IFN. However, caspase-1 and IL-1β maturation induced by transfected DNA in macrophages deficient in IFNRI occurred almost as efficiently as in wild-type cells (Fig. 3d). Furthermore, IRF-3 activation triggered by transfected DNA and adenovirus remained intact in NALP3- and ASC-deficient macrophages (Fig. 3e and Supplementary Fig. 9) and after inflammasome blockade by glyburide and extracellular potassium in THP-1 cells (Fig. 3c). Together, these results confirm that DNA sensing by the inflammasome is distinct from type I IFN pathways.

The above experiments predicted that ASC and NALP3 would be important mediators of the innate immune response to the adenovirus *in vivo*, and thus experiments were performed using an established model of innate immunity to adenovirus in mice[7]. NALP3-, ASC- and caspase-1-deficient mice or their wild-type littermates were injected intraperitoneally with first-generation adenovirus vectors. Compared to wild-type mice, the intrapentoneal administration of AdGFP to $Nalp3^{-/-}$ mice resulted in a significant reduction of nuclear factor-κB-dependent inflammatory gene expression such as pro-IL-1β (*Il1b*), MIP-1β (*Mip1b*, also called *Ccl4*) or IP-10 (*IP-10*, also called *Cxcl10*) in the liver at 6 h (Fig. 4a, b). Notably, protein levels of IL-1β, IL-6 and MIP-1β were decreased (Fig. 4c, d). Similarly, in ASC- and caspase-1-deficient mice, the early

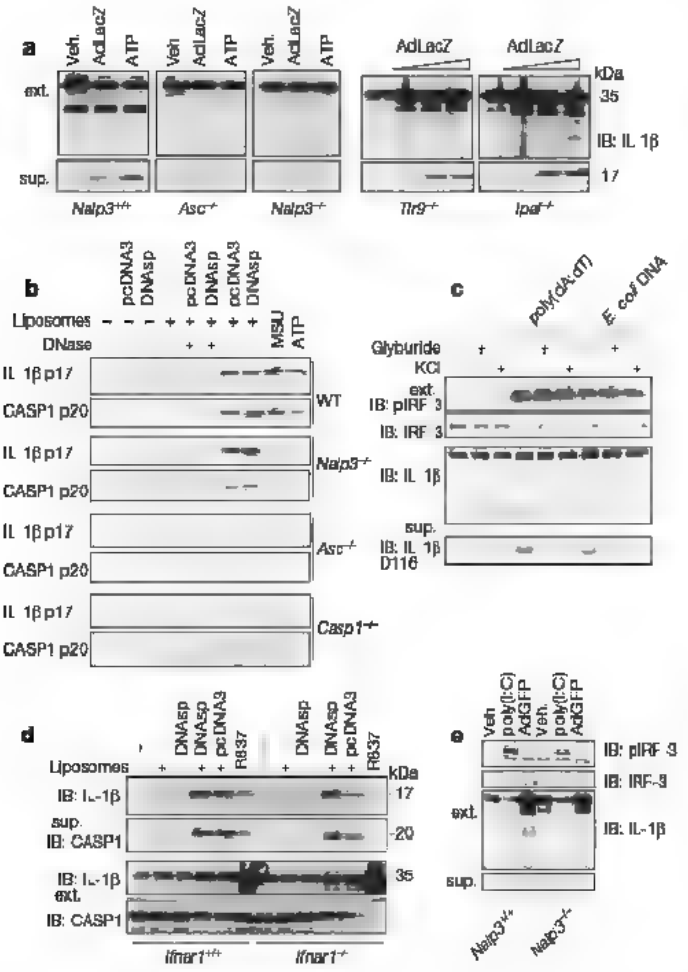

Figure 3 | Role of NALP3 and ASC in adenovirus and DNA activation of IL-1β. **a**, Immunoblotting for IL-1β in cell extracts (ext.) or supernatants (sup.) from LPS-primed murine wild type, $Nalp3^{-/-}$, $Asc^{-/-}$, $Tlr9^{-/-}$ or $Ipaf^{-/-}$ peritoneal macrophages 6 h after transduction with AdLacZ or vehicle (veh.). ATP (5 mM) served as a positive control. $Tlr9^{-/-}$ and $Ipaf^{-/-}$ macrophages were challenged with an increasing titre of AdLacZ (range 5×10^3 to 5×10^4 particles per cell) or vehicle. **b**, Effect of liposome-mediated transfection of salmon sperm or plasmid DNA (DNAsp, pcDNA3) in wild-type, $Nalp3^{-/-}$, $Asc^{-/-}$ and $Casp1^{-/-}$ macrophages with and without DNase treatment. Monosodium urate (MSU) crystals and ATP were used as controls. **c**, IL-1β and phospo-IRF3 immunoblotting in THP-1 cells transfected with poly(dA:dT) or *E. coli* DNA. Cells were pre-treated with KCl (100 mM) or the potassium channel inhibitor glyburide (100 μM). **d**, IL-1β and caspase-1 immunoblotting in IFNR1-deficient ($Ifnar1^{-/-}$) macrophages transfected with DNA or challenged with the TLR7/8 agonist and inflammasome activating R837 (10 μg ml^{-1}). **e**, Phospho-IRF3 and IL-1β immunoblotting in wild-type and $Nalp3^{-/-}$ macrophages stimulated with AdGFP or transfected with poly(I:C) at 6 h

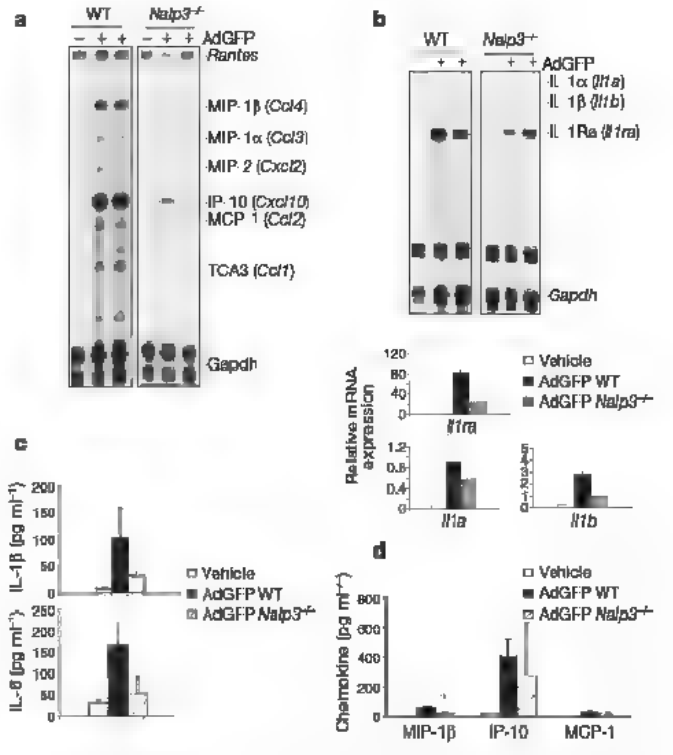

Figure 4 | Role of NALP3 in adenovirus-vector-induced inflammation *in vivo*. **a**, **b**, RNase protection assay of total liver RNA probing for chemokine and cytokine genes at 6 h in wild-type and $Nalp3^{-/-}$ mice receiving AdGFP intraperitoneally. $Nalp3^{-/-}$ mice displayed blunted liver cytokine mRNA levels in response to adenovirus vectors. Quantifications are based on phosphorimaging and are normalized to housekeeping genes (mean ± s.d., $n = 3$–5). **c**, **d**, ELISA of spleen IL-1β, IL-6, MIP-1β (CCL4), IP-10 (CXCL10) and MCP-1 (CCL2) from wild-type and $Nalp3^{-/-}$ mice 6 h after AdGFP administration (mean ± s.d., $n = 3$–5; asterisk, $P < 0.05$)

inflammatory response in the liver was blunted after intraperitoneal administration of AdLacZ compared to wild-type controls (Supplementary Fig. 9). These results show that the NALP3 inflammasome and IL-1β are mediators of the innate immune response to the adenovirus virion *in vivo*. However, the partial reduction in the inflammatory response observed in mice deficient in inflammasome components is consistent with redundant mechanisms that exist in the innate response to adenovirus[19].

Our data demonstrate that the internalized adenovirus DNA activates intracellular NALP3 and downstream signalling that involves ASC and caspase-dependent activation of IL-1β. This is in line with findings that IL-1β and the IL-1RI have a significant role in the innate immune response to adenovirus[8], and is also consistent with the requirement for adenoviral DNA to mediate the innate response[20]. Similarly, the inflammasome-dependent IL-18 was shown to have a major role in the protection against HSV-1 (ref. 21). The identification of the inflammasome as an antiviral innate mechanism is also consistent with data demonstrating a PYD-containing protein (M13L) encoded by myxoma virus that disrupts the NALP–ASC interaction and caspase-1 activation[22], an important immunomodulatory strategy to circumvent host antiviral responses.

In addition to detecting viral DNA, the inflammasome also responded to cytoplasmic mammalian genomic DNA, bacterial DNA and synthetic DNA. Unexpectedly, the response to transfected cytoplasmic DNA occurred in a NALP3-independent manner, but relied on ASC and caspase-1. Because ASC is part of the NALP inflammasome complex, it is likely that NALP inflammasomes constitute the sensing platform of cytoplasmic DNA. Alternatively, a NALP-independent mechanism, requiring only ASC for the activation of the inflammasome as recently proposed, cannot be excluded[23]. How the DNA is sensed is currently not clear. We have no evidence that the only characterized cytosolic DNA sensor, DAI, is involved (data not shown).

Our data clearly identify the NALP/ASC inflammasomes and IL-1β as an alternative innate mechanism to type I IFN capable of sensing cytoplasmic DNA and of triggering a pro-inflammatory response. This has a number of implications. First, it is likely that the NALP3 inflammasome has an important role in the host response to DNA virus infection in general. Second, our data raise the possibility that autoimmune diseases such as systemic lupus erythematosus (SLE) might involve the dysregulation of the inflammasome. Because many patients of such diseases form immune complexes to dsDNA by means of autoreactive antibodies, the elevated IL-1β levels observed during active disease might be explained via this mechanism[24]. Similarly, chronic arthritis caused by mammalian DNA that escapes from degradation is associated with increased levels of IL-1β and IL-18. Indeed, one form of SLE and rheumatoid arthritis was recently found to be associated with mutations in the *NALP1* gene[25]. The identification of the inflammasome as a general sensor of cytoplasmic DNA may therefore lead to new antiviral therapies and to new insights and treatments for nucleic-acid-dependent autoimmune diseases.

METHODS SUMMARY

Viruses and viral vectors. Wild-type serotype 5, serotype 3 adenovirus, serotype 5 adenovirus vectors and helper-dependent adenovirus vectors were propagated and purified as previously described[26–28]. Empty serotype 5 adenovirus capsids were generated using the helper-dependent adenovirus vector system and 293-Cre cells, as previously described[13].

Animal studies. Mice genetically deficient for caspase-1 (*Casp1*), *Asc*, *Nalp3*, *Ipaf*, interferon receptor 1 (*Ifnar1*) or *Tlr9* were on a C57BL/6 background[29,30]. For *in vivo* studies, mice were injected intraperitoneally with 2×10^{11} particles of adenovirus vectors.

Cell culture. Human THP-1 cells were differentiated for 24 h with PMA (100 nM). Mouse peritoneal macrophages were isolated using 4–10% thioglycollate solution and stimulated with 1–10 ng ml^{-1} ultra-pure LPS (Invivogen). Viral infection/transduction was performed using 10^4 particles per cell for adenovirus vectors or multiplicity of infection 100:1 for wild-type adenovirus 3 and 5.

DNA isolation, plasmids and transfections. Human and viral genomic DNA was isolated from THP-1 cells and adenovirus by standard protocol. DNA of varying length was amplified in standard PCR reactions using oligonucleotides specific to the mouse *Gapdh* gene and to regions of the human *RANTES* (*Ccl5*) and mouse IP-10 (*Cxcl10*) promoters. PCR products were pooled, ethano. precipitated and re-suspended in water. Complimentary sense and antisense oligonucleotides (40 bp) were synthesized and annealed to obtain dsDNA fragments. Bacterial DNA was isolated from *E. coli*. To remove contaminating LPS from the DNA preparation, *E. coli* DNA was incubated with polymyxin B (50 μg ml^{-1}) at room temperature for 30 min. DNA was ethanol precipitated twice and re-suspended in endotoxin-free water. Single-stranded DNA, poly(deoxyadenosine: deoxythymidine) (poly(dA:dT)) DNA, CpG oligonucleotides, poly(inosine: cytosine) (poly(I:C)) and R837 were obtained from commercial sources. Transfections were performed using Lipofectamine 2000 (4 μl ml^{-1}) as per the manufacturer's protocol (Invitrogen). All transfections were performed using 1–2 μg of DNA.

Full Methods and any associated references are available in the online version of the paper at www.nature.com/nature.

Received 9 June 2007; accepted 4 January 2008.
Published online 20 February 2008.

1. Kawai, T. & Akira, S. TLR signaling. *Cell Death Differ.* 13, 816–825 (2006).
2. Ishii, K. J. & Akira, S. Innate immune recognition of, and regulation by, DNA. *Trends Immunol.* 27, 525–532 (2006).
3. Stetson, D. B. & Medzhitov, R. Recognition of cytosolic DNA activates an IRF3-dependent innate immune response. *Immunity* 24, 93–103 (2006).
4. Takaoka, A. *et al.* DAI (DLM-1/ZBP1) is a cytosolic DNA sensor and an activator of innate immune response. *Nature* 448, 501–505 (2007).
5. Sergerie, Y., Rivest, S. & Boivin, G. Tumor necrosis factor-α and interleukin-1-β play a critical role in the resistance against lethal herpes simplex virus encephalitis. *J. Infect. Dis.* 196, 853–860 (2007).
6. Kay, M. A., Glorioso, J. C. & Naldini, L. Viral vectors for gene therapy: the art of turning infectious agents into vehicles of therapeutics. *Nature Med.* 7, 33–40 (2001).
7. Muruve, D. A., Barnes, M. J., Stillman, I. E. & Libermann, T. A. Adenoviral gene therapy leads to rapid induction of multiple chemokines and acute neutrophil-dependent hepatic injury *in vivo*. *Hum. Gene Ther.* 10, 965–976 (1999).
8. Shayakhmetov, D. M., Li, Z. Y., Ni, S. & Lieber, A. Interference with the IL-1-signaling pathway improves the toxicity profile of systemically applied adenovirus vectors. *J. Immunol.* 174, 7310–7319 (2005).
9. Fritz, J. H., Ferrero, R. L., Philpott, D. J. & Girardin, S. E. Nod-like proteins in immunity, inflammation and disease. *Nature Immunol.* 7, 1250–1257 (2006).
10. Petrilli, V., Dostert, C., Muruve, D. A. & Tschopp, J. The inflammasome: a danger sensing complex triggering innate immunity. *Curr. Opin. Immunol.* 19, 615–622 (2007).
11. Franchi, L. *et al.* Intracellular NOD-like receptors in innate immunity, infection and disease. *Cell. Microbiol.* 10, 1–8 (2008).
12. Cotter, M. J., Zaiss, A. K. & Muruve, D. A. Neutrophils interact with adenovirus vectors via Fc receptors and complement receptor 1. *J. Virol.* 79, 14622–14631 (2005).
13. Stilwell, J. L., McCarty, D. M., Negish, A., Superfine, R. & Samulski, R. J. Development and characterization of novel empty adenovirus capsids and their impact on cellular gene expression. *J. Virol.* 77, 12881–12885 (2003).
14. Kanneganti, T. D. *et al.* Critical role for cryopyrin/Nalp3 in activation of caspase-1 in response to viral infection and double-stranded RNA. *J. Biol. Chem.* 281, 36560–36568 (2006).
15. Boyden, E. D. & Dietrich, W. F. Nalp1b controls mouse macrophage susceptibility to anthrax lethal toxin. *Nature Genet.* 38, 240–244 (2006).
16. Franchi, L., Kanneganti, T. D., Dubyak, G. R. & Nunez, G. Differential requirement of P2X7 receptor and intracellular K^+ for caspase-1 activation induced by intracellular and extracellular bacteria. *J. Biol. Chem.* 282, 18810–18818 (2007).
17. Petrilli, V. *et al.* Activation of the NALP3 inflammasome is triggered by low intracellular potassium concentration. *Cell Death Differ.* 14, 1583–1589 (2007).
18. Henry, T., Brotcke, A., Weiss, D. S., Thompson, L. J. & Monack, D. M. Type I interferon signaling is required for activation of the inflammasome during *Francisella* infection. *J. Exp. Med.* 204, 987–994 (2007).
19. Zhu, J., Huang, X. & Yang, Y. Innate immune response to adenoviral vectors is mediated by both TLR-dependent and -independent pathways. *J. Virol.* 81, 3170–3180 (2007).
20. Nociari, M., Ocheretina, O., Schoggins, J. W. & Falck-Pedersen, E. Sensing infection by adenovirus: toll-like receptor-independent viral DNA recognition signals activation of the interferon regulatory factor 3 master regulator. *J. Virol.* 81, 4145–4157 (2007).
21. Fujioka, N. *et al.* Interleukin-18 protects mice against acute herpes simplex virus type 1 infection. *J. Virol.* 73, 2401–2409 (1999).
22. Johnston, J. B. *et al.* A poxvirus-encoded pyrin domain protein interacts with ASC-1 to inhibit host inflammatory and apoptotic responses to infection. *Immunity* 23, 587–598 (2005).

23. Fernandes-Alnemri, T. *et al.* The pyroptosome: a supramolecular assembly of ASC dimers mediating inflammatory cell death via caspase-1 activation. *Cell Death Differ.* 14, 1590–1604 (2007)
24. Sun, K. H., Yu, C. L., Tang, S. J. & Sun, G. H. Monoclonal anti-double-stranded DNA autoantibody stimulates the expression and release of IL-1β, IL-6, IL-8, IL-10 and TNF-α from normal human mononuclear cells involving in the lupus pathogenesis. *Immunology* 99, 352–360 (2000)
25. Jin, Y. *et al.* NALP1 in vitiligo-associated multiple autoimmune disease. *N. Engl. J. Med.* 356, 1216–1225 (2007)
26. Tibbles, L. A. *et al.* Activation of p38 and ERK signaling during adenovirus vector cell entry lead to expression of the C-X-C chemokine IP-10. *J. Virol.* 76, 1559–1568 (2002)
27. Cotten, M. *et al.* Psoralen treatment of adenovirus particles eliminates virus replication and transcription while maintaining the endosomolytic activity of the virus capsid. *Virology* 205, 254–261 (1994)
28. Muruve, D. A. *et al.* Helper-dependent adenovirus vectors elicit intact innate but attenuated adaptive host immune responses *in vivo*. *J. Virol.* 78, 5966–5972 (2004)
29. Manathasan, S. *et al.* Differential activation of the inflammasome by caspase-1 adaptors ASC and Ipaf. *Nature* 430, 213–218 (2004).
30. Martinon, F., Petrilli, V., Mayor, A., Tardivel, A. & Tschopp, J. Gout-associated uric acid crystals activate the NALP3 inflammasome. *Nature* 440, 237–241 (2006).

Supplementary Information is linked to the online version of the paper at www.nature.com/nature.

Acknowledgements This work was supported by the Alberta Heritage Foundation for Medical Research, operating and group grants from the Canadian Institutes for Health Research, the Swiss Committee for Technology and Innovation and MUGEN. D.A.M. is the recipient of an AHFMR Scholar Award; A.K.Z. is the recipient of a Heart and Stroke Foundation of Canada Studentship; V.P. is the recipient of a Marie Curie training award. We thank R. Castillo for technical assistance, V. Dixit, A. Trumpp and S. Akira for knockout mice and P. Vandenabeele for the caspase-1 antibody.

Author Contributions D.A.M., V.P., A.K.Z., L.R.W., S.A.C., P.J.R. and R.J.P. conceived the research and conducted the experiments. J.T. oversaw the whole project.

Author Information Reprints and permissions information is available at www.nature.com/reprints. Correspondence and requests for materials should be addressed to J.T. (Jurg.Tschopp@unil.ch).

LETTERS

A peptide deformylase–ribosome complex reveals mechanism of nascent chain processing

Rouven Bingel-Erlenmeyer[1], Rebecca Kohler[1], Günter Kramer[2], Arzu Sandikci[2], Snježana Antolić[1]†, Timm Maier[1], Christiane Schaffitzel[1], Brigitte Wiedmann[3], Bernd Bukau[2] & Nenad Ban[1]

Messenger-RNA-directed protein synthesis is accomplished by the ribosome[1–3]. In eubacteria, this complex process is initiated by a specialized transfer RNA charged with formylmethionine ($tRNA^{fMet}$)[4–6]. The amino-terminal formylated methionine of all bacterial nascent polypeptides blocks the reactive amino group to prevent unfavourable side-reactions and to enhance the efficiency of translation initiation[7,8]. The first enzymatic factor that processes nascent chains is peptide deformylase (PDF)[9–11]; it removes this formyl group as polypeptides emerge from the ribosomal tunnel[12,13] and before the newly synthesized proteins can adopt their native fold, which may bury the N terminus. Next, the N-terminal methionine is excised by methionine aminopeptidase[14]. Bacterial PDFs are metalloproteases sharing a conserved N-terminal catalytic domain. All Gram-negative bacteria, including *Escherichia coli*, possess class-1 PDFs characterized by a carboxy-terminal α-helical extension[15]. Studies focusing on PDF as a target for antibacterial drugs[14,16] have not revealed the mechanism of its co-translational mode of action despite indications in early work that it co-purifies with ribosomes[17]. Here we provide biochemical evidence that *E. coli* PDF interacts directly with the ribosome via its C-terminal extension. Crystallographic analysis of the complex between the ribosome-interacting helix of PDF and the ribosome at 3.7 Å resolution reveals that the enzyme orients its active site towards the ribosomal tunnel exit for efficient co-translational processing of emerging nascent chains. Furthermore, we have found that the interaction of PDF with the ribosome enhances cell viability. These results provide the structural basis for understanding the coupling between protein synthesis and enzymatic processing of nascent chains, and offer insights into the interplay of PDF with the ribosome-associated chaperone trigger factor.

We probed PDF interaction with the ribosome by using a sedimentation assay in which N-terminally *Strep*-tagged PDF was incubated with purified, non-translating *E. coli* 70S ribosomes, 50S or 30S subunits. *Strep*-PDF was detected only in pellets of samples containing 70S (Supplementary Fig. 1a) or 50S (Fig. 1a and b), demonstrating a direct interaction with the large ribosomal subunit. This association is specific, with a defined stoichiometry, because even a 25-fold molar excess of *Strep*-PDF did not yield a considerably stronger signal than observed for a one-to-one complex (Fig. 1a). Also, surface plasmon resonance analysis gave best fits when using a one-to-one model (Supplementary Fig. 2). The obtained affinity of PDF for the 50S subunit (dissociation constant $K_D = 2.5 \pm 1.0\,\mu M$), agrees well with that for the entire ribosome ($K_D = 1.8 \pm 0.9\,\mu M$; Supplementary Table 1).

Our finding that the PDF–ribosome interaction is salt-sensitive (Supplementary Fig. 1b) indicated that complementary charge interactions are at least partially responsible for the association. We therefore reasoned that the positively charged C-terminal helix of PDF (Supplementary Fig. 3a), which is not critical for catalytic activity *in vitro*[18], might be responsible for interactions with the ribosome; we therefore generated a deletion construct (*Strep*-PDFΔC, Fig. 1c). We also cloned the construct *Strep*-Trx-PDFc147, in which only the C-terminal helix of PDF is fused via a flexible linker to *E. coli* thioredoxin (Trx) (Fig. 1c and d and Supplementary Fig. 1d). The truncated version *Strep*-PDFΔC lost the ability to bind the ribosome in surface plasmon resonance experiments (Supplementary Table 1) and in the sedimentation assay (Fig. 1d and Supplementary Fig. 1c). In contrast, fusing the C-terminal helix of PDF to Trx resulted in its binding to the 50S subunit (Fig. 1d) with a K_D of $1.3 \pm 0.5\,\mu M$, in agreement with the value for full-length PDF (Supplementary Table 1). These experiments demonstrate that the C-terminal helix of PDF serves as binding module for ribosome association.

On the basis of our biochemical results, we designed crystallographic experiments. We reasoned that structural data for the binding of the C-terminal helix alone would give us insights into the precise positioning of PDF at the ribosomal exit because: (1) it is the main determinant of ribosome binding and (2) it is in a fixed disposition with respect to the catalytic core domain, as is shown by a number of high-resolution X-ray structures of full-length PDF in different crystal forms (Supplementary Fig. 3b).

E. coli 70S crystals[19], diffracting to 3.7 Å resolution (Supplementary Table 2) were soaked with a synthetic peptide of the C-terminal PDF ribosome-binding helix (residues 147–168). The crystallographic data show that the binding helix of PDF is tucked into a groove between ribosomal proteins L22 and L32 in the vicinity of the C terminus of L17 (which is established as the main crosslinking partner of PDF; Supplementary Fig. 4), with L22 serving as the major docking site (Fig. 2a, Supplementary Fig. 5). We observed three main interactions between the helix and the ribosome: Leu 149 inserts into a hydrophobic pocket of L22, Arg 153 forms a salt bridge with Glu 59 of L22, and Lys 157 of PDF interacts with the helix 24 of domain I of the 23S ribosomal RNA. These residues are conserved throughout bacterial class 1 PDFs (Fig. 2b) and should be considered as major determinants for ribosome association.

To investigate the importance of the C-terminal helix for the function of PDF *in vivo*, we performed a complementation analysis by expressing PDF or PDFΔCII (lacking residues 151–168) in the *E. coli* strain MG1655, which is deficient in the authentic *def* gene encoding PDF. The expression levels of PDF in the absence of arabinose are so low that cells exhibit severely impaired growth (Fig. 3a). A gradual increase of arabinose concentration restores the growth of the cells expressing PDF and PDFΔCII. Western blot analysis demonstrated

[1]Institute of Molecular Biology and Biophysics, ETH Zurich, 8093 Zurich, Switzerland. [2]Zentrum für Molekulare Biologie (ZMBH), Universität Heidelberg, Im Neuenheimer Feld 282, 69120 Heidelberg, Germany. [3]Novartis Institutes for BioMedical Research, Inc., 500 Technology Square, Cambridge, Massachusetts, 02139 USA. †Present address: Solvias AG, Postfach, 4002 Basel, Switzerland.

the presence of equivalent expression levels of PDFΔCII and PDF (Fig. 3b). Nevertheless, we observed a clearly reduced plating efficiency and a growth rate diminished at least tenfold for cells expressing PDF lacking the C-terminal helix (Fig. 3a).

The binding studies presented here, together with earlier deletion studies[18], suggest a functional separation in *E. coli* PDF: the N-terminal domain being exclusively involved in catalytic activity, whereas the C-terminal helix mediates binding to the ribosome. Because both parts of the enzyme are structurally conserved, we propose that the C-terminal helix serves as a general ribosome-binding module for bacterial class 1 PDFs. It remains to be elucidated whether the C-terminal extension in bacterial class 2 PDFs, featuring a loop with a short β-strand, fulfils a similar function[15].

PDF adopts a unique conformation, as observed in various crystal structures (Supplementary Fig. 3b), so superimposing the structure of full-length *E. coli* PDF[20] based on its C terminus onto the structure of the ribosome-bound helix provides an accurate model for the positioning of PDF on the ribosome: PDF orients the entrance of its active site towards the ribosomal exit tunnel (Fig. 4a) at a distance of ~35 Å, equivalent to 13 amino acids in an extended conformation. Considering that about 35 amino acids are necessary to reach from the peptidyl transferase centre to the tunnel exit[21], a nascent chain of about 45 to 50 residues would be sufficiently long to reach the active site of ribosome-bound PDF, in excellent agreement with previous results[12,13].

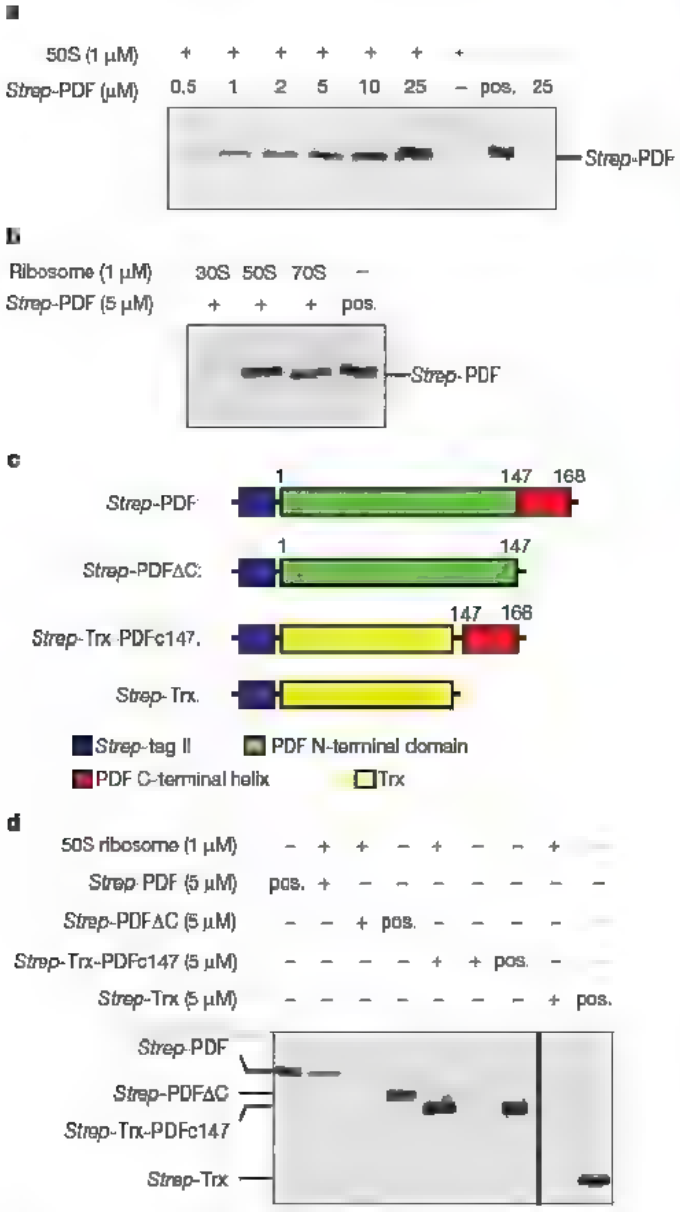

Figure 1 | PDF specifically binds to the 50S ribosomal subunit via its C-terminal helix. **a**, 50S ribosome sedimentation assay containing 1 μM of non-translating *E. coli* 50S ribosomes and different concentrations of *Strep*-tagged PDF. A positive control (pos.) was loaded as a reference (for details see Methods). **b**, Comparison of the interaction of 5 μM *Strep*-PDF with 1 μM of 30S, 50S and 70S, respectively, using the same method as in **a**. **c**, PDF constructs used in the ribosome sedimentation assays to determine the ribosome-binding region of PDF. **d**, Ribosome sedimentation assay as in **a**, using different *Strep*-tagged PDF constructs to dissect the two PDF domains for ribosome binding.

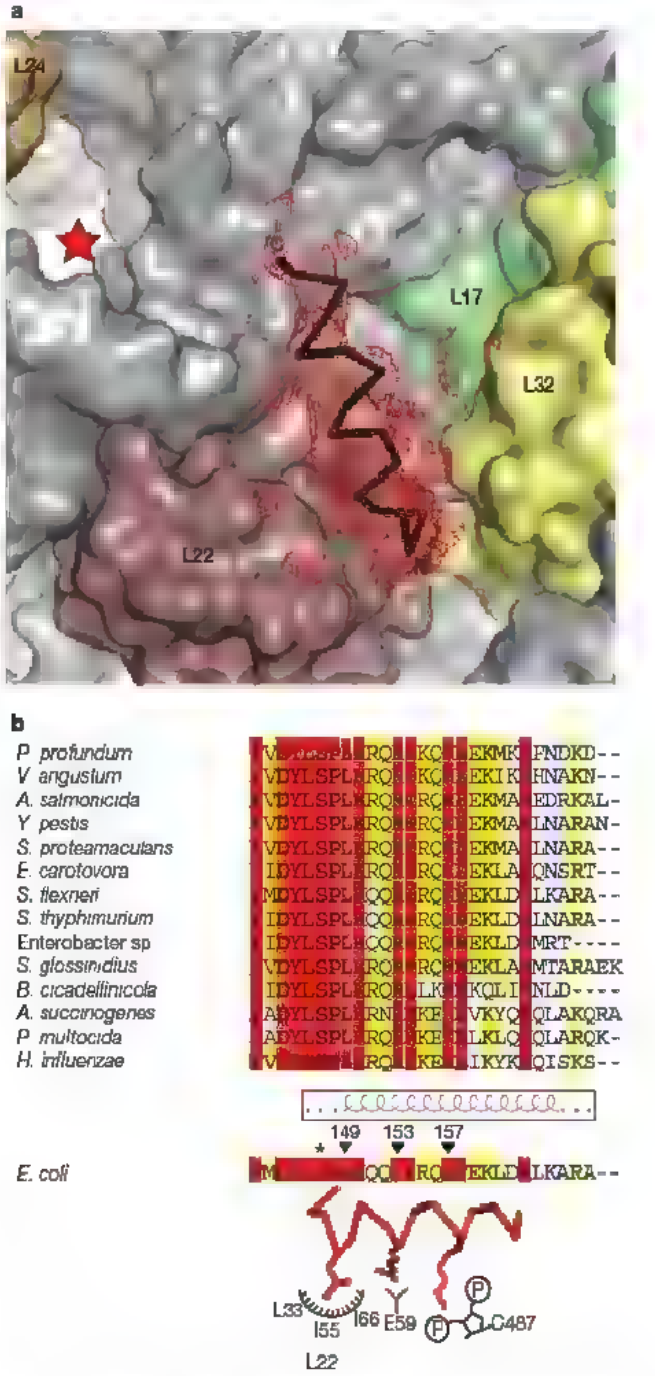

Figure 2 | Interaction of the C-terminal helix of PDF with the ribosome. **a**, Surface representation of the ribosome in the region of the exit tunnel (star) shown with an unbiased $F_o - F_c$ omit map around the bound helix (black ribbon) contoured in red at the 2.0σ level. **b**, Sequence alignment of the C-terminal helix of bacterial class 1 PDF. Conserved residues are highlighted (red, 100%; yellow, 80% conservation). Key interactions of the binding helix with ribosomal protein L22 (residues L33, I55, I66, and E59) and the phosphate backbone (P) of the ribosomal RNA are schematically shown in the lower part of the panel. The length of the peptide used in soaking experiments is marked by a frame and the α-helical secondary structure of the wild-type PDF is indicated.

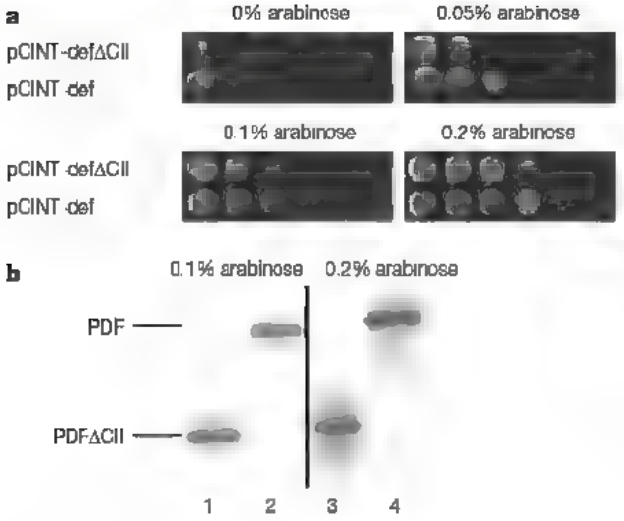

Figure 3 | Growth analysis comparing the *in vivo* complementation abilities of PDF and PDFΔCII. **a**, Spot tests of MG1655Δ*def::kan* complemented with either full-length PDF or PDFΔCII lacking the C-terminal helix. 1:10 serial dilutions of overnight cultures of both strains were spotted onto Luria-Broth (LB) plates containing the indicated L(+)-arabinose concentrations and incubated overnight at 37 °C. **b**, Steady-state levels of PDF (lanes 2 and 4) or PDFΔCII (lanes 1 and 3) in cells grown in liquid culture in LB containing the indicated L(+)-arabinose concentrations.

As observed for PDF, the ribosome-associated chaperone trigger factor interacts with nascent chains when they reach ~40 amino acids. Owing to their complementary roles in co-translational processing and folding of nascent chains, it is likely that the trigger factor and PDF work in concert. Combining the structural information on the binding of trigger factor to the ribosome[22] with the results described here, we propose a model for their simultaneous action (Fig. 4b and c). Emerging nascent chains are greeted by the chaperone trigger factor, which forms a hydrophobic molecular cradle underneath the ribosomal exit tunnel and initially delays protein folding[23]. This cradle, as a consequence of the multi-domain structure of the trigger factor[22]—which resembles a dragon with a tail, back, arms and head—is open on several sides, enabling the trigger factor to serve as a passive router that channels nascent chains into various processing steps (Fig. 4d). PDF, the first enzyme that processes nascent chains, binds to the ribosome next to the trigger factor and positions its active site towards one of the lateral openings between the arms and the ribosome-binding tail where nascent polypeptides emerge from the ribosomal tunnel (Fig. 4b and c). To reach the active site of PDF, nascent polypeptides would not have to leave this

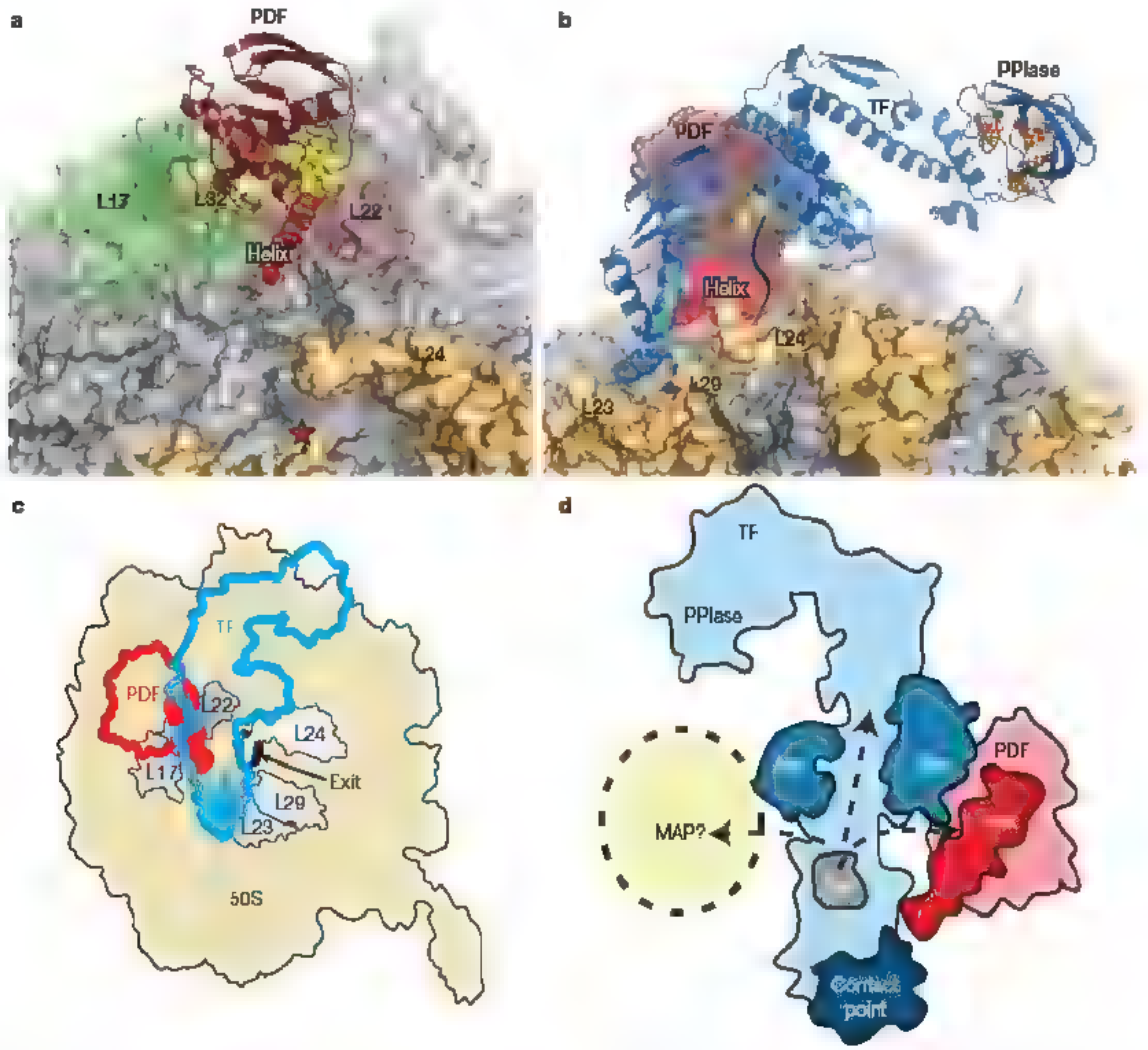

Figure 4 | Model for the concerted mechanism of PDF and trigger factor. **a**, PDF (catalytic domain in dark red, C-terminal helix in red, substrate shown as yellow spheres) superimposed onto the ribosome-bound helix. A star marks the exit tunnel. **b**, View through the cradle of the trigger factor (in blue, TF, active site residues of the peptidyl-prolyl-*cis/trans*-isomerase (PPIase) in orange spheres) across the exit tunnel towards the active site of PDF (colouring as in **a**). An arrow indicates the route from the exit tunnel to the active site of PDF. **c**, Footprints of PDF (red) and trigger factor (blue, TF) on the ribosome, from crystallographic data. Filled areas indicate binding sites for PDF and trigger factor, projections are shown as outlines in the same colours (view onto the exit tunnel). **d**, A schematic of the trigger factor (blue, TF) with its two arms and ribosome-binding domain (contact point) forming a hydrophobic nascent chain folding and processing chamber and functioning as a router, viewed from the ribosomal tunnel. Methionine-aminopeptidase (MAP) and PDF close the lateral openings of the trigger factor

shielded environment. PDF is present in sub-stoichiometric amounts relative to the ribosome, so it will use its rapid binding and dissociation, as indicated by our surface plasmon resonance measurements (Supplementary Information), to sample translating ribosomes, while the more abundant trigger factor remains attached for longer periods during ongoing protein synthesis[24].

After deformylation the unmasked N-terminal methionine is cleaved by methionine aminopeptidase, which associates with the 60S subunit in yeast[25,26], and was suggested to interact with ribosomes via ribosomal protein L24 in *Mycobacterium tuberculosis*[27]. This would position methionine aminopeptidase on the opposite site of PDF, where the second lateral opening of the trigger factor is situated (Fig. 4d). Therefore, after the removal of the formyl group the nascent peptide may be transferred to methionine aminopeptidase while still being protected by the trigger factor cradle. Nascent chains will then continue to fold, aided by the trigger factor and its peptidyl-prolyl-*cis/trans*-isomerase enzymatic activity, which is located in the vicinity of the third opening of the cradle between the arms of the trigger factor. Although transient and dynamic, such an assembly could be considered as a dedicated nascent chain folding and processing chamber at the exit of the ribosomal tunnel.

Our *in vivo* data emphasizes the importance of ribosome association mediated by the C-terminal helix in the living cell. The intracellular PDF concentration[28] is ~2.5 μM, compared to a ribosome concentration[29] of 15 μM. Therefore, it is possible that under physiological concentrations of PDF, only wild-type PDF, which is targeted with micromolar affinity to the ribosome via its C-terminal helix, will achieve local concentrations of the enzyme sufficient to ensure highly efficient processing of nascent chains.

The results presented here reveal an important cellular interaction between the ribosome and PDF. Moreover, they provide the structural framework for future studies aimed at revealing dynamic and temporal aspects of the interaction between the ribosome and various factors involved in co-translational processing and folding of nascent chains. These factors probably work on the ribosome in a highly organized and concerted manner, directed by specific interactions with the ribosome and controlled by finely balanced relative affinities and dynamics of their binding equilibria.

METHODS SUMMARY

PDF constructs bearing an N-terminal *Strep*-tag II were expressed in *E. coli* and purified using *Strep*-Tactin Sepharose and a HiLoad 16/60 Superdex75 prep grade gel filtration column. *E. coli* ribosomes were purified using ultracentrifugation steps. Ribosome sedimentation assays were carried out using a Beckman Optima Max ultracentrifuge and a TLA55 rotor. Ribosomal pellets were analysed by immuno-detection of the N-terminal *Strep*-tag II of the PDF constructs. To investigate the function of PDF *in vivo*, we performed complementation experiments using strains lacking the authentic *def* gene and expressing either PDF or PDFΔCII from a chromosomally integrated plasmid under the control of the tightly controlled arabinose promoter. *E. coli* 70S crystals were obtained as described[19] and soaked with 15 mM of a peptide purified by high-performance liquid chromatography (HPLC). Crystallographic data were collected at the SLS of the Paul Scherrer Institute. Deposited coordinates[19] were used as a starting model and refined employing PHENIX.

Full Methods and any associated references are available in the online version of the paper at www.nature.com/nature.

Received 27 September 2007; accepted 11 January 2008.
Published online 20 February 2008.

1. Ramakrishnan, V. Ribosome structure and the mechanism of translation. *Cell* 108, 557–572 (2002)
2. Moore, P. B. & Steitz, T. A. The ribosome revealed. *Trends Biochem. Sci.* 30, 281–283 (2005)
3. Liljas, A. Deepening ribosomal insights. *ACS Chem. Biol.* 1, 567–569 (2006)
4. Marcker, K. & Sanger, F. N-formyl-methionyl-s-RNA. *J. Mol. Biol.* 8, 835–840 (1964)
5. Adams, J. M. & Capecchi, M. R. N-formylmethionyl-sRNA as the initiator of protein synthesis. *Proc. Natl Acad. Sci. USA* 55, 147–155 (1966)
6. Laursen, B. S., Sorensen, H. P., Mortensen, K. K. & Sperling-Petersen, H. U. Initiation of protein synthesis in bacteria. *Microbiol. Mol. Biol. Rev.* 69, 101–123 (2005)
7. Eisenstadt, J. & Lengyel, P. Formylmethionyl-tRNA dependence of amino acid incorporation in extracts of trimethoprim-treated *Escherichia coli*. *Science* 154, 524–527 (1966).
8. Harvey, R. J. Growth and initiation of protein synthesis in *Escherichia coli* in the presence of trimethoprim. *J. Bacteriol.* 114, 309–322 (1973)
9. Fry, K. T. & Lamborg, M. R. Amidohydrolase activity of *Escherichia coli* extracts with formylated amino acids and dipeptides as substrates. *J. Mol. Biol.* 28, 423–433 (1967)
10. Adams, J. M. On the release of the formyl group from nascent protein. *J. Mol. Biol.* 33, 571–589 (1968)
11. Pine, M. J. Kinetics of maturation of the amino termini of the cell proteins of *Escherichia coli*. *Biochim. Biophys. Acta* 174, 359–372 (1969)
12. Housman, D., Gillespie, D. & Lodish, H. F. Removal of formyl-methionine residue from nascent bacteriophage f2 protein. *J. Mol. Biol.* 65, 163–166 (1972)
13. Ball, L. A. & Kaesberg, P. Cleavage of the N-terminal formylmethionine residue from a bacteriophage coat protein *in vitro*. *J. Mol. Biol.* 79, 531–537 (1973).
14. Giglione, C., Boularot, A. & Meinnel, T. Protein N-terminal methionine excision. *Cell. Mol. Life Sci.* 61, 1455–1474 (2004)
15. Guilloteau, J. P. *et al.* The crystal structures of four peptide deformylases bound to the antibiotic actinonin reveal two distinct types: a platform for the structure-based design of antibacterial agents. *J. Mol. Biol.* 320, 951–962 (2002)
16. Giglione, C., Pierre, M. & Meinnel, T. Peptide deformylase as a target for new generation, broad spectrum antimicrobial agents. *Mol. Microbiol.* 36, 1197–1205 (2000)
17. Takeda, M. & Webster, R. E. Protein chain initiation and deformylation in *B. subtilis* homogenates. *Proc. Natl Acad. Sci. USA* 60, 1487–1494 (1968)
18. Meinnel, T. *et al.* The C-terminal domain of peptide deformylase is disordered and dispensable for activity. *FEBS Lett.* 385, 91–95 (1996)
19. Schuwirth, B. S. *et al.* Structures of the bacterial ribosome at 3.5 Å resolution. *Science* 310, 827–834 (2005)
20. Becker, A. *et al.* Iron center, substrate recognition and mechanism of peptide deformylase. *Nature Struct. Biol.* 5, 1053–1058 (1998)
21. Hardesty, B. & Kramer, G. Folding of a nascent peptide on the ribosome. *Prog. Nucleic Acid Res. Mol. Biol.* 66, 41–66 (2001)
22. Ferbitz, L. *et al.* Trigger factor in complex with the ribosome forms a molecular cradle for nascent proteins. *Nature* 431, 590–596 (2004).
23. Agashe, V. R. *et al.* Function of trigger factor and DnaK in multidomain protein folding: increase in yield at the expense of folding speed. *Cell* 117, 199–209 (2004)
24. Kaiser, C. M. *et al.* Real-time observation of trigger factor function on translating ribosomes. *Nature* 444, 455–460 (2006)
25. Raue, U., Oellerer, S. & Rospert, S. Association of protein biogenesis factors at the yeast ribosomal tunnel exit is affected by the translational status and nascent polypeptide sequence. *J. Biol. Chem.* 282, 7809–7816 (2007)
26. Vetro, J. A. & Chang, Y. H. Yeast methionine aminopeptidase type 1 is ribosome-associated and requires its N-terminal zinc finger domain for normal function *in vivo*. *J. Cell. Biochem.* 85, 678–688 (2002)
27. Addlagatta, A. *et al.* Identification of an SH3-binding motif in a new class of methionine aminopeptidases from *Mycobacterium tuberculosis* suggests a mode of interaction with the ribosome. *Biochemistry* 44, 7166–7174 (2005)
28. Ragusa, S., Blanquet, S. & Meinnel, T. Control of peptide deformylase activity by metal cations. *J. Mol. Biol.* 280, 515–523 (1998).
29. Wegrzyn, R. D. & Deuerling, E. Molecular guardians for newborn proteins: ribosome-associated chaperones and their role in protein folding. *Cell. Mol. Life Sci.* 62, 2727–2738 (2005).

Supplementary Information is linked to the online version of the paper at www.nature.com/nature.

Acknowledgements Crystallographic data were collected at the beamline X06SA at the Swiss Light Source (SLS). We are grateful to C. Schulze-Briese, S. Gutmann, E. Pohl, S. Russo and T. Tomizaki for their outstanding support at the SLS. We thank B. Mikolasek for ribosome preparation, F. Parmeggiani and A. Plückthun at the University of Zurich for assistance with the surface plasmon resonance measurements and access to the Biacore 3000 instrument, R. Brunisholz at the Functional Genomics Center Zurich for mass-spectrometric analysis, D. Böhringer, J. Erzberger, S. Jenn and M. Müller for critically reading the manuscript and all members of the Ban laboratory for suggestions and discussions. This work was supported by the Swiss National Science Foundation (SNSF) and the National Center of Excellence in Research (NCCR) Structural Biology programme of the SNSF.

Author Information Atomic coordinates and structure factors of the 70S–PDF complex have been deposited in the Protein Data Bank under accession codes 2VHM, 2VHN, 2VHO and 2VHP. Reprints and permissions information is available at www.nature.com/reprints. Correspondence and requests for materials should be addressed to N.B. (ban@mol.biol.ethz.ch).

LETTERS

Transient cyclical methylation of promoter DNA

Sara Kangaspeska[1]*, Brenda Stride[1]*†, Raphaël Métivier[2], Maria Polycarpou-Schwarz[1], David Ibberson[1], Richard Paul Carmouche[1], Vladimir Benes[1], Frank Gannon[1]† & George Reid[1]

Methylation of CpG dinucleotides is generally associated with epigenetic silencing of transcription and is maintained through cellular division[1–3]. Multiple CpG sequences are rare in mammalian genomes, but frequently occur at the transcriptional start site of active genes, with most clusters of CpGs being hypomethylated[4]. We reported previously that the proximal region of the trefoil factor 1 (*TFF1*, also known as *pS2*) and oestrogen receptor α (*ERα*) promoters could be partially methylated by treatment with deacetylase inhibitors[5], suggesting the possibility of dynamic changes in DNA methylation. Here we show that cyclical methylation and demethylation of CpG dinucleotides, with a periodicity of around 100 min, is characteristic for five selected promoters, including the oestrogen (E2)-responsive *pS2* gene, in human cells. When the *pS2* gene is actively transcribed, DNA methylation occurs after the cyclical occupancy of ERα and RNA polymerase II (polII). Moreover, we report conditions that provoke methylation cycling of the *pS2* promoter in cell lines in which *pS2* expression is quiescent and the proximal promoter is methylated. This coincides with a low-level re-expression of *ERα* and of *pS2* transcripts.

Cell-specific patterns of cytosine methylation occur on approximately 60% to 90% of CpG dinucleotides within the somatic genomes of vertebrates[6]. The pattern of methylation on DNA is maintained through cellular replication, predominantly by the action of the methyltransferase DNMT1, which preferentially acts on hemimethylated CpG substrates. DNMT3a and DNMT3b have been assigned as the cellular *de novo* methyltransferases because they target unmethylated and hemimethylated substrates with comparable efficiencies[7]. We and others have shown that ERα cyclically engages with target gene promoters to initiate the sequential recruitment of

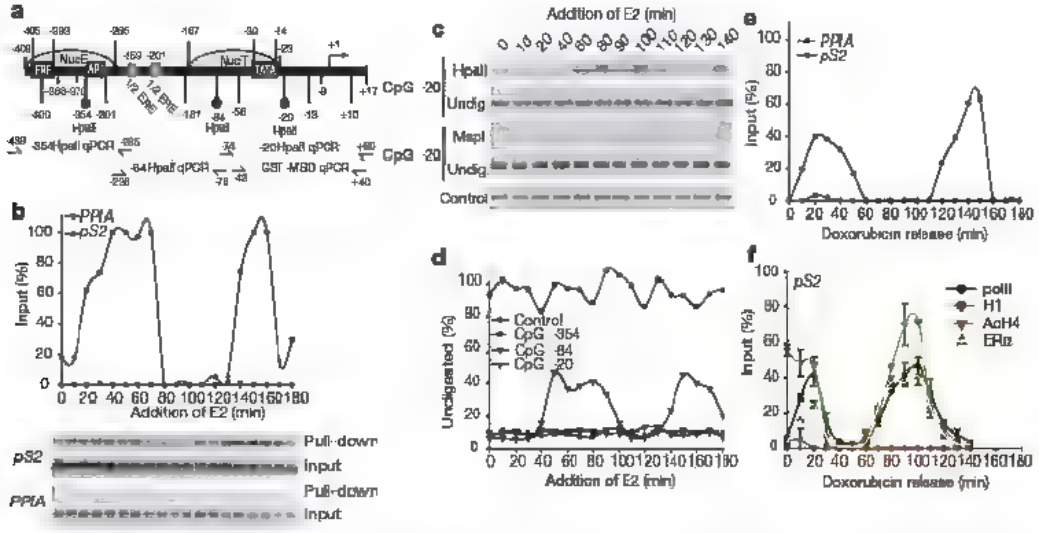

Figure 1 | The methylation status of the *pS2* promoter cycles on release from synchronization. a, A schematic overview of relevant features of the *pS2* promoter is shown. NucE and NucT are phased nucleosomes associated with the oestrogen response element (ERE) and TATA box, respectively. The positions of CpG dinucleotides are marked by vertical lines, and those within the sequence CCGG are marked as HpaII sites (filled circles) with the TSS denoted as +1. **b**, MCF-7 cells were cultured for 72 h in oestrogen-free media. E2 (1×10^{-8} M) was then added and genomic DNA subsequently prepared at ten-min intervals. After fragmentation by sonication, DNA fragments containing methylated CpG dinucleotides were selectively isolated using the MBD of human MECP2 fused to GST. The proportion of *pS2* and *PPIA* promoter DNA selectively captured, compared with total input DNA, was monitored by qPCR (**b**, top panel) and by endpoint PCR (**b**, bottom panel). **c**, The methylation status of CCGG sites close to the TSS of the *pS2* promoter were then kinetically evaluated using the methylation-sensitive restriction enzyme HpaII in conjunction with PCR. After synchronization by release from E2 deprivation, genomic DNA was digested with HpaII or with the methylation-insensitive isoschizomere MspI, and subjected to PCR with primers flanking the enzyme-recognition site encompassing the CpG at position −20 or a control region in the 5′ region of the *pS2* promoter that contains no HpaII sites. Undig., undigested. **d**, This procedure was also characterized by qPCR, however, in this case, primers were used that allow the individual HpaII sites at −20, −84 and −354 bp to be probed. **e**, **f**, MCF-7 cells were treated for 1 h with 300 nM doxorubicin, which was then removed by washing and media replacement. Serial samples were processed by the GST–MBD pull-down procedure (**e**) or by ChIP (**f**) with the antibodies as indicated. Primers specific for the *pS2* and *PPIA* promoters were used to determine the proportion of promoter DNA captured by each affinity isolation; mean values ± s.e.m. are shown, $n = 2$.

[1]European Molecular Biology Laboratory, Meyerhofstrasse 1, D-69117 Heidelberg, Germany. [2]SPARTE, UMR CNRS, 6026, Université de Rennes I, Bâtiment 13, 35042 Cedex, Rennes, France. †Present addresses: Phenex Pharmaceuticals AG, J542N Werksgelände BASF, 67056 Ludwigshafen, Germany (B.S.); Science Foundation Ireland, Wilton Park House, Wilton Place, Dublin 2, Ireland (F.G.).
*These authors equally contributed to this work

transcription factor complexes that promote and then limit transcription of responsive genes[8–10]. Here we show that, similarly, cyclical methylation of promoter DNA occurs on a timescale of tens of minutes.

Our initial observations were made on the E2-responsive *pS2* promoter, a schematic representation of which is shown in Fig. 1a. A rapid, quantitative, affinity isolation procedure using the methyl-binding domain (MBD) of methyl CpG-binding protein 2 (MECP2) was developed to characterize the methylation status of DNA (Supplementary Fig. 1). In brief, genomic DNA was isolated and fragmented by sonication to an average size of approximately 300 bp, and DNA containing symmetrically methylated $^{5\text{-Me}}$CpG was selectively isolated using the glutathione *S*-transferase (GST)–MBD fusion protein. The ERα-positive, E2-dependent cell line MCF-7 was maintained in oestrogen-free medium for three days to minimise activity of the *pS2* promoter. E2-responsive promoters were then synchronously activated by the addition of E2. Cells were collected at ten-minute intervals for three hours and subjected to the GST–MBD pull-down assay, which was evaluated using primers encompassing the *pS2* promoter close to the transcriptional start site (TSS, Fig. 1a). The *pS2* promoter is initially unmethylated (Fig. 1b and Supplementary Fig. 2), with two cycles of DNA methylation observed in the three hours after addition of E2, and broad peaks occurring between 20 and 50 min and between 120 and 150 min (Fig. 1b). By contrast, methylation of the peptidylprolyl isomerase A (*PPIA*) promoter, constitutively expressed in MCF-7 cells, was not observed (Fig. 1b).

The methylation-sensitive restriction endonuclease HpaII, which does not cleave hemimethylated or fully methylated C$^{5\text{-Me}}$CGG sequences, was used to evaluate cycling of the CCGG site at −20 relative to the TSS of the *pS2* promoter on release from E2 deprivation. Periodic methylation, similar to that observed using the GST–MBD fusion procedure, was detected by endpoint PCR evaluating the methylation status of the CpG sequence at position −20 (Fig. 1c) and by quantitative PCR (qPCR) using primer sets that individually evaluate the methylation status of CpGs at positions −354, −84 and −20 relative to the TSS (Fig. 1d). We next developed a promoter-synchronization methodology designed to facilitate the evaluation of E2-independent genes. Cells were treated for one hour with 300 nM doxorubicin, which prevents transcription by intercalating into GC-rich regions of DNA and by compromising topological changes required for the function of RNA polymerase II and topoisomerases I and II (ref. 11). Additionally, by intercalating into DNA, doxorubicin perturbs the action of DNMT1 (ref. 12) and potentially may affect the action of other components of the transcriptional machinery. Synchronous release from doxorubicin blockade was then achieved by washout. The methylation status of the 5′ proximal *pS2* promoter in doxorubicin-treated MCF-7 cells showed cyclic changes with kinetics similar to that seen after release from E2 deprivation (Fig. 1e and Supplementary Fig. 3). Additionally, doxorubicin synchronization induced cyclical changes in the occupancy of the *pS2* promoter by ERα, polII and acetylated H4 (AcH4, a marker of transcriptional permissiveness on histones), as determined by chromatin immunoprecipitation (ChIP), albeit with different kinetics to those induced when promoters are synchronized by α-amanitin, an inhibitor of polII (refs 9 and 10). Histone H1, associated with condensed chromatin, was never present on the *pS2* promoter in MCF-7 cells. Promoter methylation is coincident with, but persists longer than, the initial productive cycle. A subsequent round of methylation then occurs after the productive wave of the second cycle (Fig. 1f).

Doxorubicin promoter synchronization was then used to evaluate proximal promoter methylation of an additional four genes that are highly expressed in MCF-7 cells and that are subject to rapid turnover at the messenger RNA level (Supplementary Fig. 4). Kinetic analysis using the GST–MBD pull-down procedure was performed after doxorubicin blockade and release. All promoters analysed—*ERα* (Fig. 2a), *TFF3* (Fig. 2b), glutamate receptor, metabotropic 4 (*GRM4*, Fig. 2c) and the inwardly rectifying potassium channel J8 (*KCNJ8*, Fig. 2d)—demonstrate cyclical changes in promoter methylation after promoter synchronization with doxorubicin treatment, as analysed either by qPCR (middle panels) or by endpoint PCR (lower panels).

The discovery that periodic changes in the methylation status occur on the *pS2* promoter in oestrogen-dependent cells prompted an evaluation of the plasticity of *pS2* promoter methylation in cells in which high levels of methylation may contribute to a restriction of gene expression. High levels of *pS2* mRNA are present in the ERα-positive cell line MCF-7, but not in the ERα-negative cell line MDA-MB-231 (Fig. 4a). This correlates with an increase in the proportion of methylated CpG dinucleotides close to the TSS, as determined by bisulphite sequencing (Fig. 3a and Supplementary Fig. 2). Transient exposure to doxorubicin resulted in a reduction of methylation of the proximal *pS2* promoter in MDA-MB-231 cells, with hypomethylation occurring approximately 45 min after the addition of doxorubicin (Fig. 3b, left panel). ChIP analysis indicated that demethylation occurs after an exclusion of DNMT1, recruitment of DNMT3a and DNMT3b and the transient recruitment of thymine-DNA glycosylase (TDG; Fig. 3b, right panel). These findings are consistent with events proposed to induce cytosine demethylation[13]. Promoter release from doxorubicin blockade resulted in cyclical changes in the methylation status of the proximal promoter of the *pS2* gene in MDA-MB-231 cells (Fig. 3c, top left panel). Similar demethylation in response to doxorubicin treatment as well as cyclical methylation/demethylation in response to release from blockade were also observed on the *pS2* promoter in HeLa cells (Supplementary Fig. 5). Kinetic ChIP analysis indicates that histone H1 remained associated with the *pS2* promoter after release from doxorubicin synchronization, although cyclical changes in the acetylation status of histone H4 and low-level recruitment of polII did occur (Fig. 3c, top right panel). Synchronization by α-amanitin[14] induces cyclical methylation of the −20 CpG dinucleotide in MCF-7 cells (Fig. 3c, bottom left panel). However, unlike doxorubicin, α-amanitin did not induce demethylation of *pS2*

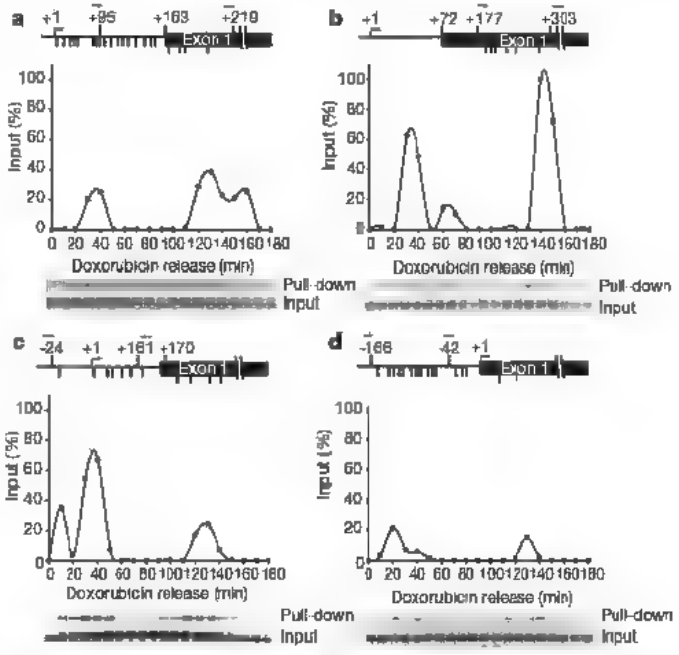

Figure 2 | Cyclical changes in methylation status occur on promoters of several genes. Serial samples of genomic DNA after synchronization with doxorubicin were subjected to GST–MBD affinity isolation, and the proportion of methylated DNA determined relative to input levels by qPCR (middle panels) and by end-point PCR (lower panels) were measured for **a**, *ERα* 5′ transcribed region, **b**, *TFF3* 5′ transcribed region; **c**, *GRM4* proximal promoter; and **d**, *KCNJ8* proximal promoter. The schemes at the top of each panel indicate the TSS, the occurrence of CpGs, the position of exon 1 and the position of the PCR primers used.

promoters in MCF-7 cells before washout and, in agreement with its inhibitory effect on polII, did not induce cyclical methylation in MDA-MB-231 cells (Fig. 3c, bottom right panel).

Transcription generally opposes a repressive environment in which multiple regulatory restrictions have to be overcome before a gene is expressed[15–17]. Functionally, cyclical changes in promoter CpG methylation may parallel changes that occur to the pattern of covalent modifications to histone tails, known as the histone code, which is a well characterized example of covalent marks that dynamically influence transcription[18,19]. We evaluated the effect that doxorubicin-induced methylation cycling in MDA-MB-231 cells has on gene expression. There is no detectable expression of *ERα* or of *pS2* in MDA-MB-231 cells (Fig. 4a), and the promoter DNA is extensively methylated (Supplementary Figs 2 and 5); however, low-level re-expression of ERα protein (Fig. 4b) and *pS2* mRNA (Fig. 4c) occur after exposure to doxorubicin for one hour. Active cytosine demethylation in response to glucocorticoid-induced development that is dependent on topoisomerase activity has been described for the tyrosine aminotransferase gene[20]. By analogy, transient inhibition of topoisomerase II activity by doxorubicin may induce similar effects on a subset of promoters, indicating that methylation cycling alone is insufficient to provoke robust mRNA expression. This is reflected in the limited re-expression of ERα protein and *pS2* mRNA, despite most of promoters in the cell population exhibiting cyclical changes in their methylation status. Kinetic ChIP analysis of the *pS2* promoter in MDA-MB-231 cells after doxorubicin synchronization suggests that local chromatin remains predominately associated with histone H1 and is likely to be condensed. By contrast, cyclical changes in the acetylation status of histones H3 (not shown) and H4 occur.

The observation that broadly similar kinetics of transitory methylation were obtained using different methodologies to synchronize the *pS2* promoter (release from E2 deprivation and from α-amanitin and doxorubicin blockade) and using five different promoters synchronized by doxorubicin treatment (*pS2*, *ERα*, *TFF3*, *GRM4* and *KCNJ8*) may indicate that common sets of events mediate promoter cycling. Further insights into the mechanism and timing of dynamic methylation events on the *pS2* promoter in response to E2 and α-amanitin treatment are provided in a related paper[13]. Transitory modifications in the methylation status of promoters may provide a mechanistic link between transcription and longer term changes in the epigenetic status of promoters. In particular, the finding that doxorubicin can be used to modify the expression of transcribed and quiescent promoters provides a general methodology to analyse the role of cyclical methylation in gene expression.

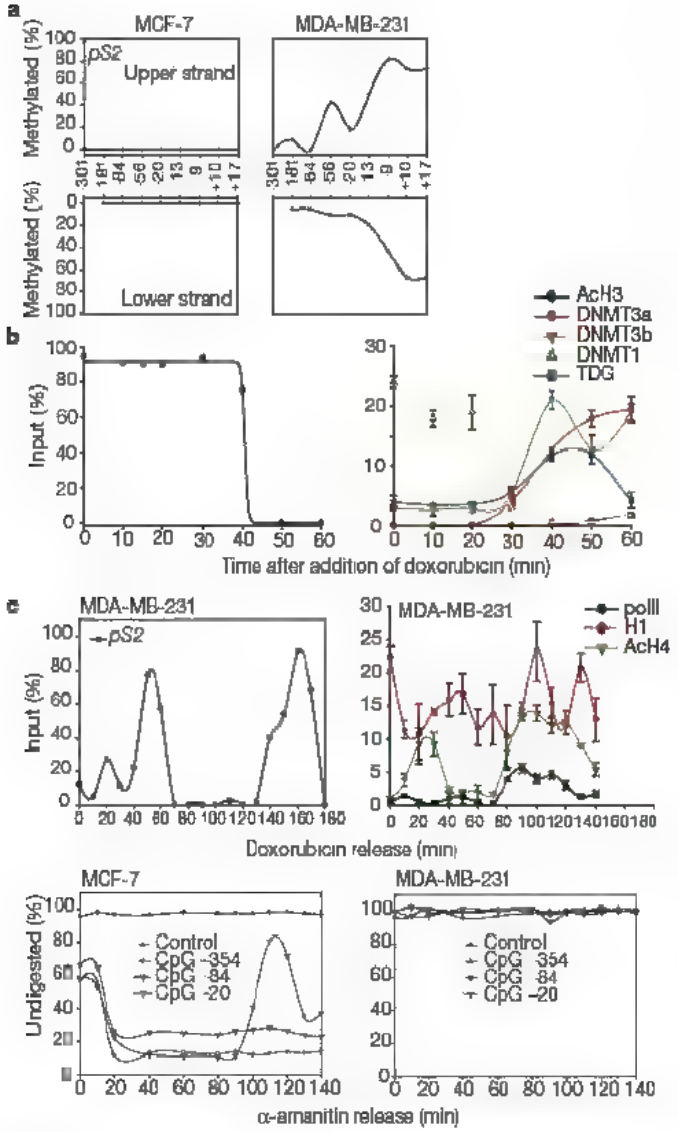

Figure 3 | Doxorubicin induces cyclical changes in the methylation status of transcriptionally inactive promoters. **a**, Bisulphite sequencing of the upper and lower strands of the *pS2* proximal promoter in MCF-7 (left) and in MDA-MB-231 (right) cells was performed to determine the proportion of CpG sites methylated at each occurrence of CpG. **b**, After addition of 300 nM doxorubicin to MDA-MB-231 cells, the methylation status of the *pS2* promoter was characterized by the GST–MBD isolation procedure (**b**, left panel). Serial samples of MDA-MB-231 cells treated with 300 nM doxorubicin were subject to ChIP analysis with the indicated antibodies; mean values ± s.e.m., $n = 2$, are shown (**b**, right panel). **c**, The methylation status of the *pS2* promoter in MDA-MB-231 cells cycles after release from doxorubicin blockade, characterized by selective purification using the GST–MBD fusion protein (**c**, top left). AcH4 and, to a lesser extent, polII, cyclically associate with the *pS2* promoter on release from doxorubicin synchronization, as determined by ChIP with the indicated antibodies (**c**, top right; mean values ± s.e.m., $n = 2$ are shown). Whereas synchronous promoter release from α-amanitin treatment induces cycling in MCF-7 cells (**c**, bottom left), it does not induce either demethylation or cyclical methylation of the *pS2* promoter in MDA-MB-231 cells (**c**, bottom right).

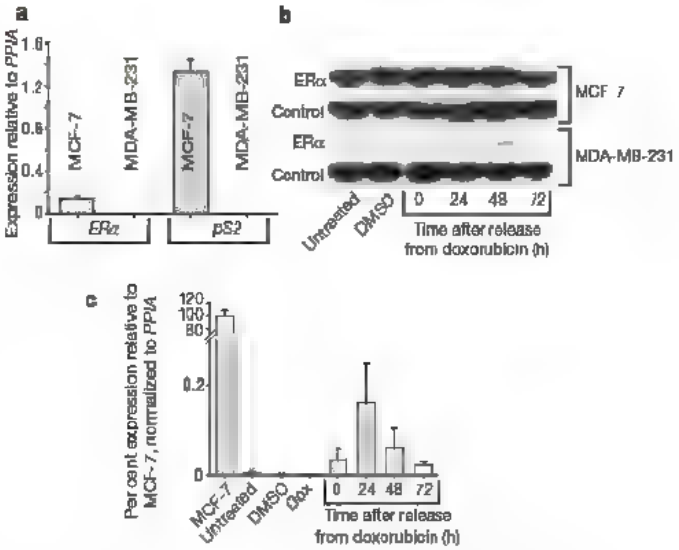

Figure 4 | *ERα* and *pS2* are re-expressed at low levels after transitory treatment with doxorubicin. **a**, The relative expression of *ERα* and *pS2* mRNA was monitored by reverse transcription (RT)–qPCR on RNA isolated from MCF-7 and MDA-MB-231 cells, shown as mean values ± s.d., $n = 3$. Levels were normalized to *PPIA* mRNA, which shows no changes in methylation status or expression under the conditions used. **b**, ERα, detected by HC-20 (Santa-Cruz) in western blot analysis, shows a small, transient re-expression after release from 1 h treatment with doxorubicin. **c**, Similarly, *pS2* mRNA shows transient, low-level re-expression on release from 1 h doxorubicin blockade; mean values ± s.d., $n = 3$, are shown. For **c**, MDA-MB 231 cells were used.

METHODS SUMMARY

Genomic DNA isolation, GST MBD pull-down assays and ChIP. Genomic DNA was isolated as described[21]. GST MBD fusion protein preparation and the GST MBD pull-down were performed as detailed in the Methods. Quantitative PCR (ABI Prism 7500 System, Applied Biosciences) was used to characterize regions of interest, with primers used reported in Supplementary Table 1 (see Methods). ChIP was performed as described previously[10].

Methylation-sensitive restriction enzyme analysis and bisulphite sequencing. Restriction endonuclease analysis and bisulphite sequencing were performed as described[22]. Primer sets used for PCR of digested samples and bisulphite sequencing are reported in Supplementary Table 1. Three biological replicates were used for each bisulphite conversion reaction, with a minimum of 12 clones per cell line, with both DNA strands subjected to sequencing.

RT–PCR and qPCR. For reverse transcription PCR, ~1×10^3 cells were lysed in TRIzol reagent (Invitrogen), and RNA isolated according to the manufacturers instructions. RNA was reverse transcribed using the Superscript III First-Strand Synthesis System (Invitrogen) and subjected to qPCR (ABI Prism7500 System, Applied Biosciences), with primers shown in Table 1 (see Methods)

Full Methods and any associated references are available in the online version of the paper at www.nature.com/nature.

Received 19 September 2007; accepted 10 January 2008.

1. Jones, P. A. & Takai, D. The role of DNA methylation in mammalian epigenetics. *Science* 293, 1068–1070 (2001).
2. Li, E. Chromatin modification and epigenetic reprogramming in mammalian development. *Nature Rev. Genet.* 3, 662–673 (2002).
3. Siegfried, Z. *et al.* DNA methylation represses transcription *in vivo*. *Nature Genet.* 22, 203–206 (1999).
4. Costello, J. F. & Plass, C. Methylation matters. *J. Med. Genet.* 38, 285–303 (2001).
5. Reid, G. *et al.* Multiple mechanisms induce transcriptional silencing of a subset of genes, including oestrogen receptor α, in response to deacetylase inhibition by valproic acid and trichostatin A. *Oncogene* 24, 4894–4907 (2005).
6. Ng, H. H. & Bird, A. DNA methylation and chromatin modification. *Curr. Opin. Genet. Dev.* 9, 158–163 (1999).
7. Duncan, B. K. & Miller, J. H. Mutagenic deamination of cytosine residues in DNA. *Nature* 287, 560–561 (1980).
8. Shang, Y. *et al.* Cofactor dynamics and sufficiency in estrogen receptor-regulated transcription. *Cell* 103, 843–852 (2000).
9. Reid, G. *et al.* Cyclic, proteasome-mediated turnover of unliganded and liganded ERα on responsive promoters is an integral feature of estrogen signaling. *Mol. Cell* 11, 695–707 (2003).
10. Metivier, R. *et al.* Estrogen receptor-α directs ordered, cyclical, and combinatorial recruitment of cofactors on a natural target promoter. *Cell* 115, 751–763 (2003).
11. Gewirtz, D. A. A critical evaluation of the mechanisms of action proposed for the antitumor effects of the anthracycline antibiotics adriamycin and daunorubicin. *Biochem. Pharmacol.* 57, 727–741 (1999).
12. Yokochi, T. & Roberson, K. D. Doxorubicin inhibits DNMT1, resulting in conditional apoptosis. *Mol. Pharmacol.* 66, 1415–1420 (2004).
13. Métivier, R. *et al.* Cyclical DNA methylation of a transcriptionally active promoter. *Nature* doi:10.1038/nature06544 (this issue).
14. Metivier, R., Reid, G. & Gannon, F. Transcription in four dimensions: nuclear receptor-directed initiation of gene expression. *EMBO Rep.* 7, 161–167 (2006).
15. Spector, D. L. The dynamics of chromosome organization and gene regulation. *Annu. Rev. Biochem.* 72, 573–608 (2003).
16. Khorasanizadeh, S. The nucleosome: from genomic organization to genomic regulation. *Cell* 116, 259–272 (2004).
17. Dillon, N. Gene regulation and large-scale chromatin organization in the nucleus. *Chromosome Res.* 14, 117–126 (2006).
18. Mellor, J. Dynamic nucleosomes and gene transcription. *Trends Genet.* 22, 320–329 (2006).
19. Jenuwein, T. & Allis, C. D. Translating the histone code. *Science* 293, 1074–1080 (2001).
20. Kress, C., Thomassin, H. & Grange, T. Active cytosine demethylation triggered by a nuclear receptor involves DNA strand breaks. *Proc. Natl Acad. Sci. USA* 103, 11112–11117 (2006).
21. Nelson, J. E. & Krawetz, S. A. Purification of cloned and genomic DNA by guanidine thiocyanate/isobutyl alcohol fractionation. *Anal. Biochem.* 207, 197–201 (1992).
22. Metivier, R. *et al.* Transcriptional complexes engaged by apo-estrogen receptor-α isoforms have divergent outcomes. *EMBO J.* 23, 3653–3666 (2004).

Supplementary Information is linked to the online version of the paper at www.nature.com/nature.

Acknowledgements The authors thank L. Cortesi, S. Denger and J. Lewis for their critical reading of this manuscript, and J. Blake for his assistance in expression array analysis. This work was supported by the EC 6th framework programme grant CRESCENDO and by the European Molecular Biology Organisation (EMBO).

Author Contributions G.R. and F.G. conceived the study, designed the experimental strategy and analysed data; S.K., B.S. and R.M. contributed to the experimental design. S.K. and B.S. prepared the GST–MBD fusion protein, validated the pull-down method, performed the MBD pull-downs and RT–PCR, and prepared DNA and chromatin for methylation analysis and for ChIP. R.M. performed restriction-sensitive methylation analysis and ChIP. M.P.-S. generated RNA for expression analysis and conducted the western blot studies. D.I., R.P.C. and V.B. produced the bisulphite sequencing results and expression array data from material provided by S.K., B.S. and M.P.-S. G.R., R.M. and F.G. wrote the paper, S.K. prepared the Supplementary Information, and all authors discussed the results and commented on the manuscript. F.G. and G.R. are joint senior authors.

Author Information The gene expression data set reported has been deposited in the NCBI Gene Expression Omnibus (GEO, http://www.ncbi.nlm.nih.gov/geo/) under accession number GSE10145. Reprints and permissions information is available at www.nature.com/reprints. Correspondence and requests for materials should be addressed to G.R. (george.reid@embl.de).

LETTERS

Structure of the DNA deaminase domain of the HIV-1 restriction factor APOBEC3G

Kuan-Ming Chen[1,2]*, Elena Harjes[1,2]*, Phillip J. Gross[1,2,3]*, Amr Fahmy[4], Yongjian Lu[1,2], Keisuke Shindo[1,2,3], Reuben S. Harris[1,2,3] & Hiroshi Matsuo[1,2]

The human APOBEC3G (apolipoprotein B messenger-RNA-editing enzyme, catalytic polypeptide-like 3G) protein is a single-strand DNA deaminase that inhibits the replication of human immunodeficiency virus-1 (HIV-1), other retroviruses and retrotransposons[1–6]. APOBEC3G anti-viral activity is circumvented by most retroelements, such as through degradation by HIV-1 Vif[7]. APOBEC3G is a member of a family of polynucleotide cytosine deaminases, several of which also target distinct physiological substrates. For instance, APOBEC1 edits *APOB* mRNA and AID deaminates antibody gene DNA[8–10]. Although structures of other family members exist, none of these proteins has elicited polynucleotide cytosine deaminase or anti-viral activity[11–16]. Here we report a solution structure of the human APOBEC3G catalytic domain. Five α-helices, including two that form the zinc-coordinating active site, are arranged over a hydrophobic platform consisting of five β-strands. NMR DNA titration experiments, computational modelling, phylogenetic conservation and *Escherichia coli*-based activity assays combine to suggest a DNA-binding model in which a brim of positively charged residues positions the target cytosine for catalysis. The structure of the APOBEC3G catalytic domain will help us to understand functions of other family members and interactions that occur with pathogenic proteins such as HIV-1 Vif.

Full-length human APOBEC3G (also known as A3G) is prone to aggregation and precipitation, especially at high concentrations[1,17]. Residues 198–384 are sufficient for DNA deamination but are similarly insoluble[18]. To circumvent this problem, we tested 31 individual lysine substitution derivatives of A3G(198–384) for activity and solubility. Activity was measured using an *E. coli*-based rifampicin-resistance (Rif^r) mutation assay, which provides a sensitive genetic readout of DNA cytosine deamination activity (for example, see refs 12 and 18). As observed previously for alanine substitutions at these positions[18], many of the lysine substitution mutants retained activity (Supplementary Fig. 1). Several variants, including L234K and F310K, had improved solubility. L234K and F310K were combined to yield a protein that was 2.4-fold more active and 4-fold more soluble (Fig. 1a and Supplementary Fig. 1, data not shown). Three additional non-detrimental substitutions[18], C243A, C321A and C356A, were added to this construct to minimize the possibility of intermolecular disulphide bond formation and to maximize long-term stability (Supplementary Fig. 2). The resulting variant was dubbed A3G-2K3A, and it was 2.7-fold more active and 4-fold more soluble than the parental protein (Fig. 1a, b). Importantly, the DNA cytosine deamination activity of A3G-2K3A was fully dependent on the catalytic glutamic acid E259 (refs 17, 19 and 20, Fig. 1a).

Gel filtration assays were used previously to show that A3G(198–384) is monomeric[18]. To bolster this finding and to assess the integrity of A3G-2K3A, the parental protein and the five-substitution derivative were compared using circular dichroism spectroscopy. The circular dichroism spectra of A3G(198–384) and A3G-2K3A virtually superimposed, indicating that the five-substitution derivative had intact secondary structures (Fig. 1c). Moreover, A3G-2K3A sedimentation velocity analytical ultracentrifugation profiles were nearly identical over a range of concentrations, providing strong evidence that a monomer–dimer or higher order equilibrium is not

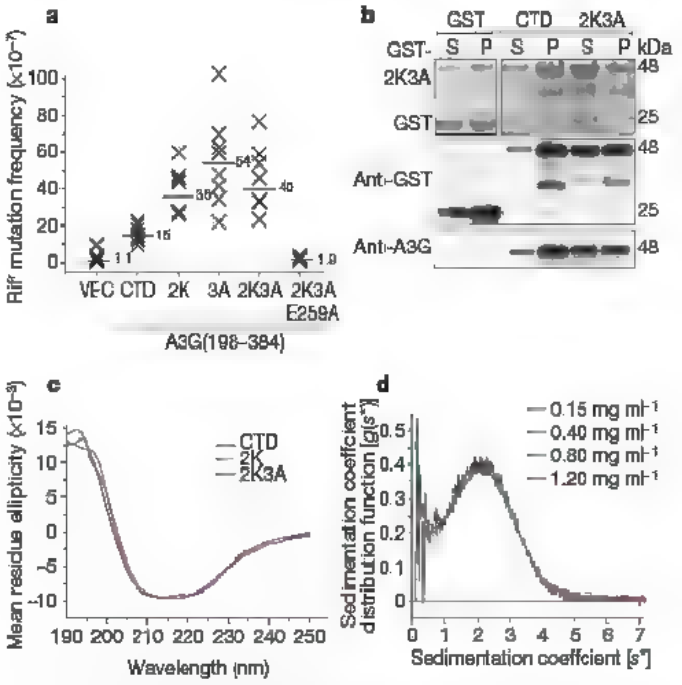

Figure 1 | Functional and biophysical properties of A3G-2K3A. **a**, Capacity of GST–A3G(198–384) (CTD), the indicated mutant derivatives or an empty vector control (VEC) to trigger Rif^r mutations in *E. coli*. Each × represents the mutation frequency of an independent culture, and the median values are indicated. **b**, Solubility of GST, GST–A3G(198–384) (CTD) and GST–A3G-2K3A, as monitored by SDS–PAGE and coomassie blue staining (top panels) or immunoblotting (anti-GST middle panel and anti-A3G bottom panel). **c**, Circular dichroism spectra of A3G(198–384) (CTD), 2K and 2K3A derivatives. **d**, Sedimentation velocity analytical ultracentrifugation profiles for A3G-2K3A. The sedimentation coefficient distribution function $g(s^*)$ is shown for various concentrations of A3G-2K3A. The single peak of the $g(s^*)$ distribution indicates that A3G-2K3A is homogenous and monomeric.

[1]Department of Biochemistry, Molecular Biology and Biophysics, [2]Institute for Molecular Virology and [3]Arnold and Mabel Beckman Center for Genome Engineering, University of Minnesota, Minneapolis, Minnesota 55455, USA. [4]Department of Biological Chemistry and Molecular Pharmacology, Harvard Medical School, 240 Longwood Avenue, Boston, Massachusetts 02115, USA
*These authors contributed equally to this work

occurring (Fig. 1d). These sedimentation velocity data were also used to calculate an A3G-2K3A molecular weight of 22.3 kDa (which is within error of the theoretical 22.6 kDa).

A3G-2K3A was used for NMR spectroscopy experiments (see Methods). A total of 2,008 distance constraints were obtained and used to calculate a solution structure (Fig. 2 and Supplementary Tables 1 and 2). The superimposition of the ten lowest-energy structures demonstrated that this enzyme has a well-defined core structure comprised of five β-strands and five α-helices, arranged from amino to carboxy terminus as β1-β2/2′-α1-β3-α2-β4-α3-β5-α4-α5 (Fig. 2a, b, c). The zinc-coordinating active site, α1-β3-α2, is anchored within the platform of β-strands. The catalytic site is further supported by the α4- and α5-helices, which make extensive stabilizing hydrophobic contacts with the β-strand platform (Fig. 2d). The secondary structural elements are connected by loops of varying lengths, with the β3-to-α2 loop being remarkably well-defined (blue in Fig. 2b). This loop consists of S284, W285, S286 and P287, residues that are conserved among DNA deaminases and that are probably important for the integrity of the active site (see Supplementary Fig. 3 and below).

The A3G catalytic domain shares some features with previously known structures. First, the α-β-α Zn^{2+}-binding motif, α1-β3-α2 in A3G-2K3A, is the clearest structural feature of this deaminase superfamily[11,13–16,21] (Fig. 3, top). Second, a subset of the superfamily members, including human A3G, *Staphylococcus aureus* transfer RNA adenosine-editing protein TadA[21] and human APOBEC2 (ref. 15) (and probably all of the other APOBEC family members), has the β-strand of the zinc-coordinating motif and the two subsequent β-strands arranged in parallel (Fig. 3, bottom). As hypothesized previously, this organization is probably a key determinant of substrate specificity, enabling a loop and additional structural elements to be accommodated between the latter two β-strands[8,15,18,22]. In contrast, cytidine deaminases of *E. coli*, *Bacillus subtilis*, *Saccharomyces cerevisiae* and humans have an anti-parallel β4-β5 organization separated by a small loop[11,13,16,23] (Fig. 3, bottom right). Finally, closer family members, such as APOBEC2 (ref. 15), have a common overall fold and similar secondary structures (Fig. 3 and Supplementary Fig. 4). Several previous reports have discussed and modelled this likelihood[8,15,16,18,22,24].

However, A3G-2K3A differs significantly from all previously reported structures. For instance, the closest family member for which we have structural information[15], APOBEC2, shares only 31% identity overall (Supplementary Fig. 3). As inferred previously[8,15,16,18,22,24], most of these residues are located within the protein core (35 out of the 86 total core residues), consistent with the likelihood that these amino acids are critical for forming the overall scaffold (Supplementary Fig. 4). In contrast, much less identity occurs among solvent-accessible residues (11 out of 68 total solvent-accessible residues), which mediate substrate recognition, catalysis and interactions with other macromolecules (Supplementary Fig. 4). This makes sense in light of evolution, because more than 400 million years have passed since these two proteins were encoded by a single gene (before vertebrate radiation)[8]. Thus, as described below, the A3G-2K3A structure will help us to understand why A3G and other family members (but apparently not APOBEC2, refs 2, 8, 12, 15 and 25) are endowed with DNA cytosine deaminase and retrovirus restriction activities.

In addition to surface residue differences, A3G-2K3A has several remarkable structural features. First, A3G-2K3A (or a derivative in which L234 is restored) has a unique β2 strand, which is interrupted with a bulge of six residues (Fig. 2c and Supplementary Figs 4 and 5; see Supplementary Discussion). In contrast, APOBEC2 has a continuous 11-residue β2 strand, which mediates dimerization through a β2 strand of another molecule[15]. The structural constraints imposed by the β2-bulge-β2′ suggest that different contacts will connect N- and C-terminal domains of A3G. Alternatively, the β2-bulge-β2′ may mediate interactions with RNA and/or other proteins (of cellular and/or viral origin), because it seems to be largely dispensable for DNA deamination activity[18] (Supplementary Figs 1 and 2). However, additional data will be needed to fully discount the possibility that the β2 bulge has a different conformation in the context of the full-length protein. Second, A3G-2K3A begins with β1, whereas APOBEC2 has a small α-helix preceding its first β-strand[15]. Amino acid alignments suggest that residues 198–202 of A3G may form an analogous α-helix (ExPASy proteomix tools, http://ca.expasy.org/),

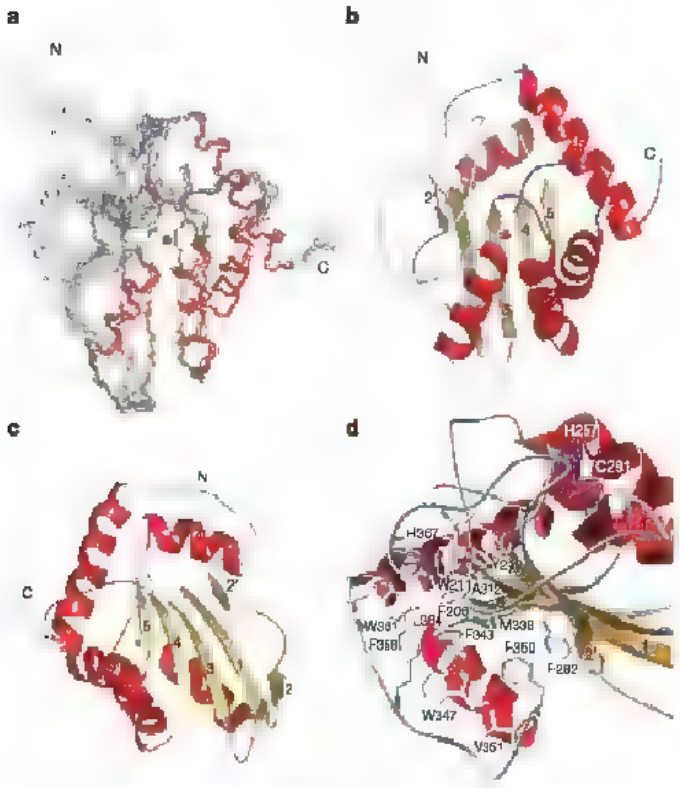

Figure 2 | NMR structure of A3G-2K3A. **a**, Superimposition of ten NMR structures showing α-helices in red, β-sheets in yellow and Zn^{2+} in purple. **b**, **c**, Ribbon diagrams of the NMR structure shown in **a** from the same (**b**) and 180° (**c**) angles, respectively. The β3-to-α2 and β4-to-α3 loops are coloured blue in **b**, and the β2-bulge-β2′ is coloured orange in **c**. **d**, Hydrophobic contacts between α4 and the β-strands and loops of the indicated regions (β1, β3, β4, N-terminal-loop, β3-α2-loop and β4-α3-loop). Amino acid side chain atoms are coloured yellow (sulphur), red (oxygen), blue (nitrogen) and white (carbon). Zn^{2+}-binding side chains are coloured purple.

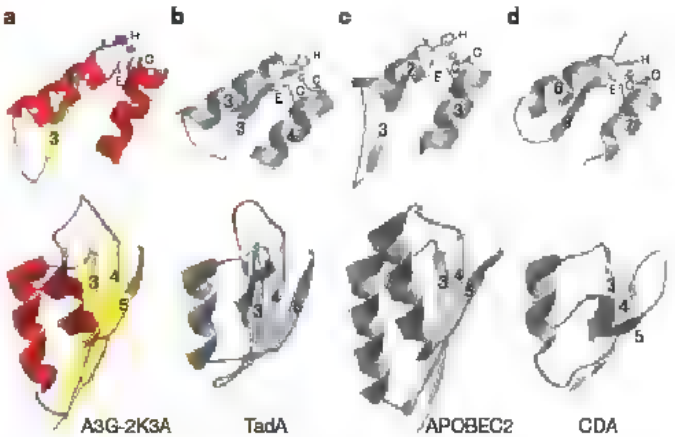

Figure 3 | The relationship of the catalytic domain of A3G to selected family members. **a**–**d**, Human A3G (2jyw), *S. aureus* TadA (2b3j), human APOBEC2 (2nyt) and *E. coli* cytidine deaminase (CDA, 1ctu) Zn^{2+}-binding motifs (top row) and β-strand organization (bottom row). The amino acid side chains of the catalytic glutamic acid (E) as well as the Zn^{2+}-binding histidine (H) and cysteines (C) are indicated.

but this prediction awaits experimental confirmation. Finally, there are many less obvious differences between A3G-2K3A and APOBEC2 (Supplementary Figs 3 and 4). For instance, the zinc-coordinating α1-helix in A3G-2K3A is considerably longer than the corresponding helix in APOBEC2, and the conserved S-W285-S motif in A3G and other DNA deaminases is an S-S-S motif in all known APOBEC2 proteins. Given the prominence of W285 within the A3G catalytic site (discussed further below), it is likely that the S-S-S motif of APOBEC2 contributes to this protein's substrate specificity.

A fundamental question is how A3G and related family members recognize single-strand DNA (ssDNA). Like many other nucleic-acid-interacting proteins, we imagined that A3G-2K3A would have a prominent positively charged surface that would define the DNA-interacting region. However, the electrostatic potential of the active-site face of A3G-2K3A was largely negative apart from a few positively charged residues arranged on an apparent brim surrounding the concave active-site region (Fig. 4a). To test directly whether any of these residues interacted with DNA, NMR chemical shift perturbation experiments were conducted with ^{15}N-labelled A3G-2K3A and varying concentrations of a 21-base ssDNA oligonucleotide, which contained an APOBEC3G 5′-CC deamination hotspot (the underlined C is heavily preferred as a deamination substrate). As expected, significant chemical shift perturbations occurred predominantly on the active-site face of A3G-2K3A (Fig. 4b and Supplementary Fig. 6). Notable perturbations were detected for conserved arginines R215 and R313 and for the catalytic glutamic acid E259. Residues adjacent to R313 (within the β4-to-α3 loop) and E259 also showed strong chemical shift perturbations. The two other brim-domain arginines, R213 and R320, could not be detected with this technique.

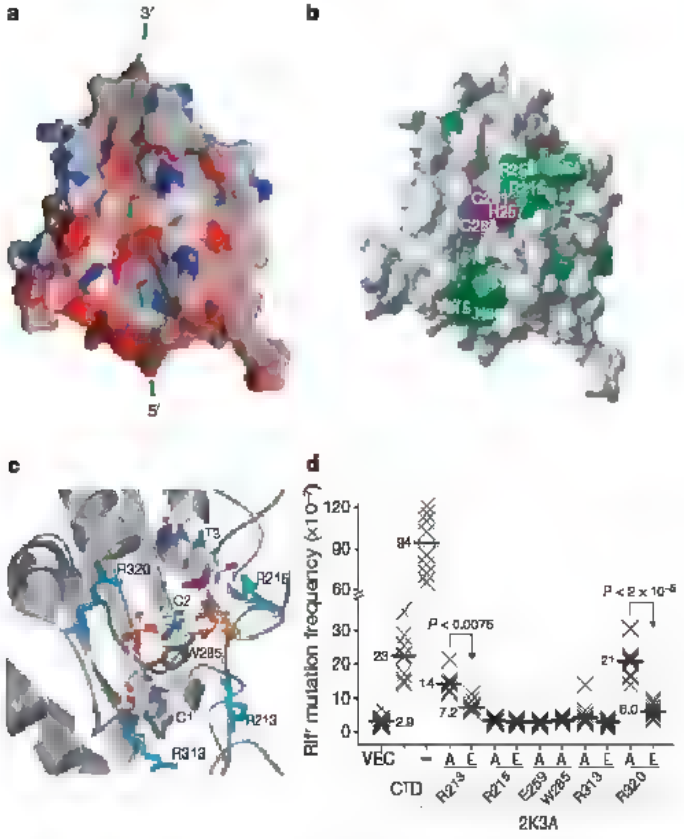

Figure 4 | A3G catalytic domain DNA interaction model. a, Surface representation of A3G-2K3A, highlighting positions of positive (blue), negative (red) or neutral (white) charge. Arginines that brim the concave active site are labelled. The hypothesized position and polarity of ssDNA is indicated (green dashed line). **b,** NMR ssDNA-titration data summary (for details, see Supplementary Fig. 6). Residues with chemical shift perturbations more than 1 s.d. above average are coloured green (E259 is perturbed but hidden by H257). H257, C288 and C291 are shaded purple. **c,** Model depicting the interaction between A3G-2K3A and ssDNA (5′-C_1-C_2-T_3-3′). H257 (purple) is shown partially stacked with the ring of the flipped-out target cytosine (C_2). W285 (grey) helps to form a hydrophobic catalytic cavity. Arginines surrounding the positively charged brim of the active site are indicated (see text for discussion). Single-stranded DNA is coloured white (carbon), blue (nitrogen), red (oxygen) and yellow (phosphate). **d,** DNA deaminase activity of A3G-2K3A derivatives. Each × represents the mutation frequency of an independent culture, and key median values are indicated (others were at background levels). The *y* axis splits to accommodate the high activity of A3G-2K3A, and therefore one CTD data point (52 7) is not shown. The significance of the A versus E substitution at R213 or R320 is indicated (Student's *t*-test).

The NMR titration data were used to build a model for ssDNA binding (Fig. 4b, c and Supplementary Fig. 6, see Methods). First we selected an A3G hotspot containing the trinucleotide 5′-C_1-C_2-T_3-3′ to model the DNA interaction. This short sequence was selected because ssDNA interactions were detected predominantly around the active site and this sequence spans that region. Second, the target cytosine (C_2) was positioned under H257, analogous to how it orients in cytidine deaminase crystal structures[26,27]. Finally, we used all residues that showed significant chemical shift perturbations to calculate the lowest energy structure of an A3G-2K3A–trinucleotide 5′-C_1-C_2-T_3-3′ complex (Fig. 4c).

One notable feature of the DNA-binding model is that the target cytosine is predicted to be flipped-out from the phosphodiester backbone (that is, without flipping, it cannot access the catalytic glutamate E259). A similar substrate contortion was described previously for TadA[21] and a number of other DNA metabolism proteins. The model further predicted that the 5′ nucleotide C_1 would be sufficiently close to interact with the conserved R313. C_1 has a large interaction surface that contributes significantly to the overall predicted trinucleotide-binding energy (−44.7 kcal mol^{-1}). This strong interaction may help to explain the observed specificity of A3G for 5′-CC dinucleotides, which underlies the retroviral genomic strand 5′-GG to 5′-AG hypermutation bias (for example, see ref. 3). We hypothesize that DNA deaminases with different dinucleotide preferences such as AID (5′-RC) or APOBEC3F (5′-TC) will make similarly robust contacts with the 5′ nucleotide. The model also predicted that the phosphate of the 3′ nucleotide T_3 would contact both R215 and R213, and that the C_2 phosphate would interact with R320.

To test this brim-domain model for DNA binding, we first asked whether conserved residues would be required for activity. The model predicted that R215 and R313 would promote DNA binding, W285 would help to form the hydrophobic active site, and E259, as shown previously, would mediate catalysis. As expected, all of these residues proved essential for activity (Fig. 4d and Supplementary Fig. 2). Second, because R213 and R320 were predicted to interact with the phosphate backbone of ssDNA, we hypothesized that they would be influential but non-essential for activity. Accordingly, a non-invasive substitution at these positions might be tolerated, but a negatively charged substitution might render the protein inactive by repelling the phosphate backbone. Indeed, R213A and R320A derivatives still retained 20% of wild-type activity, whereas R213E and R320E derivatives were nearly dead (Fig. 4d and Supplementary Fig. 2). Thus, the A3G-2K3A solution structure, NMR DNA titration data, computational modelling, phylogenetic conservation and DNA cytosine deaminase activity data combined to support the brim-domain model for ssDNA binding.

The catalytic domain of the HIV-1 restriction factor A3G represents the first high-resolution ssDNA deaminase structure. This structure will facilitate studies on related proteins such as the mRNA editor APOBEC1, the antibody gene deaminase AID and other family members that elicit retroelement restriction activity. Although our data strongly support a novel model for DNA interaction, future studies are necessary to understand all of the molecular contacts and to explain major substrate differences such as the specificity for ssDNA over RNA (and *vice versa* for other family members such as APOBEC1). As a practical consideration, we anticipate that similar mutagenesis strategies may be used to improve the solubility

of other family members. Moreover, the A3G-2K3A structure may be used to build accurate models of the N-terminal, Vif-interacting domain of A3G and therefore also models of the full-length protein. The structure presented here therefore provides a crucial step towards a molecular definition of the A3G–Vif interaction, which will benefit the development of AIDS therapeutics that function by modulating this battle between host and pathogen.

METHODS SUMMARY

All expression constructs were based on pGEX6P2-A3G(198–384) (ref. 18), modified by site-directed mutagenesis and confirmed by DNA sequencing. *E. coli* Rif^r mutation assays were used to report the intrinsic activity of A3G(198–384) derivatives[12,18]. Glutathione S-transferase (GST)-based constructs were expressed in *E. coli* strain BL21 DE3 RIL (Stratagene). Unlabelled proteins were produced by expression for 17 h at 17 °C in Luria broth containing 1 mM IPTG and 200 μg ml^{-1} ampicillin. Isotope-labelled proteins were produced by expression for 17 h at 17 °C in M9 supplemented with $^{15}NH_4Cl$, ^{13}C-labelled D-glucose and ^2H water as described[28]. Proteins were purified by sonicating cell pellets in lysis buffer (100 mM NaCl, 50 mM Na_2HPO_4/NaH_2PO_4 (pH 7.0), protease inhibitor (Roche)), separating the soluble (supernatant) and insoluble (pellet) fractions by centrifugation (12,110*g*, 20 min, 4 °C), binding to glutathione sepharose (GE Healthcare), washing with lysis buffer and eluting with PreScission protease (GE Healthcare) in 1 mM dithiothreitol (DTT) and 50 mM Na_2HPO_4/NaH_2PO_4 (pH 7.4), and, finally, concentrating with Centricon filters (Millipore). Solubility was monitored by SDS–PAGE, coomassie blue staining and/or immunoblotting (anti-GST (GE Healthcare) or anti-A3G[20]). Circular dichroism spectroscopy, velocity sedimentation and NMR experiments were conducted as described previously (for example, refs 29 and 30) and details can be found online in Supplementary Information and in the Methods. The ssDNA-binding model was calculated by searching all possible rotamers of the trinucleotide 5′-dCdCdT-3′ and of the side chains of A3G-2K3A residues that showed significant chemical shift perturbations for the lowest-energy complex. The model was only constrained by positioning the target cytosine within the conserved active site, which was estimated from substrate-containing crystal structures[26,27].

Full Methods and any associated references are available in the online version of the paper at www.nature.com/nature.

Received 11 September 2007; accepted 21 December 2007.
Published online 20 February 2008.

1. Chelico, L., Pham, P., Calabrese, P. & Goodman, M. F. APOBEC3G DNA deaminase acts processively 3′ → 5′ on single-stranded DNA. *Nat. Struct. Mol. Biol.* 13, 392–399 (2006).
2. Esnault, C. *et al.* APOBEC3G cytidine deaminase inhibits retrotransposition of endogenous retroviruses. *Nature* 433, 430–433 (2005).
3. Harris, R. S. *et al.* DNA deamination mediates innate immunity to retroviral infection. *Cell* 113, 803–809 (2003).
4. Mangeat, B. *et al.* Broad antiretroviral defence by human APOBEC3G through lethal editing of nascent reverse transcripts. *Nature* 424, 99–103 (2003).
5. Sheehy, A. M., Gaddis, N. C., Choi, J. D. & Malim, M. H. Isolation of a human gene that inhibits HIV-1 infection and is suppressed by the viral Vif protein. *Nature* 418, 646–650 (2002).
6. Zhang, H. *et al.* The cytidine deaminase CEM15 induces hypermutation in newly synthesized HIV-1 DNA. *Nature* 424, 94–98 (2003).
7. Yu, X. *et al.* Induction of APOBEC3G ubiquitination and degradation by an HIV-1 Vif–Cul5–SCF complex. *Science* 302, 1056–1060 (2003).
8. Conticello, S. G., Langlois, M. A., Yang, Z. & Neuberger, M. S. DNA deamination in immunity: AID in the context of its APOBEC relatives. *Adv. Immunol.* 94, 37–73 (2007).
9. Di Noia, J. M. & Neuberger, M. S. Molecular mechanisms of antibody somatic hypermutation. *Annu. Rev. Biochem.* 76, 1–22 (2007).
10. Wedekind, J. E., Dance, G. S., Sowden, M. P. & Smith, H. C. Messenger RNA editing in mammals: new members of the APOBEC family seeking roles in the family business. *Trends Genet.* 19, 207–216 (2003).
11. Betts, L., Xiang, S., Short, S. A., Wolfenden, R. & Carter, C. W. Jr. Cytidine deaminase. The 2.3 Å crystal structure of an enzyme: transition-state analog complex. *J. Mol. Biol.* 235, 635–656 (1994).
12. Harris, R. S., Petersen-Mahrt, S. K. & Neuberger, M. S. RNA editing enzyme APOBEC1 and some of its homologs can act as DNA mutators. *Mol. Cell* 10, 1247–1253 (2002).
13. Johansson, E., Mejlhede, N., Neuhard, J. & Larsen, S. Crystal structure of the tetrameric cytidine deaminase from *Bacillus subtilis* at 2.0 Å resolution. *Biochemistry* 41, 2563–2570 (2002).
14. Ko, T. P. *et al.* Crystal structure of yeast cytosine deaminase. Insights into enzyme mechanism and evolution. *J. Biol. Chem.* 278, 19111–19117 (2003).
15. Prochnow, C., Bransteitter, R., Klein, M. G., Goodman, M. F. & Chen, X. S. The APOBEC-2 crystal structure and functional implications for the deaminase AID. *Nature* 445, 447–451 (2007).
16. Xie, K. *et al.* The structure of a yeast RNA-editing deaminase provides insight into the fold and function of activation-induced deaminase and APOBEC-1. *Proc. Natl Acad. Sci. USA* 101, 8114–8119 (2004).
17. Iwatani, Y., Takeuchi, H., Strebel, K. & Levin, J. G. Biochemical activities of highly purified, catalytically active human APOBEC3G: correlation with antiviral effect. *J. Virol.* 80, 5992–6002 (2006).
18. Chen, K. M. *et al.* Extensive mutagenesis experiments corroborate a structural model for the DNA deaminase domain of APOBEC3G. *FEBS Lett.* 581, 4761–4766 (2007).
19. Navarro, F. *et al.* Complementary function of the two catalytic domains of APOBEC3G. *Virology* 333, 374–386 (2005).
20. Newman, E. N. *et al.* Antiviral function of APOBEC3G can be dissociated from cytidine deaminase activity. *Curr. Biol.* 15, 166–170 (2005).
21. Losey, H. C., Ruthenburg, A. J. & Verdine, G. L. Crystal structure of Staphylococcus aureus tRNA adenosine deaminase TadA in complex with RNA. *Nat. Struct. Mol. Biol.* 13, 153–159 (2006).
22. Huthoff, H. & Malim, M. H. Cytidine deamination and resistance to retroviral infection: towards a structural understanding of the APOBEC proteins. *Virology* 334, 147–153 (2005).
23. Chung, S. J., Fromme, J. C. & Verdine, G. L. Structure of human cytidine deaminase bound to a potent inhibitor. *J. Med. Chem.* 48, 658–660 (2005).
24. Zhang, K. L. *et al.* Model structure of human APOBEC3G. *PLoS ONE* 2, e378 (2007).
25. Mariani, R. *et al.* Species-specific exclusion of APOBEC3G from HIV-1 virions by Vif. *Cell* 114, 21–31 (2003).
26. Teh, A. H. *et al.* The 1.48 Å resolution crystal structure of the homotetrameric cytidine deaminase from mouse. *Biochemistry* 45, 7825–7833 (2006).
27. Xiang, S., Short, S. A., Wolfenden, R. & Carter, C. W. Jr. The structure of the cytidine deaminase-product complex provides evidence for efficient proton transfer and ground-state destabilization. *Biochemistry* 36, 4768–4774 (1997).
28. Devany, M., Kotharu, N. P. & Matsuo, H. Solution NMR structure of the C-terminal domain of the human protein DEK. *Protein Sci.* 13, 2252–2259 (2004).
29. Matsuo, H. *et al.* Structure of translation factor eIF4E bound to m7GDP and interaction with 4E-binding protein. *Nat. Struct. Biol.* 4, 717–724 (1997).
30. Kim, S., Cullis, D. N., Feig, L. A. & Baleja, J. D. Solution structure of the Reps1 EH domain and characterization of its binding to NPF target sequences. *Biochemistry* 40, 6776–6785 (2001).

Supplementary Information is linked to the online version of the paper at www.nature.com/nature.

Acknowledgements We thank R. LaRue, N. Martemyanova, M. Stenglein and S. Wagner for assistance, laboratory members for discussions, V. Pathak for sharing unpublished information, and J. Lipscomb and K. Walters for comments on the manuscript. Key instrumentation was provided by the University of Minnesota NMR Facility (NSF) and Supercomputing Institute, the University of Wisconsin NMRfam (NIH) and the University of Connecticut Analytical Ultracentrifugation Facility. This work was supported by grants from the National Institutes of Health (A.F., H.M. and R.S.H.), the Medica Foundation (MN Partnership for Biotechnology and Medical Genomics (H.M. and R.S.H.)), the University of Minnesota (H.M. and R.S.H.) and the Searle Scholarship Program (R.S.H.).

Author Contributions H.M. and R.S.H. conceived the experimental designs, wrote the manuscript and assisted with experimentation. K.C., E.H., P.G., Y.L., A.F. and K.S. primarily contributed to protein purification, NMR data analyses, activity assays, site-directed mutagenesis, A3G-2K3A–DNA complex modelling and immunoblotting/purification optimization experiments, respectively. All authors contributed to data analyses, figure constructions and manuscript revisions.

Author Information The atomic coordinates for A3G-2K3A have been deposited in the Protein Data Bank under the accession number 2jyw. Reprints and permissions information is available at www.nature.com/reprints. Correspondence and requests for materials should be addressed to H.M. (matsu029@umn.edu) or R.S.H. (rsh@umn.edu).

RETRACTION

doi:10.1038/nature06819

Genetic tracing reveals a stereotyped sensory map in the olfactory cortex

Zhihua Zou, Lisa F. Horowitz, Jean-Pierre Montmayeur, Scott Snapper & Linda B. Buck

Nature 414, 173–179 (2001)

This Article described patterns of labeling observed in olfactory cortex when a transneuronal tracer was co-expressed with single odorant receptor genes in the mouse olfactory epithelium. During efforts to replicate and extend this work, we have been unable to reproduce the reported findings. Moreover, we have found inconsistencies between some of the figures and data published in the paper and the original data. We have therefore lost confidence in the reported conclusions. We regret any adverse consequences that may have resulted from the paper's publication.

Author Contributions L.B.B. and L.F.H. conceived the project, L.F.H. and J.-P.M. prepared gene-targeting constructs to generate the mice, S.S. trained Z.Z. in gene-targeting techniques, Z.Z. prepared and analysed the mice and provided all figures and data for the paper, and L.B.B. and Z.Z. wrote the paper. Correspondence and requests for materials should be addressed to L.B.B. (lbuck@fhcrc.org).

CORRIGENDUM

doi:10.1038/nature06818

Behavioural improvements with thalamic stimulation after severe traumatic brain injury

N. D. Schiff, J. T. Giacino, K. Kalmar, J. D. Victor, K. Baker, M. Gerber, B. Fritz, B. Eisenberg, T. Biondi[1], J. O'Connor, E. J. Kobylarz, S. Farris, A. Machado, C. McCagg, F. Plum, J. J. Fins & A. R. Rezai

[1]JFK Johnson Rehabilitation Institute, Edison, New Jersey 08818, USA.

Nature 448, 600–603 (2007)

In this Letter, Tracey Biondi was omitted from the author list. In addition, a sentence in the Author Contributions statement should be revised to read: 'M.G., B.F., B.E., T.B. and J.O. collected behavioural data and assisted in the development of secondary outcome measures.'.

This Cell's for You

The latest in cell separation technology

New technologies are making it easier than ever before to conduct cell separation. Instead of spending valuable time baby-sitting your experiments to obtain low yields and purity, the latest cell separation advancements give researchers the freedom to walk away with the peace of mind that they will obtain high yields of highly pure and viable cells. Now not only are the cells put through less stress, so are the researchers.

The autoMACS® Pro Separator benchtop cell sorter from Miltenyi Biotec.

Cell Sorting Instrumentation

Miltenyi's autoMACS™ Pro Separator is a benchtop magnetic cell sorter that sorts virtually any cell type from any species and can even isolate cells directly from whole blood or bone marrow. The instrument has an easy-to-use color touch screen. By automating sample uptake and elution of magnetically labeled and non-labeled cell fractions, it minimizes sample handling. State-of-the-art sensor technology monitors the instrument's status. Three different tube racks can be pre-cooled for safe handling of up to six samples. The autoMACS Pro Separator can handle sample volumes ranging from 0.2 mL to 50 mL, separate more than 10 million cells per second, and can fit into a laminar flow hood or safety cabinet.

Another system that isolates virtually any cell type from any species and any sample source is the **RoboSep®** from **STEMCELL Technologies**. This column-free cell separation instrument uses EasySep® technology in an automated format. Kim Nelson, STEMCELL Technologies' Product Manager of Cell Separation remarked, "RoboSep is the only truly automated cell separator. The researcher simply loads the instrument, presses run and can then walk away while RoboSep processes their samples". The system separates up to four samples simultaneously. There is no pre-labeling necessary so researchers only need to select the protocol from the touch screen, load samples and reagents, and let the machine do the rest. The magnetic nanoparticles are compatible for flow cytometric analysis after isolation. All tips are single-use disposable, so there is never a chance for cross contamination since there are no reusable columns or tubing.

The **BD FACSAria™ II** flow cytometry system is the latest high-performance cell-sorting instrument from **BD Biosciences**, a segment of BD (Becton, Dickinson and Company). The second generation FACSAria has several key enhancements. The fluidics and nozzle designs have been changed to improve aseptic setup and accommodate a wider range of particles. It also has a 375nm near-UV laser option to expand its applications, particularly for hematopoietic stem cell analysis. The BD FACSAria boasts configurations with up to four air-cooled, solid state lasers and can detect up to 15 parameters simultaneously, including two scatter parameters.

Upgrades to the BD FACSDiva software and physical alterations decrease setup time and ease the insertion and removal of tube holders. Pierce Norton, Principal Scientist of Instrument Research at BD Biosciences commented, "New systems are bringing the benefits of cell sorting to a broader group of researchers, offering unique and revolutionary features that minimize startup time, improve experiment-to-experiment reproducibility, and increase the sensitivity and resolution needed for multicolor applications." BD plans to offer customers with the first-generation BD FACSAria system the opportunity to upgrade to the capabilities of the new model.

The **Beckman Coulter MoFlo XDP** cell sorter offers a number of advanced functionalities that result in greater productivity and ease-of use for researchers. The MoFlo XDP claims sort rates of up to 70,000 events per second. On top of zero dead time, the MoFlo XDP features digital triggering on any parameter, digital pulse processing, and a true dynamic range of five decades. For cruise control sorting, the IntelliSort function not only allows walk-away operation, but it assures purity and yield, monitors pressure and temperature and provides excellent image quality. MoFlo XDP's Summit Software Version 5.0 determines regions with full parameter resolution, has standard and custom plate sort capability and more

Material compiled by
The Chempetitive Group

BD FACSAria™ II flow cytometry system for cell sorting by BD Biosciences.

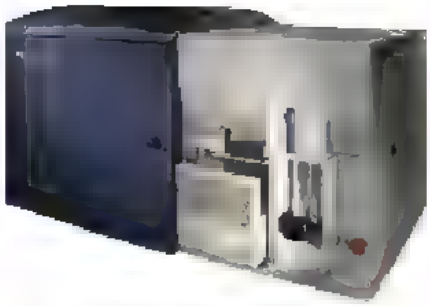

RoboSep® automated cell separation instrument from STEMCELL Technologies.

than one billion event listmode files. Further advantages are high viability, auto-compensation and an easy-to-use workspace concept. The touch screen aXcess Control Panel means user-friendly set up and sorting refinements.

Cell Isolation and Optimization Kits

Cell isolation kits are becoming more sophisticated, and less demanding on cells, allowing researchers to cost effectively sort cells of interest for downstream assays. **R&D Systems PlusCellect**™ cell isolation kits work quickly and accurately by utilizing two analyte-specific antibodies to positively select different epitopes. The kits contain biotinylated analyte-specific Selection Antibody, PE-conjugated Detection Antibody and PlusCellect Buffer. Because targeted cells are tagged with biotinylated antibodies, they work with streptavidin-ferrofluid and magnetic purification systems. Once the cells are resuspended in the PlusCellect Buffer, the efficiency of enrichment can be assessed with the PE-conjugated Detection Antibody. Both negative and positive cell fractions remain viable after separation. For greater purity of small cell populations, the PlusCellect kit can be used with negative selection prior to the positive selection step.

Invitrogen's Dynabeads® FlowComp™ cell isolation kits offer researchers a gentle, simple tube-based isolation method that yields homogeneous, contaminant-free cells. The polymer-coated magnetic Dynabeads have minimal interaction with cells during isolation, prevent the introduction of contaminants such as iron oxides, and save cells from the stress of passing through a dense column. Cells isolated with Dynabeads FlowComp kits thus keep their functional characteristics and are suitable for any downstream cell-based assay such as flow cytometry.

The kit is available for Human CD4 cells, Mouse CD4 cells, Human CD8 cells, Mouse CD8 cells, and Human NK cells. These isolated cells achieve up to 99 percent purity and more than 90 percent recovery.

Isolating Cells from Tissue

The new **Olympus SmartCut Plus** optical-based microdissection system is designed specifically for use in daily micromanipulation routines of both fixed and living cells, and is capable of isolating groups of cells, single cells and cell compartments for downstream molecular analysis. Esther Ahrent, Marketing Communications Manager of Microscopy and Diagnostics at Olympus Life Science Europa GmbH noted, "Isolating the correct biological material for downstream processing is becoming increasingly important; laser microdissection provides a quick and easy way of doing this very accurately." Ideal for pathology, forensic medicine, or teaching and educational purposes, the SmartCut Plus is fully integrated with the inverted Olympus CKX41 microscope, enabling users to simply switch on and start microdissecting. The system uses a high precision, solid-state UV laser and is based on picosecond pulses. Other new SmartCut Plus features include a unique PenDisplay option and advanced software, allowing users to reduce sample handling and possibility of contamination. The instrument incorporates the novel automated single CapLift facility with adjustable contact pressure.

Worthington Biochemical Corp.'s Cell Isolation Optimizing Kit offers a complete method development kit with an assortment of Worthington enzymes referenced in tissue dissociation and cell isolation procedures. This assortment offers versatility in developing a method of obtaining cells from many tissue types and sources in a cost-efficient manner. Also included is a guide which details commonly used tissue types, the mode of action of various enzymes, tissue culture techniques and protocol optimization guidelines. The guide lists hundreds of cell- and tissue-specific isolation references for getting started in enzymatic cell isolation, plus strategies for the handling, use and optimization of methods to achieve maximum yield of viable cells.

"New systems are bringing the benefits of cell sorting to a broader group of researchers, offering novel features that minimize startup time, improve experiment reproducibility, and increase the sensitivity and resolution needed for multicolor applications."

-Pierce Norton
Principal Scientist
Instrument Research
BD Biosciences

Companies mentioned in this Products Focus:

Beckman Coulter - www.beckmancoulter.com
Becton Dickinson - www.bd.com
Invitrogen - www.invitrogen.com
Miltenyi Biotec - www.miltenyibiotec.com
Olympus - www.microscopy.olympus.eu
R&D Systems - www.rndsystems.com
StemCell Technologies - www.stemcell.com
Worthington Biochemical - www.worthington-biochem.com

NATURE|Vol 452|6 March 2008

THE CAREERS MAGAZINE FOR SCIENTISTS

FOCUS
SPOTLIGHT
RECRUITMENT
ANNOUNCEMENTS
EVENTS

nature jobs

PROSPECTS
Scientists under attack

REGIONS
Agribiotech takes root in St Louis

JOBS FEATURES
Focus on physics

COMING SOON
Highlight on Francophone countries (20 March)

A*STAR INVESTIGATORSHIPS

A prestigious award to recruit the young scientific talent

Singapore's Agency for Science, Technology & Research (A*STAR) invites applications for the A*STAR Investigatorships

The **A*STAR Investigatorships** aim to support and promote the early independent career development of the next generation of world leaders in scientific research. Applicants should have obtained their PhD or MD within 24 months (not more than 48 months) of the application date, and should have already demonstrated a strong ability and creativity in research.

The award provides for an **independent** position for a duration of 3+3 years, with a review at the end of the 3rd year and a possibility of "fast-track" promotion. Tenable at one of A*STAR's prestigious biomedical research institutes, **A*STAR Investigators** may select a mentor from A*STAR but will conduct and publish their research independently.

A*STAR Investigators will receive attractive remuneration, support for set-up costs, research funding, research staff and have access to state-of-the-art scientific equipment and facilities including the Biopolis Shared Facilities and the Biological Resource Centre. Each **A*STAR Investigator's** laboratory would be funded with up to US$500K p.a.

Candidates are invited to apply in the following areas:

- **Imaging**
- **Protein Structure & Function**
- **Protein Engineering**
- **Bioinformatics**

The **A*STAR Investigatorship Selection Panel** is composed of:

Professor Tadataka Yamada, President, Global Health Program, Bill and Melinda Gates Foundation

Professor Sir David Lane, Chairman, Biomedical Research Council, A*STAR; Chief Scientist, Cancer Research UK

Professor Edward Holmes, Executive Deputy Chairman, Translational and Clinical Sciences, Biomedical Research Council, A*STAR; Executive Chairman, National Medical Research Council, Singapore

Professor Alex Matter, Director, Novartis Institute for Tropical Diseases

JP1246855R

Up to ten shortlisted candidates will be invited to Singapore for interviews and a review based on a scientific presentation, expected to be held in August 2008. Applications will close on **31 May 2008.**

Applicants are requested to submit their CVs, including 3 academic referees, and a 5-page research proposal (1 hard copy & 1 soft copy) to:

A*STAR Investigatorships
Agency for Science, Technology & Research
20 Biopolis Way, #08-01 Centros
Singapore 138668
Email: A-STAR_ADMIN_BMRC@a-star.edu.sg
www.a-star.edu.sg/astar_investigators

Agency for Science, Technology and Research
SINGAPORE

naturejobs

On the afternoon of 24 February, a group of masked protesters gathered outside the home of a biologist from the University of California, Santa Cruz. According to police reports, insults were hurled at the family home, the front door was battered and the biologist's husband assaulted. Although the identities of the protesters are still unknown, the events bear the hallmarks of an attack by animal-rights activists. If this is true it will be depressingly familiar. A few days earlier, for example, the University of California, Los Angeles, secured a restraining order against five activists who had been harassing a primate researcher (see *Nature* **451,** 1041; 2008).

The tactics deployed by animal-rights extremists aim to intimidate researchers, and there are signs that these activists are becoming more brazen, willing to visit homes rather than just trash laboratories. "I can't imagine, if this continues, that it's not going to give researchers pause," says Frankie Trull, president of advocacy organization the Foundation for Biomedical Research. But as yet there is no evidence of such a trend, although there has been a handful of high-profile cases in which researchers have changed their jobs after being threatened (see *Nature* **444,** 808–810; 2006).

Violent protest and threats are no way to engage in debate and dialogue, and researchers who are involved in humane animal research should bind together as a community to ensure that the extremists' approach doesn't succeed. Working together, the research community can explain to the public the value of its work — as well as promptly communicating any hints of threats to colleagues and administrators. In the United States, researchers would also be wise to tell their deans if their data are requested under the Freedom of Information Act, as this can sometimes be a sign that activists are hunting for targets. And universities need to be proactive. They should identify those researchers who are potential targets and be prepared to offer them additional security. There should be no reason to adjust careers — although for some engaged in animal research, heightened awareness and additional protection may have to become part of the daily routine.

Gene Russo, acting editor of *Naturejobs*

CONTACTS
Acting Editor: Gene Russo

US Head Office
New York
75 Varick Street, 9th Floor
New York, New York 10013-1917
Tel: +1 800 989 7718
Fax: +1 800 989 7103
e-mail: naturejobs@natureny.com

US Sales Manager/Corporations:
Peter Bless
Tel: +1 800 989 7718

San Francisco Office
Classified Sales Representative:
Michaela Bjorkman
West USA/West Corp. Canada
225 Bush Street, Suite 1453
San Francisco,
California 94104
Tel: +1 415 781 3803
Fax: +1 415 781 3805
e-mail: m.bjorkman@nature.com

India
Vikas Chawla
Tel: +91 1242881057
e-mail: v.chawla@nature.com

European Head Office, London
The Macmillan Building,
4 Crinan Street,
London N1 9XW, UK
Tel: +44 (0) 20 7843 4961
Fax: +44 (0) 20 7843 4996
e-mail: naturejobs@nature.com

European Sales Manager:
Andy Douglas (4975)
Advertising Production Manager:
Stephen Russell
To send materials use London address above.
Tel: +44 (0) 20 7843 4816
Fax: +44 (0) 20 7843 4996
e-mail: naturejobs@nature.com
***Naturejobs* web development:** Tom Hancock
***Naturejobs* online production:** Dennis Chu

Japan Head Office, Tokyo
Chiyoda Building, 2-37
Ichigayatamachi,
Shinjuku-ku, Tokyo 162-0843
Tel: +81 3 3267 8751
Fax: +81 3 3267 8746

Asia-Pacific Sales Manager:
Ayako Watanabe
Tel: +81-3-3267-8765
e-mail: a.watanabe@natureasia.com
Business Development Manager, Greater China/Singapore:
Gloria To
Tel: +852 2811 7191
e-mail: g.to@natureasia.com

JOBS OF THE WEEK

Almost in bloom

St Louis wants to become a hub of agricultural biotechnology. All it needs, says **Emma Marris**, is more start-ups and funds.

In the heart of the United States, where the rolling Midwestern plains meet the Ozark Mountains, sits Saint Louis and its environs. The area is a fledgling agricultural biotechnology hub in the midst of the farm belt. But it hasn't quite reached critical mass: the key missing factor is start-ups, which provide risk-taking ideas and young, enthusiastic workers.

Agribiotech focuses on using new tools of genetic investigation and manipulation to try to develop products that outperform traditional crops. Vocal opposition to such products as untested and unnatural has undoubtedly restrained the sector. But increasing population and climate change could spur a large market for crops that offer more nutrition per hectare with fewer inputs such as fertilizer and pesticide. As agricultural biotechnology enters its 'second wave' — in which products are enhanced for the supermarket shopper rather than just the farmer (for example, soya beans that are omega-3 enriched rather than just drought-resistant) — the St Louis area is poised to become the paramount region for the industry in the Americas. Yet challenges remain.

Perception of public resistance

There is agribiotech talent aplenty at Washington University, the various campuses of the University of Missouri, the non-profit Donald Danforth Plant Science Center and the area's industrial behemoth, Monsanto. But a combination of factors including a less-than-entrepreneurial culture and public resistance (or the perception of public resistance) to the technology's products has led to few new small companies being founded by scientists.

Much of the area's strength flows from Monsanto, where business is booming. The company is 'stacking' various yield-increasing traits together in single seed lines to rake in the cash, but its pipeline also contains second-wave crops with lipid or protein enhancements or complex traits such as drought tolerance.

In the 1990s and early 2000s, the company now known as Monsanto shed its chemical and drug parts to focus solely on agriculture. Net sales have grown each year since 2003. For fiscal year 2007, sales totalled more than US$8.5 billion, and research and development spending was $780 million, or more than $2 million a day. The company says it will invest 10% of its sales in research and development in 2008.

The advantages of working for Monsanto are many. The scientific talent and lab facilities are top-notch. The gene libraries are extensive and exclusive. At a lab in the suburb of Chesterfield, the company spends $4 million a year on electricity, mostly to run 122 growth chambers crammed with bar-coded plants and plant tissue — each one a potential blockbuster.

But Monsanto is also extremely secretive, even keeping exact employee numbers hush-hush for "competitive reasons". All employees sign a confidentiality agreement. Publication can follow only after patent protection. The tour guide at the Chesterfield lab even hints at "all kinds of fun toys I can't show you". Because of the culture of secrecy, and because of their number, scientists at Monsanto have their own internal community with poster sessions, a competitive fellows programme, and even awards, complete with ceremonies at the Ritz-Carlton Hotel.

T SPIEGEL/CORBIS

According to Karen Wishart, vice-president for human resources at Monsanto, the culture is very "team oriented", with rewards and incentives being doled out to the interdisciplinary teams that the company shuffles to keep things fresh and its employees engaged. The company is also very "results oriented", meaning it doesn't forget that the goal is to make products that farmers want to buy — and it makes sure its employees don't forget either. Monsanto employs about 3,300 scientists worldwide, double the number of four years ago. About 2,500 are in the United States, and most of those are in Missouri.

Monsanto is still hiring. "We're growing quickly," says Wishart. "And the baby boomers are retiring on top of our growth phase." According to Alexandra Doronkin, who heads recruitment for scientific and regulatory positions in Monsanto, the company's research and development corps is hiring several hundred scientists a year.

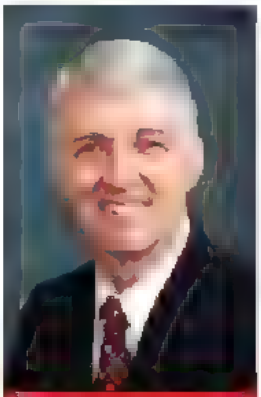

"If you ask where is the most discovery science that leads to new inventions, I think St Louis is in the top few."
Roger Beachy

DANFORTH CENTER

And Doronkin has a wish-list: researchers with the core skills that Monsanto will need for the foreseeable future — molecular biology, biochemistry, systems biology, agronomy, pathology and genetics — plus traditional plant breeders, scientists with business training and bioinformaticians. Its mammoth greenhouses are growing hectares of data that need to be mined and analysed. And sifting through millions of genes for the ones that will boost yield, resist pests, increase nutritional value and, above all, sell, requires more than just molecular biology skills; business savvy counts. But she realizes what attracts scientists. "The main draw for the scientists is the cool science, the cool technologies and the incredible impact," she says.

Humanitarian goals

Across the street from the concrete solidity of the Monsanto campus lies the non-profit Donald Danforth Center, which looks a little like a kitchen island. Here, Roger Beachy, whose disease-resistant tomato was the plump red opening note to the agricultural biotechnology era, runs a team of scientists intent on using agribiotech advances to aid humanitarian efforts. The Danforth Center is in some ways the hip young kid on the block. Established in 1998, it is just now hiring the last of its core investigators.

The Danforth, with its 19 principal investigators, is much smaller than Monsanto, and consequently hires

less, but it too is interested in bioinformatics. The most qualified people have good molecular-biology and plant skills, according to Billie Broeker, director of human resources for the organization. "We need people who can do greenhouse work and tissue-culture work in sterile conditions," she says. Researchers work with everything from mass spectrometry to exotic tissue culture. "You don't have to just work in *Arabidopsis*; you can work in corn, soya, cassava," says Jan Jaworski, vice-president for research.

Recently, Enterprise Rent-A-Car donated $25 million to the Danforth to create an institute of renewable fuels. Despite the potential downsides of corn based ethanol and other biofuels, they are likely to be a part of the energy future in the United States. The recently passed energy bill has substantial research funds: $75 million for research on "biofuel production technologies in states with low rates of ethanol production", and $50 million for university-based research on cellulosic ethanol. This year's farm bill is expected to have hundreds of millions for biofuel research.

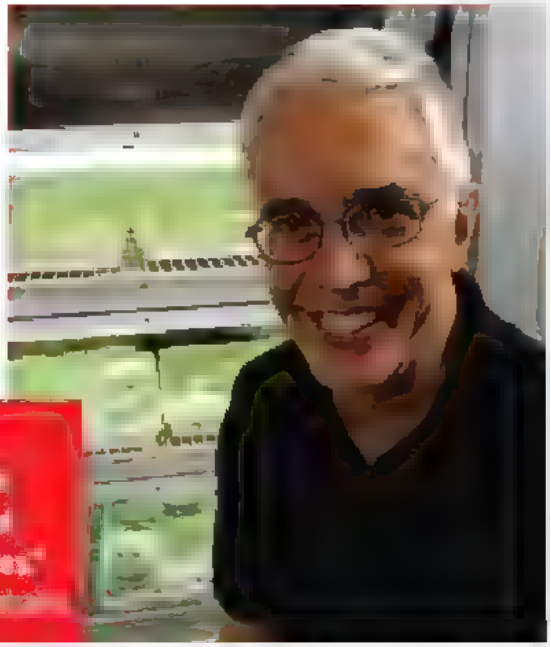

J. ANGELES/WASHINGTON UNIV

Revolutionary hopes

Beachy's office is studded with African masks and other reminders of the part of the world in which he hopes agricultural biotechnology will be most revolutionary. He seems a bit weary when it comes to questions about why European activists hate genetically modified crops. But when asked about St Louis as a possible agribiotech hub, his blue eyes engage. "If you look at it and say where is the most discovery science that leads to new inventions — I think we are in the top five," he says. He estimates there are about 500 plant-science PhDs in the St Louis area.

But Beachy admits that St Louis has yet to dominate the sector. "I lived in San Diego and felt the energy, excitement and upbeat attitude. People were starting things in garages," he recalls. "We are not there; we have to mature. And if you look at the venture-capital market, it is more conservative than it was five years ago." He laments the negative impact of the Ventria Bioscience case, in which politicians and companies such as the brewery giant Anheuser-Busch unexpectedly blocked Ventria's plans to cultivate anti-diarrhoeal genetically modified rice in Missouri. They worried the rice would contaminate other fields. "It stunned the state," says Beachy, suggesting that lawmakers bowed to the pressure too readily.

Still, rosier days could be ahead for biotech. Missouri is using some settlement money from a tobacco-company lawsuit to stock a life-sciences research trust fund. A total of $13.1 million was split among 14 projects in Missouri, including a bioplastics collaboration between the Danforth and Boston-based Metabolix, which will open an office at the Nidus Center, an incubator in St Louis.

Another project funded with tobacco money is the new International Center for Advanced Renewable Energy and Sustainability at Washington University. Run by Himadri Pakrasi, this $55-million endeavour, with a building currently under construction, will research biofuels in collaboration with scientists worldwide. "We are going after carbon sequestration, biofuels, cellulase enzymes and micro algae," he says. There will be five new endowed positions.

Washington University has had a long tradition of plant sciences, carried on by Ralph Quatrano, chairman of the biology department and co-leader of a team that has just sequenced the genome of the moss *Physcomitrella patens*. The department has strong links with the Danforth Center and the Missouri Botanical

DANFORTH CENTER; E. MARRIS, MONSANTO

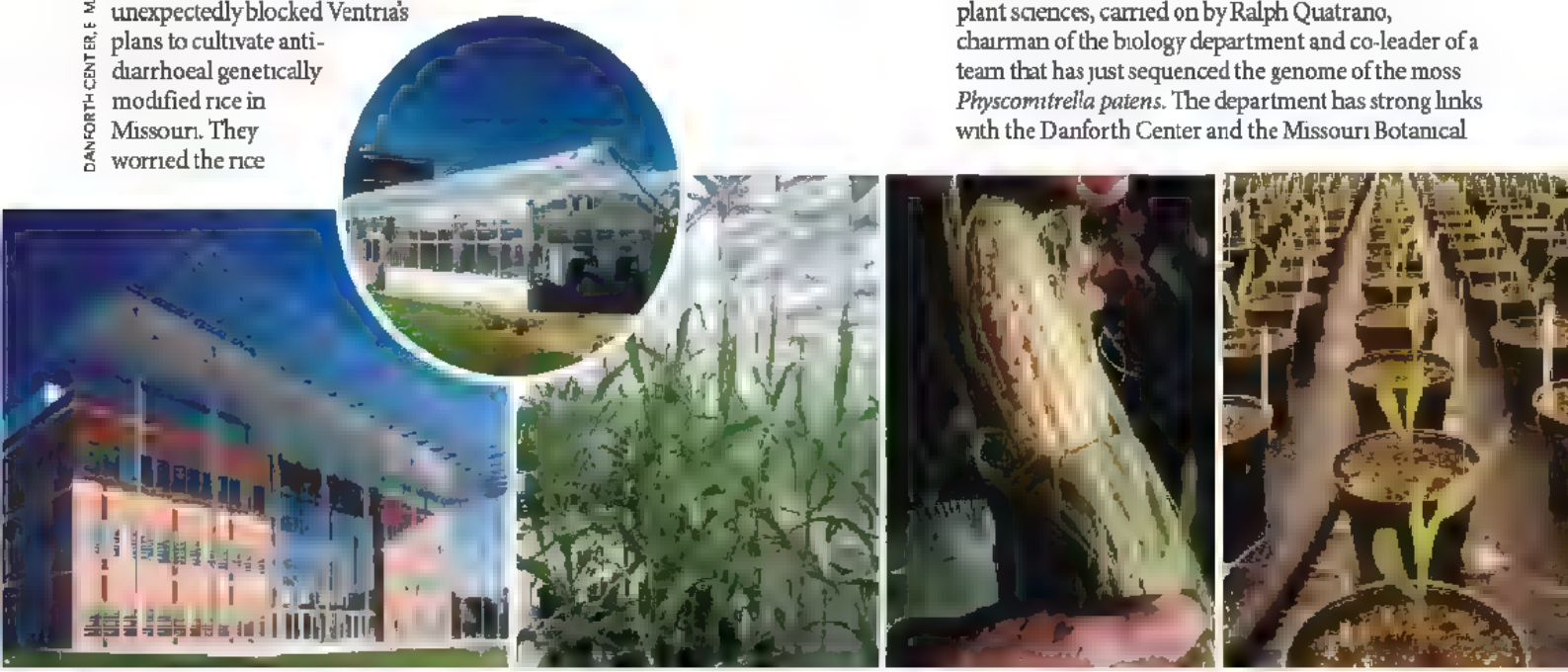

Transparency and secrecy: greenhouses (inset) at the Danforth Center (far left) and Monsanto's crops (above centre and right).

E. MARRIS, MONSANTO

St Louis is pinning its hopes on growth within the agribiotech sector with crops such as maize (left) and soya.

Garden, which specializes in plant ecology and taxonomy. "The future," says Quatrano, "is interaction with engineering and physical sciences. We have these huge data sets in the genomic age. Quantitative computational expertise is absolutely necessary."

Complex boutique crops of the future

Meanwhile, two hours' drive east of St Louis is the University of Missouri, in the college town of Columbia. Faculty members here are more explicitly focused on agricultural research, especially on creating crops that do more than pack calories into hectares. There is a spotlight on human health, such as adding nutrients and medicines to crops. "I think this is what the future of agriculture is going to be in the United States," says Thomas Payne, dean of the College of Agriculture, Food and Natural Resources. "We have a lot of competition in commodity agriculture around the world." So the United States, he says, can make the complex boutique crops.

The biggest challenge at the University of Missouri is money. The state is less generous than it once was, and federal budgets are tight at the National Institutes of Health, the National Science Foundation and the Department of Agriculture. Payne is seeing his faculty members recruited away from him. "We are the bottom of the barrel in terms of compensation," he admits. The college is letting its faculty numbers drop a bit, so it can give more to the remaining faculty members. Any new hires are likely to be what Payne calls "professional track" — faculty members eventually destined for the public sector, who pay their own way with grants.

On the same campus is the headquarters of the Illinois–Missouri Biotech Alliance — the office of Ken Schneeberger, an assistant dean under Payne. The alliance used to fund biotech science in soya and maize (corn) to the tune of $1 million a year, until Washington cut off its funds. Schneeberger hopes that it will be back in the 2009 budget. Its biggest achievement so far has been developing some lines of soya bean that are resistant to cyst nematode.

The lack of start-up companies in Missouri continues to be an issue, says Nick Kalaitzandonakes, head of the Economics and Management of Agrobiotechnology Center at the University of Missouri. Yet he is optimistic about the region. "If you read the newspaper, you would think that agricultural biotechnology is going nowhere," he says. "But if you look at the acreage being planted with it, the future looks pretty good." He blames onerous federal safety regulations and a culture that does not reward entrepreneurialism for the shortage of start-ups. "The industry has a small number of large players," he says.

Still, he says, the University of Missouri system and Washington University together will probably spend between $400 million and $600 million on research in the field. All that is needed are some business-savvy scientists to really get things humming. Kalaitzandonakes' advice to young scientists shaping their career in agribiotech is simple. "Take a few business classes. Go visit your local angel investor and put yourself out there."

Start-up activity is picking up, says Robert Calcaterra, head of the Nidus Center, which opened in 1999. He has worked with 20 baby businesses, some of them agricultural biotechs. "In 1999, I could count on two hands the number of companies in the plant biosciences," he says. Now, with Nidus, an incubator called the Center for Emerging Technologies and other fledgling companies working alone, he estimates the total could be as high as 35. Calcaterra hopes to see significant growth in another five years.

J. ANGELES/WASHINGTON U/NIV

G. CHRONIS

Optimistic: Himadri Pakrasi (top) and Nick Kalaitzandonakes.

Mean streets

St Louis itself, the centre for all this would-be entrepreneurial action, is a slightly shabby depopulated former industrial town with the classic crime-ridden core ringed by car-friendly suburbs. It is number two on the latest list of most dangerous US cities, compiled annually by *Congressional Quarterly*, although there are some revitalization schemes. According to Bob Kranz, a researcher at Washington University, it can be hard to tempt graduate students in from the coasts, despite the low cost of living.

It's one of several challenges. If St Louis is to become a hip, feisty biotech hub, it will have to overcome public perceptions about genetically modified organisms, about St Louis, and about the wisdom of betting on a fledgling biotech cluster that has yet to prove its mettle despite ample promise. Only then might it become the centre of another agricultural revolution. ■

Emma Marris is a correspondent for *Nature*.

Put Your Passion to Work:

THE MONSANTO EXPERIENCE

At Monsanto, we're passionate about using science and technology to improve agriculture. We invest about $1.5 million a day to look for and bring to market the innovative technologies that our customers tell us make a difference. It's research that's about more than just biotechnology. We use many tools – like genomics, conventional and molecular breeding, crop analytics, animal productivity, chemistry and biotechnology – to bring forward new products to answer our customers' needs, in turn, providing benefits to not only the farmer, but processors and consumers, as well.

At Monsanto, we believe in -

INNOVATION IN AGRICULTURE

Advanced science and innovative technology are at the heart of our company. We are committed to developing science based solutions to make our farmer customers more productive and profitable. Our employees are making a difference by feeding the world while preserving the environment.

EXCELLENCE

People at Monsanto are driven to do extraord nary things and are dedicated to being the best in our industry.

GREAT WORKING RELATIONSHIPS

Monsanto is team based with highly qualified professionals sharing knowledge, creating a great place to work and allowing employees to take ownership for results

To learn more about Monsanto, our passion and our opportunities, visit **www.monsanto.com**.

Come grow with us.

MONSANTO
imagine™

Monsanto values diversity and is an equal opportunity affirmative action employer M/F/D/V

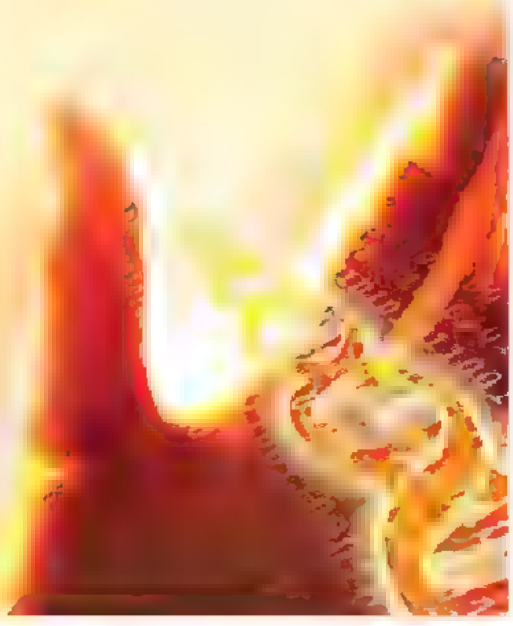

NW125349R

Sprouting Success

CULTIVATE DISCOVERIES

A national leader in plant genomics research, MU is 7th in the nation in plant sciences funding from the National Science Foundation.*

BLOOM WITH TOP SCIENTISTS AND STUDENTS

At MU nearly 50 faculty-led research teams combine genomic, proteomic, informatic, biochemical, physiological and ecological approaches to study plant biology and its application to agriculture, natural resource management and comparative medicine.

THRIVE IN A COLLABORATIVE ENVIRONMENT

State-of-the-art research facilities include:

Center, proteomic, genomic, imaging and cytology cores; 20,000-plus square feet of greenhouse and growth chamber resources; phytonutrient/phytochemical and phytotherapy centers; National Soybean Biotechnology Center; Agricultural Experiment Station; and Interdisciplinary Plant Group.

*Based on most recent comparative data from NSF

University of Missouri
www.missouri.edu

FACULTY POSITION IN CARDIOVASCULAR BIOCHEMISTRY

DEPARTMENT OF BIOCHEMISTRY AND MOLECULAR BIOLOGY
SAINT LOUIS UNIVERSITY SCHOOL OF MEDICINE

Saint Louis University, a Catholic Jesuit institution dedicated to student learning, research, health care, and service is seeking applicants for a faculty position in the Edward A. Doisy Department of Biochemistry and Molecular Biology for a tenure-track position involving research and teaching at the ASSISTANT PROFESSOR level, although outstanding candidates at a more senior level will be considered. The department is housed in the E.A. Doisy Research Center, a brand new state-of-the-art facility designed to foster collaboration between investigators. We seek applicants who use innovative approaches in the areas of cardiovascular biology, metabolism and signaling. Cardiovascular research is a growing focus area at the School of Medicine with strengths in lipidomics, cell signaling, systems biology and molecular basis of cardiovascular disease. We are interested in a highly interactive candidate whose interests will complement ongoing research programs in the cardiovascular sciences in the Department as well as the University.

The successful candidate is expected to establish a strong extramurally-funded research program. A potential for or demonstrated evidence of competing successfully for external funding will be important criterion for selection. Excellent start up funds and salary are available. Interested candidates must submit a cover letter, application and current curriculum vitae to http://jobs.slu.edu. Additionally send current curriculum vitae, description of research plans, and at least three letters of recommendation to:

Search Committee
c/o William S. Sly, M.D., Chairman
Edward A. Doisy Department of
Biochemistry and Molecular Biology
Saint Louis University School of Medicine
1100 South Grand Blvd.
St. Louis, MO 63104-1028

Saint Louis University
is an Affirmative Action, Equal Opportunity Employer, and encourages nominations and applications of women and minorities.

NW123561R

Division of Immunobiology Faculty Position

Saint Louis University, a Catholic, Jesuit institution dedicated to student learning, research, health care, and service, is seeking applicants for tenure-track faculty positions in the Division of Immunobiology, beginning immediately. The primary goal of the new Division of Immunobiology is to perform cutting-edge translational research in areas of human immunology. An internationally renowned Center for Vaccine Development has been in existence within the Saint Louis University Department of Internal Medicine for the past 20 years, and will provide important collaborative opportunities for researchers in the Division of Immunobiology. Current projects at the Center for Vaccine Development include studies of mucosal immunity, TB vaccine development, as well as vaccine development for potential pandemic influenza, small pox and hepatitis C. The Microbiology and other basic science programs at Saint Louis University have multiple investigators with ongoing active research programs in molecular virology, macrophage biology, immune-mediated pathology and innate lung immunity.

The School of Medicine has provided generous start-up packages for multiple new faculty to be recruited into this new Division of Immunobiology. Dr. Daniel F. Hoft, MD, PhD has been appointed the Director of this new Division. Dr. Hoft is an infectious Diseases expert and molecular immunologist who currently is the PI of 3 NIH grants focused on the development of vaccines for mucosally invasive intracellular pathogens, such as *Mycobacterium tuberculosis*, *Trypanosoma cruzi*, smallpox and influenza. His lab also has a special interest in studying the role of γδ2 T cells in human vaccine immunity.

Dr. Hoft is interested in recruiting MDs and MD/PhDs with clinical expertise and research interests in vaccine immunobiology, human cellular immunity, immunogenetics, autoimmunity, cancer immunobiology, transplant immunobiology and/or allergy/immunology working towards the development of prophylactic vaccines and immunotherapies effective against human diseases. It is expected that these new faculty will spend some time performing clinical work in their area of expertise, but the majority of their time will be devoted for research. This new Division of Immunobiology will be housed in a brand new 80 million dollar research complex on target to open in the Fall of 2007.

Interested candidates must apply online at http://jobs.slu.edu. All other correspondence regarding this position may be directed towards Dr. Hoft (contact information is shown below).

Daniel F. Hoft, MD, PhD, Professor and Director,
Division of Immunobiology
Departments of Internal Medicine & Molecular Microbiology
Email: hoftdf@slu.edu
Website: http://internalmed.slu.edu/immunobio/

Saint Louis University is an Affirmative Action, Equal Opportunity Employer and encourages nominations of and application from women and minorities.

NW126753R

Call for access to Synchrotron Beamline Facilities 2008 EMBL Hamburg, Germany

EMBL

We announce a call for synchrotron beam time applications in biological X-ray crystallography (PX) and small-angle scattering (SAXS). Up to 12 weeks of beam time will be available at the DORIS storage ring (DESY) during the period September 2008 until December 2008. The EMBL Outstation will operate the following beamlines:

Beamline	Type	Wavelength	Scientist responsible
X11	PX	0.80 Å	Paul Tucker
X12	PX	tuneable	Manfred Weiss
X13	PX	0.80 Å	Matthew Groves
X33	SAXS	1.5 Å	Dmitri Svergun

The deadline for submission of proposals is May 16th, 2008. An external Priorities Committee will assess the proposals.

Electronic beam proposal forms and detailed description of the beamline facilities are available via the web links **http://www.embl-hamburg.de** and **http://www.embl-hamburg.de/facilities**

In parallel, EMBL-Hamburg is constructing three new beamlines for applications in biological X-ray crystallography (PX) and small-angle scattering (SAXS) at the Petra-III synchrotron storage ring, with an expected opening in 2010/11. Further information can be obtained under **http://www.embl-hamburg.de/services/petra**.

Two of the DORIS-III beamlines (BW7A, BW7B) will be used as test beamlines for future Petra-III applications. Depending on circumstances, they may become temporarily available to the external user community.

Applications to use the EMBL-Hamburg high-throughput crystallisation facility can be made at any time at http://www.embl-hamburg.de/services/crystallisation

For further information
tel. +49-40-89902-110,
fax +49-40-89902-149 or email
beam@embl-hamburg.de (PX),
svergun@embl-hamburg.de (SAXS)

Access to the EMBL Hamburg beamline facilities is supported by the European Commission, Research Infrastructure Action under the FP6 "Structuring the European Research Area Specific Programme", Contract Number RII3-CT-2004-506008.

www.embl.org

W127008A

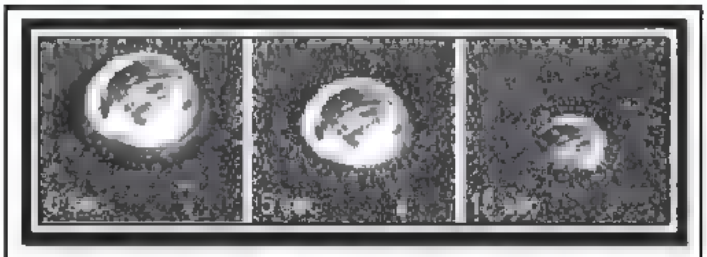

In the Disordered Media group of the Leiden Institute of Physics, a three-year postdoc position is available

The project concerns novel experiments to probe the transition from granular fluids to granular glasses. Both states will be generated in so-called split-bottom shear cells, and be probed by video imaging and rheometry. The project is part of our broader effort to investigate the slow flow and jamming of granular media and foams, focussing on the interplay between mesoscopic organization and macroscopic flow features. For details see our web page www.physics.leidenuniv.nl/sections/cm/grm/

We are looking for candidates with a PhD in experimental physics, preferably with experience in soft matter experiments. Applications, including CV, statement of interest and contact details of two or three referees should be sent by mail or e-mail to Dr. M. van Hecke, Kamerlingh Onnes Laboratories, PO Box 9504, 2300 RA Leiden, the Netherlands

W126471R

UNIVERSITY OF LIVERPOOL

Fully-funded PhD Studentships available for 2008-09*

The Physics Department of The University of Liverpool leads research at the frontline of Particle, Nuclear Condensed Matter and Accelerator Physics (http://www.liv.ac.uk/physics/research/).

The Department has achieved the top grade of excellence in three consecutive reviews by HEFCE - the national Research Assessment Exercise. It is also very well funded and currently enjoys the highest research income of any Physics department from research councils in the UK.

Physics postgraduate students at The University of Liverpool benefit from an excellent training environment comprising of advanced lectures and technical courses delivered by the Department, as well as transferable skills workshops organised by the University Graduate School (http://www.liv.ac.uk/gradschool/).

The Department of Physics is seeking outstanding applicants for PhDs in Particle, Nuclear Condensed Matter and Accelerator Physics. Studentships are awarded on a competitive basis. The University of Liverpool is committed to ensure equality of opportunities and to promote diversity.

* Eligibility criteria include UK or EU citizenship.

Contact:
Dr Mariella Chartier
Department Director of Postgraduate Research
chartier@liverpool.ac.uk
+44 (0) 151 794 6775

U126804R

We are the largest interdisciplinary research centre in Europe and work in the following research fields: Energy, Information, Life, and Environment.

For our Institute of Solid Research (IFF) we are seeking

4 Ph.D. Students for three-year projects

- code D011/2008 -

working in our research focus „highly correlated electron systems" and „nanomagnetism. The students will be inscribed at the Elite University RWTH Aachen

We expect from you:

- Completed study of physics, chemistry or materials science with a good or very good diploma or master degree
- good language skills in English
- sound knowledge of solid state physics or chemistry
- ability to work in a team as well as mobility and high motivation.

Equal opportunities is an important cornerstone of our staff policy at Research Centre Jülich, for which we have been awarded the „TOTAL E-QUALITY" award. Applications from women are therefore particularly welcome. Applications from disabled persons are welcomed

Payment will correspond to salary grade 13/2 Collective Agreement for the Civil Service (TVöD).

Please send your application with the relevant documentation to:

Mr D Schlotmann
Institut für Festkörperforschung (IFF-4)
Forschungszentrum Jülich GmbH
52425 Jülich
Telefon: 02461 61-4465

Further Informationen at:
www.fz-juelich.de

JÜLICH
FORSCHUNGSZENTRUM

W126128R

UCL

University College London
The London Centre for Nanotechnology

LCN
LONDON CENTRE FOR NANO TECHNOLOGY

Deputy Director, Business

The London Centre for Nanotechnology (LCN) is a joint venture, capitalized at around £30M, between University College London (UCL) and Imperial College London, to use nanotechnology for solving major scientific, medical and engineering problems.

The Deputy Director will manage high-value research facilities, major strategic initiatives and seek revenue opportunities in private and public sectors. In addition, he/she will take responsibility for branding, marketing, media relations and LCN business practices.

The candidate will need strong business and marketing skills and will also be an exceptional communicator with business, government, academia and the broader public. Additionally the candidate will have experience in senior management in science and technology facilities. A PhD or MSc are desirable and a degree in a technical, engineering, physical, medical or life sciences subject is considered essential.

The salary is negotiable and commensurate with the candidate's experience. Further details about the job and how to apply are available at www.london-nano.com

Closing date: 28th March 2008

We particularly welcome female applications and those from an ethnic minority as they are under-represented within UCL at this level

U126978R

Endowed Chair at Duke University in Experimental Condensed Matter Physics

The Department of Physics at Duke University invites applications and nominations for an Endowed Chair in Experimental Condensed Matter Physics, including Biological Physics, at the tenured Full Professor level to begin on or after January 2009. We are looking for candidates who have a primary interest in the fundamental physics of hard or soft condensed matter systems and demonstrated excellence in research and teaching. The successful candidate is expected to lead a world class program and will benefit from potential overlap with current university thrusts in nanoscience, imaging, and/or optics and photonics.

Applications should include a complete curriculum vitae and publication list, and a statement of research and teaching.

Application should be made via https://academicjobsonline.org

Additional material may be sent to: Prof. Robert Behringer, Chair of the Search Committee, c/o Florin Damian, Department of Physics, Duke University Box 90305, Durham, NC 27708-0305.

The search committee will begin evaluation of applicants on April 1, 2008. Duke University is an Equal Opportunity/Affirmative Action Employer; we particularly encourage applications from women and minorities.

NW126936R

Johannes Kepler University of Linz - Austria

From October 1, 2009, the permanent position of a Professor of "Theoretical Physics"

is to be filled in the Faculty of Technical and Natural Sciences.
It will be the task of the successful applicant to cover the field of Theoretical Physics in its entirety within teaching and to represent and further develop his or her special area within research. The detailed requirements are contained in a job description, that can be accessed on the Internet under the address http://www.jku.at/professuren.

A prerequisite for application is a Habilitation or equivalent qualification in the advertised subject.
The Johannes Kepler University is seeking to increase the representation of women among its scientific personnel and therefore would expressly request qualified women to apply for the post.. In the case of identical qualifications, preference will be given to a female applicant.

Taking into account the criteria stipulated in the job description, interested parties are requested to submit the required documentation and their application form electronically to the rector of the Johannes Kepler University of Linz by midnight on March 31, 2008 (mailto: bewerbung@jku.at). Should electronic communication of the documents not be possible, those are to be sent in quintuple form, to be received by the rector at latest within a period of one week after the end of the application period.

Rector Prof. Dr. Richard Hagelauer
Johannes Kepler University
A-4040 Linz, Austria.

W123667R

We are the largest interdisciplinary research centre in Europe and work in the following research fields: Energy, Information, Life, and Environment.

Within the „Jülich Aachen Research Alliance" (JARA), a collaboration in the field of molecular magnetism has been established, where several physics institutes, in particular the institutes for „Electronic Properties", for „Quantum Theory of Matter" and „Scattering Methods" of the Institute for Solid State Research are collaborating in an interdisciplinary manner with the Institute for Anorganic Chemistry of the RWTH Aachen. For this research field, we are seeking for our Institute of Solid State Research (IFF) a

PHYSICIST (PostDoc) or PHYSICAL CHEMIST (PostDoc), in Materials Science

– code 017/2008 –

- Optimisation of magnetic interaction parameters in two dimensional networks of molecular magnets on substrate surfaces also with possible future applications in quantum information technology
- besides the microscopic characterisation, the focus will be on modern scattering methods at neutron and synchrotron x-ray sources, such as polarised neutron scattering under grazing incidence or resonant x-ray scattering in the frame of the „Jülich Centre for Neutron Science" JCNS.

We expect from you:

We are particularly interested in highly motivated candidates, which can work well in a team and have an excellent knowledge of solid state physics or -chemistry. We expect mobility, in particular the willingness to perform experiments at various large scale facilities and a sound knowledge of English. We would welcome experience in the field of magnetism as well as working experience in scattering methods (neutron and synchrotron x-ray scattering).

Initially, a fixed term contract for three years will be offered.

Equal opportunities is an important cornerstone of our staff policy at Research Centre Jülich, for which we have been awarded the „TOTAL E-QUALITY" award. Applications from women are therefore particularly welcome. Applications from disabled persons are welcomed.

Salary and social benefits will conform to the provisions of the Collective Agreement for the Civil Service (TVöD).

Please send your application, giving the reference code to:

Forschungszentrum Jülich GmbH
Geschäftsbereich Personal
– Personalentwicklung –
52425 Jülich
Telefon 02461 61-5358

Further Informationen at:
www.fz-juelich.de

JÜLICH FORSCHUNGSZENTRUM

W126128R

We are the largest interdisciplinary research centre in Europe and work in the following research fields: Energy, Information, Life, and Environment.

For our Institute of Solid State Research (IFF) we are seeking a

PHYSICIST (PostDoc) or PHYSICAL CHEMIST (PostDoc), in Materials Science

– code 015/2008 –

- Working in our research focus „highly correlated electron systems", in particular on materials with colossal magnetoresistance or multiferroica
- preparation and macroscopic characterisation of the samples, e. g. with our PPMS-system
- investigation of the order and excitations of spin-, charge-, orbital- and lattice degrees of freedom by means of modern scattering methods at neutron and synchrotron radiation sources, aiming at a microscopic understanding of the macroscopic properties.

We expect from you:

We are particularly interested in highly motivated candidates, which can work well in a team and have an excellent knowledge of solid state physics. We expect mobility, in particular the willingness to perform experiments at various large scale facilities and a sound knowledge of English. We would welcome experience with preparation and characterisation of ceramics and single crystal samples of complex transition metal chalcogenides as well as working experience in scattering methods (neutron and synchrotron x-ray scattering),

as well as a

PHYSICIST (PostDoc), in Materials Science

– code 016/2008 –

- Working in our research focus „nanomagnetism"
- preparation of thin magnetic films and layer systems (metals, dilute magnetic semiconductors, complex transition metal oxides)
- structuring by means of electron beam- or interference lithography
- characterisation of the samples with MOKE, SQUID etc.
- investigation of magnetic ordering phenomena and magnetisation dynamics by means of modern scattering methods at neutron and synchrotron radiation sources.

We expect from you:

We are particularly interested in highly motivated candidates, which can work well in a team and have an excellent knowledge of solid state physics. We expect mobility, in particular the willingness to perform experiments at various large scale facilities, and a sound knowledge of English. We welcome experience with the preparation (MBE, sputtering, PLD, etc.) and characterisation of thin film systems, as well as working experience with scattering methods (neutron and synchrotron x-ray radiation).

Initially, fixed term contracts for three years will be offered.

Equal opportunities is an important cornerstone of our staff policy at Research Centre Jülich, for which we have been awarded the „TOTAL E-QUALITY" award. Applications from women are therefore particularly welcome. Applications from disabled persons are welcomed.

Salary and social benefits will conform to the provisions of the Collective Agreement for the Civil Service (TVöD).

Please send your application, giving the reference code to:

Forschungszentrum Jülich GmbH
Geschäftsbereich Personal
– Personalentwicklung –
52425 Jülich
Telefon 02461 61-5358

Further Informationen at:
www.fz-juelich.de

JÜLICH FORSCHUNGSZENTRUM

W126127R

2nd International Conference on Advanced Nano Materials (ANM-2008)

June 23rd-25th 2008, Aveiro, Portugal

The Nanotechnology Research Division (NRD) of the University of Aveiro, Portugal is pleased to announce that the second series of International conference on Advanced Nano Materials (ANM-2008) will be held at Aveiro, Portugal during 23rd-25th June 2008. This premier conference on nanotechnology will address the latest issues on cutting edge nanotechnology. The proceedings of the conference will be published in a special issue of the Journal of Nanoscience and Nanotechnology (JNN). More elaborate details on this conference are available at **http://anm2008.web.ua.pt**

Links to the highlights
NRD: http://www.mec.ua.pt/cvd/
University of Aveiro: http://www.ua.pt
JNN: http://www.aspbs.com/jnn/

W126768E

CIC nanoGUNE

nanoscience cooperative research center

The Nanoscience Cooperative Research Center CIC nanoGUNE Consolider (www.nanogune.eu) invites applications and nominations for two positions as

Group Leaders

CIC nanoGUNE Consolider, located in San Sebastian, Basque Country (Spain), is a R&D center created recently with the mission of conducting basic and applied world-class research in nanoscience and nanotechnology, fostering training and education excellence, and supporting the growth of a nanotechnology-based industry

The Group Leaders of nanoGUNE will be responsible for the design, management, and operation of their respective Research Area and laboratories. At the present time, nanoGUNE is welcoming applicants in the following disciplines

- **Nano-Scale Devices (#001)**
  All qualified candidates will be considered. Special preference might be given to candidates specializing in nano-mechanical, nano-fluidic, nano-chemical, nano-biological, nano-magnetic, or optoelectronic devices or technologies
- **Nano-Scale Imaging (#002)**
  All qualified candidates will be considered. Special preference might be given to candidates specializing in electron microscopy or scanning probe microscopy techniques

Candidates should have an outstanding track record of research, with an orientation to nanoscience and nanotechnology, a proven ability to obtain competitive research funding, and a proven record of technological transfer initiatives. Proficiency in spoken and written English is compulsory, knowledge of Spanish is not a requirement. An attractive remuneration will be offered.

Applicants should forward their CV, a summary of research interests, and a list of at least three references to director@nanogune.eu

Closing date: 15 April 2008

W125244R

nature REVIEWS MICROBIOLOGY

Associate Editor

Nature Reviews Microbiology has a vacancy for an Associate Editor. This exciting position involves working closely with the Chief Editor and other members of the journal team on all aspects of the editorial process, including commissioning and editing reviews, organizing peer-review, writing for the journal, and developing the content of the journal, both in print and online.

To meet these challenging tasks, the ideal candidate will have a broad knowledge of microbiology and hold a PhD in a relevant field. We are particularly interested in applicants with at least 2 years of postdoctoral experience, but we would welcome applications from outstanding candidates who have recently completed their Ph.D. A key aspect of the job is liaising with the scientific community and attending international conferences, so the successful candidate must be dynamic and outgoing with good interpersonal skills. Previous editorial experience would be an advantage, but is not essential

The position will be based in the London office of Nature Publishing Group, and the terms and conditions are highly competitive, reflecting the importance and responsibilities of the role. For further information about *Nature Reviews Microbiology* series visit http://www.nature.com/nrmicro

Contact Details:
To apply, please send your CV a summary of relevant experience, and current salary, quoting reference number NPG/LON/835 to: Denise Pitter, Personnel Assistant, at londonrecruitment@macmillan.co.uk

All candidates must demonstrate the right to live and work in the UK to be considered for the vacancy.

nature publishing group npg

Closing date: Friday 14th March 2008

W128131R

CALL FOR 100 PREDOCTORAL RESEARCH GRANTS AT UNIVERSITAT AUTÒNOMA DE BARCELONA

Develop your professional career in a modern and prestigious university employing 3000 researchers and located in the centre of an important scientific and technological pole.

Applications must be submitted from 14 March to 18 April 2008.

Duration of the grant: 4 years

Grant holders will participate in doctoral programmes or official master's degree courses.

For more information on the research areas offering grants and application procedures please visit:

www.uab.es/researchgrants

Universitat Autònoma de Barcelona has a gender equality policy and an action plan for the integration of disabled persons.

UAB Universitat Autònoma de Barcelona

W126760R

IMMUNOEPIDEMIOLOGIST
Tenure-Track/Tenured Investigator Position

The new Infections and Immunoepidemiology Branch (IIB, http://www.dceg.cancer.gov/iib) in the Division of Cancer Epidemiology and Genetics (DCEG), National Cancer Institute (NCI), National Institutes of Health (NIH), Department of Health and Human Services (DHHS), is recruiting for a tenure-track/tenured epidemiologist with experience and interest in the study of immunology and cancer.

Research at the IIB focuses on understanding the causes and mechanisms involved in the development of tumors linked to infectious agents and in understanding the mechanisms underlying successful immune responses as they relate to cancer risk and to successful responses to vaccination. Both infectious and host immunological factors are considered in the context of human epidemiological studies. Studies undertaken by the group are often large, international and include rich biological specimen components to permit in-depth evaluation of biological processes, including immunological and inflammatory mechanisms, involved in tumor development and vaccination responses using state-of-the-art techniques. The Branch has an active set of studies aimed at evaluating the role of numerous infectious agents (including EBV, HIV, HPV, HTLV-1 and KHSV) and tumor sites (including cervical cancer, gastric cancer, Hodgkin and non-Hodgkin lymphomas, lung cancer, nasopharyngeal carcinoma, and oral/oropharyngeal cancers). The Branch also houses the 7,500 woman community-based vaccine trial in Costa Rica designed to evaluate the efficacy and impact of a new HPV-16/18 virus-like particle vaccine, and an HPV immunology laboratory that complements field activities and allows interactive evaluation of hypotheses of immunological importance within our studies.

The successful candidate will receive research support from the intramural research program of NIH for conducting innovative studies aimed at elucidating inflammatory and immunological mechanisms of HPV-related or other cancers and/or vaccine responses. Applicants must have an M.D. and/or Ph.D. in epidemiology or a related field, and considerable post-doctoral experience in cancer epidemiology, molecular epidemiology and/or tumor or vaccine immunology. A record of peer-reviewed publications in one of these fields is required. A demonstrated ability to lead complex epidemiologic investigations is highly desirable. The successful candidate should have strong analytical skills, a good understanding of biological/immunological processes, and a demonstrated ability to collaborate across disciplines. Strong oral and written communication skills are an important requirement. Applications will be evaluated on their ability to develop a creative, independent program of epidemiological research applicable to understanding immune determinants of successful vaccination against cancer causing infections and/or immunological determinants of HPV-related or other cancers; and to collaborate effectively in a multidisciplinary setting.

Interested individuals should send a cover letter, curriculum vitae, a brief summary of research experience, accomplishments and research interests and goals, copies of three publications or preprints, and three letters of reference to: **Ms. Judy Schwadron, Division of Cancer Epidemiology and Genetics, National Cancer Institute, 6120 Executive Blvd. EPS/8073, Bethesda, MD 20892**

Candidates should submit applications by **May 30, 2008**; however, the search will continue until a qualified candidate is found. Additional information about staff and ongoing research in the Division of Cancer Epidemiology and Genetics and in the Infections and Immunoepidemiology Branch is available at **http://www.dceg.cancer.gov**. Prospective applicants should send E-mail inquiries to **Allan Hildesheim, Ph.D., Branch Chief (hildesha@exchange.nih.gov)**. This position is subject to a background investigation. DHHS and NIH are Equal Opportunity Employers.

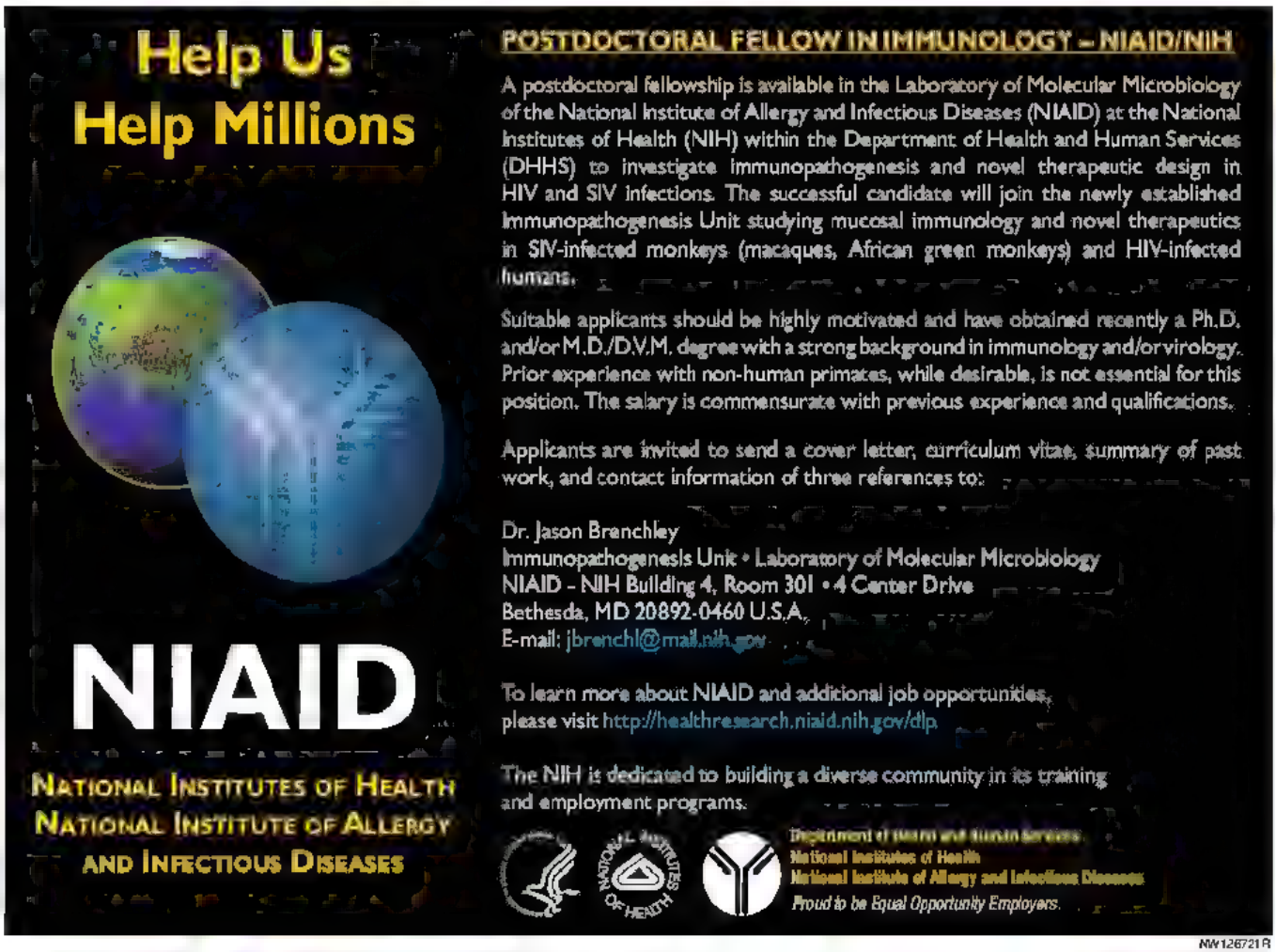

LANCASTER UNIVERSITY

Aiming for greater diversity

The School of Health and Medicine

The creation of a new School of Health and Medicine is at the heart of Lancaster University's strategic developments. The School brings together colleagues working in biomedical and life sciences, health research, and medicine, in a novel cross-disciplinary mix. We wish to appoint several academic posts in the first phase of expansion, from September 2008 or as soon as possible thereafter.

All successful candidates will have an outstanding, or emerging, research record in an area complementing existing strengths in the School and will be expected to play significant roles in research, in the delivery of the undergraduate medical degree and in the development of new undergraduate or postgraduate degree programmes.

Specifically, we wish to appoint in the following areas:

Professor in Primary Care Reference: A996

(joint with North Lancashire Teaching Primary Care Trust)

Lecturer in Medical Education Reference: A997

Lecturer in Health Care Management & Leadership Reference: A004

(For Primary Care, Medical Education and Healthcare Management & Leadership please contact Professor Anne Garden a.garden@lancaster.ac.uk)

Professor(s) in Biomedicine Reference: A998

Lecturers in Biomedicine (2 positions) Reference: A999

(For Biomedicine please contact Dr Jane Owen-Lynch j.owen-lynch@lancaster.ac.uk)

Professor in Environmental Epidemiology or Reference: A001

Public/Population Health Reference: A002

Lecturer in Public/Population Health Reference: A003

(for Epidemiology post please contact Professor Peter Diggle p.diggle@lancaster.ac.uk, for Public/Population Health please contact Professor Chris Hatton chris.hatton@lancaster.ac.uk)

We welcome expressions of interest from research groups who share our ambitions for the new School of Health and Medicine.

Salary

Professorial minimum £55,620
Lecturer Grade 7 £30,013 - £33,780
Lecturer Grade 8 £34,793 - £41,545

Closing date for all posts 28 March 2008.

To apply or receive further information please visit our website or telephone Human Resources quoting the appropriate reference on (01524) 846549 (answerphone).

www.lancs.ac.uk/hr/jobs

U126988PM

University of Erlangen-Nuremberg, Germany

1 The Faculty of Natural Sciences invites applications for a tenured

W2-Professorship in Neurobiology

in the Department of Biology

Successful candidates should represent the field in research and teaching. Applicants should have an excellent research record in mammalian neurobiology and expertise in state of the art molecular imaging techniques, ideally in combination with electrophysiology or mouse genetics. The successful candidate is expected to strengthen existing research cooperations and to contribute to new neurobiology initiatives of the university. Teaching includes lectures and courses for bachelor and master students in the fields of animal physiology and neurobiology.

The position is to be filled by April 1, 2009.

2 The Faculty of Natrual Sciences invites applications for a tenured

W3-Professorship in Genetics (chair)

(succession of Prof. Dr. G. Fey)

in the Department of Biology.

Successful candidates should represent the field of Genetics in research and teaching. Applicants must have an excellent research record in mammalian molecular genetics, preferentially by the use of genetically modified mice. State of the art animal and transgenic facilities are available on site. The successful candidate is expected to strengthen coordinated research programs at the University. Teaching responsibilities include lectures and courses in the Bachelor and Master programs of the Department of Biology.

The position is to be filled by April 1, 2010.

Qualifications include university undergraduate and doctoral degrees, good teaching skills, and a habilitation or equivalent other qualification, which may have been gained outside the University or within a "Junior Professorship".

At the time of appointment the candidate must not be older than 52 years of age. The Ministry for Science, Research and Art may allow an exception in special cases, which has to be approved by the Ministry of Finance.

The University of Erlangen-Nuremberg actively encourages applications from female candidates in an effort to increase female representation in research and teaching.

Applications from the severly disabled having the same suitability for appointment as other candidates will be given priority.

Application documents (curriculum vitae, photograph, list of publications and teaching activities, certified copies of degree certificates but no publications) and a brief statement of research interests must be sent by the latest **May 1, 2008**, to: Dekan der Naturwissenschaftlichen Fakultät der Universität Erlangen-Nürnberg, Universitätsstr. 40, 91054 Erlangen, Germany.

Friedrich-Alexander-Universität Erlangen-Nürnberg

www.uni-erlangen.de

W126987R

Need to find the ideal candidate *fast*?

Visit

www.naturejobs.com

to discover how applicants can respond directly to you by email.

nature jobs
making science work

Johnson & Johnson Pharmaceutical Research & Development (J&JPRD) is a global research and development organization with researchers both in the United States of America and Europe, of whom over a thousand are working at the company's Beerse site in Belgium.

The company sets very high qualitative and ethical standards. Johnson & Johnson Pharmaceutical Research & Development, a division of Janssen Pharmaceutica NV, is located in Beerse, at a distance of 35 km from Antwerp, a historical, cosmopolitan and international city in the center of Belgium and Europe.

Five positions are available immediatly at J&J PRD in the Neuroscience group.

(Senior) Scientist, Behavioral Pharmacology Expert (ref. 801055)

Senior/Principal Scientist, Behavioral Pharmacology Expert (ref. 801056)

Job description: • The candidate will have state-of-the-art knowledge in relevant neuropharmacology, and will be expert in behavioral pharmacology • Knowledge and hands-on experience in for example operant and/or cognitive behavioral tests aimed at investigating disturbances related to psychiatric and neurodegenerative disorders are considered an advantage. • Work will focus on drug development as well as technology development. Knowledge and some experience in the drug discovery is considered an advantage.

Profile: • Candidates should have a relevant life sciences degree and at least 5-10 years of experience in Drug Discovery and Development. • The candidates must be expert in behavioral pharmacology. • Have a proven track record in neuroscience research with emphasis on CNS disorders.

Senior/Principal Scientist, Alzheimer Expert (ref. 801058)

Job description: • The candidate will have state-of-the-art knowledge in the biology of Alzheimer's disease. • Knowledge and hands-on experience in assay development for screening of small molecules is considered an advantage. • Expertise in beta-amyloid and tau pathways is a strong asset.

Profile: • Candidates should have a PhD in Neuroscience, Biochemistry or related discipline and at least 10-15 years of experience in Neuroscience Research, including Alzheimer's disease. A minimum of 3 years experience in an industry environment is required.

(Senior) Scientist, Preclinical Imaging (ref. 801057)

Job description: • As part of a multidisciplinary project team, the candidates will be expected to establish and perform various ex-vivo functional neuroanatomical assays (receptor occupancy assay, 2-deoxyglucose autoradiography, gene and protein expression) in line with project requirements • Knowledge and hands-on experience with neuroanatomical methods such as radioligand autoradiography, in situ hybridisation and immunohistochemistry are required • Practical experience with in vivo imaging techniques (m-PET, MRI, bioluminescence) applied to psychiatry/neurology disease areas would be an asset.

Profile: • Candidates should have a PhD in Neuroscience, Neuropharmacology with at least 3 years postdoctoral experience preferably in a Pharmaceutical/Biotech environment.

Senior/Principal Scientist, Electrophysiology Expert (ref. 801053)

Job description: • The candidate will have a state-of-the-art knowledge in relevant neurophysiology and molecular biology, and will be expert in electrophysiological techniques such as patch clamp and/or brain slice recordings. • Knowledge and hands-on experience of electrophysiological applications (e.g. LTP, LTD) is considered a strong advantage.

Profile: • Candidates should have a relevant life sciences degree and at least 5-10 years of experience, ideally in drug discovery. • The candidates must have a hands-on expert attitude in electrophysiological techniques

Interested applicants should send a cover letter including statement of research interest, curriculum vitae with contact information for three references by e-mail attachment to, Kristine Declox (kdeclox@janbe.jnj.com)

Johnson & Johnson
PHARMACEUTICAL RESEARCH & DEVELOPMENT

W128813R

progress through innovation

FNP
foundation for Polish Science

HOMING PROGRAMME REINTEGRATION GRANTS FOR POLISH Ph.D.s

3rd Call for Proposals

The Foundation for Polish Science offers young **Ph.D.s returning from an extended scientific stay abroad** 2-year grants to facilitate their return to Poland. The grant consists of a stipend for the laureate and the subvention for scientific project and international cooperation.

The closing date for applications is **30 April 2008.**

For further information and application forms visit: www.fnp.eu

W126828R

Rat der Eidgenössischen Technischen Hochschulen ETH-Rat

Conseil des écoles polytechniques fédérales CEPF

Consiglio dei politecnici federali CPF

Board of the Swiss Federal Institutes of Technology ETH Board

The ETH Board invites applications for the

Director of Empa

the Swiss Federal Laboratories of Materials Testing and Research (www.empa.ch)

Empa is an interdisciplinary, application-oriented research institute in materials science and technology employing over 800 people. It is one of the four autonomous Research Institutes within the ETH Domain, the Swiss nationally funded education and research system. Empa focuses on nanotechnology, the engineering and technology development for adaptive systems, materials for health and performance, and materials for energy technologies, and questions related to natural resources and pollutants. In addition, sustainability of resource use and societal impacts in these areas are major cross-cutting research topics. As a technology center that provides scientific services, Empa plays a bridging role between academia, industry and governmental agencies.

The candidate for the Director of Empa is expected to be an internationally recognized individual with a broad scientific background and a distinguished track record in materials science and technology. A creative personality with strong leadership and managerial skills is sought. Competences in managing research groups and interdisciplinary projects in the area of science – engineering – technology are expected. Strong networks with industry and governmental agencies are essential. The successful candidate should have a demonstrated ability to translate scientific results into innovative applied technologies and new ventures and be ready to communicate and to develop strong links with the academic world, industry, governmental agencies, and the public. Familiarity with political issues related to education, research and technology transfer would be advantageous. Since the successful candidate will be considered for a professorship at ETH Zurich or EPFL (the Swiss Federal Institutes of Technology, Zurich or Lausanne, respectively), he or she should meet the criteria for a full professor at the university level.

Applicants should submit a letter of interest and a comprehensive curriculum vitae to: Chair of the Selection Committee, Dr. Fritz Schiesser, ETH Board, Haeldeliweg 15, 8092 Zurich, Switzerland. Further information may be obtained by phone (+41 44 632 20 04) or e-mail (baltensperger@ethrat.ch). All applications will be treated with strict confidence. Female candidates are particularly encouraged to apply.

W126840R

Johnson & Johnson Pharmaceutical Research & Development (J&JPRD) is a global research and development organization with researchers both in the United States of America and Europe, of whom over a thousand are working at the company's Beerse site in Belgium.

The company sets very high qualitative and ethical standards. Johnson & Johnson Pharmaceutical Research & Development, a division of Janssen Pharmaceutica NV, is located in Beerse, at a distance of 35 km from Antwerp, a historical, cosmopolitan and international city in the center of Belgium and Europe.

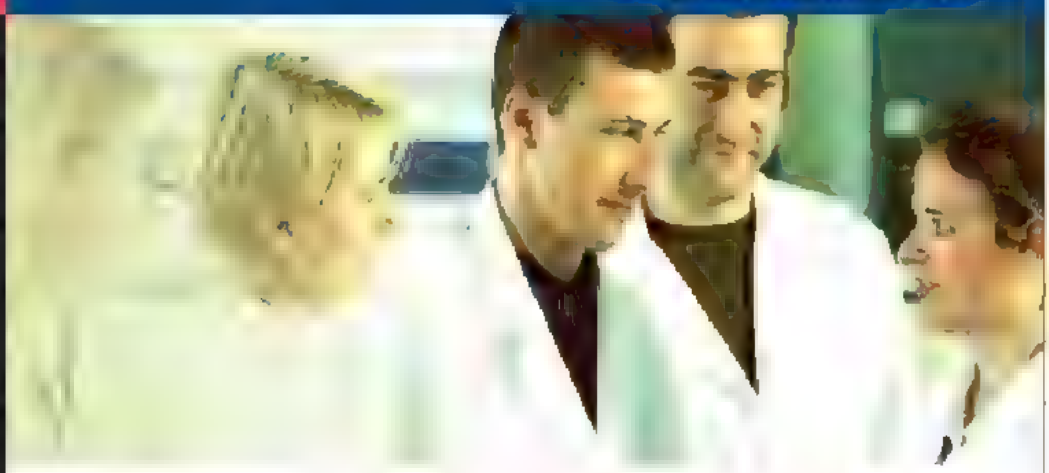

Five Post Doctoral positions are available immediately at Johnson & Johnson Pharmaceutical Research & Development in the areas of Translational Research, Target Identification and Validation in the Neuroscience group.

Postdoc 1

(ref. 802616)

The 3 year project is focused on the development of novel behavioural paradigms to study the effects of glutamatergic, cholinergic and dopaminergic systems on the role of the fronto-striatal loops in rodents in relation to neurodegenerative and psychiatric disorders, including the pharmacological characterization of novel compounds. The qualified candidate is a dedicated and highly skilled person, with a background in behavioural neuroscience/animal experimental psychology/ comparative & physiological psychology. The placement will be in the systems biology team

Postdoc 2

(ref. 802617)

The 3 year project is focused on the measurement of amyloid in brain and peripheral tissues in rodents, including transgenic mice, using novel technology that eventually should be translatable to studies in man, including the pharmacological characterization of novel compounds. The qualified candidate is a dedicated and highly skilled person, with a background in preclinical (in vivo) pharmacology. Knowledge of molecular neuroscience is considered an advantage. The placement will be in the systems biology team .

Postdoc 3

(ref. 802618)

The 2 year project is focused on the development of neuronal cell cultures for the molecular study of synaptic plasticity. The qualified candidate is a dedicated and highly skilled person, with a background in in vitro pharmacology/molecular neuroscience. The placement will be in the assay development team.

Postdoc 4

(ref. 802619)

The 2 year project is focused on the molecular analysis of the processes underlying synaptic plasticity in vitro and in vivo, including microarray and siRNA technology. The qualified candidate is a highly skilled person, with a background in molecular neuroscience/functional genomics. The placement will be in the functional genomics team.

Postdoc 5

(ref. 802620)

The 2 year project is focused on analysis and mining of data generated from genomic, proteomic and metabolomic studies in the area of synaptic plasticity. The qualified candidate is a dedicated and highly skilled person, with a background in molecular neuroscience/multivariate data analysis/bioinformatics. The placement will be in the functional genomics team.

Candidates may apply before having received their PhD or MD degree, but the selected candidate must have earned their degree before the start of the appointment. Applicants must possess excellent written and verbal skills in English. Evidence of a strong publication record is essential.
Successful applicants will join an interactive Neuroscience research environment with strong intra- and extramural collaborations in Belgium and abroad. The team conducts in vitro and in vivo pharmacology studies of different neurotransmitter systems and signaling cascades in the CNS, with a focus on schizophrenia, bipolar disorder and neurodegenerative disorders, in particular Alzheimer's disease.

Interested applicants should send a cover letter including statement of research interest, curriculum vitae with contact information for three references by e-mail attachment to Kristine Deckx (kdeckx@janbe.jnj.com)

Johnson & Johnson
PHARMACEUTICAL RESEARCH & DEVELOPMENT

W126643R

progress through innovation

An der Universität Duisburg-Essen sind im Fachbereich Biologie und Geographie, Zentrum für Medizinische Biotechnologie (ZMB), zum 01.10.2008 folgende Stellen zu besetzen:

1. W 3-Professur für „Molekularbiologie"

Bewerber/innen sollen durch exzellente Forschung auf dem Gebiet der Molekularbiologie international ausgewiesen sein und das Fach in Forschung und Lehre vertreten.

Die Forschungstätigkeit des/der zukünftigen Stelleninhabers/-in soll die bestehenden Stärken des Zentrums für Medizinische Biotechnologie ergänzen und ausbauen. Mögliche Forschungsthemen umfassen die Themenbereiche degenerative Erkrankungen, Tumorbiologie und epigenetische Mechanismen. Medizinisch relevante Grundlagenforschung und Erfahrung in der Biotechnologie oder Pharmaindustrie sind ebenfalls von Interesse. Eine Mitarbeit in lokalen SFBs und Graduiertenkollegs sowie Kooperationen mit Industriepartnern ist erwünscht.

Es wird erwartet, dass der/die Bewerber/in ein kompetitives, Drittmittel finanziertes Forschungsprogramm unterhält und die zu dieser Stelle gehörende Lehre in den Studiengängen Medizinische Biologie und Lehramt Biologie erfüllt.

Die Voraussetzungen nach § 36 Hochschulgesetz NRW (HG) sind ein abgeschlossenes Hochschulstudium, Promotion und zusätzliche wissenschaftliche Leistungen, die im Rahmen einer Juniorprofessur, einer Habilitation, einer wissenschaftlichen Tätigkeit an einer Hochschule, einer außeruniversitären Forschungseinrichtung, in Wirtschaft, Verwaltung oder einem anderen gesellschaftlichen Bereich im In- und Ausland erbracht wurden.

Weitere Auskünfte erteilt der Vorstandsvorsitzende des ZMB, Univ.-Prof. Dr. Michael Ehrmann, Tel. +49-201 183 2949, e-mail: michael.ehrmann@uni-due.de.

2. W 1-Juniorprofessur (mit Tenure Track) für „Molekularbiologie"

Die Stelle ist auf drei Jahre befristet und wird nach erfolgreicher Evaluation um weitere drei Jahre verlängert.

Der/Die Stelleninhaber/in beteiligt sich aktiv an Forschung und Lehre auf dem Gebiet der molekularen Zellbiologie.

Die Forschungstätigkeit soll die bestehenden Stärken des Zentrums für Medizinische Biotechnologie komplementieren. Diese umfassen, sind aber nicht limitiert auf, degenerative Erkrankungen, Tumorbiologie und epigenetische Mechanismen. Von besonderem Interesse sind Kandidaten/-innen, deren Grundlagenforschung zum Verständnis dieser Mechanismen beiträgt.

Es wird erwartet, dass ein kompetitives Forschungsprogramm über eingeworbene (oder einzuwerbende) Drittmittel aufgebaut wird und die zu dieser Stelle gehörende Lehre in den Studiengängen Medizinische Biologie und Lehramt Biologie erfüllt wird.

Einstellungsvoraussetzungen sind gemäß § 36 Hochschulgesetz NRW (HG) ein abgeschlossenes Hochschulstudium, eine naturwissenschaftliche Promotion mit herausragendem Ergebnis sowie wesentliche weiterführende wissenschaftliche Aktivitäten nach der Promotion (erfolgreiche Post-Doc-Phase).

Für beide Stellen gilt:
Die Universität Duisburg-Essen ist für ihre Bemühungen um die Gleichstellung von Mann und Frau mit dem „Total-E-Quality-Award" ausgezeichnet worden. Sie strebt eine Erhöhung des Anteils der Frauen am wissenschaftlichen Personal an und fordert deshalb einschlägig qualifizierte Frauen nachdrücklich auf, sich zu bewerben.

Schwerbehinderte werden bei gleicher Qualifikation bevorzugt eingestellt.

Bewerbungen mit den üblichen Unterlagen (Lebenslauf, Liste der wissenschaftlichen Veröffentlichungen, Unterlagen zum wissenschaftlichen und beruflichen Werdegang, beglaubigte Zeugniskopien, Darstellung des eigenen Forschungsprofils und der sich daraus ergebenden Perspektiven an der Universität Duisburg-Essen, Angaben über bisherige Lehrtätigkeit und Mitwirkung in der akademischen Selbstverwaltung sowie über eingeworbene Drittmittel) sowie dem ausgefüllten Informationsbogen (erhältlich unter www.uni-due.de/zmb) sind bis zum 06.04.2008 zu richten an den Dekan des Fachbereichs Biologie und Geographie der Universität Duisburg-Essen, Herrn Univ.-Prof. Dr. Peter Bayer, Universitätsstraße 2, 45141 Essen.

Weitere Informationen finden Sie unter www.uni-due.de/zmb.

W126898R

Frontiers in Genetics

UNIVERSITÉ DE GENÈVE

Frontiers in Genetics proposes an international program for doctoral training supported by the Swiss National Science Foundation. The program is based at the University of Geneva but includes participating members at the Universities of Lausanne, Zurich and Basel, at the Swiss Federal Institutes of Technology in Lausanne and Zurich, at the Swiss Institute for Experimental Cancer Research (Lausanne) and the Friedrich Miescher Institute (Basel). The program accepts students wishing to carry out a PhD starting in October 2008 and provides a strong background in molecular genetic, genomic and proteomic approaches for the study of modern biological problems.

We are seeking outstanding candidates with a degree in biological or physical sciences and a commitment to a career in research. The students selected will receive stipends for four years, subject to completion of all program requirements.

Applicants should download and send the registration form, a letter describing their interests, background and research experience, an official transcript of their university curriculum with grades, and contact information of 3 persons who can supply letters of recommendation, to:

Ms. Berénice Krebs
National Center of Competence in Research *Frontiers in Genetics*
30, Quai Ernest-Ansermet
CH - 1211 Geneva 4, Switzerland

Participating members:
Stylianos E. Antonarakis, Silvia Arber, Konrad Basler, Denis Duboule, Susan M. Gasser, Marie Gomez, Ernst Hafen, Pedro Herrera, François Karch, Ulrich K. Laemmli, Joachim Lingner, Serge Nef, Ivan Rodriguez, Botond Roska, Ariel Ruiz I Altaba, Ueli Schibler, David Shore, Pierre Spierer, Françoise Stutz, Bernard Thorens, Didier Trono, Jean-Dominique Vassalli, Walter Wahli

UNIL Université de Lausanne

ETH Eidgenössische Technische Hochschule Zürich Swiss Federal Institute of Technology Zurich

IGREC

SNF Swiss National Science Foundation

EPFL École Polytechnique Fédérale de Lausanne

UNI BASEL

University of Zurich

W126103R

DUKE NUS GRADUATE MEDICAL SCHOOL

Faculty Positions

–All Ranks –

Program in Emerging Infectious Diseases

The Duke-NUS Graduate Medical School Singapore (Duke-NUS GMS) is unique in bringing post-baccalaureate, research-intensive medical education to Asia, and represents a truly global partnership between two leading universities, National University of Singapore and Duke University. The Duke-NUS GMS shares a modern campus with Singapore's largest hospital and several national research centers. The Duke-NUS GMS is creating a world-class, academically based Program in Emerging Infectious Diseases that will both enhance health care in Singapore and serve as a national and international resource of excellence in emerging infectious diseases. The mission of the Program faculty will be to conduct high-level basic, applied and translational research, and to train graduate students, post-doctoral fellows, physician scientists and scientists in the disciplines relevant to emerging infectious diseases.

We are seeking individuals with outstanding scientific credentials for the Program. Faculty will be provided with the space and resources necessary to conduct state of the art research. The packages for faculty recruits will include full salary, generous start-up, and five years of annual research funding of up to S$500K/p.a., assuring a stable base of support that can be supplemented by competitive grant awards, which are expanding rapidly in Singapore. Areas of initial focus include dengue, influenza and zoonotic diseases. In addition to basic and physician scientists, we are seeking epidemiologists and entomologists. The faculty members will join the pioneering Duke and Singapore investigators already affiliated with the Duke-NUS GMS (see www.gms.edu.sg).

Interested candidates should send a CV and the names of three references to: **Duane J Gubler, Sc.D, Director, Program in Emerging Infectious Diseases, Duke-NUS Graduate Medical School, Singapore by email to: faculty.id@gms.edu.sg.**

For further enquiries on the faculty position, you may also email to: **Duane J Gubler at faculty.id@gms.edu.sg.**

JP125744R

HELMHOLTZ ASSOCIATION

The Helmholtz Association of German Research Centres is seeking excellent young scientists and engineers as leaders for

20 HELMHOLTZ YOUNG INVESTIGATORS GROUPS

IN SIX RESEARCH FIELDS:
ENERGY | EARTH AND ENVIRONMENT | HEALTH | KEY TECHNOLOGIES | STRUCTURE OF MATTER | TRANSPORT AND SPACE

The Helmholtz Association is Germany's largest organisation for scientific research and development. The 15 Research Centres united in the Association have a staff of 26,500 and an annual budget of about 2,3 billion euros. They perform top-rate research in strategic programmes and thus contribute to solving grand challenges which face society, science and industry.
The Association's potential for realising these ambitious objectives lies in the excellence of its personnel, its world-class large-scale facilities and scientific infrastructure and its experience in researching systems of great complexity.
The Young Investigators Groups will promote and further strengthen collaborations between the Helmholtz Centres and universities.

ELIGIBILITY: Individuals who have earned a doctoral degree within the last six years and have achieved a superior record of accomplishment during their doctoral and post-doctoral research.

DURATION: 5 years with a peer evaluation

PERSPECTIVE: Permanent employment, if evaluation attests excellence of group leaders

APPLICATION:

Step 1 Candidates contact the Helmholtz Centre of their choice with a CV, publication list and a letter of intent.

Step 2 The formal applications must be submitted by the chairman of the executive board of the Centre

For further details and application information:
www.helmholtz.de/yig

DEADLINES: For applicants: 5 May 2008
For Helmholtz Centres: 30 June 2008

The Helmholtz Association is an equal opportunity employer and is committed to increasing the percentage of women in group leader positions.

Contact: marianne.feldmann@helmholtz.de

W126551R

The Rockefeller Foundation (RF) works around the world to promote the well-being of humanity by expanding opportunities for poor and vulnerable people. With assets of almost $4 billion, it is one of the largest private foundations.

THE ROCKEFELLER FOUNDATION

Managing Director, Southeast Asia

Bangkok, Thailand

The Managing Director plays a key role in evaluating new and existing program initiatives for the Foundation and manages all day-to-day activities of the work and office in Southeast Asia. Individual will have overall responsibility for developing the regional strategy for initiative implementation, managing staff and other resources; providing leadership; ensuring effective communication and serving as a representative of the Foundation to multiple constituencies. Specific responsibility will also include helping to develop as well as leading Foundation initiatives and issues development in the "Climate Change" category.

Must have an advanced degree (PhD, JD, MA, MPP MBA) in an area related to Public Policy, Social Policy, Law, Business, Environment and Climate Science) and a minimum of 10 years related work experience, including at least 5 years in a managerial capacity. Must also possess strong leadership and strategic planning skills as well as a track record of turning ideas into measurable outcomes. Creativity and the ability to apply a new perspective to problems and opportunities are also needed. Experience with evaluative research methods helpful. The ability to travel extensively is a must.

The Rockefeller Foundation offers a generous benefits package and competitive salary commensurate with experience. For consideration please email CV, stating position of interest, by April 21, 2008, to: **hr1@rockfound.org**

The Rockefeller Foundation is an Equal Opportunity Employer

NW126398A

www.rockfound.org

nature chemical biology

Locum Assistant Editor

Nature Chemical Biology seeks a Locum Assistant Editor to join their editorial team for a period of six months to cover a maternity leave. The journal publishes high quality articles at the interface of chemistry and biology. For more information about *Nature Chemical Biology*, see our website (http://www.nature.com/naturechemicalbiology).

Candidates should have a broad interest in science, excellent communication skills, and a willingness and ability to learn new fields. Applicants should have a Ph.D. in chemistry or biology, with demonstrable research achievements. Postdoctoral experience is preferred but not required. The journal team is particularly interested in broadly trained applicants with significant knowledge of chemical and biological systems.

Key elements of the position include the selection of manuscripts for publication, and commissioning, editing and writing other content for the journal. This is a demanding and extremely stimulating position, which requires a keen interest in the practice and communication of science. The successful candidate will therefore be dynamic, motivated and outgoing, and must possess excellent interpersonal skills.

To apply, please submit a CV, a cover letter explaining your interest in the position and possible start date, along with a 'News & Views' style article (800 words or less) on a recent paper from the chemical biology literature. Applications should be sent (attached pdf files preferred) to Human Resources Department, Nature Publishing Group by e-mail: admin@natureny.com as soon as possible but not later than 17 March 2008. Position in our Boston office.

nature publishing group npg

NPG is an Equal Opportunity Employer. Additional information about Nature Publishing Group is available at http://www.nature.com.

JN126444A

Assistant Editor

Nature Biotechnology

Nature Biotechnology seeks an Assistant Editor for its editorial team based in New York. Expertise in systems biology and/or computational biology would be desirable, but not required.

Members of the editorial team evaluate manuscripts, oversee the peer review process, commission and edit secondary materials such as Reviews, and write short pieces and editorials for the journal. The successful applicant will attend scientific meetings and visit laboratories to maintain contact with the international scientific community. The position will play a key role in consolidating *Nature Biotechnology's* presence in the fields of systems biology and computational biology.

Excellent communication skills and a willingness and ability to learn new fields are a must. Applicants should have completed a Ph.D. in the biological sciences.

To apply, an interested candidate should submit a curriculum vitae, a short (500-1000 words) News and Views-style article on an exciting and newsworthy recent development in biotechnology, and a cover letter explaining their interest in the position to Human Resources Department, Nature Publishing Group.

All applications should be sent via email to: admin@natureny.com.

Please place "Assistant Editor Nature Biotechnology" in the subject line.

All applicants will be reviewed upon receipt with a close date of March 31, 2008.

Nature Publishing Group
75 Varick Street
New York, New York 10013, USA

nature publishing group npg

JN125803A

www.cam.ac.uk/jobs/
A world of opportunities

UNIVERSITY OF CAMBRIDGE

The Herchel Smith Professorship of Medicinal Chemistry

The Board of Electors to the Herchel Smith Professorship of Medicinal Chemistry invite applications for this Professorship from persons whose work falls within the general field of the Professorship, to take up appointment on October 1st 2008 or as soon as possible thereafter.

The Professorship is currently assigned to the School of Clinical Medicine. However, the Electors expect that the person appointed to the Professorship will also be associated with the Department of Chemistry, pursuing a research programme that encompasses both fundamental chemistry and clinical relevance. The Professor would also be expected to foster wider links between the Department of Chemistry and the Clinical School.

Further information may be obtained from the Academic Secretary, University Offices, The Old Schools, Cambridge, CB2 1TT, (email: ibise@admin.cam.ac.uk), to whom a letter of application should be sent, together with details of current and future research plans, a curriculum vitae, a publications list and form PD18 with details of two referees, so as to reach him no later than 18 April 2008.

Informal enquiries may be made to Professor Patrick Sissons, Regius Professor of Physic and Head of the School of Clinical Medicine (Tel: 01223 336738, e-mail regius@medschl.cam.ac.uk) and to Professor Jeremy Sanders FRS, Department of Chemistry (Tel: 01223 336411, e-mail jkms@cam.ac.uk)

The University is committed to Equality of Opportunity.

U126973A

www.naturejobs.com

Faculty of Science
School of Pharmacy and Biomedical Sciences

Senior Lecturer in Pharmaceutics

£32,796 - £40,335

We are seeking a Pharmacist or Pharmaceutical Scientist qualified to PhD level in an area related to pharmaceutics/drug delivery/formulation. The successful candidate will have a good record of publishing in peer-reviewed journals and is expected to make an active contribution to our current research interests including biomaterials and drug delivery systems. An appreciation of the application of formulation to support clinical practice would be considered highly desirable as would undergraduate and postgraduate teaching experience. Previous formulation work in either a hospital or industrial environment would also be advantageous.

The successful candidate will contribute towards the teaching of pharmaceutics including biopharmaceutics, basic and advanced drug delivery and other related subjects to students on our highly rated, fully accredited Masters degree in pharmacy and other associated pathways. In addition, a contribution to the teaching and supervision of students on a variety of postgraduate routes, e.g. MSc, MPhil, PhD and Professional Doctorate will be expected. The applicant will also be expected to make a significant input into the design and management of degree pathways. Success in obtaining research funding would also be very advantageous.

For an informal discussion, please contact the Head of School, Dr John Wong on 023 9284 3594 or email: john.wong@port.ac.uk or the Head of Pharmaceutics, Dr Michael Norris on 023 9284 2629 or email: mike.norris@port.ac.uk **Ref: ASCI 2019/N.**

2 x Senior Lecturers in Pharmacology

£32,796 - £40,335

Available from September 2008

The School of Pharmacy & Biomedical Sciences is seeking to recruit two established scientists with a background in pharmacology or physiology.

Candidates should have a first degree in an appropriate subject (pharmacology, physiology or biochemistry), and a PhD in a relevant field. You must be a self-motivated researcher with a good publication record in peer-reviewed journals. You will be expected to develop a research programme that is either related to, or complements, one of the areas of research strength in the School (neuropathology and oncology, molecular medicine, musculoskeletal pathology, respiratory, neuro and gastrointestinal pharmacology). Research in the School forms part of the University's Institute of Biomedical and Biomolecular Sciences (RAE Grade 5).

You will also contribute to high-quality teaching (scored 24 out of 24 in QAA review) in a range of undergraduate and postgraduate programmes.

For an informal discussion, please contact Dr John Wong, Head of School on 023 9284 3594 or email: john.wong@port.ac.uk or Dr James Brown, Head of Pharmacology on 023 9284 2154 or email: james.brown@port.ac.uk **Ref: ASCI 6020/N.**

To find out more about us and the roles we have on offer visit www.port.ac.uk/vacancies and apply on-line. Alternatively, telephone 023 9284 3421. Please quote the reference number on all communications.

Closing date: 21st March 2008.

Personnel Services, University House,
Winston Churchill Avenue,
Portsmouth PO1 2UP.

Committed to equality of opportunity

INVESTOR IN PEOPLE

University of Portsmouth

U127001A

Unleashing Potential

ulm university universität **uulm**

Ulm University invites applications for the

Junior-Professorship "Tropical Botany" donated by the Carl-Zeiss-Foundation

at the **Institute of Systematic Botany and Ecology** for a time span of six years.

Biodiversity and the animal-plant-interactions are one of the topics of the Biology at the Ulm University. The candidate should have an excellent record on the field of tropical biodiversity and his/her focus in one of the following fields.

- Structure and function of plant surfaces regarding their biotic and abiotic interactions
- Structural and functional diversity of plant vessels
- New materials derived from the biodiversity of plant structures and mechanical adaptations

Teaching responsibilities include providing courses in the relevant areas of biodiversity, tropical biology and his/her own research field for students of Biology at Bachelor and Master level. Courses at Master level should be taught in English. The professorship can rely on good laboratory equipment, herbarium and botanical garden with experimental facilites. The Ulm University offers also several possibilities for scientific cooperation in tropical biology, especially regarding animal-plant-interactions.

The selection and employment procedure is based on the regulations laid down by university law regarding the appointment of professors. Preconditions for employment are successful completion of academic studies at an institution of higher education, pedagogical aptitude, teaching experience and an outstanding Ph.D./doctorate.

The appointment will initially be on the basis of a temporary civil servant status (W_1) or on an employee status for four years. Following a positive evaluation, there will be a further two years' extension. Continuation in a tenure-track (W_3) is possible after successful evaluation and approval by the bodies of Ulm University and the Ministry for Research (MWK), State of Baden-Württemberg, Germany.

The University of Ulm is committed to increase the share of women in research and teaching positions and therefore explicitly encourages female candidates to apply.

Please submit your application together with a curriculum vitae, a brief description of research and teaching interests as well as a list of publications together with copies of the five most relevant publications to the Dean of the Faculty of Natural Sciences, Prof. Dr. K.-D. Spindler, Ulm University, Albert-Einstein-Allee 11, D-89081 Ulm, Germany, **no later than April 4, 2008.** More specific informations about this announcement can be obtained from Prof. Dr. M. Kazda, marian.kazda@uni-ulm.de, phone +49 731 50-22702.

Physically disabled applicants receive favourable consideration when equally qualified.

W126868A

The Center for Genomic Regulation (CRG, http://www.crg.es/) is a leading genomics research institute, associated with the University Pompeu Fabra (UPF) and located at the Parc de Recerca Biomèdica de Barcelona (PRBB, http://www.prbb.org/). The CRG contains six research programmes: Gene Regulation, Differentiation and Cancer, Cell & Development Biology, Systems Biology, Genes and Disease and Bioinformatics & Genomics, and has a partnership with the EMBL through the Systems Biology programme. The PRBB includes three other institutions devoted to biomedical research: the Department of Life and Health Sciences of the UPF (CEXS/UPF, http://www.upf.edu/cexs/), the Municipal Institute of Medical Research (IMIM, http://www.imim.es/) and the Centre for Regenerative Medicine of Barcelona (CMRB, http://www.cmrbarcelona.org/). To give support to this scientific community the CRG has built state of the art Genomics and Light microscopy facilities, as well as Screening and FACS facilities. New developments contemplate a top of the art proteomics facility. The CRG recruits academic staff and faculty internationally and encourages mobility and exchange.

Senior Scientist position in the Differentiation and Cancer Programme Ref. DC-GL 0308-01

The Senior Scientist appointment comes with an indefinite (rolling tenure) contract. Funds are provided for a Staff Scientist, a Postdoctoral position, a Technician and a Graduate Student, an equipped laboratory for up to 12 people, a start-up package, as well as funding for consumables and special equipment.
- The **Differentiation and Cancer Programme** focuses on the Epigenetic events in cancer (L. Di Croce), Epithelial homeostasis and cancer (S. Aznar-Benitah) and Hematopoietic stem cell biology and differentiation (T. Graf). We are seeking to appoint a researcher interested in the biology of mammalian stem cells and the role of transcription factors, circadian regulators and non-coding RNAs in cancer and cell reprogramming.

Three Group Leader positions in several Programmes

The Group Leader positions come with an initial contract for 5 years, renewable for 4 additional years upon review by an external scientific committee. Funds are provided for a Postdoctoral position, a Technician and a Graduate Student, an equipped laboratory for up to 7 people, a start-up package, as well as funding for consumables and special equipment. We have openings in the following programmes:

- Gene Regulation Programme - Ref. GR-GL 0308
This programme is coordinated by M. Beato and encompasses two senior groups (J. Valcárcel and R. Shiekhattar) and three group leaders (R. Méndez, F. Gebauer and J. Vilardell) that work on various aspects of transcriptional and post-transcriptional gene regulation. Additionally CRG is also implementing a transversal project on "Cell Reprogramming". We are looking for a new group leader working in any field of gene regulation that will complement the existing groups. The candidate should have an excellent scientific record, be prepared to lead an ambitious independent group and to collaborate with the local scientific community.

- Cell & Development Biology Programme - Ref. CDB-GL 0308
The programme is coordinated by V. Malhotra and comprises one senior group (I. Vernos) and one group leader (H. López-Schier), as well as the Advanced Light Microscopy Unit headed by T. Zimmermann. The CRG is recruiting an additional group leader interested in cellular and molecular aspects of development.

- Differentiation and Cancer Programme - Ref. CDC-GL 0308-02
This programme, coordinated by T. Graf, is looking for an additional group leader interested in mammalian stem cells, differentiation and mechanisms of cancer and in the fields described above.

Candidates should send a CV with list of publications, a brief research proposal and the addresses of at least 3 potential references to:

Miguel Beato, Director
Centre de Regulació Genòmica
Dr. Aiguader 88, 08003-Barcelona, Spain
rrhh@crg.es

Applications Deadline: 8 weeks after the publication of this add.

W126869R

Max-Planck-Institut
für Neurobiologie
Martinsried/München

The Department of Neuroimmunology (Director Hartmut Wekerle M.D.), Max-Planck-Institute of Neurobiology, seeks a

(neuro-) immunologist or neurobiologist

with interest in interactions between cells of the immune and nervous system. The position is on postdoctoral/senior postdoctoral level. The department, in cooperation with the Institute of Clinical Neuroimmunology, University of Munich, combines clinical and experimental approaches to study mechanisms of autoimmune responses within the central nervous system. The research is aimed to elucidate the pathogenesis of multiple sclerosis and ultimately to discover new, specific therapies. Our experimental projects combine multiphoton imaging and molecular analyses to study the behavior of autoimmune T lymphocytes within CNS and peripheral milieus, and use recently developed models of spontaneous brain autoimmunity to explore interactions between myelin-specific T and B cells. For more details please visit our website (http://www.neuro.mpg.de/english/rd/nr/research/index.html).

The ideal candidate is an enthusiastic, interactive, and creative scientist with experience in cellular or molecular immunology (T and/or B cells) or in cellular neurobiology and with the ability to integrate in a interdisciplinary team and to supervise PhD students. This position will provide an excellent opportunity for building up a scientific career including Habilitation.

Our research is funded by the Max-Planck-Society, Deutsche Forschungsgemeinschaft (SFBs) and corporate sponsors. The MPI of Neurobiology is located in the south of Munich within one of Europe's premier research campuses composed of Max-Planck-Institute, University Centers (Biology and Medicine) and a large number of biotechnological companies. Salary will be according to German tariff (TVöD).

The Max Planck Society is committed to employing more disabled individuals and especially encourages them to apply. The Max Planck Society aims to increase the number of women in those areas where they are underrepresented and urges them to apply.

Interested candidates are invited to apply with a cover letter summarizing scientific accomplishments, research and career goals, reasons for the interest in our project, and a list of three references.

Max-Planck-Institut für Neurobiologie
Am Klopferspitz 18
82152 Planegg-Martinsried

W126832R MAX PLANCK GESELLSCHAFT

School of the Environment and Natural Resources,
College of Natural Sciences,
Bangor University
and
Centre for Ecology and Hydrology
Natural Environment Research Council

Chair or Reader in Environmental Sciences/Physical Geography

Salary negotiable (minimum £48,023 p.a.)

We invite applications from candidates with an international reputation and an outstanding research record to this exciting new post in the University. The post is jointly funded for the first 5 years to facilitate closer interaction between the University and the Centre for Ecology and Hydrology Bangor station of NERC which is housed in a new, environmentally designed building on the Bangor University science site. Applications are particularly welcomed from individuals with experience in soils and sustainable land use, catchment science, hydrology or biogeochemistry.

The successful candidate will have a strong track record of publications, of attracting research funding, and of academic leadership. They will be expected to identify opportunities for collaborative research with the Centre for Ecology and Hydrology Bangor (http://www.ceh.ac.uk/sections/bef/bef.html) and to help deliver the joint vision of the **Environment Centre Wales** which has been funded to £5.8M by the University and NERC. The University is committed to developing Geography and the successful candidate will also take a leading role in developing the curriculum at undergraduate and postgraduate level.

Salary and application process. This is a permanent position. The salary is negotiable, minimum £48,023 p.a.

Application forms and further particulars should be obtained by contacting Human Resources, Bangor University; tel. (01248) 382926/388132, e-mail personnel@bangor.ac.uk; web: www.bangor.ac.uk

Please quote reference number 08-7/123 when applying.

Closing date for applications, Friday 4 April, 2008. Interviews will be held on 30 April, 2008.

For informal discussions concerning this position, candidates are encouraged to contact Professor Stephen Hawkins, Head of the College of Natural Sciences, tel. +44 (0)1248 382608; e-mail: s.hawkins@bangor.ac.uk, or Dr David Wright, Head of the School of the Environment and Natural Resources, tel: +44 (0)1248 382289; e-mail: d.wright@bangor.ac.uk

Centre for Ecology & Hydrology

PRIFYSGOL BANGOR UNIVERSITY

Wedi Ymrwymo i Gyfle Cyfartal • Committed To Equal Opportunities

U127008R

Group Leader Positions in Epigenetics & Development

MRC Clinical Sciences Centre

Two group leader positions are available in the Epigenetics and Development Section at the MRC Clinical Sciences Centre. Potential areas of research include biology of stem cells and cell commitment, chromatin biochemistry, chromosome biology, systems-based approaches to transcriptional regulation and the interface between signaling pathways and epigenetic regulators.

Applicants will have an excellent scientific reputation at or approaching international level as measured by an outstanding publication track record and high measures of esteem. Successful applicants will be expected to establish an internationally competitive research programme.

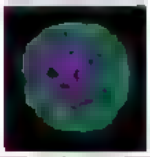

The MRC Clinical Sciences Centre is a direct funded MRC Institute located on the Hammersmith Campus of Imperial College in West London.

The Institute provides a comprehensive range of research services including transgenic, proteomic, FACS and confocal microscope facilities.

Current research in the Epigenetics and Development Section includes epigenetic regulation of gene expression, molecular mechanisms of transcriptional control, regulation of the cell cycle and mammalian development.

The research environment provides extensive opportunities for collaboration and interaction.

A generous startup package is available for successful applicants.

For more information visit our web site: www.csc.mrc.ac.uk
reference number CSC08/127

Informal enquiries can be made to
Niall Dillon e-mail: niall.dillon@csc.mrc.ac.uk

There is no formal deadline for applications although we are seeking to fill these positions by the end of 2008

U127016R

The Leeds Institute of Molecular Medicine

LEEDS

Leeds Institute of Molecular Medicine (LIMM)
Section of Experimental Therapeutics

Research Technician

Applications are invited for a technical position in Leeds Institute of Molecular Medicine (LIMM) to work on the generation and analysis of human cancer models using gene targeting in embryonic stem cells (ES cells). You will prepare and transfect targeting constructs for making mutations corresponding to chromosomal translocations (or other human tumour-associated changes) in ES cells and inject selected clones into blastocysts. In addition, transgenes will be made and injected into pro-nuclei. These projects will be carried out in collaboration with the biologists in LIMM.

The post will be held in LIMM under the supervision of Terence Rabbitts (Director of LIMM) at the St. James's University Hospital site, in the Wellcome Trust Brenner building.

The post is available immediately for a fixed term of three years.

University Grade 6 (£22,332 - £26,666 p.a.)

Applications should include a covering letter outlining the reason for the interest in the post, a CV and the name of three academic referees. The full job specification must be viewed online at http://www.limm.leeds.ac.uk/vacancies.htm Applications should be made by email to Mrs Jennifer Flowerdew email j.h.flowerdew@leeds.ac.uk

Job ref: 124027 Closing date: 25 March 2008

We welcome applications from all sections of the community. Textphone for deaf applicants only +44 (0)113 343 4353. All information is available in alternative formats, please contact +44 (0)113 343 4146.

U127002R

WORKING TOWARDS EQUALITY AND DIVERSITY www.leeds.ac.uk

UNIVERSITY OF BIRMINGHAM

School of Biosciences

Research Fellow investigating the mechanics of ape locomotion on flexible branches

Applications are invited for an NERC-supported Research Fellow position to study the mechanical interaction between arboreal bipedality and flexible branches in apes (including humans) to establish whether this behaviour could have been pre-adaptive for the adoption of habitual bipedality by early hominins. This post will include design of a portable compliant branch system and lab, zoo and computer simulation studies of the biomechanics, muscle-activity patterns and muscle-tendon-unit behaviour of human and orangutan bipedalism.

You should have a PhD and proven experience in engineering, biomechanics and/or computer modelling with an interest in biology/physical anthropology. Experience with kinematic, kinetic, EMG, ultrasound, O2 consumption and ADAMS/LifeMod and/or ABACUS computer modelling techniques is also desirable. Preference will be given to applicants that can demonstrate skills in a number of these areas.

Informal enquiries can be addressed to Dr Susannah Thorpe on email: s.k.thorpe@bham.ac.uk.

Maximum starting salary £25,134 a year, in the range of £25,134 - £32,796 a year (potential progression on performance once in post to £34,813 a year). This position is available from April 2008 for a period of 33 months.

Interviews will be held in early April.

Closing date: 28 March 2008 **Ref: H46205**

Details from ☎ 0121 415 9000 or www.hr.bham.ac.uk/jobs
HR, University of Birmingham, Edgbaston, Birmingham B15 2TT

A University of Fairness and Diversity

U126968R

AICR

Cancer knows no boundaries.
Fortunately, neither do we.

AICR International Cancer Research Fellowship

Applications are invited for the Association for International Cancer Research International Cancer Fellowship, which may be held at a research institute anywhere in the world, commencing on or after 1st January 2009.

Candidates, who may come from any country, should have a minimum of three years and normally a maximum of eight years postdoctoral research experience when they would take up the fellowship, unless they have taken a career break.

Fellowships are tenable for six years and will include a significant level of research support, of around £1million. The application will include the submission of a research proposal which may be in any area of non-clinical cancer research.

The deadline for receipt of completed applications is 30th June 2008. Further information about the fellowships and an application form can be obtained from the AICR website: http://www.aicr.org.uk/fellowships.stm

Association for International Cancer Research
Madras House, South Street, St Andrews, Fife KY16 9EH
Tel: +44 (0)1334 477910
Email: debbie.wheelans@aicr.org.uk
Charity No: SC022918

U126845R

Protein Phosphorylation Unit

MRC Medical Research Council

Postdoctoral Career Development Fellowship Position to investigate the role of the LKB1-AMPK-mTOR signal transduction pathway in cancer

£25,368 per annum

A postdoctoral position in the MRC Protein Phosphorylation Unit, School of Life Sciences University of Dundee is available to study the role of the LKB1-AMPK signalling pathway in cancer. The research will be undertaken in the group of Professor Dario Alessi at the University of Dundee. Suitable candidates should have a strong interest in signal transduction and previous experience in molecular and cellular biology, or biochemistry would be advantageous.

The MRC Unit has outstanding research facilities, provides stimulating environment in which to work and is recognised as one of the worlds leading signalling laboratories The position is for three years and starting salary will be at Band 4 of the MRC postdoctoral pay scale currently £25,368 per annum

For further information on the research being undertaken within Dario's group including recent publications please consult our web site (http://www.dundee.ac.uk/lifesciences/mrcppu/).

Applications for this role must be made online at http://jobs.mrc.ac.uk

Please include a CV and a list of publications. If you do not have internet access or experience technical difficulties, please call 01793 30 312, quoting reference number PPU08/116.

Informal enquiries may be made to the Professor Dario Alessi, MRC Protein Phosphorylation Unit via email: d.ralessi@dundee.ac.uk

Closing date: 4 April 2008.

For further information about the MRC visit www.mrc.ac.uk

The MRC is an Equal Opportunities Employer

'Leading science for better health'

U127011A

---

unicat





The cluster of excellence "UniCat - Unifying Concepts in Catalysis" offers several positions for scientific assistants (mainly PhD positions; several postdoctoral positions BAT IIa) in the fields of chemistry, physics, biology and engineering to be filled at the Technische Universität Berlin, the Freie Universität Berlin, the Humboldt-Universität zu Berlin, the Universität Potsdam (UP), the Fritz Haber Institute of the Max Planck Society and the Max Planck Institute of Colloids and Interfaces. The positions are immediately available.

Requirements: Completed scientific education with a degree in one of the areas mentioned above or a comparable qualification. Excellent written as well as spoken English is required.

Term of contracts: If not specified in the individual project, the positions terminate on 31 December 2010.

The Universities envisage to ensure equal opportunity for men and women, applications from female candidates with the advertised qualifications are explicitly solicited. Severely disabled applicants with equivalent qualifications will be given preferential treatment.

For specific information see: http://www.unicat.tu-berlin.de/jobs

Applications with necessary documents should be sent to the given addresses within 3 weeks.

If you would like to apply for several of the advertised positions, respective applications should be send separately indicating the project number in each case.

Application materials will not be returned. Therefore, applicants are requested to send only copies of all documents.

If you would like the vacancies in paper form, please write to:
Technische Universität Berlin
Sekr. C1
Straße des 17. Juni 135
10623 Berlin

W128888A

INSTITUTE OF ZOOLOGY
ZOOLOGICAL SOCIETY OF LONDON

ZSL
LIVING CONSERVATION

TWO FIXED-TERM POSTDOCTORAL FELLOWSHIPS

STARTING SALARY £28,109
(INCLUDING LONDON WEIGHTING)

Applications are invited for up to two postdoctoral research fellowships, each available from 1 May 2008. These are four-year fixed-term appointments for outstanding young researchers to undertake a programme of independent research within the Institute of Zoology's current research themes in conservation biology (http://www.zoo.cam.ac.uk/ioz/research.htm). Applications in the following areas are especially encouraged, but applicants wishing to work on other topics relevant to the Institute's research will also be considered

- The dynamics of extinctions and/or exotic introductions (Professor Tim Blackburn; Tim.Blackburn@ioz.ac.uk)
- Biodiversity and/or macroecology, including the analysis of Institute large-scale databases (Dr Chris Carbone; Chris.Carbone@ioz.ac.uk)
- The use of reproductive technologies for the conservation of threatened amphibians (Professor Bill Holt; Bill.Holt@ioz.ac.uk)
- Behavioural and/or population ecology (Dr Guy Cowlishaw; Guy.Cowlishaw@ioz.ac.uk)

Candidates must be within 5 years of completing a PhD and should be able to demonstrate their potential for successful independent research in the appropriate field. Applications should include a cover letter (stating preferred area of research of those listed if applicable), CV, a 1-2 page outline of the research they would develop over the course of the Fellowship, and the names and full contact details of three referees (including the candidate's PhD supervisor). For informal enquiries, contact the senior researcher identified within each specified area

Further details can be found at www.zsl.org/jobs

Send applications to: Human Resources, Zoological Society of London, Regent's Park, London NW1 4RY or email hr@zsl.org

Closing date: Monday, 31 March 2008.

Registered charity in England and Wales Number 208728

U127020A

THE UNIVERSITY OF
WARWICK

Warwick Centre For Analytical Science

Assistant Professor — £33,779 - £40,335 pa
Associate Professor — £41,545 - £48,161 pa
Professor — Salary negotiable

Three strategic posts are available in the new Warwick Centre for Analytical Science (WCAS), a unique multidisciplinary initiative funded by the EPSRC Science and Innovation Scheme, one in each of the following areas.

Physics - Electron Microscopy	**Ref: 34915-028**
Chemistry - Mass Spectrometry	**Ref: 34917-028**
Statistics - Statistical Methods in Physical Sciences	**Ref: 34916-028**

The new Centre will promote the growth of analytical science across the Departments of Chemistry, Physics, Statistics, Biological Sciences and the Warwick Medical School

You will have a strong track record in your respective research area, and a desire to enhance your international research profile through interdisciplinary collaboration and knowledge transfer

Appointments are expected to be made at Assistant or Associate Professorship level, but outstanding applications in Electron Microscopy and Mass Spectrometry may be considered at the Full Professor level. Each position will be supported by research personnel and all are available from 1 October 2008.

When applying please quote the relevant reference number for the specific post in which you are interested.

Informal enquiries to the WCAS Director, Prof. P. Unwin, email P.R.Unwin@warwick.ac.uk, 02476 523264

or the Heads of the Departments of:
Physics - Prof. M.J. Cooper, email M.J.Cooper@warwick.ac.uk
Chemistry - Prof. P.J. Sadler, email FRS, P.J.Sadler@warwick.ac.uk
Statistics - Prof. J. Hutton, email J.L.Hutton@warwick.ac.uk

Application packs are available from Human Resources on 024 7652 3685 (24 hour answerphone), by email recruit@warwick.ac.uk, our website below or www.jobs.ac.uk/warwick. An application form MUST be completed if you wish to be considered for this post.

Closing date for applications is 28 March 2008

J127016R

The University Values Diversity **www.warwick.ac.uk/jobs**

University of Oxford

Department of Zoology

University Lectureships in Zoology:
(1) Development/Ecology
(2) Quantitative Evolutionary Ecology

In association with Lady Margaret Hall and Wadham College

The Department of Zoology proposes to appoint two University Lectureships with effect from 1 September 2008 or as soon as possible thereafter. The successful candidates will be offered an Official Fellowship and Tutorship by Lady Margaret Hall (position 1) and Wadham College (position 2), under arrangements described in the further particulars.

Preference for position 1 will be given to applicants working at the interface of developmental biology and ecology, or ecological/evolutionary genomics. Applications for position 1 will also be considered from candidates working at the interface between any two or more of the Department's specialist research fields: behaviour, development, disease, ecology, entomology, evolution and ornithology.

Position 2 is for a quantitative evolutionary ecologist. You will be required to engage in research, which will contribute to the Department's research reputation; to teach, supervise and examine undergraduate and graduate students and to contribute to administration in the College and Department.

Further particulars, containing details of the application procedure and of the duties, may be obtained from: paul.harvey.pa@zoo.ox.ac.uk or by visiting: http://www.zoo.ox.ac.uk. The closing date for applications is 4 April 2008.

The University are Equal Opportunity Employers.
We positively encourage applications from people of all backgrounds

U128993RM

www.ox.ac.uk/jobs

Need to find the ideal candidate *fast?*

Visit

www.naturejobs.com

to discover how applicants can respond directly to you by email.

naturejobs
making science work

Max Planck Institute for Marine Microbiology

The Max Planck Institute (MPI) for Marine Microbiology in Bremen and the Center for Biotechnology (CeBiTec) of the University of Bielefeld plan to establish a research group for the investigation of microbial communities involved in the generation of energy from biomass. The group will be located at the MPI Bremen, an interdisciplinary center of environmental microbiology, but will have full access to genomics facilities of the CeBiTec Bielefeld. The group leader will be appointed associate professor at the University of Bielefeld with a reduced teaching obligation of 2 hours.

The Max Planck Institute for Marine Microbiology invites applications for an

Independent Junior Group Leader Position (W2)

in Microbiology of Sustainable Energy Production.

A particular focus is on complex anaerobic communities, microbial physiology, biochemistry, and ecology.

The position will be available for a period of five years, and includes a tenure-track option (W3) at the University of Bielefeld.

A search symposium will be held upon pre-selection of candidates (tentative date: June 2008). A Ph. D. in a related field, postdoctoral experience, and a visible record of independent research is required.

Please send your electronic application including curriculum vitae, a list of publications and a concise description of previous achievements, research plans and perspectives (up to 2 pages) before 18 April, 2008 to **snwg@mpi-bremen.de** (please use this contact also for questions regarding this position).

MAX PLANCK GESELLSCHAFT

W127005R

Technische Universität Berlin

unicat

The Cluster of Excellence (CoE) "Unifying Concepts in Catalysis" in Berlin seeks for excellent young researcher as leaders of Junior Research Groups (German salary scheme BAT Ib).

At the Technische Universität Berlin up to five research groups that will be funded by the end of October 2012 may be installed in various fields of the CoE´s programme such as, for example, Natural Product Synthesis, Surface Nanopatterning, or Molecular Modelling. Applicants having an excellent research record should submit innovative research proposals that complement the research programme of the CoE (see also: http://www.unicat.tu-berlin.de/). Applications should be addressed to Technische Universität Berlin, Unicat, Institut für Chemie, code number FO-988, Sekr. C1, Straße des 17. Juni 135, D-10623 Berlin within 4 weeks.

Additionally, two positions (German salary scheme BAT-O IIb) for Junior Research Group leaders are immediately opened at the Humboldt-Universität Berlin, Faculty of Mathematics and Natural Sciences I, Department of Chemistry in the fields of "Bioinorganic Chemistry" and "Theoretical Bioinorganic Chemistry". Applicants should have an outstanding record of achievement in important areas of the abovementioned fields which complement the existing research activities of the Department for Chemistry as well as the catalysis research within the Berlin area. Scientific exchange with research institutes within and outside Humboldt-Universität zu Berlin (HU) and with high tech companies at the science park Berlin-Adlershof and in the Berlin area will be appreciated. The candidate will be involved in the teaching of students covering the entire field of Inorganic chemistry and Theoretical Chemistry, respectively.

Applicants must be qualified by a postdoctoral research period of 2 - 4 years after graduation. HU seeks to increase the number of female employees in research and teaching and thus in particular invites qualified female scientists to apply for this vacant position. Physically handicapped persons will be preferred, if they are equally qualified.

Applications with necessary documents should be sent to Dekan der Mathematisch-Naturwissenschaftlichen Fakultät I, Humboldt-Universität zu Berlin, code number DR/067/07, 12489 Berlin, Newtonstr. 14, within 4 weeks.

Application materials will not be returned. Therefore, you are requested to send only copies of all documents.

W126865R

HUMBOLDT-UNIVERSITÄT ZU BERLIN

The Faculty of Mathematics and Natural Sciences and the Department of Biology invite applications for a

Full Professorship (W3) in Theoretical Neuroscience

Applicants should be able to establish a strong research and teaching program in computational, theoretical or cognitive neuroscience within the department's area of Theoretical Biology and Neurosciences. Candidates should have demonstrated expertise in the analysis of neural data and the modelling of experimental results, we welcome candidates who do both modelling and experiments. The successful candidate will collaborate with the Bernstein Center for Computational Neuroscience Berlin, which offers a Master's and PhD Program in "Computational Neuroscience" taught entirely in English. In addition, Berlin is host to many internationally recognized research consortia of relevance to neuroscience and provides a vibrant scientific community.

Applicants must meet the legal requirements for appointments of professors in accordance with § 100 of the "Berliner Hochschulgesetz". Applications from women and physically disabled persons are encouraged. Humboldt-Universität actively seeks to increase the number of women in research and teaching.

Applications should include three letters of recommendation, curriculum vitae, list of publications, reprints (max. 5), and a short research proposal (max. 5 pages) delineating the candidate's vision for doing theoretical neuroscience in Berlin. Materials should refer to the reference number **PR/009/08** and be sent to the following address: Humboldt-Universität zu Berlin, Dekan der Mathematisch-Naturwissenschaftlichen Fakultät I, Herrn Prof. Dr. C. Limberg, Unter den Linden 6, 10099 Berlin, Germany. Application materials will not be returned. Therefore, you are requested to send only copies of all documents. Additionally, electronic copies of all materials should be sent by email as PDFs to theorneuro@bccn-berlin.de. To ensure full consideration, applications should arrive no later than April 15, 2008.

W126863R

Telethon

Chief Scientific Officer

Job Description

Telethon is an internationally recognised Italian Foundation that funds research in the field of human genetic diseases.

Telethon invites applications for the position of Chief Scientific Officer who will coordinate the activities of its Scientific Office based in Milan.

The responsibilities of the scientific office are as follows:

a) Defining Telethon's scientific policies
b) Overseeing the peer review-based evaluation and selection of projects
c) Evaluating the results of funded projects
d) Producing key scientific documents
e) Communicating with patients' associations (to convey scientific results of the research in lay terms).

The Chief Scientific Officer will report directly to Telethon's Managing Director.

He / she will operate under the supervision and in consultation with a Scientific Advisory Board and will submit the strategic documents to the Board of Directors for final approval.

The candidate will also be part of Telethon's Managing Board, which is coordinated by the Managing Director and includes the Finance Director, the Fundraising Director and the Chief Communications Manager.

Professional/Technical Requirements

Training in a biomedical field
International experience
Research experience
Managerial experience in industrial and / or research organizations
Knowledge of international and national research models
Knowledge of peer review mechanisms in funding research
Fluency in both English and Italian
Expertise in the development of therapies is desirable

Managerial Requirements

The candidate must have the ability to develop a strategic vision in the field of Telethon's activity, i.e. research in the field of genetic diseases. Other requirements are:

Strong interpersonal skills
Leadership skills.

The Candidate must demonstrate that he / she is willing to adhere to Telethon's ethical principles and Mission.

Please submit resume to: Dr. Angelo Maramai, amaramai@telethon.it

Closing dates for applications is March 29, 2008.

W126832R

LEO

In vivo Pharmacologist

We wish to strengthen our efforts within Nephrology in our Department of Disease Pharmacology.

Therefore, we are looking for an experienced in vivo pharmacologist for our Nephrology Research Group. By participating in the group, you can play a key role in the drug discovery process.

The Nephrology Group is a dynamic team of seven research scientists and research technicians, whose main responsibility is to provide proof-of-principle studies for the evaluation in vivo of new drug candidates for nephrology indications, including chronic kidney failure.

The group is a part of the Department of Disease Pharmacology within Biological Research. In the Department of Disease Pharmacology, we work in a flexible and team-orientated manner and have state-of-the-art laboratory facilities at our disposal. The high standard of research that we provide is achieved in close collaboration with leading experts from universities and CROs and by participation in key scientific conferences.

Your Job

As a highly skilled scientist, you perform screening and characterisation of drug candidates in vivo in relation to our Nephrology Discovery Projects.

You will participate in developing, establishing and characterising in vivo models, and will validate them in relation to the diseases and targets that we focus on. Work in cross-disciplinary project teams and collaboration with external scientific partners, including CROs and universities, will be an important aspect of the job.

Your Qualifications

You:

- are a highly motivated and dynamic scientist with a background as DVM, MSc or PhD within in vivo pharmacology or a related discipline
- have solid experience with in vivo handling procedures
- have knowledge of nephrology, and preferably also inflammation research and immunology
- are able to work independently, have a good grasp for details, and excellent collaboration and communication skills within an international environment

Previous industry experience is an advantage

We offer

Unique opportunities for professional and scientific development in a dynamic, ambitious and informal research environment, together with a team of dedicated colleagues.

Other

For further information, please contact Group Leader Markus Latta on +45 7226 2296 or Head of Department Thomas Kongstad Petersen on +45 7226 2992.
To apply, please send your application and C.V. with reference no. "51351", to LEO Pharma A/S, Human Resources, Industriparken 55, DK-2750 Ballerup, no later than 17 March 2008.

W126763R

THE RAMMAL AWARD 2007 HONOURS POSTHUMOUSLY Prof. DANIEL AMIT

EUROSCIENCE's President Enric Banda announced today that, by a unanimous decision of its expert panel, the Rammal Award for the year 2007 will be awarded posthumously to Professor Daniel Amit, of Israeli and Italian citizenships, who passed away on November 3rd, 2007.

The Rammal Award, created in memory of the great Lebanese physicist Rammal Rammal (1951-1991), is awarded each year to an outstanding personality of strong scientific stature who, through his or her life and activity in a Mediterranean country (whether in fundamental or applied research, teaching, or the integration of knowledge), has elevated the level of scientific exchanges in this part of the world.

Professor Daniel Amit was 69. In 1978 he was appointed Professor at Hebrew University of Jerusalem, and was Chairman of the Racah Institute of Physics from 1984 to 1987. In 1991, he was appointed Professor at the La Sapienza University of Rome.

Daniel Amit was a high level scientist who worked at the forefronts of both elementary particle physics and statistical mechanics. His pioneering research on the modelling of neuronal networks had a strong impact on the development of computational neuroscience. He also worked tirelessly for a just and mutually acceptable peace between the Arab World (and in particular the Palestinian people) and Israel, especially through a close scientific and educational cooperation among peoples of this part of the world.

RW126463A

If Alzheimer's will end in my generation.

It's hard going through life with the thought of Alzheimer's hanging over your head. That's why for over 20 years, MetLife Foundation has supported research on this disease. Today, we are proud to honor Bart De Strooper, MD, PhD, University of Leuven and VIB Institute, Belgium; Robert Vassar, PhD, Northwestern University, Chicago and Philip C. Wong, PhD, The Johns Hopkins University School of Medicine, Baltimore. They join a growing list of scientists searching for a cure. So that one day, Alzheimer's won't follow in anybody's footsteps.

MetLife Foundation
A leader in finding an Alzheimer's cure

NW124833A

REPROGRAPHICS: CTT, London E17 6BU UK and **Alden Multimedia**, Northampton UK.
PRINTED BY: St. Ives Plymouth Ltd. UK; **Publishers Press**, Lebanon Junction, Ky, USA and **Obun Printing Co. Inc**, Tokyo, Japan

nature events

Directory 2008
get your free digital edition!

Events are essential for every scientist. From delegates discussing hot issues and opinion, through to networking and collaboration. Events provide a platform for learning and advancement.

With a burgeoning number of events across the globe, where can you find a complete resource to ensure you attend the right events in 2008?

The *Natureevents* Directory is published once a year and covers a complete range of scientific events, conferences and courses around the world.

Plan your year ahead, go to **www.natureevents.com** and download the digital edition of the 2008 *Natureevents* Directory for free.

If you are interested in advertising an event please call +44 (0)20 7014 4015
for US please call +1 800 989 7718 or email natureevents@nature.com

www.natureevents.com

---

nature events

nature publishing group npg

U12502E

Images courtesy of "SOHO (ESA & NASA)"

From Alice to everywhere, with love

A leap into the unknown.

Chaz Brenchley

JACEY

The problem was that someone had to go. Slowly, irrevocably, actually go.

The aliens, when they came, were … properly exotic. Difficult to see, difficult to understand. Their ship pulsed to indetectable rhythms; chilly computers sweated to find a pattern they could analyse.

The aliens brought a machine, the great phase-transmitter that stands on Salisbury Plain. With painful caution, they explained its function. They demonstrated; one by one, they entered the machine and were gone. Transmitted, relocated, somewhere else. Other aliens would come by return; there would be two-way traffic. The speed of light is the speed of information and light is an idler, but they would come.

It would not work for humans, yet. The phase-transmitter needed a template to work from. Uncountable numbers of these machines were spread across the Galaxy, and each of them would have to examine a living human before it could accept one in transmission.

Before humankind could take even a single phase-jump to the nearest station, someone had to go the slow way, in the ship.

Alice Temple had spent her life immersed in the science of language: first as an academic, then — since the aliens came — as a practitioner. At the same time, she had raised a husband and two children from idiocy to independence. She had achieved respect within her profession, renown outside it: and still she was unsatisfied.

Not bitter, not malcontented; short-changed, rather. She had done the best and the most that was available, and it wasn't enough. It had been too easy. Success ought not to be this cheap.

It was she who found a way to communicate with the aliens; of course, she was on the panel that decided who should leave with them. She sat through days of interviews with bright, healthy, noble young volunteers — and in the end, she said no.

"No," she said. "It has to be me."

It had needed her to make the aliens comprehensible here on Earth; it would need her again, to make humans comprehensible elsewhere.

When the others were done arguing the point, they argued outside it: her age, her responsibilities, her entitlements. She might make the journey in cold-sleep, but it would still be 30 years at sub-light speeds. She could come back through the machine, but even so: her parents would be dead, her unborn grandchildren would be having children of their own, she'd be out of her proper time, adrift. Better to dwell gracefully in her achievements, and leave adventure to the young …

It wasn't about grace, she said, nor yet adventure. It was necessary: to the project, to the planet and also to her. She needed to do this thing.

She was right, and finally they confessed it. When the alien ship left, she was the one in the cryo-tank.

She remembered being the one who went into the tank. Now she was the one coming out of it, with the deep knowledge in her bones of time and distance passed. She was still herself, this was still her body, but something had shifted between them.

This place, this time was not her own or anything like it. Just a terminal, a switching-place, a depot on a cold moon: there was a phase-transmitter constantly busy and a spaceport too, just as busy. Only living matter could go through the machine. Everything else must be carried, by old-school traders prepared to spend lifetimes in cold-sleep between brief spells ashore.

They took her to the machine, and it … engulfed her. She felt its slow and intimate examination like a reverse of the cryo-tank, endless awareness of going nowhere.

Once it had what it needed, it gave her back to herself; they said she could go home. Immediately, if she cared to: be the first human to pass this way, through the phase-transmitter to Earth.

"And then what?" she asked.

Why, then humans could transport here, at light-speed at last; and the young, the vigorous, the bold could go onward in ships to open up new routes to other planets, other vistas …

"What for me?" she said. "If I go home?"

They couldn't answer that, but she could. A little brief celebrity and a resumed lifetime of disappointment, of feeling that there should have been something more.

The alternative, of course, was to go on. Someone else could carry the message, that this portal was open to humans now. Before anyone arrived she could be well on her way to the next, beating a trail forwards.

But oh, this was a slow way to the stars, eked out, one body, one gateway at a time …

She mused, she argued with herself; at last, she asked more questions.

Yes, they said, the portal could be reconfigured, looped around to send its message to itself; but …

Yes, they said, the data stream could be divided, to make two copies of the same individual; but …

But, they said, catching on at last, the process would be lossy. Neither one of her would be what she was now. Not so sharp, not so vibrant. Less Alice.

Yes, they said, the iterations would still be perfectly good templates for the machines.

Yes, they said, if the beam could be split once, it could be split a dozen times.

But …

The next dozen cargo-ships to leave each carried a passenger. Like a starburst, Alice sent herself to a dozen other portals; and then again, a dozen each from those. And so on and on, fading and multiplying, slicing herself thinner and thinner until there was not enough Alice left to sustain a living body. Five billion living bodies.

It wasn't really humankind that flung outward to the stars. It was Alice. ■

Chaz Brenchley has been a professional writer since he was 18, working mostly in crime, horror, fantasy and science fiction. He claims to live down the dirty end of genre fiction. In fact, he lives in Newcastle upon Tyne.

25,000 Tagged ORF Clones

including the ones you want

TrueORF™

for tagged protein expression

TrueORF enables the expression of the encoded transcript as a C-terminally tagged protein with Myc and FLAG® epitopes, facilitating multiple applications that utilize an anti-tag antibody, such as protein detection, protein purification, subcellular localization, etc.

- Genome-wide coverage
- Sequence verified and guaranteed
- The C-terminal dual tag of Myc and FLAG®
- Transfection-ready: Provided as 10 ug of purified plasmid
- Easy shuttling into 20 tagged vectors using PrecisionShuttle™ system

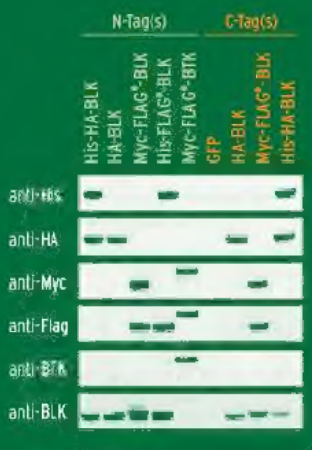

The Western blot analysis of HEK293 cell lysate over-expressing BLK or BTK tagged with indicated epitopes.

FLAG® is a registered trade mark of Sigma-Aldrich

ORIGENE
Your Gene Company

1-888-267-4436 • origene.com

DO LESS.

MAKE MORE HAPPEN.

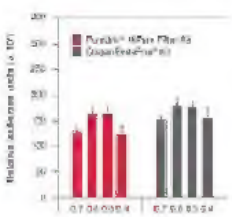

All PureLink™ HiPure Kits provide endotoxin levels and transfection efficiency equivalent to the Qiagen EndoFree Kit.

Demand more from your plasmid purification method—and get more with PureLink™ HiPure kits from Invitrogen. Purelink™ HiPure plasmid purification kits provide significantly higher yields, more effective lysate filtration, and higher final concentrations—all at a substantially lower cost. These kits also produce low-endotoxin DNA (see figure) so no matter the application, you can count on getting the plasmid you need. Every time. Just another way that Invitrogen is giving you real solutions to the problems you face every day. Get your FREE PureLink™ HiPure Plasmid Midiprep and Maxiprep Starter Kits at www.invitrogen.com/napsample.

invitrogen™